



PHYSICS & ENGINEERING EXPERIMENTS

Mechanics | Heat | Electricity | Optics | Atomic & Modern Physics | Bio- & Medical Physics

Find all experiments and products online at 3bscientific.com

DEAR VALUED CUSTOMER,



Dr. Johannes Recht

The revised Physics and Engineering Experiment catalog now contains more than 135 experiments for the modern Physics laboratory. This straightforward collection covers the whole spectrum of Physics, from classical to modern.

Each experiment includes:

- Objectives
- Easy to follow illustration of the experimental set-up
- Introduction of the theoretical and experimental background
- Summary of expected experiment results
- Detailed list of required equipment

Our web site www.3bscientific.com provides you detailed information and full product specifications.

Many of the experiments are compatible with our data logging system, VinciLab or WiLab. The powerful evaluation software Coach7, allows you to record and analyze measurement data and to perform video analysis and computational modeling.

Furthermore we are very pleased to present the new Bio- and Medical Physics chapter.

Highlights cover the following subjects:

- Fluid Mechanics
- Zeeman effect
- Installation and optimization of photovoltaic systems
- Speed of sound in solids
- Neurophysiology

If you require bespoke sets, we are able to assemble these for you on request. We strive to create experiments for all your teaching and learning needs and we are available to discuss these with you. You can contact us by telephone, e-mail or via our website 3bscientific.com. Instruction manuals and full product information can be downloaded from the website in PDF form. We will continue to be your partner when it comes to equipping your laboratory or classroom.

Yours sincerely

Dr. Johannes Recht | Director of Natural Science Business

CONNECT WITH US!



3BSCIENTIFIC.COM

Find us online! Order online, save time and find full product information! Also use our fast Quick Order!



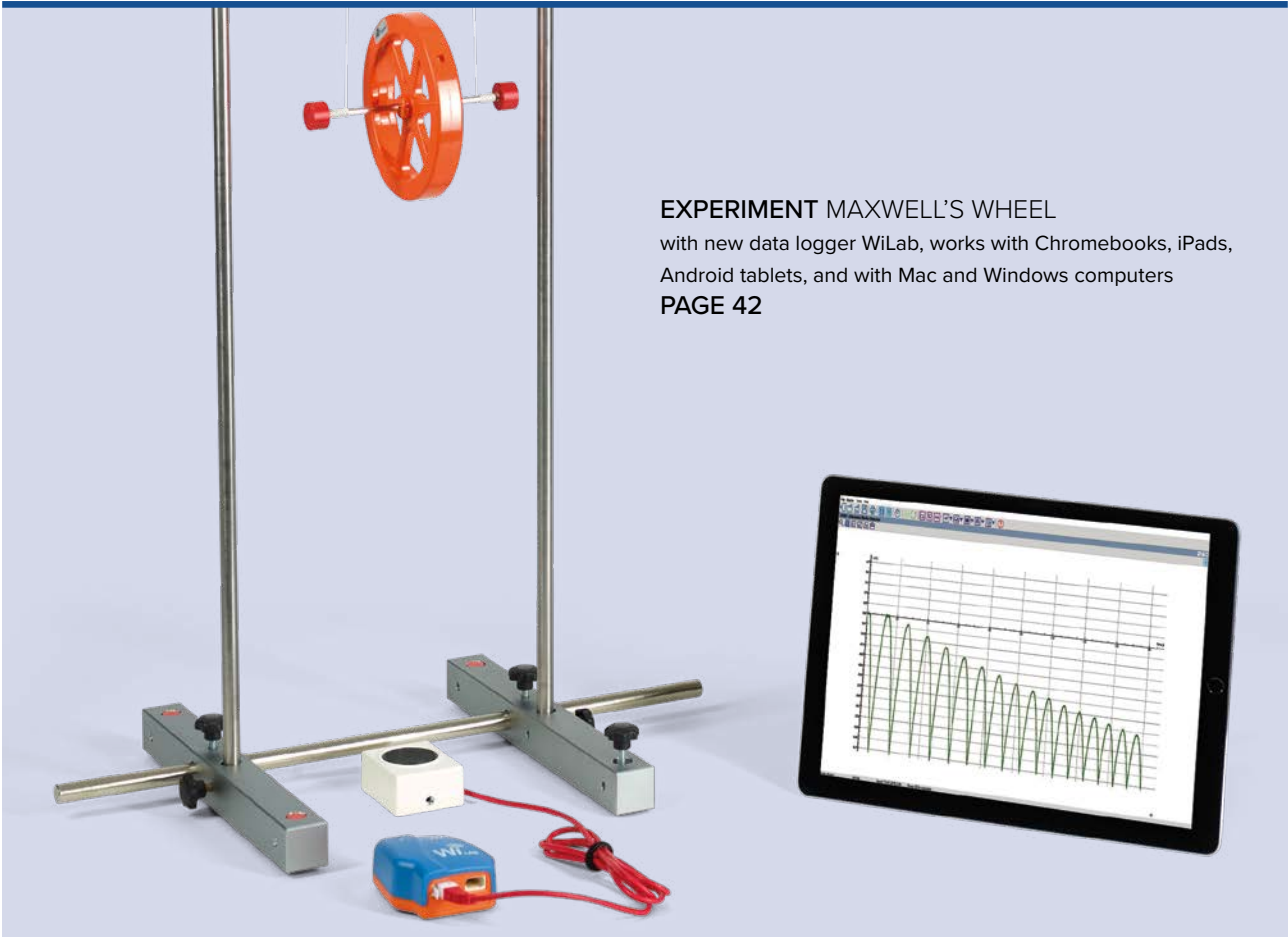
Send us an E-Mail to:
INFO@3BSCIENTIFIC.COM



Call us! We'll be happy to answer your questions!
+ 49 40 – 73966-0



Copyright © 2019 3B Scientific GmbH, Hamburg.
The unauthorized reproduction and publication of the catalog material is prohibited.



EXPERIMENT MAXWELL'S WHEEL
with new data logger WiLab, works with Chromebooks, iPads,
Android tablets, and with Mac and Windows computers
PAGE 42



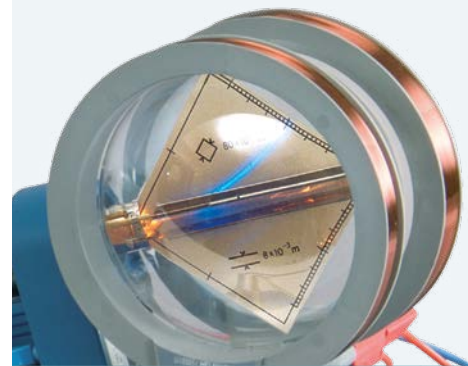
NEW EXPERIMENT ZEEMAN EFFECT PAGE 244



NEW EXPERIMENT DOPPLER SONOGRAPHY PAGE 276



CONTENT



MECHANICS

Measurement Procedures

Spherometer.....	6
Lengths and Volumes.....	8
Gravitational Constant.....	10

Force

Hooke's Law.....	12
First- and Second-Class Levers.....	14
Parallelogram of Forces.....	16
Inclined Planes.....	18
Static and Dynamic Friction.....	20

Buoyancy

Archimedes' Principle.....	22
Uniformly Accelerated Motion.....	24

Translational Motion

Motion with Uniform Acceleration.....	26
Laws of Collisions.....	28
Free Fall.....	30
Inclined Launch.....	32
Two-Dimensional Collisions.....	34

Rotational Motion

Rotational Motion with Uniform Acceleration.....	36
Moment of Inertia I.....	38
Moment of Inertia II.....	40
Maxwell's Wheel.....	42

Spinning Motion

Precession and Nutation of a Gyroscope.....	44
--	----

Oscillations

Harmonic Oscillation of a String Pendulum.....	46
Elliptical Oscillation of a String Pendulum.....	48
Variable g Pendulum.....	50
Kater's Reversible Pendulum.....	52
Foucault Pendulum.....	54
Simple Harmonic Oscillations.....	56
Pohl's Torsion Pendulum I.....	58
Pohl's Torsion Pendulum II.....	60
Coupled Oscillations.....	62
Mechanical Waves.....	64

ACOUSTICS

Wavelength and Speed of Sound

Speed of Sound in Air I.....	66
Speed of Sound in Air II.....	68
Propagation of Sound in Rods.....	70
Sound Propagation in Solids.....	72
Debye-Sears Effect.....	74

AERODYNAMICS AND HYDRODYNAMICS

Viscosity

Falling Sphere Viscosimeter.....	76
----------------------------------	----

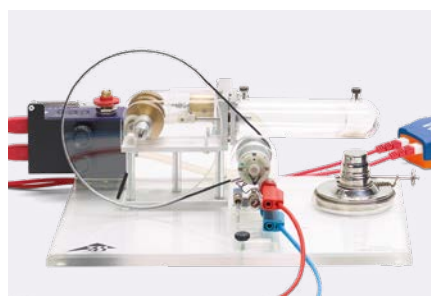
MECHANICS

Mechanics of Liquids and Gases

Surface Tension.....	78
----------------------	----

Deformation of Solid Bodies

Bending of Flat Beams.....	80
Torsion on Cylindrical Rods.....	82



THERMODYNAMICS

Thermal Expansion

Thermal Expansion of Solid Bodies.....	84
Water Anomaly.....	86

Transport of Heat

Heat Conduction.....	88
----------------------	----

Heat Transfer

Leslie Cube.....	90
------------------	----

Internal Energy

Increase of Internal Energy by Mechanical Work.....	92
Internal Energy and Electrical Work.....	94

Gas Laws

Boyle's Law.....	96
Amontons' Law.....	98
Adiabatic Index of Air.....	100
Real Gases and Critical Point.....	102

Heat Cycles

Stirling Engine D.....	104
Stirling Engine G.....	106
Heat Pumps.....	108

ELECTRICITY

Electrostatics

Electric Field in a Plate Capacitor.....	110
Voltage on a Plate Capacitor.....	112

Transport of Charge and Current

Charged Droplets of Water.....	114
Electrical Conductors.....	116
Wheatstone's Bridge.....	118
Ohm's Law.....	120
Kirchhoff's Laws.....	122

Transport of Charge and Current

Voltage Dividers.....	124
-----------------------	-----

Charge

Transport and Current.....	126
----------------------------	-----

Magnetic Fields

Lorentz Force.....	128
Electric Balance.....	130
Magnetic Field of a Cylindrical Coil.....	132
Magnetic Field of the Earth.....	134

Induction

Faraday's Law of Induction.....	136
Induction in a Moving Conductor Loop.....	138
Induction by a Varying Magnetic Field.....	140
Waltzenhofen's Pendulum.....	142

Induction

Transformers.....	144
-------------------	-----

DC and AC Circuits

Charging and Discharging a Capacitor I.....	146
Charging and Discharging a Capacitor II.....	148
Impedance of a Capacitor in an AC Circuit.....	150
Charging and Discharging a Coil.....	152
Impedance of a Coil in an AC Circuit.....	154

DC and AC

AC Resistance I.....	156
AC Resistance II.....	158
Impedances.....	160
LC Resonant Circuits.....	162

Electromagnetic Oscillations and Waves

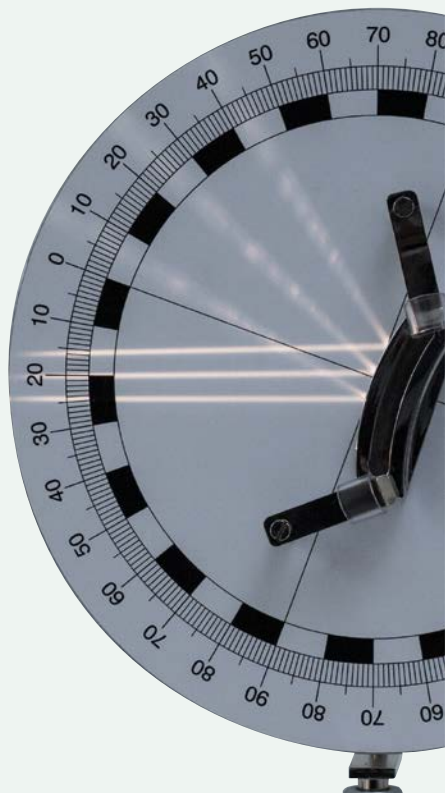
Wave Optics Using Microwaves.....	164
-----------------------------------	-----

Electron Tubes

Thermionic Diode.....	166
Thermionic Triode.....	168
Maltese-Cross Tube.....	170
Perrin Tube.....	172
Thomson Tube.....	174
Fine-Beam Tube.....	176
Training Oscilloscope I.....	178
Training Oscilloscope II.....	180

Electronics

Bipolar Transistors.....	182
Field Effect Transistors.....	184



ATOMIC AND NUCLEAR PHYSICS

Introductory Experiments in Atomic Physics

Planck's Constant.....	228
Millikan's Experiment	230

Fundamentals of Atomic Physics

Electron Diffraction	232
----------------------------	-----

Atomic Shells

Line Spectra I.....	234
Line Spectra II.....	236
Franck-Hertz Experiment for Mercury	238
Franck-Hertz Experiment for Neon	240
Critical Potentials.....	242

Electron Shell

Normal Zeeman Effect.....	244
---------------------------	-----

Magnetic Resonance

Electron Spin Resonance	246
Nuclear Magnetic Resonance.....	248

SOLID-STATE PHYSICS

Conduction Phenomena

Electrical Conduction in Semiconductors.....	250
Hall-Effect in Semiconductors.....	252
Photoconductivity	254
Seebeck Effect.....	256

X-RAY PHYSICS

Diffraction

Bragg Reflection.....	258
-----------------------	-----

Energy Spectroscopy

X-Ray Fluorescence	260
--------------------------	-----

OPTICS

Geometric Optics

Reflection in a Mirror	186
Refraction of Light.....	188
Lens Equation.....	190

Colour

Transmission Spectra.....	192
---------------------------	-----

Wave Optics

Diffraction by a Single Slit.....	194
Diffraction by Multiple Slits and Gratings	196
Fresnel Biprism	198
Newton's Rings	200

Interferometer

Michelson Interferometer	202
--------------------------------	-----

Wave Optics

Mach-Zehnder Interferometer	204
-----------------------------------	-----

Polarization

Malus' Law	206
Optical Activity	208
Pockels Effect.....	210
Faraday Effect	212

Intensity of Radiation

Inverse Square Law.....	214
Stefan-Boltzmann Law.....	216

Velocity of Light

Determination of the Velocity of Light....	218
--	-----

Laser Physics

Nd:YAG Lasers	220
Q-Switching for Nd:YAG Laser	222
Nd:YAG-Laser	224

Spectrometry

Prism Spectrometer.....	226
-------------------------	-----



BIOPHYSICS

Neurophysiology

Neurophysiology.....	268
----------------------	-----

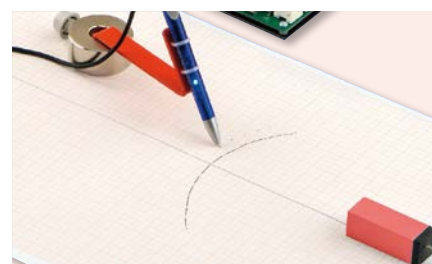
MEDICAL PHYSICS

Ultrasound

Ultrasonic Biometry	270
Ultrasonic Computer Tomography	272

Ultrasonic Doppler Effect

Fluid Mechanics.....	274
Doppler Sonography	276



STUDENT EXPERIMENTS

Student Experiment Kit Systems

Mechanical Oscillations and Waves.....	278
Ultrasonic Waves.....	280
Kröncke Optical System	282
Electricity and Magnetism	284
Electronics	286
Solar Energy	288
Sound Propagation in Solid Bodies	290

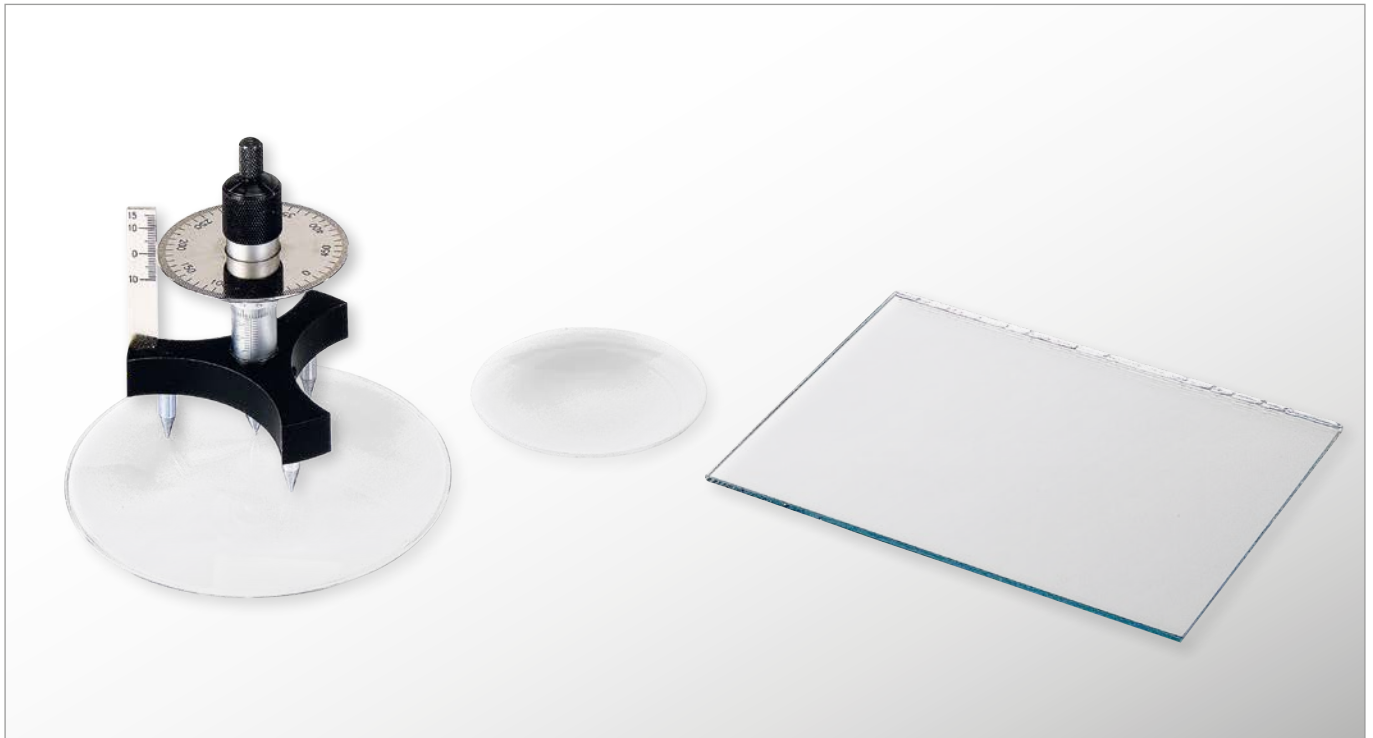


ENERGY AND ENVIRONMENT

Photovoltaics

Photovoltaic Systems.....	262–266
---------------------------	---------

UE1010100 | SPHEROMETER



> EXPERIMENT PROCEDURE

- Measure the height of the curvature h for two watch glasses for a given distance s between the tips of the spherometer legs.
- Determine the radius of curvature R of both glasses.
- Compare the methods for both convex and concave surfaces.

OBJECTIVE

Determine the radius of curvature of various watch glasses

SUMMARY

From the height h of a spherical surface above a point on a plane defined by the corners of an equilateral triangle, the radius of curvature R of the spherical surface may be determined. This can be done for both convex and concave curvatures of the sphere.

REQUIRED APPARATUS

Quantity	Description	Item Number
1	Precision Spherometer	1002947
1	Plane Mirror	1003190
1	Set of 10 Watch Glass Dishes, 80 mm	1002868
1	Set of 10 Watch Glass Dishes, 125 mm	1002869

BASIC PRINCIPLES

A spherometer consists of a tripod with the three legs tipped by steel points and forming an equilateral triangle with sides of 50 mm. A micrometer screw, the tip of which is the point to be measured, passes through the center of the tripod. A vertical rule indicates the height h of the measured point above a plane defined by the tips of the three legs. The height of the measured point can be read off to an accuracy of $1 \mu\text{m}$ with the aid of a circular scale that rotates along with the micrometer screw.

The relationship between the distance r of all three legs from the center of the spherometer, the radius of curvature R to be determined and the height h of the surface is given by the following equation:

$$(1) \quad R^2 = r^2 + (R-h)^2$$

Rearranging for R gives:

$$(2) \quad R = \frac{r^2 + h^2}{2 \cdot h}$$

The distance r can be calculated from the length s of the sides of the equilateral triangle formed by the legs:

$$(3) \quad r = \frac{s}{\sqrt{3}}$$

Thus the relevant equation for R is as follows:

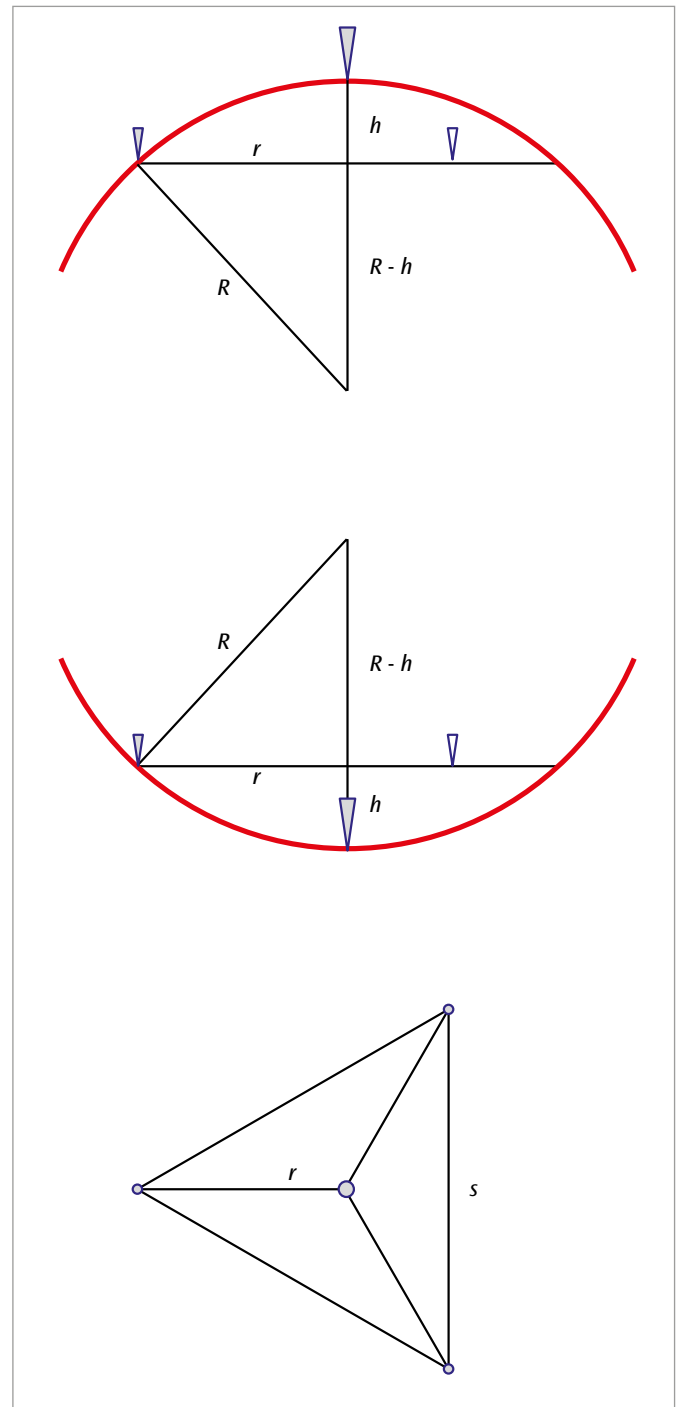
$$(4) \quad R = \frac{s^2}{6 \cdot h} + \frac{h}{2}$$

EVALUATION

The separation s between the legs of the spherometer is in this case 50 mm. When the height h is small, equation (4) can be simplified to the following:

$$R = \frac{s^2}{6 \cdot h} = \frac{2500\text{mm}^2}{6 \cdot h} \approx \frac{420\text{mm}^2}{h}$$

The scale of the spherometer allows readings for heights between 10 mm and $1 \mu\text{m}$ to an accuracy of $1 \mu\text{m}$, so that radii of curvature of about 40 mm to 400 m can be calculated.



Schematic for measurement of radius of curvature by means of a spherometer

Top: Vertical cross section for measuring an object with a convex surface

Middle: Vertical cross section for measuring an object with a concave surface

Bottom: View from above

UE1010200 | LENGTHS AND VOLUMES



EXPERIMENT PROCEDURE

- Determine the external dimensions of an irregularly shaped body.
- Determine the internal dimensions of an irregularly shaped body.
- Determine depths on an irregularly shaped body.
- Calculate and measure the volume.

OBJECTIVE

Measurement of an irregularly shaped body

SUMMARY

Callipers are used for making precise measurements of quite short lengths. They are suitable for finding internal and external dimensions and depths, as demonstrated in the measurement of an irregularly shaped body. However, calculating a body's volume from the data obtained is comparatively complex. The displacement method is an easier way to determine the volume of an irregularly shaped body.

REQUIRED APPARATUS

Quantity	Description	Item Number
1	Callipers, 150 mm	1002601
1	Object for Measurement Exercises	1006889
Additionally recommended		
1	Vessel with Overflow, Transparent	1003518
1	Graduated Cylinder, 100 ml	1002870
1	Laboratory Jack II	1002941
1	Cord for Experiments	1001055
1	Set of 10 Beakers, Tall Form	1002873

BASIC PRINCIPLES

One suitable method for determining the volume of an irregularly shaped body is the overflow method. This involves immersing the body in water inside a vessel with an overflow outlet. The water displaced by the body is then collected in a graduated measuring cylinder. The volume of water displaced is equal to the volume V of the body.

In order to avoid systematic errors, callipers must wherever possible be used in such a way that they are not tilted. The accuracy is conventionally increased to resolve fractions of a millimeter by the inclusion of a vernier scale. The full millimeter values are read off from the left of the zero mark on the vernier. The fraction following the decimal point is read off where a mark further over is in line with one of the marks on the vernier.

If you have a displacement vessel available, you can determine the volume using the displacement method. The body is completely immersed in a displacement vessel filled with water. The water displaced from this vessel then flows into a measuring cylinder. The volume of water displaced is equal to the volume V of the body.

EVALUATION

As a rule, a dimension is measured multiple times and the accepted result is obtained by taking the average of the individual readings.

To calculate the volume, it can be broken down into sub-volumes of regular shapes, which are then added or, in the case of drill holes, for example, subtracted.

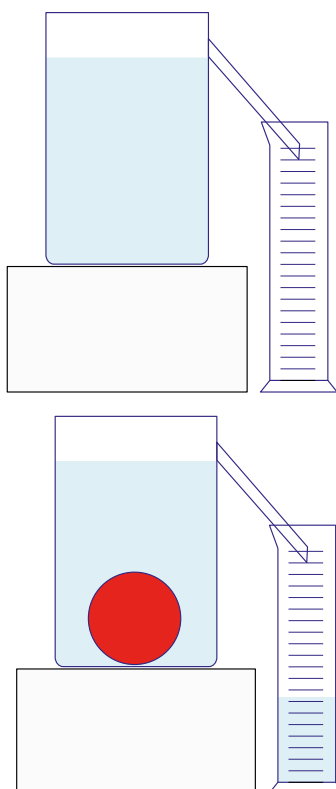


Fig. 6: Schematic illustration of the displacement method

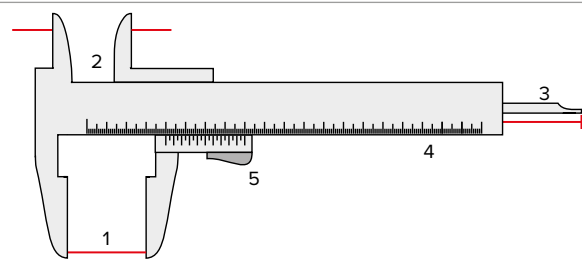


Fig. 1: Prongs for external measurements (1), Prongs (crossed over) for internal measurement (2), Bar for depth measurement (3), Millimeter scale (4), Vernier scale (5)

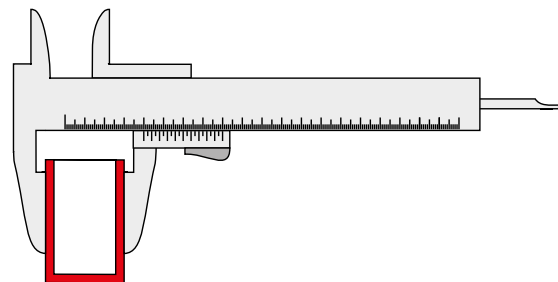


Fig. 2: Determination of external dimensions

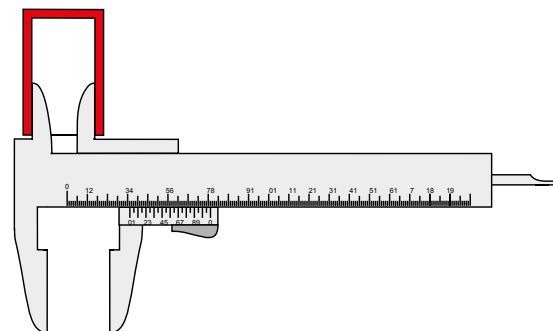


Fig. 3: Determination of internal dimensions

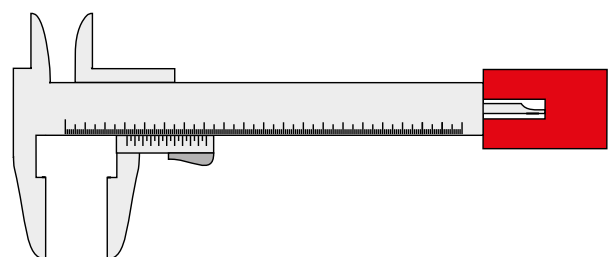


Fig. 4: Determining the depth of a drill hole

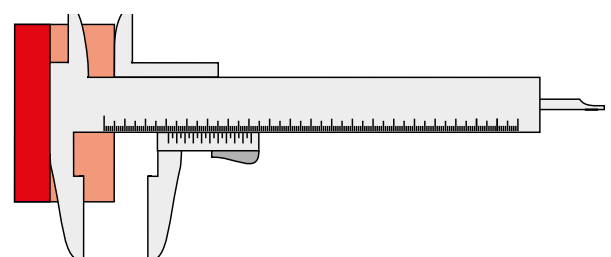


Fig. 5: Determining the height of a step

UE1010300 | GRAVITATIONAL CONSTANT



EXPERIMENT PROCEDURE

- Determine the initial equilibrium position of the torsional pendulum.
- Record the oscillation of the torsional pendulum about the final equilibrium position and determine the period.
- Determine where the final equilibrium position is.
- Calculate the gravitational constant G .

OBJECTIVE

Measure the gravitational force and determine the gravitational constant using Cavendish torsion balance

SUMMARY

The central component of a Cavendish torsion balance is a sensitive torsional pendulum with a pair of small lead spheres attached to it. Two larger lead spheres are then placed near these two small balls in order to attract them. The position of the large spheres thus determines the equilibrium position of the torsional pendulum. If the two large spheres are then moved to a second position which is symmetrical with the first with respect to the two small balls, the torsional pendulum will adopt a new equilibrium position after a short period of settling. By measuring the geometry of the set-up in both positions, it is possible to determine the gravitational constant. The decisive factor in this is the equilibrium between the gravitational force and the restoring torque of the torsional pendulum. Measurements are made of the oscillation of the torsional pendulum using a capacitive differential sensor, which suppresses noise and vibrational components of the signal to a large extent. The tungsten wire from which the pendulum is made is chosen to be so thin that the period of oscillation is of the order of a few minutes, meaning that several oscillations about the equilibrium position may be observed in the space of an hour.

REQUIRED APPARATUS

Quantity	Description	Item Number
1	Cavendish Torsion Balance	1003337
1	Laser Diode, Red 230 V	1003201 or
	Laser Diode, Red 115 V	1022208
1	Barrel Foot, 1000 g	1002834
1	Universal Clamp	1002830
1	Stainless Steel Rod 100 mm	1002932
Additionally recommended		
1	Callipers, 150 mm	1002601
1	Electronic Scale 5000 g	1003434

BASIC PRINCIPLES

When measuring the gravitational force between two masses in a laboratory, it is inevitably the case that all other masses in the vicinity have a disturbing effect on the results. The Cavendish balance largely gets around this problem since two measurements are made with the masses symmetrically positioned.

The central component of a Cavendish torsion balance is a sensitive torsional pendulum with a pair of small lead spheres attached to it. Two larger lead spheres are then placed near these two small balls in order to attract them. The position of the large spheres thus determines the equilibrium position of the torsional pendulum. If the two large spheres are then moved to a second position which is symmetrical with the first with respect to the two small balls, the torsional pendulum will adopt a new equilibrium position after a short period of settling. By measuring the geometry of the set-up in both positions, it is possible to determine the gravitational constant. The decisive factor in this is the equilibrium between the gravitational force and the restoring torque of the torsional pendulum.

The gravitational force is given by the following:

$$(1) \quad F = G \cdot \frac{m_1 \cdot m_2}{d^2}$$

G : Gravitational constant,

m_1 : Mass of one small lead sphere,

m_2 : Mass of one large lead sphere,

d : Distance between small and large lead spheres at the position where the measurement is made

The force deflects the torsional pendulum from its equilibrium position when the two large spheres are in position for the measurement. The deflecting torque is

$$(2) \quad M_1 = 2 \cdot F \cdot r$$

r : Distance of small lead sphere from its mounting point on the supporting beam

If the torsional pendulum is deflected by an angle φ , there is a restoring torque

$$(3) \quad M_2 = D \cdot \varphi$$

D : Torsion coefficient of tungsten wire

This acts due to the tungsten wire from which the support beam of the torsional balance is suspended. In the equilibrium position, M_1 and M_2 are equal.

The torsional coefficient D can be determined from the period of oscillation T for the oscillation of the torsional pendulum about its equilibrium position.

$$(4) \quad D = J \cdot \frac{4\pi^2}{T^2}$$

The moment of inertia J comprises the moment of inertia J_1 of the two small spheres and the moment of inertia J_k of the supporting beam

$$(5) \quad J = 2 \cdot m_1 \cdot r^2 + \frac{m_B}{12} \cdot (a^2 + b^2)$$

m_B : Mass of support beam

a, b : Length and width of support beam.

For the two large lead spheres, there should be two symmetrical positions where measurements are made. The angles of deflection in these two positions are φ and φ' and the two corresponding deflecting torques are equal but in opposite directions. In equilibrium, equations (2) and (3) therefore imply the following:

$$(6) \quad 4 \cdot F \cdot r = D \cdot (\varphi - \varphi') = D \cdot \Delta\varphi$$

In the course of the experiment the oscillations of the torsional pendulum are measured using a capacitive differential sensor, which suppresses noise and vibrational components of the signal to a large extent. The tungsten wire from which the pendulum is made is chosen to be so thin that the period of oscillation is of the order of a

few minutes, meaning that several oscillations about the equilibrium position may be observed in the space of an hour. A mirror attached to the torsional pendulum can be used to set up a light pointer so that the oscillations are easy to follow with the naked eye. This makes the necessary adjustment and calibration of the balance much easier.

EVALUATION

By rearranging equations (1), (4), (5) and (6):

$$G = \frac{\Delta\varphi}{m_2} \cdot \frac{d^2 \cdot \pi^2}{T^2} \cdot \left(2 \cdot r + \frac{1}{12} \cdot \frac{m_B}{m_1} \cdot \frac{a^2 + b^2}{r} \right).$$

This does not take into account that the two small spheres are also attracted by the more distant large sphere, so that the torque on the torsional pendulum is somewhat reduced in comparison with the calculations made so far. It is not difficult to introduce correction for this into equation (2), since all the distances are known.

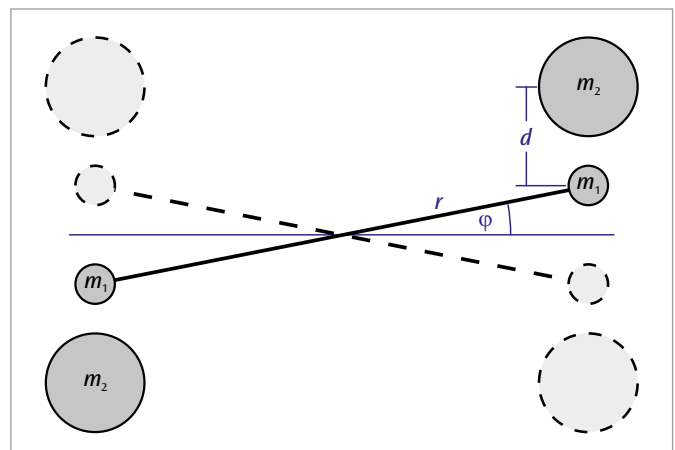


Fig. 1: Schematic of measurement set-up for the Cavendish torsional balance

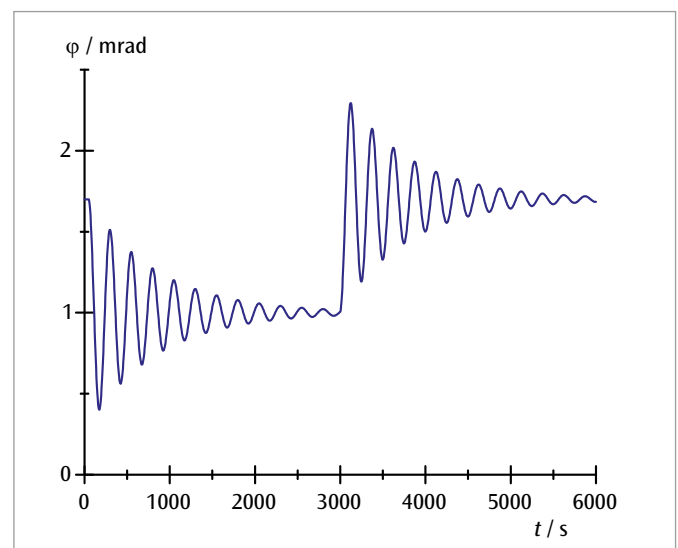


Fig. 2: Angle of deflection of torsional pendulum as a function of time when the measurement position of the two large lead spheres has been changed twice

UE1020100 | HOOKE'S LAW



OBJECTIVE

Confirm Hooke's law for coil springs under tension

EXPERIMENT PROCEDURE

- Confirm Hooke's law and determine the spring constant of five different coil springs.
- Compare the measured spring constants with those calculated theoretically.

SUMMARY

In any elastic body, extension and tension are proportional to one another. This relationship was discovered by *Robert Hooke* and is frequently demonstrated using a coil spring with weights suspended from it. The change in the length of the spring is proportional to the force of gravity F on the suspended weight. In this experiment, five different coil springs will be measured. Thanks to a suitable choice of wire diameter and coil diameter, the spring constants all span one order of magnitude. In each case, the validity of Hooke's law will be demonstrated for forces in excess of the initial tension.

REQUIRED APPARATUS

Quantity	Description	Item Number
1	Set of Helical Springs for Hooke's Law	1003376
1	Set of Slotted Weights, 20 – 100 g	1003226
1	Vertical Ruler, 1 m	1000743
1	Set of Riders for Rulers	1006494
1	Barrel Foot, 1000 g	1002834
1	Stainless Steel Rod 1000 mm	1002936
1	Tripod Stand 150 mm	1002835
1	Clamp with Hook	1002828

Additionally recommended

1	Callipers, 150 mm	1002601
1	External Micrometer	1002600

BASIC PRINCIPLES

In any elastic body, extension and tension are proportional to one another. This relationship was discovered by *Robert Hooke* and is a good description of how a large number of materials behave when the degree of deformation is sufficiently small. This law is frequently demonstrated using a coil spring with weights suspended from it. The change in the length of the spring is proportional to the force of gravity F on the suspended weight.

For the sake of greater precision, it is first necessary to determine the initial tension which may be exhibited by the spring as the result of its manufacturing process. It is necessary to compensate for this by adding a weight which applies a force F_1 , causing the spring to extend from its natural length without any weight s_0 to a length s_1 . For weights in excess of F_1 , Hooke's law applies in the following form:

$$(1) \quad F - F_1 = k \cdot (s - s_1)$$

This is so as long as the length of the spring s does not exceed a certain critical length.

The spring constant k depends on the material and the geometric dimensions of the spring. For a cylindrical coil spring with n turns of constant diameter D , the following is true:

$$(2) \quad k = G \cdot \frac{d^4}{D^3} \cdot \frac{1}{8 \cdot n}$$

d : Diameter of wire coils of spring

The shear modulus G for the steel wire forming the spring's coils is 81.5 GPa.

In this experiment, five different coil springs will be measured. Thanks to a suitable choice of wire diameter and coil diameter, the spring constants all span one order of magnitude. In each case, the validity of Hooke's law will be demonstrated for forces in excess of the initial tension.

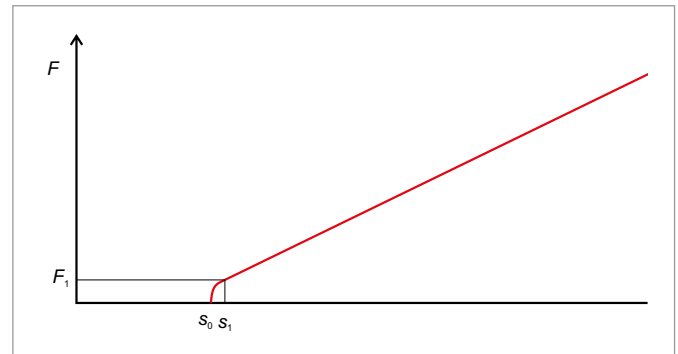


Fig. 1: Schematic of characteristic curve for a spring coil of length s with a certain initial tension

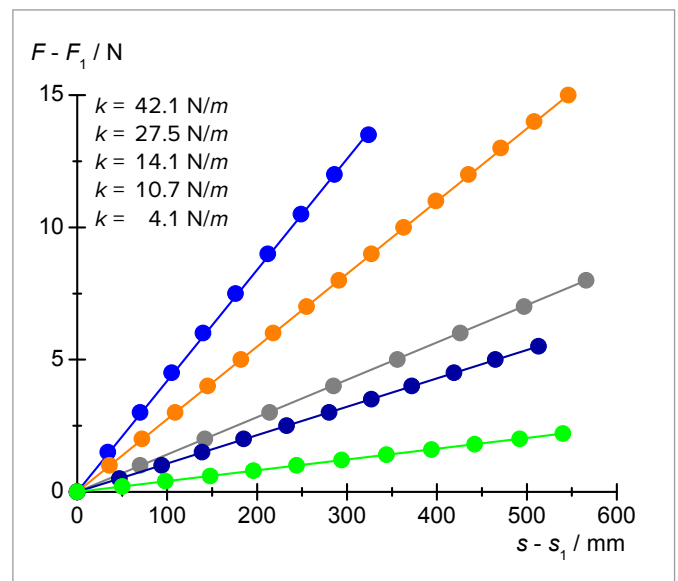


Fig. 2: Load as a function of the change in length

EVALUATION

The force of gravity F can be determined to sufficient precision from the mass m of the weight as follows:

$$F = m \cdot 10 \frac{\text{m}}{\text{s}^2}$$

UE1020200 | FIRST- AND SECOND-CLASS LEVERS



> EXPERIMENT PROCEDURE

- Measure the force F_1 as a function of the load F_2 , the distance between the load and the fulcrum x_2 and the distance between the force and the fulcrum x_1 for a second-class lever.
- Measure the force F_1 as a function of the load F_2 , the distance between the load and the fulcrum x_2 and the distance between the force and the fulcrum x_1 for a first-class lever.

OBJECTIVE

Verification of the law of the lever

SUMMARY

The law of the lever follows from the equilibrium of moments, which works for all three classes of lever. It represents the physical basis for all kinds of mechanical transmission of force.

REQUIRED APPARATUS

Quantity	Description	Item Number
1	Lever	1008539
1	Precision Dynamometer 2 N	1003105
1	Precision Dynamometer 5 N	1003106

BASIC PRINCIPLES

A lever is a fixed body which can rotate around a fixed axis and can be used to lift and move loads. A force or effort is applied at a certain point from the fulcrum in order to move a load or resistance at another point along the lever. With a second-class lever, the effort F_1 and load F_2 are both on the same side of the fulcrum and both the forces act in opposite directions. With a first-class lever, the forces are on different sides of the fulcrum and are both directed the same way.

For both types, the law of the lever follows from the equilibrium of moments:

$$(1) \quad F_1 \cdot x_1 = F_2 \cdot x_2$$

This represents the physical basis for all kinds of mechanical transmission of force.

EVALUATION

From the values measured, calculate in each case the products

$$F_1 \cdot x_1 \text{ and } F_2 \cdot x_2$$

and make a comparison between them.

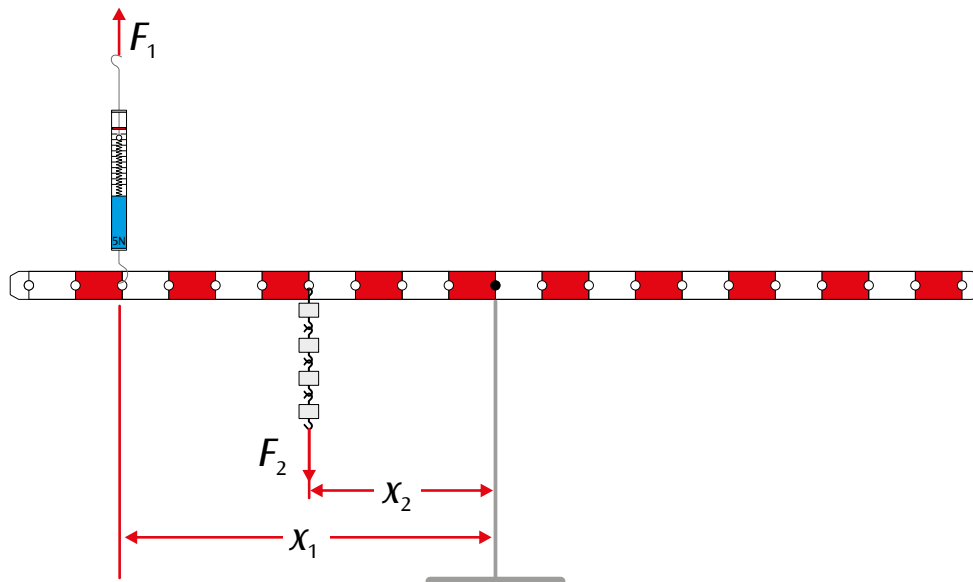


Fig. 1: 2nd-class lever

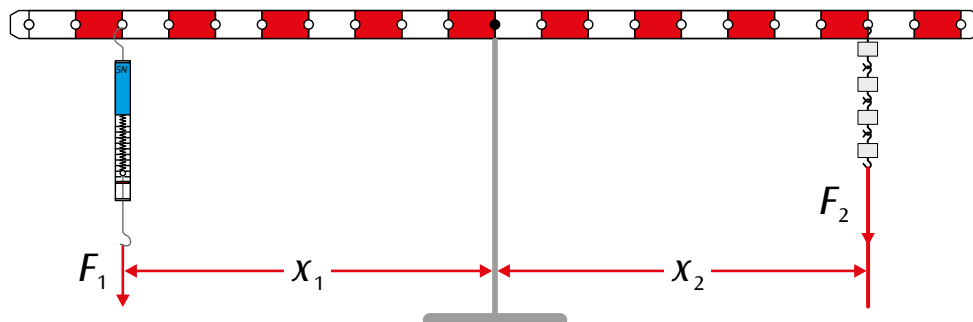


Fig. 2: 1st-class lever

UE1020300 | PARALLELOGRAM OF FORCES



EXPERIMENT PROCEDURE

- Plotting the equilibrium of three arbitrary forces on a graph.
- Analytical investigation of the point of equilibrium when forces F_1 and F_2 are symmetrical.

OBJECTIVE

Experimental investigation of the vector addition of forces

SUMMARY

The vector addition of forces can be demonstrated in a clear and simple manner on the force table. The point of action of three individual forces in equilibrium is exactly in the middle of the table. Determine the magnitude of the individual forces from the suspended weights and, using a protractor, note the angle of each force vector (the direction of each force). The result of the experiment can be evaluated analytically or represented as a graph.

REQUIRED APPARATUS

Quantity	Description	Item Number
1	Force Table	1000694

BASIC PRINCIPLES

Forces are vectors and can therefore be added using the rules of vector addition. To demonstrate the sum of two vectors on a graph, the point of origin of the second vector is placed on the final point of the first vector. The arrow from the point of origin of the first vector to the final point of the second vector represents the resultant vector. By completing the parallelogram (of which the two vector lines are sides), a diagonal drawn from the original angle to the opposite corner represents the resultant vector (also see Fig. 1).

The vector addition of forces can be demonstrated in a clear and simple manner on the force table. The point of action of three individual forces in equilibrium is exactly in the middle of the table. Determine the magnitude of the individual forces from the suspended weights and, using a protractor, note the angle of each force vector (the direction of each force).

In a state of equilibrium, the sum of the three individual forces is given by:

$$(1) \quad F_1 + F_2 + F_3 = 0$$

F_3 is therefore the sum of individual forces F_1 and F_2 (also see Fig. 2):

$$(2) \quad -F_3 = F = F_1 + F_2$$

The parallel vector components for sum F are given by

$$(3) \quad -F_3 = F = F_1 \cdot \cos \alpha_1 + F_2 \cdot \cos \alpha_2$$

and the vertical components are given by

$$(4) \quad 0 = F_1 \cdot \sin \alpha_1 + F_2 \cdot \sin \alpha_2$$

Equations (3) and (4) provide a mathematical analysis of the vector addition. For the experiment, it is advisable to align force F_3 at an angle of 0° .

For analytical observations, the equilibrium of forces can alternatively be investigated on a graph. To do so, draw lines representing all three forces diverging from the central point of action. Note the magnitude and angle of each force. Subsequently, displace forces F_2 and F_3 along a parallel path till the point of origin is at the end of the preceding vector. The resultant vector is 0 (also see Fig. 3). In the experiment, carry out this procedure for three arbitrary forces, making sure to maintain the state of equilibrium every time.

In the experiment, the analytical observation is restricted to the special situation that the two forces F_1 and F_2 are symmetric to F_3 .

EVALUATION

Equation (4) is satisfied in a symmetric case ($F_1 = F_2$ and $\alpha_1 = -\alpha_2$). From equation (3) we get the characteristic equation applied in Fig. 4 (for describing the measurement data).

$$F = 2 \cdot F_1 \cdot \cos \alpha$$

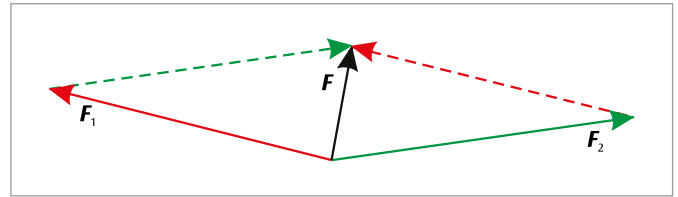


Fig. 1: Vector sum of forces (parallelogram of forces)

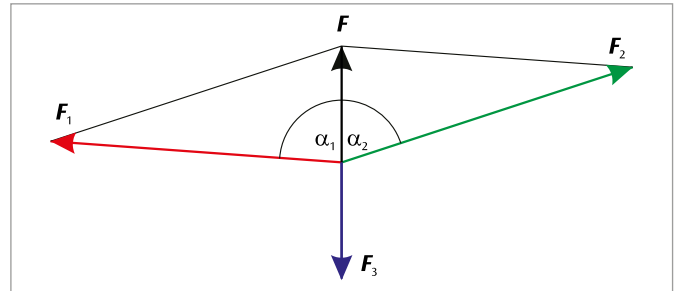


Fig. 2: Determining the sum of vectors of two forces F_1 and F_2 from equilibrium force F_3

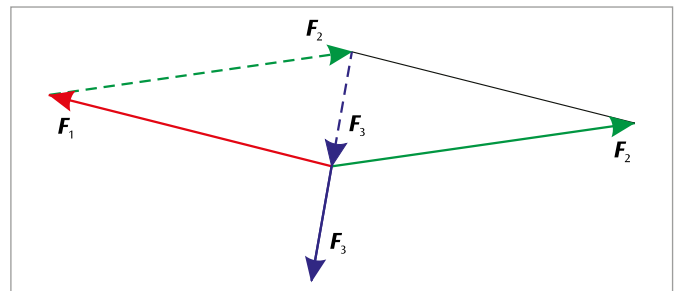


Fig. 3: Graphic investigation of the equilibrium of three arbitrary forces acting in different directions

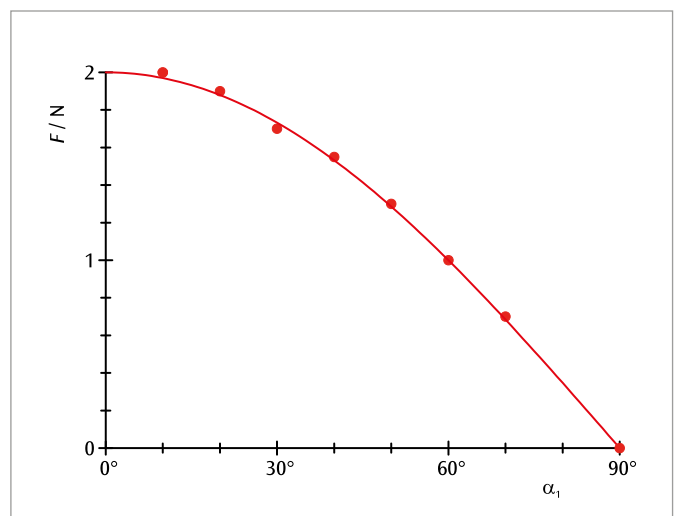


Fig. 4: Measured and calculated sums of two symmetric forces in relation to the angle α_1

UE1020400 | INCLINED PLANES



> EXPERIMENT PROCEDURE

- Measure the component F_1 of the weight of an object which acts down an inclined plane as a function of the angle of inclination α .
- Plot the ratio of the component F_1 to the weight G as a function of $\sin \alpha$.

OBJECTIVE

Determine the forces acting on an inclined plane

SUMMARY

If a body needs to be propelled up an inclined plane, it is not the body's full weight G which needs to be overcome, but only the component which acts parallel to the plane F_1 . The fact that this component is less than the weight is more pronounced the smaller the inclination α of the plane becomes.

REQUIRED APPARATUS

Quantity	Description	Item Number
1	Inclined Plane	1003213
1	Precision Dynamometer 5 N	1003106
1	Set of Weights 1 g to 500 g	1010189

BASIC PRINCIPLES

If a body needs to be propelled up an inclined plane, it is not the body's full weight G which needs to be overcome, but only the component which acts parallel to the plane F_1 . The vector differential between the weight and the component down the plane is represented by the component normal to the plane F_2 , see Fig. 1.

The magnitudes of the forces are given by the following relationships:

$$(1) \quad F_1 = G \cdot \sin \alpha$$

$$(2) \quad F_2 = G \cdot \cos \alpha$$

In this experiment, the body is suspended from a cord which runs over a pulley. The force along the plane is then compensated for by weights on a weight holder suspended from the other end of the cord. Since the friction between the body and the inclined plane is of importance, the value used for the measurements is an average of the lowest and highest values, where the component of the force down the plane is just enough to stop the body sliding down the slope and when it is just enough not to drag it up the slope.

The weight of the body G is determined in advance using a dynamometer. The weight of the weight holder is also taken into account. The angle of inclination α can simply be read from a protractor scale.

EVALUATION

In order to evaluate the data, the ratio of the parallel component of the force F_1 , as measured for various inclination angles α , and the weight of the body G is plotted on a graph against $\sin \alpha$. To within the measurement tolerances, the values all lie on a straight line passing through the origin.

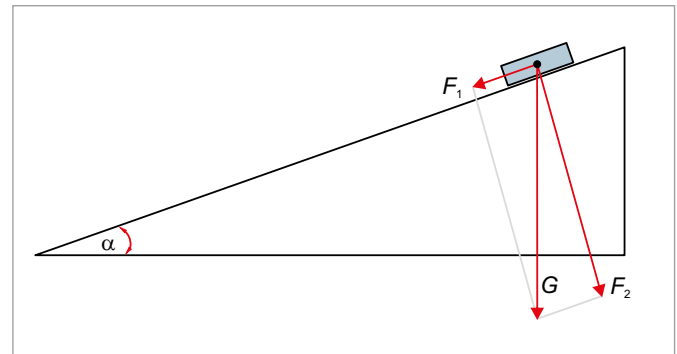


Fig. 1: Resolution of the weight G into vector components parallel to the plane, F_1 , and normal to the plane, F_2

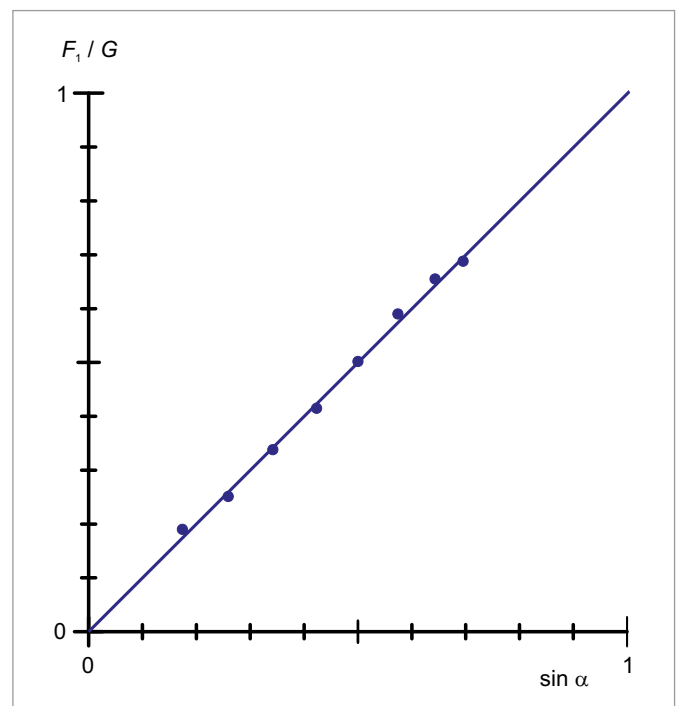
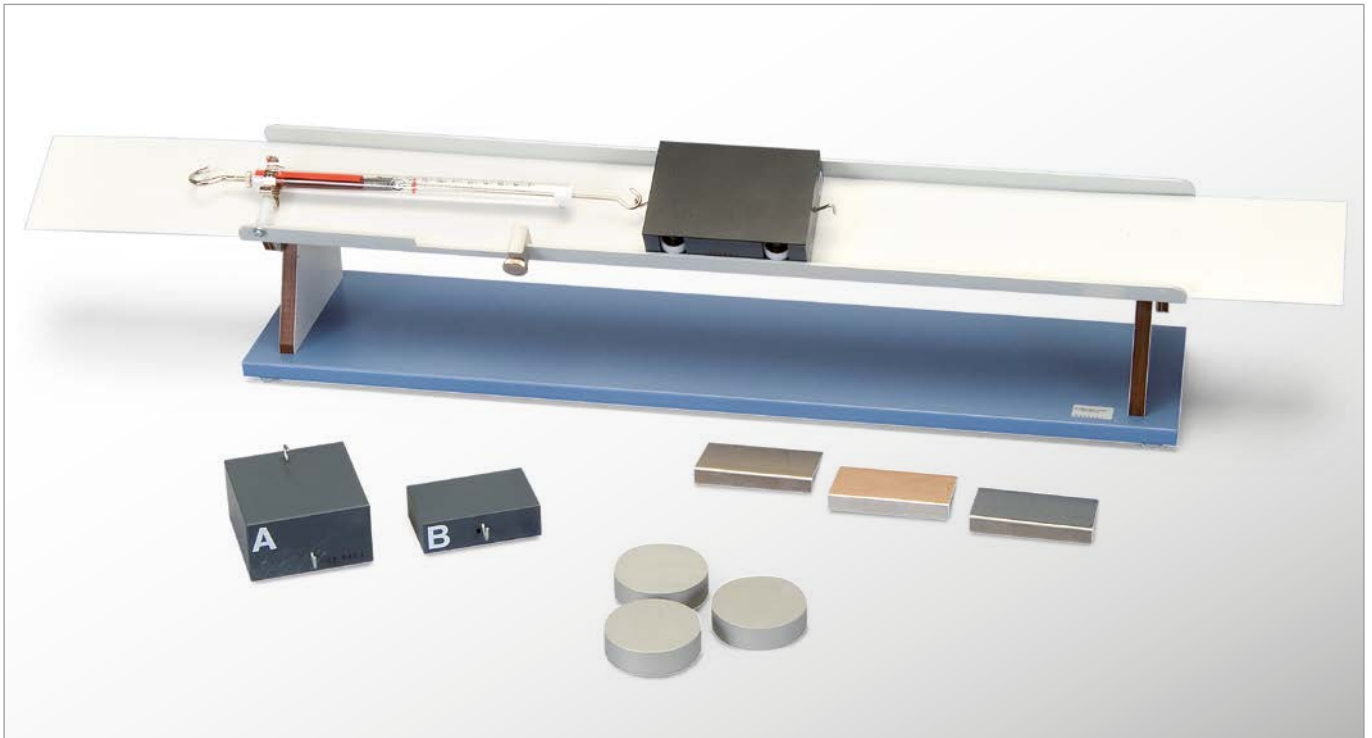


Fig. 2: The ratio between the parallel component F_1 and the weight G as a function of $\sin \alpha$.

UE1020500 | STATIC AND DYNAMIC FRICTION



> EXPERIMENT PROCEDURE

- Comparison of static and dynamic friction.
- Measurement of how dynamic friction depends on the area in contact.
- Measurement of how dynamic friction depends on the combination of materials.
- Measurement of how dynamic friction depends on the perpendicular force between the two surfaces (normal force).

OBJECTIVE

Measurement of friction forces

SUMMARY

In order to measure dynamic friction, a friction measuring apparatus is used. It is composed of movable friction strips, which are pulled from under a stationary rough body connected to a dynamometer at constant speed. In order to vary the effective weight (and therefore the normal force) of the stationary body, the angle of the track can be set to any angle.

REQUIRED APPARATUS

Quantity	Description	Item Number
1	Friction Measuring Apparatus	1009942

BASIC PRINCIPLES

In order to move an object from rest along a level surface, a force of inertia needs to be overcome. This results from static friction between the body and the surface on which it rests. If, once moving the body is to continue sliding along the surface, a force of F_{Dyn} needs to be applied to overcome the dynamic friction. This force is smaller than the initial force needed to overcome the inertia caused by static friction F_{Stat} , as the degree of contact between the sliding body and the surface beneath is less.

Neither of these forces are dependent on the area in contact, instead being determined primarily by the types of materials and the roughness of the surfaces in contact. They are also proportional to the force that is pushing the surfaces together in a plane perpendicular to that of the surfaces themselves. This is called the normal force F_N (it acts normally, i.e. perpendicular to the surface). The coefficients of static friction μ_{Stat} and dynamic friction μ_{Dyn} are thereby defined as in the following two equations:

$$(1) \quad F_{\text{Stat}} = \mu_{\text{Stat}} \cdot F_N \quad \text{and} \quad F_{\text{Dyn}} = \mu_{\text{Dyn}} \cdot F_N$$

In order to measure dynamic friction, an apparatus for measuring such friction is used, in which rough strips are pulled out at constant speed from under a body that remains stationary and is also connected to a dynamometer. Measurements are made for various combinations of materials and contact areas. To alter the normal force the track can be tipped up so that the component of the stationary body's weight that acts normally to the plane of the surface changes.

EVALUATION

If the track is tilted by an angle α , the normal force exerted by a body of mass m in the direction perpendicular to the inclined plane is as follows:

$$F_N = m \cdot g \cdot \cos \alpha$$

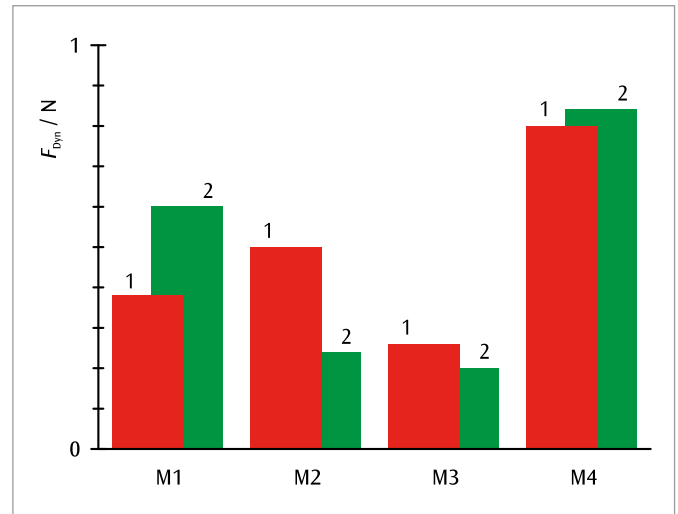


Fig. 1: Dynamic friction F_{Dyn} for four different materials on a smooth surface (1) and a rough surface (2)

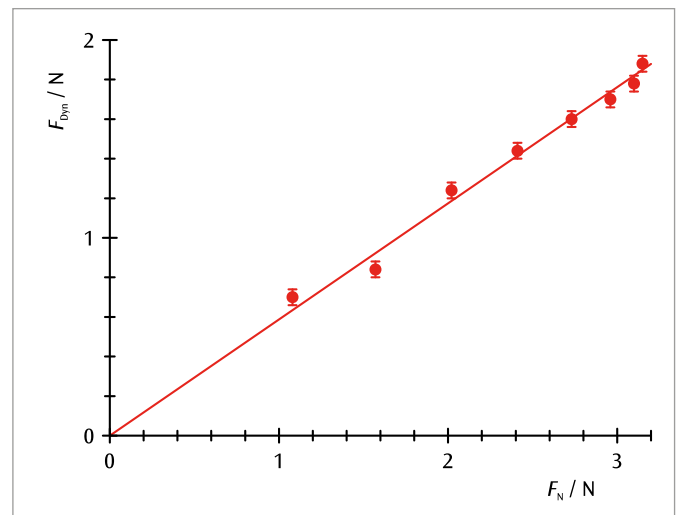


Fig. 2: Dynamic friction F_{Dyn} depending on normal force between the two surfaces F_N

UE1020850 | ARCHIMEDES' PRINCIPLE



OBJECTIVE

Determining buoyant updraft as a function of immersion depth

SUMMARY

Archimedes' principle states that a body immersed in a fluid experiences an upward force (updraft or force of buoyancy) F_G . The magnitude of this force is equal to the weight of the displaced fluid. For a regularly shaped immersed body, the updraft is proportional to the depth h to which the body is immersed as long as this is smaller than the height H of the body itself.

> EXPERIMENT PROCEDURE

- Measure the force on a body immersed in water.
- Determine the updraft and confirm that it is proportional to the depth to which the body is immersed.
- Determine the density of water.

REQUIRED APPARATUS

Quantity	Description	Item Number
1	Immersion Block Al 100 cm ³	1002953
1	Precision Dynamometer 5 N	1003106
1	Callipers, 150 mm	1002601
1	Set of 10 Beakers, Tall Form	1002873
1	Laboratory Jack II	1002941
1	Tripod Stand 150 mm	1002835
1	Stainless Steel Rod 750 mm	1002935
1	Clamp with Hook	1002828

BASIC PRINCIPLES

Archimedes' principle states that a body immersed in a fluid experiences an upward force (updraft or force of buoyancy) F_1 . The magnitude of this force is equal to the weight of the displaced fluid.

For a regularly shaped immersed body with a surface area A and height H , immersed to a depth h , the following applies:

$$(1) \quad F_G = \rho \cdot g \cdot A \cdot h, \text{ where } h < H$$

and

$$(2) \quad F_G = \rho \cdot g \cdot A \cdot H, \text{ where } h > H$$

This experiment uses a block of weight F_0 . This weight acts on a dynamometer at the same time as the block is immersed in water to a depth h , so that the total force present is given by the following:

$$(3) \quad F(h) = F_0 - F_G(h)$$

EVALUATION

The values measured for the updraft F_G as a function of the relative immersion depth h/H all lie on a straight line through the origin with the following gradient:

$$a = \rho \cdot g \cdot A \cdot H$$

The density of water can be calculated from this gradient.

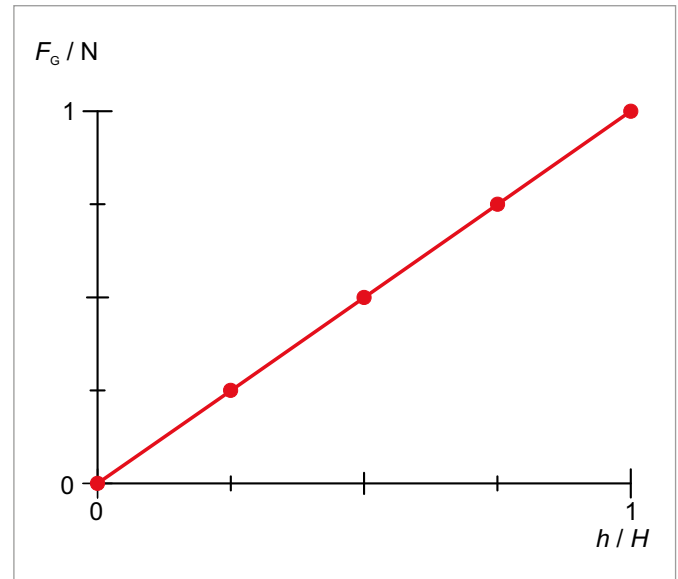


Fig. 1: Updraft F_G as a function of relative immersion depth h/H

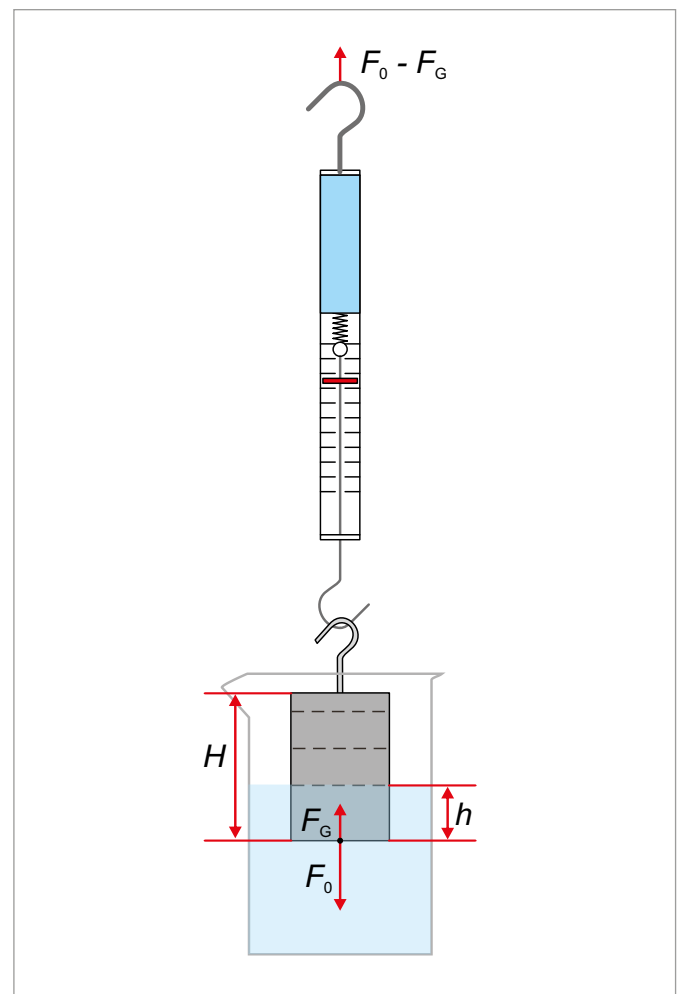
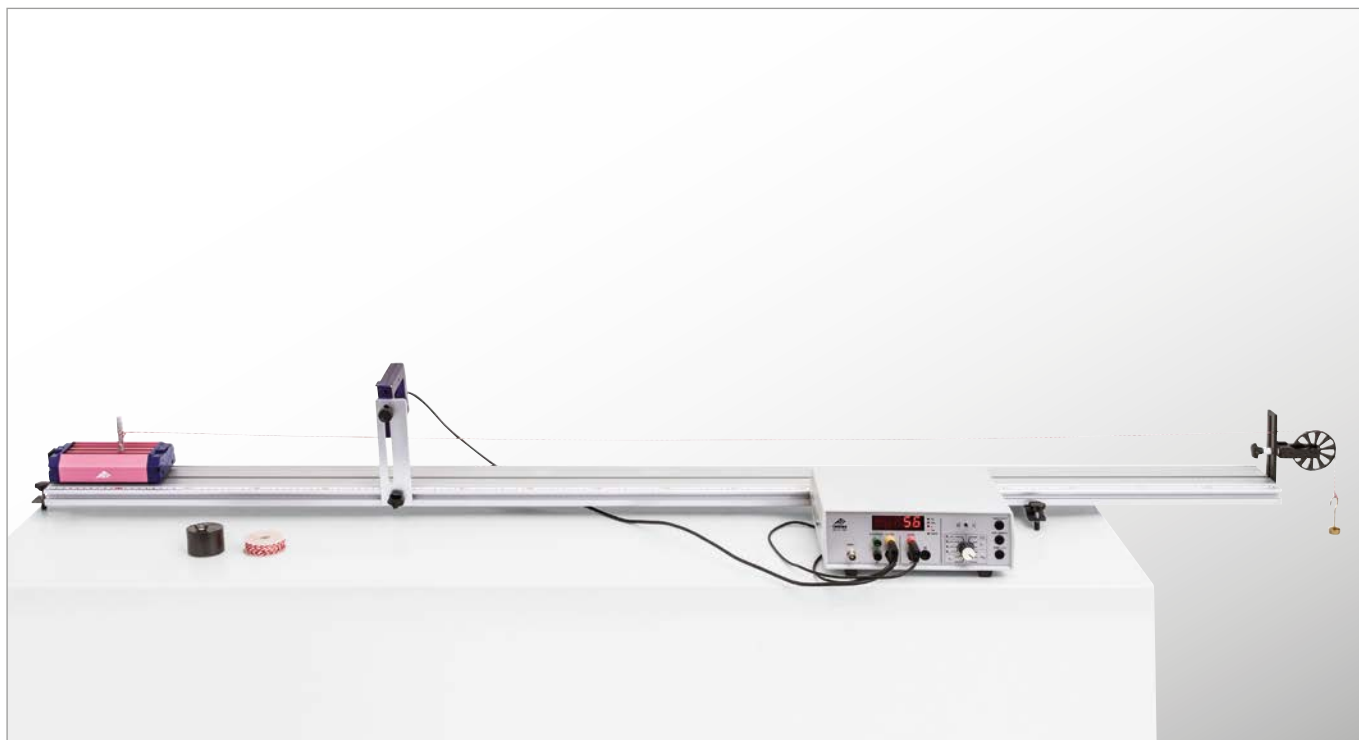


Fig. 2: Schematic representation

UE1030250 | UNIFORMLY ACCELERATED MOTION



> EXPERIMENT PROCEDURE

- Investigate uniformly accelerated motion as a function of the accelerating mass.
- Investigate uniformly accelerated motion as a function of the accelerated mass.

OBJECTIVE

Measurement of instantaneous velocity as a function of distance covered

SUMMARY

In the case of uniform acceleration, the instantaneous velocity increases as the distance covered becomes greater. The constant of proportionality between the square of the velocity and the distance covered can be used to calculate the acceleration. This will be investigated in an experiment involving a carriage rolling along a track. In order to measure the instantaneous velocity, a flag of known width attached to the wagon breaks the beam of a photoelectric sensor. The time for which the beam is broken is then measured by means of a digital counter.

REQUIRED APPARATUS

Quantity	Description	Item Number
1	Trolley Track	1018102
1	Photo Gate	1000563
1	Digital Counter (230 V, 50/60 Hz)	1001033 or
	Digital Counter (115 V, 50/60 Hz)	1001032
1	Set of Slotted Weights, 10 x 10 g	1003227
1	Pair of Safety Experiment Leads, 75 cm	1002849
1	Cord, 100 m	1007112

BASIC PRINCIPLES

In the case of uniform acceleration, the velocity v and the distance covered s increase over the course of time t . Thus the velocity increases as the distance becomes greater.

The instantaneous velocity after a period of time t is as follows:

$$(1) \quad v(t) = a \cdot t$$

The distance covered is given by

$$(2) \quad s(t) = \frac{1}{2} \cdot a \cdot t^2$$

This leads to the following conclusions:

$$(3) \quad v(s) = \sqrt{2 \cdot a \cdot s}$$

and

$$(4) \quad v^2(s) = 2 \cdot a \cdot s$$

The instantaneous velocity is given by the following:

$$(5) \quad v = \frac{\Delta s}{\Delta t}$$

In order to measure the instantaneous velocity in this experiment, an interrupter flag of known width Δs is attached to the carriage and breaks the beam of a photoelectric sensor as the carriage passes by it. The time the beam is broken Δt is measured by means of a digital counter.

EVALUATION

Plotting the squares of the instantaneous acceleration for each run, calculated from the times for which the beam is broken, against the distances covered, it is to be expected that there would be a linear relationship in the case of uniform acceleration as described by Equation 4. The gradient of the straight line through the origin plotted is equal to twice the acceleration.

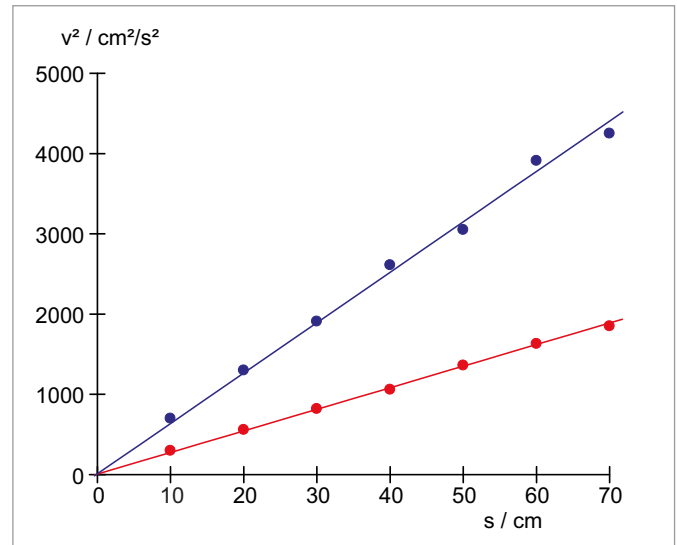


Fig. 2: v^2 - s plot for $m_2 = 500$ g. $m_1 = 10$ g (red), 20 g (blue)

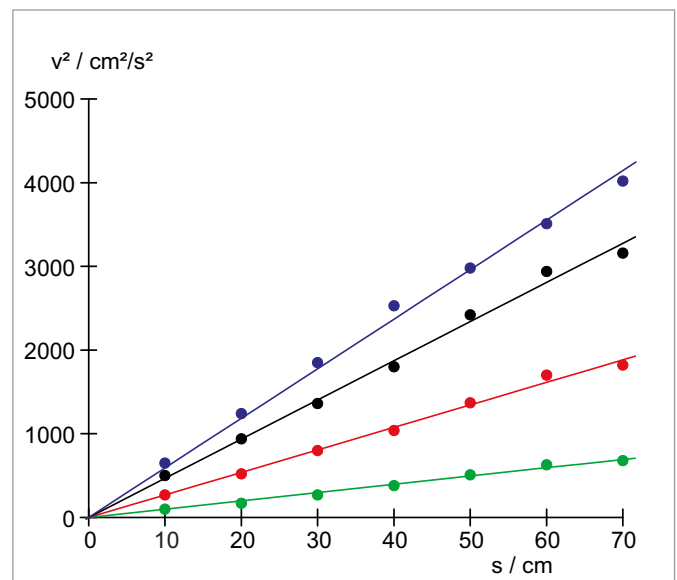


Fig. 3: v^2 - s plot for $m_2 = 1000$ g. $m_1 = 10$ g (green), 20 g (red), 30 g (black), 40 g (blue)

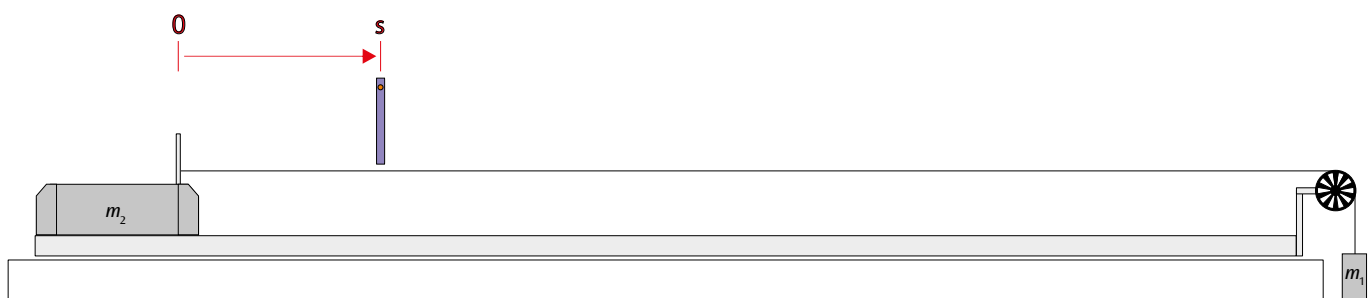
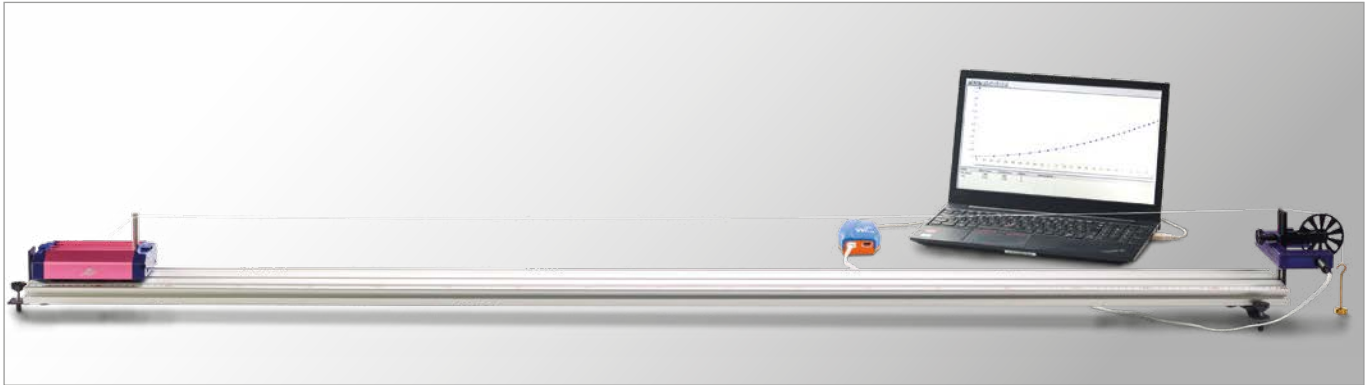


Fig. 1: Schematic representation

UE1030260

MOTION WITH UNIFORM ACCELERATION



> EXPERIMENT PROCEDURE

- Record distance as a function of time.
- Determine the speed at any given point as a function of time.
- Determine the acceleration at any given point as a function of time.
- Determine the average acceleration as a fit to the data and compare with the quotient of force and mass.

OBJECTIVE

Record and evaluate motion with uniform acceleration on a roller track

SUMMARY

When uniformly accelerated motion takes place the velocity at any instant is linearly proportional to the time, while the relationship between distance and time is quadratic. These relationships are to be recorded in an experiment using a roller track with the combination of a spoked wheel employed as a pulley and a photoelectric light barrier.

REQUIRED APPARATUS

Quantity	Description	Item Number
1	Trolley Track	1018102
1	WiLab *	1022284
1	Connecting Lead MiniDIN8 – BT	1021688
1	Photo Gate	1000563
1	Cord, 100 m	1007112
Additionally required		
1	Coach 7 License	

* Alternative: 1 VinciLab 1021477

BASIC PRINCIPLES

The velocity v and acceleration a at any given point in time are defined as first and second-order differentials of the distance s covered after a time t . This definition can be verified experimentally by using differential quotients instead of the actual differentials on a plot with the distance sampled at close intervals where the displacement points s are matched with measurements of time t_n . This provides a framework for experimentally investigating, for example, uniformly accelerated motion.

For constant acceleration a , the instantaneous velocity v increases in proportion to the time t , assuming the center of gravity was initially at rest:

$$(1) \quad v = a \cdot t$$

The distance covered s increases in proportion to the square of the time:

$$(2) \quad s = \frac{1}{2} \cdot a \cdot t^2$$

Constant acceleration results from a constant accelerating force F , as long as the mass m being accelerated does not change:

$$(3) \quad a = \frac{F}{m}$$

These relationships are to be investigated in an experiment using a carriage on a roller track. The carriage is accelerated uniformly because it is pulled by a thread subjected to a constant force, which is provided by a weight of known mass attached to the other end of the thread, see Fig. 1. The pulley for the thread takes the form of a spoked wheel and the spokes periodically interrupt a photoelectric light barrier. A measuring interface is attached which measures the times t_n when the spokes break the beam and sends that data to a computer for evaluation. The evaluation software calculates the distance covered at times t_n , along with the corresponding values for the time and acceleration at that instant.

$$(4a) \quad s_n = n \cdot \Delta$$

$$(4b) \quad v_n = \frac{\Delta}{t_{n+1} - t_{n-1}}$$

$$(4c) \quad a_n = \frac{\frac{\Delta}{t_{n+1} - t_n} - \frac{\Delta}{t_n - t_{n-1}}}{\frac{t_{n+1} - t_{n-1}}{2}}$$

$\Delta = 20$ mm: distance between spokes

Measurements are made for various combinations of accelerating force F and accelerated mass m .

EVALUATION

The evaluation software can display the values s , v and a as a function of time t . Applicability of equations (1) and (2) is checked by matching the results with various expressions using the acceleration a as a parameter.

If m_1 is the mass of the carriage and m_2 is the mass of the weight hanging from the thread. Since the mass m_2 also undergoes acceleration, then the values to be used in equation (3) are:

$$F = m_2 \cdot g \quad \text{and} \quad m = m_1 + m_2$$

This implies:
$$a = \frac{m_2}{m_1 + m_2} \cdot g$$

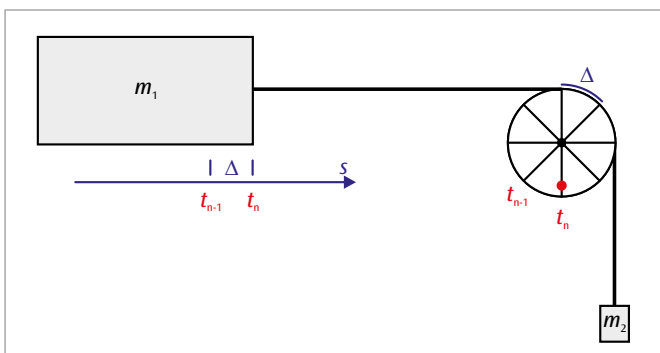


Fig. 1: Schematic illustration of measuring principle

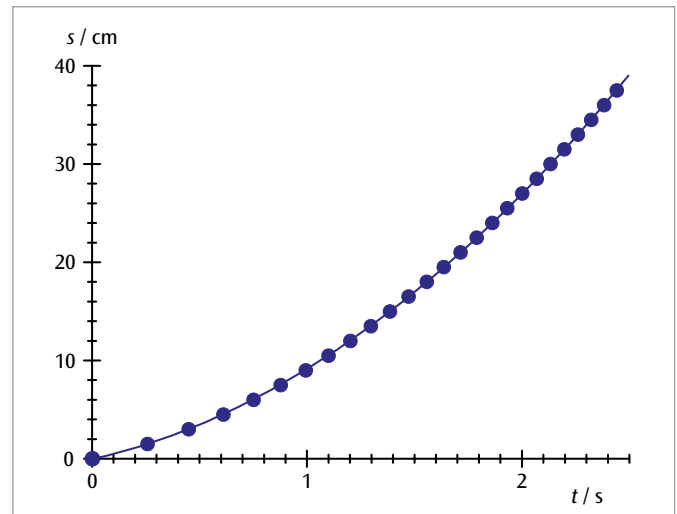


Fig. 2: Distance as a function of time

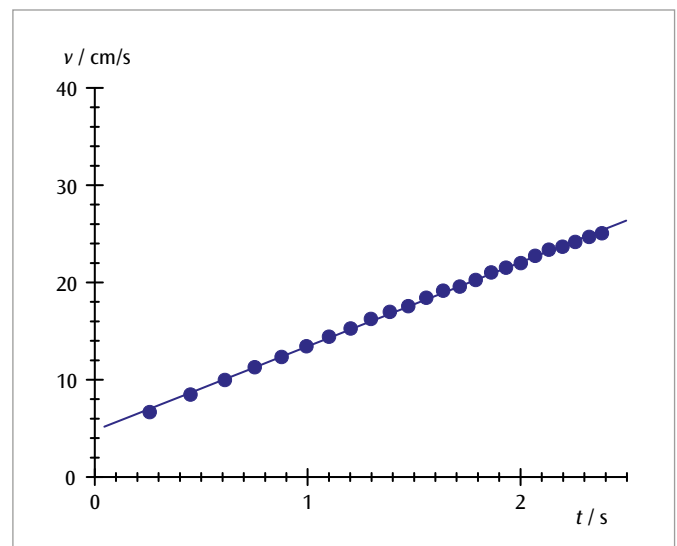


Fig. 3: Velocity as a function of time

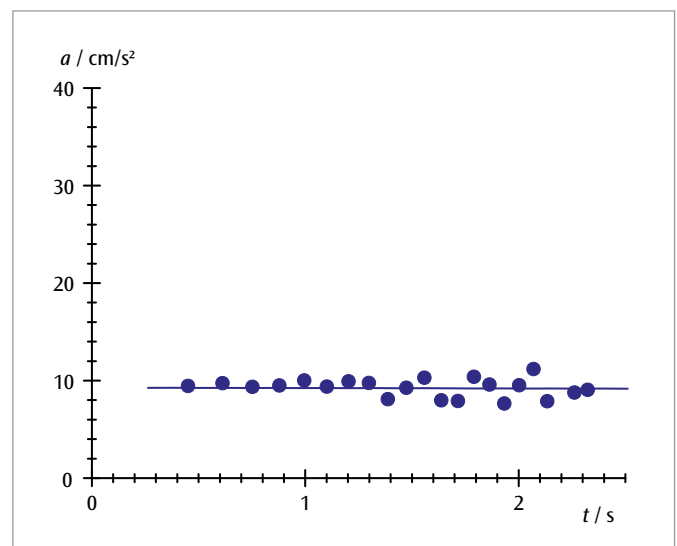


Fig. 4: Acceleration as a function of time

UE1030280 | LAWS OF COLLISIONS



OBJECTIVE

Investigate uni-dimensional collisions on an air track

SUMMARY

One important consequence of Newton's third law is the conservation of momentum in collisions between two bodies. One way of verifying this is to investigate collisions between two sliders on an air track. When all of the kinetic energy is conserved, we speak of elastic collisions. In cases where kinetic energy is only conserved for the common center of gravity of the two bodies, we use the term inelastic collisions. In this experiment, the individual velocities of the sliders are determined from the times that photoelectric light barriers are interrupted and the momentum values are calculated from these speeds.

> EXPERIMENT PROCEDURE

- Investigate elastic and inelastic collisions between two sliders on an air track.
- Demonstrate conservation of momentum for elastic and inelastic collisions and observe the individual momenta for elastic collisions.
- Investigate how energy is distributed in elastic and inelastic collisions.

REQUIRED APPARATUS

Quantity	Description	Item Number
1	Air Track	1021090
1	Air Flow Generator (230 V, 50/60 Hz)	1000606 or
	Air Flow Generator (115 V, 50/60 Hz)	1000605
1	WiLab *	1022284
2	Connecting Lead MiniDIN8 – BT	1003122
2	Photo Gate	1000563
2	Barrel Foot, 1000 g	1002834
2	Universal Clamp	1002830
2	Stainless Steel Rod 470 mm	1002934
Additionally required		
1	Coach 7 License	
Additionally recommended		
1	Mechanical Balance 610	1003419

* Alternative: 1 VinciLab 1021477

BASIC PRINCIPLES

One important consequence of Newton's third law is the conservation of momentum in collisions between two bodies. One way of verifying this is to investigate collisions between two sliders on an air track.

In the frame of reference of their common center of gravity, the total momentum of two bodies of masses m_1 and m_2 is zero both before and after the collision.

$$(1) \quad \vec{p}_1 + \vec{p}_2 = \vec{p}'_1 + \vec{p}'_2 = 0$$

\vec{p}_1, \vec{p}_2 : Individual momenta before collision, \vec{p}'_1, \vec{p}'_2 : Individual momenta after collision

The kinetic energy of the two sliders in the same frame of reference is given by

$$(2) \quad \tilde{E} = \frac{\tilde{p}_1^2}{2m_1} + \frac{\tilde{p}_2^2}{2m_2}$$

Depending on the nature of the collision, this may be converted partially or even wholly into other forms of energy. When all of the kinetic energy is conserved in frame of reference of the common center of gravity, we speak of elastic collisions. In an inelastic collision, all the energy is converted into another form.

Using the track itself as the frame of reference, conservation of momentum is described by the following equation:

$$(3) \quad p_1 + p_2 = p'_1 + p'_2 = p = \text{const.}$$

p_1, p_2 : Individual momenta before collision

p'_1, p'_2 : Individual momenta after collision

As a result of conservation of momentum, the velocity of the center of gravity

$$(4) \quad v_c = \frac{p}{m_1 + m_2}$$

and its kinetic energy

$$(5) \quad E_c = \frac{m_1 + m_2}{2} \cdot v_c^2$$

are also conserved. This is true of both elastic and inelastic collisions. In this experiment, the second slider is initially at rest before the collision. Therefore the conservation of momentum (equation 3) is given by

$$(6) \quad p = m_1 \cdot v_1 = m_1 \cdot v'_1 + m_2 \cdot v'_2,$$

Here v'_1 and v'_2 have different values after an elastic collision, but are the same subsequent to an inelastic collision. In an elastic collision, a flat buffer on the first slider collides with a stretched rubber band on the second slider. An inelastic collision involves a long pointed spike being pushed into some modelling clay. The masses of the sliders can be modified by adding weights.

After an elastic collision the following relationships apply:

$$(7) \quad p'_1 = \frac{m_1 - m_2}{m_1 + m_2} \cdot p, \quad p'_2 = \frac{2 \cdot m_2}{m_1 + m_2} \cdot p$$

and

$$(8) \quad E = \frac{m_1}{2} \cdot v_1^2 = \frac{m_1}{2} \cdot v_1'^2 + \frac{m_2}{2} \cdot v_2'^2$$

In the case of an inelastic collision only the kinetic energy of the center of gravity remains conserved. This can be calculated using equations (4), (5) and (6)

$$(9) \quad E_c = \frac{m_1}{m_1 + m_2} \cdot \frac{m_1}{2} \cdot v_1^2 = \frac{m_1}{m_1 + m_2} \cdot E$$

EVALUATION

The time intervals Δt recorded by the software are to be matched with experimental procedures. The following applies to the velocities of the sliders

$$v = \frac{25 \text{ mm}}{\Delta t}$$

A precise consideration of the velocity and momentum distributions should also take into account frictional losses. For the momentum values obtained here, they should amount to some 5% and for the energy values 10%, see Figs. 1 to 5.

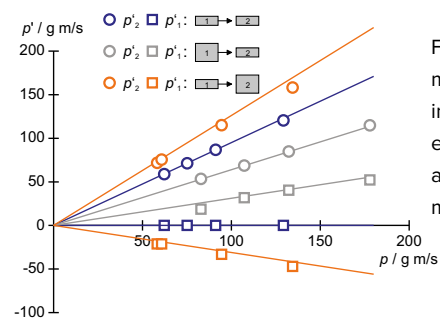


Fig. 1: Individual momenta for colliding bodies after an elastic collision as a function of initial momentum

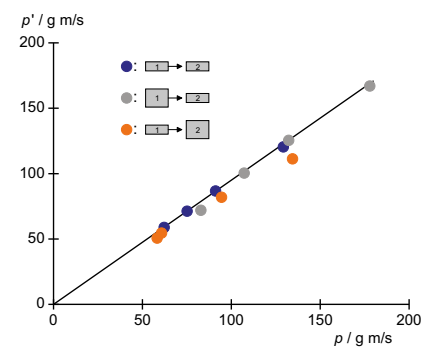


Fig. 2: Total momentum for colliding bodies after an elastic collision as a function of initial momentum

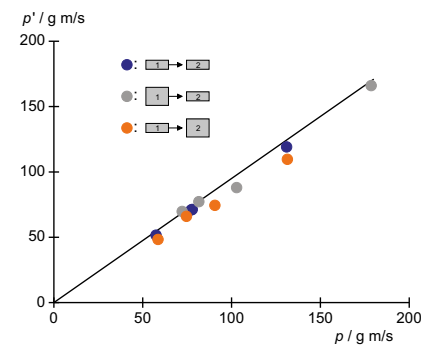


Fig. 3: Total momentum for colliding bodies after an inelastic collision as a function of initial momentum

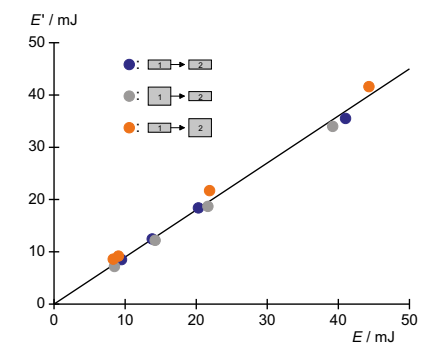


Fig. 4: Total energy for colliding bodies after an elastic collision as a function of initial energy

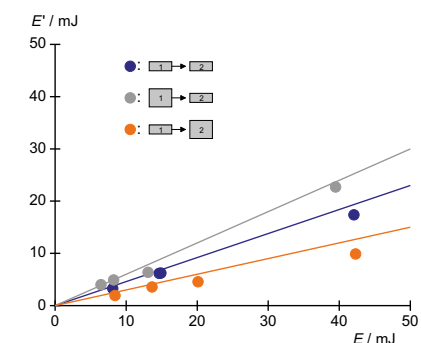
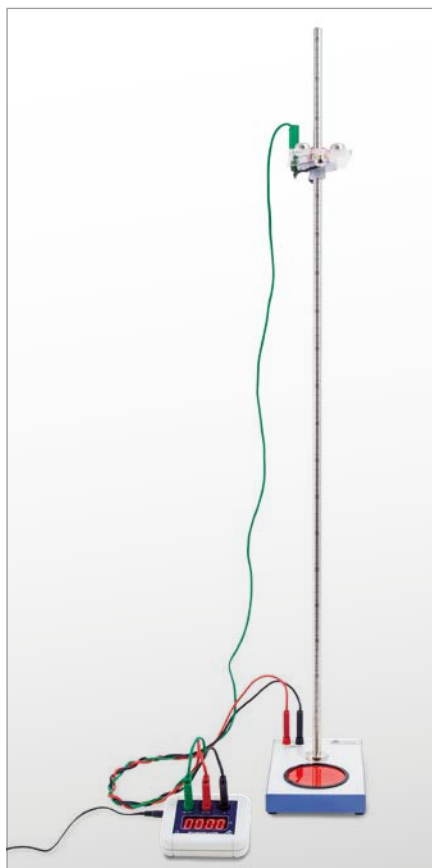


Fig. 5: Total energy for colliding bodies after an inelastic collision as a function of initial energy

UE1030300 | FREE FALL



> EXPERIMENT PROCEDURE

- Measure the time t that a ball takes to fall a distance h between a release mechanism and a target plate at the bottom.
- Draw points for a displacement/time graph for a uniformly accelerating motion.
- Verify that the distance fallen is proportional to the square of the time.
- Calculate the acceleration due to gravity g .

OBJECTIVE

Determine the gravitational acceleration

SUMMARY

In free fall the distance fallen h is proportional to the square of the time t taken to fall that distance. The coefficient of that proportionality can be used to calculate the gravitational acceleration g .

REQUIRED APPARATUS

Quantity	Description	Item Number
1	Free-fall Apparatus	1000738
1	Millisecond Counter (230 V, 50/60 Hz)	1012833 or
	Millisecond Counter (115 V, 50/60 Hz)	1012832
1	Set of 3 Safety Experiment Leads	1002848

BASIC PRINCIPLES

If a body falls to the ground in the Earth's gravitational field from a height h , it undergoes a constant acceleration g , as long as the speed of the fall is slow so that friction can be ignored. Such a falling motion is called free fall.

In this experiment a steel ball is suspended from a release mechanism. As soon as it is released into free fall, an electronic timer is started. After it has fallen a distance h the ball hits a target plate at the bottom which stops the time measurement at a time t .

Since the ball is not moving before it starts to fall at time $t_0 = 0$ its initial velocity is zero, i.e. $v_0 = 0$. Therefore the distance covered in time t is given as follows

$$(1) \quad h = \frac{1}{2} \cdot g \cdot t^2$$

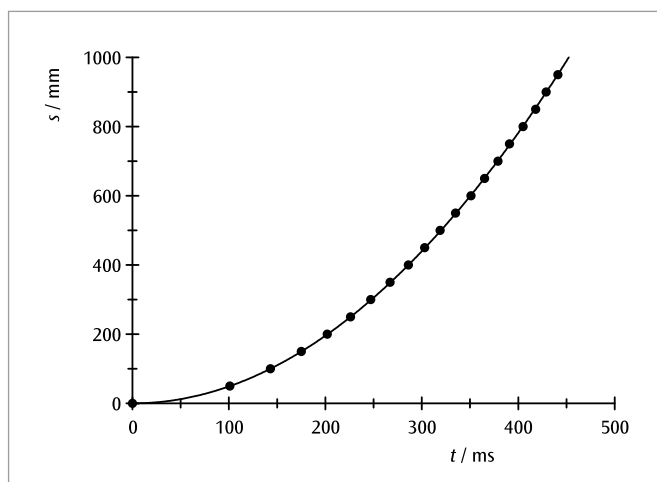


Fig . 1: Time-displacement diagram for free fall

EVALUATION

First variant:

Fall times change in the ratio 2:1 if the height of the fall changes in the ratio 4:1. This confirms that the height is proportional to the square of the time.

Second variant:

Measurements for various heights of fall should be plotted on a displacement/time graph. The height h is not linearly proportional to the time t , as can be confirmed by attempting to match the curve to a line then to a parabola. To obtain a straight line, the height should be plotted against the square of the time. The straight-line relationship found in this way confirms equation (1). The gradient of such a line corresponds to the acceleration due to gravity.

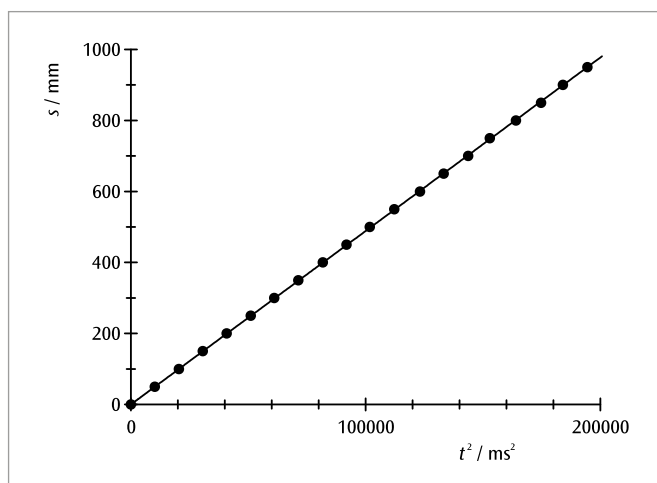
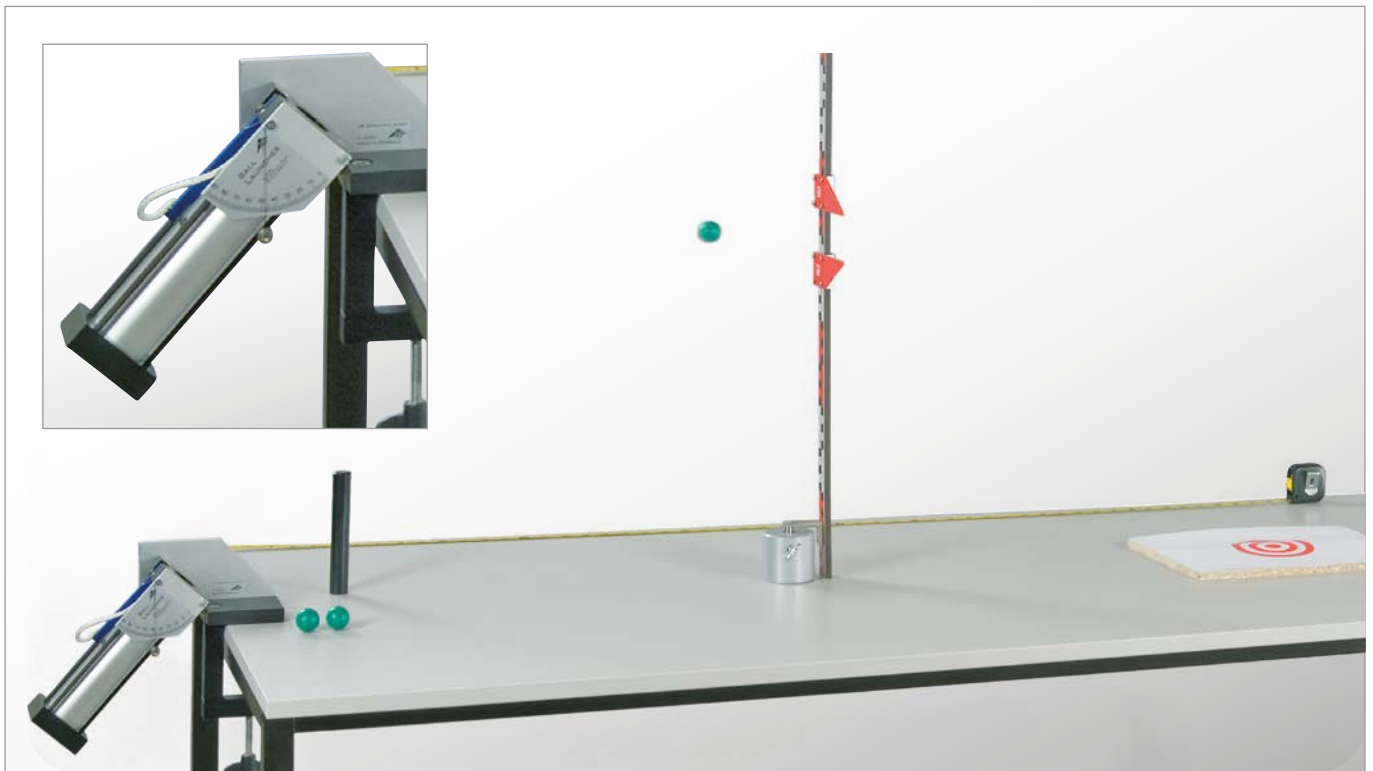


Fig. 2: Height plotted against the square of time

UE1030400 | INCLINED LAUNCH



> EXPERIMENT PROCEDURE

- Measuring the width of the trajectory as a function of the throwing angle and the initial velocity.
- Calculating the initial velocity from the maximum width of the trajectory.
- Point-by-point plotting of the “parabolic” trajectory as a function of the throwing angle and the initial velocity.
- Verification of the principle of superposition.

OBJECTIVE

Plotting the “parabolic” trajectories point by point

SUMMARY

The motion of a ball that is thrown upward at an angle to the horizontal in the earth’s gravitational field follows a parabolic curve whose height and width depend on the throwing angle and the initial velocity. The curve is measured point by point using a height scale with two pointers.

REQUIRED APPARATUS

Quantity	Description	Item Number
1	Projectile Launcher	1002654
1	Clamp for Projectile Launcher	1002655
1	Vertical Ruler, 1 m	1000743
1	Set of Riders for Rulers	1006494
1	Barrel Foot, 900 g	1002834
1	Pocket Measuring Tape, 2 m	1002603

BASIC PRINCIPLES

According to the principle of superposition, the motion of a ball that is thrown upward at an angle to the horizontal in the earth's gravitational field is the combination of a motion at a constant speed in the direction of throwing and a gravitational falling motion. This results in a parabolic flight curve, whose height and width depend on the throwing angle α and the initial velocity v_0 .

To calculate the theoretical flight curve, for simplicity we take the center of the spherical ball as the origin of the coordinate system, and we neglect the frictional drag of the air on the ball. Thus the ball retains its initial velocity in the horizontal direction

$$(1) \quad v_x(t) = v_0 \cdot \cos \alpha$$

and therefore at time t the horizontal distance travelled is

$$(2) \quad x(t) = v_0 \cdot \cos \alpha \cdot t$$

In the vertical direction, under the influence of the gravitational field, the ball is subjected to gravitational acceleration g . Therefore, at time t its vertical velocity is

$$(3) \quad v_y(t) = v_0 \cdot \sin \alpha - g \cdot t$$

and the vertical distance travelled is

$$(4) \quad y(t) = v_0 \cdot \sin \alpha \cdot t - \frac{1}{2} \cdot g \cdot t^2$$

The flight curve of the ball has the form of a parabola, as it conforms to the equation

$$(5) \quad y(x) = \tan \alpha \cdot x - \frac{1}{2} \cdot \frac{g}{(v_0 \cdot \cos \alpha)^2} \cdot x^2$$

At time t_1 given by

$$(6) \quad t_1 = \frac{v_0 \cdot \sin \alpha}{g}$$

the ball reaches the highest point of the parabola, and at time t_2 given by

$$(7) \quad t_2 = 2 \cdot \frac{v_0 \cdot \sin \alpha}{g}$$

it is again at the initial height 0. Thus, the height of the parabola is

$$(8) \quad h = y(t_1) = \frac{v_0^2}{2 \cdot g} \cdot \sin^2 \alpha$$

and the width is

$$(9) \quad s = x(t_2) = 2 \cdot \frac{v_0^2}{g} \cdot \sin \alpha \cdot \cos \alpha$$

In the experiment, the flight curves of a ball are measured point by point as a function of the throwing angle and the initial velocity, using a height scale with two pointers.

EVALUATION

The maximum width of all the flight curves, s_{\max} , is reached when the throwing angle α is 45° . From this maximum width, it is possible to calculate the initial velocity. By using Equation 9, we get

$$v_0 = \sqrt{g \cdot s_{\max}}$$

An exact analysis of the experimental data shows that the frictional drag of the air on the ball must be taken into account, and that the flight curves actually depart slightly from the parabolic shape.

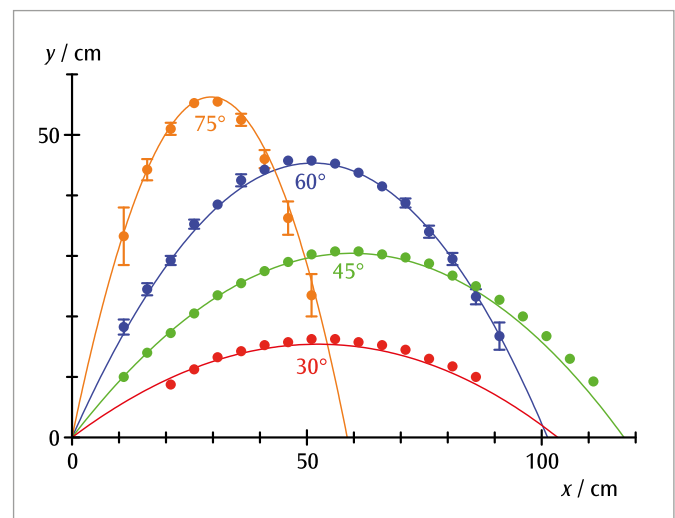


Fig. 1: Flight curves for the smallest initial velocity and different throwing angles, measured experimentally, and calculated theoretically with air friction taken into account

UE1030600 | TWO-DIMENSIONAL COLLISIONS



> EXPERIMENT PROCEDURE

- Determine the velocities before and after a collision.
- Verify the conservation of momentum for elastic and inelastic collisions.
- Verify the conservation of energy for elastic and inelastic collisions.
- Investigate the motion of the centers of gravity in the system.

OBJECTIVE

Investigate elastic and inelastic collisions between two objects on a plane

SUMMARY

In any collision between two bodies, the colliding objects must obey the laws of conservation of energy and conservation of momentum. With the help of these two conserved quantities it is possible to describe how the bodies will behave after the collision. In the case of a flat plane, the velocity and momentum need to be expressed as vectors. A particularly simple description can be obtained by switching to a system which focuses on the mutual center of gravity of the two bodies. In this experiment, two discs of specific mass are allowed to collide on an air cushion table and the velocities are then recorded and analyzed by inkjet marking or video tracking.

REQUIRED APPARATUS

Quantity	Description	Item Number
1	Air Cushion Platform with Inkjet Pucks	1021623
Additionally recommended		
1	Mechanical Balance 610	1003419
1	Ruler, 50 cm	
1	Goniometer	
1	Video Camera	
1	Video Analysis Software, e.g. Coach 7	

BASIC PRINCIPLES

A collision refers to a brief interaction between two bodies. It is assumed that this interaction takes place in the space of a certain, short length of time and that the bodies do not affect one another in any other way. If no other forces are present, the two bodies will move at constant velocities both before and after the collision. Since the two bodies may be regarded as a closed system, the interaction must obey the laws of conservation of momentum and conservation of energy.

The velocities of bodies 1 and 2 before the collision are represented by the vectors v_1 and v_2 . Those after the collision are represented by v'_1 and v'_2 . The corresponding momentum is represented by p_i and p'_i ($i = 1, 2$). The masses of both bodies remain constant over time and are labelled m_1 and m_2 .

Due to conservation of momentum, the following must be true:

$$(1) \quad m_1 \cdot \mathbf{v}_1 + m_2 \cdot \mathbf{v}_2 = m_1 \cdot \mathbf{v}'_1 + m_2 \cdot \mathbf{v}'_2$$

In addition, when the collisions are elastic, the overall kinetic energy in the system is also conserved:

$$(2) \quad \frac{1}{2} \cdot m_1 \cdot v_1^2 + \frac{1}{2} \cdot m_2 \cdot v_2^2 = \frac{1}{2} \cdot m_1 \cdot v_1'^2 + \frac{1}{2} \cdot m_2 \cdot v_2'^2$$

If body 2 is at rest before the collision, it is possible to select a coordinate system in which the motion of body 1 is along the x-axis ($v_{1y} = 0$). This does not in any way affect the generality of the description. First let us consider a collision in line with the centers of gravity of both objects, where $d = 0$, see Fig. 1. The bodies will then move along the x-axis and the velocities after the collision are given by:

$$(3) \quad v'_1 = \frac{m_1 - m_2}{m_1 + m_2} \cdot v_1$$

and

$$(4) \quad v'_2 = \frac{2m_1}{m_1 + m_2} \cdot v_1$$

For identical masses, $m_1 = m_2$, the following conditions are true:

$$(5) \quad v'_1 = 0$$

and

$$(6) \quad v'_2 = v_1$$

If collisions are off-center but the masses are the same, the bodies will separate from one another at an angle of 90° , i.e.

$$(7) \quad \theta_1 + \theta_2 = 90^\circ$$

Additionally, if $v_{1y} = 0$ and $m_1 = m_2$, then equation (1) provides the following result:

$$(8) \quad v'_{1y} = -v'_{2y}$$

The position vector for the center of gravity is as follows:

$$(9) \quad \mathbf{r}_s = \frac{m_1 \cdot \mathbf{r}_1 + m_2 \cdot \mathbf{r}_2}{m_1 + m_2}$$

Since the total momentum is conserved, the velocity of the center of gravity is constant and is given by the following equation:

$$(10) \quad \mathbf{v}_s = \frac{m_1 \cdot \mathbf{v}_1 + m_2 \cdot \mathbf{v}_2}{m_1 + m_2}$$

The total momentum corresponds to the momentum of a single mass $m_s = m_1 + m_2$, which moves at the same velocity as the center of gravity.

It often makes sense to transform the frame of reference to a system centered on the combined center of gravity of the two bodies. Then, before the collision, the two bodies will converge towards one another in such a way that the overall momentum is zero. After an elastic collision, they then separate in such a way that the total momentum continues to be zero. After a completely inelastic collision, they stick together and rotate about their mutual center of gravity. The kinetic energy of the system is also conserved in this case. In this experiment, two discs of known mass are allowed to collide on a cushion of air. The motion they undergo is recorded with the help of a spark generator.

EVALUATION

Calculation of the kinetic energy indicates that some energy is lost. This is due to the slight deformation of the bodies when they collide and any intrinsic rotation of the pucks which has not been taken into account.

The magnitude of the velocities can be calculated using the following relationship: $v = \Delta \cdot f$

Δ : Distance between two points,
 f : Frequency of the plotter

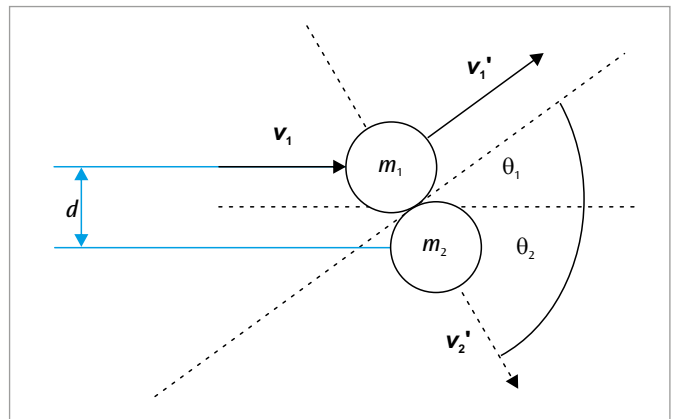


Fig. 1: Schematic representation of an off-center collision between two bodies

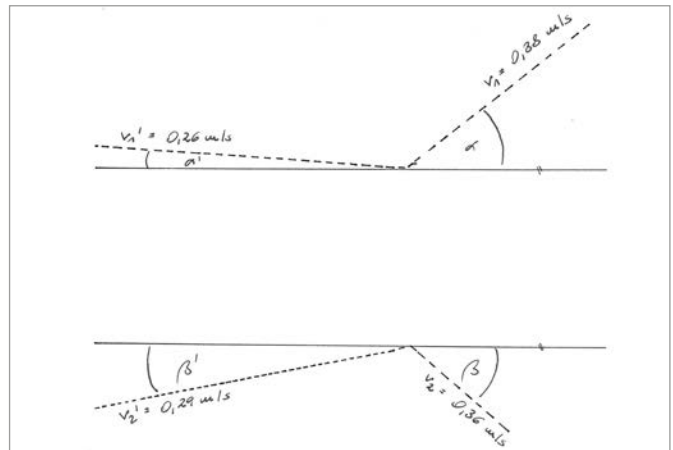


Fig. 2: Recording and evaluation of an off-center collision between two bodies of unequal mass and initial velocities $v_1 \neq 0$ and $v_2 \neq 0$

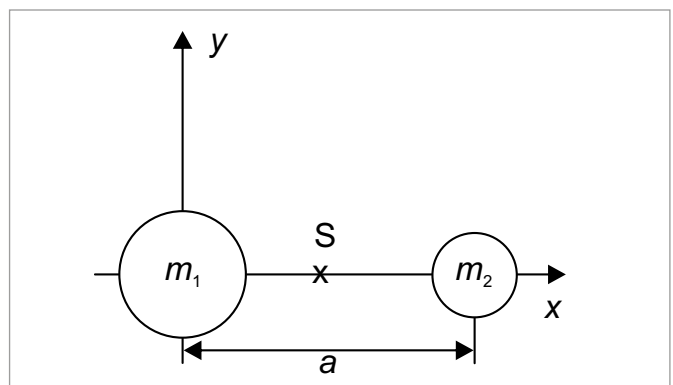


Fig. 3: Motion of center of gravity S before and after collision

UE1040101 | ROTATIONAL MOTION WITH UNIFORM ACCELERATION



EXPERIMENT PROCEDURE

- Plot the angle of rotation point by point as a function of time for a uniformly accelerated rotational motion.
- Confirm the proportionality between the angle of rotation and the square of the time.
- Determine the angular acceleration as a function of the torque and confirm agreement with Newton's equation of motion.
- Determine the angular acceleration as a function of the moment of inertia and confirm agreement with Newton's equation of motion.

OBJECTIVE

Confirm Newton's equation of motion

SUMMARY

For a body that rotates about a fixed axis with uniform acceleration, the angle of rotation φ increases in proportion to the square of the time t . From this proportionality factor it is possible to calculate the angular acceleration α , which in turn depends, according to Newton's equation of motion, on the accelerating torque (turning moment) and the moment of inertia of the rigid body.

REQUIRED APPARATUS

Quantity	Description	Item Number
1	Rotating System on Air Bed (230V, 50/60 Hz)	1000782 or
	Rotating System on Air Bed (115V, 50/60 Hz)	1000781
1	Laser Reflection Sensor	1001034
1	Digital Counter (230 V, 50/60 Hz)	1001033 or
	Digital Counter (115 V, 50/60 Hz)	1001032

BASIC PRINCIPLES

The rotation of a rigid body about a fixed axis can be described in a way that is analogous to a one-dimensional translational motion. The distance s is replaced by the angle of rotation φ , the linear velocity v by the angular velocity ω , the acceleration a by the angular acceleration α , the accelerating force F by the torque M acting on the rigid body, and the inertial mass m by the rigid body's moment of inertia J about the axis of rotation.

In analogy to Newton's law of motion for translational motion, the relationship between the torque (turning moment) M that is applied to a rigid body with a moment of inertia J , supported so that it can rotate, and the angular acceleration α is:

$$(1) \quad M = J \cdot \alpha$$

If the applied torque is constant, the body undergoes a rotational motion with a constant rate of angular acceleration.

In the experiment, this behavior is investigated by means of a rotating system that rests on an air-bearing and therefore has very little friction. The motion is started at the time $t_0 = 0$ with zero initial angular velocity $\omega = 0$, and in the time t it rotates through the angle

$$(2) \quad \varphi = \frac{1}{2} \cdot \alpha \cdot t^2$$

The torque M results from the weight of an accelerating mass m_M acting at the distance r_M from the axis of rotation of the body, and is therefore:

$$(3) \quad M = r_M \cdot m_M \cdot g$$

the gravitational acceleration constant

$$g = 9.81 \frac{\text{m}}{\text{s}^2}$$

If two additional weights of mass m_J are attached to the horizontal rod of the rotating system at the same fixed distance r_J from the axis of rotation, the moment of inertia is increased to:

$$(4) \quad J = J_0 + 2 \cdot m_J \cdot r_J^2$$

J_0 : moment of inertia without additional weights.

A number of weights are provided, both for producing the accelerating force and for increasing the moment of inertia. The distances r_M and r_J can also be varied. Thus, it is possible to investigate how the angular acceleration depends on the torque and the moment of inertia in order to confirm the relationship (1).

EVALUATION

The proportionality of the angle of rotation to the square of the time is demonstrated by measuring the times for the angles of rotation 10° , 40° , 90° , 160° and 250° .

To determine the angular acceleration α as a function of the variables M and J , measure the time $t(90^\circ)$ needed for an angle of rotation of 90° with different values of the variable in both cases. For this special case the angular acceleration is

$$\alpha = \frac{\pi}{t(90^\circ)^2}$$

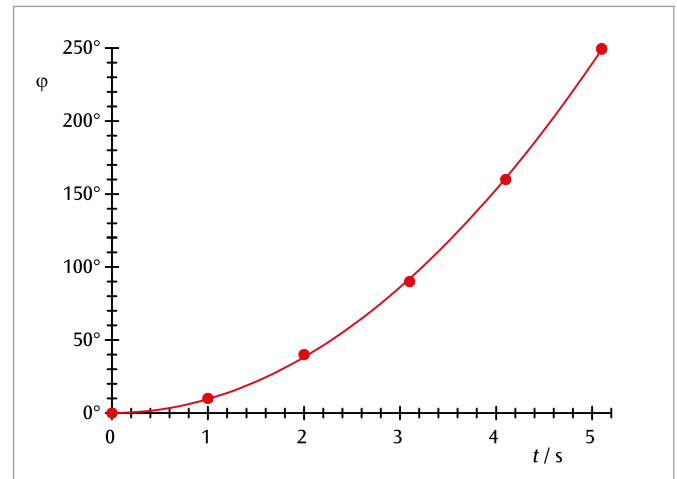


Fig. 1: Angle of rotation as a function of time for a uniformly accelerated rotational motion

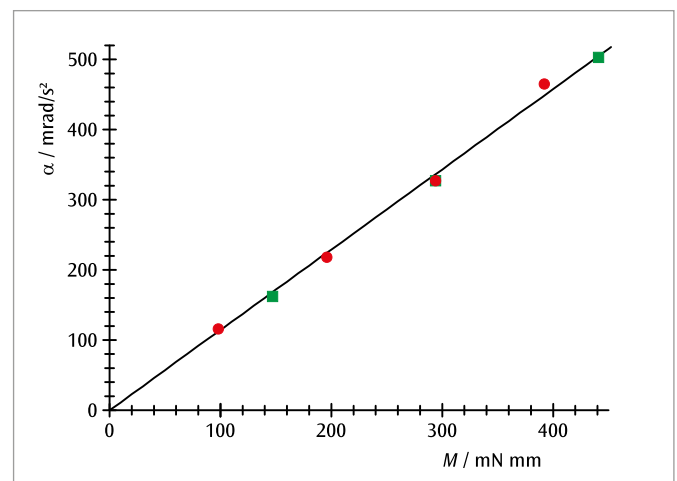


Fig. 2: Angular acceleration α as a function of the torque M

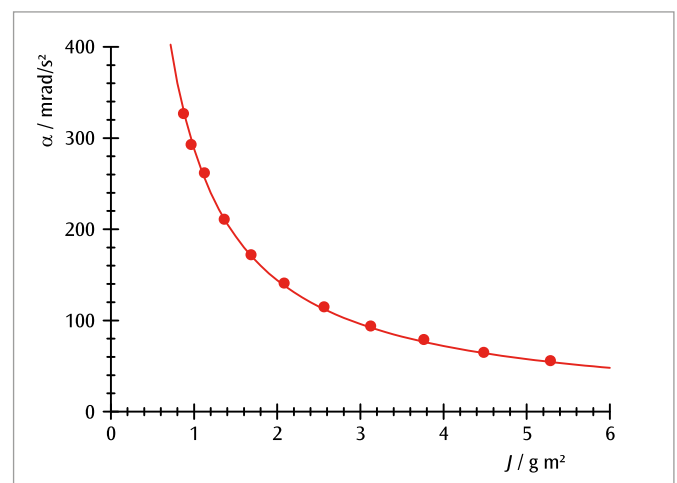


Fig. 3: Angular acceleration α as a function of the moment of inertia J

UE1040201 | MOMENT OF INERTIA I



> EXPERIMENT PROCEDURE

- Determine the torsional coefficient D_r of the coupled spring.
- Determine the moment of inertia J as a function of the distance r of the added weights from the axis of rotation.
- Determine the moment of inertia J as a function of the value m of the added weights.

OBJECTIVE

Determine the moment of inertia of a horizontal rod with additional weights attached

SUMMARY

The moment of inertia of a body about its axis of rotation depends on the distribution of its weight in relation to the axis. This is to be investigated for the case of a horizontal rod to which two additional weights are attached symmetrically about the axis of rotation. The rod is coupled to a torsion spring, and its period of oscillation increases as its moment of inertia, which is determined by the additional weights and their distance from the axis, is raised.

REQUIRED APPARATUS

Quantity	Description	Item Number
1	Rotating System on Air Bed (230 V, 50/60 Hz)	1000782 or
	Rotating System on Air Bed (115 V, 50/60 Hz)	1000781
1	Supplementary Kit for Rotating System on Air Bed	1000783
1	Laser Reflection Sensor	1001034
1	Digital Counter (230 V, 50/60 Hz)	1001033 or
	Digital Counter (115 V, 50/60 Hz)	1001032

BASIC PRINCIPLES

The inertia of a rigid body that acts against a change of its rotational motion about a fixed axis is described by the moment of inertia J . It depends on the distribution of weight in relation to the axis of rotation. The greater the distance of a weight from the axis of rotation the greater also is the moment of inertia it causes.

In the experiment, this is investigated using the example of a rotating disc carrying a horizontal rod, to which two additional weights of mass m are attached symmetrically at a distance r from the axis of rotation. For this system the moment of inertia is:

$$(1) \quad J = J_0 + 2 \cdot m \cdot r^2$$

J_0 : moment of inertia without the additional weights.

If the rotating disc is coupled elastically by a coil spring to a rigid stand, the moment of inertia can be determined from the period of torsional oscillation of the disc about its rest position. The relationship is as follows:

$$(2) \quad T = 2\pi \cdot \sqrt{\frac{J}{D_r}}$$

D_r : torsional coefficient of the coil spring.

Thus, the greater the moment of inertia J of the disc with the attached horizontal rod, as dependent on the mass m and the distance r , the longer the period of oscillation T .

EVALUATION

From (2) the following equation is derived to determine the moment of inertia:

$$J = D_r \cdot \frac{T^2}{4\pi^2}$$

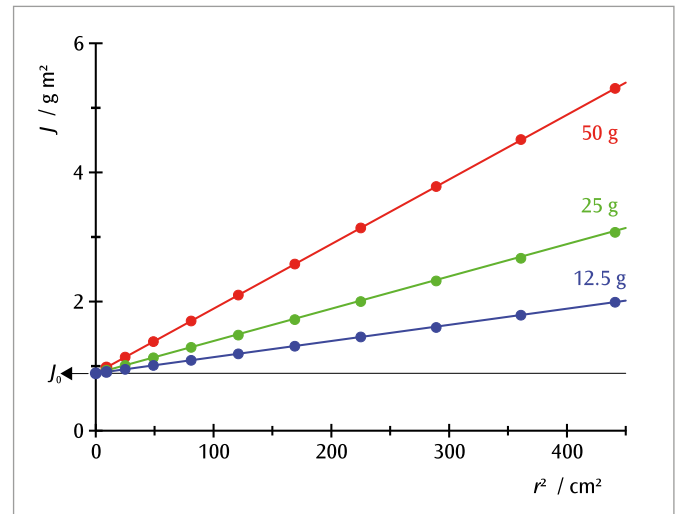
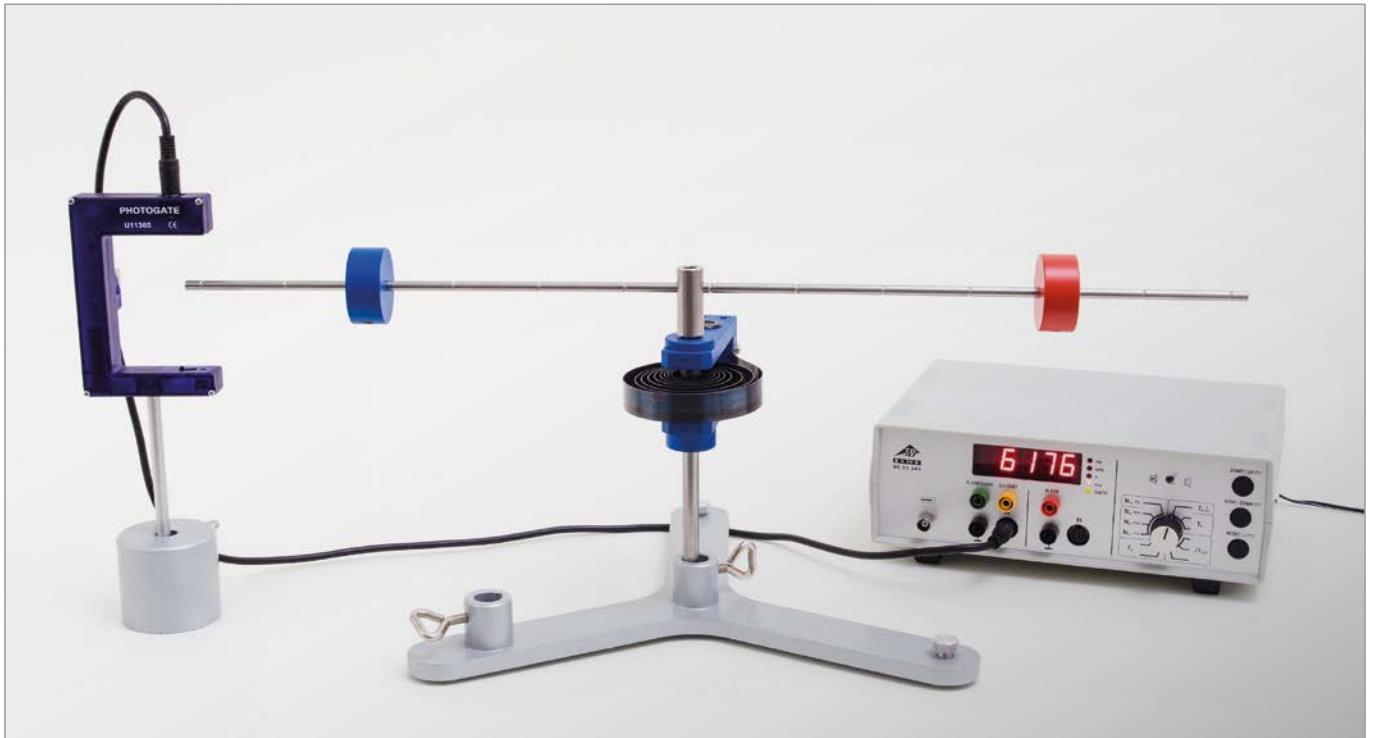


Fig. 1: Moment of inertia J of rotating disc with horizontal rod as a function of the square of the distance r from the axis of rotation for three different additional weights of mass m

UE1040205 | MOMENT OF INERTIA II



> EXPERIMENT PROCEDURE

- Determine the torsional coefficient D_t between for the springs used to couple the objects.
- Determine the moment of inertia J for a dumbbell bar without any added weights.
- Determine the moment of inertia J as a function of distance r of a weight from its axis of rotation.
- Determine the moment of inertia J for a circular wooden disc, a wooden sphere and both solid and hollow cylinders.

OBJECTIVE

Determine the moment of inertia for various test bodies

SUMMARY

A body's moment of inertia around an axis of rotation depends on how the mass of the object is distributed with respect to the axis. This will be investigated for a dumbbell, which has two weights symmetrically aligned either side of the axis, for a circular wooden disc, a wooden sphere and both solid and hollow cylinders. The period of oscillation of the test bodies is dependent on the mass distribution and the effective radius of the object.

REQUIRED APPARATUS

Quantity	Description	Item Number
1	Torsion Axle	1008662
1	Photo Gate	1000563
1	Digital Counter (230 V, 50/60 Hz) Digital Counter (115 V, 50/60 Hz)	1001033 or 1001032
1	Barrel Foot, 1000 g	1002834
1	Tripod Stand 185 mm	1002836
1	Precision Dynamometer 1 N	1003104
1	Set of Test Bodies for Torsion Axle	1021752

BASIC PRINCIPLES

The inertia of a rigid body with respect to a change in its rotational motion around a fixed axis is given by its moment of inertia J . This is dependent on the distribution of mass in the body relative to the axis of rotation and increases at greater distance from the axis of rotation itself.

In general, moment of inertia is defined by means of a volume integral:

$$(1) \quad J = \int_V r_s^2 \cdot \rho(r) \cdot dV$$

r_s : component of r perpendicular to the axis of rotation

$\rho(r)$: Distribution of mass in the body

Using as an example a dumbbell set, which has two weights of mass m symmetrically arranged at a distance r from the axis of rotation, then the moment of inertia is as follows:

$$(2) \quad J = J_0 + 2 \cdot m \cdot r^2$$

J_0 : Moment of inertia of dumbbell bar without weights

Now we can attach various test bodies to a twisting axis so that they can oscillate. If the period of oscillation is T , then the following is true:

$$(3) \quad T = 2\pi \cdot \sqrt{\frac{J}{D_r}}$$

D_r : Torsional coefficient of coil springs

This means that the period of oscillation T will be greater when the moment of inertia J is larger.

The torsional coefficient of the coil springs can be determined with the help of a spring dynamometer:

$$(4) \quad D_r = \frac{F \cdot r}{\alpha}$$

α : Deflection from equilibrium state

EVALUATION

From equation (3) it is possible to obtain a formula for determining the moment of inertia:

$$J = D_r \cdot \frac{T^2}{4\pi^2}$$

For the set-up involving the dumbbell, it is then necessary to subtract the moment of inertia of the bar itself:

$$J(\text{weights}) = J(\text{bar} + \text{weights}) - J(\text{bar}).$$

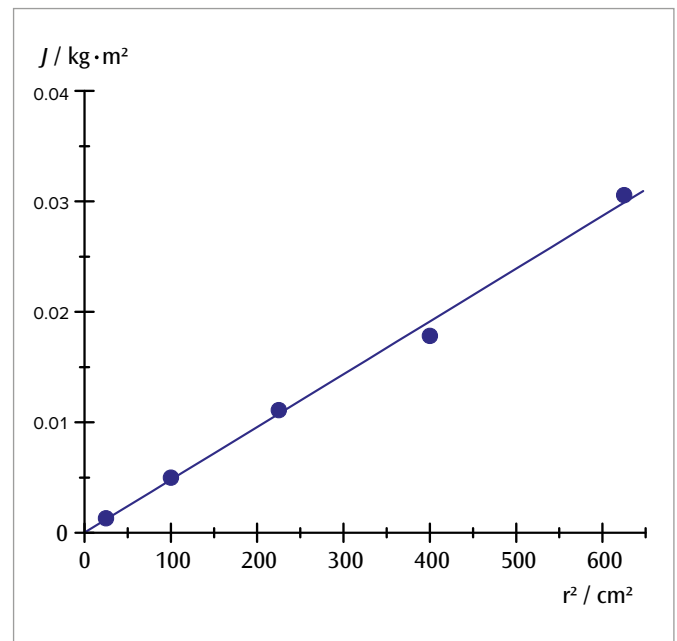


Fig. 1: Moment of inertia J of weights as a function of their radius r from the axis of rotation

UE1040320 | MAXWELL'S WHEEL



OBJECTIVE

Confirm the conservation of energy with the help of Maxwell's wheel

SUMMARY

Maxwell's wheel is suspended from threads at both ends of its axle in such a way that it can roll along the threads. In the course of its motion, potential energy is converted into kinetic energy and back again. The process of rolling up and down is repeated until the potential energy derived from the initial height of the wheel is entirely lost due to reflection losses and friction. In this experiment the movement of Maxwell's wheel is recorded with an ultrasonic motion sensor. From the resulting displacement versus time graph the instantaneous speed of the wheel can be determined and thereby its kinetic energy can be calculated.

EXPERIMENT PROCEDURE

- Plot a graph of displacement against time and another of speed against time for the first downward roll.
- Determine the acceleration and the moment of inertia.
- Determine the kinetic energy and potential energy during upward and downward motions.
- Confirm the conservation of energy taking into account losses due to reflection and friction.

REQUIRED APPARATUS

Quantity	Description	Item Number
1	Maxwell's Wheel	1000790
1	WiLab *	1022284
1	Motion Sensor for WiLab *	1022288
1	Stand with H-Shaped Base	1018874
2	Stainless Steel Rod 1500 mm	1002937
2	Universal Clamp	1002830

Additionally required

1	Coach 7 License
---	-----------------

Additionally recommended

1	Electronic Scale 5000 g	1003434
1	Callipers, 150 mm	1002601

* Alternatives: 1 €Motion 1021673 or 1 VinciLab 1021477 and 1 Motion Sensor 1021683

BASIC PRINCIPLES

Maxwell's wheel is suspended from threads at both ends of its axle in such a way that it can roll along the threads. As it moves, potential energy is increasingly converted into kinetic energy of the spinning wheel. Once the threads are fully wound out, though, they then start to wind up the opposite way round and the wheel rises, whereby the kinetic energy is converted back into potential energy until all of it is reconverted. The wheel then keeps rolling down and back up again until the potential energy derived from the initial height of the wheel is entirely lost due to reflection losses and friction.

As it rolls up and down, the wheel moves at a velocity v . The velocity obeys the following fixed relationship to the angular velocity ω with which the wheel rotates about its axle:

$$(1) \quad v = \omega \cdot r \quad \text{where } r: \text{ radius of axle.}$$

The total energy is therefore given by

$$(2) \quad E = m \cdot g \cdot h + \frac{1}{2} \cdot I \cdot \omega^2 + \frac{1}{2} \cdot m \cdot v^2 \\ = m \cdot g \cdot h + \frac{1}{2} \cdot m \cdot \left(\frac{I}{m \cdot r^2} + 1 \right) \cdot v^2$$

m : mass, I : moment of inertia,

h : height above lower point of reversal,

g : acceleration due to gravity

This describes a translational motion with an acceleration downwards given by

$$(3) \quad \dot{v} = a = \frac{g}{\frac{I}{m \cdot r^2} + 1}$$

This acceleration is determined in the experiment from the distance covered in time t

$$(4) \quad s = \frac{1}{2} \cdot a \cdot t^2$$

It can also be determined from the instantaneous speed attained after a time t

$$(5) \quad v = a \cdot t$$

In this experiment the movement of Maxwell's wheel is recorded with an ultrasonic motion sensor. From the resulting displacement versus time graph the instantaneous speed of the wheel can be determined and thereby its kinetic energy can be calculated.

EVALUATION

If the mass of the wheel m and the radius of its axle r are known, the moment of inertia can be determined from the acceleration a . From equation (3), the following must be true:

$$I = m \cdot r^2 \cdot \left(\frac{g}{a} - 1 \right).$$

The instantaneous velocities v can be determined by deriving the displacement versus time graph. The kinetic energies E_{kin} are calculated as follows:

$$E_{\text{kin}} = \frac{1}{2} \cdot m \cdot \left(\frac{I}{m \cdot r^2} + 1 \right) \cdot v^2.$$

The potential energy is given by

$$E_{\text{pot}} = m \cdot g \cdot h.$$

The energy losses which are clearly apparent from Fig. 3 are described quite well by assuming a constant force of friction acting in opposition to the direction of motion and an appreciable loss of energy when the direction changes at the bottom of the motion.

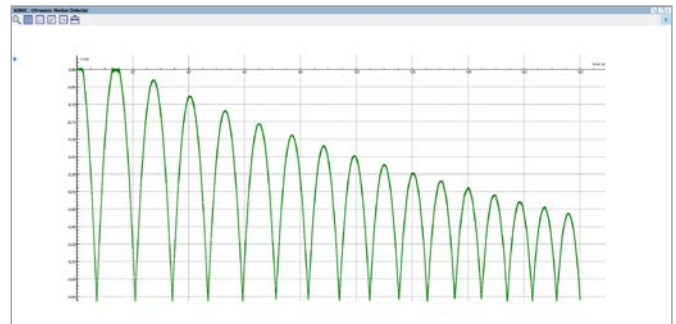


Fig. 1: Graph of displacement versus time

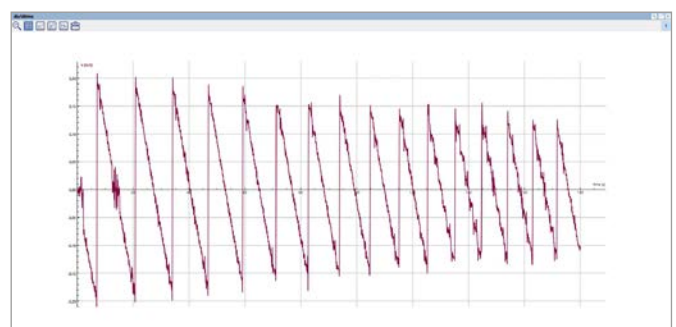


Fig. 2: Graph of velocity versus time

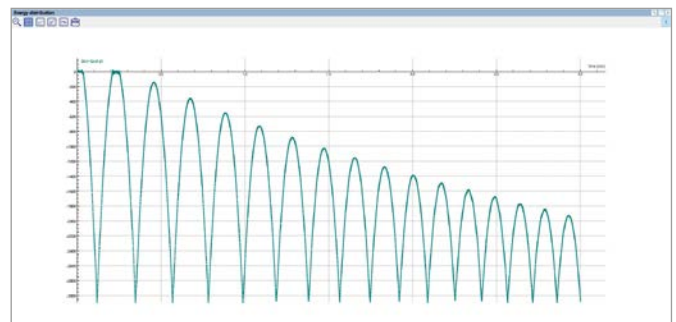


Fig. 3: Energy distribution as a function of time

UE1040500

PRECESSION AND NUTATION OF A GYROSCOPE



OBJECTIVE

Experimental investigation of precession and nutation of a gyroscope and determination of moment of inertia

> EXPERIMENT PROCEDURE

- Verify that the frequency of rotation f_R of a rotating disc is proportional to the period of precession of a gyroscope T_P and determine the moment of inertia by plotting $f_R (T_P)$.
- Verify that the frequency of rotation f_R of a rotating disc is proportional to the frequency of nutation f_N by plotting $f_N (f_R)$ or the corresponding periods $T_R (T_N)$.

SUMMARY

A spinning disc exhibits motions known as precession and nutation in addition to its rotational motion, depending on whether there is an external force, and thereby an additional torque, acting upon its axle or if the axle of a disc spinning in an equilibrium state is then deflected from its equilibrium position. The period of precession is inversely proportional to the period of rotation while the period of nutation is directly proportional to the period of rotation. The way the period of precession depends on the period of rotation makes it possible to determine the moment of inertia of the rotating disc.

REQUIRED APPARATUS

Quantity	Description	Item Number
1	Gyroscope	1000695
2	Photo Gate	1000563
1	Laser Diode, Red 230 V	1003201 or
	Laser Diode, Red 115 V	1000540
1	WiLab *	1022284
2	Connecting Lead MiniDIN8 – BT	1021688
3	Tripod Stand 150 mm	1002835
3	Universal Clamp	1002830
3	Stainless Steel Rod 750 mm	1002935

Additionally required

1	Coach 7 License
---	-----------------

* Alternative: 1 VinciLab 1021477

BASIC PRINCIPLES

A spinning top is a rigid body which spins around an axis fixed at a given point. If an external force acts upon the axis, its torque causes a change in the angular momentum. The top then moves in a direction perpendicular to the axis and the force acting upon it. Such a motion is called precession. If a top is pushed away from its axis of rotation it starts to undergo a tipping motion. This motion is called nutation. In general, both these motions occur superimposed on one another.

In this experiment, a gyroscope is used rather than a top. Its large rotating disc rotates with low friction about an axis which is fixed at a certain bearing point. A counterweight is adjusted in such a way that the bearing point coincides with the center of gravity. If the gyroscope is in equilibrium and the disc is set spinning, the momentum L will be constant:

$$(1) \quad L = I \cdot \omega_R$$

I : moment of inertia, ω_R : angular velocity

The moment of inertia of the rotating disc of the gyroscope is given by:

$$(2) \quad I = \frac{1}{2} \cdot M \cdot R^2$$

M : mass of disc, R : radius of disc

If extra weight is put on the axis of rotation by addition of a mass m , the additional weight causes a torque τ which changes the angular momentum:

$$(3) \quad \tau = m \cdot g \cdot r = \frac{dL}{dt}$$

r : distance from bearing point of axis of rotation to where the weight of the additional mass acts.

The axis of rotation then moves as shown in Fig. 2 by the following angle:

$$(4) \quad d\varphi = \frac{dL}{L} = \frac{m \cdot g \cdot r \cdot dt}{L}$$

It also starts to precess. The angular velocity of the precession motion can then be derived:

$$(5) \quad \omega_p = \frac{d\varphi}{dt} = \frac{m \cdot g \cdot r}{L} = \frac{m \cdot g \cdot r}{I \cdot \omega_R}$$

$$\text{where } \omega = 2\pi/T = 2\pi f$$

$$(6) \quad \frac{1}{T_R} = f_R = \frac{m \cdot g \cdot r}{I} \cdot T_p$$

If the disc is set spinning in the absence of any extra external torque and the axis of rotation is slightly deflected to one side, the gyroscope will exhibit nutation. The angular velocity of the nutation is then directly proportional to the angular velocity of the rotation:

$$(7) \quad \omega_N = C \cdot \omega_R \text{ and } T_R = C \cdot T_N$$

C : constant

This experiment involves racing the rotational, precessive and nutative motions with the help of photoelectric light barriers, whereby the way the pulses change over time is recorded and displayed by an interface and its software.

EVALUATION

The periods of rotation, precession and nutation are determined from the recordings of how the pulses change over time. According to equation (6), the period of precession is inversely proportional to that of the rotation, while (7) says that the period of nutation is directly proportional to that of the rotation. On the respective graphs, the measured values will therefore lie along a straight line through the origin. From the slope of a line matched to these values $f_R(T_p)$ it is possible to obtain the moment of inertia of the gyroscope's rotating disc by experiment and then compare it with the theoretical value calculated using equation (2).

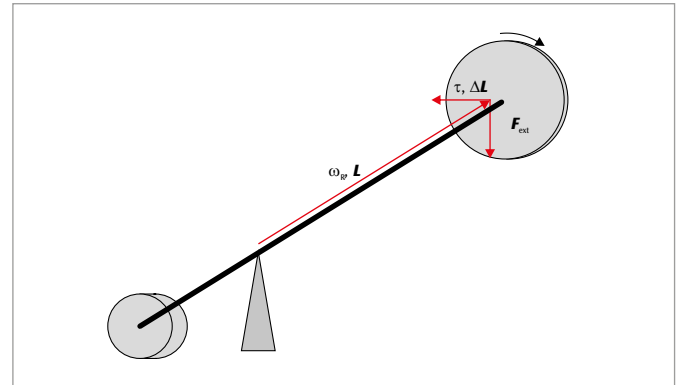


Fig. 1: Schematic of a gyroscope illustrating precession

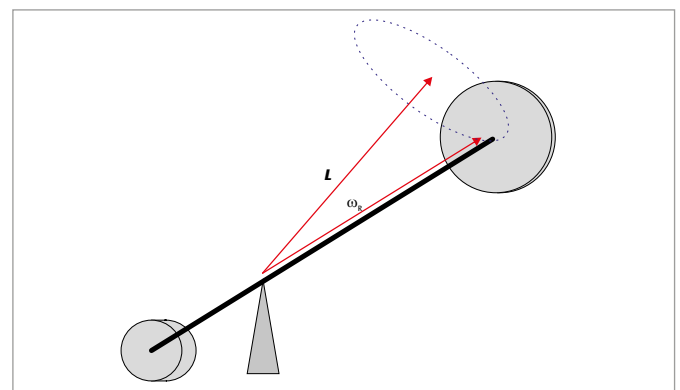


Fig. 2: Schematic of a gyroscope illustrating nutation

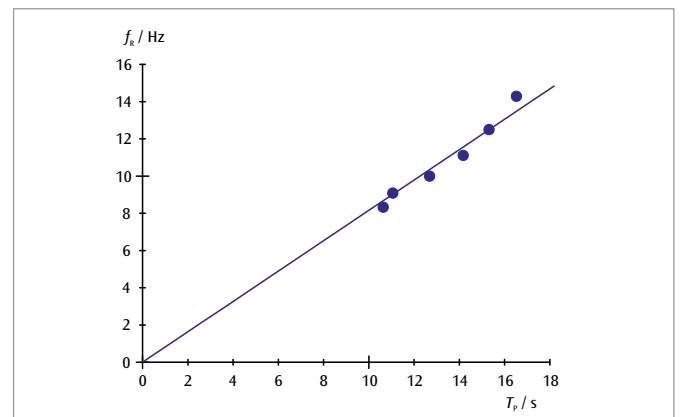


Fig. 3: Frequency of rotation f_R of a rotating disc as a function of the period of precession T_p

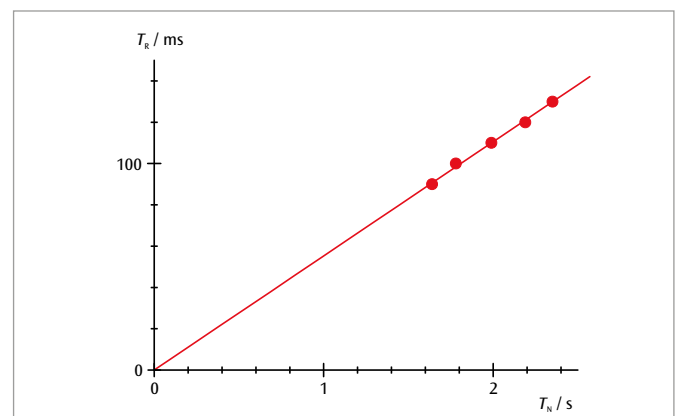
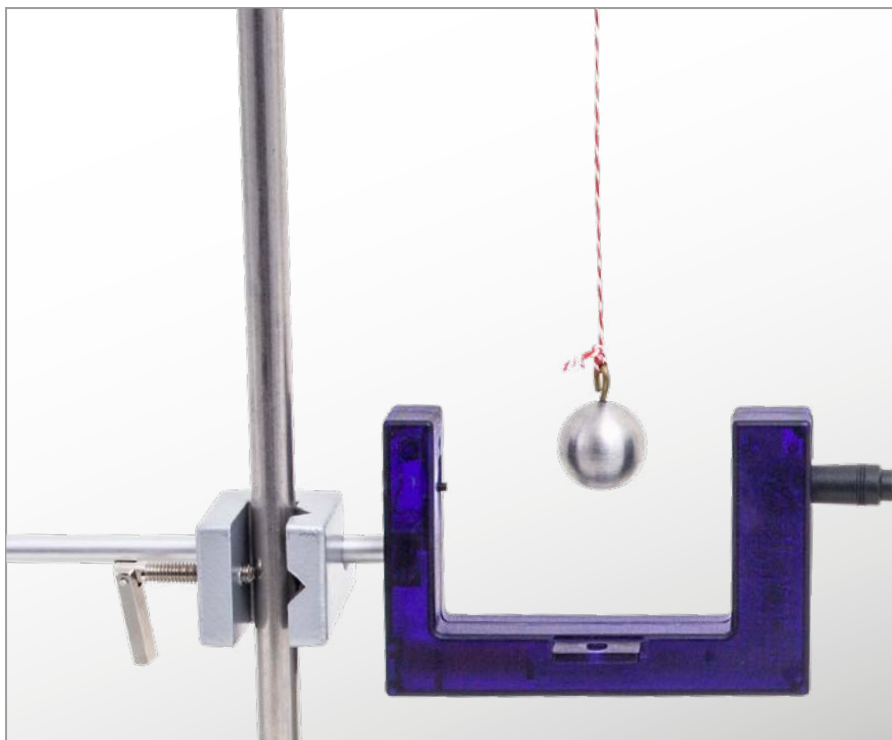


Fig. 4: Period of rotation T_R as a function of period of nutation T_N

UE1050101

HARMONIC OSCILLATION OF A STRING PENDULUM



> EXPERIMENT PROCEDURE

- Measure the period of oscillation T of a string pendulum as a function of the length of the pendulum L .
- Measure the period of oscillation T of a string pendulum as a function of the mass of the pendulum bob m .
- Determine the acceleration due to gravity g .

OBJECTIVE

Measuring the period of oscillation of a string pendulum with bobs of various masses

SUMMARY

The period of oscillation T for a string pendulum is dependent on the length of the pendulum L , but does not depend on the mass of the bob m . This is to be verified by a series of measurements in which the period of oscillation of such a pendulum is measured by means of a photoelectric sensor connected to a digital counter.

REQUIRED APPARATUS

Quantity	Description	Item Number
1	Set of 4 Pendulum Bobs	1003230
1	Cord for Experiments	1001055
1	Tripod Stand 185 mm	1002836
1	Stainless Steel Rod 1500 mm	1002937
1	Stainless Steel Rod 100 mm	1002932
1	Clamp with Hook	1002828
2	Universal Clamp	1002830
1	Photo Gate	1000563
1	Digital Counter (230 V, 50/60 Hz)	1001033 or
	Digital Counter (115 V, 50/60 Hz)	1001032
1	Pocket Measuring Tape, 2 m	1002603
1	Electronic Scale 200 g	1003433

BASIC PRINCIPLES

A string pendulum with a bob of mass m and a length L will exhibit simple harmonic oscillation about its rest point as long as the angle of deflection is not too great. The period T , i.e. the time it takes for the pendulum to swing from one end of its motion to the other end and back, is dependent solely on the length of the pendulum L and not on the mass m .

If the pendulum is deflected from its rest position by an angle φ , the restoring force is as follows:

$$(1a) \quad F_1 = -m \cdot g \cdot \sin \varphi.$$

For small angles φ , this closely approximates to the following:

$$(1b) \quad F_1 = -m \cdot g \cdot \varphi$$

The moment of inertia of the accelerated mass is given by

$$(2) \quad F_2 = m \cdot L \cdot \ddot{\varphi}$$

Both these forces are equal, thus the result is equivalent for the equation of motion for simple harmonic oscillation:

$$(3) \quad \ddot{\varphi} + \frac{g}{L} \cdot \varphi = 0$$

For the period of oscillation T the following applies:

$$(4) \quad T = 2\pi \cdot \sqrt{\frac{L}{g}}$$

In this experiment the period of oscillation will be measured for various lengths of pendulum and masses of bob with the help of a photoelectric sensor connected to a digital counter. The digital counter's internal programming is such that it halts the time measurement after each complete swing of the pendulum.

EVALUATION

The measurements are plotted on a graph of T against L and another one of T against m . These graphs will show that the period of oscillation depends on the pendulum's length and not on the mass of the bob, as expected.

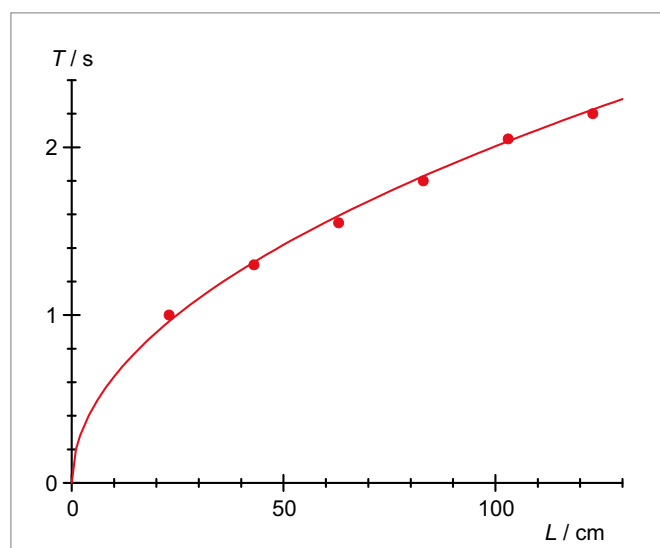


Fig. 1: Period of oscillation T as a function of the pendulum length L

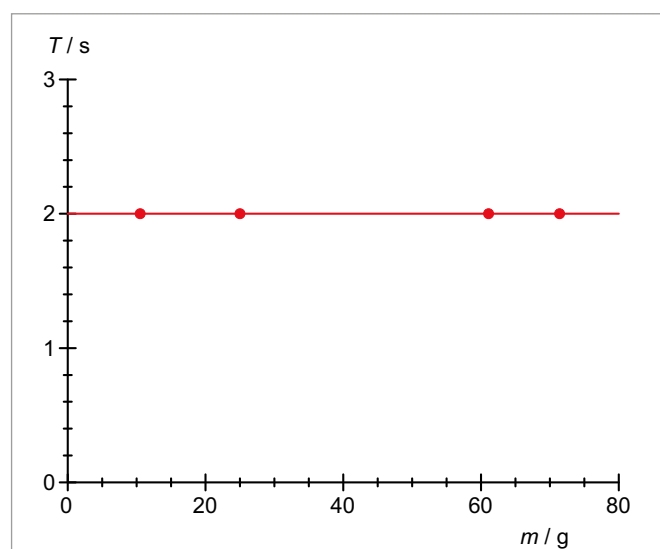
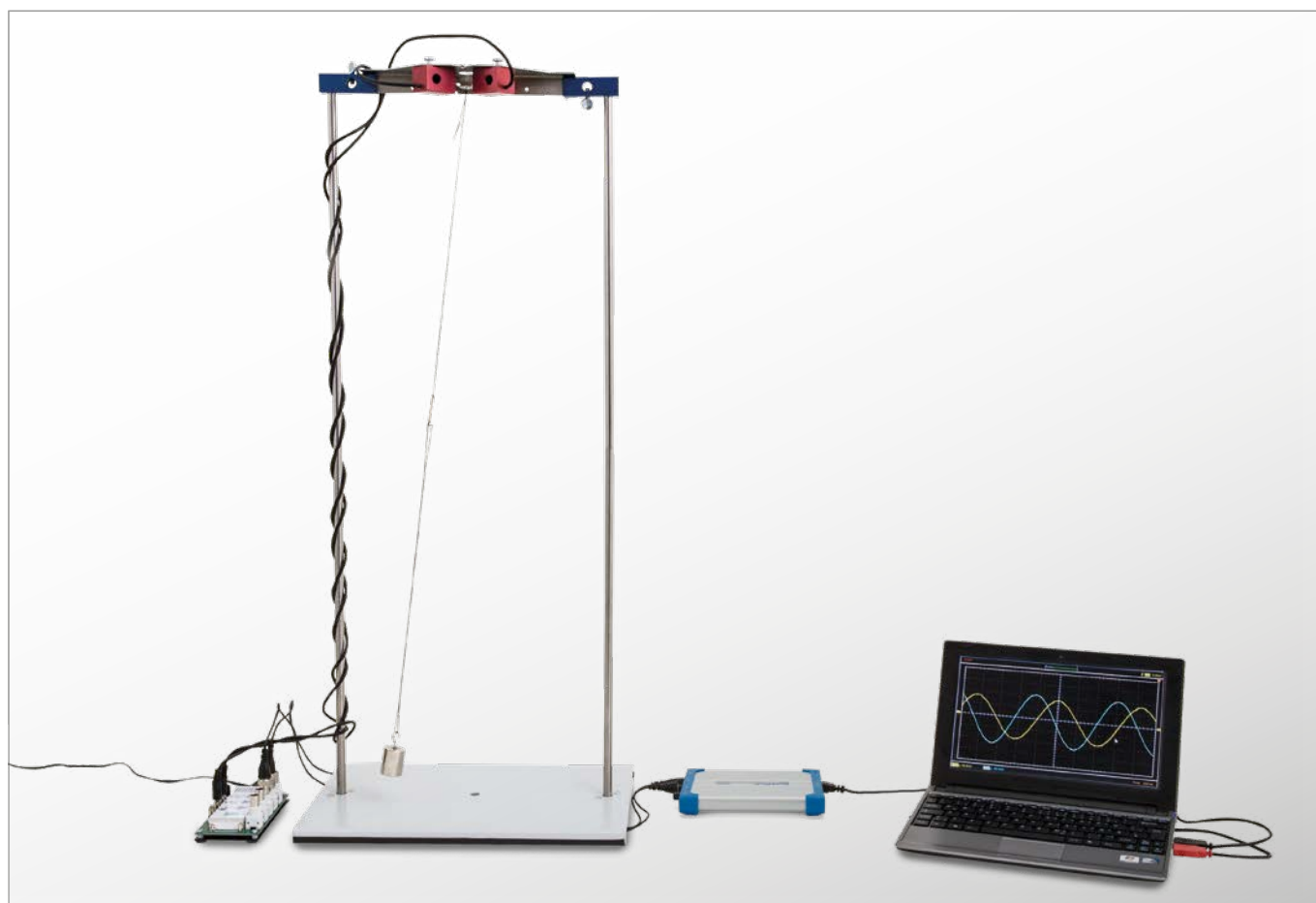


Fig. 2: Period of oscillation T as a function of the pendulum mass m

UE1050121

ELLIPTICAL OSCILLATION OF A STRING PENDULUM



> EXPERIMENT PROCEDURE

- Plot the elliptical oscillation of a string pendulum in the form of two perpendicular components for a variety of initial conditions.

OBJECTIVE

Description of elliptical oscillations of a string pendulum as the superimposition of two components perpendicular to one another

SUMMARY

Depending on the initial conditions, a suitable suspended string pendulum will oscillate in such a way that the bob's motion describes an ellipse for small pendulum deflections. If the motion is resolved into two perpendicular components, there will be a phase difference between those components. This experiment will investigate the relationship by measuring the oscillations with the help of two perpendicularly mounted dynamic force sensors. The amplitude of the components and their phase difference will then be evaluated.

REQUIRED APPARATUS

Quantity	Description	Item Number
1	SW String Pendulum Set	1012854
1	SW Stand Equipment Set	1012849
1	SW Sensors Set (230 V, 50/60 Hz)	1012850 or
	SW Sensors Set (115 V, 50/60 Hz)	1012851
1	1 PC Oscilloscope, 2x25 MHz	1020857

BASIC PRINCIPLES

Depending on the initial conditions, a suitable suspended string pendulum will oscillate in such a way that the bob's motion describes an ellipse for small pendulum deflections. If the motion is resolved into two perpendicular components, there will be a phase difference between those components.

This experiment will investigate the relationship by measuring the oscillations with the help of two perpendicularly mounted dynamic force sensors. The amplitude of the components and their phase difference will then be evaluated. The phase shift between the oscillations will be shown directly by displaying the oscillations on a dual-channel oscilloscope.

Three special cases shed light on the situation:

- If the pendulum swings along the line bisecting the two force sensors, the phase shift $\varphi = 0^\circ$.
- If the pendulum swings along a line perpendicular to that bisecting the two force sensors, the phase shift $\varphi = 180^\circ$.
- If the pendulum bob moves in a circle, the phase shift $\varphi = 90^\circ$.

EVALUATION

The oscillations are recorded by means of a storage oscilloscope and frozen on screen. The amplitude of the components and their phase difference will then be evaluated.

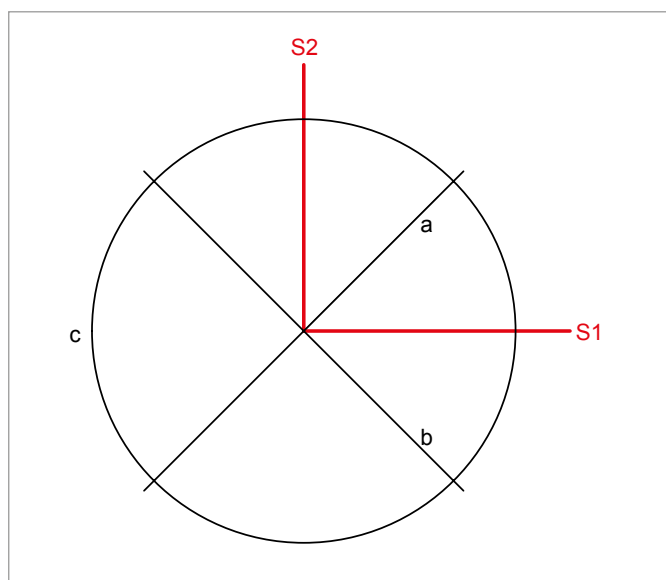


Fig. 1: The alignment of sensors S1 and S2, including the oscillation directions of the string pendulum under investigation

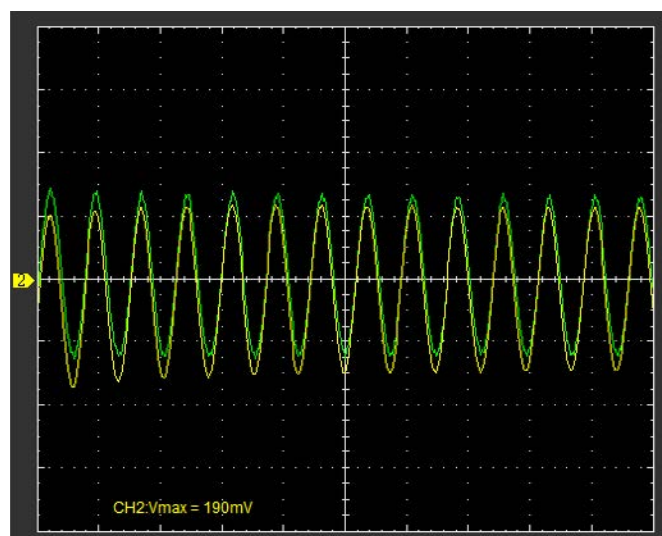


Fig. 2: Oscillation components for a string pendulum swinging along the line bisecting the two force sensors

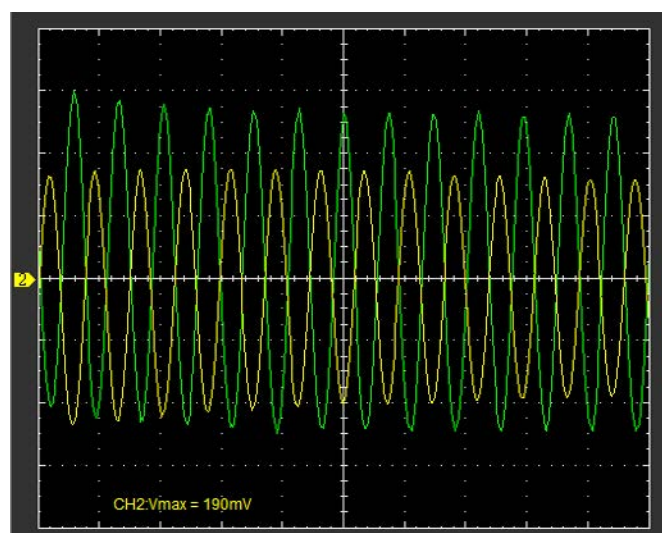


Fig. 3: Oscillation components for a string pendulum swinging along the line perpendicular to that bisecting the two force sensors

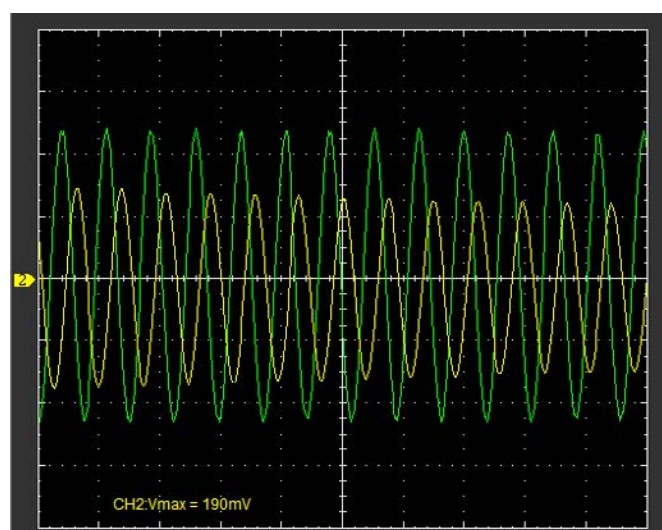


Fig. 4: Oscillation components for a string pendulum describing a circle

UE1050201 | VARIABLE g PENDULUM



> EXPERIMENT PROCEDURE

- Measure the period T as a function of the effective component of the gravitational acceleration g_{eff} .
- Measure the period T for various pendulum lengths L .

OBJECTIVE

Measure the period of an oscillating pendulum as a function of the effective component of the gravitational acceleration

SUMMARY

The period of a pendulum is lengthened by tilting its axis away from the horizontal, since the effective component of the gravitational acceleration is reduced.

REQUIRED APPARATUS

Quantity	Description	Item Number
1	Variable g Pendulum	1000755
1	Support for Photogate	1000756
1	Photo Gate	1000563
1	Digital Counter (230 V, 50/60 Hz)	1001033 or
	Digital Counter (115 V, 50/60 Hz)	1001032
1	Tripod Stand 150 mm	1002835
1	Stainless Steel Rod 470 mm	1002934

BASIC PRINCIPLES

The period of a pendulum is determined mathematically by the length of the pendulum L and the acceleration due to gravity g . The effect of the gravitational acceleration can be demonstrated by tilting the axis of the pendulum so that it is no longer horizontal.

When the axis is tilted, the component of the gravitational acceleration g that is parallel to the axis g_{par} is rendered ineffective by the fact that axis is fixed (see Fig.1). The remaining component that is effective g_{eff} is given by the following equation:

$$(1) \quad g_{\text{eff}} = g \cdot \cos \alpha$$

α : is the inclination of the axis to the horizontal

When the pendulum is deflected by an angle φ from its rest position a suspended weight of a mass m experiences a returning force of the following magnitude:

$$(2) \quad F = -m \cdot g_{\text{eff}} \cdot \sin \varphi$$

For small angles the equation of motion of the pendulum comes out as the following:

$$(3) \quad m \cdot L \cdot \ddot{\varphi} + m \cdot g_{\text{eff}} \cdot \varphi = 0$$

The pendulum's angular frequency of oscillation is therefore:

$$(4) \quad \omega = \sqrt{\frac{g_{\text{eff}}}{L}}$$

EVALUATION

Equation (4) implies that the period of the pendulum is as follows:

$$T = 2\pi \sqrt{\frac{L}{g_{\text{eff}}}}$$

Thus, shortening the pendulum causes the period to be shorter and reducing the effective component of the gravitational acceleration makes the period longer.

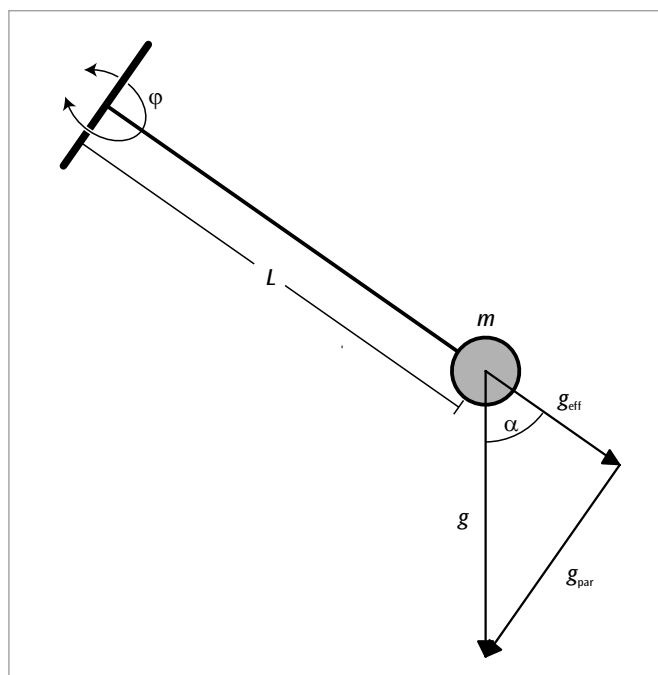


Fig. 1: Variable g pendulum (schematic)

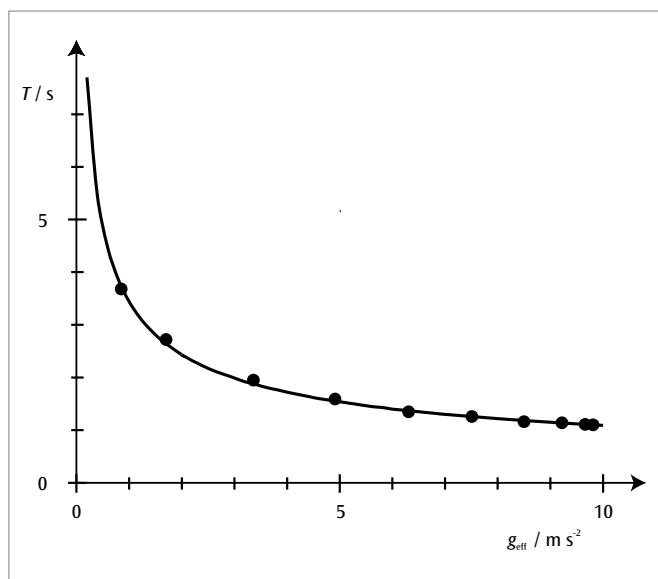


Fig. 2: Period of the pendulum as a function of the effective component of the gravitational acceleration. Line calculated for pendulum length $L = 30 \text{ cm}$

UE1050221 | KATER'S REVERSIBLE PENDULUM



> EXPERIMENT PROCEDURE

- Configure a reversible pendulum such that the periods of oscillation are the same from both mounting points.
- Determine the period of oscillation and calculate the local acceleration due to gravity.

OBJECTIVE

Work out the local acceleration due to gravity with the help of a reversible pendulum

SUMMARY

A reversible pendulum is a special design of a normal physical pendulum. It is able to swing from either of two mounting points and can be set up in such a way that the period of oscillation is the same from both these points. The reduction in the length of the pendulum then matches the distance between the two mounting points. This makes it easier to determine the local acceleration due to gravity from the period of oscillation and the reduced pendulum length. Matching of the reversing pendulum is achieved by moving a weight between the mounts as appropriate while a rather larger counterweight outside that length remains fixed.

REQUIRED APPARATUS

Quantity	Description	Item Number
1	Kater's Reversible Pendulum	1018466
1	Photo Gate	1000563
1	Digital Counter (230 V, 50/60 Hz)	1001033 or
	Digital Counter (115 V, 50/60 Hz)	1001032

BASIC PRINCIPLES

A reversible pendulum is a special design of a normal physical pendulum. It is able to swing from either of two mounting points and can be set up in such a way that the period of oscillation is the same from both these points. The reduction in the length of the pendulum then matches the distance between the two mounting points. This makes it easier to determine the local acceleration due to gravity from the period of oscillation and the reduced pendulum length.

If a physical pendulum oscillates freely about its rest position with a small deflection φ then its equation of motion is as follows:

$$(1) \quad \frac{J}{m \cdot s} \cdot \ddot{\varphi} + g \cdot \varphi = 0$$

J : Moment of inertia around axis of oscillation,

g : Acceleration due to gravity, m : Mass of pendulum,

s : Distance between axis of oscillation and center of gravity

The reduced length of the physical pendulum is

$$(2) \quad L = \frac{J}{m \cdot s}$$

A mathematical pendulum of this length oscillates with the same period of oscillation.

Steiner's law gives us the moment of inertia:

$$(3) \quad J = J_s + m \cdot s^2$$

J_s : Moment of inertia about center of gravity axis

For a reversible pendulum with two mounting points separated by a distance d , the reduced lengths to be assigned are therefore

$$(4) \quad L_1 = \frac{J_s}{m \cdot s} + s \quad \text{and} \quad L_2 = \frac{J_s}{m \cdot (d - s)} + d - s$$

They match up if the reversible pendulum is configured in such a way that the period of oscillation is the same for both mounting points. In that case, the following is true:

$$(5) \quad s = \frac{d}{2} \pm \sqrt{\left(\frac{d}{2}\right)^2 - \frac{J_s}{m}}$$

and

$$(6) \quad L_1 = L_2 = d$$

In this case, the period of oscillation T is given by

$$(7) \quad T = 2\pi \cdot \sqrt{\frac{d}{g}}$$

In the experiment, matching of the reversible pendulum is accomplished by moving a weight of mass $m_2 = 1$ kg between the mounting points as appropriate. A second large counterweight of mass $m_1 = 1.4$ kg is fixed outside the mounts. Measurement of the period of oscillation is handled electronically with the lower end of the pendulum periodically interrupting a photoelectric gate. By this means, the periods of oscillation T_1 and T_2 associated with the reduced pendulum lengths L_1 and L_2 are measured as a function of the position x_2 of weight m_2 .

EVALUATION

The two curves derived from the measurements $T_1(x_2)$ and $T_2(x_2)$ intersect twice at the value $T = T_1 = T_2$. In order to determine the intersection points precisely, an interpolation between the measuring points required. Acceleration due to gravity is calculated from the measurements as follows:

$$g = \left(\frac{2\pi}{T}\right)^2 \cdot d, \quad d = 0.8 \text{ m}$$

with relative precision of 0.3 per thousand.

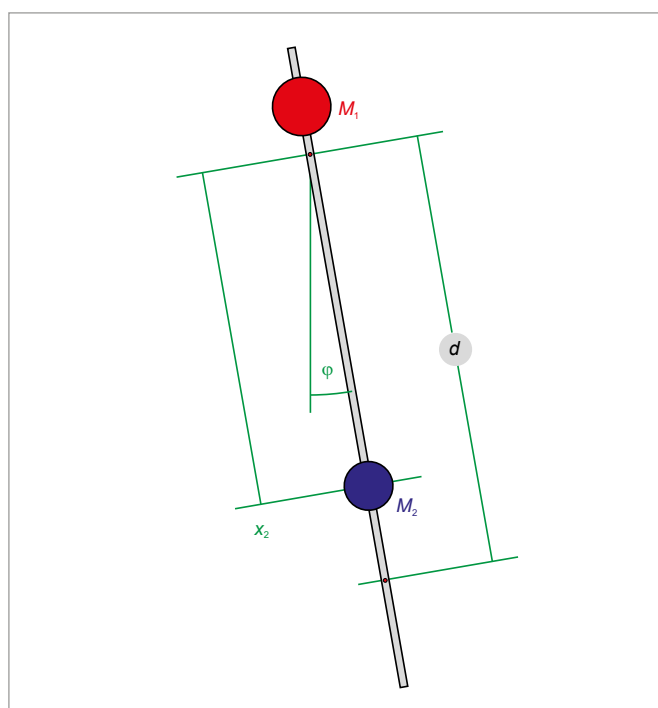


Fig. 1: Schematic diagram of a reversible pendulum

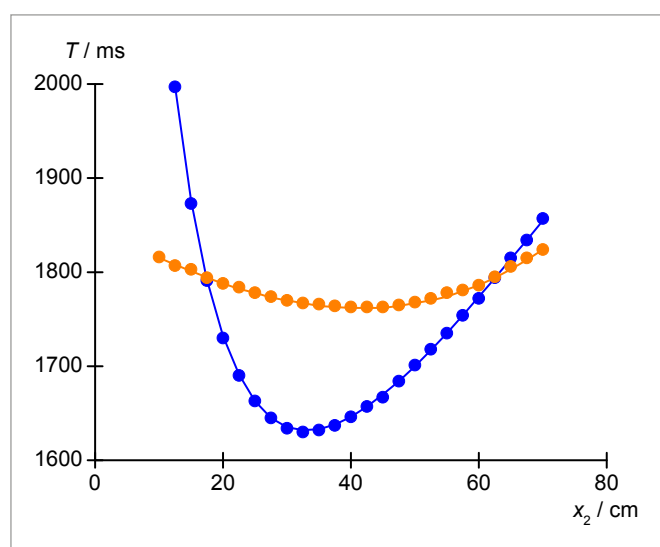


Fig. 2: Measured periods of oscillation T_1 and T_2 as a function of position of weight 2.

UE1050250 | FOUCAULT PENDULUM



OBJECTIVE

Demonstrate the rotation of the earth with a Foucault pendulum

SUMMARY

A Foucault pendulum is a long string pendulum with a heavy bob, which can be used to demonstrate the rotation of the earth. In this experiment, a pendulum 1.2 meters in length is used. The direction of its oscillations can be very accurately determined by projecting the pendulum's shadow. For long periods of observation, any damping of the oscillation can be compensated for with the aid of an adjustable electromagnetic system to provide additional momentum.

> EXPERIMENT PROCEDURE

- Measure the direction of the oscillation as a function of time.
- Determine the speed of the rotation.
- Determine the latitude where the experiment is taking place.

REQUIRED APPARATUS

Quantity	Description	Item Number
1	Foucault Pendulum (230 V, 50/60 Hz)	1000748 or
	Foucault Pendulum (115 V, 50/60 Hz)	1000747
1	Digital Stopwatch	1002811

BASIC PRINCIPLES

A Foucault pendulum is a long string pendulum with a heavy bob, which can be used to demonstrate the rotation of the earth. It is named after *Jean Foucault*, who in 1851 discovered that the direction of the oscillation of a pendulum 2 m in length would change over the course of time. This experiment was later repeated with ever longer and heavier pendulums.

Since the earth rotates on its axis, when using an earth-based coordinate system, a force called the Coriolis force arises, which then acts on the moving pendulum in a direction perpendicular to the direction of the oscillation:

$$(1) \quad \mathbf{F} = 2 \cdot m \cdot \boldsymbol{\Omega}_0 \times \mathbf{v}$$

m : mass of pendulum bob

$\boldsymbol{\Omega}_0$: vector describing angular velocity of earth

\mathbf{v} : velocity vector of oscillating pendulum

This causes the plane of the oscillation to turn with an angular frequency dependent on the angle of latitude φ of the point from which the pendulum is suspended:

Because the Foucault pendulum is only deflected by a small angle α , the pendulum bob can be assumed to move exclusively in the horizontal plane, which can be seen in Fig. 1, and moves between an axis N aligned with north and an axis E aligned with east. The observation is concerned only with horizontal deflections since the pendulum bob is hanging from a thread. For this reason, only the vertical component of the vector $\boldsymbol{\Omega}_0$ is relevant:

$$(2) \quad \Omega(\varphi) = \Omega_0 \cdot \sin\varphi$$

The equation of motion for an oscillating Foucault pendulum is therefore as follows:

$$(3) \quad \frac{d^2\alpha}{dt^2} \cdot \mathbf{e}_p + 2 \cdot \Omega_0 \cdot \sin\varphi \cdot \frac{d\alpha}{dt} \cdot \mathbf{e}_v + \frac{g}{L} \cdot \alpha \cdot \mathbf{e}_p = 0$$

L : length of pendulum, g : acceleration due to gravity

\mathbf{e}_p : horizontal unit vector parallel to the current direction of oscillation

\mathbf{e}_v : horizontal unit vector perpendicular to current direction of oscillation

The solution to this can be separated into a solution for the angle of deflection α and a solution for the turning unit vector \mathbf{e}_p parallel to the current direction of oscillation:

$$(4a) \quad \alpha(t) = \cos(\omega \cdot t + \beta) \quad \text{where} \quad \omega = \sqrt{\frac{g}{L}}$$

$$(4b) \quad \mathbf{e}_p(t) = \mathbf{e}_E \cdot \cos(\psi(t)) + \mathbf{e}_N \cdot \sin(\psi(t))$$

where $\psi(t) = \Omega_0 \cdot \sin\varphi \cdot t + \psi_0$: direction of oscillation

\mathbf{e}_E : horizontal unit vector aligned with east

\mathbf{e}_N : horizontal unit vector aligned with north

The plane of the oscillation therefore rotates over the course of time with a frequency as given by equation (2). In the northern hemisphere the rotation is clockwise and in the southern hemisphere it is counter-clockwise. The speed of the rotation is at its highest at the poles, whereas at the equator there is no rotation at all.

In this experiment, a pendulum 1.2 meters in length is used. In order to avoid the oscillations becoming elliptical, the pendulum thread is allowed to collide with a so-called Charon ring every time it swings. The direction of oscillation can be seen by projecting the shadow of the thread onto an angle scale whereby the angle can be read off with great accuracy. It is possible to observe the rotation of the plane of oscillation after only a few minutes. For long periods of observation, any damping of the oscillation can be compensated for with the aid of an adjustable electromagnetic system to provide additional momentum.

EVALUATION

The angle of the oscillation plane φ is in linear proportion to the time, see Fig. 2. The value we are seeking $\Omega(\varphi)$ is the gradient of the straight lines through the measurements. The latitude in degrees can be calculated by rearranging equation (2):

$$\varphi = \frac{180^\circ}{\pi} \cdot \arcsin\left(\frac{86400 \text{ s}}{360 \text{ grad}} \cdot \Omega(\varphi)\right)$$

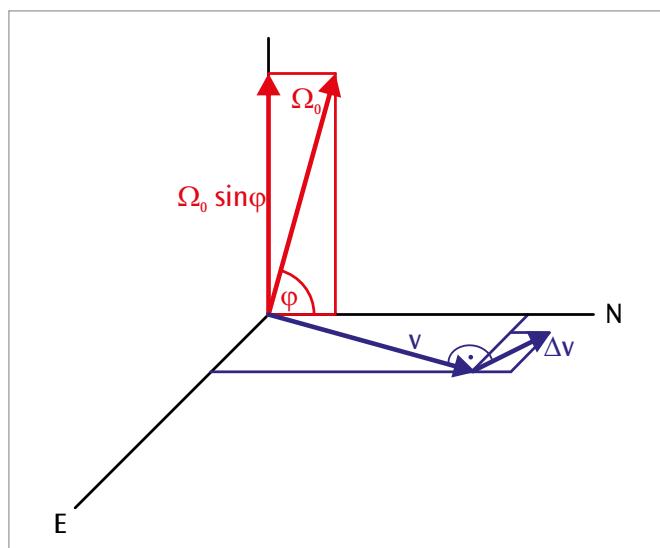


Fig. 1: Illustration of Foucault pendulum in fixed earth-based coordinate system

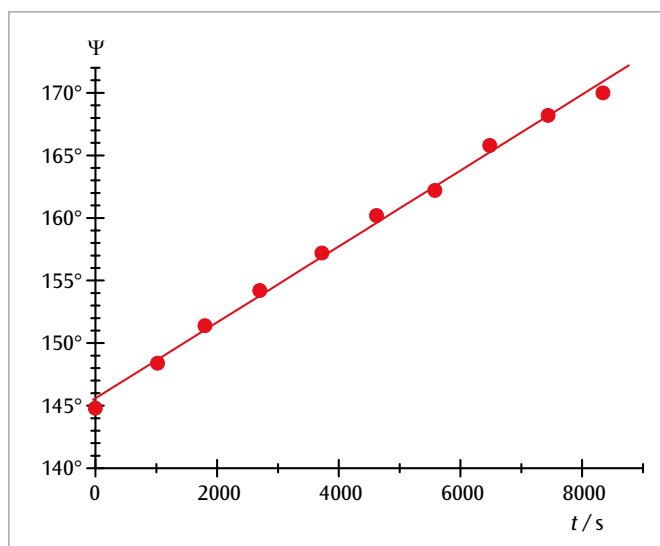


Fig. 2: Measured curve recorded at latitude of $\varphi = 50^\circ$

UE1050311 | SIMPLE HARMONIC OSCILLATIONS



> EXPERIMENT PROCEDURE

- Record the harmonic oscillation of a coil spring pendulum as a function of time using an ultrasonic motion sensor.
- Determine the period of oscillation T for various combinations of spring constant k and mass m .

OBJECTIVE

Measure the oscillations of a coil spring pendulum using an ultrasonic motion sensor

SUMMARY

The oscillations of a coil spring pendulum are a classic example of simple harmonic oscillation. In this experiment, those oscillations are recorded by an ultrasonic motion sensor, which detects the distance to the weight suspended from the spring pendulum.

REQUIRED APPARATUS

Quantity	Description	Item Number
1	Set of Helical Springs for Hooke's Law	1003376
1	Set of Slotted Weights, 10 x 10 g	1003227
1	Set of Slotted Weights, 5 x 100 g	1003229
1	Tripod Stand 150 mm	1002835
1	Stainless Steel Rod 1000 mm	1002936
1	Clamp with Hook	1002828
1	€Motion *	1021673
1	Pocket Measuring Tape, 2 m	1002603

Additionally required

1	Coach 7 License
---	-----------------

* Alternatives: 1 WiLab 1022284 and 1 motion sensor 1022288 or
1 VinciLab 1021477 and 1 Motion Sensor 1021683

BASIC PRINCIPLES

Oscillations occur when a system disturbed from its equilibrium position is affected by a force which acts to restore it to equilibrium. This is known as simple harmonic oscillation if the restoring force is proportional to the deviation from the equilibrium position at all times. The oscillations of a coil spring pendulum are one classic example of this. The proportionality between the deviation and the restoring force is described by Hooke's law.

The law states that the relationship between the deviation x and the restoring force F is given by

$$(1) \quad F = -k \cdot x$$

where k = spring constant

For a weight of mass m suspended from the spring, the following therefore holds:

$$(2) \quad m \cdot \frac{d^2x}{dt^2} + k \cdot x = 0$$

This applies as long the mass of the spring itself and any friction that might arise can be neglected.

In general, solutions to this equation of motion take the following form:

$$(3) \quad x(t) = A \cdot \sin\left(\sqrt{\frac{k}{m}} \cdot t + \varphi\right)$$

This will be verified by experiment by recording the harmonic oscillations of a coil spring pendulum as a function of time with the help of an ultrasonic motion sensor and matching the measured data to a sine function.

The ultrasonic motion sensor detects the distance between itself and the weight suspended from the spring. Other than an offset for the zero point, which can be compensated for by calibration, the measurement corresponds directly to the variable $x(t)$ included in equation 3.

The period of oscillation T is defined as the interval between two points where a sine wave crosses the zero axis in the same direction.

From equation (3) it can therefore be seen to be equal to:

$$(4) \quad T = 2\pi \cdot \sqrt{\frac{m}{k}}$$

In order to verify equation (4), the measurements are made for various combinations of mass m and spring constant k , whereby the period of oscillation is determined from where a curve matching the data crosses the zero axis.

EVALUATION

The following can be deduced from equation 4:

$$T^2 = \frac{4\pi^2}{k} \cdot m$$

Measurements are therefore plotted using various spring constants k as parameters in a graph of T^2 against m . Within measurement tolerances, they lie on a straight line through the origin, the gradient of which can be calculated using a second graph

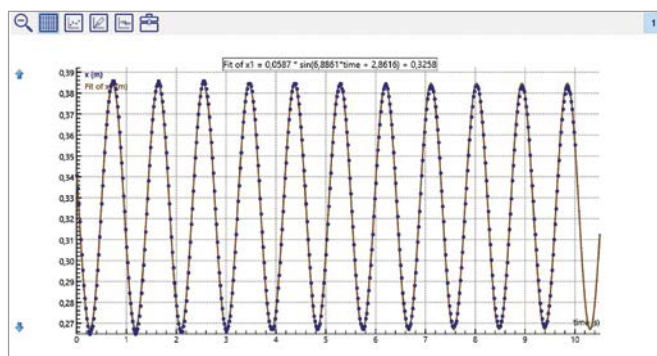


Fig. 1: Recorded oscillation data after matching to a sine function

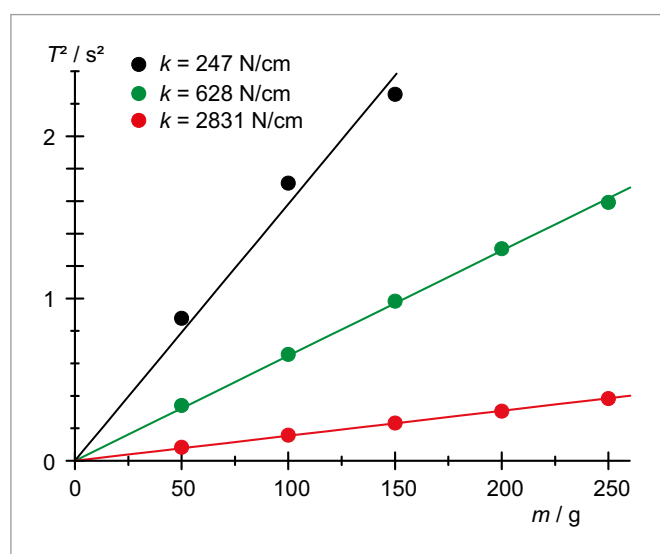


Fig. 2: T^2 as a function of m

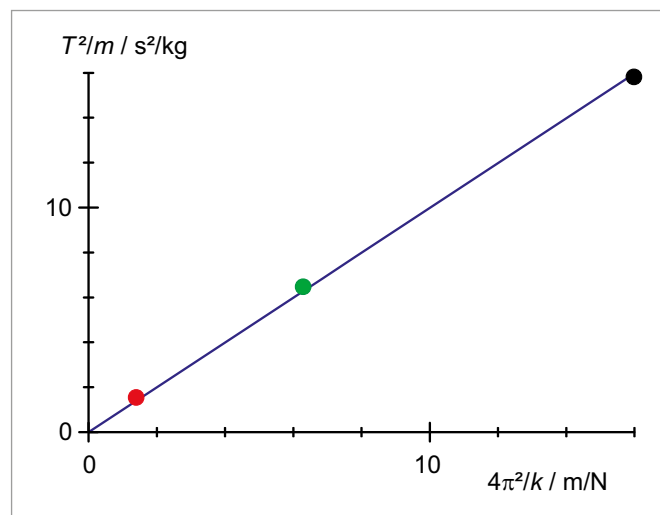
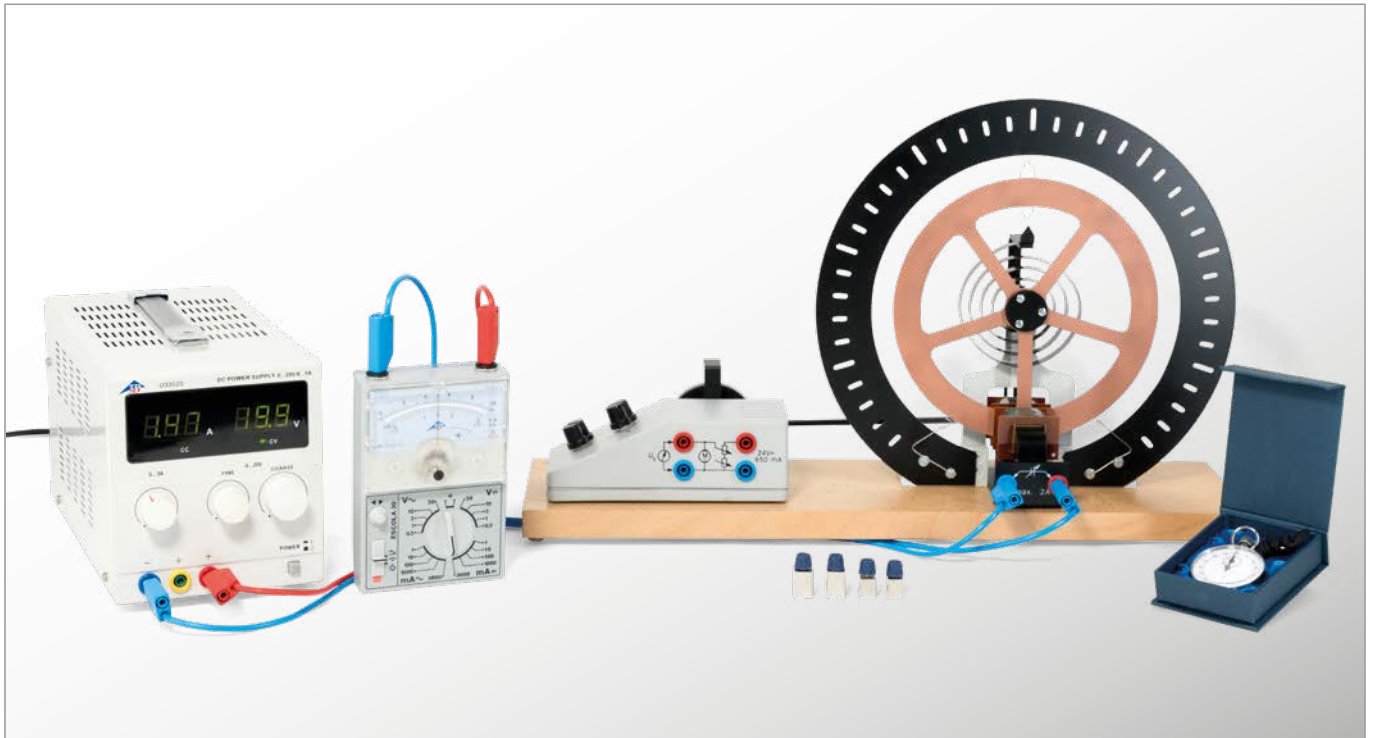


Fig. 3: $\frac{T^2}{m}$ as a function of $\frac{4\pi^2}{k}$

UE1050500 | POHL'S TORSION PENDULUM I



> EXPERIMENT PROCEDURE

- Measure period of oscillation T for various initial deflections and velocities.
- Determine the damping constant δ when the rotating pendulum is damped.

OBJECTIVE

Measurement and analysis of simple harmonic rotary oscillation

SUMMARY

Pohl's wheel or rotating (torsional) pendulum allows for the investigation of simple harmonic rotary oscillation. The only forces acting on the wheel are the restoring torque provided by a spiral spring and damping torque supplied by means of an eddy current brake with an adjustable current. This experiment demonstrates how the period of oscillation is not dependent on the initial deflection or the initial velocity, and analyzes the amplitudes of the oscillations.

REQUIRED APPARATUS

Quantity	Description	Item Number
1	Pohl's Torsion Pendulum	1002956
1	Mechanical Stopwatch, 15 min	1003369
1	DC Power Supply 0 – 20 V, 0 – 5 A (230 V, 50/60 Hz)	1003312 or
	DC Power Supply 0 – 20 V, 0 – 5 A (115 V, 50/60 Hz)	1003311
1	Analog Multimeter Escola 30	1013526
1	Set of 15 Safety Experiment Leads, 75 cm	1002843

BASIC PRINCIPLES

Pohl's wheel or rotating (torsional) pendulum allows for the investigation of simple harmonic rotary oscillation. The only forces acting on the wheel are the restoring torque provided by a spiral spring and damping torque supplied by means of an eddy current brake with an adjustable current.

The equation of motion for the angle of deflection φ of a freely oscillating, but damped torsional pendulum is as follows:

$$(1) \quad \frac{d^2\varphi}{dt^2} + 2 \cdot \delta \cdot \frac{d\varphi}{dt} + \omega_0^2 \cdot \varphi = 0,$$

$$\text{where } \delta = \frac{k}{2J} \quad \omega_0^2 = \frac{D}{J}$$

J : moment of inertia

D : spring constant

k : damping coefficient

As long as the damping is not excessive and the condition $\delta < \omega_0$ is fulfilled, the equation of motion has the following solution:

$$(2) \quad \varphi(t) = \varphi_0 \cdot e^{-\delta t} \cdot \cos(\omega \cdot t + \psi)$$

$$\text{where } \omega = \sqrt{\omega_0^2 - \delta^2}$$

The initial amplitude φ_0 and the phase angle ψ are arbitrary parameters which are dependent on the deflection and speed of the rotary pendulum at a time $t = 0$. The pendulum will therefore move back and forth with the following period of oscillation:

$$(3) \quad T = \frac{2\pi}{\omega}$$

The amplitude of the oscillations decreases over time according to the following equation:

$$(4) \quad \hat{\varphi}(t) = \varphi_0 \cdot e^{-\delta t}$$

In this experiment oscillations are investigated with various levels of damping, which can be set up by varying the current to the eddy current brake. The period of oscillation is measured with the aid of a stopwatch. It will be shown that the period of oscillation is not dependent on the initial deflection or velocity.

In order to determine the damping, the decreasing deflections of the pendulum to the left and right are noted. For the sake of simplicity, the pendulum starts without initial speed.

EVALUATION

In equation (4) the amplitude of the oscillation is defined as a positive value. This implies that the absolute values for the limits of the motion to the left and right should be considered. If the natural logarithms of these values are plotted against time, a straight line with a gradient $-\delta$ should be obtained. In fact certain deviations from such linear behavior will be observed, since the force of friction is not exactly proportional to the speed as assumed here.

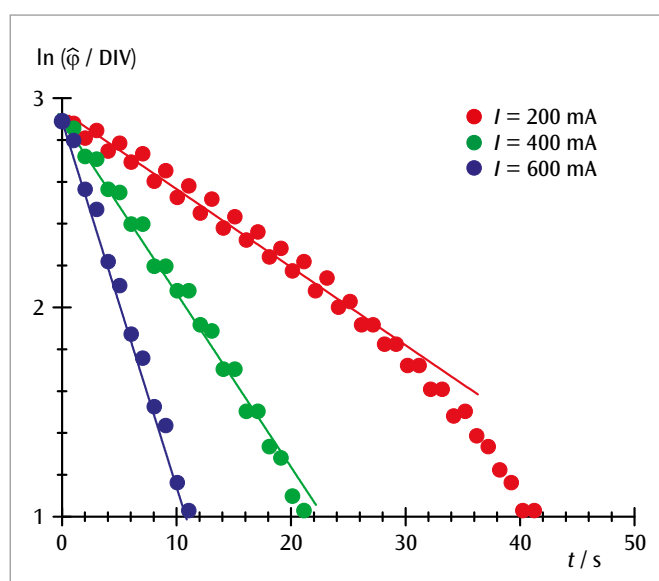
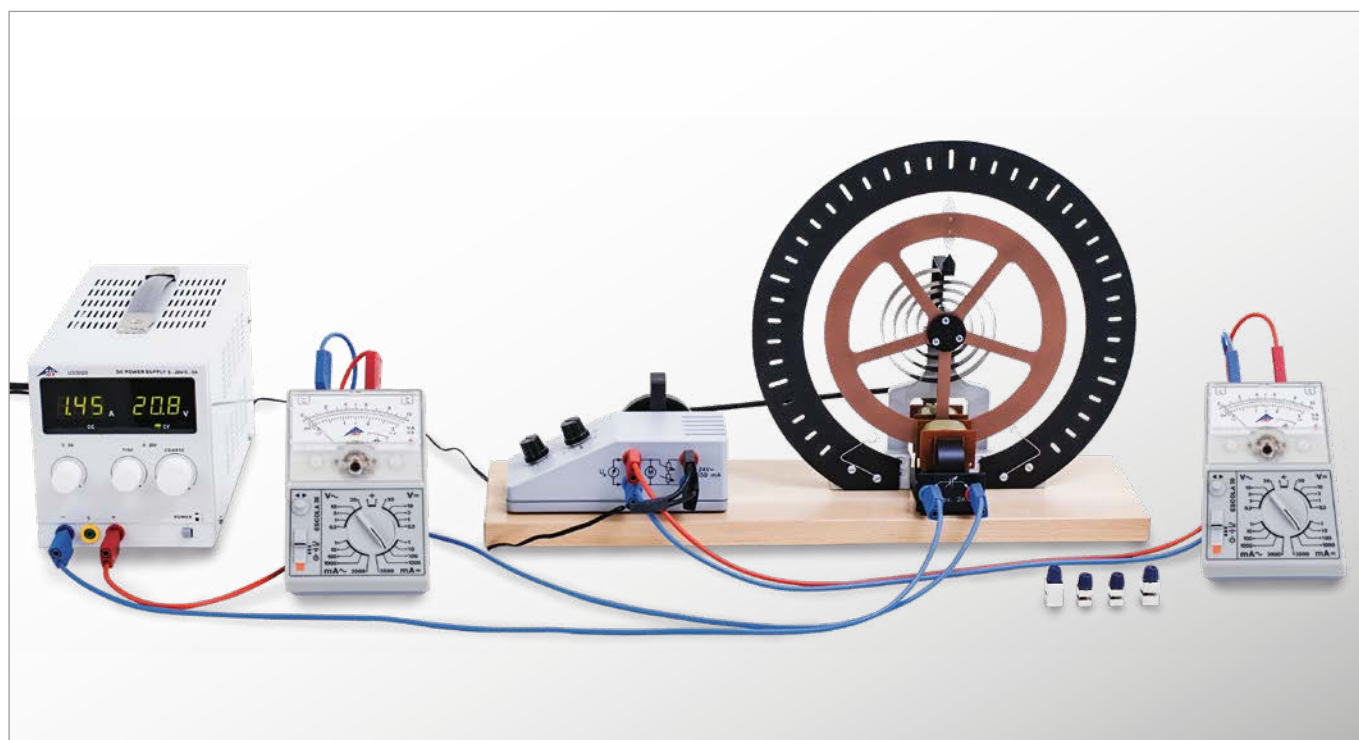


Fig. 1: $\ln(\hat{\varphi})$ as a function of time for various degrees of damping

UE1050550 | POHL'S TORSION PENDULUM II



EXPERIMENT PROCEDURE

- Measure the amplitude of forced oscillations as a function of the excitation frequency for various degrees of damping.
- Observe the phase shift between the excitation and the actual oscillation for excitation frequencies which are very small and other which are very large.

OBJECTIVE

Measurement and analysis of forced harmonic rotary oscillation

SUMMARY

Pohl's wheel or rotating (torsional) pendulum allows for the investigation of forced harmonic rotary oscillation. For this purpose, the oscillating system is connected to an excitation linkage which is driven by an adjustable-speed DC motor so that the restoring spring periodically extends and compresses. In this experiment the amplitude is measured as a function of the excitation frequency for various degrees of damping and the phase shift between the excitation and the actual oscillation is observed.

REQUIRED APPARATUS

Quantity	Description	Item Number
1	Pohl's Torsion Pendulum	1002956
1	Mechanical Stopwatch, 15 min	1003369
1	Plug In Power Supply 24 V, 0.7 A (230 V, 50/60 Hz)	1000681 or
	Plug In Power Supply 24 V, 0.7 A (115V, 50/60 Hz)	1000680
1	DC Power Supply 0 – 20 V, 0 – 5 A (230 V, 50/60 Hz)	1003312 or
	DC Power Supply 0 – 20 V, 0 – 5 A (115 V, 50/60 Hz)	1003311
2	Analog Multimeter Escola 30	1013526
1	Set of 15 Safety Experiment Leads, 75 cm	1002843

BASIC PRINCIPLES

Pohl's wheel or rotating (torsional) pendulum allows for the investigation of forced harmonic rotary oscillation. For this purpose, the oscillating system is connected to an excitation linkage which is driven by an adjustable-speed DC motor so that the restoring spring periodically extends and compresses.

The equation of motion for this system is as follows

$$(1) \quad \frac{d^2\varphi}{dt^2} + 2 \cdot \delta \cdot \frac{d\varphi}{dt} + \omega_0^2 \cdot \varphi = A \cdot \cos(\omega_E \cdot t)$$

where $\delta = \frac{k}{2J}$, $\omega_0^2 = \frac{D}{J}$, $A = \frac{M_0}{J}$

J : moment of inertia

D : spring constant

k : damping coefficient

M_0 : amplitude of external torque

ω_E : angular frequency of external torque

The solution to this equation is composed of a uniform and a non-uniform component. The uniform component is equivalent to damped simple harmonic motion, as investigated in experiment UE1050500. This decreases exponentially over time and can be neglected by comparison with the non-uniform component after a short period of settling.

The non-uniform component

$$(2) \quad \varphi(t) = \varphi_E \cdot \cos(\omega_E \cdot t - \psi_E)$$

is linked to the external torque, however, and remains non-negligible as long as that torque is present: Its amplitude is as follows:

$$(3) \quad \varphi_E = \frac{A_0}{\sqrt{(\omega_0^2 - \omega_E^2)^2 + 4 \cdot \delta^2 \cdot \omega_E^2}}$$

This becomes increasingly high the closer the excitation frequency ω_E is to the intrinsic resonant frequency ω_0 of the rotating pendulum. Resonance is said to occur when $\omega_E = \omega_0$.

The phase shift is shown below:

$$(4) \quad \psi_E = \arctan\left(\frac{2 \cdot \delta \cdot \omega_E}{\omega_0^2 - \omega_E^2}\right)$$

This indicates that the deflection of the pendulum lags behind the excitation. For low frequencies it is close to zero but as the frequency increases, it rises, reaching 90° at the resonant frequency. For very high excitation frequencies, the excitation and oscillation frequencies end up being 180° out of phase.

EVALUATION

The amplitudes of the damped oscillations are plotted against the excitation frequency. This results in a selection of curves which can be described by equation (4) as long as the appropriate damping parameter δ is chosen.

There will be slight deviations from the damping values measured in experiment UE1050500. This is mainly due to the fact that the force of friction is not exactly proportional to the speed as assumed here.

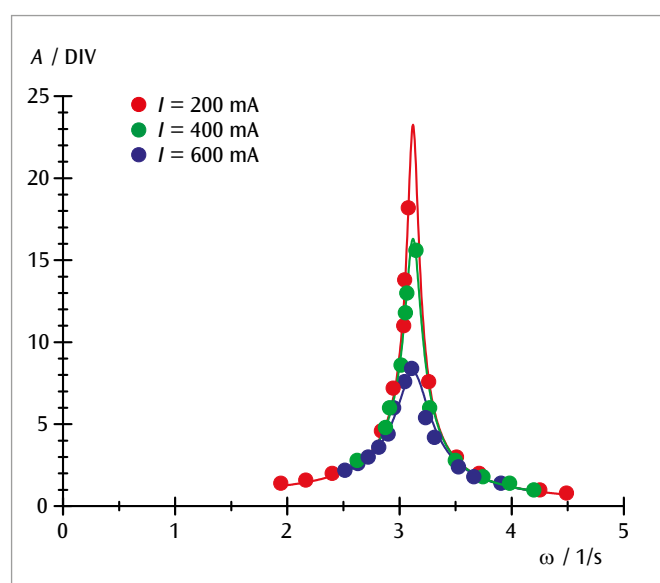


Fig. 1: Resonance curves for various degrees of damping

UE1050600 | COUPLED OSCILLATIONS



OBJECTIVE

Record and evaluate oscillation of two identical coupled pendulums

SUMMARY

The oscillation of two identical, coupled pendulums is distinguished by the period of oscillation and the beat period. The beat period is the interval between two points in time when one pendulum is swinging at its minimum amplitude. Both values can be calculated from the natural periods of oscillation for the coupled pendulums when the oscillations are in phase and out of phase.

EXPERIMENT PROCEDURE

- Record the oscillations when they are in phase and determine the period T_+ .
- Record the oscillations when they are out of phase and determine the period T_- .
- Record a coupled oscillation and determine the oscillation period T and the beat period T_Δ .
- Compare the values obtained for those calculated for the natural periods T_+ and T_- .

REQUIRED APPARATUS

Quantity	Description	Item Number
2	Pendulum Rods with Angle Sensor (230 V, 50/60 Hz)	1000763 or
	Pendulum Rods with Angle Sensor (115 V, 50/60 Hz)	1000762
1	Helical Springs 3,0 N/m	1002945
2	Table Clamps	1002832
2	Stainless Steel Rods 1000 mm	1002936
1	Stainless Steel Rod 470 mm	1002934
4	Universal Clamp	1002830
2	Adaptor, BNC Plug/4 mm Jacks	1002750
1	WiLab *	1022284
2	Voltage Sensor 500 mV, Differential	1021681
2	Sensor Cable	1021514

Additionally required

1	Coach 7 License
---	-----------------

* Alternative: 1 VinciLab 1021477

BASIC PRINCIPLES

For oscillation of two coupled pendulums, the oscillation energy is transferred from one pendulum to the other and back again. If both pendulums are identical and oscillation is begun so that one pendulum is initially at rest while the other is swinging, the energy is actually transferred in its entirety, i.e. one pendulum always comes to rest while the other is swinging at its maximum amplitude. The time between two such occurrences of rest for one pendulum or, more generally, the time between any two instances of minimum amplitude is referred to as the beat period T_Δ .

The oscillation of two identical coupled ideal pendulums can be regarded as a superimposition of two natural oscillations. These natural oscillations can be observed when both pendulums are fully in phase or fully out of phase. In the first case, both pendulums vibrate at the frequency that they would if the coupling to the other pendulum were not present at all. In the second case, the effect of the coupling is at a maximum and the inherent frequency is greater. All other oscillations can be described by superimposing these two natural oscillations.

The equation of motion for the pendulums takes the form:

$$(1) \quad \begin{aligned} L \cdot \varphi_1 + g \cdot \varphi_1 + k \cdot (\varphi_1 - \varphi_2) &= 0 \\ L \cdot \varphi_2 + g \cdot \varphi_2 + k \cdot (\varphi_2 - \varphi_1) &= 0 \end{aligned}$$

g : Acceleration due to gravity, L : length of pendulum,
 k : coupling constant

For the motions $\varphi_- = \varphi_1 - \varphi_2$ and $\varphi_+ = \varphi_1 + \varphi_2$ (initially chosen arbitrarily) the equation of motion is as follows:

$$(2) \quad \begin{aligned} L \cdot \varphi_+ + g \cdot \varphi_+ &= 0 \\ L \cdot \varphi_- + (g + 2k) \cdot \varphi_- &= 0 \end{aligned}$$

The solutions

$$(3) \quad \begin{aligned} \varphi_+ &= a_+ \cdot \cos(\omega_+ t) + b_+ \cdot \sin(\omega_+ t) \\ \varphi_- &= a_- \cdot \cos(\omega_- t) + b_- \cdot \sin(\omega_- t) \end{aligned}$$

give rise to angular frequencies

$$(4) \quad \begin{aligned} \omega_+ &= \sqrt{\frac{g}{L}} \\ \omega_- &= \sqrt{\frac{g + 2k}{L}} \end{aligned}$$

corresponding to the natural frequencies for in phase or out of phase motion ($\varphi_+ = 0$ for out of phase motion and $\varphi_- = 0$ for in-phase motion). The deflection of the pendulums can be calculated from the sum or the difference of the two motions, leading to the solutions

$$(5) \quad \begin{aligned} \varphi_1 &= \frac{1}{2} \cdot (a_+ \cdot \cos(\omega_+ t) + b_+ \cdot \sin(\omega_+ t) + a_- \cdot \cos(\omega_- t) + b_- \cdot \sin(\omega_- t)) \\ \varphi_2 &= \frac{1}{2} \cdot (a_+ \cdot \cos(\omega_+ t) + b_+ \cdot \sin(\omega_+ t) - a_- \cdot \cos(\omega_- t) - b_- \cdot \sin(\omega_- t)) \end{aligned}$$

Parameters a_+ , a_- , b_+ and b_- are arbitrary coefficients that can be calculated from the initial conditions for the two pendulums at time $t = 0$. It is easiest to consider the following case where pendulum 1 is moved at time 0 from rest to an initial angular velocity ψ_0 while pendulum 2 remains at rest.

$$(6) \quad \begin{aligned} \varphi_1 &= \frac{1}{2} \cdot \left(\frac{\psi_0}{\omega_+} \cdot \sin(\omega_+ t) + \frac{\psi_0}{\omega_-} \cdot \sin(\omega_- t) \right) \\ \varphi_2 &= \frac{1}{2} \cdot \left(\frac{\psi_0}{\omega_+} \cdot \sin(\omega_+ t) - \frac{\psi_0}{\omega_-} \cdot \sin(\omega_- t) \right) \end{aligned}$$

The speed of both pendulums is then given by:

$$(7) \quad \begin{aligned} \dot{\varphi}_1 &= \frac{\psi_0}{2} \cdot (\cos(\omega_+ t) + \cos(\omega_- t)) \\ \dot{\varphi}_2 &= \frac{\psi_0}{2} \cdot (\cos(\omega_+ t) - \cos(\omega_- t)) \end{aligned}$$

which can be rearranged to give

$$(8) \quad \begin{aligned} \varphi_1 &= \psi_0 \cdot \cos(\omega_\Delta t) \cdot \cos(\omega t) & \text{where (9)} & \quad \omega_\Delta = \frac{\omega_- - \omega_+}{2} \\ \varphi_2 &= \psi_0 \cdot \sin(\omega_\Delta t) \cdot \cos(\omega t) & & \quad \omega = \frac{\omega_+ + \omega_-}{2} \end{aligned}$$

This corresponds to an oscillation of both pendulums at identical angular frequency ω , where the velocity amplitudes ψ_1 and ψ_2 are modulated at an angular frequency ω_Δ :

$$(10) \quad \begin{aligned} \psi_1(t) &= \psi_0 \cdot \cos(\omega_\Delta t) \\ \psi_2(t) &= \psi_0 \cdot \sin(\omega_\Delta t) \end{aligned}$$

EVALUATION

Equation (4) can be used to calculate the natural oscillation periods T_+ and T_- for in-phase and out-of-phase oscillation:

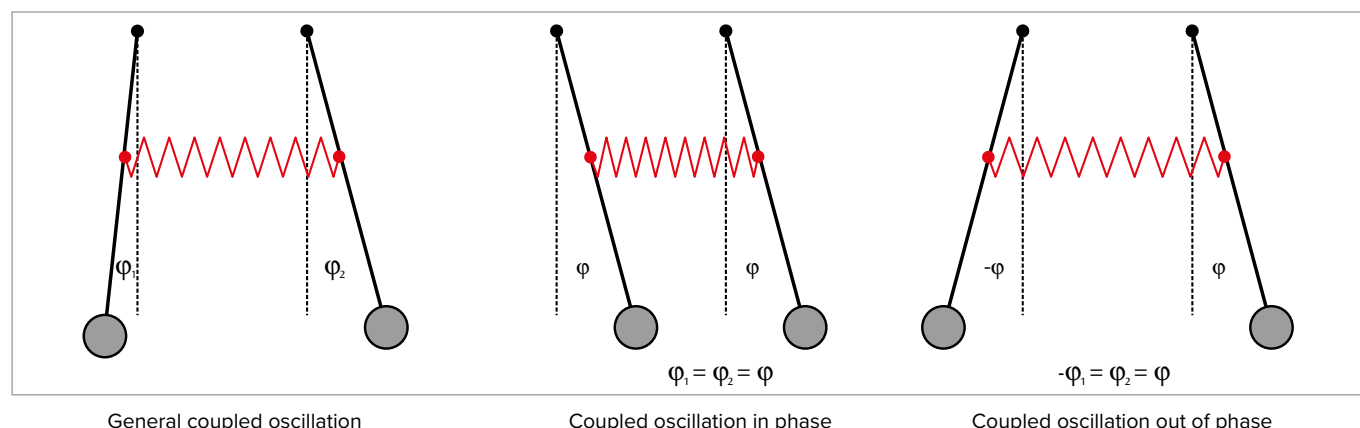
$$T_+ = \frac{2\pi}{\omega_+} = 2\pi \sqrt{\frac{L}{g}} \quad \text{and} \quad T_- = \frac{2\pi}{\omega_-} = 2\pi \sqrt{\frac{L}{g + 2k}}$$

For a period T for coupled oscillation, equation (9) implies the following:

$$\frac{2\pi}{T} = \omega = \frac{\pi}{T_+} + \frac{\pi}{T_-} \quad \text{and therefore} \quad T = 2 \cdot \frac{T_+ \cdot T_-}{T_- + T_+}$$

The amplitude modulation given in equation (10) is usually stipulated in terms of its period T_Δ corresponding to the time between successive points where one pendulum stands still:

$$\frac{2\pi}{2T_\Delta} = \omega_\Delta = \frac{\pi}{T_-} - \frac{\pi}{T_+} \quad \text{and therefore} \quad T_\Delta = \frac{T_+ \cdot T_-}{T_+ - T_-}$$



UE1050700 | MECHANICAL WAVES



EXPERIMENT PROCEDURE

- Generate standing longitudinal waves in a coil spring and standing transverse waves along a rope.
- Measure the intrinsic frequency f_n as a function of number of nodes n .
- Determine the corresponding wavelength λ_n and speed of propagation of the waves c .

OBJECTIVE

Investigate standing waves along a stretched coil spring and a taut rope.

SUMMARY

Some examples of where mechanical waves arise include a stretched coil spring, where the waves are longitudinal, or a taut rope where the waves are transverse. In either case, standing waves will be set up if one end of the carrier medium is fixed. This is because the incoming wave and the wave reflected at the fixed end have the same amplitude and are superimposed on one another. If the other end is also fixed, the only way that waves can propagate is if resonance conditions are met. In this experiment the coil spring and the rope are fixed at one end. The other end, a distance L from the fixed point, is fixed to a vibration generator, which uses a function generator to drive small-amplitude oscillations of variable frequency f . This end can also be regarded as a fixed point to a good approximation. The intrinsic frequency of the vibration will be measured as a function of the number of nodes in the standing wave. The speed of propagation of the wave can then be calculated from this data.

REQUIRED APPARATUS

Quantity	Description	Item Number
1	Accessories for Spring Oscillations	1000703
1	Accessories for Rope Waves	1008540
1	Vibration Generator	1000701
1	Function Generator FG 100 (230 V, 50/60 Hz)	1009957 or
	Function Generator FG 100 (115 V, 50/60 Hz)	1009956
1	Precision Dynamometer, 2 N	1003105
1	Pocket Measuring Tape, 2 m	1002603
1	Pair of Safety Experimental Leads, 75 cm, red/blue	1017718

BASIC PRINCIPLES

Some examples of where mechanical waves arise include a stretched coil spring or a taut rope. The waves arising in the spring are longitudinal waves since the deflection of the coil is in the direction of propagation. The waves along a rope by contrast are transverse waves. This is because the incoming wave and the wave reflected at the fixed end have the same amplitude and are superimposed on one another. If the other end is also fixed, the only way that waves can propagate is if resonance conditions are met.

Let $\xi(x,t)$ be the longitudinal or transverse deflection at a point x along the carrier medium at a point in time t . The following is then true:

$$(1) \quad \xi_1(x,t) = \xi_0 \cdot \cos(2\pi \cdot f \cdot t - \frac{2\pi}{\lambda} \cdot x)$$

This applies to a sinusoidal wave travelling from left to right along the carrier medium. The frequency f and wavelength λ are related in following way:

$$(2) \quad c = f \cdot \lambda$$

c: Propagation velocity of wave

If such a wave, travelling from left to right, should be reflected from a fixed point at $x = 0$, a wave travelling from right to left direction then arises.

$$(3) \quad \xi_2(x,t) = -\xi_0 \cdot \cos(2\pi \cdot f \cdot t + \frac{2\pi}{\lambda} \cdot x)$$

The two waves are then superimposed to create a standing wave.

$$(4) \quad \xi(x,t) = 2\xi_0 \cdot \sin(2\pi \cdot f \cdot t) \cdot \sin(\frac{2\pi}{\lambda} \cdot x)$$

These considerations are valid regardless of the nature of the wave or of the carrier medium.

If the other end is also fixed at a position $x = L$, then the following resonance condition needs to be fulfilled at all times t .

$$(5) \quad \xi(L,t) = 0 = \sin(\frac{2\pi}{\lambda} \cdot L)$$

This only applies if the wavelength meets the following conditions:

$$(6a) \quad \frac{2\pi}{\lambda_n} \cdot L = (n+1) \cdot \pi, \quad \lambda_n = 2 \cdot \frac{L}{n+1}$$

$$\text{or } L = (n+1) \cdot \frac{\lambda_n}{2}$$

According to equation (2), the frequency is then

$$(6b) \quad f_n = (n+1) \cdot \frac{c}{2 \cdot L}$$

This implies that the condition for resonance (5) is only fulfilled if the length L is an integer multiple of half the wavelength. The resonant frequency must correspond to this wavelength. In this case, n is the number of nodes in the oscillation. This is zero if there is only one anti-node in the fundamental oscillation (see Fig. 2).

In this experiment, the carrier medium is either a spring or a rope which is fixed at one end. The other end is connected to a vibration generator at a distance L from this fixed point. This uses a function generator to drive small-amplitude oscillations of variable frequency f . This end can also be regarded as a fixed point to a good approximation.

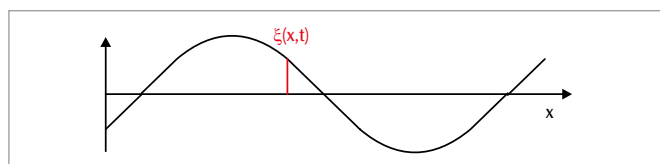


Fig. 1: Illustration of how the localised deflection $\xi(x,t)$ is defined

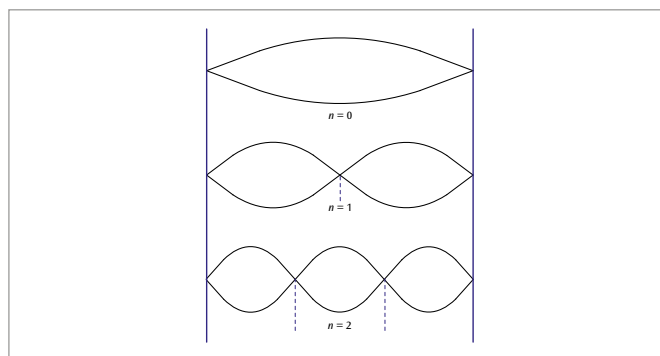


Fig. 2: Standing waves

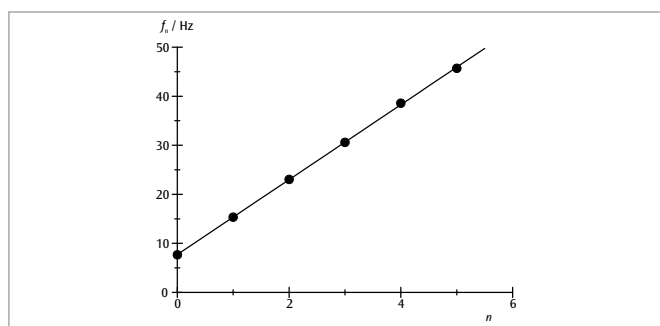


Fig. 3: Resonant frequency as a function of the number of nodes for waves along a coil spring

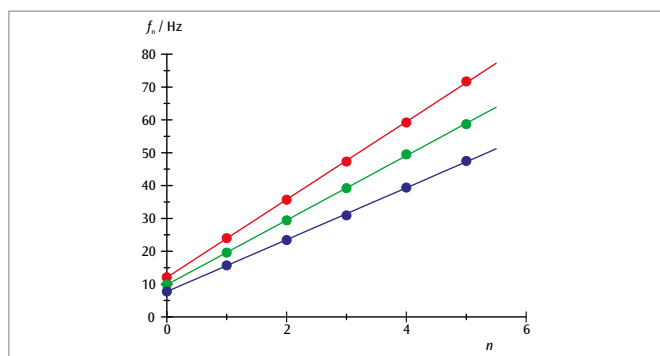


Fig. 4: Resonant frequency as a function of the number of nodes for waves along a rope

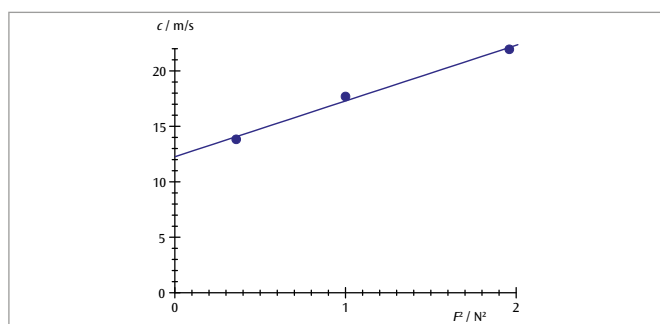


Fig. 5: Wave velocity c as a function of F^2 for the waves along a rope

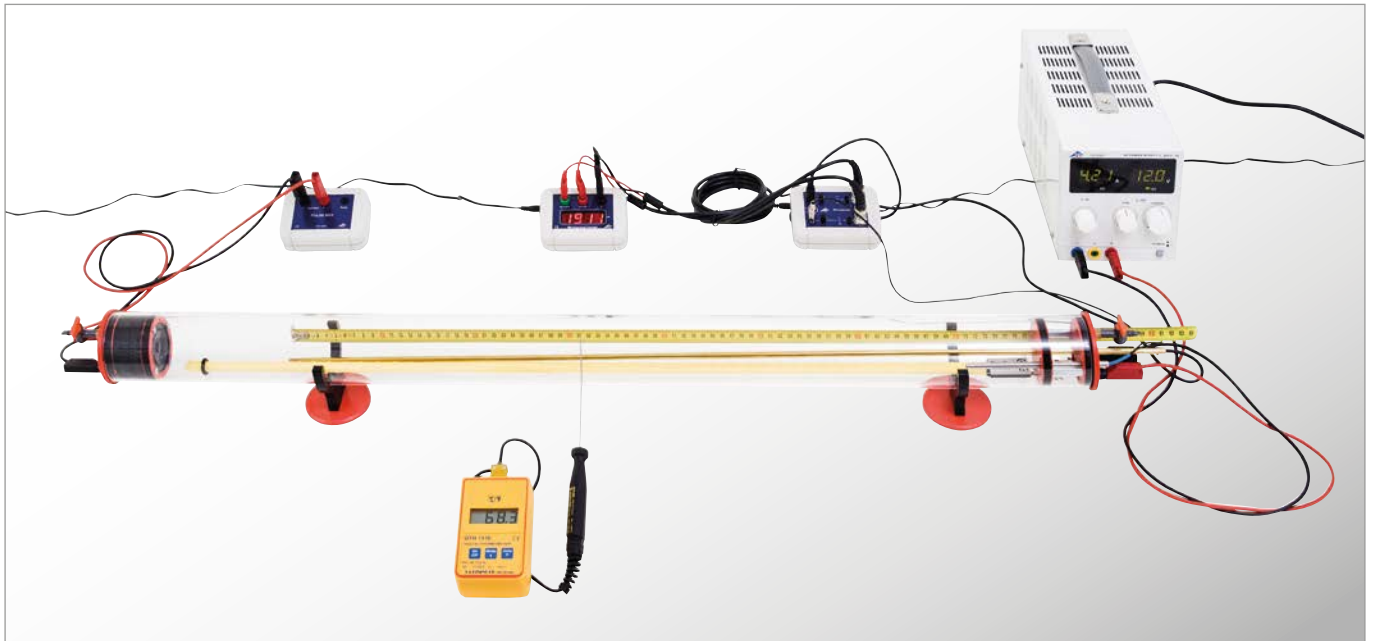
EVALUATION

If resonant frequency is plotted against the number of nodes, the points will all lie along a straight line of gradient

$$\alpha = \frac{c}{2 \cdot L}$$

Therefore, as long as the length L is known, it is possible to calculate the speed of propagation of the wave c . With all other parameters being equal it is dependent on the tensile force F , as Fig. 5 demonstrates for the waves along the rope.

UE1070310 | SPEED OF SOUND IN AIR I



EXPERIMENT PROCEDURE

- Measuring the propagation time t of a sound pulse in air at room temperature as a function of the distance s between two microphone probes.
- Confirming the linear relationship between s and t .
- Measuring the propagation time t of a sound pulse in air as a function of the temperature T over a fixed distance between two microphone probes.
- Determining the speed of sound (group velocity) as a function of temperature.
- Comparing the result with Laplace's derivation.

OBJECTIVE

Measuring the propagation time of sound pulses in Kundt's tube

SUMMARY

Sound waves propagate longitudinally in gases. The group velocity here is equal to the phase velocity. In this experiment, we will measure the propagation time of a sound pulse between two microphone probes in Kundt's tube, and use the result to calculate the speed of sound. The temperature dependence of the speed of sound is examined between room temperature and 50°C. The measurement result matches the result of Laplace's derivation.

REQUIRED APPARATUS

Quantity	Description	Item Number
1	Kundt's Tube E	1017339
1	Pulse Box K	1017341
1	Probe Microphone, long	1017342
1	Microphone Probe, short	4008308
1	Microphone Box (230 V, 50/60 Hz)	1014520 or
	Microphone Box (115 V, 50/60 Hz)	1014521
1	Microsecond Counter (230 V, 50/60 Hz)	1017333 or
	Microsecond Counter (115 V, 50/60 Hz)	1017334
1	Heating Rod K	1017340
2	Patch Cord BNC/4mm, 0.5 m	4008293
1	DC Power Supply 0 – 20 V, 0 – 5 A (230 V, 50/60 Hz)	1003312 or
	DC Power Supply 0 – 20 V, 0 – 5 A (115 V, 50/60 Hz)	1003311
1	Digital Quick Response Pocket Thermometer	1002803
1	K-Type NiCr-Ni Immersion Sensor, -65°C – 550°C	1002804
1	Pair of Safety Experiment Leads, 75 cm	1002849

Additionally recommended

A Variety of Technical Gases

BASIC PRINCIPLES

Sound waves are elastic waves within a deformable medium. The wave velocity depends on the medium's elastic properties. In simple gases, sound propagates exclusively as longitudinal waves, the group velocity being equal to the phase velocity.

In a derivation according to Laplace, sound waves in gases are considered as changes in adiabatic pressure or density. The speed of sound is determined as being:

$$(1) \quad c = \sqrt{\frac{c_p \cdot p}{c_v \cdot \rho}}$$

p : Pressure. ρ : Density.

c_p, c_v : Heat capacities of the gas

For an ideal gas at absolute temperature T :

$$(2) \quad \frac{p}{\rho} = \frac{R \cdot T}{M}$$

$$R = 8,314 \frac{\text{J}}{\text{Mol} \cdot \text{K}} \quad \text{: Universal gas constant.}$$

M : Molar mass

The speed of sound in this gas is therefore:

$$(3) \quad c = \sqrt{\frac{c_p \cdot R \cdot T}{c_v \cdot M}}$$

For temperature differences ΔT which are not too large compared to a reference temperature T_0 , the speed of sound is a linear function of the temperature change ΔT :

$$(4) \quad c = \sqrt{\frac{c_p \cdot R \cdot T_0}{c_v \cdot M}} \cdot \left(1 + \frac{\Delta T}{2 \cdot T_0}\right)$$

For dry air as an ideal gas, the speed of sound is accordingly often expressed as follows:

$$(5) \quad c(T) = \left(331,3 + 0,6 \cdot \frac{\Delta T}{\text{K}}\right) \frac{\text{m}}{\text{s}}$$

$T_0 = 273,15 \text{ K} = 0^\circ\text{C}$

In the experiment, we will measure the propagation time t of a sound pulse between two microphone probes spaced at a distance s . The sound pulse is produced by a sudden movement of a loudspeaker diaphragm controlled by a voltage pulse with steep edge. High-resolution measurement of the propagation time using a microsecond counter starts when the sound pulse reaches the first microphone probe, and stops when the second microphone probe at a distance s is reached. A heating element is used to heat the air in Kundt's tube to up to 50°C for measurements of propagation time as a function of temperature. The temperature distribution during the cooling process is sufficiently homogeneous. It is therefore sufficient to measure the temperature at one point in Kundt's tube.

A tube connector can be used to supply Kundt's tube with technical gases other than air.

EVALUATION

The speed of sound is calculated as the quotient of the travelled distance s and the propagation time t :

$$c = \frac{s}{t}$$

Figure 2 represents it as the reciprocal of the slope.

The temperature dependence of the speed of sound is described by equation 3 with the following parameters:

$$M = 28,97 \frac{\text{g}}{\text{Mol}}, \quad \frac{c_p}{c_v} = \frac{7}{5}$$

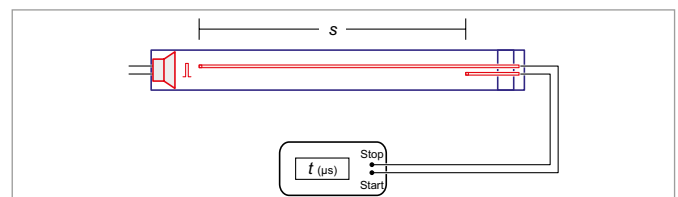


Fig. 1: Schematic of the experiment setup

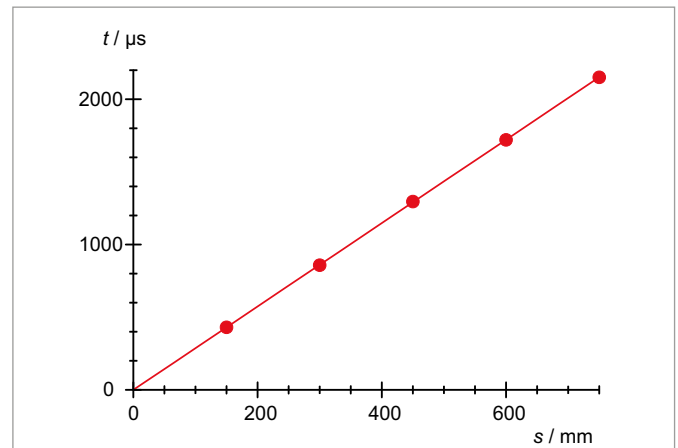


Fig. 2: Sound propagation time t in air as a function of the travelled distance s at room temperature

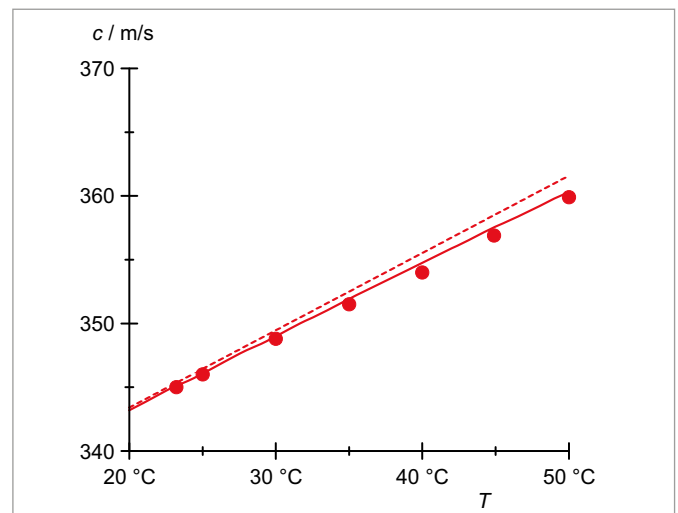
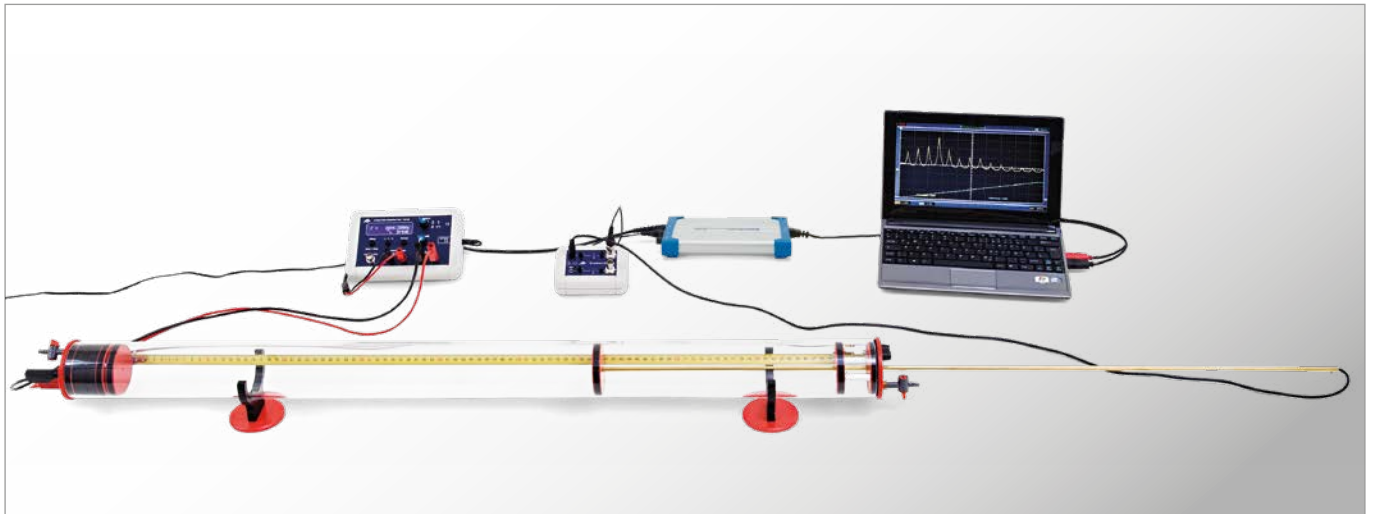


Fig. 3 Speed of sound c in air as a function of the temperature T
 Solid line: Calculation according to equation 3
 Dashed line: Calculation according to equation 5

UE1070320 | SPEED OF SOUND IN AIR II



EXPERIMENT PROCEDURE

- Generate standing waves in Kundt's tube with both ends closed off.
- Measure the fundamental frequency as a function of the length of the Kundt's tube.
- Measure the frequencies of the fundamental and overtones for a fixed length of tube.
- Determine the speed of propagation of the wave from the resonant frequencies.

OBJECTIVE

Generate and measure standing sound waves in Kundt's tube

SUMMARY

Sound waves propagate in gases in the form of longitudinal waves. The overall velocity is equivalent to the phase velocity. In this experiment a standing wave is generated inside Kundt's tube with both ends closed off. The fundamental frequency is measured as a function of the length of the tube, and the frequencies of the fundamental and overtones are also measured for a fixed length of tube.

REQUIRED APPARATUS

Quantity	Description	Item Number
1	Kundt's Tube E	1017339
1	Probe Microphone, long	1017342
1	Microphone Box (115 V, 50/60 Hz)	1014521 or
	Microphone Box (230 V, 50/60 Hz)	1014520
1	Function Generator FG 100 (230 V, 50/60 Hz)	1009957 or
	Function Generator FG 100 (115 V, 50/60 Hz)	1009956
1	PC Oscilloscope, 2x25 MHz	1020857
1	Analog Multimeter ESCOLA 30	1013526
1	Patch Cord BNC/4mm, 0.5 m	4008293
1	Pair of Safety Experiment Leads, 75 cm	1002849

BASIC PRINCIPLES

It is possible to generate standing waves in Kundt's tube by producing waves of a suitable resonant frequency from a loudspeaker at one end of the tube, which are then reflected by the cap at the other end. If the length of the tube is known, it is possible to determine the speed of propagation of the waves from the resonant frequency and the number of the harmonics.

Sound waves propagate in air and other gases by means of rapid changes in pressure and density. It is easiest to describe them on the basis of the sound pressure, which is superimposed on top of atmospheric pressure. As an alternative to the sound pressure p , the sound velocity v can

also be used to describe a sound wave. That is the average velocity of gas molecules at a given point x in the oscillating medium at a point in time t . Pressure and velocity of sound are linked, for example by an Euler equation of motion:

$$(1) \quad -\frac{\partial p}{\partial x} = \rho_0 \cdot \frac{\partial v}{\partial t}$$

ρ_0 : Density of gas

In Kundt's tube, sound waves propagate along the length of the tube, i.e. they can be described with the help of a one-dimensional wave equation, which applies to both sound pressure and velocity:

$$(2) \quad \frac{\partial^2 p(x,t)}{\partial t^2} = c^2 \cdot \frac{\partial^2 p(x,t)}{\partial x^2} \quad \text{or} \\ \frac{\partial^2 v(x,t)}{\partial t^2} = c^2 \cdot \frac{\partial^2 v(x,t)}{\partial x^2}$$

c : speed of sound

This experiment studies harmonic waves, which are reflected at the end of the Kundt's tube. To find the solutions to the wave equation, the superposition of the outgoing and reflected waves needs to be taken into account:

$$(3) \quad p = p_{0>} \cdot e^{2\pi i \left(ft - \frac{x}{\lambda} \right)} + p_{0<} \cdot e^{2\pi i \left(ft + \frac{x}{\lambda} \right)}$$

$p_{0>}, v_{0>}$: Amplitudes of outgoing wave,

$p_{0<}, v_{0<}$: Amplitudes of returning wave

f : Frequency, λ : Wavelength

In this case

$$(4) \quad f \cdot \lambda = c$$

By substituting these solutions into equation (1) and considering the outgoing and returning waves separately, the following can be derived:

$$(5) \quad p_{0>} = v_{0>} \cdot Z \quad \text{and} \quad p_{0<} = v_{0<} \cdot Z$$

The quantity

$$(6) \quad Z = c \cdot \rho_0$$

is known as the sound impedance and corresponds to the resistance to the waves from the medium itself. It plays a key role in considerations of the reflection of a sound wave by walls with an impedance of W :

The following then applies:

$$(7) \quad r_v = \frac{v_{0<}}{v_{0>}} = \frac{Z - W}{Z + W} \quad \text{and} \quad r_p = \frac{p_{0<}}{p_{0>}} = \frac{Z + W}{Z - W}$$

In this experiment W is much higher than Z so that we may assume $r_v = 1$ and $r_p = -1$.

If the reflecting wall is selected, for simplicity's sake, to be at $x = 0$, the spatial component of the sound wave can be derived from equation (3) as follows:

$$(8) \quad p = p_{0>} \cdot \left(e^{-2\pi i \frac{x}{\lambda}} + e^{+2\pi i \frac{x}{\lambda}} \right) \cdot e^{-2\pi i f t} \\ = 2 \cdot p_{0>} \cdot \cos\left(\frac{2\pi}{\lambda} \cdot x\right) \cdot e^{-2\pi i f t}$$

and

$$v = v_{0>} \cdot \left(e^{-2\pi i \frac{x}{\lambda}} - e^{+2\pi i \frac{x}{\lambda}} \right) \cdot e^{-2\pi i f t} \\ = -2 \cdot i \cdot v_{0>} \cdot \sin\left(\frac{2\pi}{\lambda} \cdot x\right) \cdot e^{-2\pi i f t}$$

Only the real components of these terms have any actual physical relevance. They correspond to standing sound waves which have a pressure anti-node at the end wall (i.e. at $x = 0$), while the sound velocity

at that point has a node in its oscillation. The velocity is phase shifted ahead of the pressure by 90° .

Sound waves are generated by a loudspeaker at a distance L from the wall. These waves oscillate with frequency f . At this point, too the pressure has an anti-node and the velocity has a node. Such boundary conditions are only fulfilled when L is an integer multiple of half the wavelength:

$$(9) \quad L = n \cdot \frac{\lambda_n}{2}$$

From equation (3) then, the frequencies must fulfil the following condition for resonance:

$$(10) \quad f_n = n \cdot \frac{c}{2 \cdot L}$$

During the experiment, the frequency f of the speaker is continuously varied while a microphone sensor measures the sound pressure at the reflecting wall. Resonance then occurs when the microphone signal is at its maximum amplitude.

EVALUATION

According to equation (9) the resonant frequencies determined f_n should have wavelengths

$$\lambda_n = \frac{2 \cdot L}{n}$$

In order to verify equation (3) and determine the wavelength, the wavelength values should be plotted on a graph of f against λ .

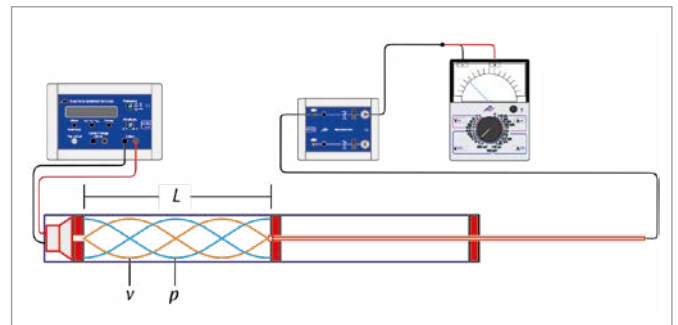


Fig. 1: Schematic of experiment set-up

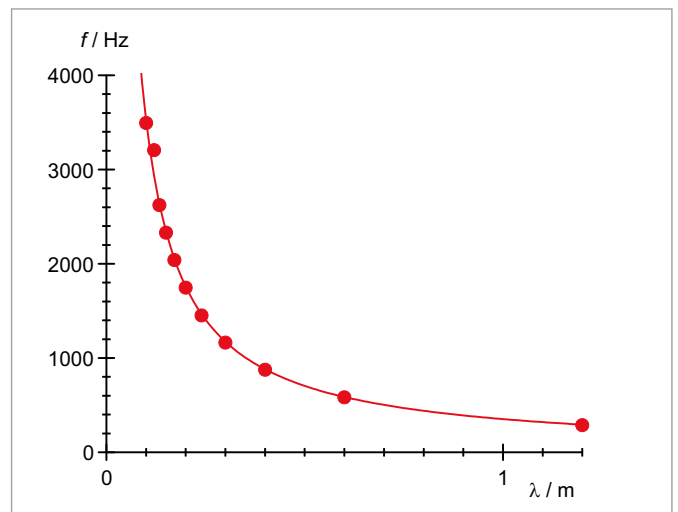
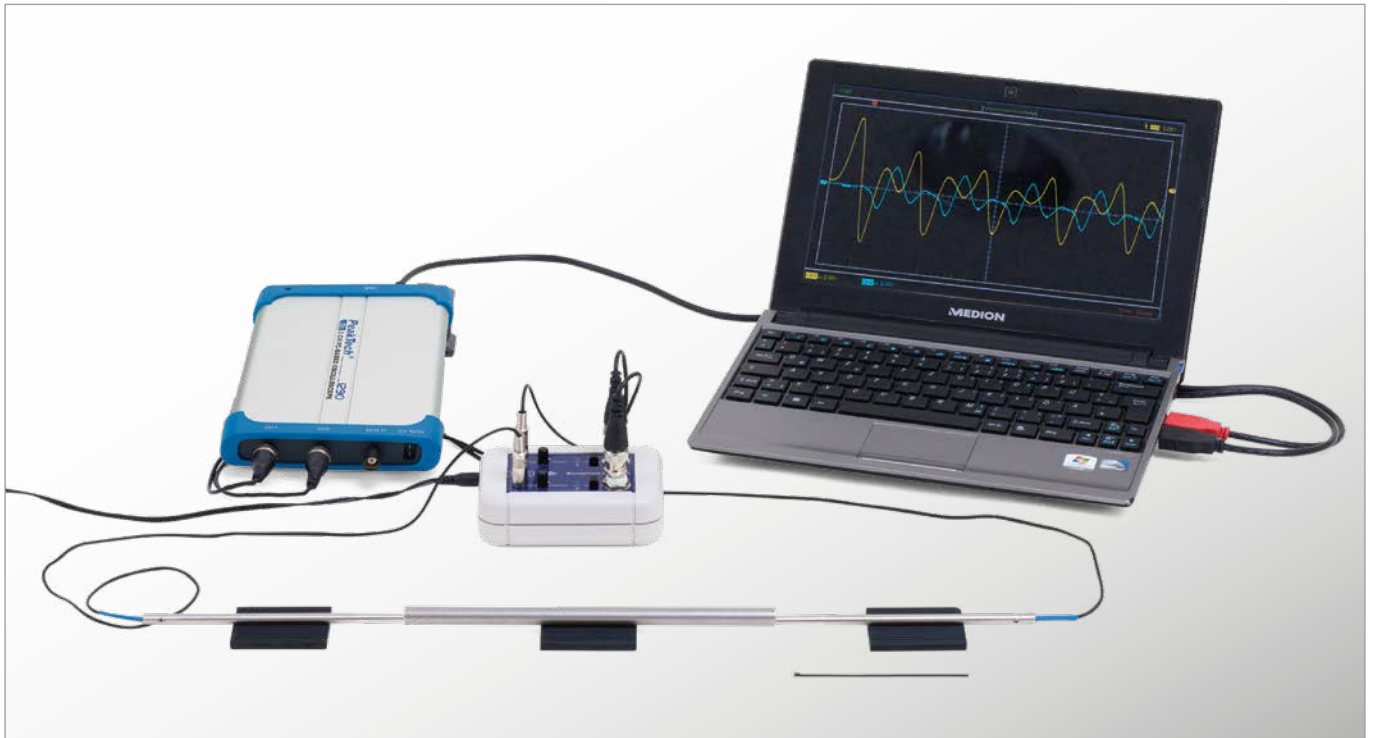


Fig. 2: Graph of frequency against wavelength

UE1070410 | PROPAGATION OF SOUND IN RODS



EXPERIMENT PROCEDURE

- Excite pulses of longitudinal sound waves in rods and use two microphone probes to detect them.
- Analyze how the sound pulses are affected by the material and length of the rods by means of an oscilloscope.
- Determine the speed of propagation of longitudinal sound waves in the materials from the time it takes the pulses to travel through them.
- Determine the modulus of elasticity of the materials from the propagation velocity of longitudinal waves and their density.

OBJECTIVE

Investigation of longitudinal sound waves in cylindrical rods and determination of propagation velocity for longitudinal sound waves

SUMMARY

Sound waves can propagate through solids in the form of longitudinal, transverse, dilatational or flexural waves. An elastic longitudinal wave propagates along a rod by means of a periodic sequence of expansion and contraction along the length of the rod. The speed of propagation depends only on the modulus of elasticity and the density of the material when the diameter of the rod is small in comparison to its length. In this experiment, it will be determined from the time it takes sound pulses to travel along the rod.

REQUIRED APPARATUS

Quantity	Description	Item Number
1	Equipment Set "Sound Propagation in Rods" (230 V, 50/60 Hz)	1018469 or
	Equipment Set "Sound Propagation in Rods" (115 V, 50/60 Hz)	1018468
1	PC Oscilloscope, 2x25 MHz	1020857

BASIC PRINCIPLES

Sound waves can not only propagate in gases or liquids, but also in solid bodies.

Longitudinal, transverse, dilatational or flexural waves can all occur in solids.

An elastic longitudinal wave propagates along a rod by means of a periodic sequence of expansion and contraction along the length of the rod. The expansion is caused by atoms being excited out of their rest positions. In a rod where the diameter is much smaller than the length, the contraction in the transverse direction is negligible, i.e. Poisson $\mu = 0$ to a good approximation.

In this case, the relationship between the changes in time and space of the compressive tension σ and the extension ξ is given by the following equations:

$$(1) \quad \frac{\partial \sigma}{\partial x} = \rho \cdot \frac{\partial v}{\partial t} \quad \text{and} \quad \frac{\partial v}{\partial x} = \frac{1}{E} \cdot \frac{\partial \sigma}{\partial t} \quad \text{where} \quad v = \frac{\partial \xi}{\partial t}$$

ρ : density of material of rod,
 E : modulus of elasticity for material of rod

This results in the following wave equations:

$$(2) \quad \frac{\partial^2 \sigma}{\partial t^2} = \frac{E}{\rho} \cdot \frac{\partial^2 \sigma}{\partial x^2} \quad \text{and} \quad \frac{\partial^2 v}{\partial t^2} = \frac{E}{\rho} \cdot \frac{\partial^2 v}{\partial x^2}$$

The speed of propagation of longitudinal waves is

$$(3) \quad c_L = \sqrt{\frac{E}{\rho}}$$

In this experiment, longitudinal sound waves are excited in rods of various materials and lengths in the form of pulses. The pulses are then detected at the end of the rod being excited and at the other end by means of microphone sensors and displayed on an oscilloscope. The ends of the rod act as reflective surfaces for sound, such that the sound pulses reflect back and forth along the rods. The time it takes for pulses to travel from one end of the rod to the other is determined from the oscilloscope traces.

In long rods the multiply reflected sound pulses are clearly separated in time. In short rods, they could easily be superimposed and form "standing waves".

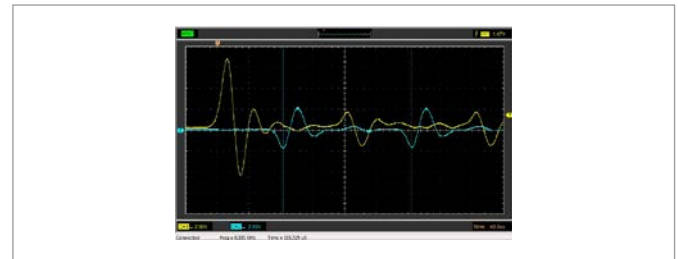


Fig. 1: Propagation of a sound pulse, signal at the excited end of the rod (yellow), (stainless steel rod, 400 mm)

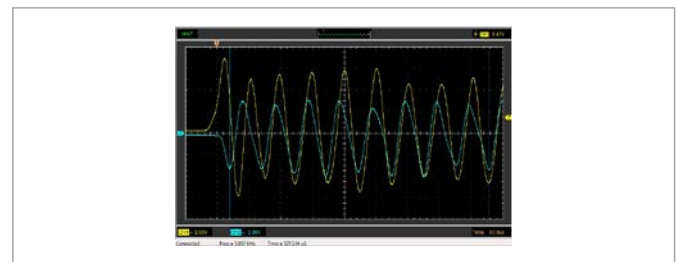


Fig. 2: Standing wave, signal at the excited end of the rod (yellow), (stainless steel rod, 100 mm)



Fig. 3: Propagation of a sound pulse (top: PVC rod, 200 mm, bottom: glass rod, 200 mm), signal at the opposite end of the rod from the excitation (cyan)

EVALUATION

The velocity of the longitudinal sound waves is determined from the time they take to travel the length of the rod and back by means of the following equation:

$$(4) \quad c_L = \frac{2 \cdot L}{T}, \quad L: \text{Length of rod}$$

This is because the sound pulse travels the length of the rod twice (to the other end and back) in a time T .

The modulus of elasticity for each of the materials is determined using equation (3) from the speed of propagation measured and the density of the rods, as determined by weighing them.

Table 1: Speed of longitudinal sound waves c_L in various materials of density ρ and modulus of elasticity E .

Material	c_L (m / s)	ρ (g / cm ³)	E (m / s)
Glass	5370	2.53	73
Aluminium	5110	2.79	73
Wood (beech)	5040	0.74	19
Stainless steel	4930	7.82	190
Copper	3610	8.84	115
Brass	3550	8.42	106
Transparent acrylic (perspex)	2170	1.23	6
PVC	1680	1.50	4

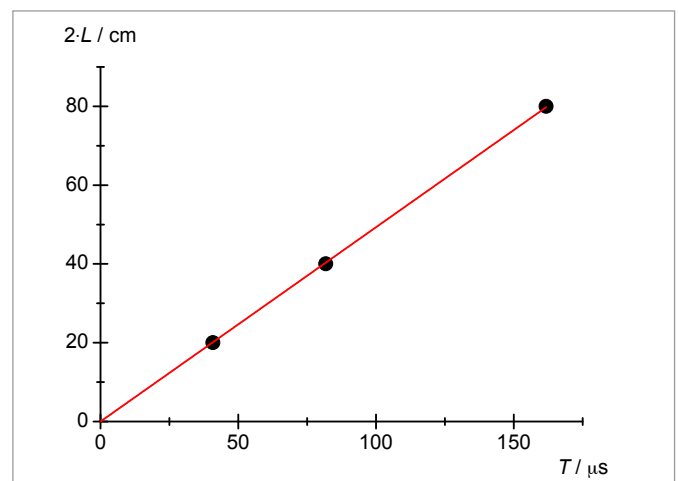
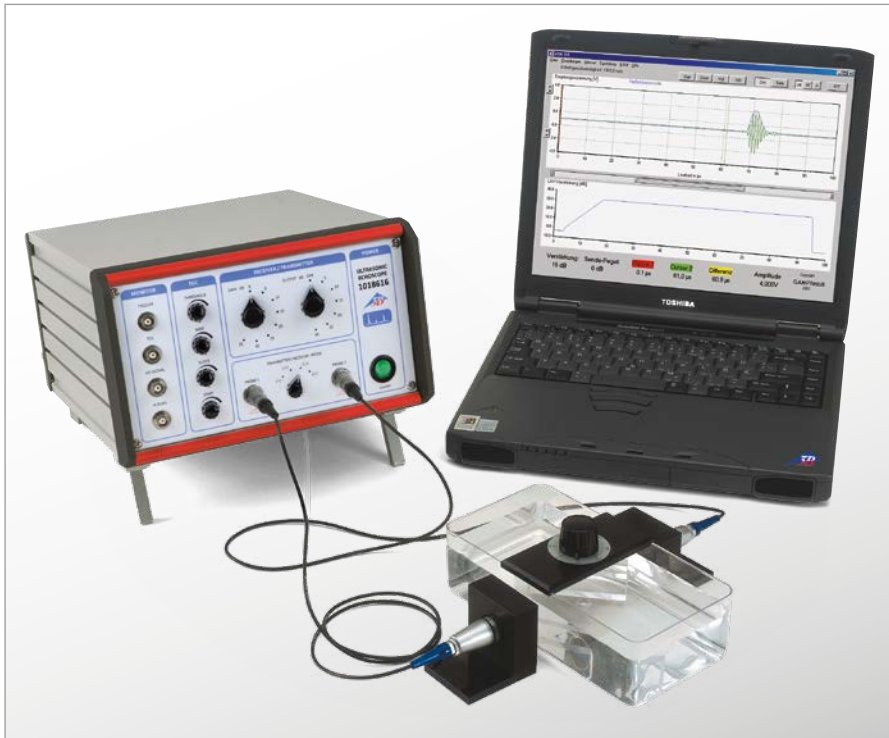


Fig. 4: Twice the length of the rods $2 \cdot L$ as a function of the time of travel T for stainless steel rods

UE1070530 | SOUND PROPAGATION IN SOLIDS



OBJECTIVE

Determine the speeds of sound propagated by longitudinal and transverse waves in solids

SUMMARY

In solids, sound is propagated in the form of longitudinal and transverse waves. However, there is a considerable difference in the speed of the two types of sound waves, since longitudinal sound waves are determined by the elastic modulus of the solid, whereas transverse sound waves are dependent on the shear modulus of the solid. By measuring the speed of the two wave types, it is possible to determine the elastic constant of the solid.

EXPERIMENT PROCEDURE

- To determine the speed of sound for longitudinal waves in polyacrylic from the propagation time of a 1-MHz ultrasound signal.
- To measure the transmission of longitudinal and transverse sound waves in solids through an inclined, plane-parallel plate.
- To determine the speed of sound for longitudinal and transverse waves from the critical angle of total reflection.
- To determine the elastic modulus E , the shear modulus G and Poisson's ratio of a solid μ from the two speeds.

REQUIRED APPARATUS

Quantity	Description	Item Number
1	Ultrasonic Echoscope GS200	1018616
2	Ultrasonic Probe, 1 MHz, GS200	1018617
1	Equipment Set "Ultrasound in Solids"	1002584
1	Aluminium Test Block with Protractor Scale	1002585
1	Set of 3 Cylinders	1002588
1	Ultrasonic Coupling Gel	1008575

BASIC PRINCIPLES

In gases and liquids, sound is propagated exclusively in the form of longitudinal waves. In the process, the sound pressure oscillates around an equilibrium value and generates oscillating regions of compression and rarefaction. Sound also penetrates solids in the form of transverse waves in which the shear stress oscillates. Transverse waves can propagate through solids because solids possess the necessary shear force required for conducting sound.

Longitudinal and transverse waves possess different speeds which depend on the density ρ and the elastic constant of the solid. The speed of longitudinal waves, given by

$$(1) \quad c_L = \sqrt{\frac{E}{\rho} \cdot \frac{1-\mu}{(1+\mu)(1-2\mu)}}$$

E : elastic modulus, μ : Poisson's ratio

is greater than that of transverse waves

$$(2) \quad c_T = \sqrt{\frac{G}{\rho}}$$

G : shear modulus

The relation between the elastic modulus E , shear modulus G of a solid and Poisson's ratio is given by the following equation:

$$(3) \quad \frac{E}{G} = 2 \cdot (1 + \mu)$$

It is therefore possible to calculate all three magnitudes of elasticity, given that the two sound speeds c_L and c_T are known.

In the experiment, first measure the propagation time t of a 1-MHz ultrasound signal through three polyacrylic cylinders of different lengths s . Plot the values in an s - t graph (see Fig. 1). From the inclination of the best-fit line through the measured values, we get the longitudinal sound speed in polyacrylic.

Subsequently, fill a trough with water and place it in the path of the wave. Measure the transit time. The transit time is reduced by placing a thin plane-parallel plate made of polyacrylic or aluminium in the path of the wave. This is due to the fact that sound propagates faster in the plate material than in water. Take accurate readings behind the water trough for the two distinct ultrasound signals caused due to the different propagation times for longitudinal and transversal sound waves in solids (see Fig. 2).

If the plate is inclined at an angle α to the incident wave, then, according to Snell's law, the wave is refracted and the two refracted waves are at angles β_L and β_T (see Fig. 3).

$$(4) \quad \frac{c}{\sin \alpha} = \frac{c_L}{\sin \beta_L} = \frac{c_T}{\sin \beta_T}$$

c: speed of sound in water

As the two sound speeds c_L and c_T through the solid are greater than the speed of sound c in water, we can eventually observe the phenomenon of total reflection – distinctly for longitudinal and transverse waves – in which the transmitted signals fully disappear. The corresponding speeds can be measured from the critical angles α_L for longitudinal waves and α_T for transverse waves:

$$(5) \quad c_L = \frac{c}{\sin \alpha_L} \quad \text{and} \quad c_T = \frac{c}{\sin \alpha_T}$$

EVALUATION

- The readings from the first series of propagation time measurements are not on a straight line through the origin on the s - t graph. This is because the propagation time required by the signal to pass through the adaptation and protective layer of the ultrasonic transducer is also measured systematically.
- From equations 1 to 3, we get the characteristic equation for Poisson's ratio μ

$$\mu = \frac{\frac{1}{2} \cdot \left(\frac{c_L}{c_T} \right)^2 - 1}{\left(\frac{c_L}{c_T} \right)^2 - 1}$$

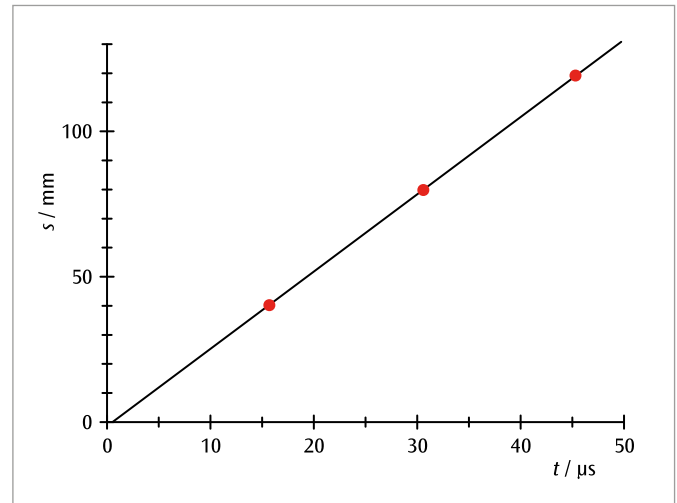


Fig. 1: s - t graph of an ultrasound signal in polyacrylic

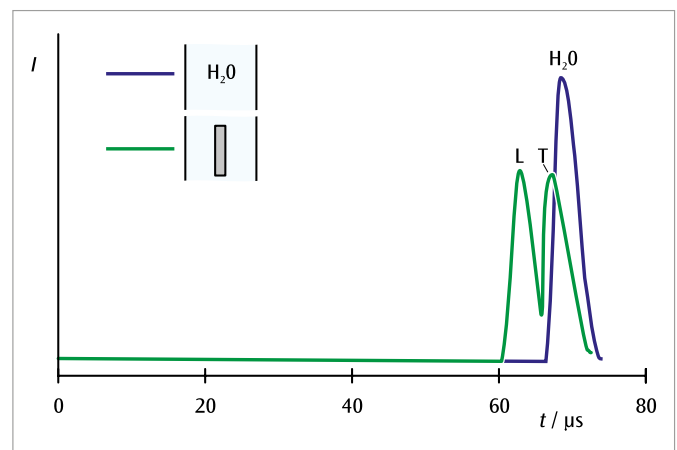


Fig. 2: Ultrasound signal after penetrating a water trough (blue: without plane-parallel plate, green: with plane-parallel plate)

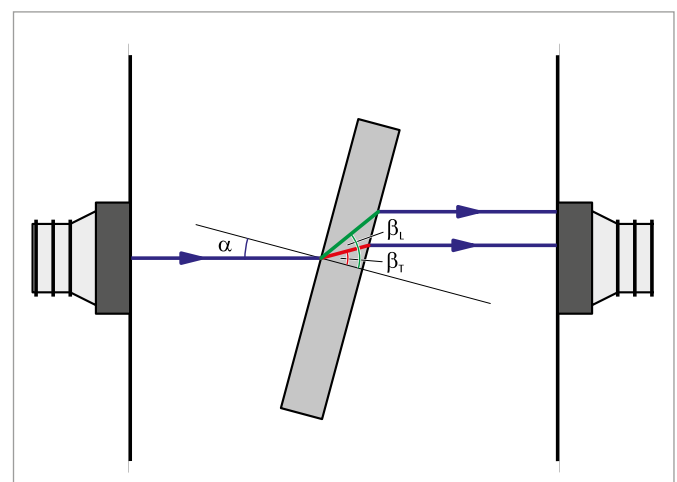
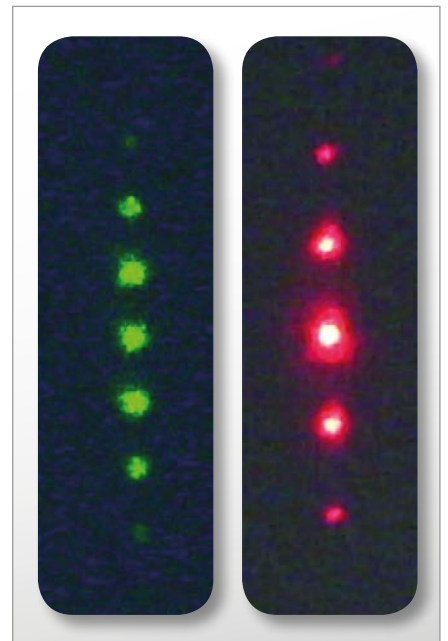


Fig. 3: Experimental set-up for determining the speed of sound for longitudinal and transverse waves from the critical angles of total reflection

UE1070550 | DEBYE-SEARS EFFECT



> EXPERIMENT PROCEDURE

- Observing the diffraction pattern at a fixed ultrasound frequency for two different light wavelengths.
- Observing the diffraction pattern for different ultrasound frequencies between 1 MHz and 12 MHz.
- Determining the corresponding sound wavelengths and the velocity of sound.

OBJECTIVE

Determine the velocity of ultrasonic waves in liquids

SUMMARY

The periodic variations of density caused by an ultrasonic standing wave pattern in a liquid act as an optical grating for the diffraction of a monochromatic parallel light beam that is transmitted in the direction perpendicular to the direction of the ultrasound wave. From the diffraction pattern and the known wavelength of the light, it is possible to determine the sound wavelength and use that to calculate the velocity of sound in the liquid.

REQUIRED APPARATUS

Quantity	Description	Item Number
1	Ultrasonic cw Generator	1002576
1	Test Vessel	1002578
1	Laser Diode for Debye-Sears Effect, Red	1002577
1	Laser Diode for Debye-Sears Effect, Green	1002579
1	Pocket Measuring Tape, 2 m	1002603
1	Ultrasonic Coupling Gel	1008575

BASIC PRINCIPLES

The diffraction of light by ultrasonic waves in liquids was predicted by Brillouin in 1922, and the effect was confirmed experimentally in 1932 by Debye and Sears and also by Lucas and Biquard. It is caused by the periodic variations in the refractive index of the liquid that are produced by ultrasonic waves. If a light beam is passed through the liquid perpendicular to the ultrasound direction, the arrangement acts as a phase grating, which moves depending on the velocity of sound. Its grating constant corresponds to the wavelength of the ultrasound, and thus depends on its frequency and the velocity of sound in the medium. The movement of the phase grating can be neglected if the effect is observed on a screen at a large distance.

In the experiment, a vertically orientated generator couples ultrasonic waves at frequencies between 1 MHz and 12 MHz into the test liquid. A monochromatic parallel light beam passes through the liquid in the horizontal direction and is diffracted by the phase grating. The diffraction pattern contains several diffraction maxima spaced at regular distances.

The k -th-order maximum of the diffraction pattern is found at the diffraction angle α_k , defined by

$$(1) \quad \tan \alpha_k = k \cdot \frac{\lambda_L}{\lambda_S}$$

λ_L : light wavelength, λ_S : ultrasound wavelength.

Thus, the ultrasound wavelength λ_S can be determined from the separation between the diffraction maxima. Furthermore, according to the relationship

$$(2) \quad c = f \cdot \lambda_S$$

it is possible to calculate the velocity of sound c in the liquid, since the frequency f of the ultrasonic waves is also known.

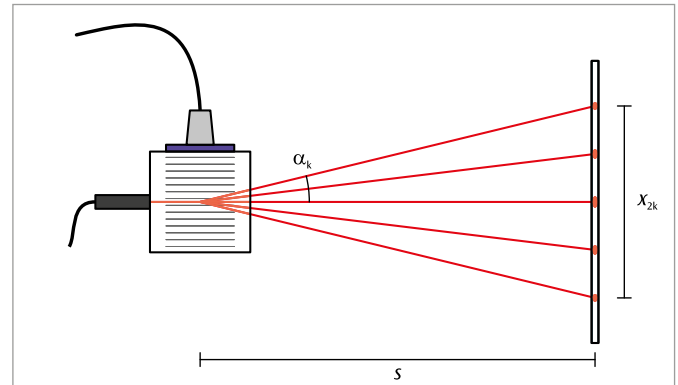


Fig. 1: Diagram showing the diffraction of light by a phase grating that is produced in a liquid by ultrasonic waves (Debye-Sears effect)

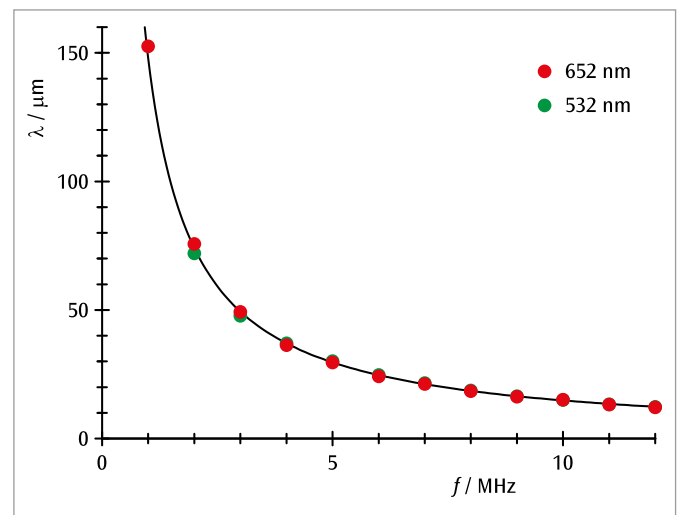


Fig. 2: Sound wavelength λ_S in water as a function of the frequency f

EVALUATION

It is necessary to measure the distance s between the ultrasound generator and the screen used to observe the diffraction pattern, and the distance x_{2k} between the $-k$ th and the $+k$ th diffraction maxima. From these two distances, it is possible to calculate the diffraction angle α_k for the k th-order maximum, given by:

$$\tan \alpha_k = \frac{x_{2k}}{2 \cdot s}$$

This leads to the following equation for determining the ultrasound wavelength λ_S :

$$\lambda_S = \frac{2 \cdot k \cdot s}{x_{2k}} \cdot \lambda_L$$

UE1080350 | FALLING SPHERE VISCOSIMETER



> EXPERIMENT PROCEDURE

- Measure the time it takes a sphere to fall through an aqueous solution of glycerine as a function of temperature.
- Determine the dynamic viscosity and compare it with values quoted in literature.
- Compare the way the dynamic viscosity depends on temperature with the predictions of the Andrade equation and determine the activation energy.

OBJECTIVE

Determine the dynamic viscosity of an aqueous solution of glycerine

SUMMARY

Dynamic viscosity, the coefficient of proportionality between velocity gradient and shear stress in a liquid, characterises how difficult it is for an object to flow through the liquid. This can be measured using a falling sphere viscosimeter of a type designed by Höppler. It is also possible to make temperature-independent measurements in conjunction with a circulation thermostat. Measurements are made in an experiment involving an aqueous solution of glycerine. This allows the way that viscosity depends on temperature to be described by the Andrade equation.

REQUIRED APPARATUS

Quantity	Description	Item Number
1	Falling Sphere Viscometer	1012827
1	Digital Stopwatch	1002811
1	Immersion/Circulation Thermostat (230 V, 50/60 Hz)	1008654 or
	Immersion/Circulation Thermostat (115 V, 50/60 Hz)	1008653
2	Tubing, Silicone 6 mm	1002622
1	Glycerine, 85%, 250 ml	1007027
Additionally recommended		
1	Set of 10 Beakers, Low Form	1002872
2	Graduated Cylinder, 100 ml	1002870
1	Funnel	
	Distilled Water, 5 l	

BASIC PRINCIPLES

The viscosity of a fluid results from the mutual bonding interaction between the fluid's atoms or molecules. The component particles are less mobile the stronger the bonding. It then requires a greater shear stress for a velocity gradient to form in a flow profile. The proportionality between the velocity gradient and the shear stress is a measure of how viscous the fluid is, in this case its dynamic or shear viscosity. Fluids in which the dynamic viscosity is not dependent on the shear stress are known as Newtonian fluids.

The dynamic viscosity η of most fluids decreases with increasing temperature. This decrease can often be described with the help of the Andrade equation.

$$(1) \quad \eta = \eta_0 \cdot \exp\left(\frac{E_A}{R \cdot T}\right)$$

E_A : activation energy of atoms/molecules in the fluid
 T : absolute temperature

$$R = 8,314 \frac{\text{J}}{\text{mol} \cdot \text{K}} : \text{universal gas constant}$$

Dynamic viscosity is often measured by observing how a sphere sinks through a fluid as a result of gravity. The sinking is slowed by so-called Stokes' drag

$$(2) \quad F_1 = \eta \cdot 6\pi \cdot r \cdot v$$

r : radius of sphere

This causes it to fall with a constant velocity v . The effect of gravity is lessened by the updraft of the fluid on the sphere:

$$(3) \quad F_2 = \frac{4\pi}{3} \cdot r^3 \cdot (\rho_0 - \rho) \cdot g$$

ρ_0 : density of sphere

ρ : density of fluid being investigated

g : acceleration due to gravity

This results in equilibrium between the forces F_1 and F_2 :

$$(4) \quad \eta = \frac{2}{9} \cdot r^2 \cdot g \cdot (\rho_0 - \rho) \cdot \frac{t}{s}$$

s : distance

t : time taken to sink the above distance

In fact, equation (2) only describes the drag on the sphere in cases where the diameter of the measuring cylinder filled with the fluid is much greater than that of the sphere. This would necessitate using a large quantity of the test fluid. In practice therefore, it is common to use a Höppler falling sphere viscosimeter, which uses a cylinder inclined to the vertical, such that the sphere descends by rolling and slipping down the side of the tube. In this case, the equation for the dynamic viscosity is as follows:

$$(5) \quad \eta = t \cdot (\rho_0 - \rho) \cdot K$$

The calibration factor K is individually quoted for each sphere supplied by the manufacturer. In order to avoid any systematic errors, the measuring cylinder can be inverted, so that the time the sphere takes to sink back to where it started can be measured as well.

This experiment studies common or garden glycerine, which is actually made up of an aqueous solution of glycerine with a glycerine content of roughly 85%. This dilution is intentional, since the viscosity of pure glycerine is too high for many applications. The viscosity is measured as a function of temperature. For this purpose, the viscosimeter is linked to a circulation thermostat. By diluting the glycerine solution to

a specific extent with distilled water, it is also possible to measure how the viscosity depends on concentration.

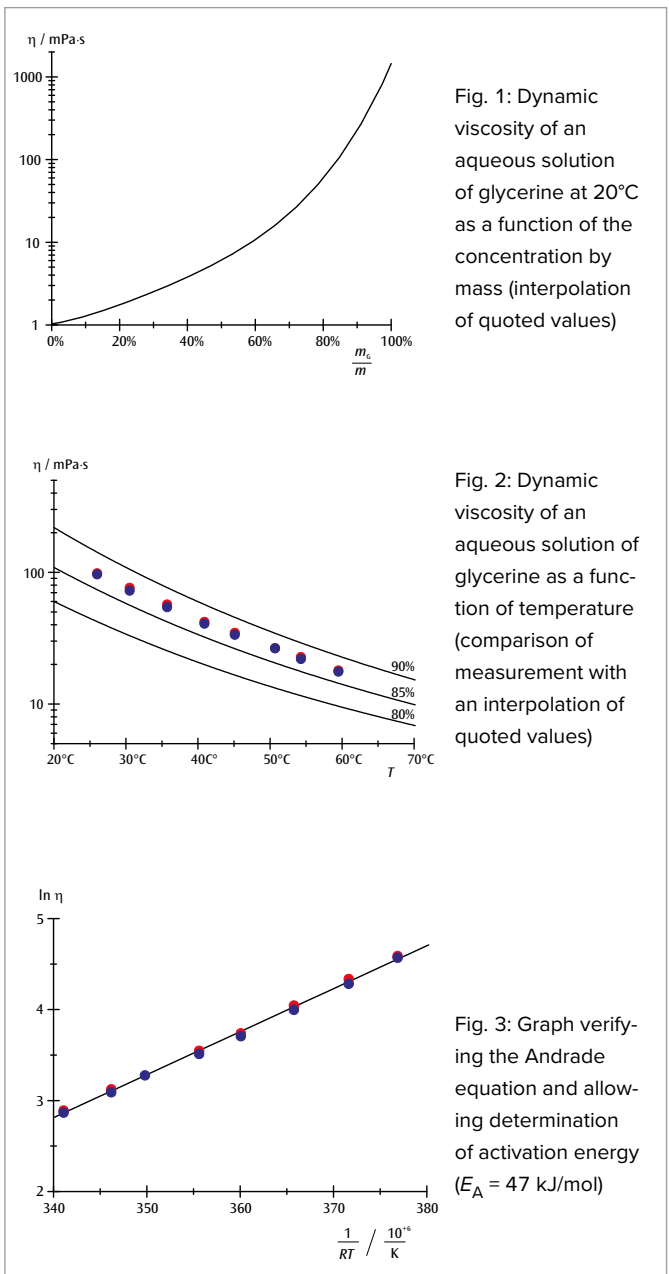
EVALUATION

Comparing the measured viscosity with values quoted in literature confirms the values specified by the manufacturer.

Equation (1) can be rearranged into the following form:

$$\ln \eta = \ln \eta_0 + E_A \cdot \frac{1}{R \cdot T}$$

This means $y = \ln \eta$ can be plotted against $x = \frac{1}{R \cdot T}$ and the activation energy E_A can be determined from the gradient of the resulting straight lines.



UE1080400 | SURFACE TENSION



OBJECTIVE

Measure the surface tension by the “break-away” method

SUMMARY

To determine the surface tension of a liquid, a blade is immersed horizontally in the liquid and is slowly pulled out upwards while measuring the pulling force. The lamella of liquid that forms at the blade “breaks away” when the force exceeds a certain value. From this force and the length of the blade one can calculate the surface tension.

> EXPERIMENT PROCEDURE

- Forming a lamella of liquid between a ring-shaped blade and the surface of the liquid by slowly lifting the ring out of the liquid.
- Measuring the pulling force shortly before the liquid lamella breaks away.
- Determining the surface tension from the measured pulling force.

REQUIRED APPARATUS

Quantity	Description	Item Number
1	Surface Tension Ring	1000797
1	Precision Dynamometer 0,1 N	1003102
1	Beaker	1002872
1	Laboratory Jack II	1002941
1	Tripod Stand 150 mm	1002835
1	1 Stainless Steel Rod 750 mm	1002935
1	Clamp with Hook	1002828
1	Callipers, 150 mm	1002601

BASIC PRINCIPLES

The surface tension of a liquid is a property of the interface between the liquid and the air in contact with it. It results from the fact that a molecule of the liquid at the surface only experiences the forces from its neighboring molecules at one side, whereas a molecule within the liquid experiences forces from all sides (see Fig. 1). Consequently, the molecule at the surface experiences a net force perpendicular to the surface towards the interior of the liquid. Therefore, in order to increase the surface area by bringing more molecules to the surface, a supply of energy is required.

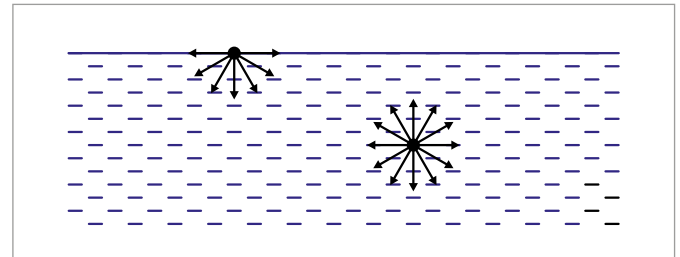


Fig. 1: Interaction forces exerted by neighboring molecules on a liquid molecule at the surface and a molecule in the interior of the liquid

The quotient

$$(1) \quad \sigma = \frac{\Delta E}{\Delta A}$$

resulting from energy ΔE added at a constant temperature divided by the increase in the surface area ΔA , is called surface tension or surface energy density.

To illustrate the meaning of this definition, consider the example of the ring-shaped blade which is initially completely immersed in the liquid. If the ring is slowly pulled out of the liquid, a lamella of liquid is also drawn upwards at its bottom edge (see Fig. 2). When the ring is lifted by an additional distance Δx , the total surface area of the lamella at the outside and inside of the ring increases by

$$(2) \quad \Delta A = 4 \cdot \pi \cdot R \cdot \Delta x$$

where R : radius of the ring.

For this, a force

$$(3) \quad F_0 = \frac{\Delta E}{\Delta x}$$

must be applied. If the force applied while lifting the ring exceeds F_0 , the liquid lamella breaks away.

In the experiment, a metal ring with a sharp lower edge hangs in a horizontal position from a precision dynamometer. At first, the ring is completely immersed in the test liquid (e.g. water), then it is slowly pulled upwards out of the liquid. The lamella of liquid breaks away when the pulling force F exceeds the limiting value F_0 .

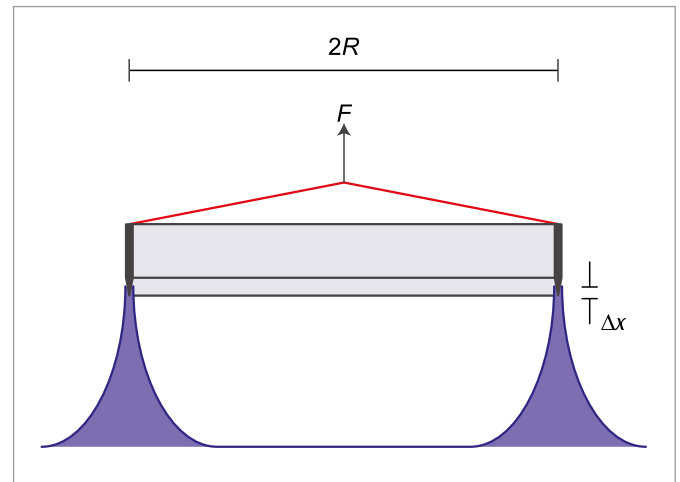


Fig. 2: Schematic diagram

EVALUATION

From Equations (1), (2) and (3),

$$F_0 = \frac{\Delta E}{\Delta x} = 4 \cdot \pi \cdot R \cdot \sigma$$

Thus, the equation for determining surface tension is

$$\sigma = \frac{F_0}{4 \cdot \pi \cdot R}$$

UE1090200 | BENDING OF FLAT BEAMS



OBJECTIVE

Measurement of deformation of flat beams supported at both ends and determination of modulus of elasticity

SUMMARY

A flat, level beam's resistance to deformation in the form of bending by an external force can be calculated mathematically if the degree of deformation is much smaller than the length of the beam. The deformation is proportional to the modulus of elasticity E of the material from which the beam is made. In this experiment, the deformation due to a known force is measured and the results are used to determine the modulus of elasticity for both steel and aluminium.

> EXPERIMENT PROCEDURE

- Measure the deformation profile with loads in the center and loads away from the center.
- Measure the deformation as a function of the force.
- Measure the deformation as a function of the length, width and breadth as well as how it depends on the material and determine the modulus of elasticity of the materials.

REQUIRED APPARATUS

Quantity	Description	Item Number
1	Apparatus for Measuring Young's Modulus	1018527
1	Young's Modulus Supplementary Set	1018528
1	Pocket Measuring Tape, 2 m	1002603
1	External Micrometer	1002600

BASIC PRINCIPLES

A flat, level beam's resistance to deformation in the form of bending by an external force can be calculated mathematically if the degree of deformation is much smaller than the length of the beam. The deformation is proportional to the modulus of elasticity E of the material from which the beam is made. Therefore the deformation due to a known force can be measured and the results are used to determine the modulus of elasticity.

For the calculation, the beam is sliced into parallel segments which are compressed on the inside by the bending and stretched on the outside. Neutral segments undergo no compression or extension. The relative extension or compression ϵ of the other threads and the associated tension σ depends on their distance z from the neutral segments:

$$(1) \quad \epsilon(z) = \frac{s + \Delta s(z)}{s} = \frac{z}{\rho(x)} \quad \text{and} \quad \sigma(z) = E \cdot \epsilon(z)$$

$\rho(x)$: Local radius of curvature due to bending

The curvature therefore involves the local bending moment:

$$(2) \quad M(x) = \int_A \sigma(z) \cdot z \cdot dA = \frac{1}{\rho(x)} \cdot E \cdot I$$

where $I = \int_A z^2 \cdot dA$: Area moment of inertia

As an alternative to the radius of curvature $\rho(x)$, in this experiment the deformation profile $w(x)$, by which the neutral segments are shifted from their rest position, will be measured. This can be calculated as follows, as long as the changes $dw(x)/dx$ due to the deformation are sufficiently small:

$$(3) \quad \frac{d^2 w}{dx^2}(x) = \frac{1}{\rho(x)} = \frac{M(x)}{E \cdot I}$$

the deformation profile is obtained from this by double integration. A typical example is to observe a beam of length L , which is supported at both ends and to which a downward force F acts at a point a . In a state of equilibrium the sum of all the forces acting is zero:

$$(4) \quad F_1 + F_2 - F = 0$$

Similarly, the sum of all the moments acting on the beam at an arbitrary point x is also zero:

$$(5) \quad M(x) - F_1 \cdot x - F_2 \cdot (L-x) + F \cdot (a-x) = 0$$

No curvature or deformation arises at the ends of the beam, i.e. $M(0) = M(L) = 0$ and $w(0) = w(L) = 0$. This means that $M(x)$ is fully determinable:

$$(6) \quad M(\zeta) = \begin{cases} F \cdot L \cdot (1-\alpha) \cdot \zeta; & 0 \leq \zeta \leq \alpha \\ F \cdot L \cdot \alpha \cdot (1-\zeta); & \alpha < \zeta \leq 1 \end{cases}$$

$$\text{where } \zeta = \frac{x}{L} \text{ and } \alpha = \frac{a}{L}$$

The deformation profile is obtained by double integration

$$(7) \quad w(\zeta) = \frac{F \cdot L^3}{E \cdot I} \cdot \left[(1-\alpha) \cdot \frac{\zeta^3}{6} - \left(\frac{\alpha^3}{6} - \frac{\alpha^2}{2} + \frac{\alpha}{3} \right) \cdot \zeta \right]$$

$$\frac{F \cdot L^3}{E \cdot I} \cdot \left[\frac{\alpha^3}{6} - \left(\frac{\alpha^3}{6} + \frac{\alpha}{3} \right) \zeta + \frac{\alpha}{2} \cdot \zeta^2 - \frac{\alpha}{6} \zeta^3 \right]$$

In the experiment the shape of this profile is checked for load at the center ($\alpha = 0.5$) and off-center ($\alpha < 0.5$).

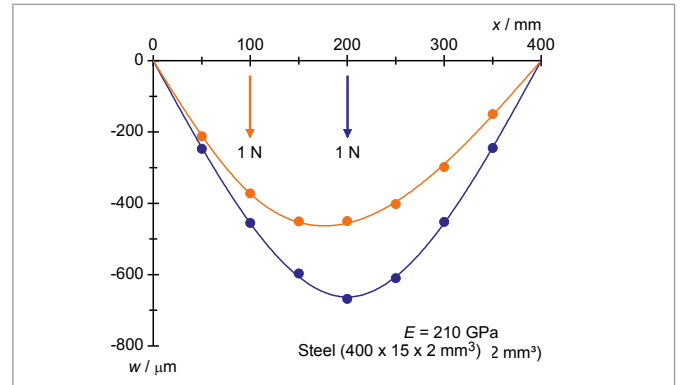


Fig. 2: Measured and calculated deformation profile for load acting at center and off-center

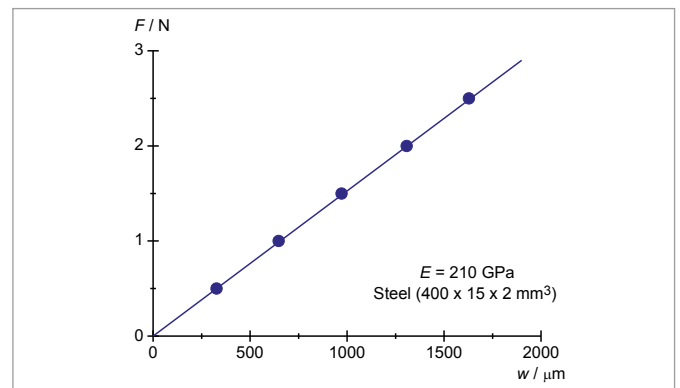


Fig. 3: Confirmation of Hooke's law

EVALUATION

When the load is in the center, then $w(x = \frac{L}{2}, a = \frac{L}{2}) = -\frac{F \cdot L^3}{48 \cdot E \cdot I}$.

For a rectangle of width b and height d , the following calculation is made:

$$I = \int_A z^2 \cdot dA = \int_{-\frac{d}{2}}^{\frac{d}{2}} z^2 \cdot b \cdot dz = \frac{d^3}{12} \cdot b$$

$$\text{Then } w(x = \frac{L}{2}, a = \frac{L}{2}) = -\frac{1}{4} \cdot \frac{F}{E} \cdot \frac{L^3}{d^3} \cdot \frac{1}{b}$$

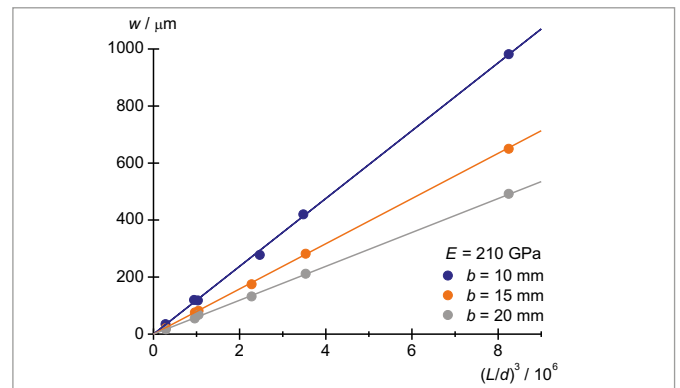


Fig. 4: How the deformation depends on $(L/d)^3$

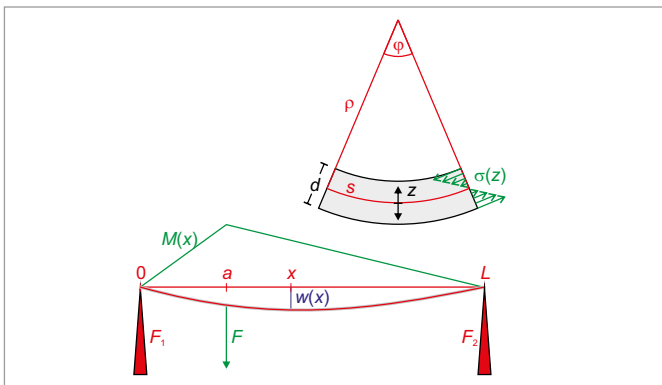


Fig. 1: Sketch of the deformation profile.

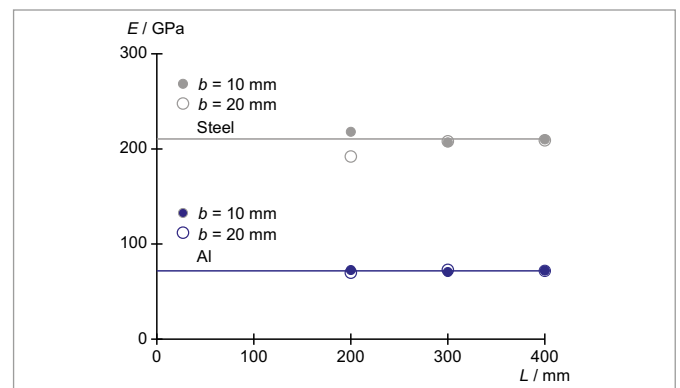


Fig. 5: Modulus of elasticity of steel and aluminium

UE1090300 | TORSION ON CYLINDRICAL RODS

OBJECTIVE

Determination of torsional coefficients and shear modulus

SUMMARY

In order for solid bodies to be deformed, an external force needs to be applied. This acts against the body's own resistance to deformation, which is dependent on the material from which the body is made, as well as its geometry and the direction of the applied force. The deformation is reversible and proportional to the applied force as long as that force is not too great. One example which is often investigated is torsion applied to a uniform cylindrical rod which is fixed at one end. The resistance of the rod to deformation can be numerically analyzed and determined by building a set-up which is capable of oscillating involving the rod itself and a pendulum disc and then measuring the period of the oscillation.



> EXPERIMENT PROCEDURE

- Determine the torsional coefficients of cylindrical rods as a function of their length.
- Determine the torsional coefficients of cylindrical rods as a function of their diameter.
- Determine the torsional coefficients of cylindrical rods made of various materials and also find their shear modulus.

REQUIRED APPARATUS

Quantity	Description	Item Number
1	Torsion Apparatus	1018550
1	Supplementary Set for Torsion Apparatus	1018787
1	Photo Gate	1000563
1	Digital Counter (230 V, 50/60 Hz)	1001033 or
	Digital Counter (115 V, 50/60 Hz)	1001032

BASIC PRINCIPLES

In order for solid bodies to be deformed, an external force needs to be applied. This acts against the body's own resistance to deformation, which is dependent on the material from which the body is made, as well as its geometry and the direction of the applied force. The deformation is elastic, reversible and proportional to the applied force as long as that force is not too great.

One example which is often investigated is torsion applied to a uniform cylindrical rod which is fixed at one end because the resistance of the rod to deformation can be numerically analyzed. This involves considering the rod broken down into radial and cylindrical segments of length L . As long as the rod does not bend, then the torsion applied to the rod at the non-fixed end which twists that end of the rod by a small angle ψ causes each of the segments, which are all of radius r , to twist by the following angle:

$$(1) \quad \alpha_r = \frac{r}{L} \cdot \psi$$

(see Fig. 1). The shearing stress would then be:

$$(2) \quad \tau_r = \frac{dF_{r,\varphi}}{dA_{r,\varphi}} = G \cdot \alpha_r$$

G: Shear modulus of the rod's material

The component of the force $dF_{r,\varphi}$ acting in tangential direction at the face of the rod:

$$(3) \quad \Delta A_{r,\varphi} = r \cdot d\varphi \cdot dr$$

is given by:

$$(4) \quad dF_{r,\varphi} = G \cdot \frac{r^2}{L} \cdot \psi \cdot d\varphi \cdot dr$$

It is then easy to calculate the force dF_r required for the torsion to twist the whole of a hollow cylinder of radius r by an angle ψ along with the corresponding torque dM_r :

$$(5) \quad dM_r = r \cdot dF_r = G \cdot 2\pi \cdot \frac{r^3}{L} \cdot \psi \cdot dr$$

Then for a solid rod of radius r_0 , the torsion can be found as follows:

$$(6) \quad M = \int_0^{r_0} dM_r = D \cdot \psi \quad \text{where} \quad D = G \cdot \frac{\pi}{2} \cdot \frac{r_0^4}{L}$$

The torque M remains proportional to the angle of twist resulting from the torsion ψ , i.e. the torsional coefficient D is constant, as long as the torque M is not too large. If the torque is too high, then the deformation becomes plastic and irreversible.

In order to determine the torsional coefficient in this experiment, a pendulum disc is coupled to the non-fixed end of the rod. As long as the angle of deflection is not too great, the disc will oscillate about the torsional axis with a period

$$(7) \quad T = 2\pi \cdot \sqrt{\frac{J}{D}}$$

J : Moment of inertia of pendulum disc

As long as the moment of inertia is known, the torsional coefficient can be determined from the period of oscillation. To be more precise, the overall moment of inertia is split into the moment of inertia J_0 for the pendulum disc and the moment of inertia of the two additional weights m , which are situated at a radius R around the torsional axis:

$$(8) \quad J = J_0 + 2 \cdot m \cdot R^2$$

The period of oscillation T for the pendulum disc with the additional weights is then measured along with the period of oscillation T_0 for the pendulum disc without the weights.

EVALUATION

The equation for determining the torsional coefficient is derived from equations (7) and (8) as follows:

$$D = 4\pi^2 \cdot \frac{2 \cdot m \cdot R^2}{T^2 - T_0^2}$$

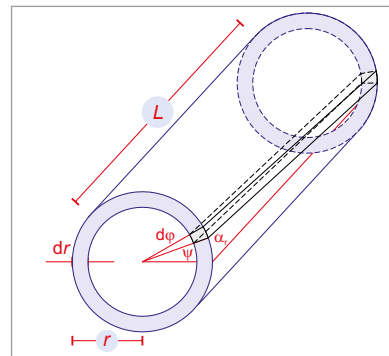


Fig. 1: Schematic for the calculation of the torque dM_r needed to apply torsion on a hollow cylinder of length L , radius r and shell thickness d_r .

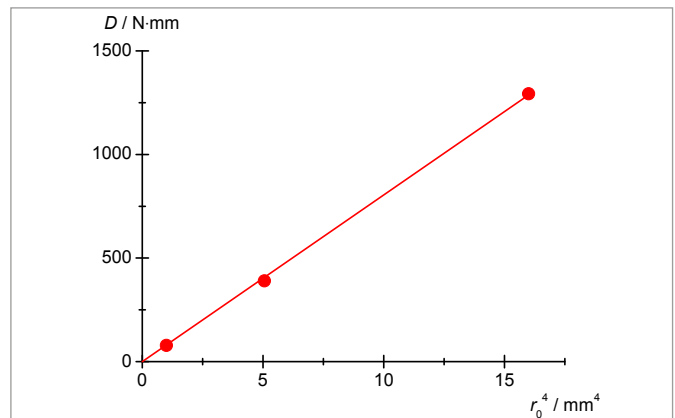


Fig. 2: Torsional coefficient of aluminium rods 500 mm in length as a function of r_0^4 .

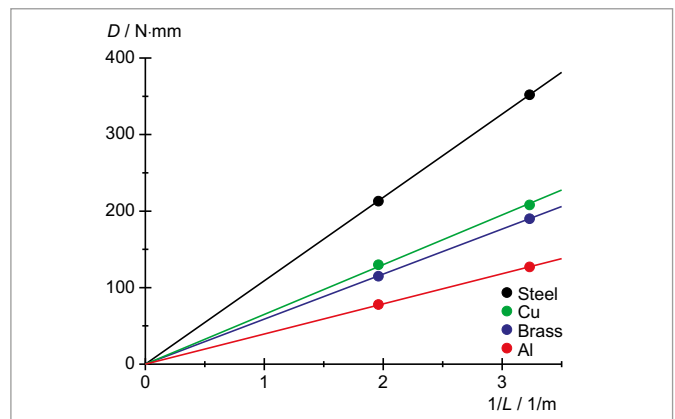


Fig. 3: Torsional coefficient of cylindrical rods as a function of $1/L$.

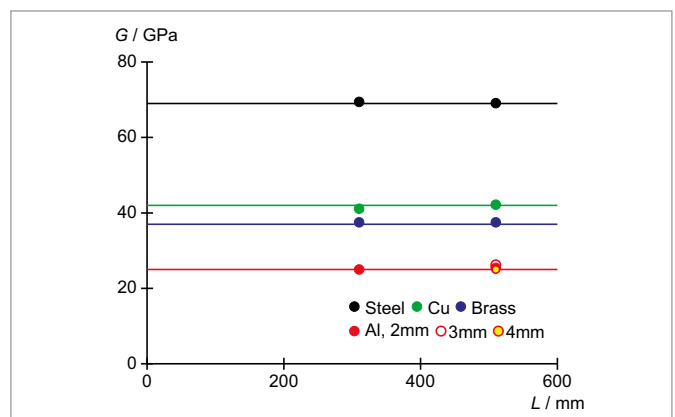


Fig. 4: Shear modulus G of the rods as a function of Length L of the rods as a function of L

UE2010130

THERMAL EXPANSION OF SOLID BODIES



EXPERIMENT PROCEDURE

- Measure thermal expansion in length for tubes made of brass, steel and glass.
- Determine linear expansion coefficients for these materials and compare them with values quoted in literature.

OBJECTIVE

Determine the coefficients of expansion for brass, steel and glass

SUMMARY

If solid bodies are heated up, they generally expand to a greater or lower degree. In this experiment, hot water is allowed to flow through tubes made of brass, steel and glass. The expansion in their length is measured using a dial gauge. The linear expansion coefficients for the three materials are then calculated from the change in their length.

REQUIRED APPARATUS

Quantity	Description	Item Number
1	Linear Expansion Apparatus D	1002977
1	Immersion/Circulation Thermostat (230 V, 50/60 Hz)	1008654 or
	Immersion/Circulation Thermostat (115 V, 50/60 Hz)	1008653
1	Gauge with Adapter	1012862
2	Tubing, Silicone 6 mm	1002622

NOTE

If it is deemed sufficient to measure the difference in length between room temperature and the temperature of boiling water, a steam generator can be used instead of the circulation thermostat bath.

BASIC PRINCIPLES

In a solid body, each atom vibrates around its equilibrium position. The oscillation is not harmonic because the potential energy is greater when two atoms which have moved from their equilibrium positions happen to get close to one another as opposed to when they are further apart. At higher temperatures, where the oscillation energy is also greater, the atoms vibrate in such a way that the average distance between two neighboring atoms is greater than the distance between their equilibrium positions. This effect becomes more predominant as the temperature increases, causing the solid body to expand even more as the temperature rises. It is normal in these circumstances to observe relative changes in length and to calculate the change in volume from this.

The coefficient of linear expansion is defined as:

$$(1) \quad \alpha = \frac{1}{L(\vartheta)} \cdot \frac{dL}{d\vartheta}$$

L : length

ϑ : temperature in °C

This coefficient depends strongly on the nature of the material and is usually less responsive to the temperature. This leads to the following conclusion:

$$(2) \quad L(\vartheta) = L_0 \cdot \exp(\alpha \cdot \vartheta)$$

$$L_0 = L(0^\circ\text{C})$$

If the temperature is not very high:

$$(3) \quad L(\vartheta) = L_0 \cdot (1 + \alpha \cdot \vartheta)$$

In this experiment measurements are carried out on thin tubes made of brass, steel and glass, through which hot water is passed in order to increase their temperature. A circulation thermostat is used to ensure that the water temperature can be adjusted to a constant value. Since one end of the tubes will be fixed in the expansion apparatus, a dial gauge can be used to read off the increase in length at the other end, using room temperature as the reference temperature.

EVALUATION

In the temperature range under investigation $\alpha \cdot \vartheta \ll 1$.

Equation (3) can therefore be modified where

$$\Delta L = L(\vartheta_1) \cdot \alpha \cdot \Delta\vartheta \quad \text{where} \quad \Delta\vartheta = \vartheta_2 - \vartheta_1$$

$$L(\vartheta_1) = 600 \text{ mm}$$

The linear expansion coefficients we are seeking can therefore be determined from the gradient of the straight lines through the origin, as shown in Fig. 1.

The derivation of equation (3) breaks down, though, when higher temperatures are observed, since α proves to be no longer constant, instead being dependent on the temperature. Indeed, strictly speaking that is also the case at the temperatures we are observing. Since the measurement of the linear expansion is measured to an accuracy of 0.01 mm, precise analysis shows that the measurements are not exactly linear, especially for brass, and that the linear expansion coefficients increase slightly with temperature.

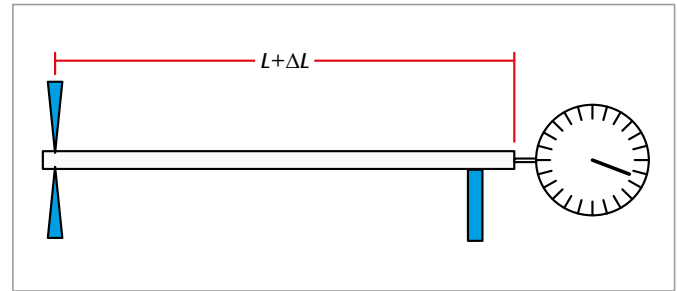


Fig. 1: Schematic of the set-up for the measurements

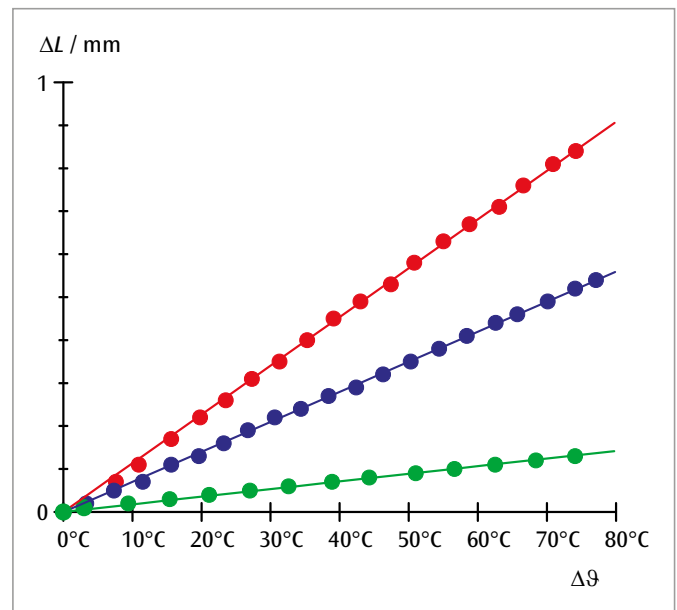


Fig. 2: Change in length of brass (red), steel (blue) and glass (green) as a function of the difference in temperature



Fig. 3: Set-up with steam generator

UE2010301 | WATER ANOMALY



EXPERIMENT PROCEDURE

- Measure the thermal expansion of water over a temperature range between 0°C and 15°C.
- Demonstrate the thermal anomaly.
- Determine the temperature when the density is at a maximum.

OBJECTIVE

Determine the temperature where water reaches its maximum density

SUMMARY

When temperature is raised from 0°C to about 4°C the volume of a mass of water initially becomes smaller and only begins to expand thermally at higher temperatures. The density of water is therefore at its greatest at around 4°C.

REQUIRED APPARATUS

Quantity	Description	Item Number
1	Device for Demonstrating the Anomaly of Water	1002889
1	Plastic Trough	4000036
1	Magnetic Stirrer	1002808
1	Digital Thermometer, 1 Channel	1002793
1	K-Type NiCr-Ni Immersion Sensor, -65°C – 550°C	1002804
Additionally recommended		
1	Tubing, Silicone 6 mm	1002622
1	Stainless Steel Rod 470 mm	1002934
1	Clamp with Jaw Clamp	1002829
1	Tripod Stand 150 mm	1002835
1	Funnel	

BASIC PRINCIPLES

Water is unlike most other materials in that up to a temperature of about 4°C it initially contracts and only starts expanding at higher temperatures. Since the density is inversely related to the volume of a mass, water thus reaches its maximum density at about 4°C.

The experiment involves measuring the expansion of water in a vessel with a riser tube. The height h to which water rises up the tube is measured as a function of the water temperature ϑ . Neglecting the fact that the glass vessel also expands at higher temperatures, the total volume of the water in the vessel and in the tube is given by:

$$(1) \quad V(\vartheta) = V_0 + \pi \cdot \frac{d^2}{4} \cdot h(\vartheta)$$

d : Internal diameter of tube, V_0 : Volume of vessel

If the expansion of the vessel is taken into account, equation (1) becomes

$$(2) \quad V(\vartheta) = V_0 \cdot (1 + 3 \cdot \alpha \cdot \vartheta) + \pi \cdot \frac{d^2}{4} \cdot h(\vartheta)$$

$\alpha = 3.3 \cdot 10^{-6} \text{ K}^{-1}$: Linear expansion coefficient of glass

EVALUATION

Water density ρ is derived from equations (1) and (2) as follows:

$$\frac{\rho(\vartheta)}{\rho(0^\circ\text{C})} = \frac{V_0 + \pi \cdot \frac{d^2}{4} \cdot h(0^\circ\text{C})}{V_0 \cdot (1 + 3 \cdot \alpha \cdot \vartheta) + \pi \cdot \frac{d^2}{4} \cdot h(\vartheta)}$$

The maximum for this expression is at $\vartheta = 3.9^\circ\text{C}$.

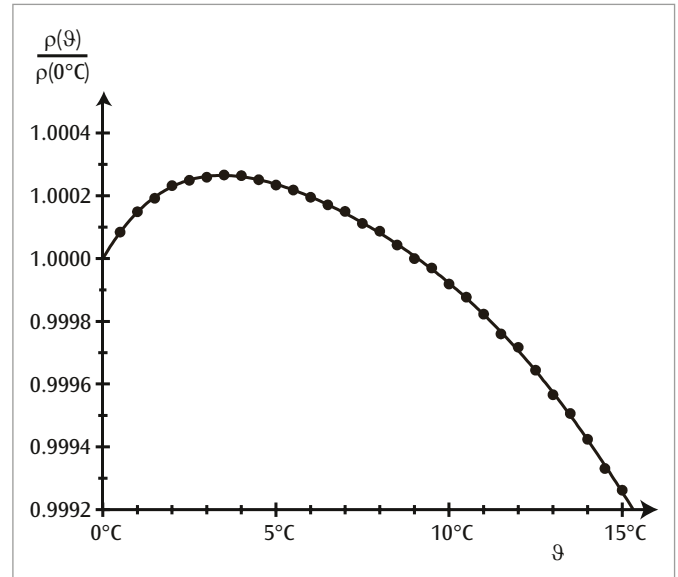


Fig. 1: Relative density of water as a function of temperature

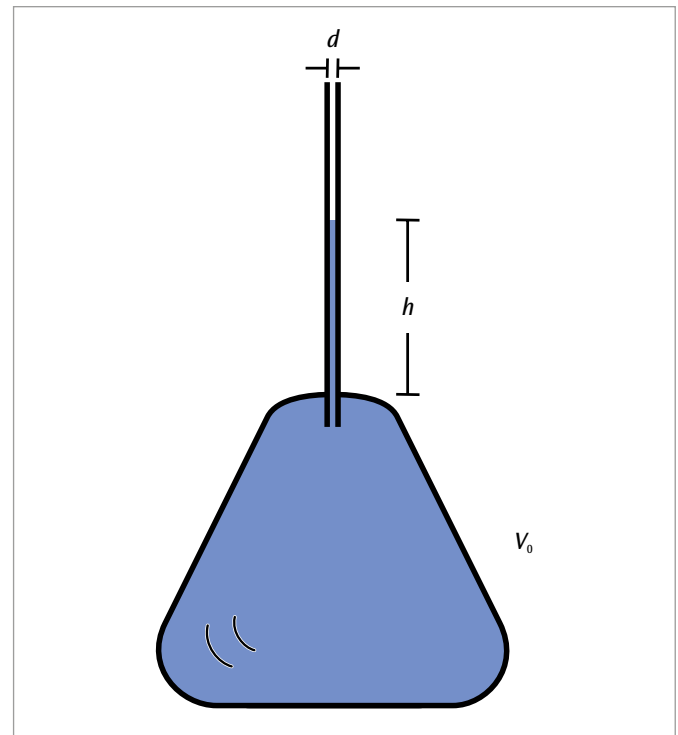


Fig. 2: Vessel with riser tube

UE2020100 | HEAT CONDUCTION



EXPERIMENT PROCEDURE

- Measure how temperature changes with time along metal bars which are heated at one end but remain cool at the other in both dynamic and steady states.
- Measure the flow of heat in the steady state.
- Determine the heat conductivity of the material from which the bar is made.

OBJECTIVE

Measure conduction of heat in metal bars

SUMMARY

Conduction of heat involves heat being transferred from a hotter part of an object to a colder area by means of the interaction between neighboring atoms or molecules, although the atoms themselves remain in place. In a cylindrical metal bar with ends maintained at different temperatures, a temperature gradient will emerge along the bar after a while. The temperature decreases uniformly from the warm end to the cold end and a constant flow of heat arises through the bar. The way the situation changes from a dynamic state to a steady state is observed by means of repeated measurements to determine the temperatures at various measurement points. The metal bars are electrically heated so that the flow of heat in the steady state can be determined from the electrical power supplied.

REQUIRED APPARATUS

Quantity	Description	Item Number
1	Heat Conduction Equipment Set	1017329
1	Heat Conducting Rod Al	1017331
1	Heat Conducting Rod Cu	1017330
1	DC Power Supply 0 – 20 V, 0 – 5 A (230 V, 50/60 Hz)	1003312 or
	DC Power Supply 0 – 20 V, 0 – 5 A (115 V, 50/60 Hz)	1003311
1	Digital Quick Response Pocket Thermometer	1002803
1	K-Type NiCr-Ni Immersion Sensor, -65°C – 550°C	1002804
1	Pair of Safety Experimental Leads, 75 cm, red/blue	1017718
1	Set of 10 Beakers, Low Form	1002872

BASIC PRINCIPLES

Heat can be transported from a hotter area to a colder one by conduction, radiation or convection. Conduction of heat involves heat being transferred from a hotter part of an object to a colder area by means of the interaction between neighboring atoms or molecules, although the atoms themselves remain in place. For instance, when a metal bar is heated, the atoms at the hotter end vibrate more vigorously than those at the cooler end, i.e. they vibrate with more energy. Energy is transferred due to collisions between neighboring atoms, passing the energy from one atom to another and thereby conducting it along the bar. Metals are particularly good conductors of heat since collisions also occur between atoms and free electrons.

In a bar with a cross-sectional area of A , when the ends are maintained at different temperatures, after a while a temperature gradient emerges along the bar, whereby the temperature decreases uniformly along the length towards the cold end. In a time period dt a quantity of heat dQ flows through the cross-section of the bar and there arises a constant flow of heat P_Q :

$$(1) \quad P_Q = \frac{dQ}{dt} = \lambda \cdot A \cdot \frac{dT}{dx}$$

P_Q : Flow of heat (measured in watts)
 A : Cross-sectional area of bar

λ : Heat conductivity of material from which the bar is made
 T : Temperature, x : Coordinate of length along the bar

Before the constant temperature gradient arises, the temperature distribution at a specific time t is given by $T(x,t)$, which gradually becomes closer to the steady state. The following differential equation then applies

$$(2) \quad \lambda \cdot \frac{\partial^2 T}{\partial x^2}(x,t) - c \cdot \rho \cdot \frac{\partial T}{\partial t}(x,t) = 0$$

c : Specific heat capacity
 ρ : Density of material from which bar is made

In the steady state the situation is in agreement with equation (1)

$$(3) \quad \frac{\partial T}{\partial t}(x,t) = 0 \quad \text{and} \quad \lambda \cdot \frac{\partial T}{\partial x}(x,t) = \text{const.} = \frac{P_Q}{A}$$

In this experiment the bar is heated at one end by electrical means. An electronically regulated source of heat provides the bar with an amount of heat which can be determined by measuring the heater voltage U and current I :

$$(4) \quad P_{el} = U \cdot I$$

Electronic regulation of the current ensures that this end of the bar rapidly reaches a temperature of about 90°C and this temperature is then maintained constant.

The other end of the bar is kept at the temperature of melting ice or simply water at room temperature via its cooling baffles. This allows the heating to be determined by calorimetry.

An insulating sleeve minimises the loss of heat from the bar to its surroundings and ensures the temperature profile is more linear in the steady state. Using an electronic thermometer that determines temperature within a second, temperatures are measured at pre-defined measurement points along the bar. Both a copper bar and an aluminum bar are provided.

EVALUATION

The flow of heat P_Q corresponds to the electrical power P_{el} minus a small quantity of power dissipated due to losses

$$P_Q; P_Q = P_{el} - P_l$$

$$\text{Therefore: } \lambda = \frac{P_{el} - P_l}{A} \cdot \frac{L}{T(0) - T(L)}$$

(L : Distance between selected temperature measurement points)

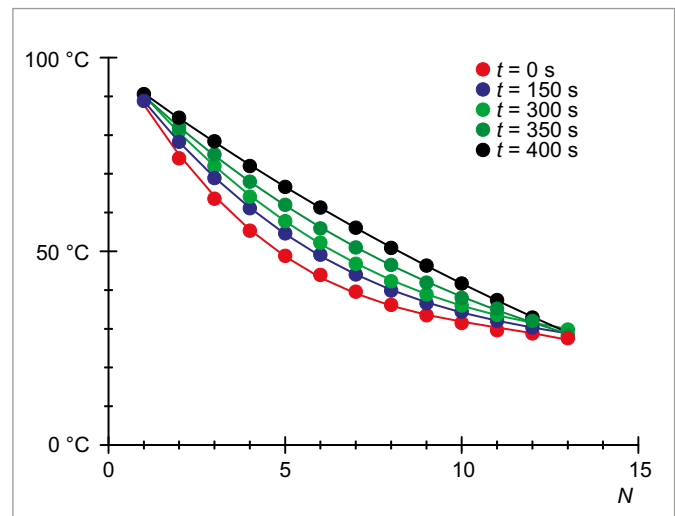


Fig. 1: Temperatures along the aluminum rod in five sets of measurements made at time intervals of 150 s



EXPERIMENT PROCEDURE

- Detect radiation from a Leslie cube with a Moll thermopile.
- Measure intensity of heat radiated by four different surfaces in relation to one another as a function of temperature.
- Confirm that the radiation intensities are proportional to T^4 .

OBJECTIVE

Measure the heat radiated by a Leslie cube

SUMMARY

The radiation emitted by a body depends on its temperature and the nature of its surface. More specifically, according to Kirchhoff's law, the ratio between emissivity and absorptivity is identical for all bodies at a given temperature and corresponds to emissivity of a black body E_{SB} at this temperature. In this experiment, we will heat a Leslie cube by filling it with water to a temperature of 100°C and ascertain the radiated intensity in a relative measurement using a Moll thermopile.

REQUIRED APPARATUS

Quantity	Description	Item Number
1	Leslie's Cube	1000835
1	Rotating Base for Leslie cube	1017875
1	Moll-Type Thermopile	1000824
1	Measurement Amplifier U (230 V, 50/60 Hz)	1020742 or
	Measurement Amplifier U (115 V, 50/60 Hz)	1020744
1	Digital Multimeter P3340	1002785
1	Digital Quick Response Pocket Thermometer	1002803
1	K-Type NiCr-Ni Immersion Sensor, $-65^\circ\text{C} - 550^\circ\text{C}$	1002804
2	Pair of Safety Experiment Leads, 75 cm	1002849
2	Barrel Foot, 500 g	1001046
1	Pocket Measuring Tape, 2 m	1002603

BASIC PRINCIPLES

Heat is exchanged between a body and its surroundings by the emission and absorption of heat radiation. The radiation depends on the body's temperature and the nature of its surface, as can be demonstrated by means of a Leslie cube.

The emitted intensity is described by the body's emissivity E . The absorptivity A is the ratio between absorbed and incident radiation intensity. It turns out that absorptivity increases with emissivity. More specifically, according to Kirchhoff's law, the ratio between emissivity and absorptivity is identical for all bodies at a given temperature, and corresponds to emissivity of a black body E_{SB} at this temperature:

$$(1) \quad \frac{E(T)}{A} = E_{SB}(T) = \sigma \cdot T^4$$

σ : Stefan-Boltzmann constant

T : Temperature in Kelvin

The degree to which absorptivity depends on temperature is generally negligible. Therefore the emissivity of a body can be described as follows:

$$(2) \quad E(T) = A \cdot \sigma \cdot T^4$$

If the body has the same temperature T_0 as its surroundings, the intensity of the heat radiated by the body into the surroundings is equal to that of the heat it absorbs from them:

$$(3) \quad E(T_0) = A \cdot \sigma \cdot T_0^4$$

If the body's temperature is higher, the intensity of the radiation absorbed from the surroundings does not change as long as the ambient temperature remains constant. Therefore, the energy radiated by a body per unit of surface and time and measurable by means of a radiation detector is as follows:

$$(4) \quad \Delta E(T) = A \cdot \sigma \cdot (T^4 - T_0^4)$$

In this experiment, a Leslie cube equipped with one white, one black, one matt and one shiny surface is heated by filling it with water boiled to a temperature of 100°C. The radiated intensity is then ascertained by means of a relative measurement using a Moll thermopile. The measured values for the four different surfaces are monitored during the entire process of cooling to room temperature.

EVALUATION

Plotting the readings against the quantity $x = T^4 - T_0^4$ results in four lines which pass through the origin and have slopes corresponding to the respective absorptivities of the surfaces.

In the investigated temperature range up to 100°C, there is no great difference between the black and white surfaces or between the matte and glossy surfaces, even though the visual distinction is clear. Obviously, the surfaces do not differ significantly in the infra-red wavelength range.

1: White surface. 2: Black surface. 3: Matt surface. 4: Shiny surface.

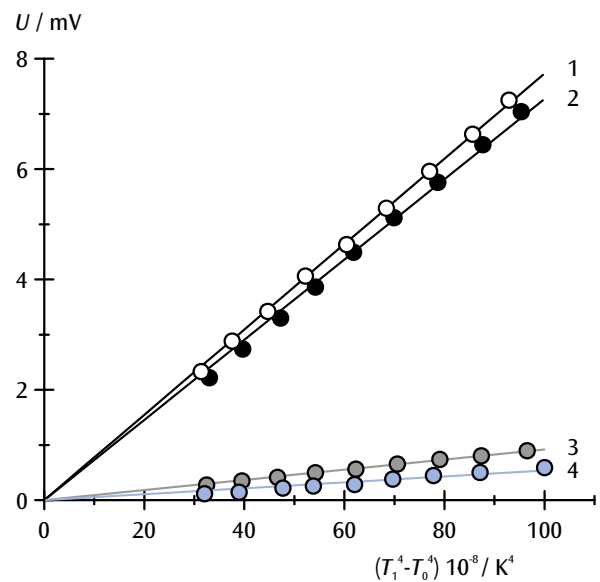


Fig 1: Radiated intensity from a Leslie cube as a function of $x = T^4 - T_0^4$

UE2030300 | INCREASE OF INTERNAL ENERGY BY MECHANICAL WORK



OBJECTIVE
Verifying the First Law of Thermodynamics

› EXPERIMENT PROCEDURE

- Measuring the temperature of the aluminum body as a function of the number of rotations against the friction cord.
- Investigating the proportionality between the temperature change and the frictional work, and thereby verifying the First Law of Thermodynamics.
- Determining the specific heat capacity of aluminum.

SUMMARY

The experiment is to investigate the increase of internal energy of an aluminum body caused by friction. The increase can be observed by measuring the increase in the temperature of the body, which is proportional to the work done, as the body undergoes no change in the state of aggregation and no chemical reaction occurs. To eliminate the effect of heat exchange between the aluminum body and the environment as far as possible, begin the series of measurements slightly below room temperature and end the series at a temperature slightly above room temperature. The difference below and above room temperature prior to starting the measurements and at the point of concluding them should approximately be the same.

REQUIRED APPARATUS

Quantity	Description	Item Number
1	Heat Equivalent Apparatus	1002658
1	Digital Multimeter P1035	1002781
1	Pair of Safety Experiment Leads, 75 cm	1017718

BASIC PRINCIPLES

According to the First Law of Thermodynamics, the change of the internal energy of a system ΔE is equal to the sum of the work performed ΔW and the transferred heat ΔQ . It can be measured as the proportional change in the temperature of the system ΔT , provided that there is no change in the state of aggregation and that no chemical reaction occurs.

The experiment is conducted to investigate the increase in the internal energy of an aluminum body caused by mechanical work. The cylindrical body is rotated about its axis by means of a hand-operated crank. A cord running over the curved surface provides the friction to heat the body. The frictional force F corresponds to the weight of a mass that is suspended from the end of the friction cord. The suspended mass is balanced by the frictional force. Therefore, the work performed against friction during n revolutions of the body is

$$(1) \quad \Delta W_n = F \cdot \pi \cdot d \cdot n$$

d : Diameter of the cylindrical body.

During the n revolutions, the frictional work raises the temperature of the body from the initial value T_0 to the final value T_n . At the same time the internal energy is increased by

$$(2) \quad \Delta E_n = m \cdot c_{Al} \cdot (T_n - T_0)$$

m : Mass of the body

c_{Al} : Specific heat capacity of aluminum.

To avoid a net exchange of heat with the environment as far as possible, the body is cooled, before starting the measurement, to an initial temperature T_0 that is only slightly below room temperature. The measurement is concluded as soon as the body reaches a final temperature T_n that is slightly above room temperature.

Note: The difference below and above room temperature prior to starting the measurements and at the point of concluding them should approximately be the same.

This ensures that the conversion of internal energy matches the work done. Thus, we have the following relation:

$$(3) \quad \Delta E_n = \Delta W_n$$

EVALUATION

From Equations 2 and 3, we derive the relation

$$T_n = T_0 + \frac{1}{m \cdot c_{Al}} \cdot \Delta W_n$$

It is therefore necessary to plot the measured final temperatures T_n as functions of the work performed W_n on a graph (see Fig. 1). The values measured in the vicinity of room temperature lie on a straight line. It is possible to determine the specific heat capacity of aluminum from its gradient. In the region below room temperature, the measured temperatures rise faster than would correspond to the gradient of the straight line, as the aluminum body absorbs heat from the surroundings. Conversely, in the region above room temperature heat is lost to the surroundings.

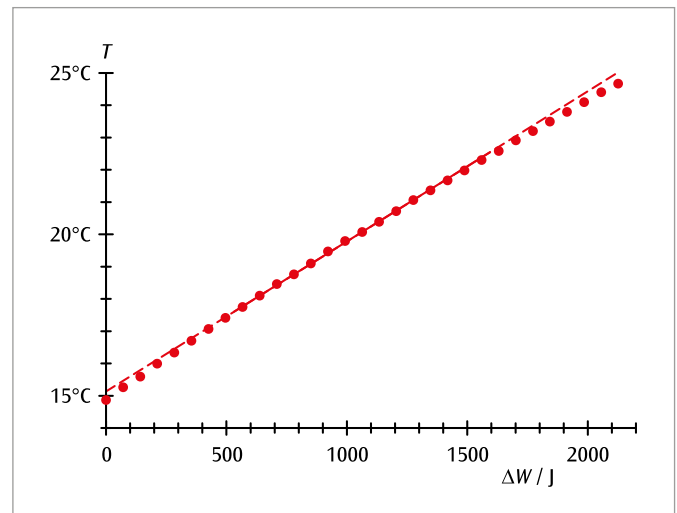


Fig. 1: The temperature of the aluminum body as a function of work performed against friction

UE2030400

INTERNAL ENERGY AND ELECTRICAL WORK



> EXPERIMENT PROCEDURE

- Measure the temperature of aluminum and copper calorimeters as a function of the electrical work done.
- Check that the change in temperature is proportional to the electrical work and verify the first law of thermodynamics.
- Determine the specific heat capacities of copper and aluminum.

OBJECTIVE

Increase internal energy by means of electrical work

SUMMARY

This experiment investigates how the internal energy of copper and aluminum calorimeters can be increased by electrical work. As long as the aggregate state does not change and no chemical reactions occur, it is possible to determine the increase in internal energy from the rise in temperature to which it is proportional. In order to prevent heat being transferred from the calorimeters to their surroundings, the series of measurements should start at a temperature somewhat below the ambient temperature and finish at a temperature only slightly above that of the surroundings.

REQUIRED APPARATUS

Quantity	Description	Item Number
1	Copper Calorimeter	1002659
1	Aluminum Calorimeter	1017897
1	Temperature Sensor	1017898
1	Pair of Adapter Cables with 4 mm Safety Plugs/2 mm Plugs	1017899
1	Pair of Safety Experimental Leads, 75 cm, red/blue	1017718
1	Digital Multimeter P1035	1002781
1	DC Power Supply 0 – 20 V, 0 – 5 A (230 V, 50/60 Hz)	1003312 or
	DC Power Supply 0 – 20 V, 0 – 5 A (115 V, 50/60 Hz)	1003311

BASIC PRINCIPLES

The internal energy of a system can be increased not only by mechanical work but also by electrical work. In both cases, the temperature of the system rises in linear proportion to the work done, as long as there is no change in the aggregate state and no chemical reactions occur.

This experiment investigates how the internal energy of copper and aluminum calorimeters is increased by electrical work. This is proportional to the applied voltage U , the current I which flows and the time the measurement is made t :

$$(1) \quad \Delta W_E(t) = U \cdot I \cdot t$$

This electrical work causes the temperature of the calorimeter to rise from an initial value T_0 to a final value T_n . Therefore the internal energy rises by the following amount:

$$(2) \quad \Delta E(t) = m \cdot c \cdot (T(t) - T_0)$$

m : mass of calorimeter

c : specific heat capacity of material

In order to minimise transfer of heat to the surroundings as far as possible, the calorimeter is initially cooled down to a start temperature of T_0 before any measurements are made. This should be only slightly lower than the ambient temperature. Measurement is halted when a final temperature T_n is attained, which is equally as far above the ambient temperature as the initial temperature was below it.

Under such conditions, the change in internal energy should be equal to the work done, meaning that the following applies:

$$(3) \quad \Delta E(t) = \Delta W_E(t)$$

EVALUATION

An NTC temperature sensor is used to measure the temperature T by measuring its resistance, which depends on the temperature. The following applies

$$T = \frac{217}{R^{0.13}} - 151$$

The temperatures measured in this way are plotted against the electrical work. The heat capacity of the calorimeters can be determined from the slope of straight lines in the graphs and as long as their mass is known, it is then possible to calculate the specific heat capacity.

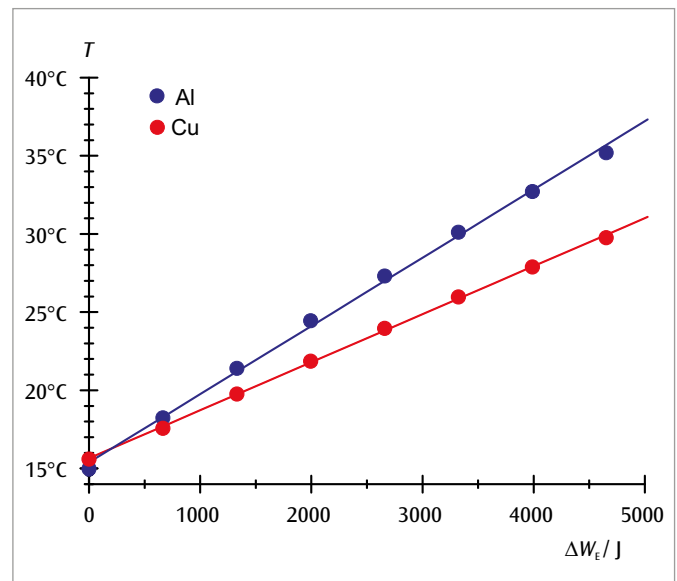


Fig. 1: Calorimeter temperature as a function of electrical work

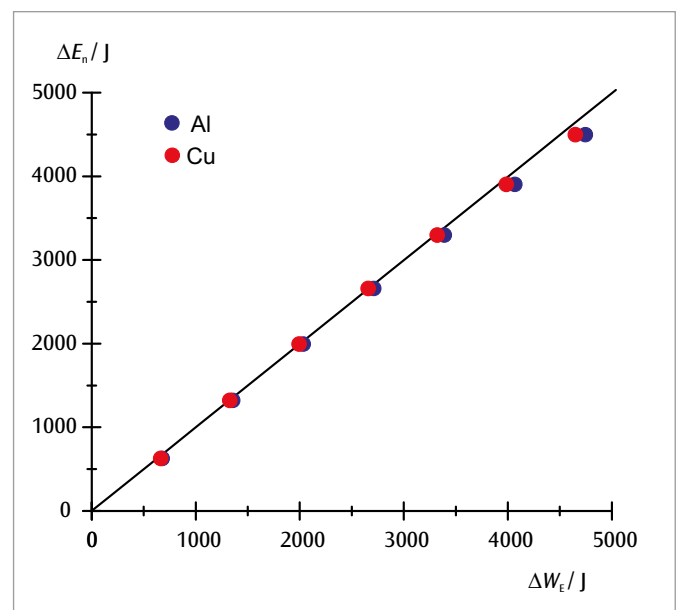


Fig. 2: Change in internal energy as a function of electrical work done

UE2040100 | BOYLE'S LAW



> EXPERIMENT PROCEDURE

- Measuring the pressure p of the enclosed air at room temperature for different positions s of the piston.
- Displaying the measured values for three different quantities of air in the form of a p - V diagram.
- Verifying Boyle's Law.

OBJECTIVE

Measurement at room temperature in air as an ideal gas

SUMMARY

The experiment verifies Boyle's Law for ideal gases at room temperature, taking air as an ideal gas in this experiment. The volume of a cylindrical vessel is varied by the movement of a piston, while simultaneously measuring the pressure of the enclosed air.

REQUIRED APPARATUS

Quantity	Description	Item Number
1	Boyle's Law Apparatus	1017366

BASIC PRINCIPLES

The volume of a fixed quantity of a gas depends on the pressure acting on the gas and on the temperature of the gas. If the temperature remains unchanged, the product of the volume and the temperature remains constant in many cases. This law, discovered by Robert Boyle and Edme Mariotte, is valid for all gases in the ideal state, which is when the temperature of the gas is far above the point that is called its critical temperature.

The law discovered by Boyle and Mariotte states that:

$$(1) \quad p \cdot V = \text{const.}$$

and is a special case of the more general law that applies to all ideal gases. This general law describes the relationship between the pressure p , the volume V , the temperature T referred to absolute zero, and the quantity n of the gas:

$$(2) \quad p \cdot V = n \cdot R \cdot T$$

$$R = 8.314 \frac{\text{J}}{\text{mol} \cdot \text{K}} \quad (\text{the universal gas constant}).$$

From the general equation (2), the special case (1) is derived given the condition that the temperature T and the quantity of the gas n do not change.

In the experiment, the validity of Boyle's Law at room temperature is demonstrated by taking air as an ideal gas. The volume V of air in a cylindrical vessel is varied by the movement of a piston, while simultaneously measuring the pressure p of the enclosed air.

The quantity n of the gas depends on the initial volume V_0 into which the air is admitted through an open valve before starting the experiment.

EVALUATION

As the cross-sectional area A of the piston is constant, the volume V of the enclosed air can easily be calculated from the distance s travelled by the piston relative to the zero-volume position. For an exact analysis, the unavoidable dead volume V_1 of the air in the manometer should also be taken into account.

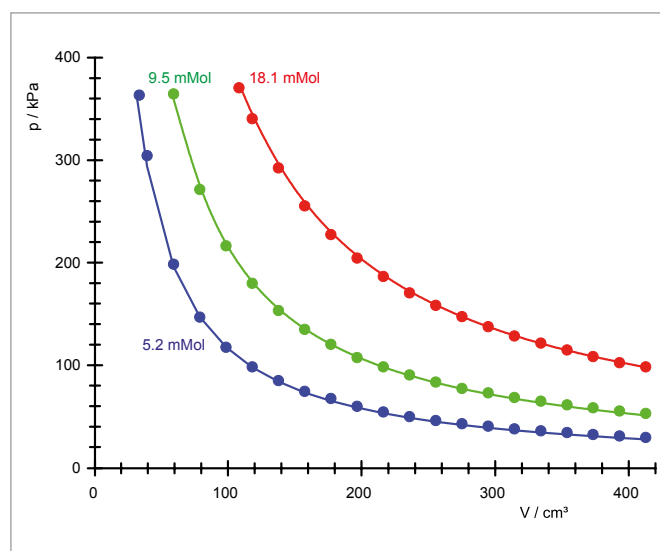


Fig. 1: Pressure/volume diagrams for three different quantities of air at room temperature

UE2040120 | AMONTONS' LAW



> EXPERIMENT PROCEDURE

- Point-by-point measurement of the pressure p of the enclosed air as a function of the temperature T .
- Plotting the measured values in a p - T diagram.
- Verification of Amontons' law.

OBJECTIVE

Verify the linear relationship between the pressure and temperature of an ideal gas

SUMMARY

The validity of Amontons' law for ideal gases is demonstrated using normal air. To demonstrate this, a volume of enclosed air located in a hollow metallic sphere is heated with the aid of a water bath while the temperature and pressure are being measured at the same time.

REQUIRED APPARATUS

Quantity	Description	Item Number
1	Jolly's Bulb and Gauge	1012870
1	Magnetic Stirrer with Heater (230 V, 50/60 Hz)	1002807 or
	Magnetic Stirrer with Heater (115 V, 50/60 Hz)	1002806
1	Digital Quick Response Pocket Thermometer	1002803
1	K-Type NiCr-Ni Immersion Sensor, -65°C – 550°C	1002804
1	Set of 10 Beakers, Low Form	1002872
1	Tripod Stand 150 mm	1002835
1	Stainless Steel Rod 250 mm	1002933
1	Bosshead	1002827
1	Universal Jaw Clamp	1002833

BASIC PRINCIPLES

The volume of a quantity of gas depends on the pressure the gas is under and on its temperature. When the volume and the gas quantity remain constant, the quotient comprising the pressure and the temperature remains constant. The law discovered by *Guillaume Amontons* applies for gases in the ideal state, i.e. when the temperature of the gas is far in excess of its so-called critical temperature.

The law discovered by Amontons

$$(1) \quad \frac{p}{T} = \text{const.}$$

is a special case of the universal gas law valid for all ideal gases, which describes the relationship between the pressure p , the volume V , temperature T relative to absolute zero and the mass n of a gas:

$$(2) \quad p \cdot V = n \cdot R \cdot T$$

$$R = 8,314 \frac{\text{J}}{\text{mol} \cdot \text{K}} : \text{universal gas constant}$$

Based on the generally applicable Equation (2), the special case (1) can be derived under the precondition that the volume V and the mass of the enclosed gas n do not change.

In the experiment the validity of Amontons' law is demonstrated using air as the ideal gas. To do this the enclosed volume of air located in a hollow metal sphere is heated up with the aid of a water bath. At the same time the temperature ϑ is measured in °C using a digital thermometer and the pressure p is measured using a manometer attached to the hollow sphere.

EVALUATION

The linear relationship between pressure and temperature is confirmed by fitting a straight line

$$(3) \quad p = a \cdot \vartheta + b$$

to the measurement points. By extrapolating the pressure p up to a value of 0, the absolute zero temperature can be determined:

$$(4) \quad \vartheta_0 = -\frac{b}{a} \text{ [}^\circ\text{C]}$$

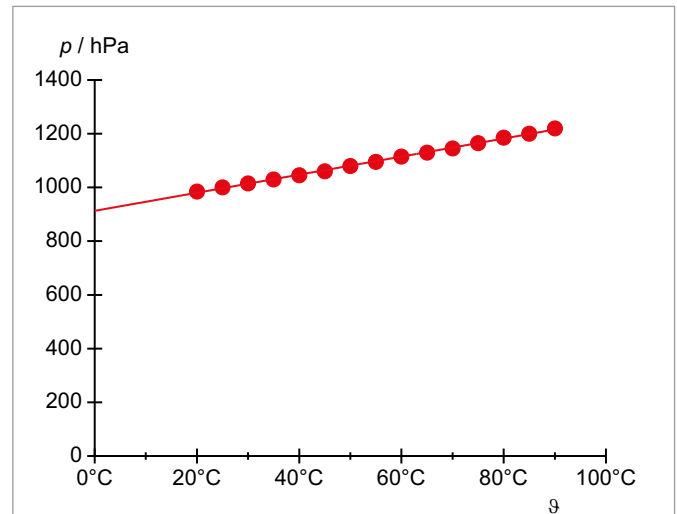


Fig. 1: Pressure-temperature diagram of air at constant volume and constant mass.

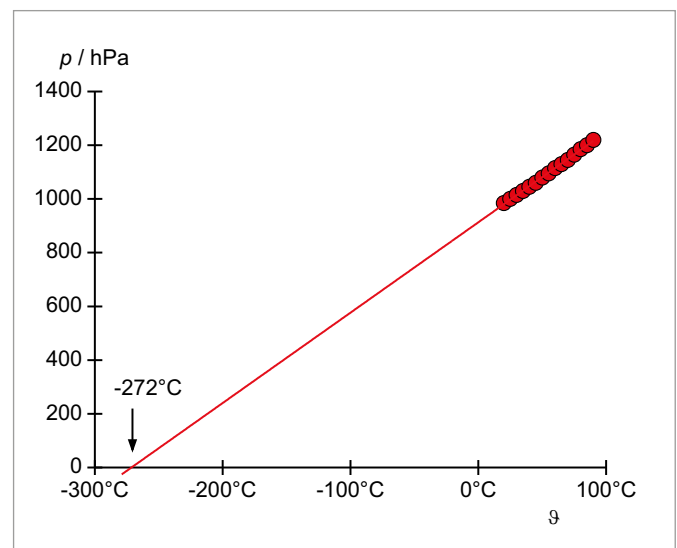


Fig. 2: Extrapolation of the pressure to a value of $p = 0$.

UE2040200 | ADIABATIC INDEX OF AIR



OBJECTIVE

Determine the adiabatic index C_p/C_v for air using Rüchardt's method

SUMMARY

In this experiment an aluminum piston inside a precision-manufactured glass tube extending vertically from on top of a glass vessel undergoes simple harmonic motion on top of the cushion formed by the volume of air trapped inside the tube. From the period of oscillation of the piston, it is possible to calculate the adiabatic index.

> EXPERIMENT PROCEDURE

- Measure the period of oscillation of the aluminum piston.
- Determine the equilibrium pressure within the enclosed volume of air.
- Determine the adiabatic index of air and compare your result with the value quoted in literature.

REQUIRED APPARATUS

Quantity	Description	Item Number
1	Mariotte Flask	1002894
1	Oscillation Tube	1002895
1	Mechanical Stopwatch, 15 min	1003369
1	Vacuum Hand Pump	1012856
Additionally recommended		
1	Callipers, 150 mm	1002601
1	Electronic Scale 200 g	1003433
1	Aneroid Barometer F	

BASIC PRINCIPLES

In a classic experiment designed by Rüchardt, it is possible to determine the adiabatic index for air from the vertical oscillations of a piston resting on a cushion of air inside a glass tube of constant cross-sectional area. The piston itself fits snugly and forms an airtight seal. Disturbing the piston from its equilibrium position causes the air inside the tube to become expanded or compressed, causing the pressure inside to rise above or below atmospheric pressure, the effect of which is to restore the piston to its equilibrium position. The restoring force is proportional to the deviation from the equilibrium position, meaning that the piston exhibits simple harmonic oscillation.

Since there is no exchange of heat with the surroundings, the oscillations are associated with adiabatic changes of state. The following equation describes the relationship between the pressure p and the volume V of the enclosed air:

$$(1) \quad p \cdot V^\gamma = \text{const.}$$

The adiabatic index γ is the ratio between the specific heat capacity at constant pressure C_p and constant volume C_v :

$$(2) \quad \gamma = \frac{C_p}{C_v}$$

From equation (1), the following relationship can be derived for changes in pressure and volume Δp and ΔV

$$(3) \quad \Delta p + \gamma \cdot \frac{p}{V} \cdot \Delta V = 0.$$

By substituting the internal cross-sectional area A of the tube, the restoring force ΔF can be calculated from the change in pressure. Similarly the deflection of the piston from its equilibrium position can be determined from the change in volume.

Therefore, the following applies:

$$(4) \quad \Delta F = -\gamma \cdot \frac{p}{V} \cdot A^2 \cdot \Delta s = 0.$$

This leads to the equation of motion for the oscillating piston.

$$(5) \quad m \cdot \frac{d^2 \Delta s}{dt^2} + \gamma \cdot \frac{p}{V} \cdot A^2 \cdot \Delta s = 0$$

$m = \text{Mass of piston}$

Solutions to this classical equation of motion for simple harmonic oscillators are oscillations with the following period:

$$(6) \quad T = 2\pi \sqrt{\frac{1}{\gamma} \cdot \frac{V}{p} \cdot \frac{m}{A^2}}$$

From this, the adiabatic index can be calculated as long as all the other variables are known.

In this experiment, a precision-made glass tube of small cross section A is set up vertically in a hole through the stopper for a glass vessel of large volume V and a matching aluminum piston of known mass m is allowed to slide up and down inside the tube. The aluminum piston exhibits simple harmonic motion atop the air cushion formed by the enclosed volume. It is possible to calculate the adiabatic index from the period of oscillation of the piston.

EVALUATION

The equilibrium volume V corresponds to the volume of the gas vessel, since that of the tube is small enough to be disregarded.

$$\gamma = \left(\frac{2\pi}{T} \right)^2 \cdot \frac{m}{A^2} \cdot \frac{V}{p}$$

The equilibrium pressure p is obtained from the external air pressure p_0 and the pressure exerted by the aluminum piston on the enclosed air in its rest state:

$$p = p_0 + \frac{m \cdot g}{A}, \text{ where } g = \text{acceleration due to gravity}$$

The expected result is therefore $\gamma = \frac{7}{5} = 1.4$, since air predominantly consists of diatomic molecules with 5 degrees of freedom for the absorption of heat energy.

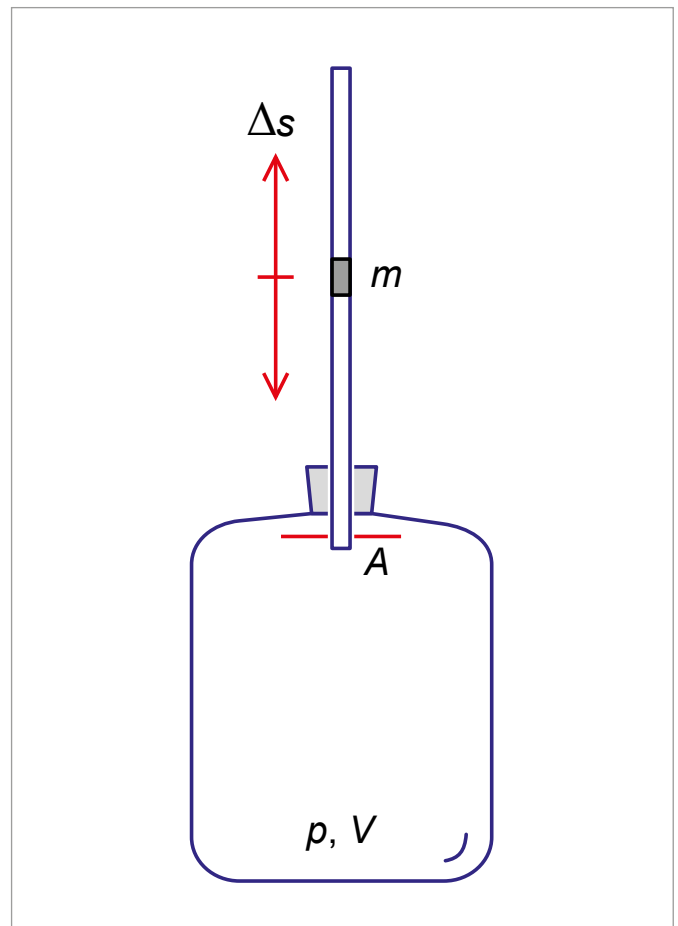
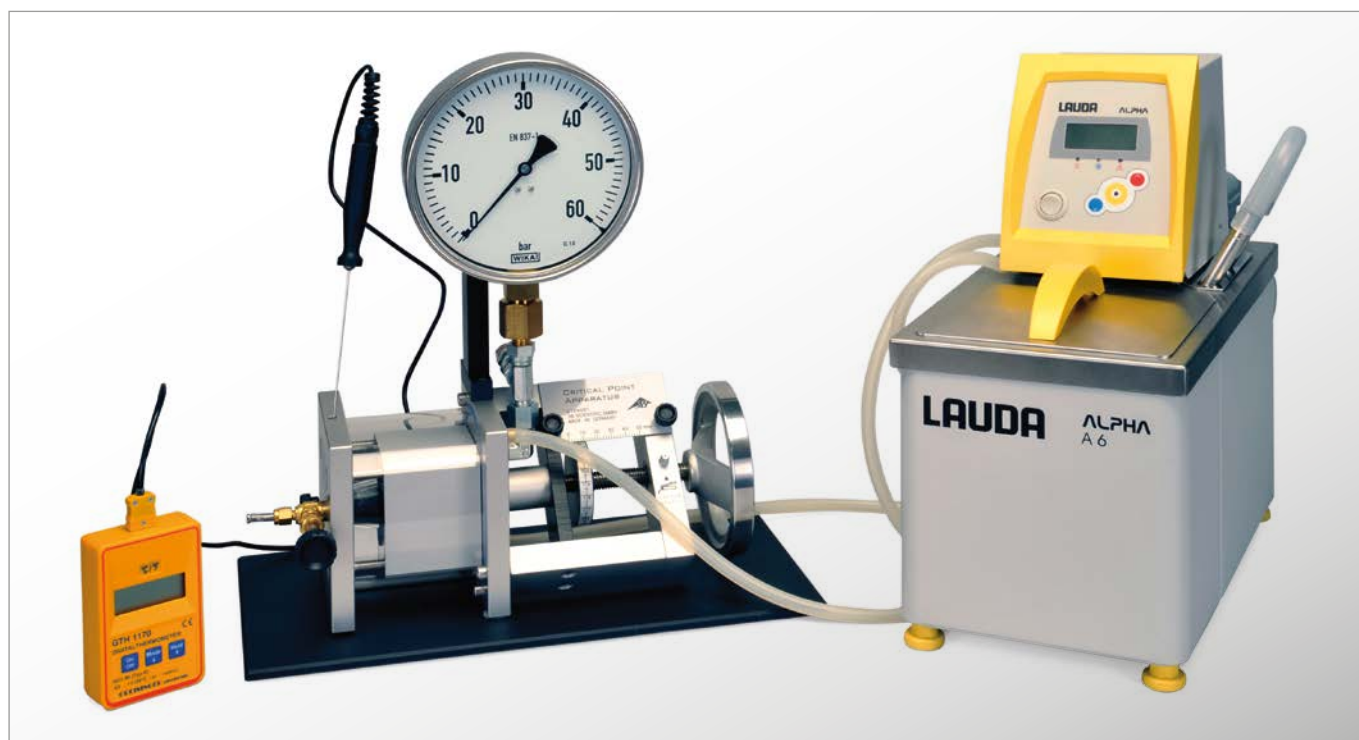


Fig. 1: Schematic of experiment set-up

UE2040300 | REAL GASES AND CRITICAL POINT



> EXPERIMENT PROCEDURE

- Observing sulphur hexafluoride in both the liquid and gaseous states.
- Plotting isotherms in a p - V diagram and a pV - p diagram.
- Observing how the behavior of real gases deviates from that for the ideal gas state.
- Determining the critical point.
- Plotting pressure curves for a saturated vapor.

OBJECTIVE

Quantitative analysis of a real gas and determination of its critical point

SUMMARY

Sulphur hexafluoride (SF_6) serves as a real gas and is examined in a measurement cell with only a minimal dead volume. Sulphur hexafluoride is especially suitable for this experiment, as its critical temperature ($T_C = 319$ K) and its critical pressure ($p_C = 37.6$ bar) are both relatively low. It is also non-toxic and is quite safe for use in teaching and in practical classes.

REQUIRED APPARATUS

Quantity	Description	Item Number
1	Critical Point Apparatus	1002670
1	Immersion/Circulation Thermostat (230 V; 50/60 Hz)	1008654 or
	Immersion/Circulation Thermostat (115 V; 50/60 Hz)	1008653
1	Digital Quick Response Pocket Thermometer	1002803
1	K-Type NiCr-Ni Immersion Sensor, -65°C – 550°C	1002804
2	Tubings, Silicone 6 mm	1002622

Additionally required

Sulphur Hexafluoride (SF_6)

NOTE

In accordance with the principles of good laboratory practice, it is recommended that the gas connections should be made by rigid metal pipework, especially if the critical point apparatus is to be used regularly. For connecting to an appropriate gas cylinder, use the 1/8" (SW 11) threaded pipe connector that is supplied.

BASIC PRINCIPLES

The critical point of a real gas is characterised by the critical temperature T_C , the critical pressure p_C , and the critical density ρ_C . Below the critical temperature the substance is gaseous at large volumes and liquid at small volumes. At intermediate volumes it can exist as a liquid-gas mixture, in which changing the volume under isothermal conditions causes a change of state: the gaseous fraction increases as the volume is increased, while the pressure of the mixture remains constant. As the liquid and the vapor have different densities, they are separated by the gravitational field. As the temperature rises, the density of the liquid decreases and that of the gas increases until the two densities converge at the value of the critical density. Above the critical temperature, the gas can no longer be liquefied. However, under isothermal conditions the gas does not obey Boyle's Law until the temperature is raised considerably above the critical temperature.

Sulphur hexafluoride (SF_6) is especially suitable for investigating the properties of real gases, as its critical temperature ($T_C = 319\text{ K}$) and its critical pressure ($p_C = 37.6\text{ bar}$) are both relatively low. It is also non-toxic and is quite safe for use in teaching and in practical classes. The apparatus for investigating the critical point consists of a transparent measurement cell, which has very thick walls and can withstand high pressures. The internal volume of the cell can be changed by turning a handwheel, which allows one to make fine adjustments and can be read with a precision down to 1/1000 of the maximum volume. Pressure is applied by a hydraulic system using castor oil of pharmaceutical quality. The hydraulic system is separated from the cell by a conical rubber seal, which rolls up when the volume is changed. This form of construction ensures that the pressure difference between the measurement cell and the oil space is practically negligible. Therefore, instead of measuring the gas pressure directly, a manometer measures the oil pressure, which avoids having a dead volume in the gas space. The measurement cell is enclosed within a transparent water jacket. During the experiment a thermostatic water bath maintains a precisely controlled and adjustable constant temperature, which is measured by a digital thermometer.

During observations of the transition from the gaseous to the liquid phase and the reverse process, the fact that there is very little dead volume makes it possible to observe the formation of the first drop of liquid or the disappearance of the last bubble of gas.

EVALUATION

The pressure as a function of the volume is measured point-by-point at constant temperature, and the results are plotted as a p - V diagram (Clapeyron diagram) and as a pV - p diagram (Amegat diagram). The deviation from the behavior of an ideal gas is immediately obvious and striking.

From the diagrams, the parameters of the critical point can easily be determined, and it is possible to obtain a clear experimental verification of the behavior of a real gas.

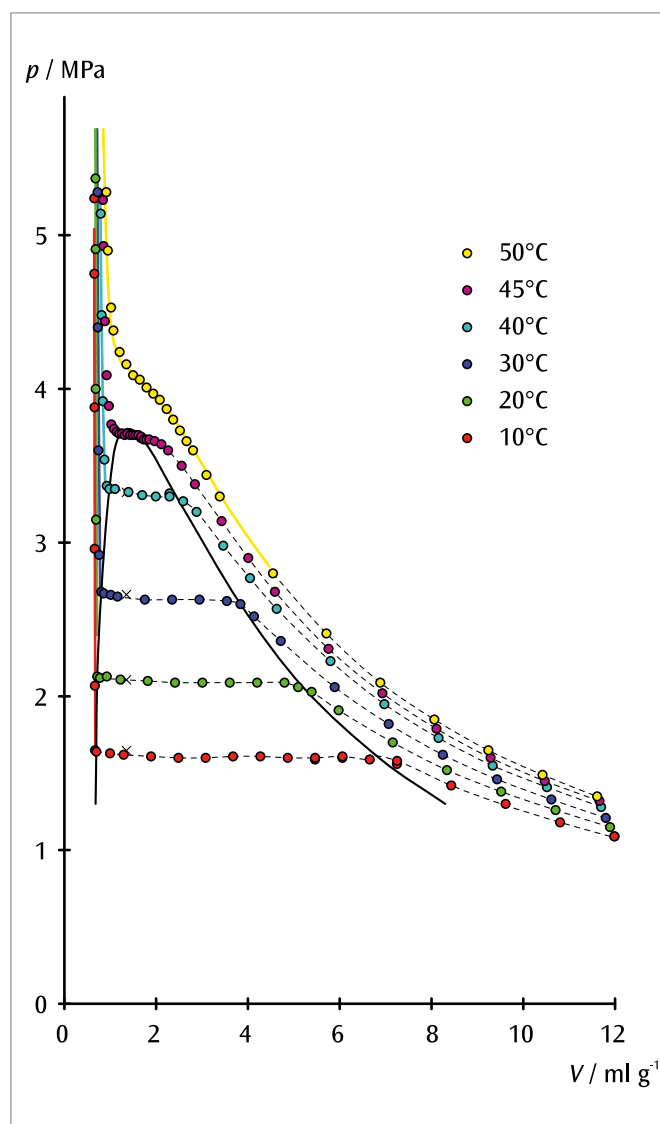
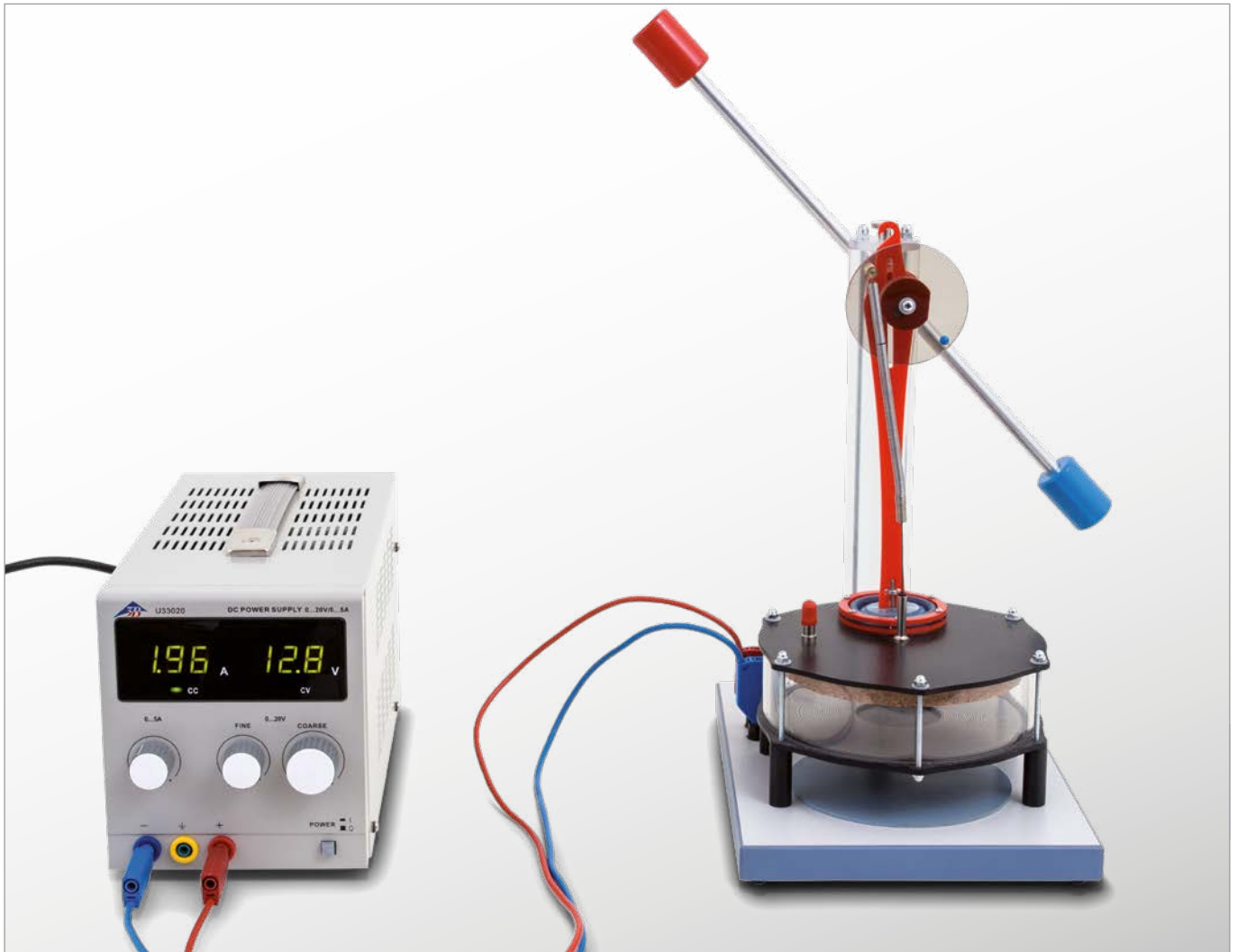


Fig. 1: p - V diagram of Sulphur hexafluoride

UE2060100 | STIRLING ENGINE D



EXPERIMENT PROCEDURE

- Operate the hot-air engine as a heat engine.
- Demonstrate how thermal energy is converted into mechanical energy.
- Measure the no-load speed as a function of the thermal power.

OBJECTIVE

Operate a functional model of a Stirling engine as a heat engine

SUMMARY

A hot-air engine is a classical example of a heat engine. In the course of a thermodynamic cycle thermal energy is fed in from a high temperature reservoir and then partially converted into useable mechanical energy. The remaining thermal energy is then transferred to a reservoir at a lower temperature.

REQUIRED APPARATUS

Quantity	Description	Item Number
1	Wilke-Type Stirling Engine	1000817
1	DC Power Supply 0 – 20 V, 0 – 5 A (230 V, 50/60 Hz)	1003312 or
	DC Power Supply 0 – 20 V, 0 – 5 A (115 V, 50/60 Hz)	1003311
1	Set of 15 Safety Experiment Leads, 75 cm	1017718
1	Mechanical Stopwatch, 30 min	1003369

BASIC PRINCIPLES

The thermodynamic cycle of a hot-air engine (invented by *R. Stirling, 1816*) can be simplified by breaking the cycle down into the separate processes of heating, expansion, cooling and compression. These processes are depicted schematically in Figs. 1 – 4 for the functional model under investigation.

If the hot-air engine is operated without any mechanical load, it rotates at its no-load speed, which is restricted by internal friction and is dependent on the amount of thermal energy supplied. The speed drops as soon as the mechanical power is tapped. This can be demonstrated most clearly by applying a frictional force to the crankshaft.

EVALUATION

Heating:

Heat is introduced when the displacement piston extends thereby pushing air into the heated region of the large cylinder. During this operation the working piston is at its bottom dead center position since the displacement piston is ahead of the working piston by 90°.

Expansion:

The heated air expands and causes the working piston to retract. At the same time mechanical work is transferred to the flywheel rod via the crankshaft.

Cooling:

While the working piston is in its top dead center position: the displacement piston retracts and air is displaced towards the top end of the large cylinder so that it cools.

Compression:

The cooled air is compressed by the working piston extending. The mechanical work required for this is provided by the flywheel rod.

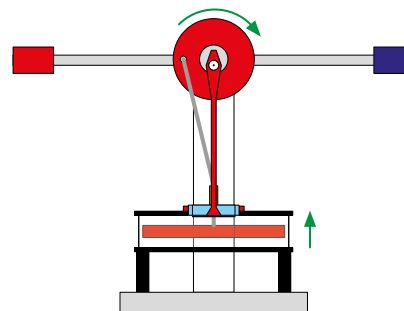


Fig. 1: Heating

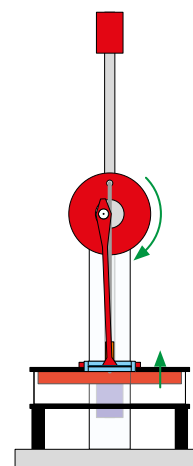


Fig. 2: Expansion

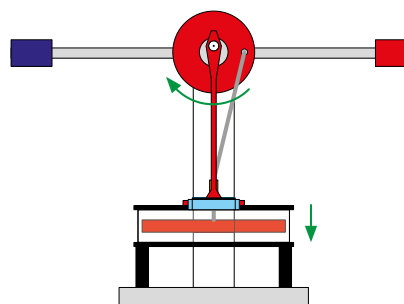


Fig. 3: Cooling

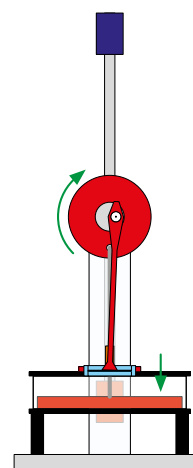
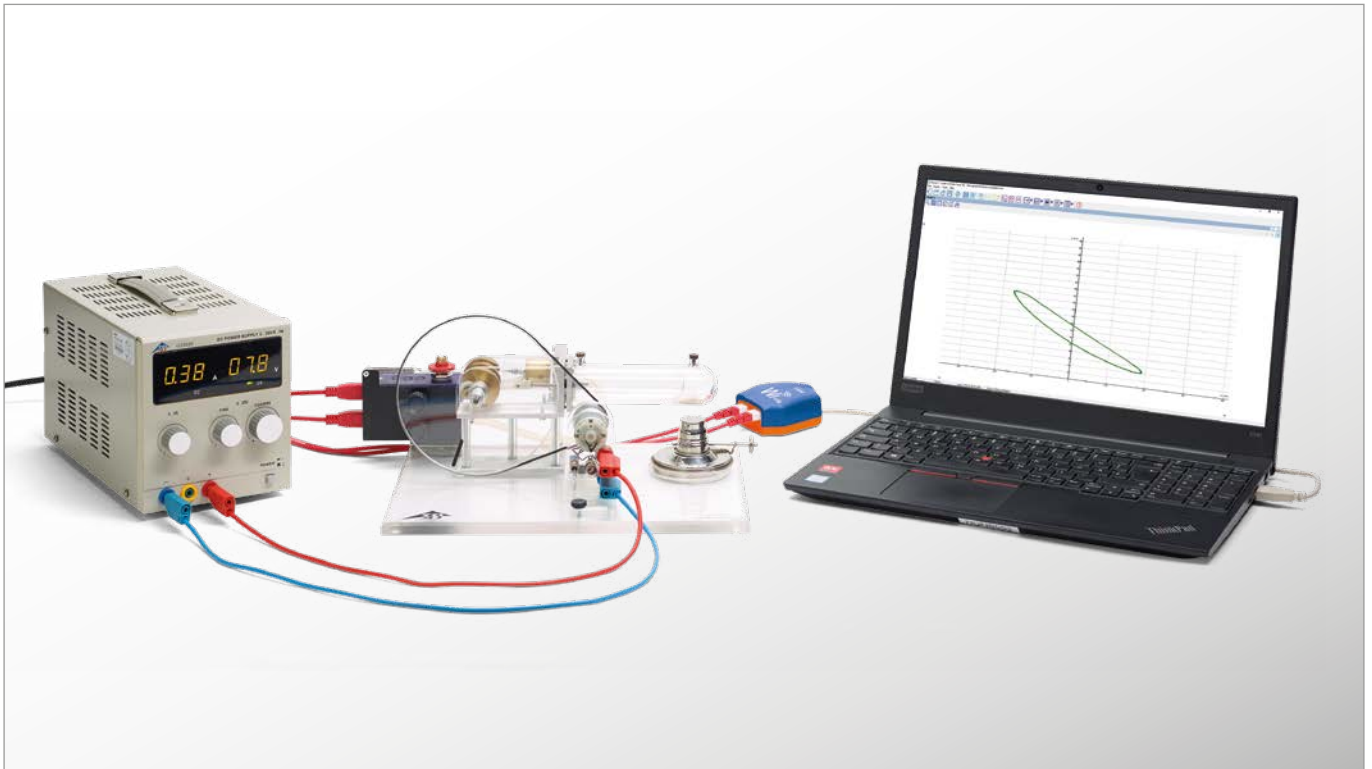


Fig. 4: Compression

UE2060250 | STIRLING ENGINE G



EXPERIMENT PROCEDURE

- Record a p - V diagram.
- Determine the mechanical power associated with a full cycle and calculate the mechanical work.

OBJECTIVE

Record a p - V diagram.

SUMMARY

Cyclic processes in thermodynamics can be plotted as a closed loop in a p - V diagram. The area enclosed by the curve corresponds to the mechanical work taken from the system. Alternatively, the mechanical power associated with a complete cycle can be determined and then the mechanical work can be calculated from that by means of an integration over time. This will be investigated in the course of an experiment using a Stirling engine.

REQUIRED APPARATUS

Quantity	Description	Item Number
1	Stirling Engine G	1002594
1	Sensor Holder for Stirling Engine G	1008500
1	Displacement Sensor FW	1021534
1	Relative Pressure Sensor FW, ± 1000 hPa	1021533
1	WiLab *	1022284
2	Sensor Cable	1021514
1	DC Power Supply 0 – 20 V, 0 – 5 A (230 V, 50/60 Hz)	1003312 or
	DC Power Supply 0 – 20 V, 0 – 5 A (115 V, 50/60 Hz)	1003311
1	Pair of Safety Experimental Leads, 75 cm, red/blue	1017718
Additionally required:		
1	Coach 7 License	

* Alternative: 1 VinciLab 1021477

BASIC PRINCIPLES

Cyclic processes in thermodynamics can be plotted as a closed loop in a p - V diagram. The area enclosed by the curve corresponds to the mechanical work W taken from the system. Alternatively, the mechanical power P associated with a complete cycle can be determined and then the mechanical work can be calculated from that by means of an integration over time.

The following equations apply:

$$(1) \quad W = \oint p dV$$

or

$$(2) \quad W = \int_{t_1}^{t_2} P dt \quad \text{with} \quad P(t) = p \frac{dV}{dt}$$

For the experiment we will choose the second variant to determine the mechanical power output in each cycle by a glass Stirling engine specifically designed for educational purposes. To determine the pressure p in the main cylinder, a relative pressure sensor is fitted, which measures the difference in cylinder pressure from the ambient pressure. The volume V is calculated from the distance s travelled by the main piston and its cross-sectional area A . A displacement sensor is attached to the main piston for this purpose.

EVALUATION

To verify the cyclic process, the measurement results are plotted in a p - V diagram. In order to determine the mechanical power output, it is plotted in a second graph as a function of time. On this second graph, it is easy to identify the cycles of the process. This is important when choosing the limits for the integration in order to calculate the mechanical work per cycle, see (2).

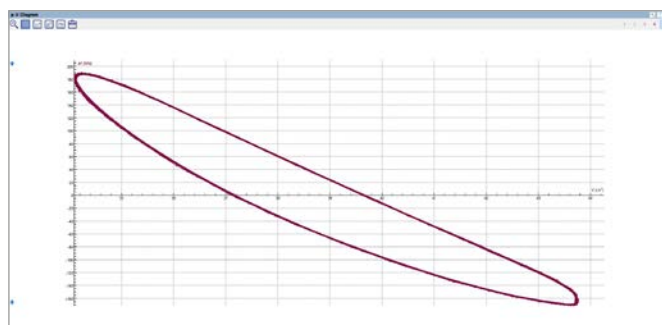


Fig. 1: p - V diagram for Stirling engine G

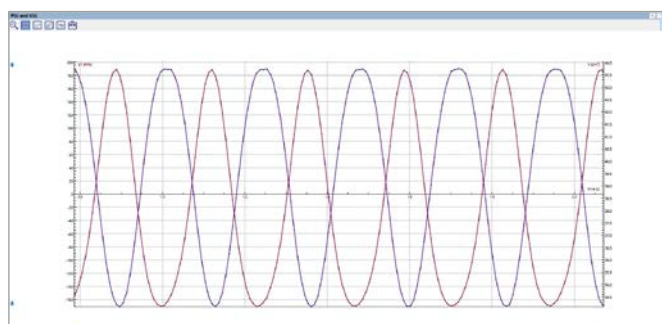
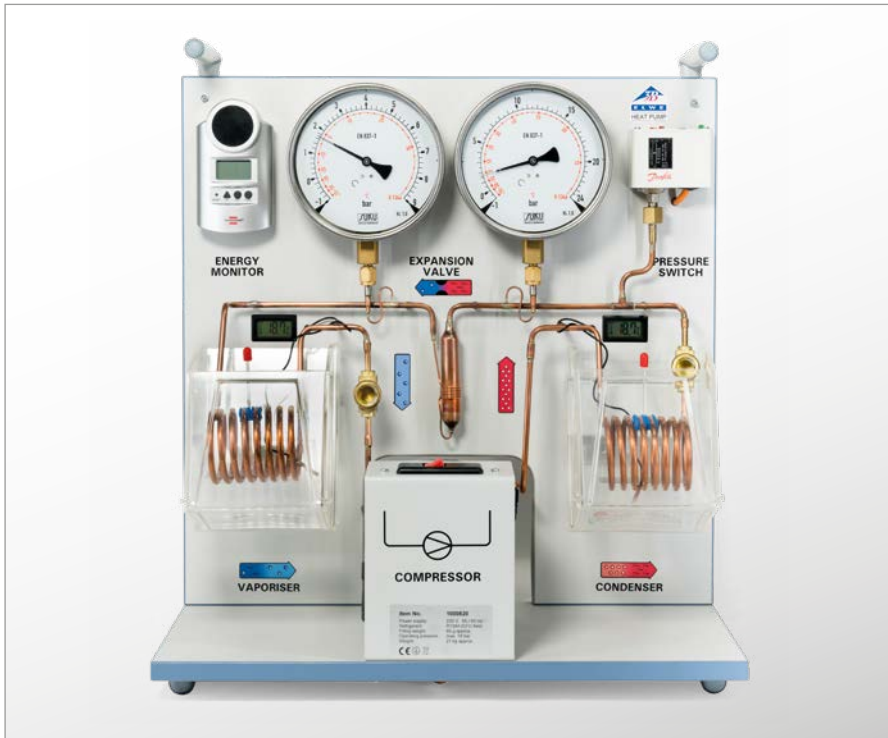


Fig. 2: $V(t)$ and $P(t)$ plot for Stirling engine G

UE2060300 | HEAT PUMPS



OBJECTIVE

Record and analyze the pressure-enthalpy diagram for a compression heat pump

EXPERIMENT PROCEDURE

- Demonstrate how an electric compression heat pump works.
- Quantitatively investigate of the related cyclical process.
- Record and analyze the pressure-enthalpy diagram for a compression heat pump.

SUMMARY

An electric compression heat pump consists of a compressor with a drive motor, a condenser, an expansion valve and an evaporator. Its functioning is based on a cyclical process with phase transition, through which the working medium in the pump passes; ideally, this process can be divided into the four steps comprising compression, liquefaction, depressurisation and evaporation. The theoretical performance coefficient of an ideal cyclical process can be calculated from the specific enthalpies h_1 , h_2 and h_3 read from a Mollier diagram. Determining the enthalpies h_2 and h_3 of an ideal cyclical process and the quantity of heat ΔQ_2 supplied to the hot water reservoir per time interval Δt makes it possible to estimate the mass flow of the working medium.

REQUIRED APPARATUS

Quantity	Description	Item Number
1	Heat Pump D (230 V, 50/60 Hz)	1000820 or
	Heat Pump D (115 V, 50/60 Hz)	1000819
4	Temperature Sensor NTC with Measurement Terminal	1021797
1	VinciLab	1021477

Additionally required:

1	Coach 7 License
---	-----------------

BASIC PRINCIPLES

An electric compression heat pump consists of a compressor with a drive motor, a condenser, an expansion valve and an evaporator. Its operation is based on a cyclical process a phase transition, which the working medium inside the pump undergoes. Ideally, this process can be divided into four steps, comprising compression, liquefaction, depressurisation and evaporation.

For the compression part of the cycle, the gaseous working medium is drawn in by the compressor and compressed without any change in entropy ($s_1 = s_2$) from p_1 to p_2 , during which process the medium heats up (see Figs. 1 and 2). The temperature accordingly rises from

T_1 to T_2 . The mechanical compression work performed per unit of mass is $\Delta w = h_2 - h_1$.

Inside the condenser, the working medium cools considerably and condenses. The heat released as a result (excess heat and latent heat of condensation) per unit of mass is $\Delta q_2 = h_2 - h_3$. It raises the temperature of the surrounding reservoir.

The condensed working medium reaches the release valve, where it is depressurized (without doing any mechanical work). In this process, the temperature also decreases due to the work which needs to be performed in opposition to the molecular forces of attraction inside the working medium (Joule-Thomson effect). The enthalpy remains constant ($h_4 = h_3$).

As it absorbs heat inside the evaporator, the working medium evaporates fully. This cools the surrounding reservoir. The heat absorbed per unit of mass is $\Delta q_1 = h_1 - h_4$.

A Mollier diagram of the working medium is often used to represent the cycle of a compression heat pump. This diagram plots the pressure p against the specific enthalpy h of the working medium (enthalpy is a measure of the working medium's heat content and generally rises with the pressure and gas content).

Also specified are the isotherms ($T = \text{constant}$) and isentropes ($S = \text{constant}$), as well as the relative proportion by mass of the working medium in the liquid phase. The working medium condenses fully to the left of the vaporisation phase boundary line. The medium is present as superheated steam to the right of the condensation phase boundary and as a mixture of liquid and gas between the two lines. The two lines make contact at the critical point.

To depict the system in a Mollier diagram, the ideal cycle described above can be determined by measuring the pressures p_1 and p_2 respectively before and after the expansion valve, as well as the temperatures T_1 and T_3 respectively before the compressor and expansion valve.

The components in this experiment are connected via a copper pipe to form a closed system, and mounted on a base board. Thanks to the clarity of the set-up, it is easy to associate them with the sequence of phase changes taking place in the heat pump cycle. The evaporator and condenser are designed as coiled copper tubes and they are each immersed in a separate water bath which serves as a reservoir for determining absorbed or emitted heat. Two large manometers indicate the pressures on the refrigerant in the two heat exchangers. Two analog thermometers allow you to measure temperature in the two water baths. Temperature sensors with specially designed measuring terminals are used to register the temperatures in the copper tube before the compressor and the expansion valve.

The theoretical performance coefficient for an ideal cyclical process can be calculated from the specific enthalpies h_1 , h_2 and h_3 read from a Mollier diagram:

$$(1) \quad \eta_{\text{th}} = \frac{\Delta q_2}{\Delta w} = \frac{h_2 - h_3}{h_2 - h_1}$$

Determining the enthalpies h_2 and h_3 of the ideal cyclical process and the quantity of heat ΔQ_2 supplied to the hot water reservoir per time interval Δt makes it possible to estimate the mass flow of the working medium.

$$(2) \quad \frac{\Delta m}{\Delta t} = \frac{\Delta Q_2}{\Delta t} \cdot \frac{1}{h_2 - h_3}$$

EVALUATION

T_1 and p_1 determine point 1 in the Mollier diagram. The intersection where the relevant isentrope crosses the horizontal line $p_2 = \text{constant}$ determines point 2. The intersection with the vaporisation boundary line determines point 3, while a perpendicular to the horizontal line $p_4 = \text{constant}$ determines point 4. Additional measurement of the temperature T_3 provides an advanced insight into the processes taking place in the heat pump. T_3 does not coincide with the temperature reading on the related manometer's temperature scale. This temperature scale is based on the vapor pressure curve for the working medium. The measurement therefore shows that the working medium before the expansion valve does not comprise a mixture of liquid and gas, but is entirely liquid.

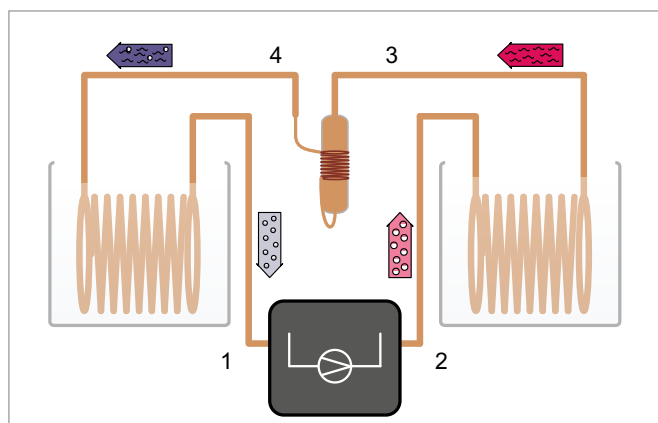


Fig. 1: Schematic representation of the heat pump with a compressor (1, 2), condenser (2, 3), expansion valve (3, 4) and evaporator (4, 1)

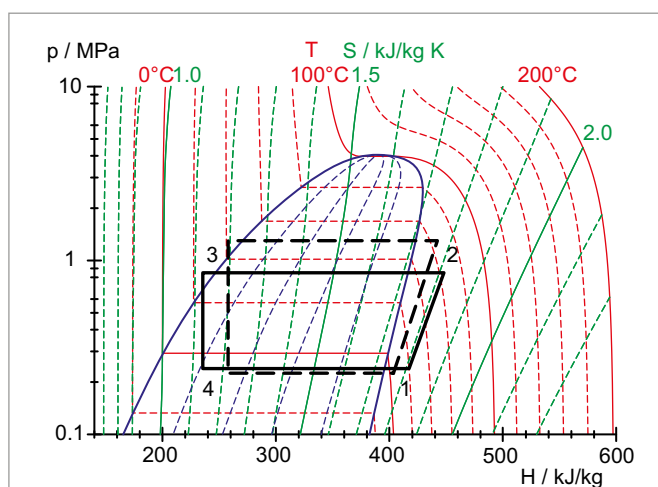


Fig. 2: Representation of ideal cyclical process for heat pump in a Mollier diagram

UE3010700

ELECTRIC FIELD IN A PLATE CAPACITOR



> EXPERIMENT PROCEDURE

- Measuring the electric field within a plate capacitor as a function of the distance between the plates.
- Measuring the electric field within a plate capacitor as a function of the applied voltage.

OBJECTIVE

Measure the electric field in a plate capacitor using the electric field meter

SUMMARY

The electric field meter can be used to measure the electric field within a plate capacitor directly. In this experiment a rotating sector disc interrupts the electrostatic flux falling on an induction plate, which forms part of a capacitor plate. The voltage pulses that are thereby generated are amplified to give an output voltage, which is then rectified to give a DC voltage that is proportional to the electric field E acting on the induction plate.

REQUIRED APPARATUS

Quantity	Description	Item Number
1	Electric Field Meter (230 V, 50/60 Hz)	1021405 or
	Electric Field Meter (115 V, 50/60 Hz)	1021406
1	DC Power Supply 450 V (230 V, 50/60 Hz)	1008535 or
	DC Power Supply 450 V (115 V, 50/60 Hz)	1008534
1	Digital Multimeter E	1018832
1	Analog Multimeter ESCOLA 30	1013526
1	Set of 15 Safety Experiment Leads, 75 cm	1002843

BASIC PRINCIPLES

The electric field meter can be used to measure electric fields directly. In front of an induction plate with four sectors in a star-shaped arrangement, a fan-like disc of similar shape is rotated. It continually interrupts the electrostatic flux, and thereby causes periodic induced charges, which are allowed to dissipate through a large resistance. The voltage pulses that are thereby generated are amplified to give an output voltage, which is then rectified to give a DC voltage that is proportional to the electric field E acting on the induction plate.

In the experiment, the electric field strength

$$(1) \quad E = \frac{U}{d}$$

in a plate capacitor is measured using the electric field meter. The applied voltage U and the distance d between the plates are varied in separate experimental runs.

EVALUATION

In applying Equation 1, one must take into account the fact that the induction plate is about 1 mm below the lower capacitor plate. Therefore, Equation 1 must be replaced by:

$$E = \frac{U}{d_{\text{eff}}} = \frac{U}{d + 1 \text{ mm}}$$

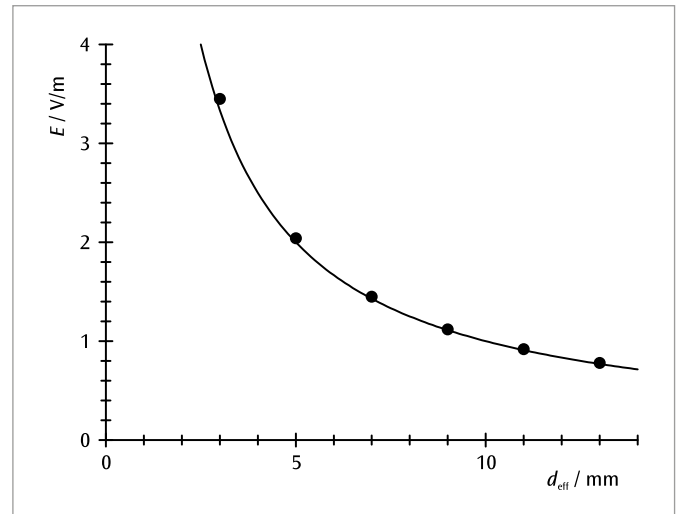


Fig. 1: Electric field inside the plate capacitor as a function of the effective distance between the plates

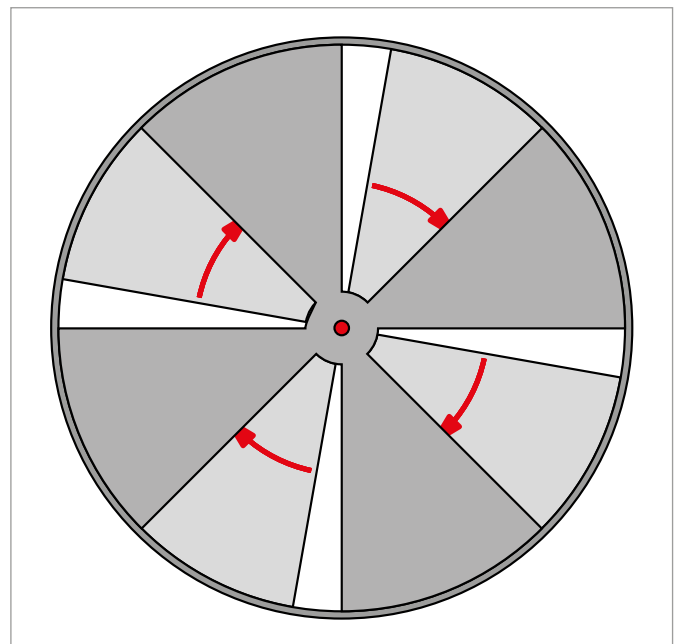
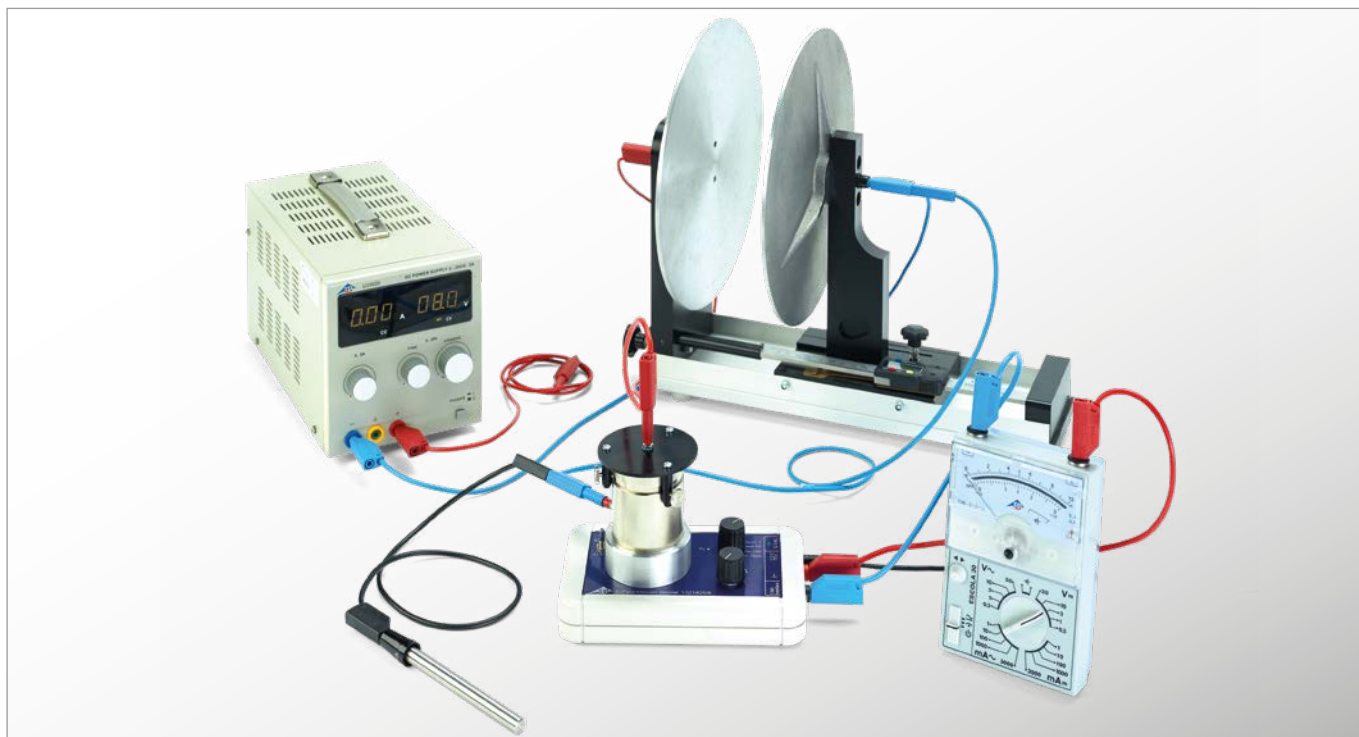


Fig. 2: Rotating sectored disc of the electric field meter

UE3010800 | VOLTAGE ON A PLATE CAPACITOR



EXPERIMENT PROCEDURE

- Measuring the electrostatic voltage on a plate capacitor as a function of the distance between the plates.
- Confirming the proportionality between the voltage and the distance between the plates for small plate distances.

OBJECTIVE

Measure the electrostatic voltage as a function of the distance between the plates

SUMMARY

To increase the distance between the charged plates of a plate capacitor after removing their external connections, mechanical work must be performed. This can be demonstrated by measuring the resulting increase of the voltage between the plates using an electrostatic voltmeter.

REQUIRED APPARATUS

Quantity	Description	Item Number
1	Electric Field Meter (230 V, 50/60 Hz)	1021405 or
	Electric Field Meter (115 V, 50/60 Hz)	1021406
1	Plate Capacitor D	1006798
1	DC Power Supply 0 – 20 V, 0 – 5 A (230 V, 50/60 Hz)	1003312 or
	DC Power Supply 0 – 20 V, 0 – 5 A (115 V, 50/60 Hz)	1003311
1	Analogue Multimeter ESCOLA 30	1013526
1	Set of 15 Experiment Leads, 75 cm, 2.5 mm ²	1002841

BASIC PRINCIPLES

The charged plates of a plate capacitor exert an attractive force on each other. Therefore, to increase the distance between the plates of a capacitor that has been charged and its external connections removed, mechanical work must be performed. The additional energy supplied to the capacitor in this way can be measured as an increase of the voltage between the plates, provided that no current flows between the plates during the measurement.

A more precise description of this relation is obtained by considering the homogeneous electric field E between the plates of the capacitor, which carry the charges Q and $-Q$. The electric field strength is:

$$(1) \quad E = \frac{1}{\epsilon_0} \cdot \frac{Q}{A}$$

A : Area of each plate,

$$\epsilon_0 = 8.85 \cdot 10^{-12} \frac{\text{V} \cdot \text{s}}{\text{A} \cdot \text{m}} : \text{Permittivity of free space}$$

If no current can flow if the plate distance d is changed, the charge Q and thus also the electric field E remain unchanged.

For small distances, for which the electric field can be assumed to be homogeneous, the voltage U on the capacitor and the electric field E are given by:

$$(2) \quad U = E \cdot d$$

d : Distance between the plates.

Thus, the voltage U is proportional to the distance between the plates d . In the experiment, this relationship is tested by using the electric field meter as an electrostatic voltmeter. This method ensures that no current can flow through the voltmeter between the capacitor plates and the charge Q on the plates remains unchanged.

EVALUATION

From Equation 2, a plot of U against d will give a straight line passing through the origin and through the measurement points, with a gradient corresponding to the constant electric field E . Deviations can be attributed to the fact that the electric field can no longer be assumed to be homogeneous with an increasing distance between the plates.

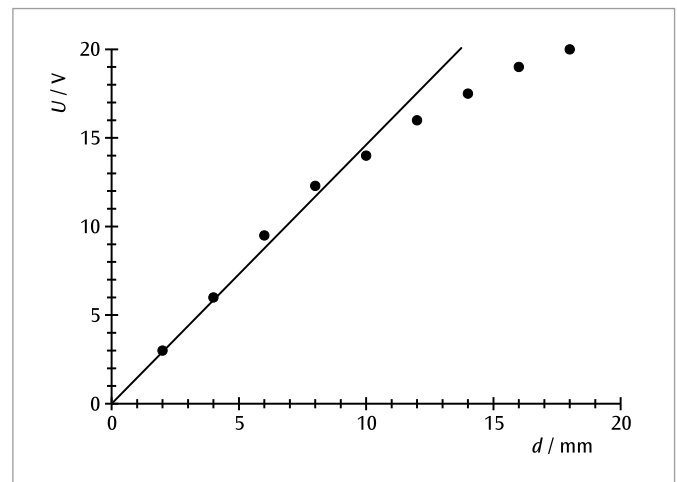


Fig. 1: Voltage U on the plate capacitor as a function of distance d between the plates

UE3020100 | CHARGED DROPLETS OF WATER



OBJECTIVE

Demonstrate the electric current generated by the motion of charged droplets of water

SUMMARY

Electric current arises due to an amount of charge being transported during a given interval of time. A flow of current can be simply illustrated with the help of charged droplets of water. In order to carry out the measurement, a burette and a Faraday cup connected to an electrometer will be used. The charge accumulated in the Faraday cup in a certain period of time is measured with the help of the voltage which drops across the capacitor. This allows the charge per droplet and the current to be determined.

> EXPERIMENT PROCEDURE

- Measure the charge transferred to a Faraday cup by charged droplets of water dripping from a burette as a function of the time.
- Determine the current generated by the movement of the charged water droplets.
- Determine the charge on each droplet.

REQUIRED APPARATUS

Quantity	Description	Item Number
1	Electrometer (230 V, 50/60 Hz)	1001025 or
	Electrometer (115 V, 50/60 Hz)	1001024
1	Electrometer Accessories	1006813
1	Analog Multimeter ESCOLA 30	1013526
1	Burette, 10 ml	1018065
1	Constantan Wire 0.2 mm / 100 m	1000955
1	DC Power Supply 450 V (230 V, 50/60 Hz)	1008535 or
	DC Power Supply 450 V (115 V, 50/60 Hz)	1008534
1	Digital Multimeter P3340	1002785
1	Digital Stopwatch	1002811
1	Tripod Stand 150 mm	1002835
1	Stainless Steel Rod 1000 mm	1002936
2	Universal Clamp	1002830
1	Universal Jaw Clamp	1002833
1	Crocodile Clip 4 mm, Not Insulated	1002844
1	Set of 3 Safety Experiment Leads for Free Fall Apparatus	1002848
2	Pair of Safety Experimental Leads, 75 cm, red/blue	1017718
1	Peleus Ball, standard	1013392
1	Set of 10 Beakers, low form	1002872
Additionally recommended		
1	WiLab *	1022284
1	Voltage Sensor 10V, differential	1021680
1	Coach 7 license	

* Alternative: 1 VinciLab 1021477

BASIC PRINCIPLES

Electric current arises due to an amount of charge being transported during a given interval of time. A flow of current can be simply illustrated with the help of charged droplets of water.

In this experiment a number of charged water droplets N drips at a constant rate of roughly one droplet per second from a burette into a Faraday cup connected to an electrometer and a capacitor. The charge Q accumulated in the Faraday cup causes the capacitor to charge up. The resulting voltage across the capacitor is observed and measured using an analogue multimeter for a certain period of time t . The high-resistance input of the operational amplifier in the electrometer ensures that the capacitor does not discharge via that path.

Observation of the analogue multimeter indicates that the voltage across the capacitor increases by about the same amount with every droplet collected in the Faraday cup, i.e. each of the droplets carries approximately the same charge:

$$(1) \quad q = \frac{Q}{N}$$

The current transported is given by

$$(2) \quad I = \frac{Q}{t}$$

As an option, the voltage across the capacitor can be recorded with the help of an interface and a voltage sensor as a function of time t and displayed in the form of a graph.

EVALUATION

The charge Q accumulated in the Faraday cup is determined by reading of the voltage U and calculating Q from that:

$$Q = C \cdot U \text{ where } C = 1 \text{ nF: capacitance of capacitor}$$

Using an interface and corresponding software the time characteristic $Q(t)$ can be measured. It is step-shaped whereby the individual steps mark the charge q that accumulates with each individual droplet per time interval Δt . The fact that each water droplet carries almost the same charge is reflected in the constant step height of the characteristic.

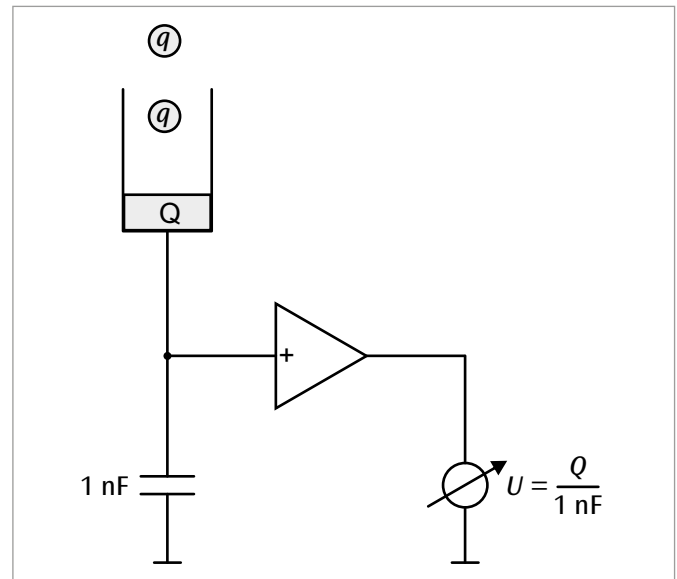


Fig. 1: Schematic illustrating the principle behind the measurement

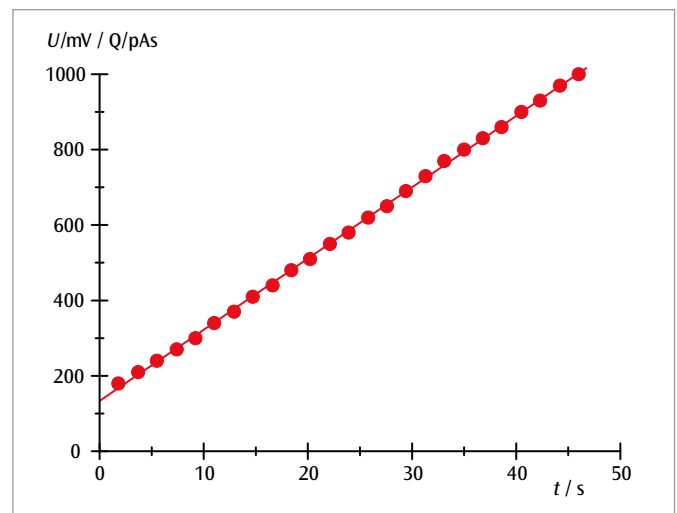


Fig. 2: Accumulated charge Q as a function of time t

UE3020200 | ELECTRICAL CONDUCTORS



> EXPERIMENT PROCEDURE

- Measure voltage drop U as a function of distance d between contact points at a constant current I .
- Measure voltage drop U as a function of current I for a fixed distance d between contact points.
- Determine the electrical conductivity of copper and aluminum and make a comparison with values quoted in literature.

OBJECTIVE

Determine the electrical conductivity of copper and aluminum

SUMMARY

Electrical conductivity of a material is highly dependent on the nature of the material. It is defined as the constant of proportionality between the current density and the electric field in the material under investigation. In this experiment, four-terminal sensing is used to measure current and voltage in metal bars of known cross section and length.

REQUIRED APPARATUS

Quantity	Description	Item Number
1	Heat Conducting Rod Al	1017331
1	Heat Conducting Rod Cu	1017330
1	DC Power Supply 1 - 32 V, 0-20 A (230 V, 50/60 Hz)	1012857 or
	DC Power Supply 0 - 40 V, 0-40 A (115 V, 50/60 Hz)	1022289
1	Measurement Amplifier U (230 V, 50/60 Hz)	1020742 or
	Measurement Amplifier U (115 V, 50/60 Hz)	1020744
2	Digital Multimeter E	1018832
1	Set of 15 Experiment Leads, 75 cm, 2.5 mm ²	1002841

BASIC PRINCIPLES

Electrical conductivity of a material is highly dependent on the nature of the material. It is defined as the constant of proportionality between the current density and the electric field in the respective material. In metals it is determined by the number density and mobility of electrons in the conduction band and is also dependent on temperature.

For a long metal conductor of cross-sectional area A and length d , a relationship between current I through the conductor and the voltage U which drops over a distance d along it can be deduced from the following formula:

$$(1) \quad j = \sigma \cdot E$$

j : current density, E : electric field

That relationship is as follows:

$$(2) \quad I = j \cdot A = A \cdot \sigma \cdot \frac{U}{d}$$

In the experiment, this relationship is used to determine the conductivity of metal bars using four-terminal sensing. This involves feeding in a current I through two wires and measuring the drop in voltage U between two contact locations separated by a distance d . Since the area of the cross section A is known, it is possible to calculate the conductivity σ .

The experiment uses the same metal bars investigated in the experiment on heat conduction, UE2020100. Two measurement probes are used to measure the voltage drop between the contact points, which can also be used to measure temperature along the bars.

NOTE

By comparing the measurements with the heat conductivity values obtained in experiment UE2020100 it is possible to verify the Wiedemann-Franz law. This states that thermal conductivity is proportional to electrical conductivity in metals and the factor is a universal value temperature-dependent coefficient.

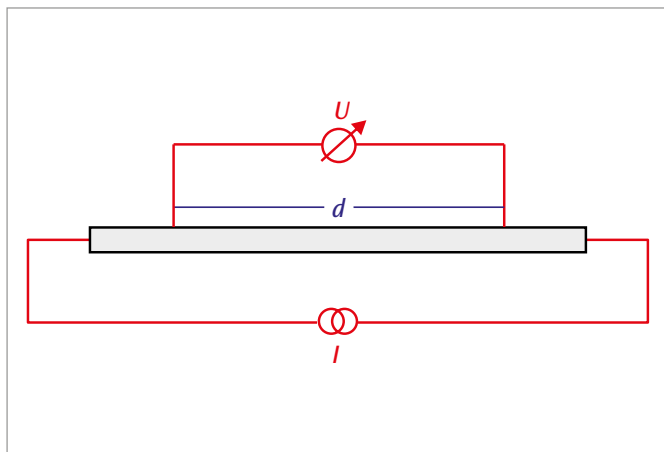


Fig. 3: Schematic of four-terminal sensing measurement

EVALUATION

The values measured for constant current I are plotted in a graph of U against d . Contact voltages between the measurement probes and the metal bar may become apparent by causing the straight lines to be shifted away from the origin. According to equation (2), the following is true

$$\alpha = \frac{I}{A \cdot \sigma}$$

Since I and A are known, it is possible to calculate the conductivity:

$$\sigma = \frac{I}{A \cdot \alpha}$$

The gradient of the U - I graph is

$$\beta = \frac{d}{A \cdot \sigma}$$

This implies that

$$\sigma = \frac{d}{A \cdot \beta}$$

Comparing the results with values quoted in literature for pure copper and aluminum, it can be seen that these metal bars are not made of pure metal but are actually copper or aluminum alloys.

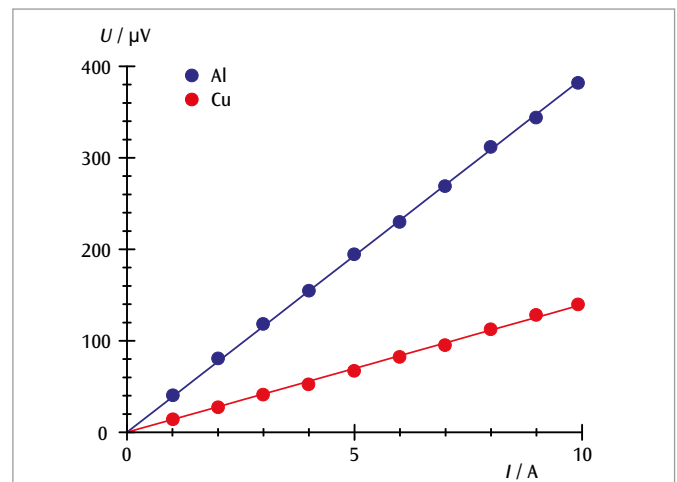


Fig. 1: Plot of U against I for copper and aluminum

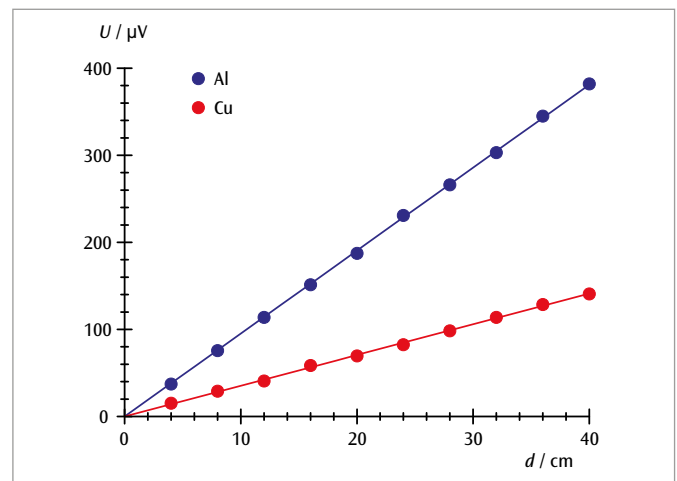
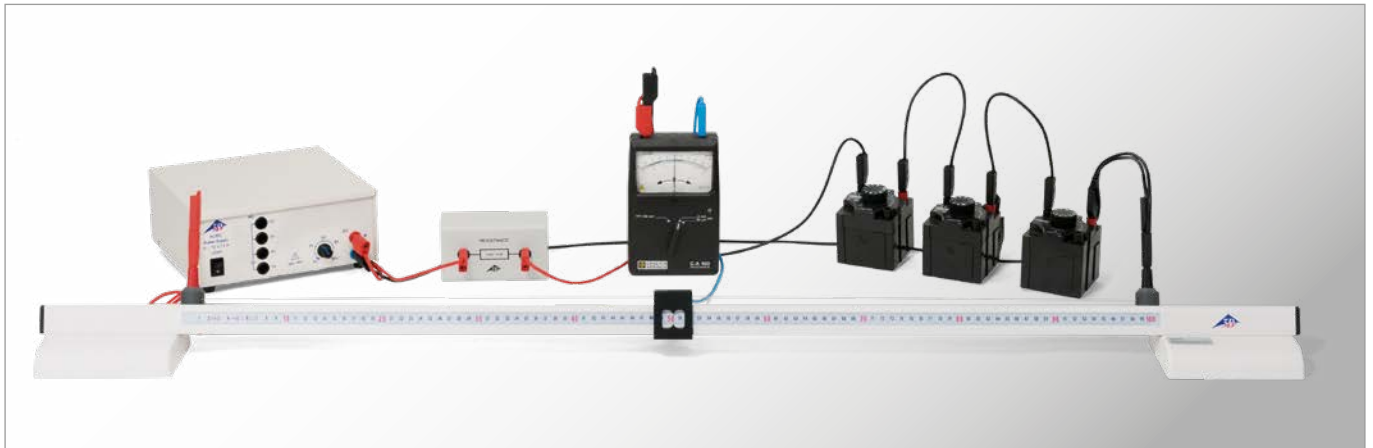


Fig. 2: Plot of U against d for copper and aluminum

UE3020300 | WHEATSTONE'S BRIDGE



EXPERIMENT PROCEDURE

- Determine resistances using a Wheatstone Bridge.
- Estimate the accuracy of the measurements.

OBJECTIVE

Determine the value of certain resistances

SUMMARY

An arrangement in which two voltage dividers are connected in parallel and connected to the same DC voltage source can be used to obtain the values of certain resistors. The first voltage divider consists of the resistance that is to be measured along with a reference resistance, while the second consists of a resistance wire 1 m in length that is divided into two sections by a sliding contact. The ratio between the two sections is adjusted until the current across the diagonal between the two voltage dividers becomes zero.

REQUIRED APPARATUS

Quantity	Description	Item Number
1	Resistance Bridge	1009885
1	AC/DC Power Supply 0 – 12 V, 3 A (230 V, 50/60 Hz)	1021091 or
	AC/DC Power Supply 0 – 12 V, 3 A (115 V, 50/60 Hz)	1021092
1	Zero Point Galvanometer CA 403	1002726
1	Resistance Decade 100 Ω	1002732
1	Resistance Decade 1 k Ω	1002733
1	Resistance Decade 10 k Ω	1002734
1	Precision Resistor 100 Ω	1009886
1	Precision Resistor 1 Ω	1009887
1	Set of 15 Safety Experiment Leads, 75 cm	1002843

BASIC PRINCIPLES

A classical method for measuring resistances uses a voltage balancing bridge named after *Charles Wheatstone* to compare the unknown resistance with a reference resistance. This involves setting up a circuit consisting of two voltage dividers in parallel, with a single DC voltage source connected across the whole. The first voltage divider consists of the resistance R_x that is to be measured and a reference resistance R_{ref} , while the second consists of two resistances R_1 and R_2 , the sum of which remains constant during the balancing process (see Fig. 1).

The ratio between the resistances R_1 and R_2 and – if necessary – the value of the reference resistance R_{ref} are varied until the current across the diagonal is reduced to zero. This occurs when the ratio between the resistances is the same for both voltage dividers. This balance condition leads to the following expression for the unknown resistance R_x :

$$(1) \quad R_x = R_{ref} \cdot \frac{R_1}{R_2}$$

The accuracy of the result depends on the precision of the reference resistance R_{ref} , the resistance ratio R_1/R_2 and the sensitivity of the null-detecting galvanometer.

In this experiment the second voltage divider consists of a resistance wire 1 m in length, which is divided into two sections of lengths s_1 and s_2 by a sliding contact. As the sum $R_1 + R_2$ remains constant, the reference resistance should, so far as possible, be chosen so that the two sections have about the same length, and therefore similar resistance.

EVALUATION

As the two resistances R_1 and R_2 correspond to the two sections of the resistance wire, Equation (1) can be rewritten as

$$R_x = R_{ref} \cdot \frac{s_1}{s_2} = R_{ref} \cdot \frac{s_1}{1\text{ m} - s_1}$$

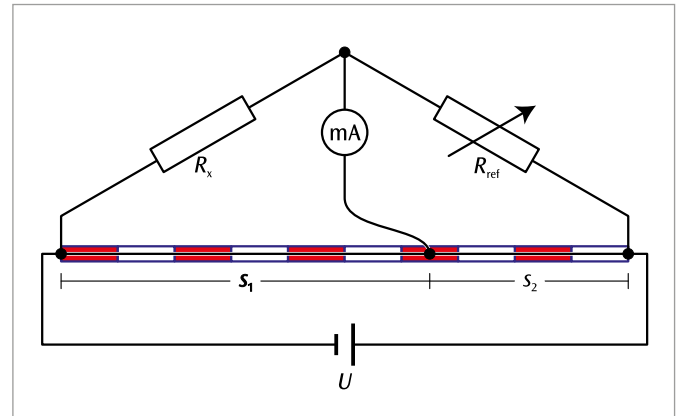
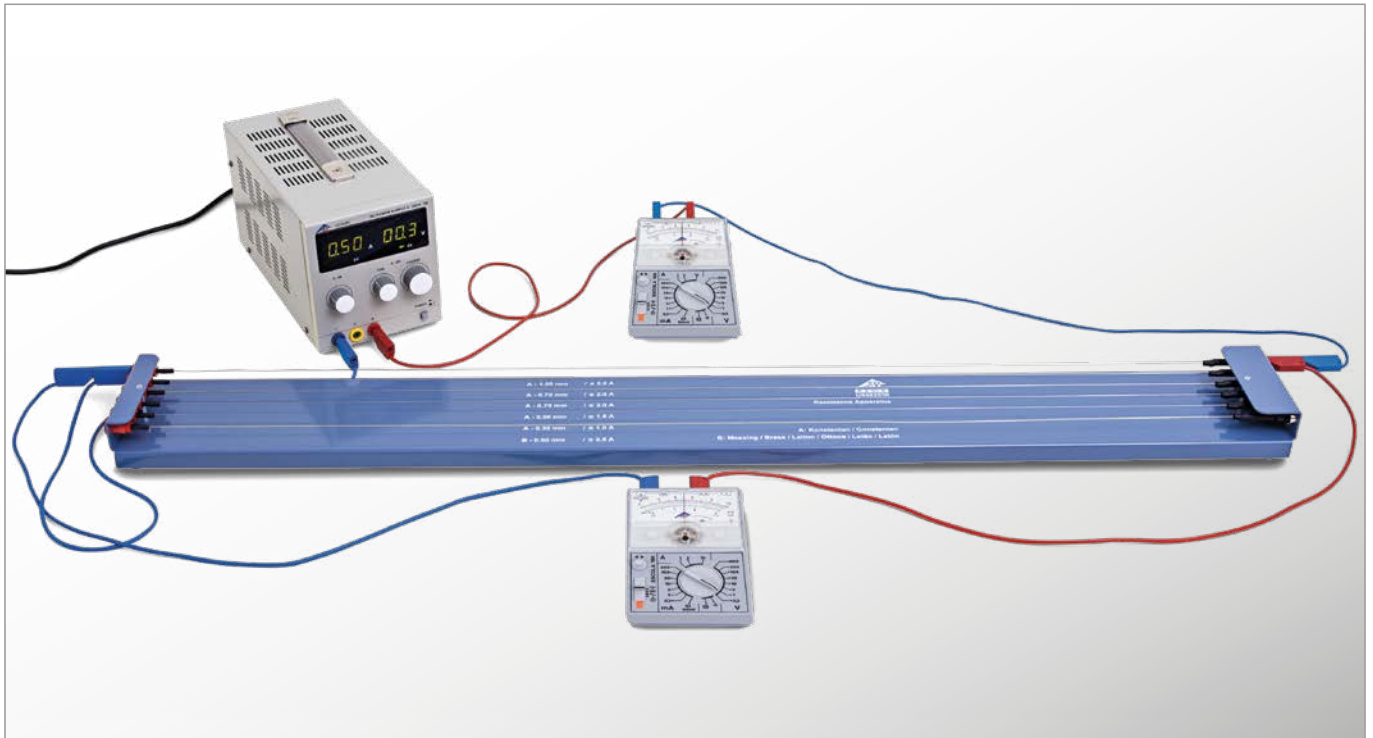


Fig. 1: Schematic diagram of a Wheatstone bridge

UE3020320 | OHM'S LAW



EXPERIMENT PROCEDURE

- Verification of Ohm's law for a constantan wire and a brass wire.
- Verification of Ohm's law for constantan wires of various lengths.
- Verification of Ohm's law for constantan wires of various thickness.

OBJECTIVE

Verification of Ohm's law

SUMMARY

In simple electrical conductors, the current I which passes through the conductor is proportional to the applied voltage U . The constant of proportionality, the ohmic resistance R , is dependent on the length x of the conductor, its cross-sectional area A and the nature of the material. This relationship is to be investigated using constantan and brass wires.

REQUIRED APPARATUS

Quantity	Description	Item Number
1	Resistance Apparatus	1009949
1	DC Power Supply 0 – 20 V, 0 – 5 A (230 V, 50/60 Hz)	1003312 or
	DC Power Supply 0 – 20 V, 0 – 5 A (115 V, 50/60 Hz)	1003311
2	Analog Multimeter ESCOLA 30	1013526
1	Set of 15 Safety Experiment Leads, 75 cm	1002843

BASIC PRINCIPLES

Georg Simon Ohm was the first in 1825 to show that the current flowing through a simple conductor is proportional to the voltage applied.

This means that Ohm's law applies:

$$(1) \quad U = R \cdot I$$

The constant of proportionality R is the resistance of the conductor. For a metal wire of length x and cross-sectional area A , the resistance R is given by the following formula:

$$(2) \quad R = \rho \cdot \frac{x}{A}$$

The specific resistivity ρ depends on the material of which the wire is made.

In order to verify this fundamental relationship, an experiment is to be carried out to investigate the proportionality between current and voltage for metal wires of varying thickness, length and material. The resistivity will also be determined and compared with values quoted in literature,

EVALUATION

The cross-sectional area A is calculated from the thickness d of the wires:

$$A = \frac{\pi}{4} \cdot d^2$$

The measurements are to be plotted in three graphs of U against I . In each of these, one of the parameters ρ , x or d will be varied.

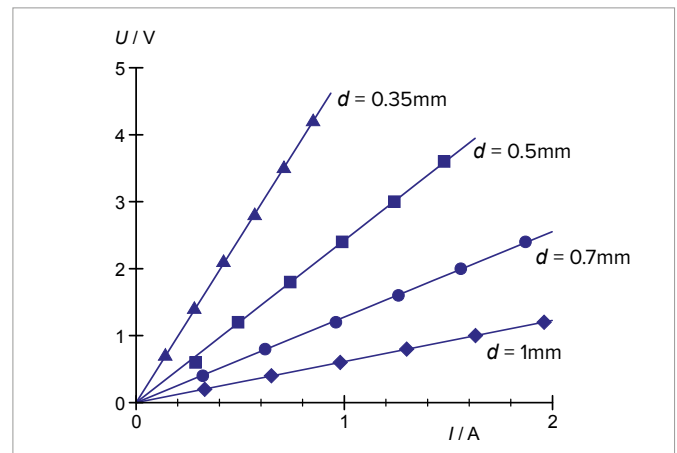


Fig. 3: Graph of U against I for constantan wires of various thickness

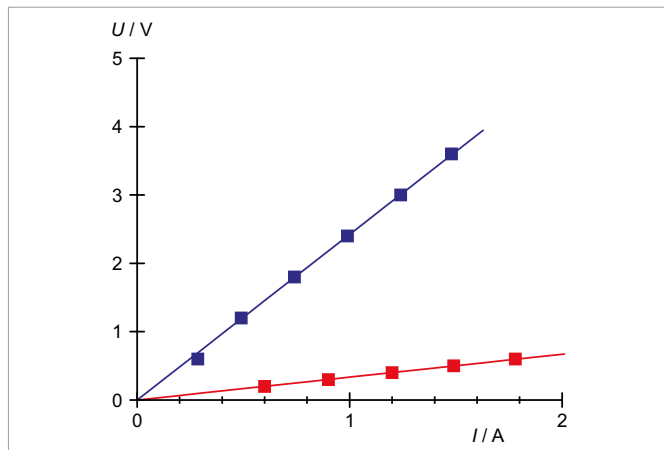


Fig. 1: Graph of U against I for constantan wire (blue) and brass wire (red)

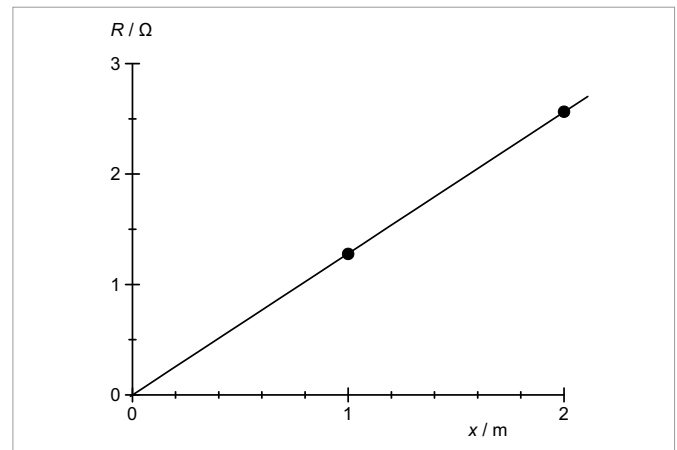


Fig. 4: Resistance R as a function of length

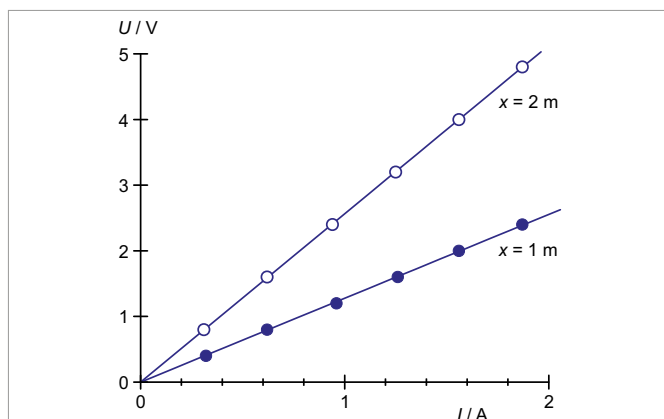


Fig. 2: Graph of U against I for constantan wires of various lengths

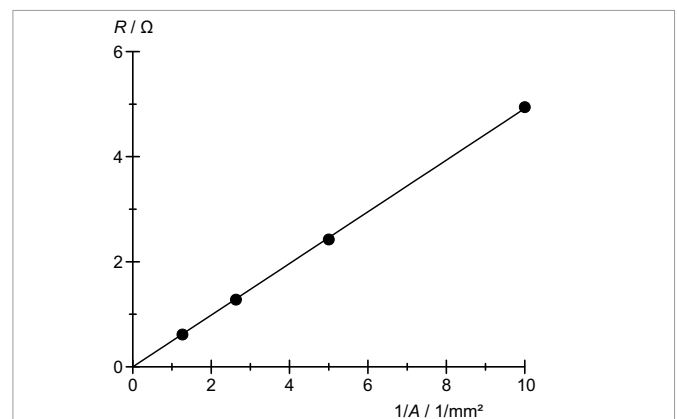
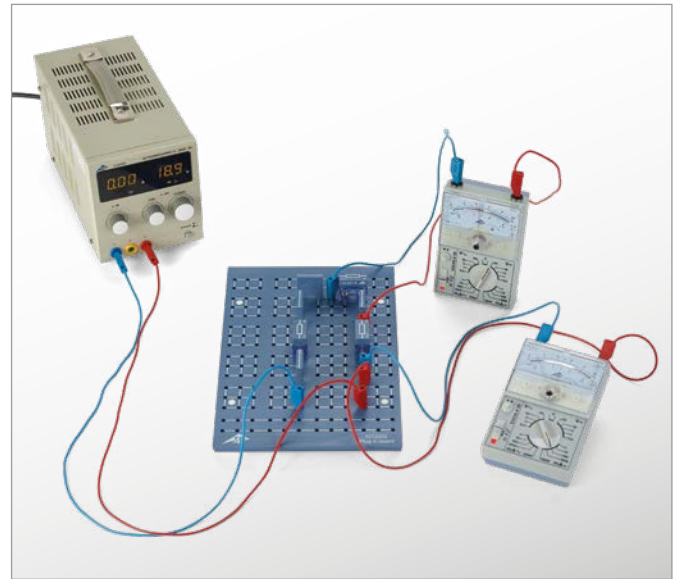
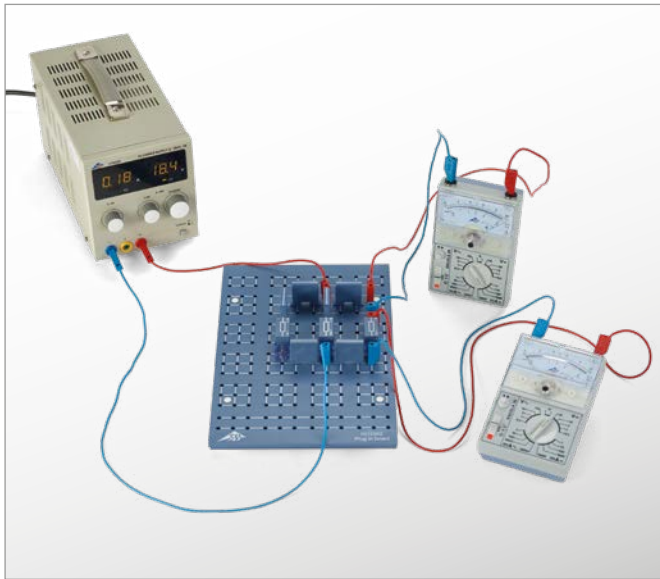


Fig. 5: Resistance R as a function of the inverse of the cross-sectional area A

UE3020330 | KIRCHHOFF'S LAWS



EXPERIMENT PROCEDURE

- Verify Kirchhoff's laws for a circuit featuring resistors in series.
- Determine the overall resistance of a series circuit.
- Verify Kirchhoff's laws for a circuit featuring resistors in parallel.
- Determine the overall resistance of a parallel circuit.

OBJECTIVE

Measure voltage and current in circuits featuring resistors in series and in parallel

SUMMARY

Kirchhoff's laws are of key importance for calculating current and voltage in various parts of a circuit with multiple branches. In this experiment, Kirchhoff's laws will be verified by measuring voltage and current in various parts of circuits featuring resistors in series and parallel.

REQUIRED APPARATUS

Quantity	Description	Item Number
1	Plug-In Board for Components	1012902
1	Resistor 220 Ω , 2 W, P2W19	1012912
1	Resistor 330 Ω , 2 W, P2W19	1012913
1	Resistor 470 Ω , 2 W, P2W19	1012914
1	Resistor 1 k Ω , 2 W, P2W19	1012916
1	Resistor 6.8 k Ω , 2 W, P2W19	1012921
1	Resistor 10 k Ω , 0.5 W, P2W19	1012922
1	Resistor 100 k Ω , 0.5 W, P2W19	1012928
1	Set of 10 Jumpers, P2W19	1012985
1	DC Power Supply 0 – 20 V, 0 – 5 A (230 V, 50/60 Hz)	1003312 or
	DC Power Supply 0 – 20 V, 0 – 5 A (115 V, 50/60 Hz)	1003311
2	Analog Multimeter ESCOLA 30	1013526
1	Set of 15 Experiment Leads, 75 cm, 1 mm ²	1002840

BASIC PRINCIPLES

In 1845 *Gustav Robert Kirchhoff* formulated laws describing the relationship between voltage and current in electric circuits which include multiple branches. Kirchhoff's 1st law (current law or junction rule) states that at every point where a circuit branches the sum of the currents flowing towards the junction are equal to the sum of currents flowing away from it. His 2nd law (voltage law, loop or mesh rule) states that, for any loop in any closed circuit, the sum of the voltages in all the branches is equal to the overall voltage provided by the source to that loop. For such loops, a direction of flow is defined. Currents flowing around the loop in the defined direction and voltages which cause such current to flow are considered to be positive, whereas if the currents flow in the opposite direction they are considered to be negative, along with the voltages driving them. These rules can, for example, be applied to circuits featuring resistors in series or in parallel.

In a circuit with n resistors in series, the current I is identical at every point in the circuit. According to Kirchhoff's second law, the sum of the voltages across each resistor will be equal to the voltage of the source to which they are connected.

$$(1) \quad U = U_1 + \dots + U_n$$

Therefore the following applies with respect to the overall resistance R_{ser} :

$$(2) \quad R_{\text{ser}} = \frac{U}{I} = \frac{U_1 + \dots + U_n}{I} = R_1 + \dots + R_n$$

For a circuit featuring resistors in parallel, so-called nodes or junctions arise for the current. Measurements at those nodes show that the sum of the current flowing towards them is equal to the sum of the currents flowing away from them. The voltages at each of these nodes are identical. Kirchhoff's 2nd law makes it possible to determine unknown currents at a node. The sum of the currents flowing through the resistors in each branch is equal to the overall current I , whereby the following is true:

$$(3) \quad I = I_1 + \dots + I_n$$

Therefore the following applies with respect to the overall resistance R_{par} :

$$(4) \quad \frac{1}{R_{\text{par}}} = \frac{I}{U} = \frac{I_1 + \dots + I_n}{U} = \frac{1}{R_1} + \dots + \frac{1}{R_n}$$

In this experiment, series and parallel circuits both featuring three resistors are investigated. To verify Kirchhoff's laws, the overall current and the current in each section will be measured along with the overall voltage and the voltage in each section.

EVALUATION

From the measurements on the series and parallel circuits, the overall resistance R is first to be calculated and then compared with the theoretical values obtained from equations (2) and (4).

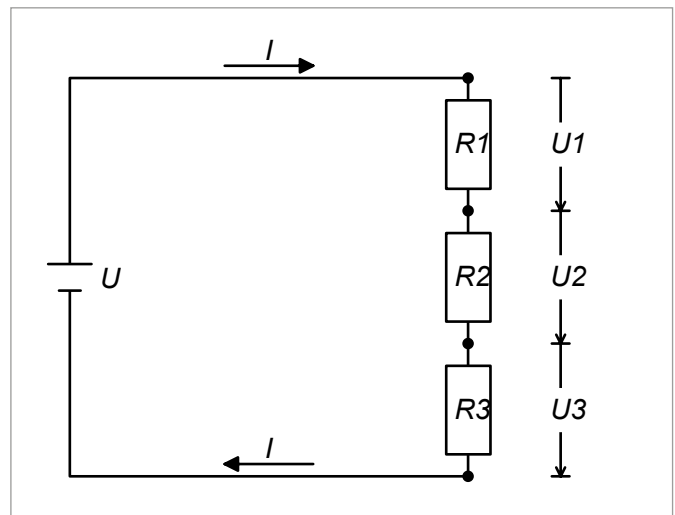


Fig. 1: Schematic for Kirchhoff's laws as applied to a circuit featuring resistors in series

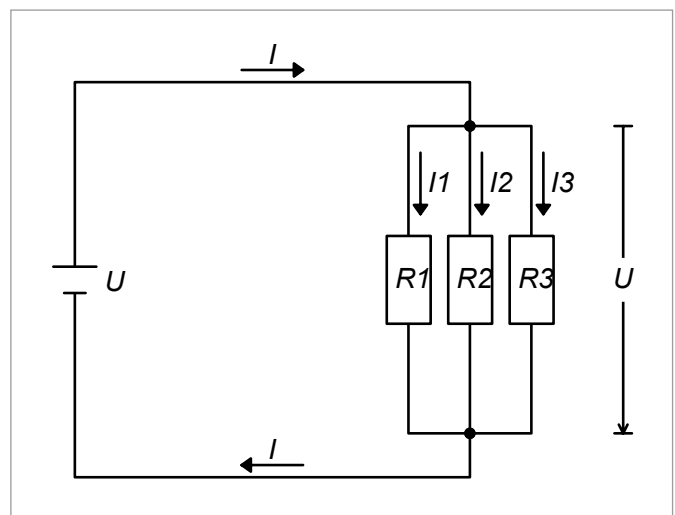


Fig. 2: Circuit diagram for a circuit featuring resistors in parallel

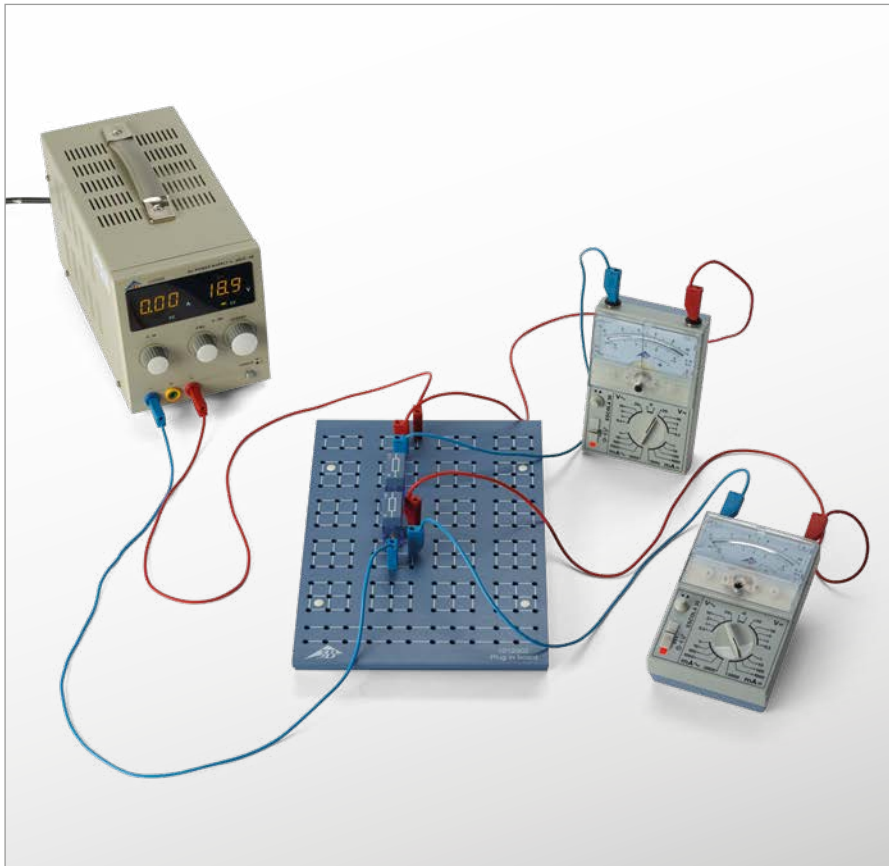
UE3020340 | VOLTAGE DIVIDERS

OBJECTIVE

Measure the voltage and current for a voltage divider with and without a load

SUMMARY

A voltage divider in its simplest form consists of a pair of resistors connected in series, whereby the total voltage across the two of them is divided into two parts. A voltage divider is considered to be loaded when a further resistance is connected in parallel with one of the pair. The current and voltage in each part of the circuit are calculated as in any other series or parallel circuit using Kirchhoff's laws. When there is no load on the divider, the portions of the voltage can vary between 0 volts and the total voltage, depending on the individual resistors. There is a marked difference, however, when the circuit is loaded with very small loads. Then the voltage across the part of the circuit including the load will be very small regardless of the resistors in the divider.



EXPERIMENT PROCEDURE

- Measure voltage and current for a voltage divider with no load as a function of the resistance R_2 .
- Measure voltage and current for a voltage divider with no load for a constant overall resistance $R_1 + R_2$.
- Measure voltage and current for a voltage divider with a load as a function of the load resistance R_L .

REQUIRED APPARATUS

Quantity	Description	Item Number
1	Plug-In Board for Components	1012902
1	Resistor 47 Ω , 2 W, P2W19	1012908
2	Resistor 100 Ω , 2 W, P2W19	1012910
1	Resistor 150 Ω , 2 W, P2W19	1012911
1	Resistor 470 Ω , 2 W, P2W19	1012914
1	Potentiometer 220 Ω , 3 W, P4W50	1012934
1	DC Power Supply 0 – 20 V, 0 – 5 A (230 V, 50/60 Hz)	1003312 or
	DC Power Supply 0 – 20 V, 0 – 5 A (115 V, 50/60 Hz)	1003311
2	Analog Multimeter ESCOLA 30	1013526
1	Set of 15 Experiment Leads, 75 cm, 1 mm ²	1002840

BASIC PRINCIPLES

A voltage divider in its simplest form consists of a pair of resistors connected in series, whereby the total voltage across the two of them is divided into two parts. A voltage divider is considered to be loaded when a further resistance is connected in parallel with one of the pair. The current and voltage in each part of the circuit are calculated as in any other series or parallel circuit using Kirchhoff's laws.

When there is no load on the divider, the overall resistance is given by the following equation (see Fig. 1)

$$(1) \quad R = R_1 + R_2$$

The same current flows through both resistors

$$(2) \quad I = \frac{U}{R_1 + R_2}$$

U : Overall voltage

Therefore the voltage across R_2 is given by the following:

$$(3) \quad U_2 = I \cdot R_2 = U \cdot \frac{R_2}{R_1 + R_2}$$

When the divider is loaded, the load resistance R_L also needs to be taken into account (see Fig. 2), whereby the value of R_2 in the above equation is replaced by the following expression:

$$(4) \quad R_p = \frac{R_2 \cdot R_L}{R_2 + R_L}$$

Thus the voltage U_2 in that part of the circuit is now given by

$$(5) \quad U_2 = I \cdot R_p = U \cdot \frac{R_p}{R_1 + R_p}$$

In this experiment, an unloaded voltage divider is assembled using two discrete resistors R_1 and R_2 with resistors of various different values being used as R_2 . Alternatively, a potentiometer can be used, in which case the total resistance $R_1 + R_2$ is inherently constant and the value of R_2 depends on the position of the potentiometer's sliding contact. The voltage source supplies a constant value U , which remains unchanged for the whole experiment. In each case the voltage and the current is measured for each section of the circuit.

EVALUATION

In a voltage divider without a load, the voltage U_2 corresponds to the overall voltage U , if R_2 is very much larger than R_1 but is close to zero if R_2 is very small in comparison.

For a voltage divider with a load of comparatively large magnitude, the resistance of the parallel section effectively equates to $R_p = R_2$ and the voltage in the section U_2 is then given by equation (3). The situation is very different if the load resistance is very small. In that case $R_p = R_L$, since most of the current flows through the load. The voltage U_2 then becomes very small regardless of the value of R_2 .

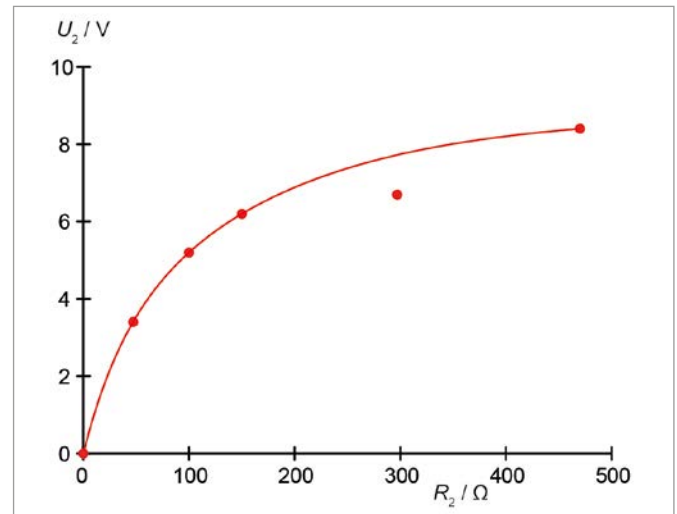


Fig. 3: Voltage U_2 as a function of resistance R_2 in a voltage divider with no load

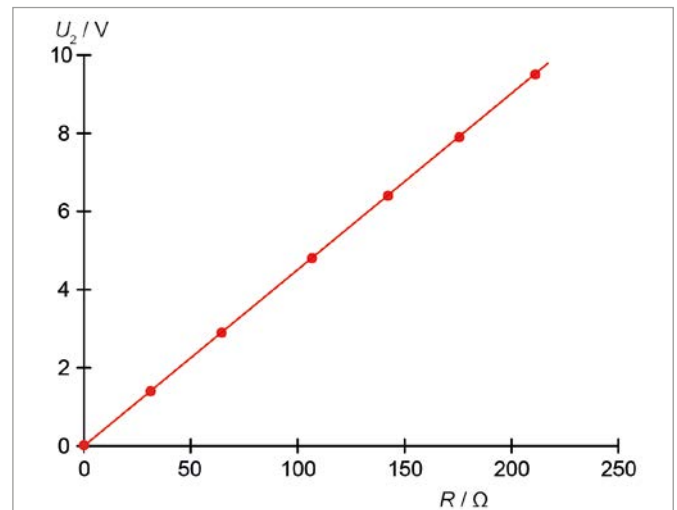


Fig. 4: Voltage U_2 as a function of resistance R_2 in a voltage divider with no load and a constant overall resistance $R_1 + R_2$

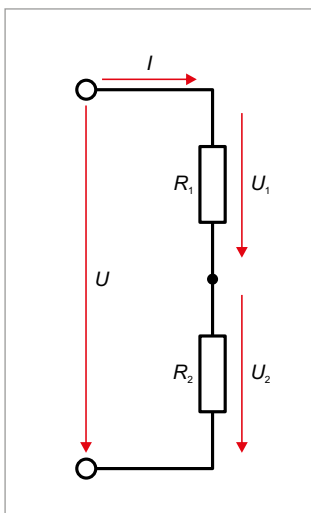


Fig. 1: Circuit diagram of a voltage divider with no load

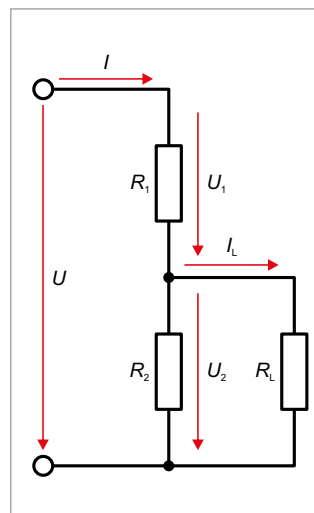


Fig. 2: Circuit diagram of a voltage divider with a load

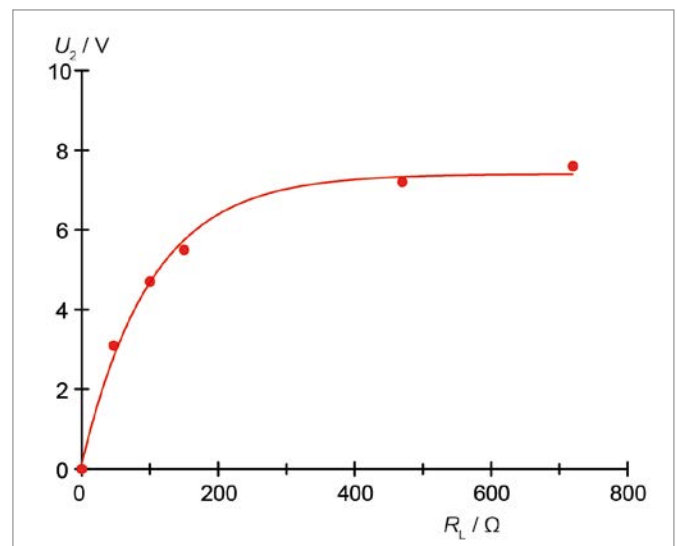


Fig. 5: Voltage U_2 as a function of resistance R_2 in a voltage divider with a load

UE3020700 | TRANSPORT AND CURRENT



EXPERIMENT PROCEDURE

- Generating hydrogen by electrolysis and measuring the volume of hydrogen V .
- Measuring the electrical work W needed to generate the hydrogen at a constant voltage U_0 .
- Calculating the Faraday constant F .

OBJECTIVE

Determine the Faraday constant

SUMMARY

The Faraday constant is determined by measuring the quantities of hydrogen and oxygen generated by the electrolysis of water and the electric charge that is transported during the process.

REQUIRED APPARATUS

Quantity	Description	Item Number
1	Electrolysis Apparatus	1002899
1	Digital Multimeter P3415	1008631
1	DC Power Supply 0 – 20 V, 0 – 5 A (230 V, 50/60 Hz)	1003312 or
	DC Power Supply 0 – 20 V, 0 – 5 A (115 V, 50/60 Hz)	1003311
1	Set of 15 Experiment Leads, 75 cm, 1 mm ²	1002840

Additionally required

Sulphuric Acid, 1 mol/l

BASIC PRINCIPLES

Electrolysis is the breakdown of a chemical compound by the action of an electric current. When this occurs, the process of electrical conduction is accompanied by a release of material, and the quantity of material released, n is proportional to the transported charge Q . The proportionality constant is called the Faraday constant F and it is a universal constant of nature.

For a fuller and more accurate description of the proportionality relationship between the charge Q and the molar quantity n of material that is released, one must also take into account the valence number z of the ions that are released. Thus

$$(1) \quad Q = F \cdot n \cdot z$$

In this manner, the Faraday Constant can be determined by measuring the charge Q and the molar quantity n for an electrolytic process, provided the valence number is known.

In the experiment, water is electrolyzed to generate a specific quantity of hydrogen and oxygen. To determine the charge Q that is transported, the electrical work

$$(2) \quad W = Q \cdot U_0$$

that is performed at constant voltage U_0 to achieve electrolysis is measured.

The molar quantity n_H of hydrogen ions that is released at room temperature T and external pressure p is determined from the measured volume V_{H_2} of the gas. However, one must take into account the fact that the hydrogen is collected in molecular form, and for each hydrogen molecule collected, two hydrogen ions have been released. Thus, from the equation of state for an ideal gas we have:

$$(3) \quad n_H = 2 \cdot \frac{p \cdot V_{H_2}}{R \cdot T}$$

$$R = 8.314 \frac{\text{J}}{\text{mol} \cdot \text{K}} : \text{the universal gas constant.}$$

EVALUATION

The valence number of hydrogen ions is $z_H = 1$. Therefore, from Equations 1, 2 and 3, we obtain the following equation for determining the Faraday constant:

$$F = \frac{W}{U_0} \cdot \frac{R \cdot T}{2 \cdot p \cdot V_{H_2} \cdot n_H} = \frac{W}{U_0} \cdot \frac{R \cdot T}{2 \cdot p \cdot V_{H_2}}$$

For comparison, we can also measure the volume of oxygen that is collected, V_{O_2} . It is only half of the hydrogen volume, because each water molecule that is electrolyzed releases two hydrogen ions and one oxygen ion. However, the valence number for oxygen ions is $z_O = 2$.

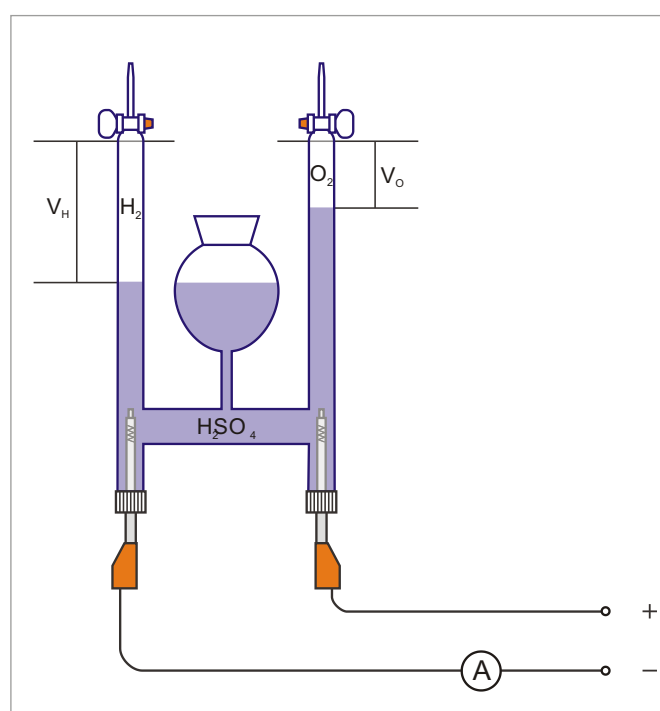


Fig. 1: Schematic diagram

UE3030300 | LORENTZ FORCE



EXPERIMENT PROCEDURE

- Determine the direction of the Lorentz force.
- Measure the force as a function of the current.
- Measure the force as a function of the effective length of the conductor.
- Measure the force as a function of the distance between the poleshoes of the permanent magnet.

OBJECTIVE

Measure the force on a current-carrying conductor in a magnetic field

SUMMARY

The experiment involves measuring the Lorentz force on a current-carrying copper rod suspended in a horizontal position from a pair of vertical wires (like a swing) and subjected to a magnetic field. When the current is switched on the “swing” is deflected from the vertical position and the Lorentz force can be calculated from the angle of deflection. The current through the rod, the magnetic field strength and the effective length of the conductor in the magnetic field are varied and the effects are measured.

REQUIRED APPARATUS

Quantity	Description	Item Number
1	Equipment Set Electromagnetism	1002661
1	Permanent Magnet with Adjustable Pole Spacing	1002660
1	DC Power Supply 0 – 20 V, 0 – 5 A (230 V, 50/60 Hz)	1003312 or
	DC Power Supply 0 – 20 V, 0 – 5 A (115 V, 50/60 Hz)	1003311
1	Pair of Safety Experimental Leads, 75 cm, red/blue	1017718

BASIC PRINCIPLES

Electrons moving in a magnetic field are deflected in a direction perpendicular to the magnetic field and also perpendicular to the direction of motion. However, the deflecting force on a single electron – the Lorentz force – cannot easily be measured in practice, as it is extremely small, even for an electron moving very fast in a very strong magnetic field. A different situation exists when a current-carrying conductor is placed in a uniform magnetic field. In the conductor there are a large number of charge-carriers, all moving with the same drift velocity v . A force then acts on the conductor, which results from the sum of the Lorentz force components on all the individual charge-carriers.

In a straight conductor of length L and cross-sectional area A , the total number of electrons is:

$$(1) \quad N = n \cdot A \cdot L$$

n : Electrons per unit volume

If the electrons move with a drift velocity v in the direction of the length of the conductor, the current I through it is as follows:

$$(2) \quad I = n \cdot e \cdot A \cdot v$$

e : Elementary charge of an electron.

If the conductor is in a magnetic field of flux density B , the combined Lorentz force on all the “drifting” electrons is as follows:

$$(3) \quad F = N \cdot e \cdot v \times B$$

If the axis of the conductor is perpendicular to the magnetic field direction, Equation (3) can be simplified to the following:

$$(4) \quad F = I \cdot B \cdot L$$

Then the force F is perpendicular to the axis of the conductor and to the magnetic field.

The experiment involves measuring the Lorentz force F on a current-carrying copper rod, suspended in a horizontal position from a pair of vertical wires (like a swing) and subjected to a magnetic field (see Fig. 1). When the current is switched on the “swing” is deflected by an angle ϕ from the vertical position by the Lorentz force F , which can then be calculated from Equation (5).

$$(5) \quad F = m \cdot g \cdot \tan \phi$$

$m = 6.23$ g, the mass of the copper rod.

The magnetic field B is provided by a permanent magnet, and can be varied by altering the distance d between the pole-shoes of the magnet. It is also possible to rotate the pole-shoes through 90° , thus changing the width b along the direction of the conductor and thereby the effective length L of the conductor, i.e. the part of it that is inside the magnetic field. This effective length L is slightly greater than the width b of the space between the pole-shoes, as the magnetic field “bulges out”, forming a non-uniform region beyond the edges of the pole-shoes. The extent of this non-uniform part of the field increases with the distance d between the pole-shoes. To a good approximation:

$$(6) \quad L = b + d$$

EVALUATION

The angle ϕ can be determined from the length of the pendulum s (the supporting wires) and the horizontal deflection x of the copper rod:

$$\frac{x}{\sqrt{s^2 - x^2}} = \tan \phi$$

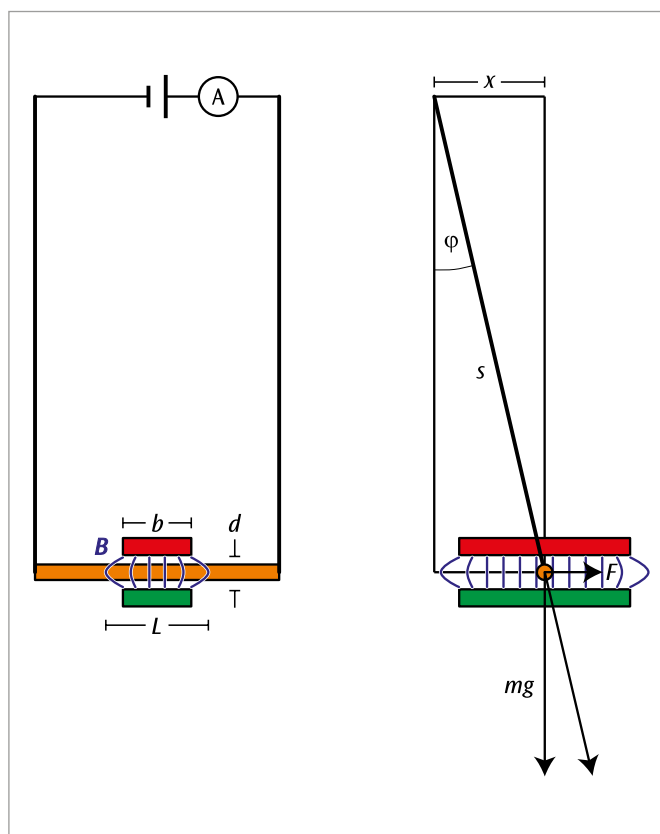


Fig. 1: Experiment set-up, viewed from the side and from the front

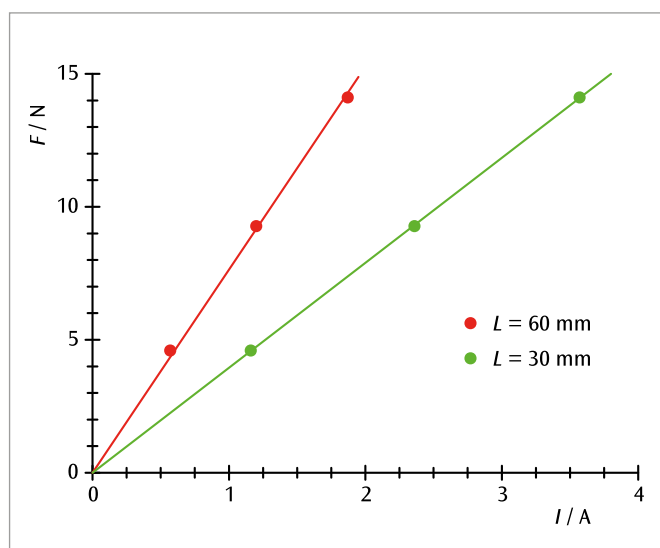


Fig. 2: Force on a current-carrying conductor as a function of current I for two different effective conductor lengths L . The gradients of the straight lines through the origin are proportional to L

UE3030350 | ELECTRIC BALANCE



> EXPERIMENT PROCEDURE

- Measurement of the force exerted on a current-carrying conductor as a function of the amperage.
- Measurement of the force exerted on a current-carrying conductor as a function of its length.
- Calibration of the magnetic field.

OBJECTIVE

Measurement of the force exerted on a current-carrying conductor located inside a magnetic field

SUMMARY

The electric balance is based on *André-Marie Ampère's* experiments on electric current. It measures the electro-dynamic force sometimes referred to as the Lorentz force on a current carrying conductor situated in a magnetic field using a balance. In this experiment the current conductor is suspended from a rigid suspension system and exerts the equal and opposite force on the permanent magnets as the electro-dynamic force generated by the magnetic field. The result is the apparent change in weight of the permanent magnets.

REQUIRED APPARATUS

Quantity	Description	Item Number
1	Current Balance Equipment Set	1021822
1	Electronic Scale Scout SKX 420 g	1020859
1	DC Power Supply 0 – 20 V, 0 – 5 A (230 V, 50/60 Hz)	1003312 or
	DC Power Supply 0 – 20 V, 0 – 5 A (115 V, 50/60 Hz)	1003311
1	Stainless Steel Rod 250 mm	1002933
1	Tripod Stand 150 mm	1002835
1	Two-pole Switch	1018439
3	Pair of Experiment Leads, 75 cm	1002850

BASIC PRINCIPLES

The electric balance is based on *André-Marie Ampères'* experiments on electrical current. It measures the force exerted on a current-carrying conductor located in a magnetic field with the aid of a balance. In the experiment a modern electronic precision balance weighs a permanent magnet. The weight measured changes in accordance with Newton's 3rd law when an electro-dynamic force is exerted on a current-carrying conductor entering a magnetic field. On the balance lies a permanent magnet which generates a horizontal magnetic field B . In this arrangement a horizontal current conductor of length L and suspended from a rigid bar is dipped vertically into the magnetic field. The electro-dynamic force from the magnet acts on the conductor

$$(1) \quad F_L = N \cdot e \cdot v \times B$$

e : elementary charge

N : total number of all electrons participating in electrical conduction

The mean drift velocity v is all the greater, the greater the current I flowing through the conductor:

$$(2) \quad I = n \cdot e \cdot A \cdot v$$

n : number of all electrons involved in the current conduction,

A : cross-section of the conductor

From

$$(3) \quad N = n \cdot A \cdot L$$

L : length of the conductor

we obtain

$$(4) \quad F_L = I \cdot L \cdot e \times B$$

or

$$(5) \quad F_L = I \cdot L \cdot B$$

since the unit vector e pointing in the direction of the conductor is located perpendicular to the magnetic field. In accordance with Newton's third law, an equal and opposite force F is exerted on the permanent magnet. Depending on the sign, the weight G of the permanent magnet measured on the balance is either increased or decreased. Thanks to the balance's tare function, the weight G can be electronically offset so that the balance immediately displays the opposing force F .

EVALUATION

It has been demonstrated that the current dependency of the electro-dynamic force or Lorentz force can be accurately described by a straight line through the origin (Fig. 2). This is not the case for conductor length dependency (Fig. 3) due to the fact that here boundary effects play a role at the ends of the conductor. The magnetic field of the fully assembled permanent magnet is computed from the linear gradients $a_2 = B L$ in Fig. 2 and $a_3 = B I$ in Fig. 3.

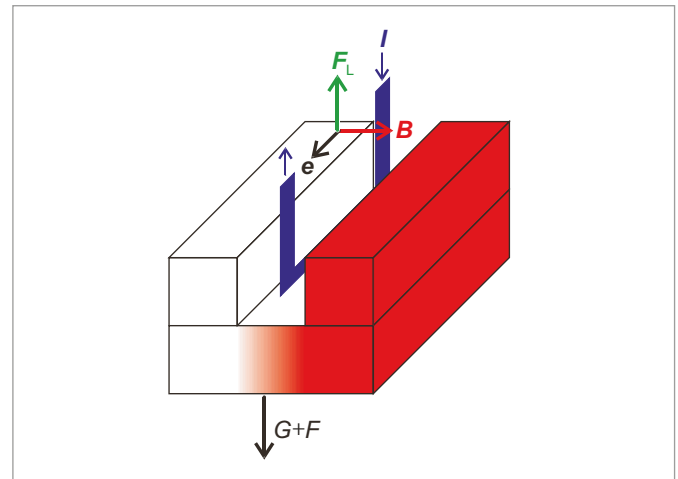


Fig. 1: Schematic depiction of the electro-dynamic force F_L on the current-carrying conductor and the total force $G + F$ on the balance.

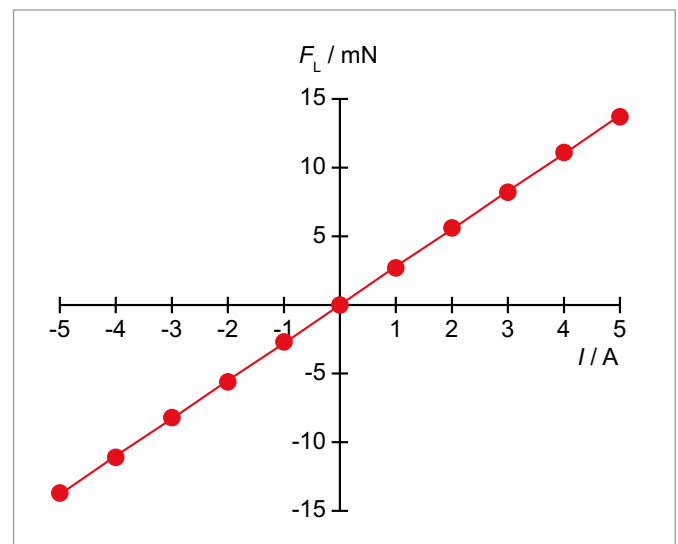


Fig. 2: Force F_L as a function of the amperage I

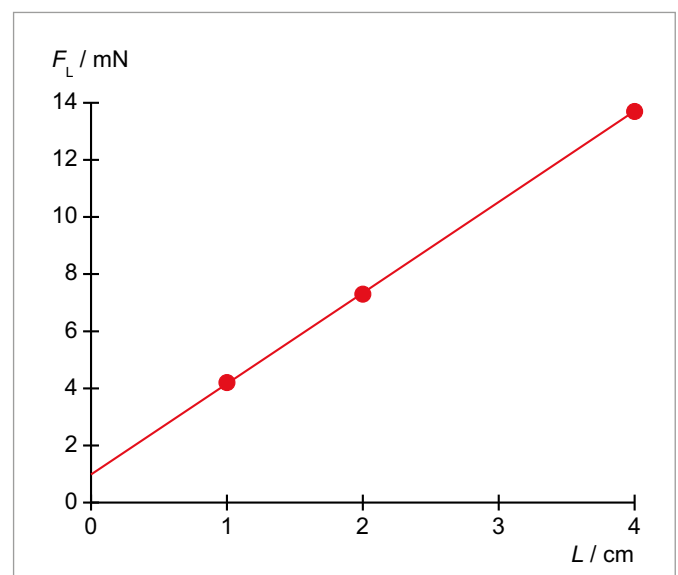
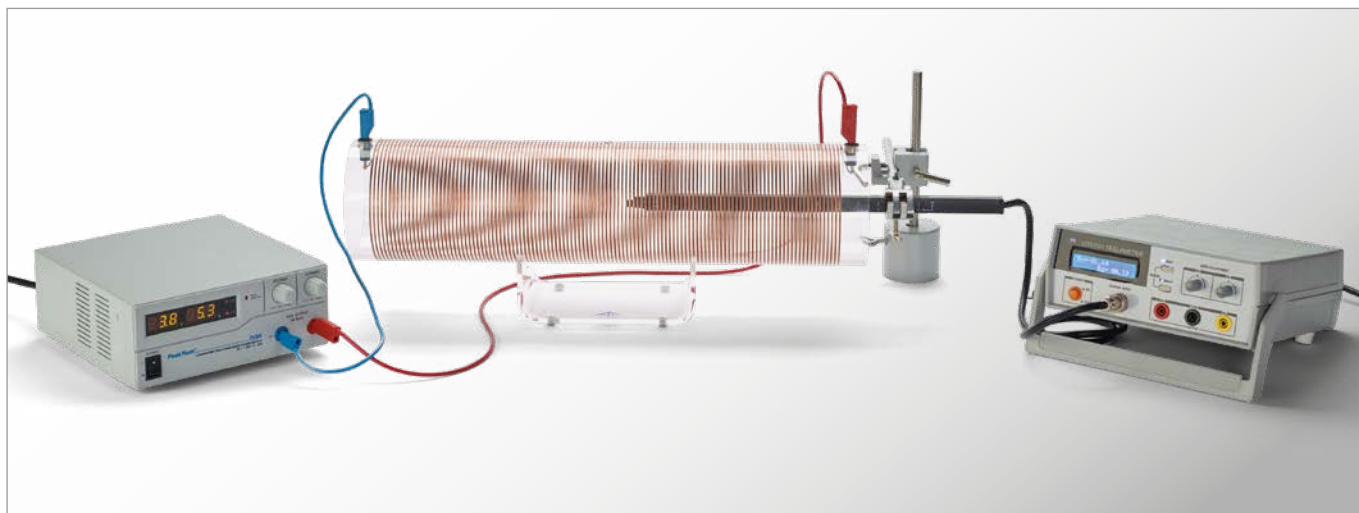


Fig. 3: Force F_L as a function of the conductor length L

UE3030500

MAGNETIC FIELD OF A CYLINDRICAL COIL



EXPERIMENT PROCEDURE

- Determine the magnetic flux density B inside a cylindrical coil as a function of the current I .
- Measure the magnetic flux density B inside a cylindrical coil with coils that can be moved closer together or farther apart as a function of the current I .
- Determine that for long coils, the magnetic flux density is proportional to the density of the windings (how close they are together).

OBJECTIVE

Determine the magnetic field generated by coils of various lengths

SUMMARY

The magnetic flux density inside a long cylindrical coil is directly proportional to the current through the coil and how close together the coil windings are, but is not dependent on the radius of the coil as long as the length of the coil is comparatively much greater than its diameter. That will be demonstrated in this experiment using two coils of different diameter and another coil in which the separation of the coil windings can be increased or decreased.

REQUIRED APPARATUS

Quantity	Description	Item Number
1	Field Coil 100 mm	1000591
1	Field Coil 120 mm	1000592
1	Coil with Variable Number of Turns per Unit Length	1000965
1	Stand for Cylindrical Coils	1000964
1	Teslameter N (230 V, 50/60 Hz)	1021669 or
	Teslameter N (115 V, 50/60 Hz)	1012857
1	DC Power Supply, 1 – 32 V, 0 – 20 A (230 V, 50/60 Hz)	1012857 or
	DC Power Supply, 1 – 40V, 0 – 40 A (115 V, 50/60 Hz)	1022289
1	Set of 15 Experiment Leads, 75 cm, 2.5 mm ²	1002841
1	Barrel Foot, 1000 g	1002834
1	Stainless Steel Rod 250 mm	1002933
1	Universal Clamp	1002830
1	Universal Jaw Clamp	1002833

BASIC PRINCIPLES

The Biot-Savart law describes the relationship between magnetic flux density B and electric current I through a conductor of any arbitrary geometry. The calculation involves adding the contributions of infinitesimally small sections of conductor to find the overall magnetic flux density. The overall field is then determined by integrating over the geometry of the conductor. In some cases, e.g. for a long cylindrical coil, there is a simple analytical solution to this integration.

According to the Biot-Savart law, an infinitesimally small section of conductor ds through which a current I is flowing, generates the following magnetic flux density at the point r

$$(1) \quad dB(r) = \frac{\mu_0}{4\pi} \cdot I \cdot \frac{ds \times r}{r^3}$$

B : magnetic flux density

$$\mu_0 = 4\pi \cdot 10^{-7} \frac{\text{Vs}}{\text{Am}} \quad \text{: permeability of free space}$$

Inside the cylindrical coil, the magnetic flux density is aligned parallel to the axis of the cylinder and is given by the following expression:

$$(2) \quad B = \mu_0 \cdot \frac{N}{L} \cdot I$$

N : number of windings, L : length of coil

This applies as long as the length of the coil is much greater than its radius. The magnetic flux density does not therefore depend on the diameter of the coil and is proportional to the density of the windings, i.e. the number of windings per unit length, and the current through the coil.

The experiment involves using an axial teslameter to measure the magnetic flux density inside long coils for currents of up to 20 A. It demonstrates that the flux density does not depend on the coil diameter but is proportional to the current and the winding density. In order to prove the latter, a coil is provided which allows the windings to be moved closer together or farther apart, i.e. varying the number of windings per unit length.

EVALUATION

All the measurements confirm that the magnetic flux density B is proportional to the current I through the coil.

The flux density is confirmed to be proportional to the windings per unit length as long as the length of the coil is more than three times its radius.

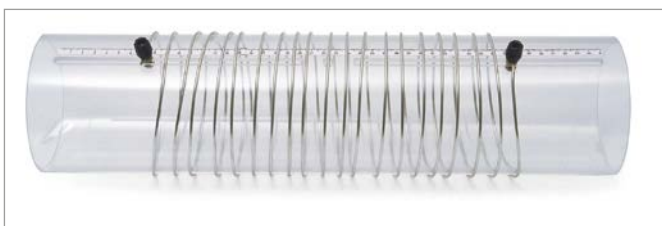


Fig. 1: Coil with variable number of windings per unit length

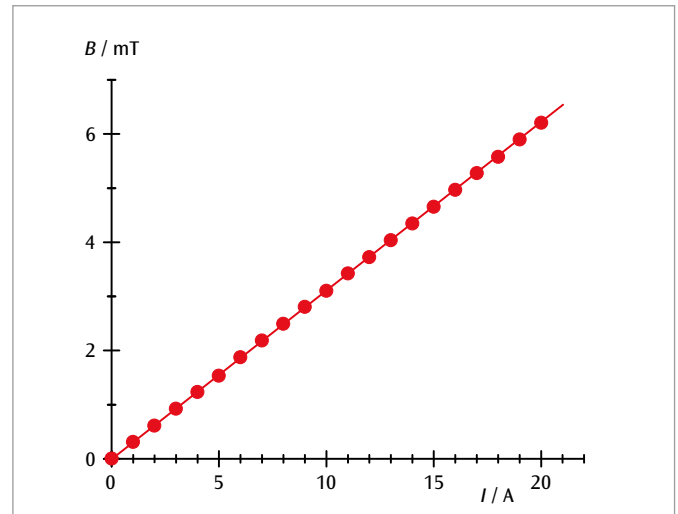


Fig. 2: Magnetic flux density B as a function of current I

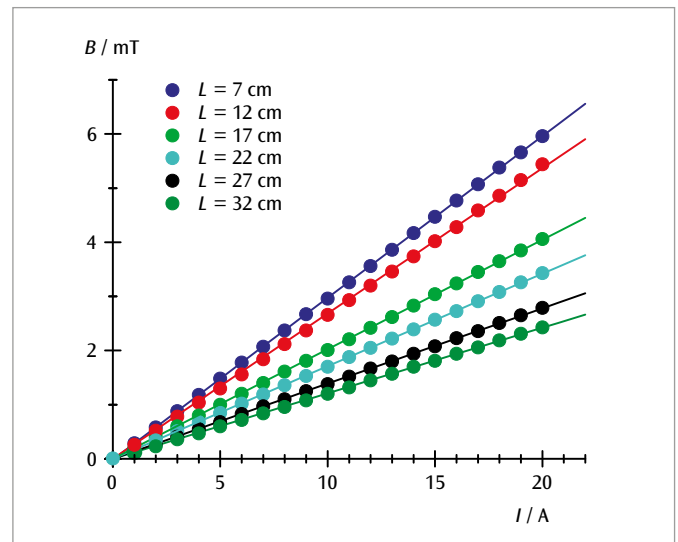


Fig. 3: Magnetic flux density B as a function of current I using the coil with a variable number of windings per unit length for various lengths of coil L

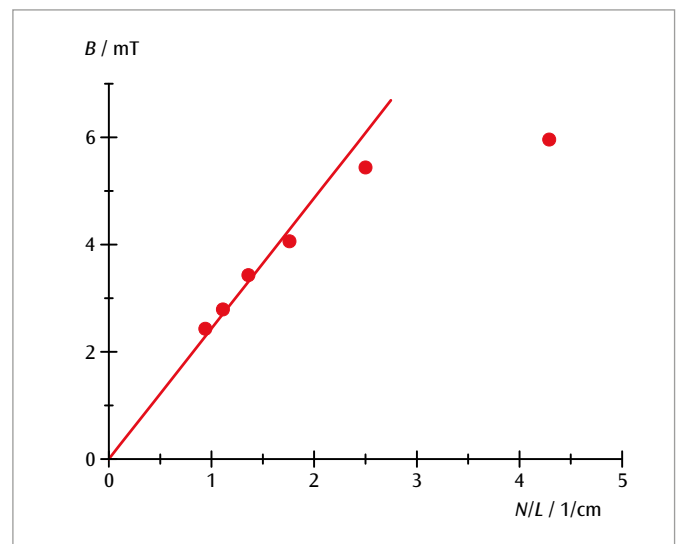


Fig. 4: Magnetic flux density B as a function of number of windings per unit length N/L when $I = 20$ A

UE3030700 | MAGNETIC FIELD OF THE EARTH



EXPERIMENT PROCEDURE

- Measure the angle of rotation of a compass needle initially aligned parallel with the horizontal component of earth's magnetic field when a second horizontal magnetic field is superimposed with the help of a pair of Helmholtz coils.
- Determine the horizontal component of the earth's magnetic field.
- Measure the inclination and vertical component and calculate the overall magnitude of the earth's magnetic field.

OBJECTIVE

Determine the horizontal and vertical components of the earth's magnetic field

SUMMARY

This experiment involves determining the inclination and magnitude of the earth's magnetic field as well as its horizontal and vertical components at the point where the measurement is made. The horizontal component of the earth's field can be found from the turning of a compass needle when an additional magnetic field is applied by means of a pair of Helmholtz coils. By measuring the angle of inclination, it is also possible to work out the vertical component and calculate the overall magnitude of the earth's magnetic field.

REQUIRED APPARATUS

Quantity	Description	Item Number
1	Helmholtz Coils 300 mm	1000906
1	DC Power Supply 0 – 20 V, 0 – 5 A (230 V, 50/60 Hz)	1003312 or
	DC Power Supply 0 – 20 V, 0 – 5 A (115 V, 50/60 Hz)	1003311
1	Digital Multimeter P1035	1002781
1	Inclination Instrument E	1006799
1	Rheostat 100 Ω	1003066
1	Set of 15 Safety Experiment Leads, 75 cm	1002843

BASIC PRINCIPLES

The earth is surrounded by a magnetic field generated by a so-called geo-dynamo effect. Close to the surface of the earth, this field resembles that of a magnetic dipole with field lines emerging from the South Pole of the planet and circling back towards the North Pole. The angle between the actual magnetic field of the earth and the horizontal at a given point on the surface is called the inclination. The horizontal component of the earth's field roughly follows a line running between geographical north and south. Because the earth's crust exhibits magnetism itself, there are localized differences which are characterized by the term declination.

This experiment involves measuring the inclination and the absolute magnitude of the earth's magnetic field along with the horizontal and vertical components of it at the point where the measurement is made. The following relationships apply:

$$(1) \quad B_v = B_h \cdot \tan \alpha$$

α : inclination

B_h : horizontal component

B_v : vertical component

and

$$(2) \quad B = \sqrt{B_h^2 + B_v^2}$$

It is therefore sufficient to determine the values B_h and α , since the other values can simply be calculated.

The inclination α is determined with the aid of a dip needle. In order to obtain the horizontal component B_h , the dip needle is aligned in horizontal plane in such a way that its needle points to 0° when parallel to the horizontal component 0° . An additional horizontal magnetic field B_{HH} , which is perpendicular to B_h , is generated by a pair of Helmholtz coils and this field causes the compass needle to turn by an angle β . According to Fig. 1 the following is then true:

$$(3) \quad \frac{B_{HH}}{B_h} = \tan \beta$$

In order to improve the accuracy, this measurement is carried out for a variety of angles β .

EVALUATION

From equation (3) the following can be deduced:

$$B_{HH} = B_h \cdot \tan \beta.$$

The horizontal component B_h is therefore equivalent to the gradient of a line through points plotted on a graph of B_{HH} against $\tan \alpha$.

The magnetic field of the Helmholtz coils B_{HH} can be determined easily. Inside the pair of coils it is highly uniform and is proportional to the current I through either of the coils:

$$B_{HH} = k \cdot I \quad \text{with} \\ k = \left(\frac{4}{5}\right)^{\frac{3}{2}} \cdot 4\pi \cdot 10^{-7} \frac{\text{Vs}}{\text{Am}} \cdot \frac{N}{R}$$

$N = 124$: number of windings, $R = 147,5 \text{ mm}$: radius

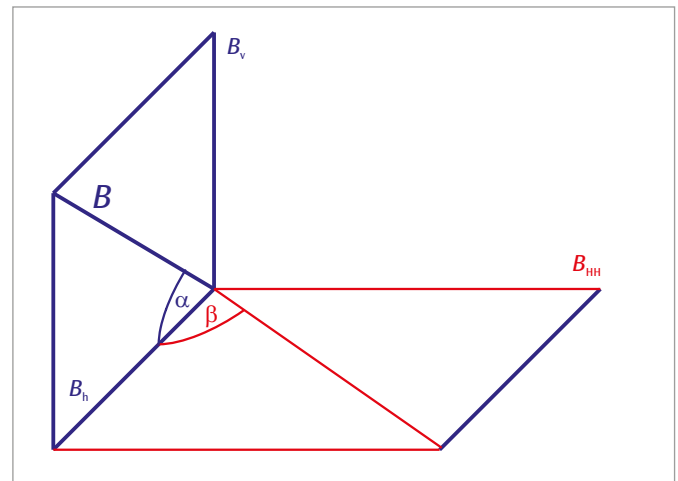


Fig. 1: Components of the magnetic fields observed in the experiment and definition of the corresponding angles

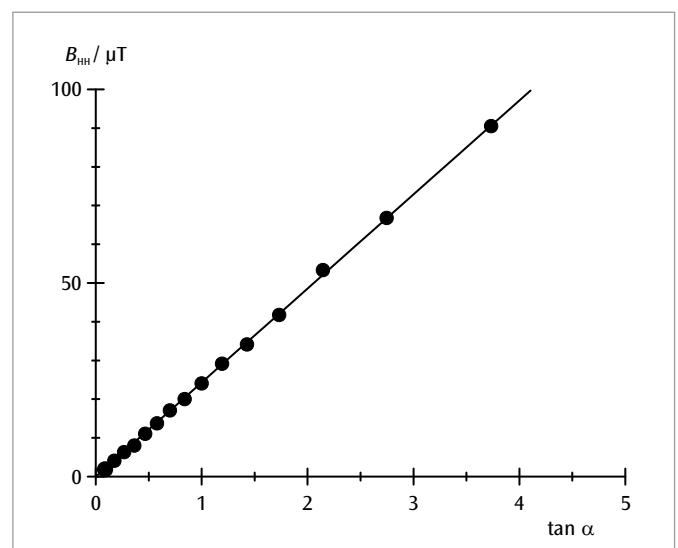
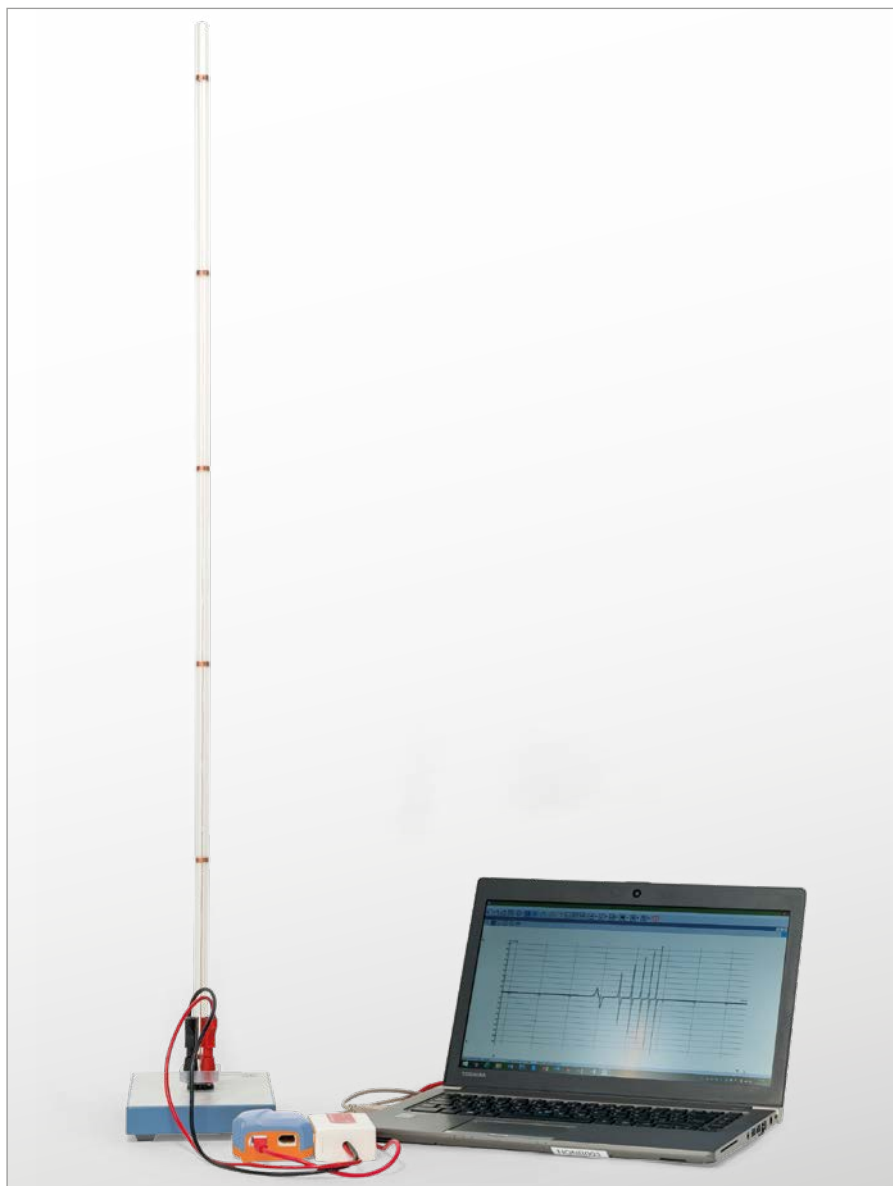


Fig. 2: $B_{HH} - \tan \alpha$ -graph to determine the horizontal component of the earth's magnetic field

UE3040100 | FARADAY'S LAW OF INDUCTION



OBJECTIVE

Generating a voltage pulse in a conducting loop by the motion of a permanent magnet

SUMMARY

When a permanent bar magnet is allowed to fall in succession through a set of identical induction coils connected in series, a voltage is induced in each of the coils. The voltage amplitude increases from coil to coil as the magnet moves through each coil, as the velocity of the magnet increases steadily. However, the magnetic flux that is calculated by integrating over the observed voltage curve has the same value for all the coils.

> EXPERIMENT PROCEDURE

- Observing the motion of a permanent bar magnet through a set of induction coils connected in series.
- Measuring the induced voltage as a function of time.
- Calculating the magnetic flux as a function of time.

REQUIRED APPARATUS

Quantity	Description	Item Number
1	Tube with 6 Induction Coils	1001005
1	WiLab *	1022284
1	Voltage Sensor 500 mV, Differential	1021681
1	Sensor Cable	1021514
Additionally required		
1	Coach 7 license	

* Alternative: 1 VinciLab 1021477

BASIC PRINCIPLES

Any change of the magnetic flux through a closed conducting loop induces in it an electrical voltage. Such a change is produced, for example, when a permanent bar magnet moves through a stationary conducting loop.

In this case it is instructive to consider not only the time-dependent induced voltage

$$(1) \quad U(t) = - \frac{d\Phi}{dt}(t)$$

Φ : Magnetic flux

but also its integral over time, viz. the voltage pulse

$$(2) \quad \int_{t_1}^{t_2} U(t) \cdot dt = \Phi(t_1) - \Phi(t_2)$$

This corresponds to the difference between the magnetic flux at the beginning (t_1) and that at the end (t_2) of the observed process.

In the experiment, a permanent bar magnet is allowed to fall through six identical induction coils that are connected in series. The induced voltage is recorded as a function of time (see Fig. 2). The voltage amplitude increases from coil to coil as the magnet moves through each coil, because the velocity of the magnet increases steadily. The areas under all the positive and negative voltage signals are equal. They correspond to the maximum flux Φ produced by the permanent magnet inside each individual coil.

EVALUATION

The experimental set-up is such that the induced voltage is negative when the magnet is introduced into the coil. The induced voltage is once again zero when the magnet reaches the center of the coil, and therefore the magnetic flux has its maximum value at that point. During the subsequent exit phase of the magnet, a positive voltage is induced. From the voltage measurements, we can calculate the magnetic flux at any point in time t by integration, using Equation 2:

$$\Phi(t) = \Phi(0) - \int_0^t U(t') \cdot dt'$$

The maximum flux reached during the magnet's fall is the same for all the coils, subject to the limitation of the precision of the measurements (see Fig. 2).

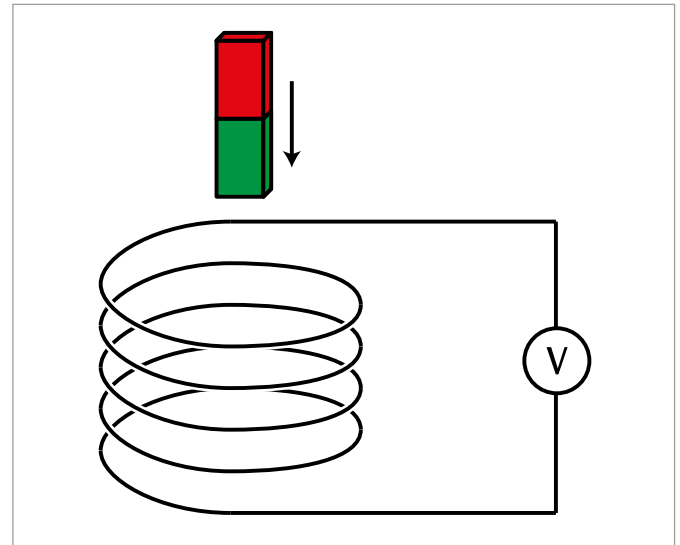


Fig. 1: Principle for measurement



Fig. 2: Induced voltage U as a function of time

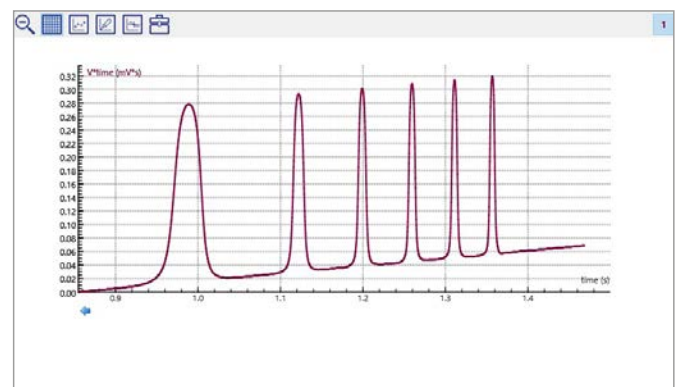
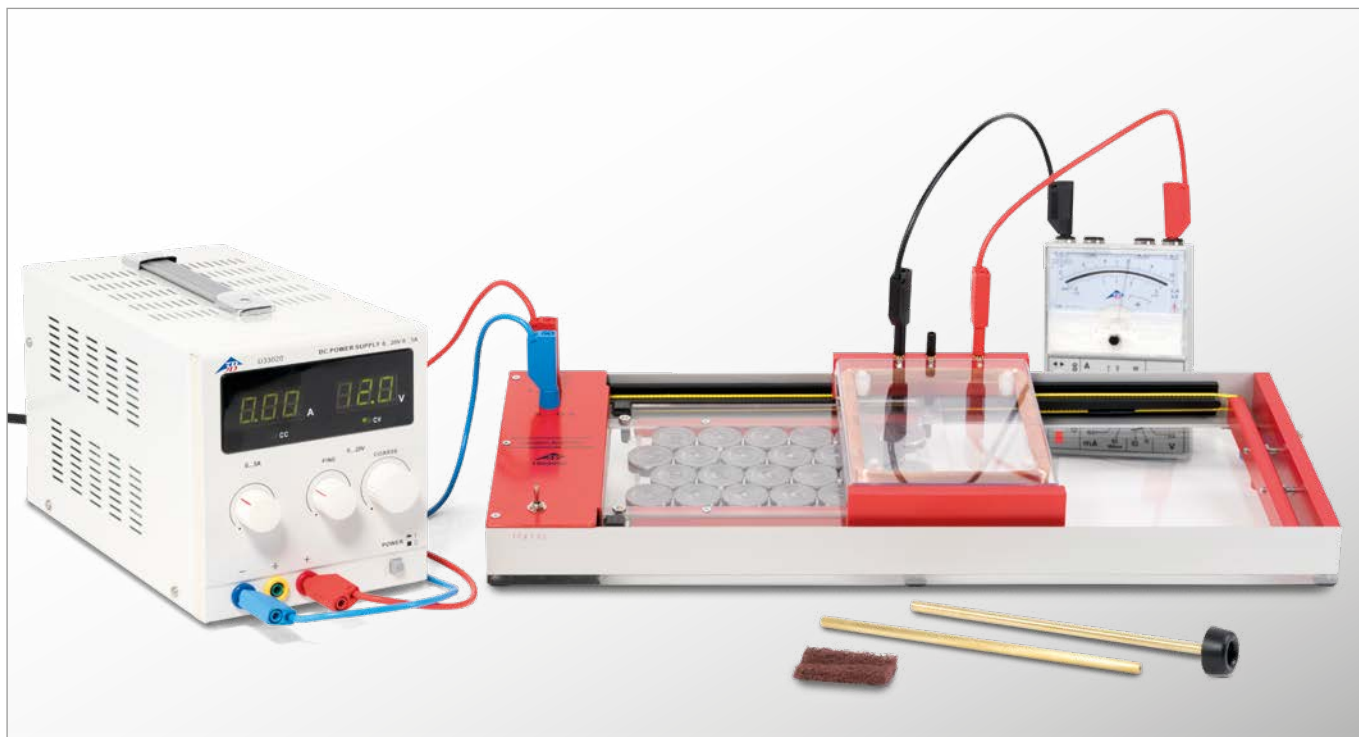


Fig. 3: Magnetic flux Φ as a function of time

UE3040200

INDUCTION IN A MOVING CONDUCTOR LOOP



EXPERIMENT PROCEDURE

- Measure the induced voltage as a function of the velocity of the conductor loop.
- Measure the induced voltage as a function of the number of turns in the conductor loop.
- Compare the sign of the induced voltage when moving the conductor loop into the field or out of it.
- Compare the sign of the induced voltage when the direction of motion is changed.
- Measure the induced voltage in a conductor loop with a single turn of variable area.

OBJECTIVE

Measure the induced voltage in a conductor made into a loop as it moves through a magnetic field

SUMMARY

The change in magnetic flux that is needed to induce a voltage in a conductor loop can be caused by a movement of the loop. Such a situation results, for example, when a conductor loop orientated with its plane perpendicular to a homogeneous magnetic field is moved into the magnetic field or withdrawn from it at a constant velocity. In the first case the magnetic flux increases at a rate determined by the relevant parameters, whereas in the second case it decreases in a similar way. Therefore the induced voltages are of opposite signs.

REQUIRED APPARATUS

Quantity	Description	Item Number
1	Induction Apparatus	1000968
1	DC Power Supply 0 – 20 V, 0 – 5 A (230 V, 50/60 Hz)	1003312 or
	DC Power Supply 0 – 20 V, 0 – 5 A (115 V, 50/60 Hz)	1003311
1	Analogue Multimeter ESCOLA 100	1013527
1	Set of 15 Safety Experiment Leads, 75 cm	1002843
1	Mechanical Cumulative Stopwatch	1002810
Additionally recommended		
1	Measurement Amplifier U (230 V, 50/60 Hz)	1020742 or
	Measurement Amplifier U (115 V, 50/60 Hz)	1020744

BASIC PRINCIPLES

The term **electromagnetic induction** refers to the process whereby an electric voltage is generated around a conductor loop when the magnetic flux passing through the loop is changed. Such a change in flux can result from a change in the magnetic field strength or from movement of the conductor loop.

To describe the relationships involved, a U-shaped conductor loop with a moveable crossbar is often considered. The plane of this loop is aligned perpendicular to a homogeneous magnetic field of flux density B (see Fig. 1). The magnetic flux through the area limited by the cross-bar is

$$(1) \quad \Phi = B \cdot a \cdot b$$

a : Width, b : Length of the loop.

If the cross-bar is moved with a velocity v , the flux changes, since the length of the loop is changed. The rate of change of the flux is

$$(2) \quad \frac{d\Phi}{dt} = B \cdot a \cdot v$$

and in the experiment it is observed as a voltage

$$(3) \quad U = -B \cdot a \cdot v$$

which is in the order of microvolts but can be measured using the amplifier that is recommended as additional equipment.

A much greater induced voltage is obtained if a conducting loop with multiple turns on a rigid frame is moved through the magnetic field. When the frame is only partly projecting into the magnetic field, the situation is as shown schematically in Figure 1. The movement of the loop into the magnetic field results in a change of flux at the following rate

$$(4) \quad \frac{d\Phi_1}{dt} = B \cdot N \cdot a \cdot v$$

N : Number of turns,

and this can be measured as an induced voltage.

$$(5) \quad U_1 = -B \cdot N \cdot a \cdot v$$

As soon as the conductor loop is completely in the magnetic field, the induced voltage returns to zero. No further change occurs until the loop begins to move out of the magnetic field. Now the magnetic flux is decreasing and the induced voltage is of opposite sign compared to the initial situation. A change of sign also occurs if the direction of motion of the loop is reversed.

In this experiment, the voltage driving an electric motor used to pull the conductor loop along is varied. This provides a range of different constant velocities. The direction of rotation of the motor can also be reversed. The coil provided also has an intermediate tapping point, so that the induced voltage can be measured for three different values of N , the number of turns.

EVALUATION

Calculate the velocity from the time t required for the conductor loop to move completely through the magnetic field and the corresponding distance L

$$v = \frac{L}{t}$$

Then draw a graph of the induced voltage U as a function of the velocity v . The data will be found to lie on a straight line through the origin (see Fig. 2).

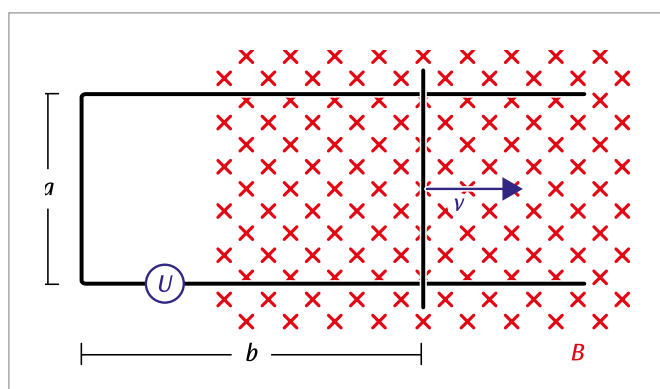


Fig. 1: The change of the magnetic flux through the conducting loop when its area is altered

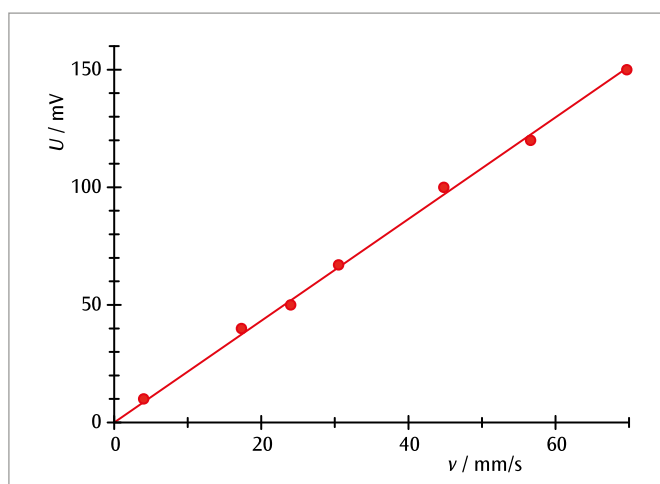
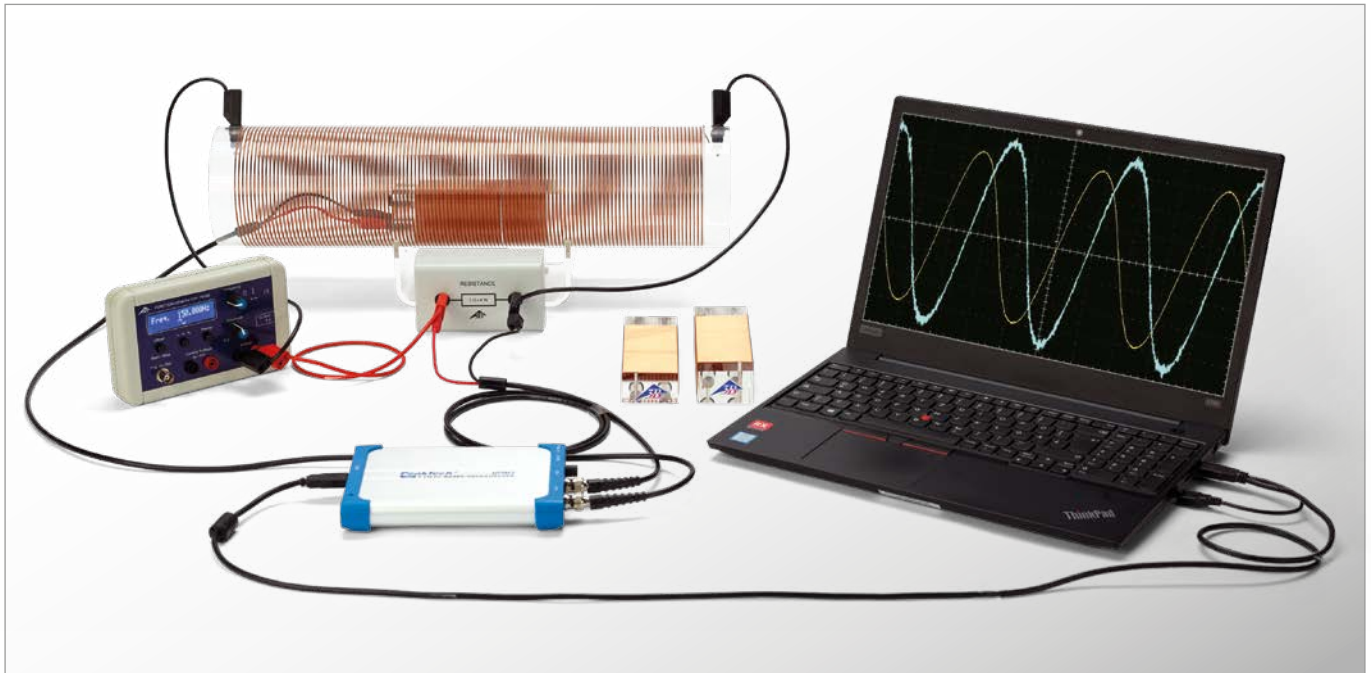


Fig. 2: Induced voltage as a function of the velocity of the conducting loop

UE3040300

INDUCTION BY A VARYING MAGNETIC FIELD



EXPERIMENT PROCEDURE

- Measure the induced voltage as a function of the number of turns N of the induction coil.
- Measure the induced voltage as a function of the cross-sectional area A of the induction coil.
- Measure the induced voltage as a function of the amplitude I_0 of the alternating current applied for induction.
- Measure the induced voltage as a function of the frequency f of the alternating current applied for induction.
- Measure the induced voltage as a function of the waveform of the alternating current applied for induction.

OBJECTIVE

Measuring the voltage induced in an induction coil

SUMMARY

If a closed conductor loop with N windings is located in a cylinder coil through which an alternating current flows, then an electrical voltage is induced by the variable magnetic flux through the conductor loop. This induction voltage is dependent on the number of windings and the cross-sectional area of the conductor loop as well as the frequency, amplitude and waveform of alternating current applied to the field coil. These dependencies are explored and compared with the principle theory.

REQUIRED APPARATUS

Quantity	Description	Item Number
1	Set of 3 Induction Coils	1000590
1	Field Coil 120 mm	1000592
1	Stand for Cylindrical Coils	1000964
1	Precision Resistor 1 Ω	1009843
1	Function Generator FG 100 (230 V, 50/60 Hz) Function Generator FG 100 (115 V, 50/60 Hz)	1009957 or 1009956
1	PC-Oszilloskop 2x25 MHz	1020857
2	HF Patch Cord, BNC/4 mm Plug	1002748
1	Pair of Safety Experiment Leads, 75 cm, black	1002849
1	Pair of Safety Experimental Leads, 75 cm, red/blue	1017718

BASIC PRINCIPLES

Every change in the magnetic flux through a closed conductor loop with N turns induces an electrical voltage in said loop. Such a variation is evoked, for example, if the conductor loop is located in a cylinder coil which has alternating current flowing through it.

According to Faraday's law of induction the following applies for an induced voltage dependent on rate of change:

$$(1) \quad U(t) = -N \cdot \frac{d\Phi}{dt}(t)$$

The magnetic flux Φ through an area A is given by:

$$(2) \quad \Phi = B \cdot A$$

B : Magnetic flux density

if the magnetic flux density B permeates the area A perpendicularly. Consequently, from Equation (1) we obtain:

$$(3) \quad U(t) = -N \cdot A \cdot \frac{dB}{dt}(t)$$

The field coil generates the following magnetic flux density in the conductor loop:

$$(4) \quad B = \mu_0 \cdot \frac{N_f}{L_f} \cdot I$$

$\mu_0 = 4\pi \cdot 10^{-7} \text{ N/A}^2$: Vacuum permeability,

N_f : Number of turns in the field coil, L_f : Length of the field coil,

I : Current flowing through the field coil

Accordingly, from Equation (3) we arrive at:

$$(5) \quad U(t) = -\mu_0 \cdot N \cdot A \cdot \frac{N_f}{L_f} \cdot \frac{dI}{dt}(t)$$

In the experiment a function generator is used first to apply a sinusoidal signal to the field coil. The amplitude I_0 of the current $I(t)$ is determined by the field coil with the aid of a resistor connected in series between the coil and generator. The amplitude U_0 of the induced voltage $U(t)$ is measured as a function of the number of windings N and cross-sectional area A of the induction coils as well as the frequency f of the sinusoidal signal and the amplitude I_0 of the current flowing through the field coil. Besides the sinusoidal signal, a triangular and a square-wave signal are also applied to the field coil for an induced voltage on a coil with fixed number of turns and cross-sectional area as well as a constant frequency, and from these measurements screen shots are made for each.

EVALUATION

For sinusoidal current: $I = I(t) = I_0 \cdot \sin(2 \cdot \pi \cdot f \cdot t)$,

the following applies: $U(t) = U_0 \cdot [-\cos(2 \cdot \pi \cdot f \cdot t)]$

with: $U_0 = 2 \cdot \pi \cdot \mu_0 \cdot \frac{N_f}{L_f} \cdot N \cdot A \cdot I_0 \cdot f$.

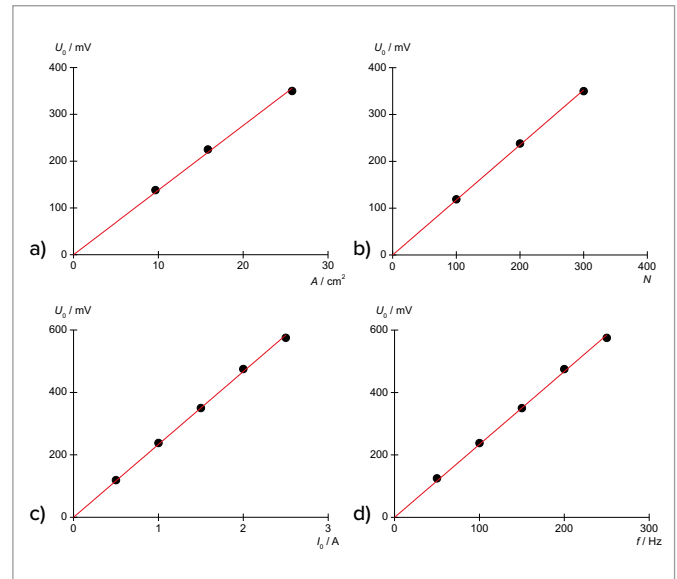


Fig. 1: Amplitude of the induced voltage as a function of the cross-sectional area of the induction coil (a), the number of turns (b), the amplitude of the current flowing through the field coil (c) and the frequency of the sinusoidal signal applied to the field coil (d).

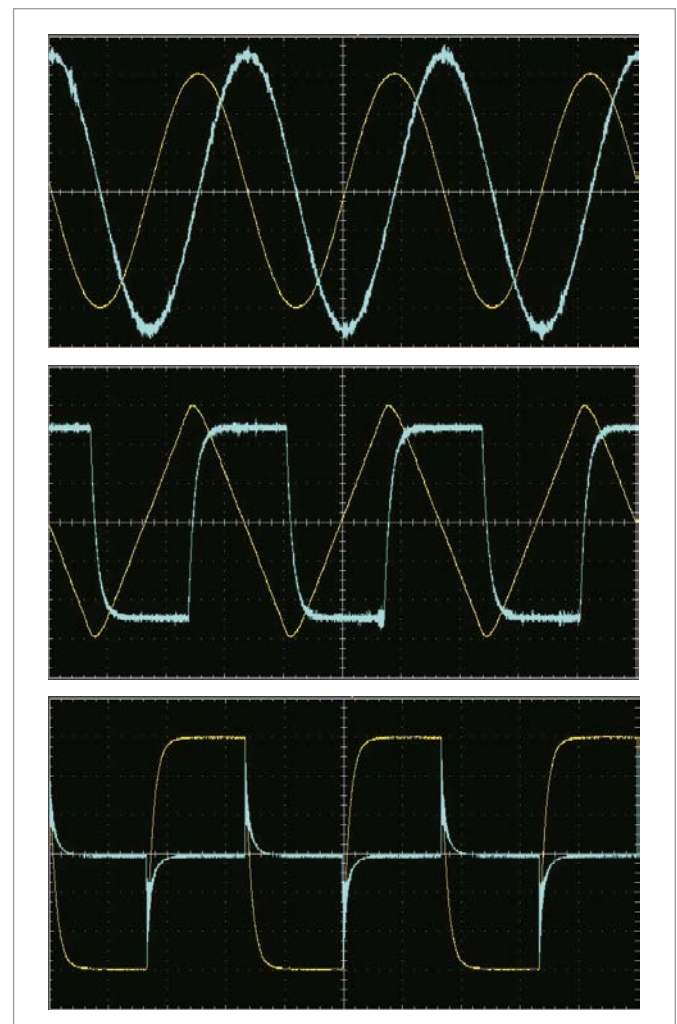


Fig. 2: Screen shots of the characteristics of the induced voltage as a function of time for a sinusoidal (top), triangular (middle) and square-wave signal (bottom) applied to the field coil

UE3040400 | WALTENHOFEN'S PENDULUM



> EXPERIMENT PROCEDURE

- Investigate the braking of a Waltenhofen pendulum due to eddy currents in a uniform magnetic field.
- Demonstrate the suppression of eddy currents in a disc with slots.

OBJECTIVE

Demonstrate and investigate how an eddy-current brake works

SUMMARY

In a metal disc moving through a uniform magnetic field, eddy currents get induced. The uniform magnetic field exerts a force due to these currents that causes the disc to slow down.

REQUIRED APPARATUS

Quantity	Description	Item Number
1	Waltenhofen's Pendulum	1000993
1	Tripod Stand 150 mm	1002835
1	Stainless Steel Rod 750 mm	1002935
1	Universal Clamp	1002830
1	DC Power Supply 0 – 20 V, 0 – 5 A (230 V, 50/60 Hz)	1003312 or
	DC Power Supply 0 – 20 V, 0 – 5 A (115 V, 50/60 Hz)	1003311
1	U Core	1000979
1	Pair of Pole Shoes	1000978
1	Pair of Clamps	1000977
2	Coil D with 1200 Taps	1000989
1	Set of 15 Safety Experiment Leads, 75 cm	1002843

BASIC PRINCIPLES

When a metal disc moves through a uniform magnetic field each section of the disc experiences constantly changing magnetic flux and an eddy voltage is induced therein. This causes electrical eddy currents to flow all over the disc. These are subject to Lorentz forces within the magnetic field that act to slow down the motion of the disc. These eddy currents are drastically reduced if the metal disc has slots in it. This means that the current has to flow from one segment to the next by a more circuitous route. Such a disc is slowed down only slightly.

The emergence and suppression of eddy currents can be clearly demonstrated using a Waltenhofen pendulum. This includes a partially slotted metal disc that oscillates inside a uniform magnetic field.

I (A)	Number of oscillations	
	disc without slots	disc with slots
0.25	21	90
0.5	6	59
0.75	3	46
1	2	37
1.25	1	30

Tab. 1: Number of oscillations of the aluminium disc in the magnetic field after being deflected from its state of rest. The pole pieces are at a distance of 8 mm and the deflection is approx. 7 cm.

EVALUATION

When a metal disc without slots moves through the uniform magnetic field, its oscillation is damped. The damping increases with the magnitude of the magnetic field. Eddy currents are induced within the disc and the magnetic field itself exerts a force as a result that opposes the motion (cf. Lenz's law).

If the slotted disc moves through the field, the damping of the motion is only slight since it is much more difficult for the eddy currents to form.

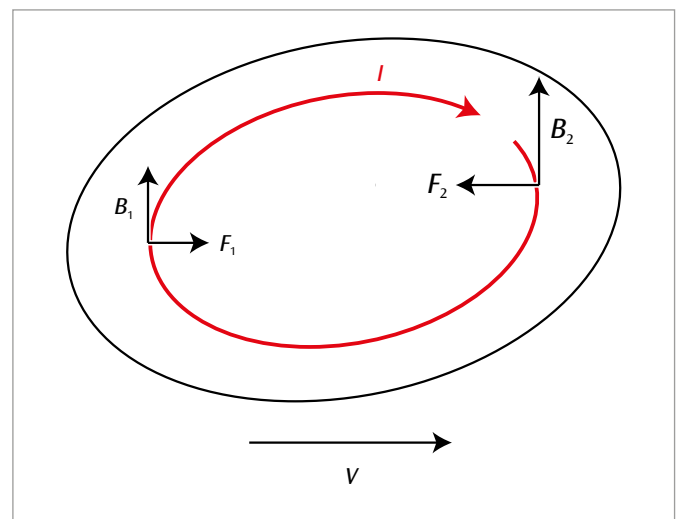


Fig. 1: Eddy current I in a metal disc moving at speed v through a uniform magnetic field. Indicated are the magnetic fields on both limbs of the eddy (B_1 and B_2) and the resulting Lorentz forces (F_1 and F_2). The force acting against the motion is greater than the one operating in the direction of motion

UE3040500 | TRANSFORMERS



EXPERIMENT PROCEDURE

- Measure the voltage across the secondary coil as a function of the voltage across the primary with no load for a fixed number of windings.
- Measure the current in the primary coil as a function of the current in the secondary with a fixed number of windings and a short-circuited output.
- Measure the primary voltage, the primary current, the secondary voltage and the secondary current, for a specific load resistance.
- Determine the power loss and the efficiency.

OBJECTIVE

Make measurements on a transformer with and without load

SUMMARY

Transformers are devices based on Faraday's law of induction which are used for converting voltages. One major use is for the transmission of electrical power over large distances, whereby power losses can be minimized by converting the voltage up to the highest possible levels thus reducing the current to a minimum. This experiment investigates the way the voltage and current depend on the number of windings with and without a load and with the output short-circuited. You will also calculate the power losses and efficiency.

REQUIRED APPARATUS

Quantity	Description	Item Number
1	Coil D with 600 Taps	1000988
1	Coil D with 1200 Taps	1000989
1	Transformer Core D	1000976
1	Transformer with Rectifier 2/ 4/ 6/ 8/ 10/ 12/ 14 V, 5 A (230 V, 50/60 Hz)	1003558 or
	Transformer with Rectifier 2/ 4/ 6/ 8/ 10/ 12/ 14 V, 5 A (115 V, 50/60 Hz)	1003557
2	Digital Multimeter P3340	1002785
1	Set of 15 Safety Experiment Leads, 75 cm	1002843

BASIC PRINCIPLES

Transformers are devices based on Faraday's law of induction which are used for converting voltages. One major use is for the transmission of electrical power over large distances, whereby power losses can be minimized by converting the voltage up to the highest possible levels thus reducing the current to a minimum.

The simplest form of transformer consists of two coils coupled together, a primary coil with N_1 winding turns and a secondary coil with N_2 winding turns, both of which are wound around a common iron core. This means that the magnetic flux Φ_1 resulting from the current I_1 flowing in the primary coil fully surrounds the secondary coil.

The following treatment considers an ideal, i.e. loss-free, transformer. When there is no load on the transformer, no current flows in the secondary, i.e. $I_2 = 0$. If an alternating voltage U_1 is applied to the primary coil, a no-load or open-circuit current I_1 flows, thereby generating a magnetic flux Φ_1 and inducing a voltage U_{ind} . Kirchhoff's 2nd law implies that this induced voltage is opposite to and equal to U_1 since ($U_1 + U_{\text{ind}} = 0$):

$$(1) \quad U_{\text{ind}} = -L_1 \cdot \frac{dI_1}{dt} = -N_1 \cdot \frac{d\Phi_1}{dt} = -U_1$$

L_1 : inductance of primary coil

Φ_1 : magnetic flux generated by I_1

Since the magnetic flux Φ_1 completely encompasses the secondary coil, a voltage is induced there:

$$(2) \quad U_2 = -N_2 \cdot \frac{d\Phi_1}{dt}$$

Equations (1) and (2) then lead to the following conclusion:

$$(3) \quad \frac{U_2}{U_1} = -\frac{N_2}{N_1}$$

The negative sign indicates that U_1 and U_2 are phase-shifted by 180° when the windings are in the same direction. If the windings are wound the opposite way round, the voltages will be in phase.

When there is a load on the transformer, a current $I_2 = U_2 / R$ flows in the secondary coil. R is the resistance of the load. This current gives rise to a magnetic flux Φ_2 which, according to Lenz's law, is opposed to the magnetic flux Φ_1 generated by the primary current I_1 . Since the primary voltage U_1 remains constant, the primary current I_1 therefore increases. In the ideal case, the power output of the secondary coil P_2 is equal to the power input to the primary P_1 :

$$(4) \quad P_1 = U_1 \cdot I_1 = U_2 \cdot I_2 = P_2$$

Combining this with equation (3) the following results:

$$(5) \quad \frac{I_1}{I_2} = \frac{N_2}{N_1}$$

The first part of the experiment involves connecting a voltmeter to the secondary side of the transformer and measuring the secondary voltage U_{2o} as a function of the primary voltage U_{1o} without any load (hence $I_{2o} = 0$). The ratio of the number of coil windings remains fixed at $N_1/N_2 = 1/2$. Then the secondary side is shorted through an ammeter (such that $U_{2c} = 0$) and the primary current I_{1c} is measured as a function of the secondary current I_{2c} , again for a fixed winding ratio $N_1/N_2 = 1/2$. Finally a load resistor $R = 2 \Omega$ is connected across the secondary and the primary voltage U_1 , primary current I_1 , secondary voltage U_2 and secondary current I_2 are all measured, still with a fixed winding ratio $N_1/N_2 = 1/2$.

EVALUATION

From equation (3) it follows for the voltages that

$$U_2 = \frac{N_2}{N_1} \cdot U_1$$

and from equation (5) correspondingly for the currents that

$$I_1 = \frac{N_2}{N_1} \cdot I_2$$

Consequently, the linear gradients found in the diagrams in Figures 2 and 3 are determined by the ratio of the number of windings.

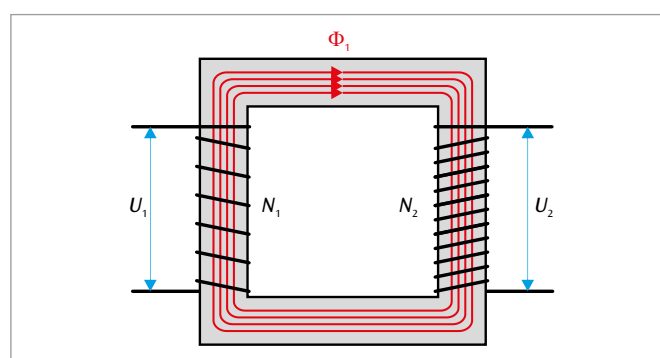


Fig. 1: Schematic depiction of the transformer

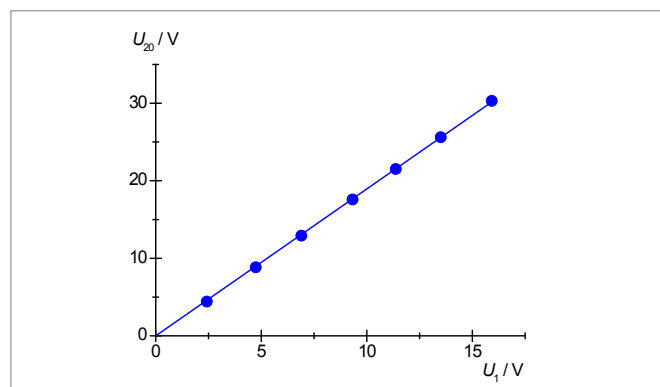


Fig. 2: Secondary voltage U_{2o} as a function of primary voltage U_{1o} with no load ($I_{2o} = 0$), $N_1 = 600$, $N_2 = 1200$

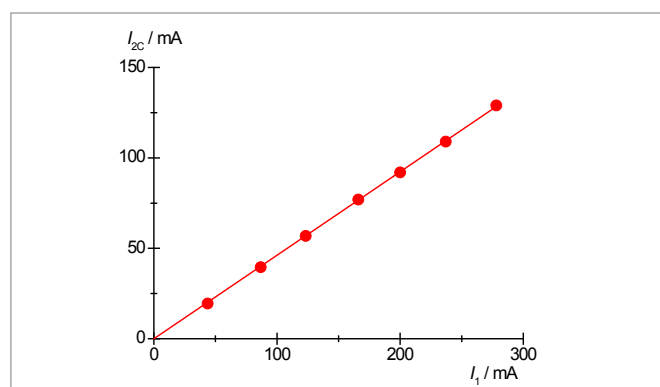
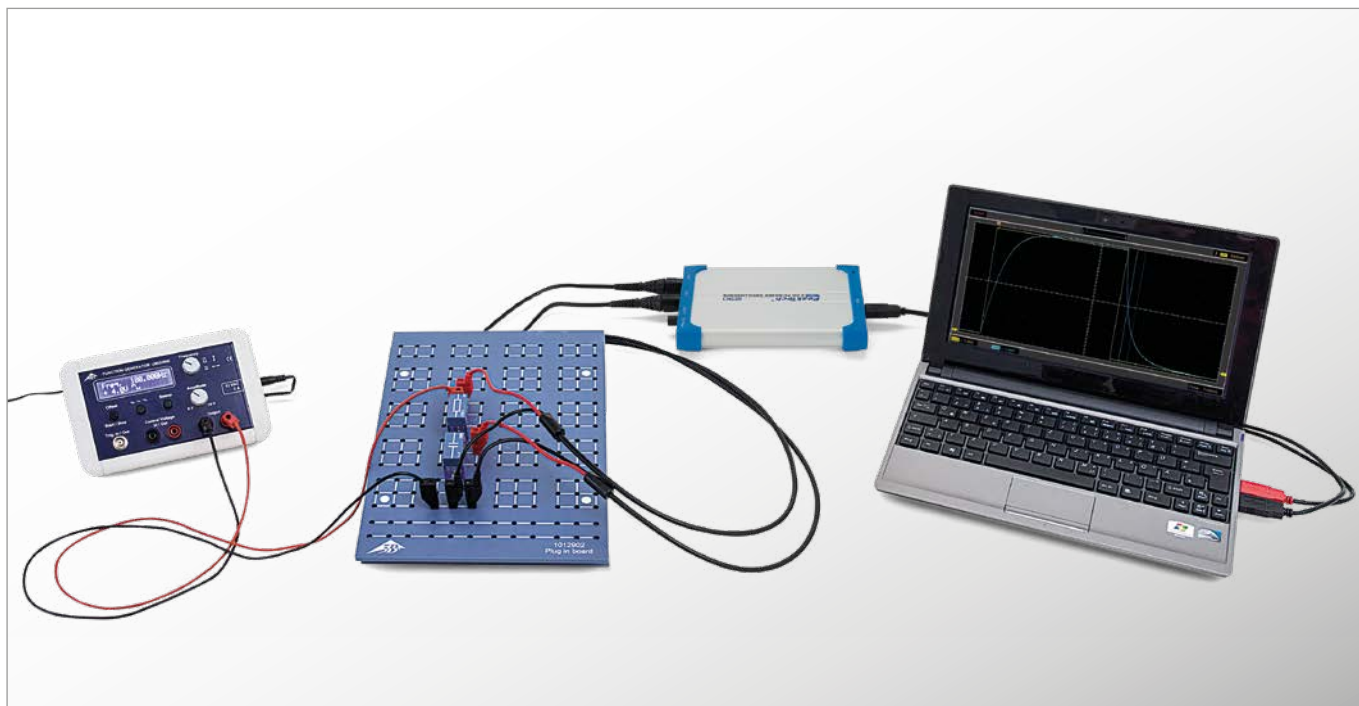


Fig. 3: Primary current I_{1c} as a function of secondary current I_{2c} with short-circuited secondary ($U_{2c} = 0$), $N_1 = 600$, $N_2 = 1200$

UE3050101

CHARGING AND DISCHARGING A CAPACITOR



> EXPERIMENT PROCEDURE

- Measure the voltage across a capacitor as it charges and discharges when the DC supply voltage to a circuit is turned on and off.
- Determine the half-life period for charging and discharging.
- Investigate how the half-life period depends on the capacitance and the resistance.

OBJECTIVE

Investigation of how the voltage across a capacitor changes over time when the capacitor is charging or discharging

SUMMARY

In a DC circuit, current only flows through a capacitor at the point in time when the power is turned on or off. The current causes the capacitor to charge up until the voltage across it is equal to the voltage applied. When the power is switched off, the capacitor will discharge till the voltage across it drops to zero. A plot of the capacitor voltage against time can be shown as an exponential curve, i.e. the voltage drops by half in the space of a fixed period $T_{1/2}$ called the half-life. The same period elapses when the voltage drops from a half to a quarter and from a quarter to an eighth. The half-life period is proportional to the capacitance and the resistance through which the capacitor discharges.

REQUIRED APPARATUS

Quantity	Description	Item Number
1	Plug-In Board for Components	1012902
1	Resistor 470 Ω , 2 W, P2W19	1012914
1	Resistor 1 k Ω , 2 W, P2W19	1012916
1	Resistor 2.2 k Ω , 2 W, P2W19	1012918
3	Capacitor 1 μ F, 100 V, P2W19	1012955
1	Function Generator FG 100 (230 V, 50/60 Hz)	1009957 or
	Function Generator FG 100 (115 V, 50/60 Hz)	1009956
1	PC Oscilloscope, 2x25 MHz	1020857
2	HF Patch Cord, BNC/4 mm Plug	1002748
1	Set of 15 Experiment Leads, 75 cm, 1 mm ²	1002840
1	Set of 10 Jumpers, P2W19	1012985

BASIC PRINCIPLES

In a DC circuit, current only flows through a capacitor at the point in time when the power is turned on or off. The current causes the capacitor to charge up until the voltage across it is equal to the voltage applied. When the power is switched off, the capacitor will discharge till the voltage across it drops to zero. A plot of the capacitor voltage against time can be shown as an exponential curve.

For a DC circuit featuring a capacitance C , resistance R and a DC voltage U_0 , the following applies when the supply is turned on:

$$(1) \quad U(t) = U_0 \cdot \left(1 - e^{-\frac{t \ln 2}{T_{1/2}}}\right)$$

The following applies when the power supply is switched off:

$$(2) \quad U(t) = U_0 \cdot e^{-\frac{t \ln 2}{T_{1/2}}}$$

where

$$(3) \quad T_{1/2} = \ln 2 \cdot R \cdot C$$

$T_{1/2}$ is the half-life period, i.e. the time, within the voltage across the discharging capacitor will be reduced in the half of its initial value. The same period elapses when the voltage drops from a half to a quarter and from a quarter to an eighth.

These aspects will be investigated in the experiment. How the capacitor voltage changes over time is recorded using a storage oscilloscope. Since the DC voltage U_0 is set to 8 V, it is easy to read off a half, a quarter and an eighth of that value.

EVALUATION

The fact that the results measured for the length of the half-life over the various sections of the charging and discharging traces all match verifies that the curve is of the expected exponential nature, see (1) and (2). Plots of the half-life periods measured as a function of the resistance and of the capacitance show that they can fit along a straight line through the origin in either case, see (3).

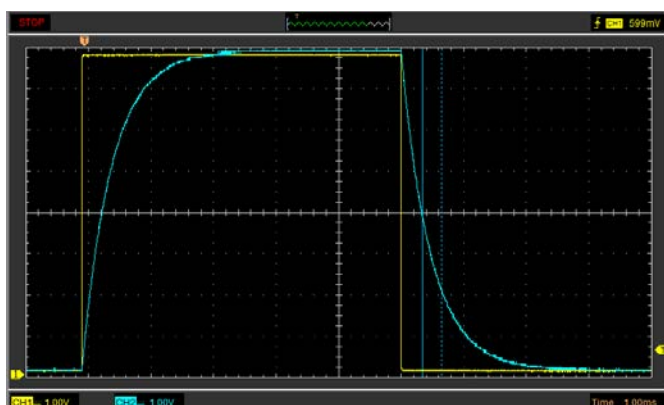


Fig. 1: Traces of voltage across a capacitor while charging and discharging recorded with an oscilloscope

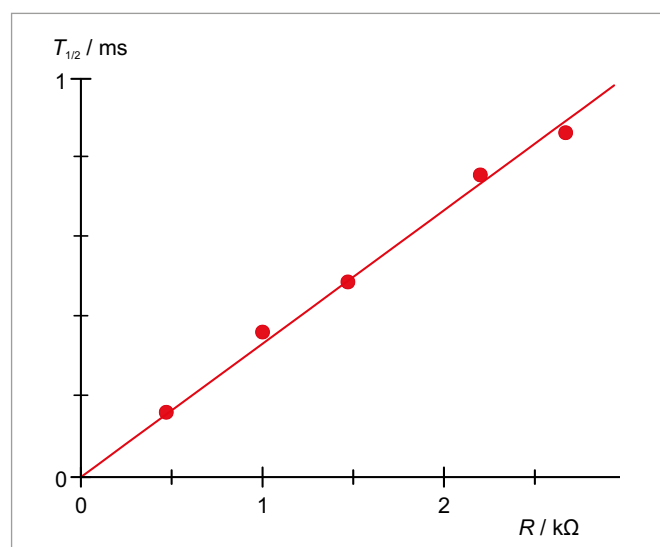


Fig. 2: Half-life $T_{1/2}$ as a function of resistance R

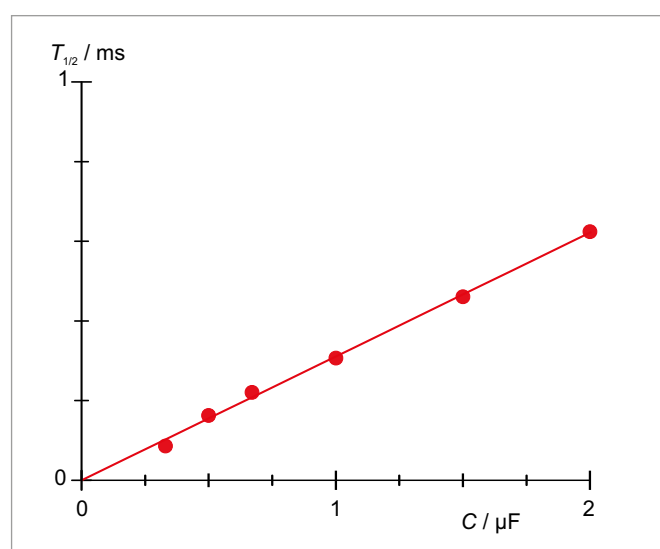


Fig. 3: Half-life $T_{1/2}$ as a function of capacitance C

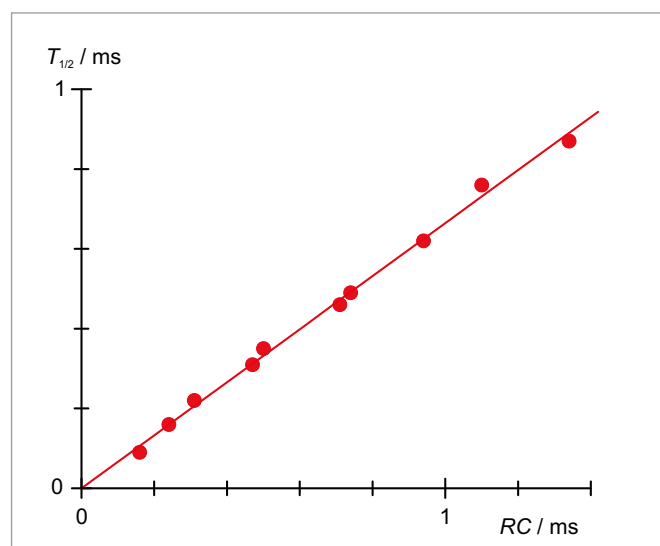


Fig. 4: Half-life $T_{1/2}$ as a function of the product of $R \cdot C$

UE3050105

CHARGING AND DISCHARGING A CAPACITOR



EXPERIMENT PROCEDURE

- Record the change in the capacitor voltage over time while a capacitor is charging by measuring the time taken to reach specific points.
- Record the change in the capacitor voltage over time while a capacitor is discharging by measuring the time taken to reach specific points.
- Determine resistance and capacitance by measuring the times it takes to charge and discharge and make a comparison with known external parameters.

OBJECTIVE

Determine the charging and discharging times

SUMMARY

The discharge curve of a capacitor is to be derived by measuring the times taken for certain voltages to be reached to obtain sample points. The charging curve is to be measured in the same way. The measurements will then be used to determine data regarding the resistors and capacitors being used.

REQUIRED APPARATUS

Quantity	Description	Item Number
1	Charge and Discharge Apparatus (230 V, 50/60 Hz)	1017781 or
	Charge and Discharge Apparatus (115 V, 50/60 Hz)	1017780
1	Capacitor 1000 μ F, 16 V, P2W19	1017806
1	Resistor 10 k Ω , 0.5 W, P2W19	1012922
Additionally required		
1	Digital Multimeter P1035	1002781

BASIC PRINCIPLES

In a DC circuit, current only flows through a capacitor while it is being turned on or off. The current causes the capacitor to charge when the circuit is switched on until it reaches the full voltage applied. When the circuit is turned off, the capacitor is discharged until its voltage falls to zero.

For a DC circuit with capacitance C , resistance R and DC voltage U_0 , the following applies when the circuit is switched on:

$$(1) \quad U(t) = U_0 \cdot (1 - e^{-\frac{t}{\tau}})$$

The following applies when the circuit is switched off:

$$(2) \quad U(t) = U_0 \cdot e^{-\frac{t}{\tau}}$$

In both cases the time constant is

$$(3) \quad \tau = R \cdot C$$

To check these relationships, the time to reach certain pre-determined comparison voltages is measured during the course of the experiment. A stopwatch is started at the same time as the circuit is switched on or off and then stopped by means of a comparator circuit once the comparison voltage has been reached. By measuring the times for various comparison voltages, the charging and discharging curves can be sampled and plotted point by point.

In practice, the following time is also of interest:

$$(4) \quad t_{5\%} = -\ln(5\%) \cdot R \cdot C \approx 3 \cdot R \cdot C$$

This is the time it takes for the capacitor voltage to reach 5% of the initial voltage U_0 during discharge or to reach within 5% of the final value U_0 when charging. By measuring $t_{5\%}$ it is possible to determine the parameters R and C , for example.

EVALUATION

For a known external resistance R_{ext} , the external capacitance C_{ext} can be calculated using the time $t_{5\%}$ by means of Equation (4):

$$C_{\text{ext}} = \frac{t_{5\%}}{3 \cdot R_{\text{ext}}}$$

The external capacitance determined in this way will be connected in parallel with the internal capacitance C_{int} in order to determine the latter by comparing the charging and discharging times.

Finally the three remaining unknown internal resistances $R_{\text{int}, i}$ can be obtained from the relevant charging and discharging times:

$$R_{\text{int}, i} = \frac{t_{5\%, i}}{3 \cdot C_{\text{int}}} \quad \text{where } i = 1, 2, 3$$

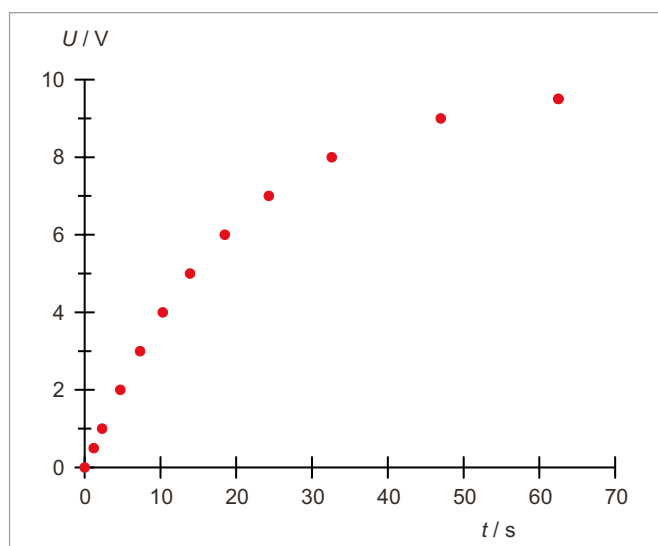


Fig. 1: Charging curve for internal RC pair

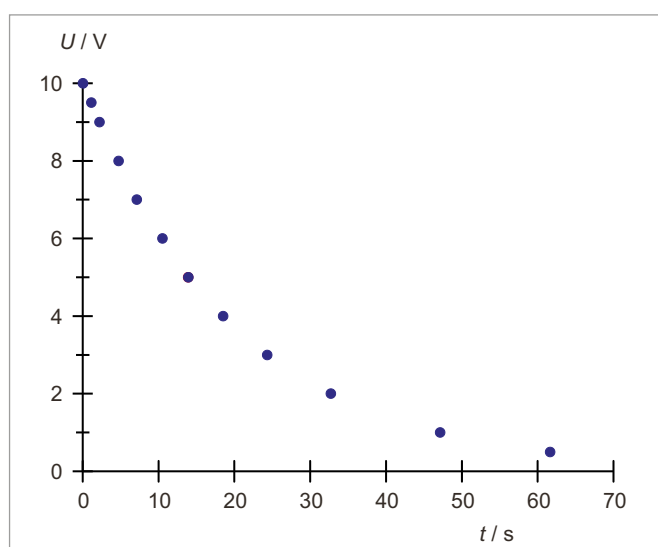
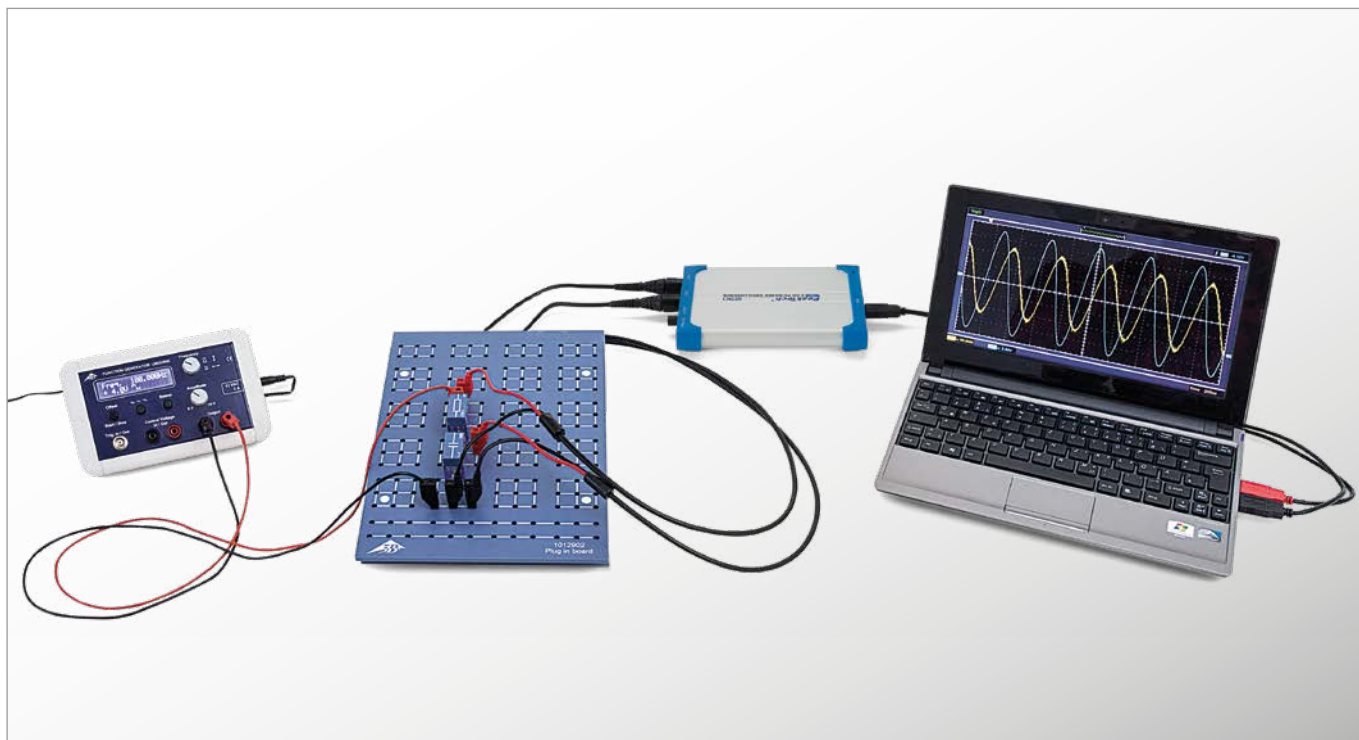


Fig. 2: Discharging curve for internal RC pair

UE3050111

IMPEDANCE OF A CAPACITOR IN AN AC CIRCUIT



> EXPERIMENT PROCEDURE

- Determine the amplitude and phase of capacitive impedance as a function of the capacitance.
- Determine the amplitude and phase of capacitive impedance as a function of the frequency.

OBJECTIVE

Determine the impedance of a capacitor as a function of capacitance and frequency

SUMMARY

Any change in voltage across a capacitor gives rise to a flow of current through the component. If an AC voltage is applied, alternating current will flow which is shifted in phase with respect to the voltage. In this experiment, a frequency generator supplies an alternating voltage with a frequency of up to 3 kHz. A dual-channel oscilloscope is used to record the voltage and current, so that the amplitude and phase of both can be determined. The current through the capacitor is given by the voltage drop across a resistor with a value which is negligible in comparison to the impedance exhibited by the capacitor itself.

REQUIRED APPARATUS

Quantity	Description	Item Number
1	Plug-In Board for Components	1012902
1	Resistor 1 Ω , 2 W, P2W19	1012903
1	Resistor 10 Ω , 2 W, P2W19	1012904
3	Capacitor 1 μF , 100 V, P2W19	1012955
1	Capacitor 0.1 μF , 100 V, P2W19	1012953
1	Function Generator FG 100 (230 V, 50/60 Hz)	1009957 or
	Function Generator FG 100 (115 V, 50/60 Hz)	1009956
1	PC Oscilloscope, 2x25 MHz	1020857
2	HF Patch Cord, BNC/4 mm Plug	1002748
1	Set of 15 Experiment Leads, 75 cm, 1 mm ²	1002840

BASIC PRINCIPLES

Any change in voltage across a capacitor gives rise to a flow of current through the component. If an AC voltage is applied, alternating current, which is shifted in phase with respect to the voltage will flow across the capacitor. In mathematical terms, the relationship can be expressed most easily if current, voltage and impedance are regarded as complex values, whereby the real components need to be considered.

The capacitor equation leads directly to the following:

$$(1) \quad I = C \cdot \frac{dU}{dt}$$

I : Current, U : Voltage, C : Capacitance

Assume the following voltage is applied:

$$(2) \quad U = U_0 \cdot \exp(i \cdot 2\pi \cdot f \cdot t)$$

This gives rise to a current as follows:

$$(3) \quad I = i \cdot \omega \cdot C \cdot U_0 \cdot \exp(i \cdot 2\pi \cdot f \cdot t)$$

Capacitor C is then assigned the complex impedance

$$(4) \quad X_c = \frac{U}{I} = \frac{1}{i \cdot 2\pi \cdot f \cdot C}$$

The real component of this is measurable, therefore

$$(5a) \quad U = U_0 \cdot \cos \omega t$$

$$(6a) \quad I = 2\pi \cdot f \cdot C \cdot U_0 \cos\left(\omega t + \frac{\pi}{2}\right) \\ = I_0 \cos\left(\omega t + \frac{\pi}{2}\right)$$

$$(7a) \quad X_c = \frac{U_0}{I_0} = \frac{1}{2\pi \cdot f \cdot C}$$

In this experiment, a frequency generator supplies an alternating voltage with a frequency of up to 3 kHz. A dual-channel oscilloscope is used to record the voltage and current, so that the amplitude and phase of both can be determined. The current through the capacitor is related to the voltage drop across a resistor with a value which is negligible in comparison to the impedance exhibited by the capacitor itself.

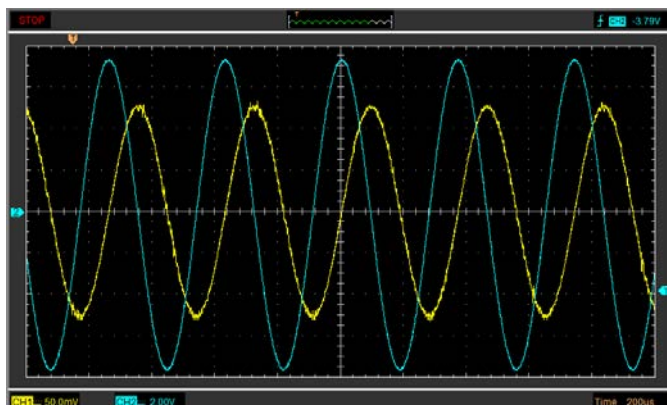


Fig. 1: Capacitor in AC circuit: trace of voltage and current

EVALUATION

The capacitive impedance X_c is proportional to the inverse of the frequency f and the inverse of the capacitance C (see equation 4). In the relevant graphs, the measurements therefore lie along a straight line through the origin within the measurement tolerances.

The phase of the current is 90° ahead of that for the voltage, since charging current (positive sign) and discharge current (negative sign) reach their maxima when the voltage passes through zero.

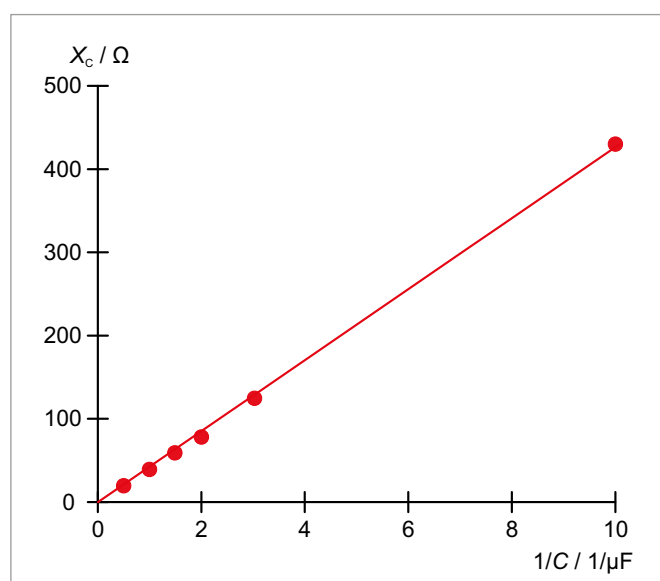


Fig. 2: Capacitive impedance X_c as a function of the inverse of the capacitance C

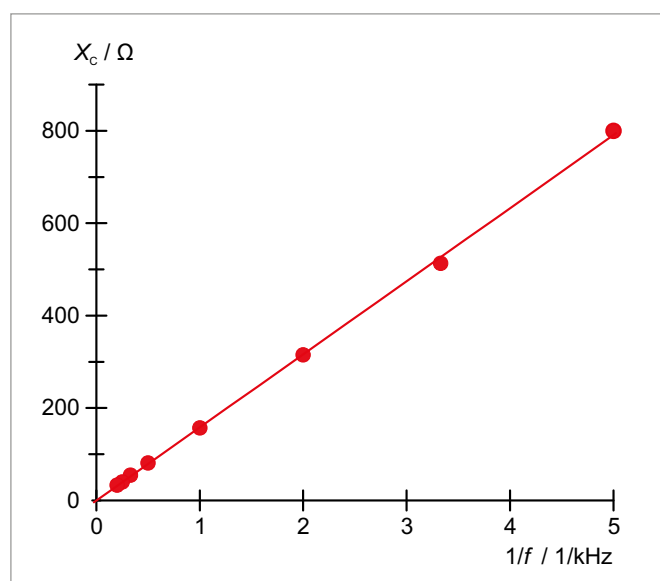
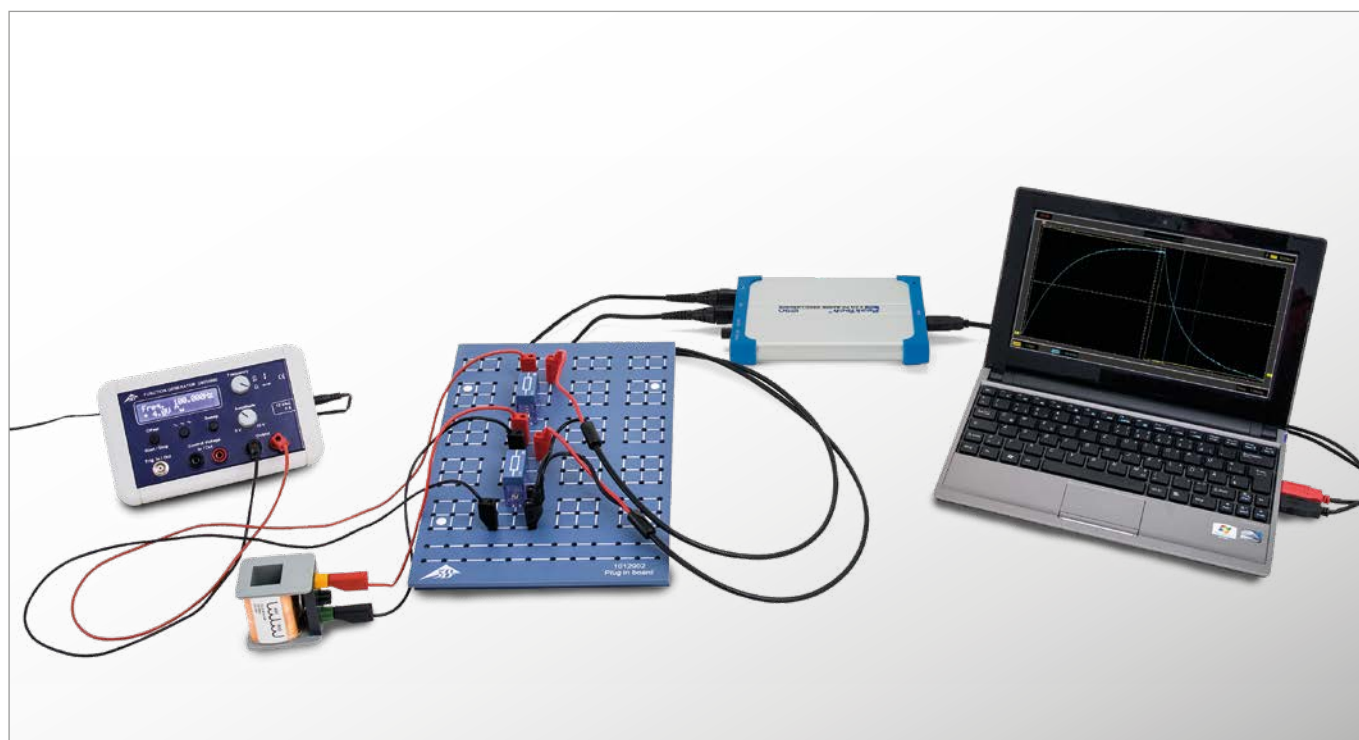


Fig. 3: Capacitive impedance X_c as a function of the inverse of the frequency f

UE3050201

CHARGING AND DISCHARGING A COIL



EXPERIMENT PROCEDURE

- Measure the current in a coil when a DC supply is turned on and when it is turned off.
- Determine the half-life period when a DC supply is turned on and when it is turned off.
- Investigate how the half-life depends on inductance and resistance.

OBJECTIVE

Investigation of how the current through a coil changes over time when the DC supply is turned on and off

SUMMARY

The behavior of a coil in a DC circuit changes as soon as the DC supply is turned on or off. The change in current is delayed by self-induction of the coil until it reaches its final value when turning on or zero when turning off. A plot of the coil current against time can be shown to be an exponential curve, i.e. the current through the coil drops by half in the space of a fixed period $T_{1/2}$ called the half-life. The same period elapses when the current drops from a half to a quarter and from a quarter to an eighth. The half-life period is proportional to the inductance and the resistance of the circuit.

REQUIRED APPARATUS

Quantity	Description	Item Number
1	Plug-In Board for Components	1012902
1	Resistor 1 Ω , 2 W, P2W19	1012903
1	Resistor 10 Ω , 2 W, P2W19	1012904
1	Resistor 22 Ω , 2 W, P2W19	1012907
1	Resistor 47 Ω , 2 W, P2W19	1012908
1	Resistor 150 Ω , 2 W, P2W19	1012911
1	Set of 10 Jumpers, P2W19	1012985
2	Coil S with 1200 Taps	1001002
1	Function Generator FG 100 (230 V, 50/60 Hz)	1009957 or
	Function Generator FG 100 (115 V, 50/60 Hz)	1009956
1	PC Oscilloscope, 2x25 MHz	1020857
2	HF Patch Cord, BNC/4 mm Plug	1002748
1	Set of 15 Experiment Leads, 75 cm, 1 mm ²	1002840

BASIC PRINCIPLES

The behavior of a coil in a DC circuit changes as soon as the DC supply is turned on or off. The change in current is delayed by self-induction of the coil until it reaches its final value when turning on or zero when turning off. A plot of the coil current against time can be shown to be an exponential curve.

For a DC circuit featuring an inductance L , resistance R and DC voltage U_0 , the following applies when the supply is switched on:

$$(1) \quad I(t) = I_0 \cdot \left(1 - e^{-\frac{t \ln 2}{T_{1/2}}}\right)$$

The following applies when the power is supply off:

$$(2) \quad I(t) = I_0 \cdot e^{-\frac{t \ln 2}{T_{1/2}}}$$

where

$$(3) \quad T_{1/2} = \ln 2 \cdot \frac{L}{R}$$

$T_{1/2}$ is the half-life period, i.e. the current through the coil will halve within a time $T_{1/2}$. The same period elapses when the current drops from a half to a quarter and from a quarter to an eighth.

These aspects will be investigated in the experiment. How the coil current changes over time is recorded using a storage oscilloscope. The current is measured by means of the voltage drop across a resistor R_M . The current I_0 has been selected such that a half, a quarter and an eighth of this current are easy to read off.

EVALUATION

The fact that the measured results for the length of the half-life over the various sections of the charging and discharging traces all match verifies that the curve is of the expected exponential nature, see (1) and (2). Plots of the half-life periods measured as a function of the resistance and of the inductance show that they can fit along a straight line through the origin in either case, see (3).

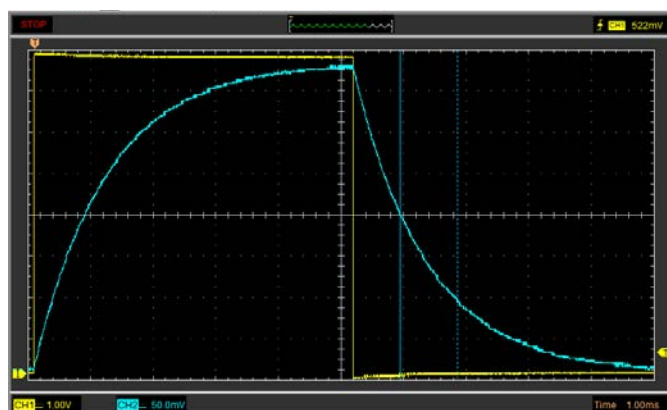


Fig. 1: Traces of current through a coil while charging and discharging recorded with an oscilloscope

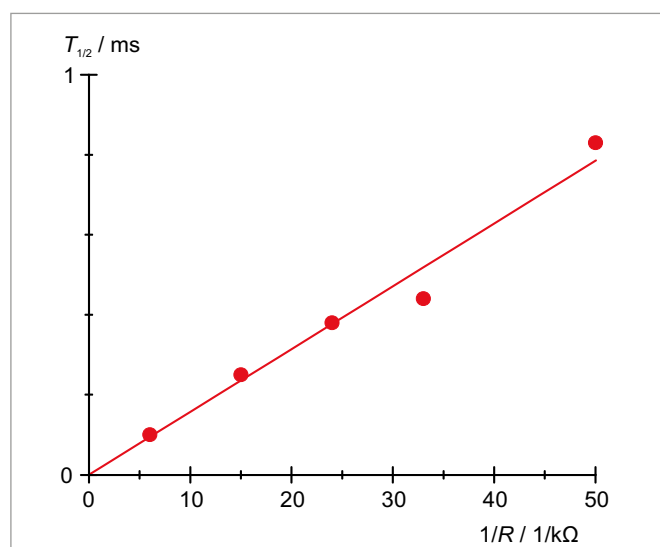


Fig. 2: Half-life $T_{1/2}$ as a function of the inverse of resistance R

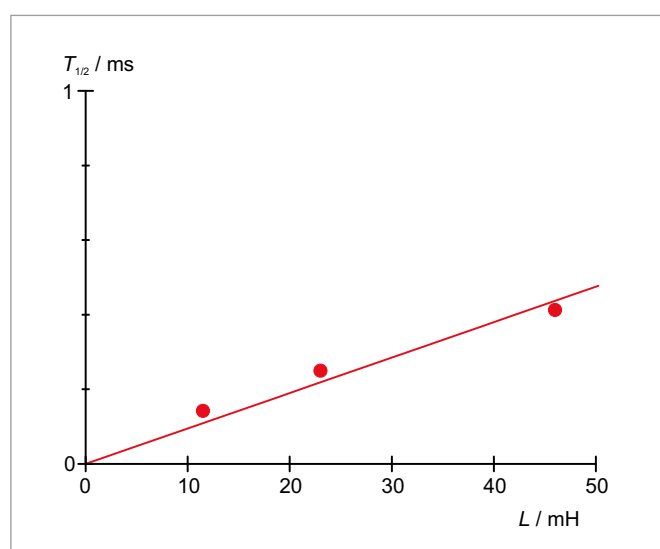


Fig. 3: Half-life $T_{1/2}$ as a function of inductance L

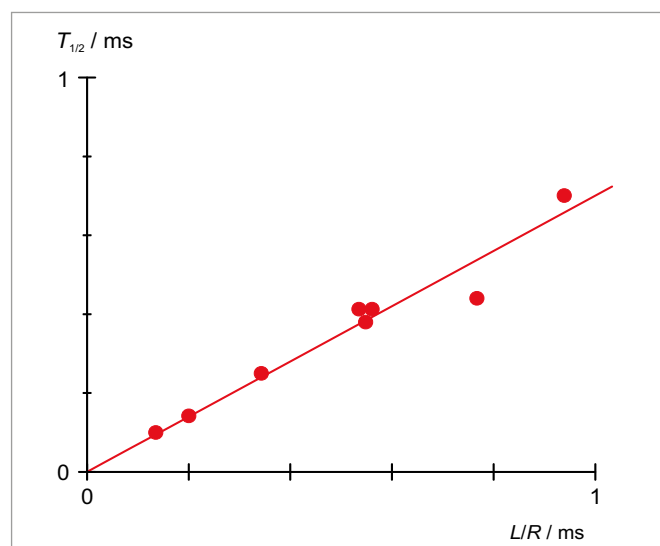
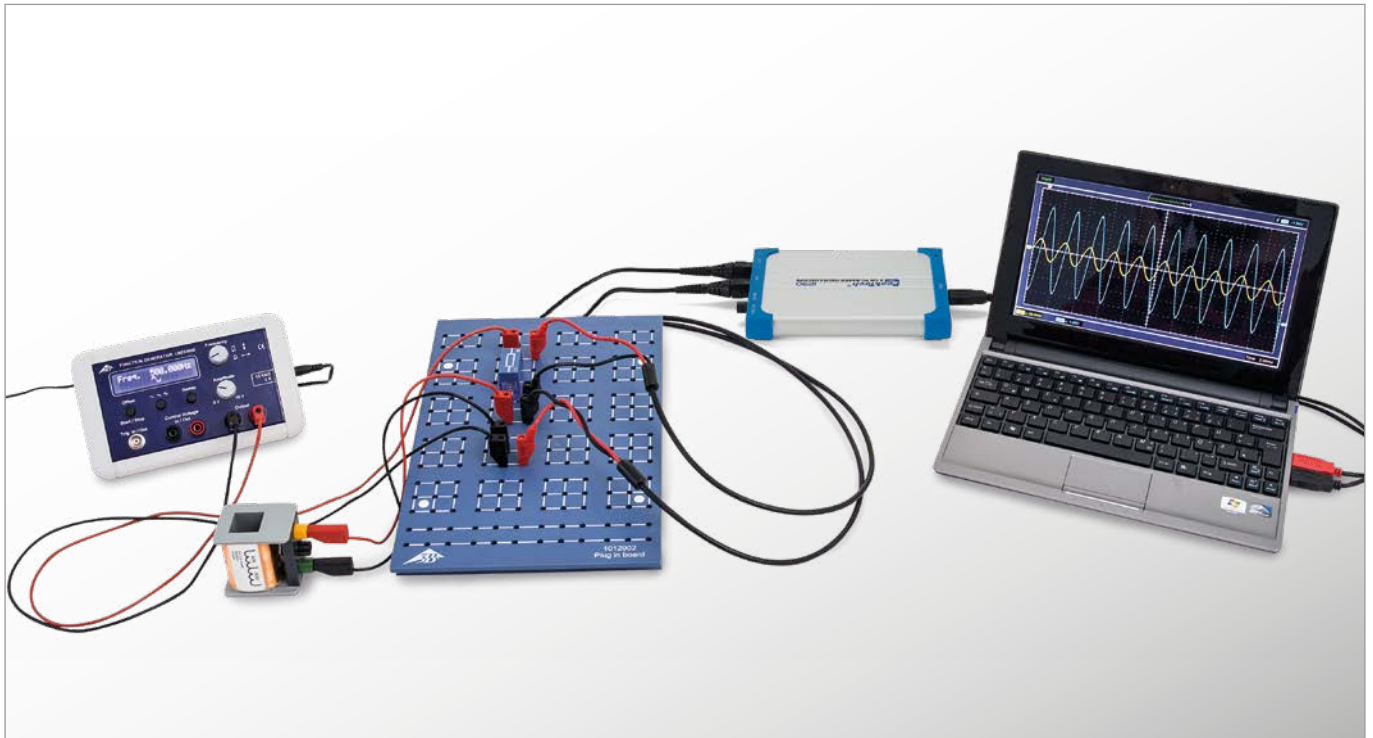


Fig. 4: Half-life $T_{1/2}$ as a function of $\frac{L}{R}$

UE3050211

IMPEDANCE OF A COIL IN AN AC CIRCUIT



EXPERIMENT PROCEDURE

- Determine the amplitude and phase of inductive impedance as a function of the inductance.
- Determine the amplitude and phase of inductive impedance as a function of the frequency

OBJECTIVE

Determine inductive impedance as a function of inductance and frequency

SUMMARY

Any change in the current through a coil induces a voltage. If an alternating current flows, an AC voltage will be induced, which is shifted in phase with respect to the current. In mathematical terms, the relationship can be expressed most easily if current, voltage and impedance are regarded as complex values, whereby the real components need to be considered. In this experiment, a frequency generator supplies an alternating voltage with a frequency of up to 2 kHz. A dual-channel oscilloscope is used to record the voltage and current, so that the amplitude and phase of both can be determined. The current through the coil is given by the voltage drop across a resistor with a value which is negligible in comparison to the inductive impedance exhibited by the coil itself.

REQUIRED APPARATUS

Quantity	Description	Item Number
1	Plug-In Board for Components	1012902
2	Coil S with 1200 Taps	1001002
1	Resistor 10 Ω , 2 W, P2W19	1012904
1	Function Generator FG 100 (230 V, 50/60 Hz)	1009957 or
	Function Generator FG 100 (115 V, 50/60 Hz)	1009956
1	PC Oscilloscope, 2x25 MHz	1020857
2	HF Patch Cord, BNC/4 mm Plug	1002748
1	Set of 15 Experiment Leads, 75 cm, 1 mm ²	1002840

BASIC PRINCIPLES

Any change in the current through a coil induces a voltage which acts such as to oppose the change in current. If an alternating current flows, an AC voltage will be induced, which is shifted in phase with respect to the current. In mathematical terms, the relationship can be expressed most easily if current, voltage and impedance are regarded as complex values, whereby the real components need to be considered.

The relationship between current and voltage for a coil is as follows:

$$(1) \quad U = L \cdot \frac{dI}{dt}$$

I : Current, U : Voltage, L : Inductance

Assume the following voltage is applied:

$$(2) \quad U = U_0 \cdot \exp(i \cdot 2\pi \cdot f \cdot t)$$

This gives rise to a current as follows:

$$(3) \quad I = \frac{U_0}{i \cdot 2\pi \cdot f \cdot L} \cdot \exp(i \cdot 2\pi \cdot f \cdot t)$$

The impedance associated with the inductor L can then be defined as in the following equation:

$$(4) \quad X_L = \frac{U}{I} = i \cdot 2\pi \cdot f \cdot L$$

The real component of this is measurable, therefore

$$(5a) \quad U = U_0 \cdot \cos \omega t$$

$$(6a) \quad I = \frac{U_0}{2\pi \cdot f \cdot L} \cos\left(\omega t - \frac{\pi}{2}\right)$$

$$= I_0 \cos\left(\omega t - \frac{\pi}{2}\right)$$

$$(7a) \quad X_L = \frac{U_0}{I_0} = 2\pi \cdot f \cdot L$$

In this experiment, a frequency generator supplies an alternating voltage with a frequency of up to 2 kHz. A dual-channel oscilloscope is used to record the voltage and current, so that the amplitude and phase of both can be determined. The current through the capacitor is related to the voltage drop across a resistor with a value which is negligible in comparison to the inductive impedance exhibited by the coil itself.

EVALUATION

As per equation (4), the inductive impedance X_L is proportional to the frequency f and the inductance L . In the relevant graphs, the measurements therefore lie along a straight line through the origin within the measurement tolerances.

The phase of the current through the coil is 90° behind that of the voltage, since every change in current induces an opposing voltage.

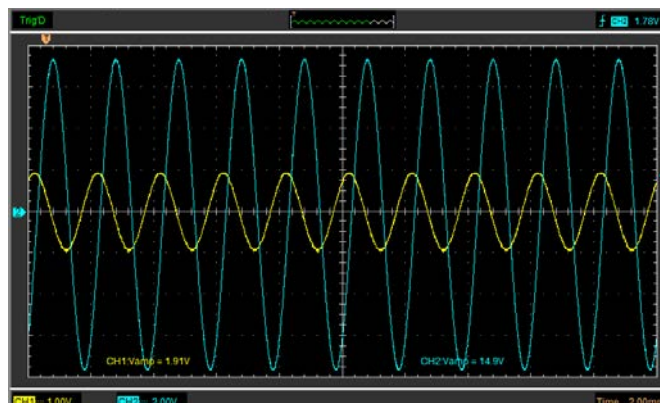


Fig. 1: Coil in an AC circuit: Current and voltage over time

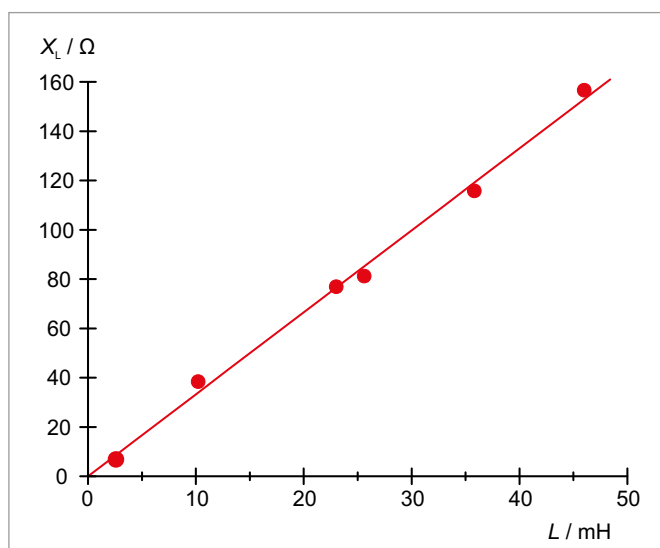


Fig. 2: Inductive impedance X_L as a function of inductance L

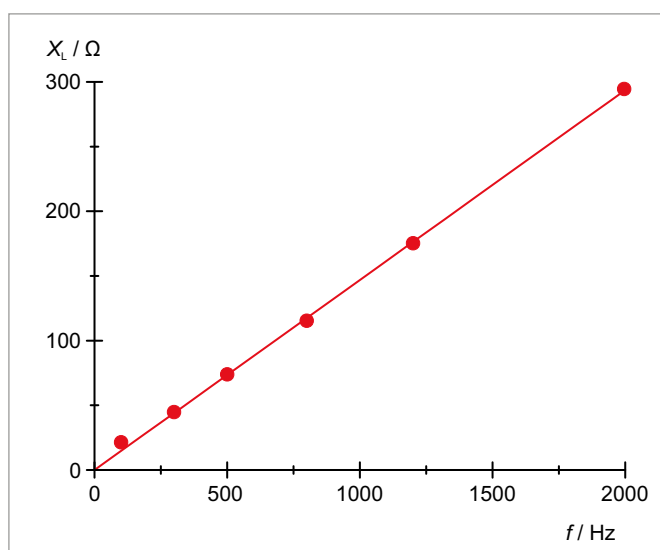
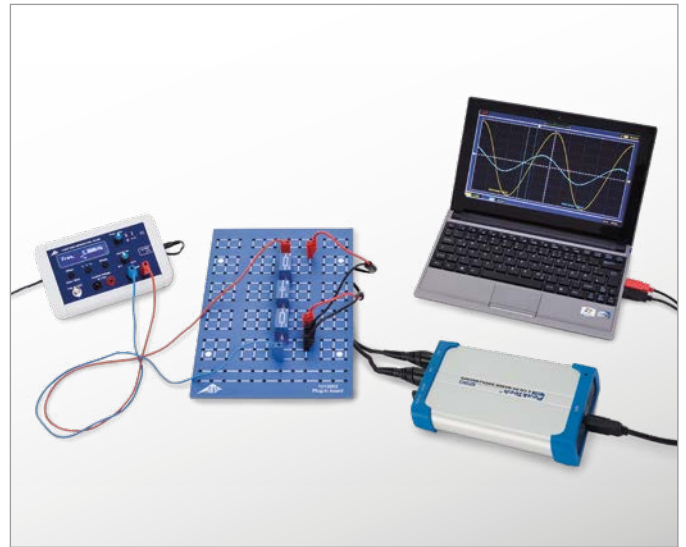
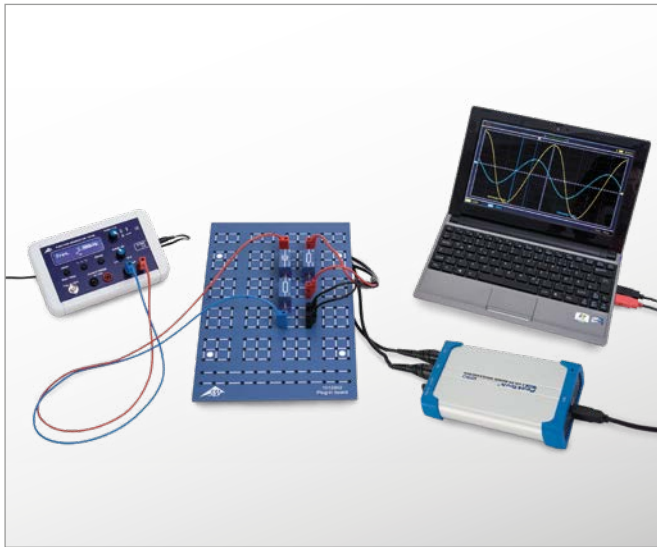


Fig. 3: Inductive impedance X_L as a function of frequency f

UE3050301 | AC RESISTANCE



EXPERIMENT PROCEDURE

- Determine the amplitude and phase of the overall resistance as a function of frequency for a series circuit.
- Determine the amplitude and phase of the overall resistance as a function of frequency for a parallel circuit.

OBJECTIVE

Determine the AC resistance in a circuit with capacitive and resistive loads

SUMMARY

In AC circuits not only ohmic resistance needs to be taken into account, but also the resistance due to capacitive loads. The combination of the two may be connected in series or parallel. This has an effect on both the amplitudes and phase of the current and voltage. In the experiment, this will be investigated using an oscilloscope and a function generator supplying alternating current with frequencies between 50 and 2000 Hz.

REQUIRED APPARATUS

Quantity	Description	Item Number
1	Plug-In Board for Components	1012902
1	Resistor 1 Ω , 2 W, P2W19	1012903
1	Resistor 100 Ω , 2 W, P2W19	1012910
1	Capacitor 10 μF , 35 V, P2W19	1012957
1	Capacitor 1 μF , 100 V, P2W19	1012955
1	Capacitor 0.1 μF , 100 V, P2W19	1012953
1	Function Generator FG 100 (230 V, 50/60 Hz)	1009957 or
	Function Generator FG 100 (115 V, 50/60 Hz)	1009956
1	PC Oscilloscope, 2x25 MHz	1020857
2	HF Patch Cord, BNC/4 mm Plug	1002748
1	Set of 15 Experiment Leads, 75 cm, 1 mm ²	1002840

BASIC PRINCIPLES

In AC circuits it is common to use complex numbers to describe the resistance in circuits with capacitors, because this actually makes calculation easier. This is because not only the amplitude of the current and voltage is a factor, but also because the phase relationships between the two need to be taken into account (this complex resistance is usually called impedance). Series and parallel circuits with both ohmic and capacitive resistance can then be described quite easily, although in each case, only the real component is measurable).

The complex resistance (impedance) of a capacitor with capacitance C in a circuit with an alternating current of frequency f is as follows:

$$(1) \quad X_c = \frac{1}{i \cdot \omega \cdot C}$$

Angular frequency $\omega = 2\pi \cdot f$

Therefore series circuits containing a capacitor and an ohmic resistor R will have the following overall resistance:

$$(2) \quad Z_s = \frac{1}{i \cdot \omega \cdot C} + R$$

A parallel circuit can be assigned the following overall resistance

$$(3) \quad Z_p = \frac{1}{i \cdot \omega \cdot C + \frac{1}{R}}$$

The usual way of expressing this is as follows:

$$(4) \quad Z = Z_0 \cdot \exp(i \cdot \varphi)$$

This becomes

$$(5) \quad Z_s = \frac{\sqrt{1 + (\omega \cdot C \cdot R)^2}}{\omega \cdot C} \cdot \exp(i \cdot \varphi_s)$$

where $\tan \varphi_s = -\frac{1}{\omega \cdot C \cdot R}$ and

$$(6) \quad Z_p = \frac{R}{\sqrt{1 + (\omega \cdot C \cdot R)^2}} \cdot \exp(i \cdot \varphi_p)$$

where $\tan \varphi_p = -\omega \cdot C \cdot R$

In this experiment a function generator supplies an AC voltage with a frequency f , which is adjusted between 50 and 2000 Hz. Voltage U and current I are recorded on an oscilloscope, whereby, I is displayed in the form of the voltage drop across a small auxiliary resistor. This allows to measure the real components of the voltage across the relevant resistance Z .

$$(7) \quad U = U_0 \cdot \exp(i \cdot \omega \cdot t)$$

The resulting current is as follows:

$$(8) \quad I = \frac{U_0}{Z_0} \cdot \exp(j \cdot (\omega \cdot t - \varphi)) \\ = I_0 \cdot \exp(i \cdot (\omega \cdot t - \varphi))$$

The amplitudes I_0 and U_0 , plus the phase shift φ can all be read from the oscilloscope.

EVALUATION

The magnitude of the overall resistance (impedance) $Z_0 = \frac{U_0}{I_0}$ is displayed as a function of frequency f or of the capacitive resistance $X_c = \frac{1}{2\pi \cdot f \cdot C}$.

At low frequencies the resistance of the series circuit corresponds to the capacitive resistance and that of the parallel circuit corresponds to the ohmic resistance. The phase shift is between 0° and 90° and equals 45° if the ohmic and capacitive resistance values are the same.

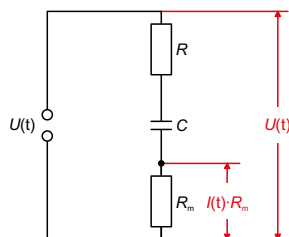


Fig. 1: Measurement set-up for series circuit

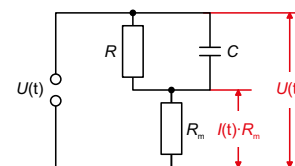


Fig. 2: Measurement set-up for parallel circuit

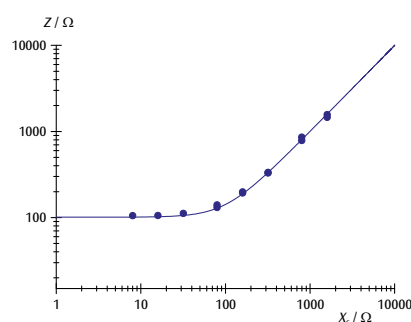


Fig. 3: Overall resistance for series circuit

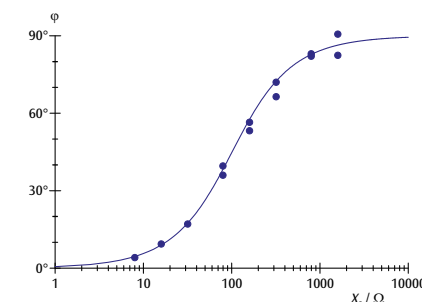


Fig. 4: Phase shift for series circuit

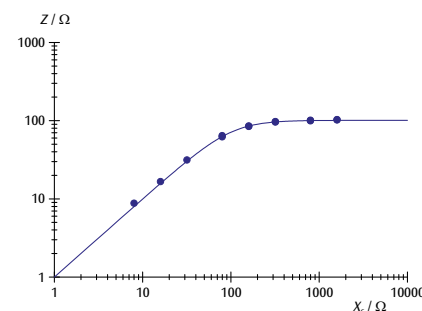


Fig. 5: Overall resistance for parallel circuit

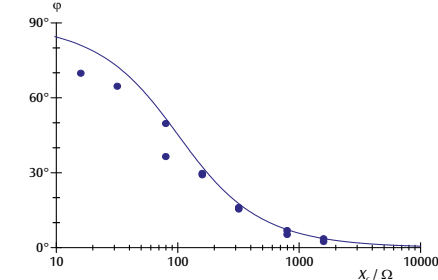
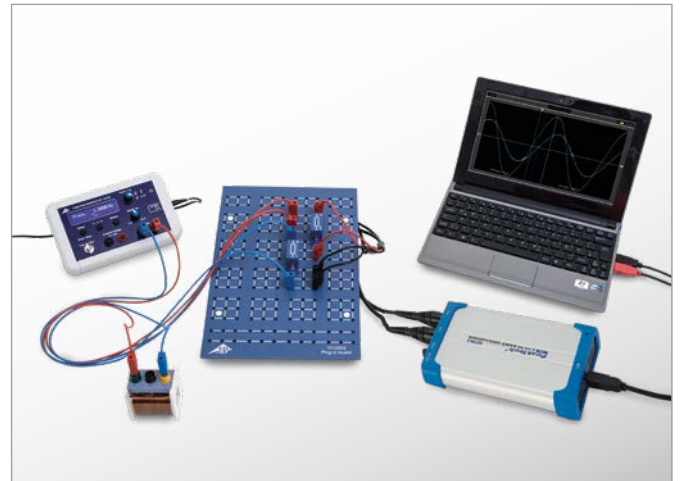
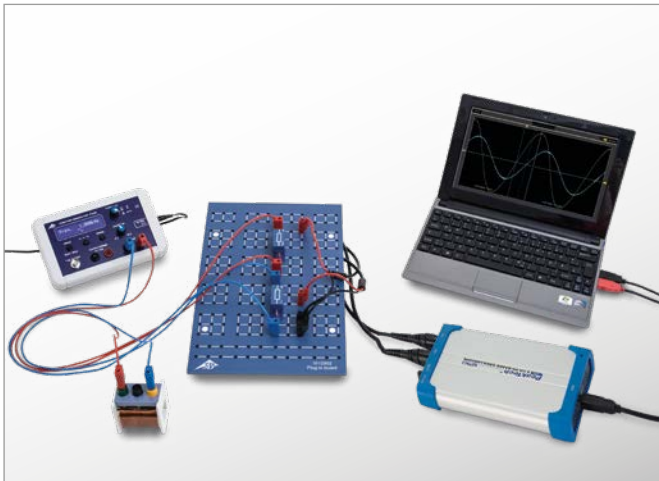


Fig. 6: Phase shift for parallel circuit

UE3050311 | AC RESISTANCE



EXPERIMENT PROCEDURE

- Determine the amplitude and phase of the overall resistance as a function of frequency for a series circuit.
- Determine the amplitude and phase of the overall resistance as a function of frequency for a parallel circuit.

OBJECTIVE

Determine the AC resistance in a circuit with inductive and resistive loads

SUMMARY

In AC circuits, not only ohmic resistance needs to be taken into account but also the resistance due to inductive loads. The combination of the two may be connected in series or parallel. This has an effect on both the amplitudes and phase of the current and voltage. In the experiment, this will be investigated using an oscilloscope and a function generator supplying alternating current with frequencies between 50 and 10000 Hz.

REQUIRED APPARATUS

Quantity	Description	Item Number
1	Plug-In Board for Components	1012902
1	Resistor 1 Ω , 2 W, P2W19	1012903
1	Resistor 100 Ω , 2 W, P2W19	1012910
1	Function Generator FG 100 (230 V, 50/60 Hz)	1009957 or
	Function Generator FG 100 (115 V, 50/60 Hz)	1009956
1	PC Oscilloscope, 2x25 MHz	1020857
1	HF Patch Cord, BNC/4 mm Plug	1002748
1	Set of 15 Experiment Leads, 75 cm, 1 mm ²	1002840
1	1 Coil S with 800 Taps	1001001
2	Coil S with 1200 Taps	1001002

BASIC PRINCIPLES

In AC circuits, it is common to use complex numbers to describe the resistance in circuits with inductors because this actually makes calculation easier. This is because not only the amplitude of the current and voltage is a factor, but also the phase relationships between the two need to be taken into account (this complex resistance is usually called impedance). Series and parallel circuits with both ohmic and inductive resistance can then be described quite easily, although in each case, only the real component is measurable.

The complex resistance (impedance) of a coil of inductance L in a circuit with an alternating current of frequency f is as follows:

$$(1) \quad X_L = i \cdot 2\pi \cdot f \cdot L$$

Angular frequency $\omega = 2\pi \cdot f$

Therefore the total resistance (impedance) of a series circuit containing a coil with a resistance R is

$$(2) \quad Z_s = i \cdot 2\pi \cdot f \cdot L + R$$

For a parallel circuit, the total resistance can be assigned thus:

$$(3) \quad Z_p = \frac{1}{\frac{1}{i \cdot 2\pi \cdot f \cdot L} + \frac{1}{R}}$$

The usual way of writing this is as follows:

$$(4) \quad Z = Z_0 \cdot \exp(i \cdot \varphi)$$

This becomes

$$(5) \quad Z_s = \sqrt{(2\pi \cdot f \cdot L)^2 + R^2} \cdot \exp(i \cdot \varphi_s)$$

where $\tan \varphi_s = \frac{2\pi \cdot f \cdot L}{R}$ and

$$(6) \quad Z_p = \frac{2\pi \cdot f \cdot L \cdot R}{\sqrt{(2\pi \cdot f \cdot L)^2 + R^2}} \cdot \exp(i \cdot \varphi_p)$$

where $\tan \varphi_p = \frac{R}{2\pi \cdot f \cdot L}$

In this experiment a function generator supplies an AC voltage with an frequency f , which is adjusted between 50 and 10000 Hz. Voltage U and current I are recorded on an oscilloscope, whereby, I is displayed in the form of the voltage drop across a small auxiliary resistor. This allows the real components of the voltage across the relevant resistance Z to be measured.

$$(7) \quad U = U_0 \cdot \exp(i \cdot 2\pi \cdot f \cdot t)$$

The resulting current is as follows:

$$(8) \quad I = \frac{U_0}{Z_0} \cdot \exp(i \cdot (2\pi \cdot f \cdot t - \varphi)) \\ = I_0 \cdot \exp(i \cdot (2\pi \cdot f \cdot t - \varphi))$$

The amplitudes I_0 and U_0 , plus the phase shift φ can all be read from the oscilloscope.

EVALUATION

The magnitude of the overall resistance is $Z_0 = \frac{U_0}{I_0}$ displayed as a function of frequency f or of the inductive resistance $X_L = 2\pi \cdot f \cdot L$. If the inductive impedance is large, the resistance of the series circuit will have the value of the inductive resistance and the parallel circuit will have the value of the ohmic resistance. The phase shift is between 0° and 90° and equals 45° if the ohmic and inductive resistance values are the same.

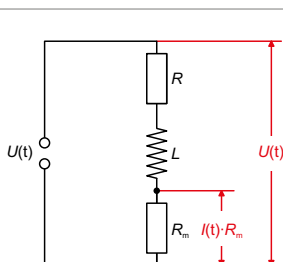


Fig. 1: Measurement set-up for series circuit

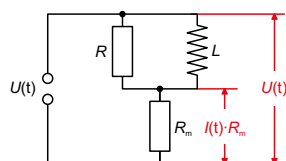


Fig. 2: Measurement set-up for parallel circuit

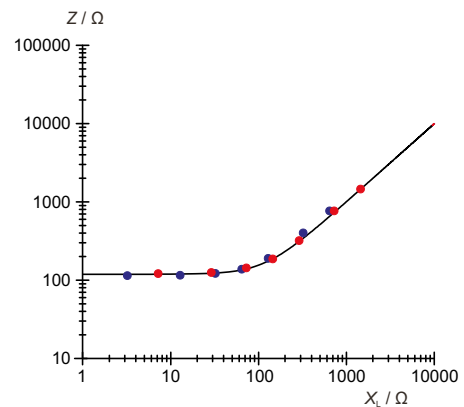


Fig. 3: Overall resistance for series circuit

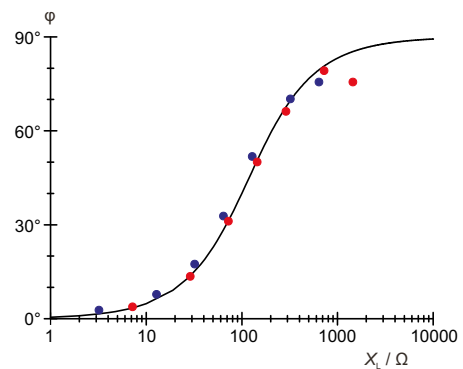


Fig. 4: Phase shift for series circuit

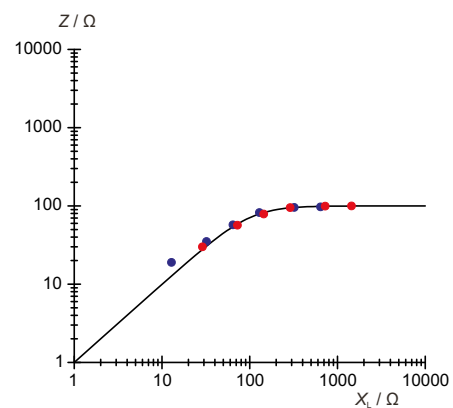


Fig. 5: Overall resistance for parallel circuit

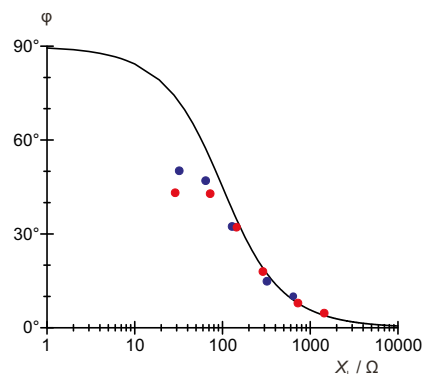
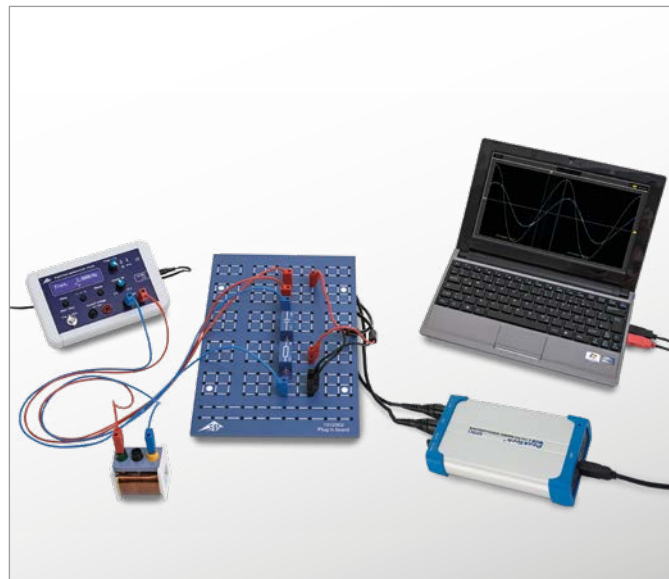
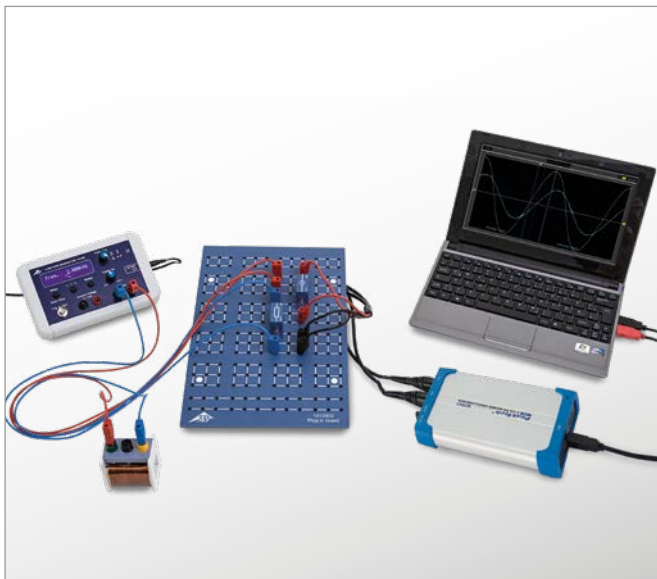


Fig. 6: Phase shift for parallel circuit

UE3050321 | IMPEDANCES



EXPERIMENT PROCEDURE

- Determining the impedances of series and parallel connections of capacitive and inductive reactances as a function of frequency.
- Determining resonant frequency as a function of inductance and capacitance.
- Observing changes in phase shift between voltage and current at the resonant frequency.

OBJECTIVE

Determining impedance in a circuit with an inductive and a capacitive reactance

SUMMARY

AC circuits with inductive and capacitive reactances show resonant behavior. At the resonant frequency, the impedance of a series connection of an inductive and a capacitive reactance is zero, whereas the impedance of a parallel connection is infinite. This experiment examines this phenomenon with the help of an oscilloscope and a function generator which supplies voltages between 50 Hz and 20,000 Hz.

REQUIRED APPARATUS

Quantity	Description	Item Number
1	Plug-In Board for Components	1012902
1	Capacitor 1 μF , 100 V, P2W19	1012955
1	Capacitor 4.7 μF , 63 V, P2W19	1012946
1	Coil S with 800 Taps	1001001
1	Coil S with 1200 Taps	1001002
1	Resistor 10 Ω , 2 W, P2W19	1012904
1	Function Generator FG 100 (230 V, 50/60 Hz) Function Generator FG 100 (115 V, 50/60 Hz)	1009957 or 1009956
1	PC Oscilloscope, 2x25 MHz	1020857
2	HF Patch Cord, BNC/4 mm Plug	1002748
1	Set of 15 Experiment Leads, 75 cm, 1 mm ²	1002840

BASIC PRINCIPLES

As the frequency of an AC circuit's current rises, the inductive reactance rises too, while the capacitive reactance drops. Series and parallel connections of capacitive and inductive reactances therefore exhibit resonant behavior. One speaks here of a resonant circuit, its current and voltage oscillating back and forth between the capacitance and inductance. An additional ohmic resistor dampens these oscillations.

To simplify calculations for series and parallel connections, inductances L are assigned the following complex reactance:

$$(1) \quad X_L = i \cdot 2\pi \cdot f \cdot L$$

f : Alternating current's frequency

Furthermore, capacitances C are assigned the following complex reactance:

$$(2) \quad X_C = \frac{1}{i \cdot 2\pi \cdot f \cdot C}$$

The total impedance of a series connection without an ohmic resistance therefore is:

$$(3) \quad Z_s = i \cdot \left(2\pi \cdot f \cdot L - \frac{1}{2\pi \cdot f \cdot C} \right)$$

The corresponding calculation for a parallel connection is:

$$(4) \quad \frac{1}{Z_p} = -i \cdot \left(\frac{1}{2 \cdot \pi \cdot f \cdot L} - 2 \cdot \pi \cdot f \cdot C \right)$$

At the resonant frequency

$$(5) \quad f_r = \frac{1}{2 \cdot \pi \cdot \sqrt{L \cdot C}}$$

the impedance Z_s of the series connection comprising inductive and capacitive reactances therefore vanishes, i.e. the voltages across both individual reactances are opposite and equal. By contrast, the value of a parallel connection's impedance Z_p becomes infinite, i.e. the individual currents are opposite and equal. At the resonant frequency, the sign of the phase shift between the voltage and current furthermore changes.

In the experiment, resonant circuits are set up as a series/parallel connections of capacitors and inductors. A function generator serves as a voltage source with an adjustable frequency and amplitude. An oscilloscope is used to measure current and voltage as functions of the set frequency. The voltage U and current I are displayed on the oscilloscope; I corresponds to the voltage drop across a small load resistor.

EVALUATION

For each frequency f , the phase shift φ as well as the amplitudes I_0 and U_0 are read on the oscilloscope. The readings are used to calculate the total impedance: $Z_0 = \frac{U_0}{I_0}$.

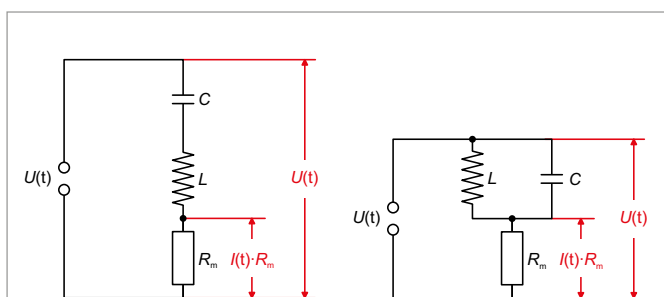


Fig. 1: Measurement setup for a series connection

Fig. 2: Measurement setup for a parallel connection

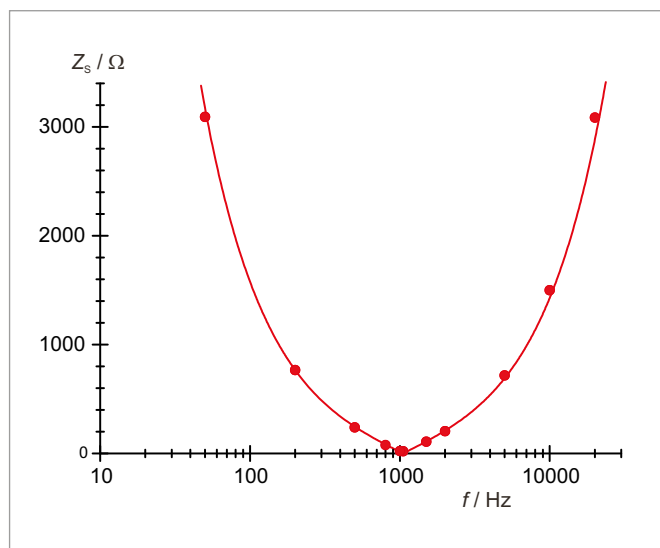


Fig. 3: Impedance of a series connection as a function of frequency

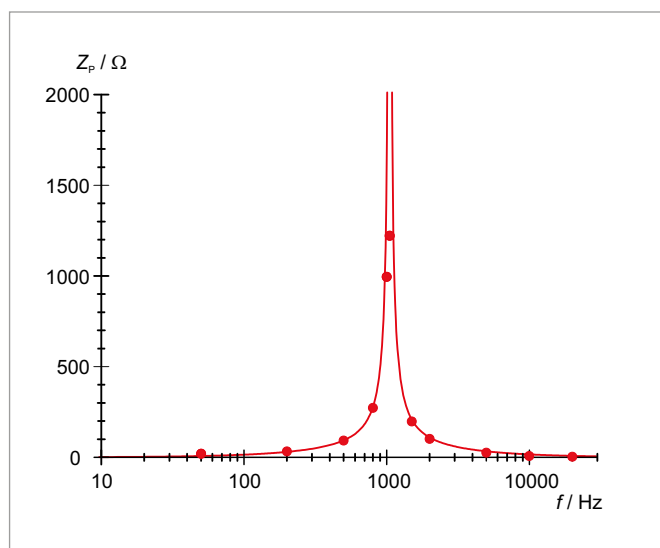


Fig. 4: Impedance of a parallel connection as a function of frequency

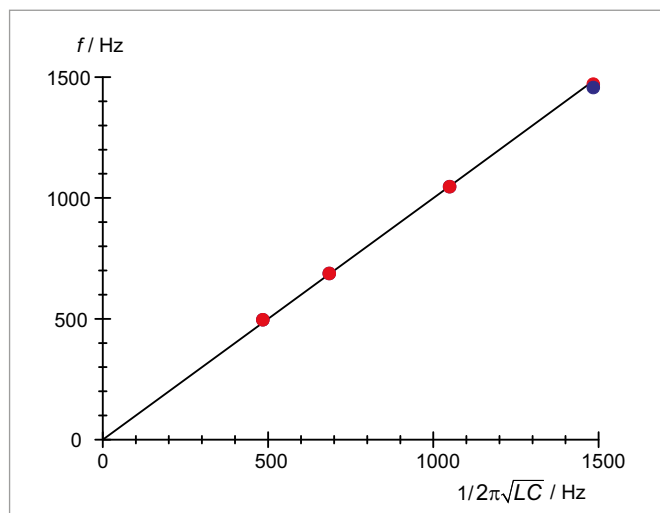


Fig. 5: Comparison between measured and calculated resonant frequencies for a series connection (red) and a parallel connection (blue)

UE3050400 | LC RESONANT CIRCUITS



EXPERIMENT PROCEDURE

- Record an amplitude resonance curve for a series LC resonant circuit with various degrees of damping.
- Determine the resonant frequency of the series LC resonant circuit.

OBJECTIVE

Investigate the resonance response of a series LC resonant circuit

SUMMARY

An electric resonant (also resonance or tuned) circuit is a circuit which is capable of resonating at a specific frequency. It comprises an inductor and a capacitor. In this experiment an AC voltage is generated with the help of a function generator and fed to a series resonant circuit. What will be measured is the amplitude resonance curve, i.e. the current as a function of the frequency at a constant voltage amplitude. If the capacitance is known, it is possible to calculate the unknown inductance of the circuit.

REQUIRED APPARATUS

Quantity	Description	Item Number
1	Basic Experiment Board (230 V, 50/60 Hz)	1000573 or
	Basic Experiment Board (115 V, 50/60 Hz)	1000572
1	VinciLab	1021477
1	Voltage Sensor 10 V, differential	1021680
1	Current Sensor 500 mA	1021679
1	Function Generator FG 100 (230 V, 50/60 Hz)	1009957 or
	Function Generator FG 100 (115 V, 50/60 Hz)	1009956
1	Set of 15 Experiment Leads, 75 cm, 1 mm ²	1002840

Additionally required

1	Coach 7 license
---	-----------------

BASIC PRINCIPLES

An electric resonant circuit is a circuit consisting of an inductor with inductance L and a capacitor with capacitance C . The periodic transfer of energy between the magnetic field of the coil and the electric field of the capacitor results in oscillation of the electric circuit. This transfer results in alternating instances where there is maximum current through the coil or maximum voltage across the capacitor.

If the resonant circuit is not oscillating freely, but is excited by an external sine-wave signal, it oscillates at the same frequency as the excitation signal and the amplitude of the current and voltage across the individual components are dependent on the frequency. The current I can be deduced from Ohm's law as follows:

$$(1) \quad I = \frac{U}{Z} = \frac{U_0 \cdot e^{i\omega t}}{Z}$$

U : sinusoidal input voltage

U_0 : amplitude, ω : angular frequency

Z : total impedance

In a series circuit, the total impedance is made up of the sum of the impedances of the individual components. In addition there is an ohmic resistance R , which covers the losses which inevitably occur in a real resonant circuit and which may also have any external resistance added to it. The following expression therefore arises:

$$(2) \quad Z = R + i\omega L + \frac{1}{i\omega C}$$

From equation (1) and (2) the current is given by

$$(3) \quad I(\omega) = \frac{U_0 \cdot e^{i\omega t}}{R + i\left(\omega L - \frac{1}{\omega C}\right)}$$

The magnitude of the current corresponds to its amplitude, which is frequency-dependent:

$$(4) \quad I_0(\omega) = \frac{U_0}{\sqrt{R^2 + \left(\omega L - \frac{1}{\omega C}\right)^2}}$$

This reaches its maximum value at the resonant frequency

$$(5) \quad f_r = \frac{\omega_r}{2\pi} = \frac{1}{2\pi \cdot \sqrt{L \cdot C}}$$

At that point, its magnitude is

$$(6) \quad I_0(\omega_r) = \frac{U_0}{R}$$

Therefore, in the case of resonance, the resonant circuit behaves as if it consisted solely of an ohmic resistance. In particular, an inductor and capacitor connected in series act as if they were a short circuit when resonance is occurring.

This experiment involves an AC voltage generated by a function generator being used to excite the tuned circuit. The current I is measured as a function of the frequency f while the amplitude of the voltage remains constant. The current is measured using a measuring interface and recorded by means of measurement and evaluation software which allows it to be displayed graphically. The amplitude resonance curve of the current, i.e. the way the amplitude of the current depends on the frequency, is recorded automatically.

EVALUATION

The resonant frequency f_r can be read off from the amplitude resonance curve. Since the capacitance C is known, it is possible to calculate the size of the inductor being used by means of equation (5):

$$L = \frac{1}{4\pi^2 \cdot f_r^2 \cdot C}$$

Using equation (6), the ohmic resistance R can be calculated from the amplitude of the resonance curve. If no external resistor is connected, R represents the ohmic losses inherent in a real resonant circuit.

$$R = \frac{U_0}{I_0(\omega_r)}$$

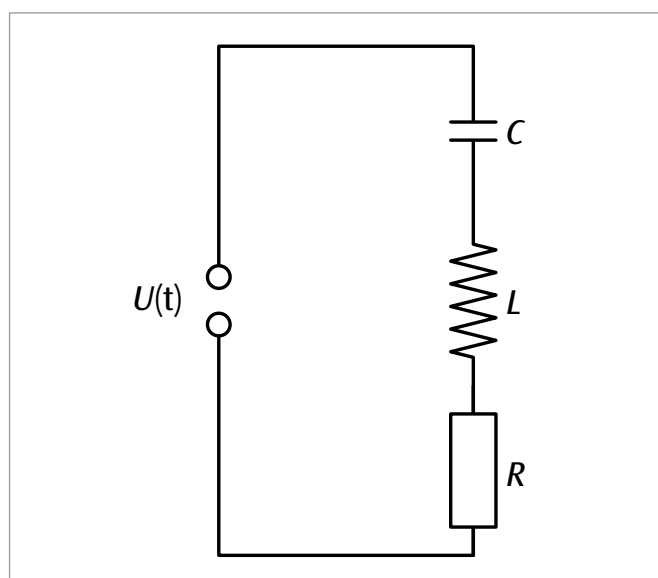


Fig. 1: Circuit diagram sketch for series LC resonant circuit

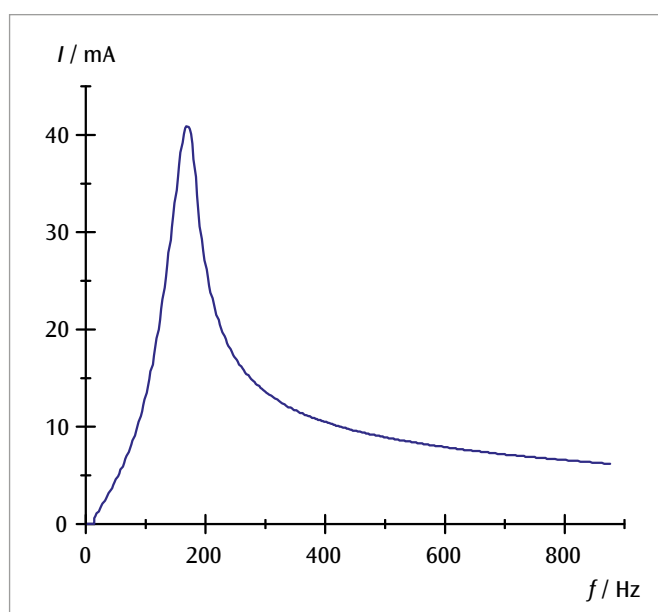
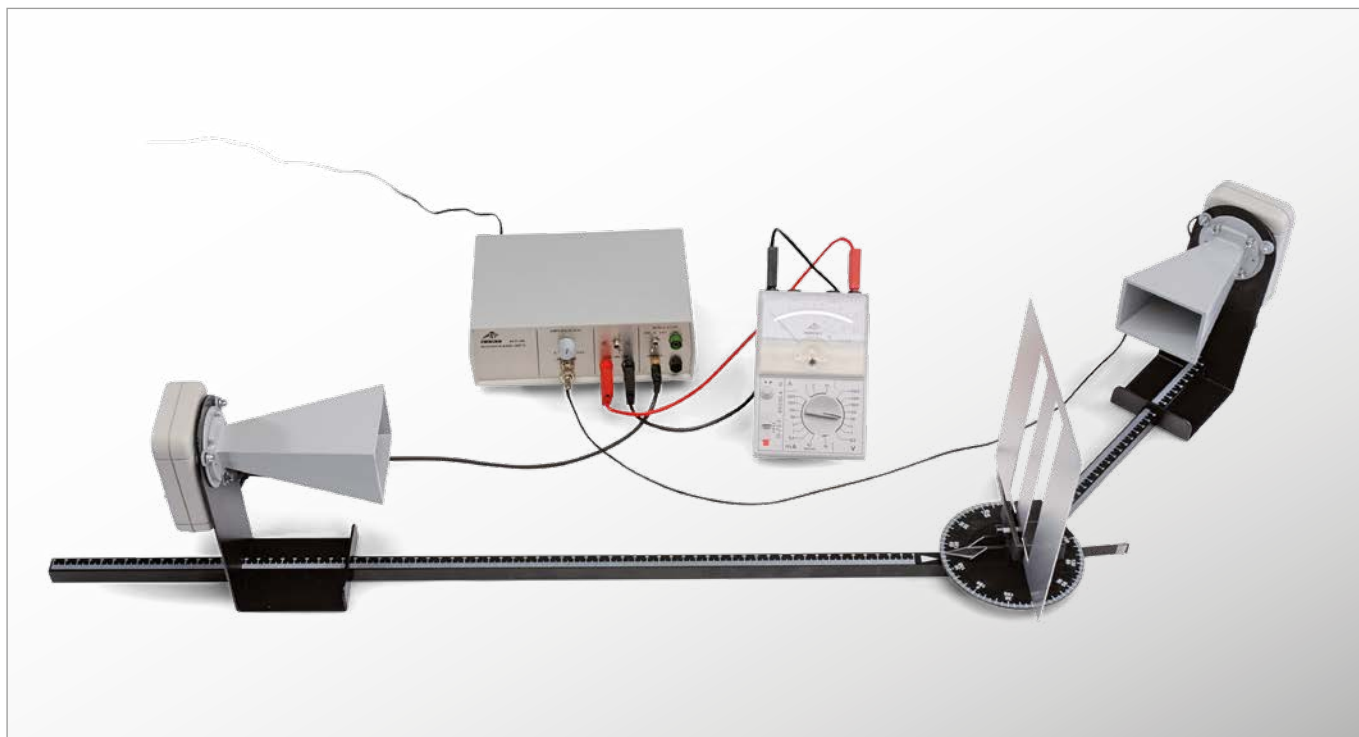


Fig. 2: Amplitude resonance curve of the current ($R_{\text{ext}} = 0$)

UE3060300 | WAVE OPTICS USING MICROWAVES



› EXPERIMENT PROCEDURE

- Take point-by-point measurements of the intensity when microwaves are diffracted at a pair of slits.
- Determine the positions of the maxima for different diffraction orders.
- Determine the wavelength when the distance between the slits is known.
- Investigate the polarisation of the emitted microwaves and modify it.

OBJECTIVE

Demonstrate and investigate the phenomena of interference, diffraction and polarisation using microwaves

SUMMARY

Using microwaves, many experiments can be conducted on interference, diffraction and polarisation, as an aid to understanding these phenomena for visible light. Diffracting objects and polarisation gratings can be used which possess a structure that can be seen with the unaided eye and easily understood. So it can be observed that in case of a double slit maximum intensity can be measured precisely if the receiver is not irradiated straight from the transmitter.

REQUIRED APPARATUS

Quantity	Description	Item Number
1	Microwave Set 9.4 GHz (230 V, 50/60 Hz)	1009951 or
	Microwave Set 10.5 GHz (115 V, 50/60 Hz)	1009950
1	Analogue Multimeter ESCOLA 30	1013526
1	Pair of Safety Experimental Leads, 75 cm, red/blue	1017718

BASIC PRINCIPLES

In wave optics light is regarded as consisting of transverse electromagnetic waves. This explains the phenomena of interference, diffraction and polarisation. Microwaves too are electromagnetic waves and they exhibit the same phenomena, but the wavelengths are much greater than those of visible light. Consequently, wave optics experiments can also be carried out using microwaves with diffraction objects and polarisation grids, the internal structure of which is obvious to the unaided eye.

This experiment investigates the diffraction of microwaves of wavelength λ at a pair of slits separated by a distance d of several centimeters. Measure the characteristic intensity distribution for diffraction by a pair of slits (see Fig. 1), with maxima at the angles α_m , as written below in formula (1):

$$(1) \quad \sin \alpha_m = m \cdot \frac{\lambda}{d}, \quad m = 0, \pm 1, \pm 2, \dots$$

Evidently the maximum intensity is observed when the detector is positioned exactly behind the central strip between the slits ($\alpha = 0, m = 0$), where it could not have detected radiation travelling along a straight-line path from the transmitter. This phenomenon can be explained as the result of interference between the partial wave beams from the two slits and is clear evidence for the wave nature of the microwaves. By rotating the detector about the direction of the source, clear evidence for the linear polarisation of the emitted microwaves can be obtained. When the planes of the transmitter and the detector are crossed at 90° the observed intensity falls to zero. If one of the polarising grids is then placed in the beam at an orientation of 45° to the other, the detector again detects radiation, although with a smaller amplitude than before. The grid transmits that component of the electric field vector of the incoming microwaves that vibrates parallel to the direction of the polarising grid. In this way the component vibrating in the direction parallel to the plane of the detector can be measured.

NOTE

Experiments on the absorption, reflection, refraction and polarisation of microwaves can be performed using the same equipment.

EVALUATION

Measure the diffraction angles α_m for the different intensity maxima and plot a graph of $\sin \alpha_m$ against the diffraction order m . The experimental measurements lie on a straight line through the origin, the gradient of which corresponds to the ratio λ/d .

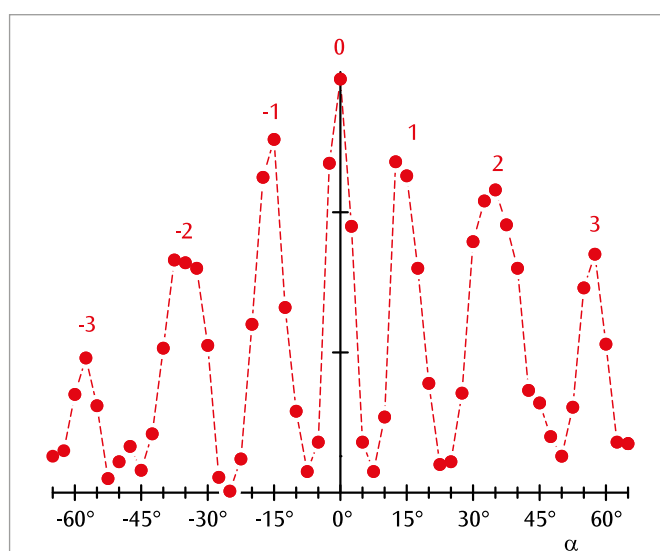


Fig. 1: Intensity distribution resulting from the diffraction of microwaves at a pair of slits

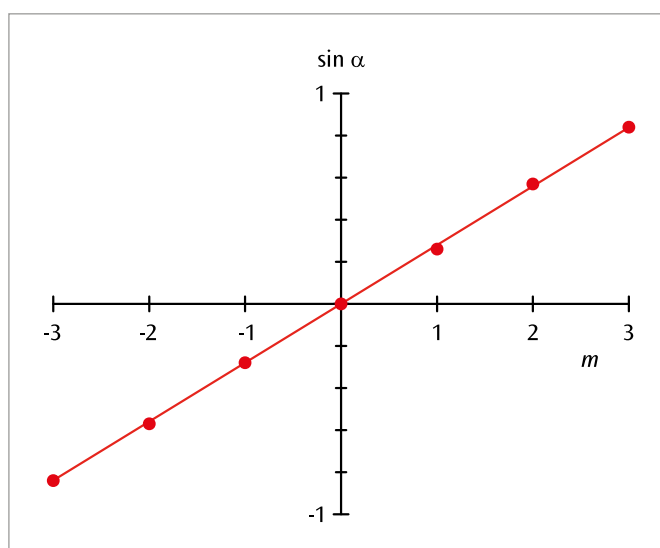


Fig. 2: Positions of the intensity maxima as a function of the diffraction order m

UE3070100 | THERMIONIC DIODE



EXPERIMENT PROCEDURE

- Record the characteristic for a thermionic diode at three different cathode heater voltages.
- Identify the space charge and saturation regions.
- Confirm the *Schottky-Langmuir* law.

OBJECTIVE

Record the characteristic for a thermionic diode

SUMMARY

In a thermionic diode, free electrons carry a flow of current between the heated cathode and the anode when a positive voltage is applied between the cathode and anode. The current increases along with the voltage until a saturation point is reached. However, if the voltage is negative, the current is zero.

REQUIRED APPARATUS

Quantity	Description	Item Number
1	Diode S *	1000613
1	Tube Holder S	1014525
1	DC Power Supply 0 – 500 V (230 V, 50/60 Hz)	1003308 or
	DC Power Supply 0 – 500 V (115 V, 50/60 Hz)	1003307
1	Analog Multimeter ESCOLA 100	1013527
1	Set of 15 Safety Experiment Leads, 75 cm	1002843

* Please ask also for a quote with our electron tubes D.

BASIC PRINCIPLES

A thermionic diode is an evacuated glass tube that contains two electrodes, a heated cathode that emits electrons due to the thermoelectric effect and an anode (see Fig. 1). A positive voltage between cathode and anode causes a current flow due to the transport of these emitted electrons from the cathode to the anode. If the voltage is low, the anode current is prevented from flowing since the charge of the emitted electrodes around the cathode, the space charge, shields the field of the cathode itself. As the anode voltage rises, the field lines penetrate more deeply into the space around the cathode and the anode current increases. It continues to rise until the space around the cathode is fully discharged so that the anode current reaches saturation level. When the voltage is sufficiently negative, however, electrons cannot get to the anode at all so that the anode current is zero in this case.

The way the anode current I_A depends on the anode voltage U_A is called the characteristic of the diode (see Fig. 2). There are three distinct areas, the reverse-bias region (a), the space charge region (b) and the saturation region (c).

In the reverse bias region the anode is at a negative voltage with respect to the cathode. Electrons are then unable to move against the electric field.

In the space charge region the anode current depends on the anode voltage in accordance with the *Schottky-Langmuir* law:

$$(1) \quad I_A \sim U_A^{\frac{3}{2}}$$

In the saturation region the anode current depends on the temperature of the cathode. By increasing the heater voltage U_F the anode current can be made to increase.

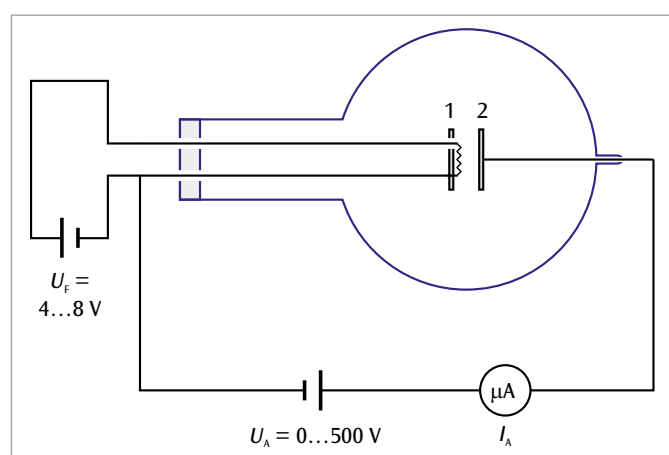


Fig. 1: Circuit for recording the characteristic of a thermionic diode.
1: Cathode, 2: Anode

EVALUATION

Reverse bias region:

Since electrons are emitted from the cathode with a kinetic energy $E_{kin} > 0$ a current flows in the anode only until the voltage of the anode is sufficiently negative that even the fastest of the emitted electrons is unable to overcome the field to reach the anode.

Space charge region:

For weak field strengths, not all the electrons emitted from the cathode are transported to the anode. They occupy the space around the cathode in a cloud creating a negative space charge. When the voltage is low, field lines for the anode thus reach only as far as the electrons in the cloud and not the cathode itself. The latter is thus shielded from the anode field. Only as the voltage increases do the field lines penetrate further into the cathode causing the anode current to rise. The increase continues until the space charge around the cathode is dissipated, at which point the anode current is saturated.

Saturated region:

In the saturation region the anode current does not depend on the anode voltage at all. It can nevertheless be increased by increasing the number of electrons emitted from the cathode in unit time. This can be achieved by raising the temperature of the cathode. The saturation current therefore depends on the heater voltage.

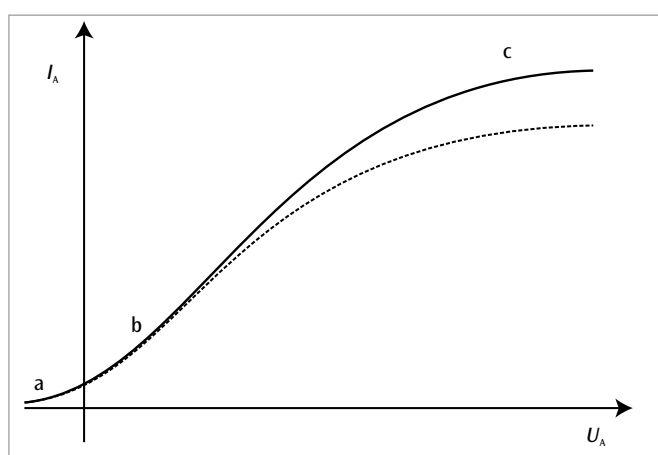


Fig. 2: Characteristic of a thermionic diode
a: Reverse bias region, b: Space charge region, c: Saturation region

UE3070200 | THERMIONIC TRIODE



EXPERIMENT PROCEDURE

- Record the anode current/anode voltage characteristics for a thermionic triode at various constant grid voltages.
- Record the anode current/grid voltage characteristics for a thermionic triode at various constant anode voltages.

OBJECTIVE

Record characteristics for a thermionic triode

SUMMARY

In a thermionic triode, free electrons carry a flow of current between the heated cathode and the anode when a positive voltage is applied between the cathode and anode. This current can be controlled by applying a positive or negative voltage to an intervening grid.

REQUIRED APPARATUS

Quantity	Description	Item Number
1	Triode S*	1000614
1	Tube Holder S	1014525
1	DC Power Supply 0 – 500 V (230 V, 50/60 Hz)	1003308 or
	DC Power Supply 0 – 500 V (115 V, 50/60 Hz)	1003307
1	Analog Multimeter ESCOLA 100	1013527
1	Set of 15 Safety Experiment Leads, 75 cm	1002843

* Please ask also for a quote with our electron tubes D.

BASIC PRINCIPLES

A thermionic triode is an evacuated glass tube that contains three electrodes, a heated cathode that emits electrons due to the thermo-electric effect and an anode with a grid placed in between them. At sufficiently high positive voltage between the cathode and anode (anode voltage), free electrons from the cathode can pass through the grid to reach the anode. The anode current generated in this way can be modulated by varying another voltage between the cathode and the grid. Depending on whether the grid is at positive or negative potential to the cathode, the anode current is either amplified or weakened. A thermionic triode can thus be used for amplifying AC voltages.

This experiment involves recording the set of characteristics for a thermionic triode. These incorporate the way the anode current I_A depends on the anode voltage U_A and on the grid voltage U_G . There are two common ways of portraying these characteristics (see Figs. 2 and 3): Fig. 2 shows the anode current as a function of the anode voltage at various constant grid voltages and Fig. 3 shows the anode current as a function of the grid voltage at various different constant anode voltages.

EVALUATION

The anode current rises as the anode voltage or the grid voltage rises. Even slight changes in the grid voltage of the order of a few volts can lead to large variations in the anode current. The grid voltage can thus be used to control the anode current.

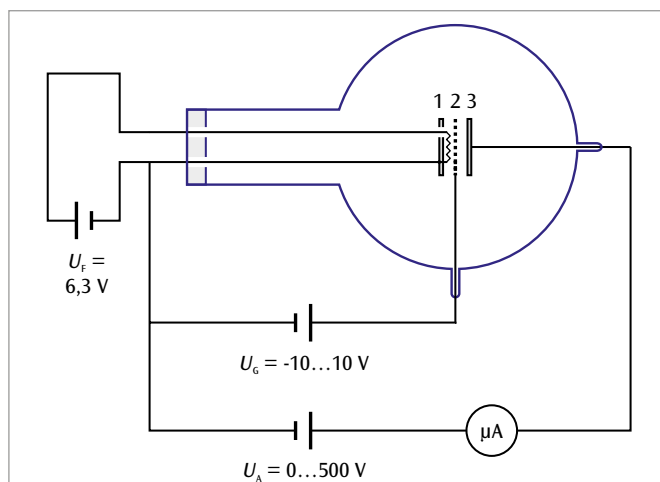


Fig. 1: Circuit for recording the characteristics of a thermionic triode
1: Cathode, 2: Grid, 3: Anode

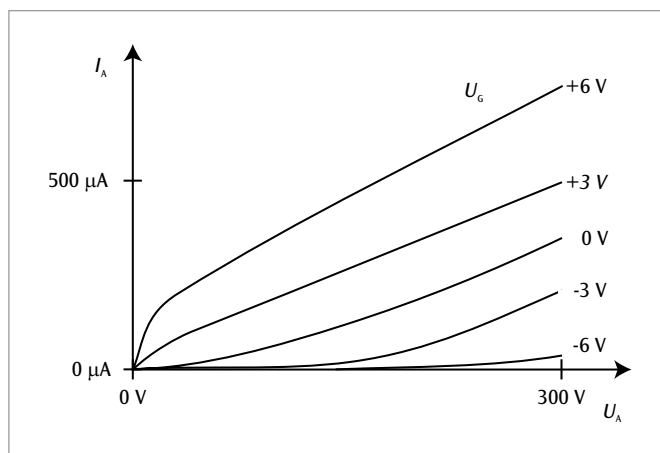


Fig. 2: Anode current/anode voltage characteristics

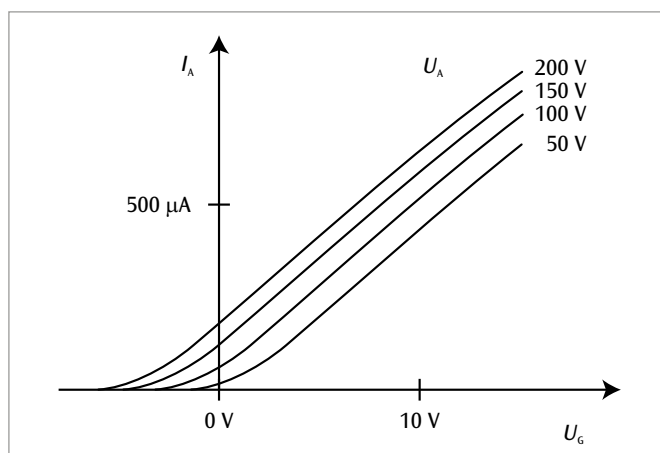
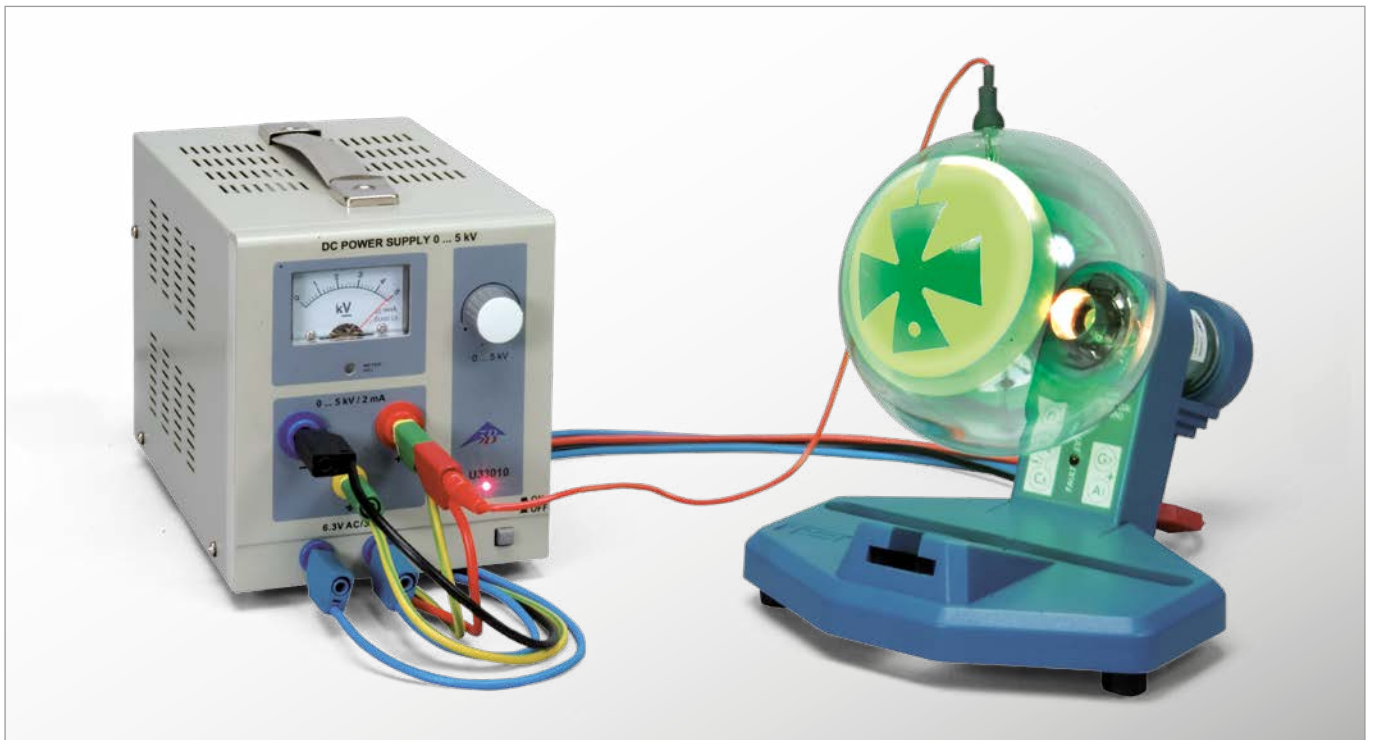


Fig. 3: Anode current/grid voltage characteristics

UE3070300 | MALTESE-CROSS TUBE



> EXPERIMENT PROCEDURE

- Demonstrate the straight-line propagation of electrons in the absence of a field.
- Demonstrate the deflection of electrons by a magnetic field.
- Introduction to electron optics.

OBJECTIVE

Demonstrate the straight-line propagation of electrons in the absence of any field

SUMMARY

Straight-line propagation of electrons in the absence of a field can be demonstrated in a Maltese-cross tube by showing how the shadow of the electron beam coincides with the shadow due to a light beam. Any deviation from the straight-line propagation of the beam, due to a magnetic field for example, can be seen since the shadow is then caused to move.

REQUIRED APPARATUS

Quantity	Description	Item Number
1	Maltese Cross Tube S *	1000011
1	Tube Holder S	1014525
1	High Voltage Power Supply 5 kV (230 V, 50/60 Hz)	1003310 or
	High Voltage Power Supply 5 kV (115 V, 50/60 Hz)	1003309
1	Set of 15 Safety Experiment Leads, 75 cm	1002843
Additionally recommended for generating an axially aligned magnetic field		
1	Helmholtz Pair of Coils S	1000611
1	DC Power Supply 0 – 20 V, 0 – 5 A (230 V, 50/60 Hz)	1003312 or
	DC Power Supply 0 – 20 V, 0 – 5 A (115 V, 50/60 Hz)	1003311

* Please ask also for a quote with our electron tubes D.

BASIC PRINCIPLES

In a Maltese-cross tube, a divergent electron beam from a cathode ray gun can be seen on a fluorescent screen by observing the shadow on the screen of an object (a Maltese cross) that is opaque to cathode rays. The position of the shadow changes when the straight-line propagation of the electrons towards the screen is disturbed.

If the anode and the Maltese-cross are at the same potential, there will be no field within the tube and electrons will propagate in a straight line. The electron shadow of the cross will then be coincident with its shadow in the light that is emitted from the glowing cathode.

How this straight-line propagation is disturbed when a field is present within the tube can be easily seen by disconnecting the lead between the anode and the cross. The cross then becomes statically charged and the electron shadow on the screen becomes blurred.

If the electrons are deflected by a magnetic field on their way to the screen, the electron shadow can be seen to shift or rotate.

The deflecting force F depends on the velocity v of the electrons, on the magnetic field B and is a result of the Lorentz-force:

$$(1) \quad F = -e \cdot v \times B$$

EVALUATION

In the absence of a field the electrons propagate in a straight line. The electron shadow exactly matches the shadow from the light.

In a magnetic field electrons are deflected and the electron shadow is shifted with respect to the shadow from the light. The deflecting force is perpendicular to the direction of motion of the electrons and to the magnetic field itself.

If the magnetic field is aligned axially, the electrons are deflected into spiral paths and the shadow rotates and becomes smaller.

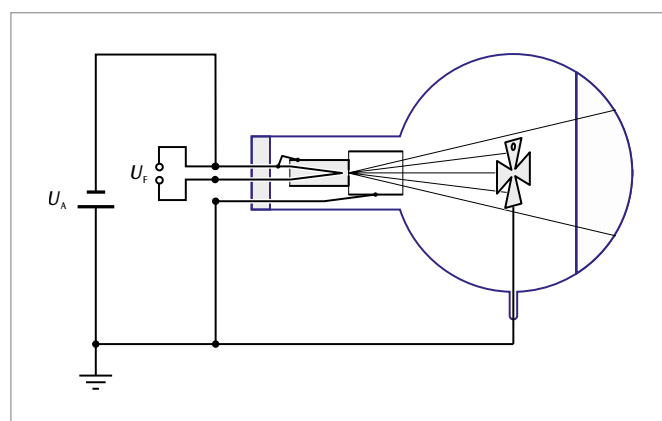


Fig. 1: Schematic of Maltese cross tube



Fig. 2: Rotation of the electron shadow through deflection of electrons in the axially aligned magnetic field

UE3070400 | PERRIN TUBE



EXPERIMENT PROCEDURE

- Observing the thermionic emission of charge-carriers from a heated cathode.
- Determining the polarity of the emitted charge-carriers.
- Estimating the specific charge (charge-to-mass ratio) of the charge-carriers.

OBJECTIVE

Determine the polarity of the charge-carriers

SUMMARY

In the Perrin tube, the electron beam can be deflected into a Faraday cup by applying a homogeneous magnetic field. The charge of the electrons can be observed by connecting an electrostatic deflection apparatus to the Faraday cup, and its polarity can be determined by comparison with an electric charge of known polarity.

REQUIRED APPARATUS

Quantity	Description	Item Number
1	Perrin Tube S *	1000616
1	Tube Holder S	1014525
1	Helmholtz Pair of Coils S	1000611
1	High Voltage Power Supply 5 kV (230 V, 50/60 Hz)	1003310 or
	High Voltage Power Supply 5 kV (115 V, 50/60 Hz)	1003309
1	DC Power Supply 0 – 20 V, 0 – 5 A (230 V, 50/60 Hz)	1003312 or
	DC Power Supply 0 – 20 V, 0 – 5 A (115 V, 50/60 Hz)	1003311
1	Kolbe's Electrostatic Deflection Apparatus	1001027
1	Set of 15 Safety Experiment Leads, 75 cm	1002843

* Please ask also for a quote with our electron tubes D.

BASIC PRINCIPLES

In the Perrin tube, a focused electron beam falls onto a fluorescent screen, where it is observed as a bright dot. A Faraday cup is placed at 45° to the electron beam, and the electrons can then be deflected into it by applying a magnetic field. The flow of charge can be measured through a separate electrical connection.

In the experiment, the electron beam is deflected by the homogeneous magnetic field of a Helmholtz coil pair into the Faraday cup, which is connected to an electroscope. From the observed charging or discharging of the electroscope by the electron beam entering the Faraday cup, it is possible to determine the polarity of the charge-carriers. It is also possible to estimate the specific charge of the charge-carriers, since the radius of curvature r of the curved path into the Faraday cup is known. The centripetal force acting on the charge-carriers in this curved path is given by the Lorentz force as follows:

$$(1) \quad m \cdot \frac{v^2}{r} = e \cdot v \cdot B$$

e : Carrier charge, m : Mass of the charge-carrier,

B : Magnetic flux density.

Also, the velocity v of the charge-carriers depends on the anode voltage U_A as follows:

$$(2) \quad v = \sqrt{2 \cdot \frac{e}{m} \cdot U_A}$$

Combining Equations 1 and 2 gives the following expression for the specific charge (charge-to-mass ratio) of the charge-carriers:

$$(3) \quad \frac{e}{m} = \frac{2 \cdot U_A}{(B \cdot r)^2}$$

EVALUATION

The radius of curvature r of the curved path to the Faraday cup is 160 mm. The anode voltage U_A is known.

The magnetic field B is generated by a Helmholtz coil pair and is proportional to the current I_H through each of the coils. The proportionality factor k can be calculated from the coil radius $R = 68$ mm and the number of turns on each coil, which is $N = 320$. Thus:

$$B = k \cdot I_H \quad \text{with} \quad k = \left(\frac{4}{5}\right)^{\frac{3}{2}} \cdot 4\pi \cdot 10^{-7} \frac{\text{Vs}}{\text{Am}} \cdot \frac{N}{R}$$

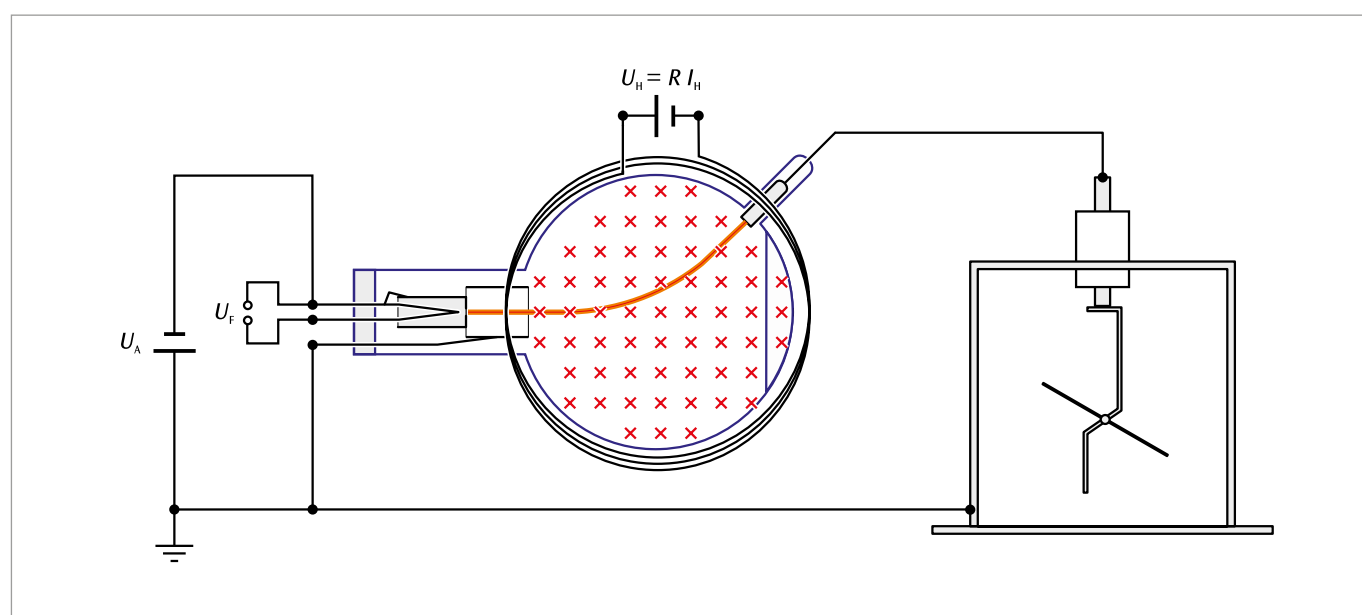
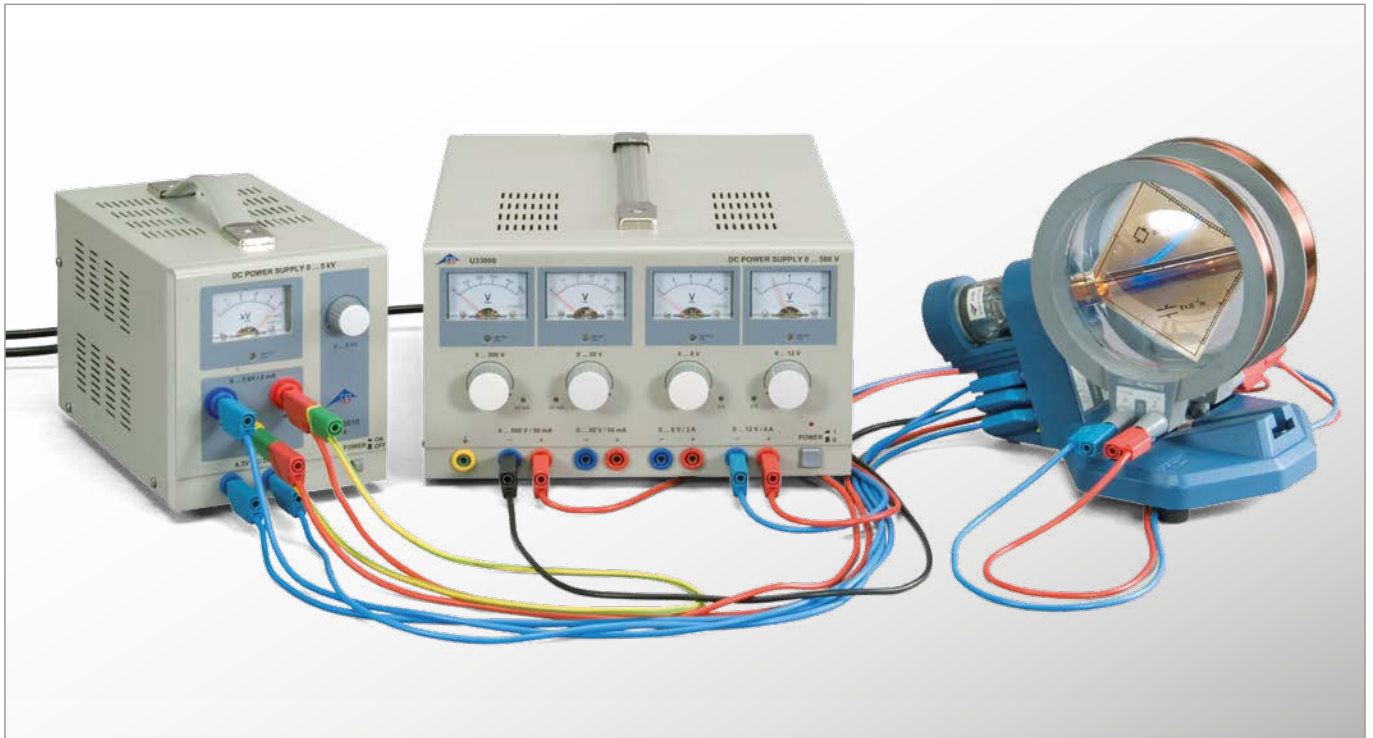


Fig. 1: Schematic diagram of the Perrin tube

UE3070500 | THOMSON TUBE



EXPERIMENT PROCEDURE

- Investigate the deflection of an electron beam by a magnetic field.
- Estimate the specific charge of an electron.
- Investigate the deflection of an electron beam by an electric field.
- Construct a velocity filter using orthogonal electric and magnetic fields.

OBJECTIVE

Investigate the deflection of electrons by electric and magnetic fields

SUMMARY

In a Thomson tube the vertical deflection of a horizontal electron beam can be observed on a fluorescent screen. Such a deflection can be generated by a vertical electric field or by a horizontal magnetic field that is perpendicular to the direction of motion in the horizontal plane.

REQUIRED APPARATUS

Quantity	Description	Item Number
1	Thomson Tube S *	1000617
1	Tube Holder S	1014525
1	Helmholtz Pair of Coils S	1000611
1	High Voltage Power Supply 5 kV (230 V, 50/60 Hz)	1003310 or
	High Voltage Power Supply 5 kV (115 V, 50/60 Hz)	1003309
1	DC Power Supply 0 – 500 V (230 V, 50/60 Hz)	1003308 or
	DC Power Supply 0 – 500 V (115 V, 50/60 Hz)	1003307
1	Set of 15 Safety Experiment Leads, 75 cm	1002843

* Please ask also for a quote with our electron tubes D.

BASIC PRINCIPLES

In a Thomson tube electrons pass horizontally through a slit behind the anode and impinge upon a fluorescent screen placed at an angle to the electron beam on which they can be observed. Beyond the slot there is a plate capacitor. The electric field between its two plates deflects the electron beam in a vertical direction. In addition Helmholtz coils can be used to create a magnetic field in a horizontal direction perpendicular to the motion of the electrons that also deflects them in a vertical direction.

An electron moving with velocity \mathbf{v} through a magnetic field \mathbf{B} is subject to a Lorentz force given by

$$(1) \quad \mathbf{F} = -e \cdot \mathbf{v} \times \mathbf{B}$$

e : Charge of an electron

The force acts in a direction perpendicular to a plane defined by the direction of motion and the magnetic field. This causes the beam to be deflected vertically, if both the direction of motion and the magnetic field are in the horizontal plane (see Fig. 1). If the direction of motion is perpendicular to a uniform magnetic field, electrons are deflected in a circular path with a centripetal force resulting from the Lorentz-force.

$$(2) \quad m \cdot \frac{v^2}{r} = e \cdot v \cdot B$$

m : Mass of an electron, r : Radius of path.

The velocity of the electrons depends on the anode voltage U_A so that:

$$(3) \quad v = \sqrt{2 \cdot \frac{e}{m} \cdot U_A}$$

This means that measuring the radius of the path allows the specific charge of an electron to be determined as long as the homogenous magnetic field B and the anode voltage U_A are both known. Equations (2) and (3) can be combined to give an expression for the specific charge of an electron:

$$(4) \quad \frac{e}{m} = \frac{2 \cdot U_A}{(B \cdot r)^2}$$

If a voltage U_p is being applied to the plate capacitor, electrons are deflected vertically by its electric field \mathbf{E} with a force

$$(5) \quad \mathbf{F} = -e \cdot \mathbf{E}$$

e : Charge of an electron

This deflection is also vertical (see Fig. 2). The electric field can thus be adjusted in such a way that it precisely cancels out the deflection due to the magnetic field:

$$(6) \quad e \cdot E + e \cdot v \cdot B = 0$$

In this case it is easy to determine the velocity of each electron:

$$(7) \quad v = \frac{|E|}{|B|}$$

Such an arrangement of orthogonal electric and magnetic fields in which the deflection of the beam, is cancelled out is sometimes called a velocity filter.

EVALUATION

The magnetic field B is generated by a pair of Helmholtz coils and is proportional to the current I_H passing through each coil individually. The coefficient of proportionality k can be determined from the coil radius $R = 68 \text{ mm}$ and the number of turns in the coil $N = 320$ per coil:

$$B = k \cdot I_H \text{ where } k = \left(\frac{4}{5}\right)^{\frac{3}{2}} \cdot 4\pi \cdot 10^{-7} \frac{\text{Vs}}{\text{Am}} \cdot \frac{N}{R}$$

The electric field can be calculated from the voltage U_p and the separation of plates d :

$$E = \frac{U_p}{d}$$

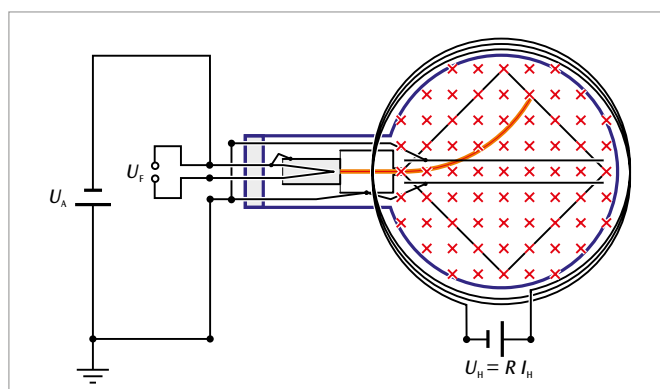


Fig. 1: Schematic of a Thomson tube in a magnetic field

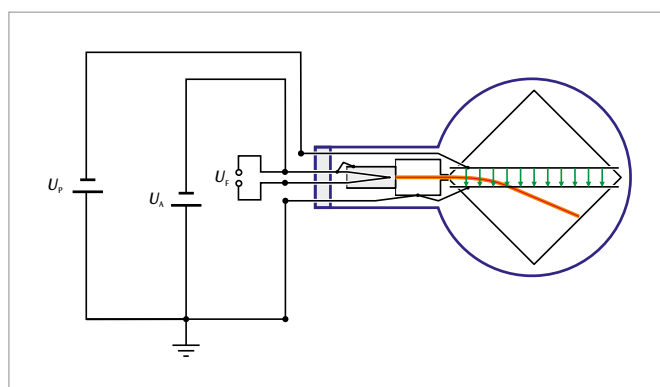


Fig. 2: Schematic of a Thomson tube in an electric field

UE3070700 | FINE-BEAM TUBE



EXPERIMENT PROCEDURE

- Demonstrate the deflection of electrons in a uniform magnetic field into a closed circular path.
- Determine the Helmholtz current I_H as a function of the accelerating voltage of the electron gun U for a constant path radius r .

OBJECTIVE

Determine the specific charge of an electron

SUMMARY

In the fine-beam tube, the path of electrons in a uniform magnetic field can be observed as a clearly delineated ray. This means that the radius of the circular path can be directly measured with a simple ruler. From the path radius r , the magnetic field B and the electron gun's accelerating voltage U the specific charge of an electron e/m can be calculated.

REQUIRED APPARATUS

Quantity	Description	Item Number
1	Fine Beam Tube on Connection Base	1019957
1	Helmholtz Coils 300 mm	1000906
1	DC Power Supply 0 – 500 V (230 V, 50/60 Hz)	1003308
	DC Power Supply 0 – 500 V (115 V, 50/60 Hz)	1003307
1	Analog Multimeter ESCOLA 100	1013527
1	Set of 15 Safety Experiment Leads, 75 cm	1002843

BASIC PRINCIPLES

Electrons in a fine-beam tube are deflected into a circular path by a uniform magnetic field. The tube contains neon gas at a precisely defined pressure so that gas atoms become ionized by collision with electrons along the path thus causing them to emit light. This means the path of the electrons can be viewed directly and the radius of the curvature can simply be measured with a ruler. Since the accelerating voltage of the electron gun U and the magnetic field strength B are both known, the radius of the path r can be used to determine the specific charge of an electron e/m :

An electron moving at velocity v in a direction perpendicular to a magnetic field B is subject to a Lorentz-force that acts in a direction orthogonal to both the movement and the magnetic field:

$$(1) \quad F = e \cdot v \cdot B$$

e : Charge on an electron

This gives rise to a centripetal force on the electron

$$(2) \quad F = \frac{m \cdot v^2}{r}$$

m : Mass of an electron

such that it moves in a circular path of radius r . Therefore

$$(3) \quad e \cdot B = \frac{m \cdot v}{r}$$

The velocity v is dependent on the accelerating voltage U applied to the electron gun:

$$(4) \quad v = \sqrt{2 \cdot \frac{e}{m} \cdot U}$$

Therefore the specific charge of the electron is given by:

$$(5) \quad \frac{e}{m} = \frac{2 \cdot U}{(r \cdot B)^2}$$

EVALUATION

The magnetic field B is generated by a pair of Helmholtz-coils and is proportional to the current I_H that passes through each of the coils. The coefficient of proportionality k can be determined from the coil radius $R = 147.5$ mm and the number of turns in the coil $N = 124$ per coil:

$$B = k \cdot I_H \quad \text{where} \quad k = \left(\frac{4}{5}\right)^{\frac{3}{2}} \cdot 4\pi \cdot 10^{-7} \frac{\text{Vs}}{\text{Am}} \cdot \frac{N}{R}$$

This means that all the components needed to calculate the specific charge are known.

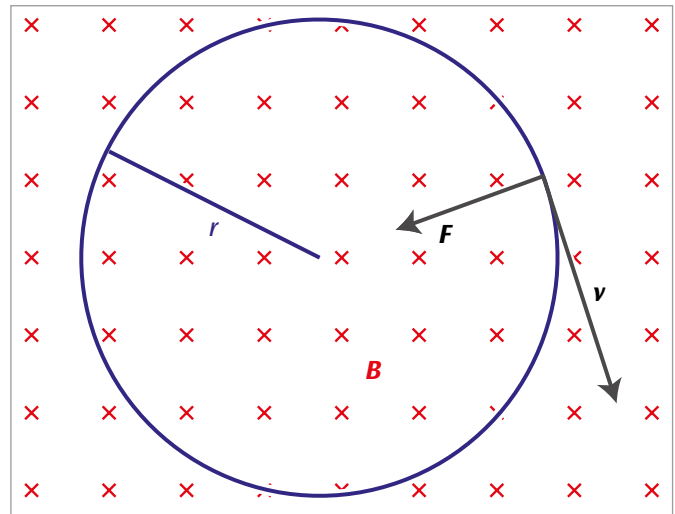


Fig. 1: Deflection of electron of velocity v in a magnetic field B by a Lorentz-force F into a closed circular path of radius r

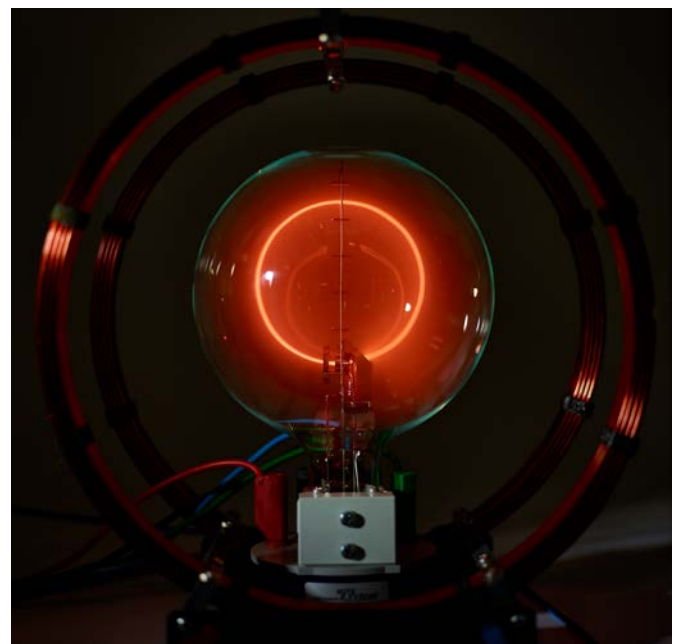
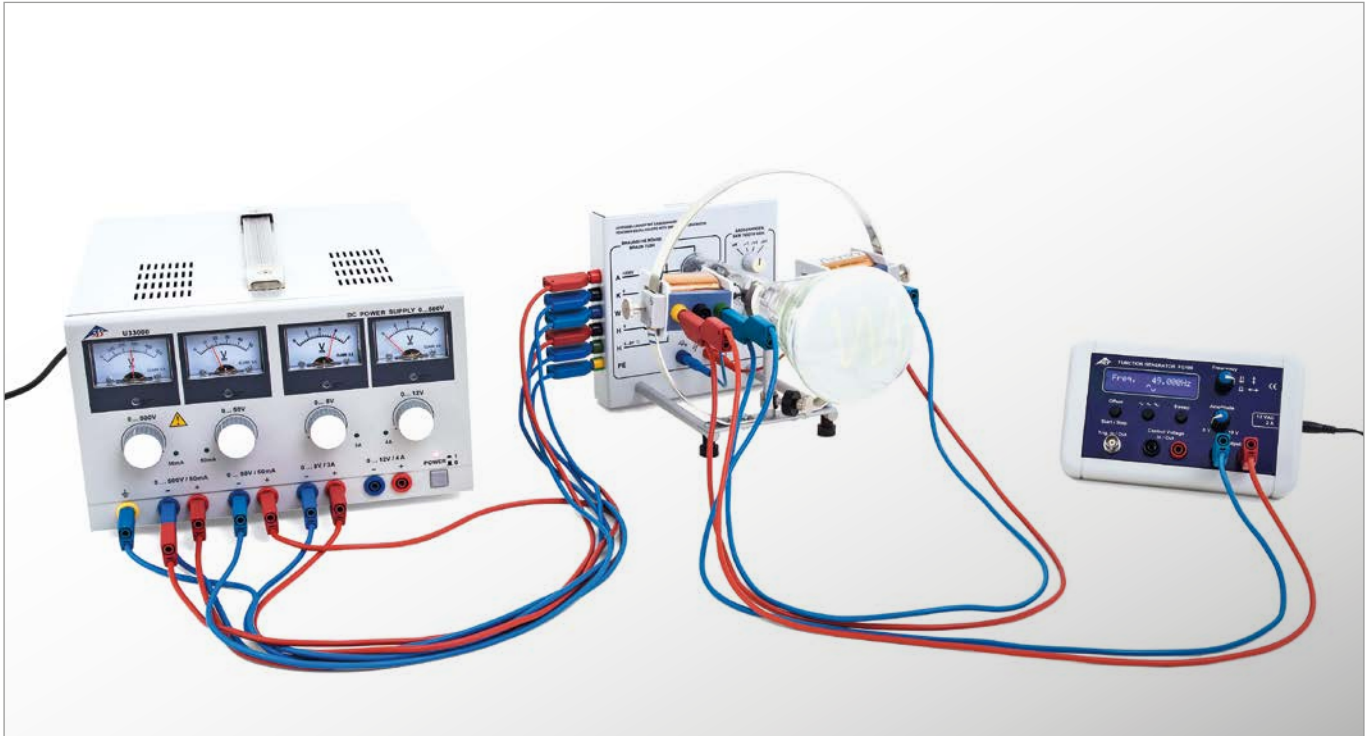


Fig. 2: Fine-beam tube with spherically-shaped luminous trace of electrons in the magnetic field

UE3070800 | TRAINING OSCILLOSCOPE I



EXPERIMENT PROCEDURE

- Investigating the deflection of an electron beam in an electric field.
- Investigating the deflection of an electron beam in a magnetic field.
- Demonstrating the display of signals on an oscilloscope, using the periodic signal from a function generator.
- Calibrating the frequency control of the sawtooth generator.

OBJECTIVE

Study the physical principles of the time-resolved display of electrical signals using an oscilloscope

SUMMARY

The student oscilloscope can be used to study the physical principles of the time-resolved display of electrical signals on a fluorescent screen. In a Braun tube, a focused electron beam is generated, and the point at which it falls on the fluorescent screen is observed as a spot of green light. When the electron beam is deflected by a sawtooth voltage applied between a pair of plates, it moves at a constant speed from left to right across the screen, then flies back to the starting point. This process is repeated cyclically at a frequency that can be adjusted. The time-dependent voltage that is to be displayed is applied to a coil outside the tube, so that the beam is deflected vertically in the magnetic field of the coil. The time-dependence of the signal is resolved by the simultaneous horizontal motion of the electron beam and displayed on the fluorescent screen.

REQUIRED APPARATUS

Quantity	Description	Item Number
1	Training Oscilloscope	1000902
1	DC Power Supply 0 – 500 V (230 V, 50/60 Hz)	1003308 or
	DC Power Supply 0 – 500 V (115 V, 50/60 Hz)	1003307
1	Function Generator FG 100 (230 V, 50/60 Hz)	1009957 or
	Function Generator FG 100 (115 V, 50/60 Hz)	1009956
1	Set of 15 Safety Experiment Leads, 75 cm	1002843

BASIC PRINCIPLES

An important application of thermionic emission in a high vacuum is the cathode ray oscilloscope, in which the Braun tube is an essential component. In the form used in the student oscilloscope, the electron-optical system of the Braun tube, which is visible from the outside, consists of a thermionic cathode surrounded by a “Wehnelt cylinder” and a pinhole disc at the anode potential. A proportion of the electrons that are accelerated towards the anode pass through the pinhole disc and form a beam, which is observed on the tube’s fluorescent screen as a green spot of light. Because the tube is filled with neon at a low pressure, the electron beam is concentrated through collisions with gas atoms, and is visible as thin threads emitting reddish light. A negative voltage that is applied to the Wehnelt cylinder also contributes to the concentration of the beam. Technical oscilloscopes usually have additional arrangements for post-acceleration (intensification) and focusing of the beam, but for simplicity and clarity these are not present in the student oscilloscope.

Behind the anode, there is a pair of plates with their planes parallel to the electron beam, which can be connected to a sawtooth generator (see Fig. 1). The electric field produced by the sawtooth voltage $U_x(t)$ deflects the beam horizontally, so that it moves across the fluorescent screen from left to right at a constant speed, then flies back to the starting point. This process is repeated cyclically at a frequency that can be adjusted.

During its left-to-right movement, the electron beam can also be deflected vertically by a magnetic field, and for this a voltage $U_y(t)$ is applied to the coils that are external to the tube. If this voltage is time-dependent, the time-resolved variations are displayed on the screen (see Fig. 2). Such time-dependent voltages might be, for example, the periodic output voltage from a function generator, or the amplified signals from a microphone.

In the experiment, the periodic signals from a function generator are investigated. The most useful display is obtained when the sawtooth frequency is adjusted so that its ratio to that of the function generator is a whole number.

EVALUATION

If the frequencies are adjusted so that exactly one cycle of the signal is displayed on the screen, then its frequency matches that of the sawtooth generator.

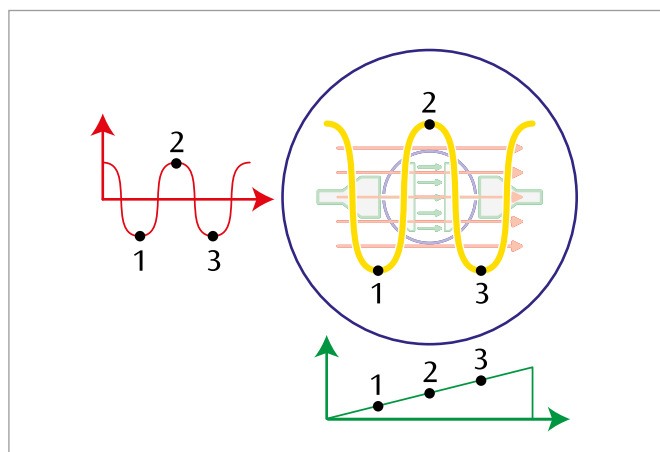


Fig. 2: Time-resolved display of a periodic signal

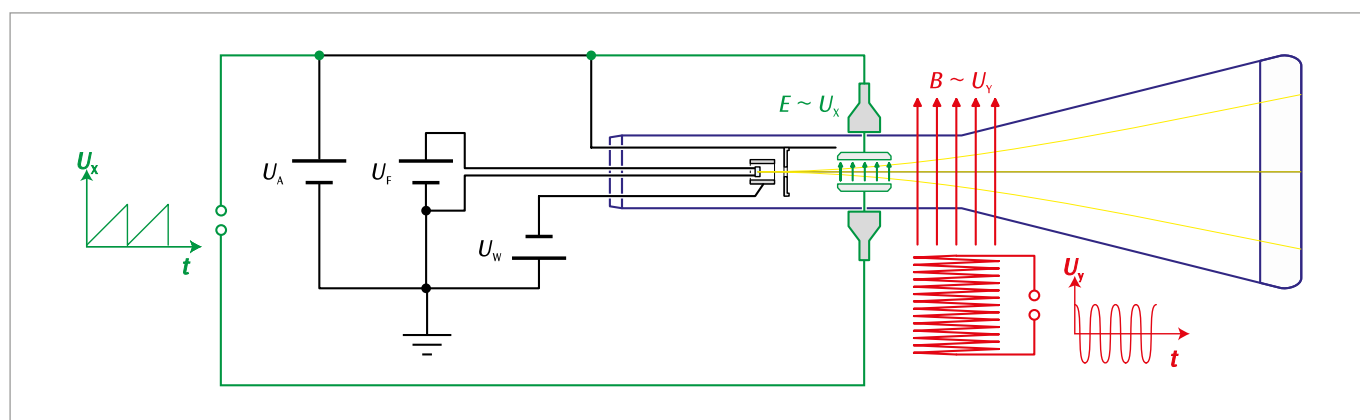


Fig. 1: Schematic diagram of the student oscilloscope, viewed from above

UE3070850 | TRAINING OSCILLOSCOPE II



EXPERIMENT PROCEDURE

- Superposing magnetic fields with the same and different frequencies, and observing the displacement of the focused spot on the screen of the tube.
- Generating closed Lissajous' figures.
- Checking the frequency of the mains supply.

OBJECTIVE

Demonstrate the superposition of magnetic fields in a vacuum

SUMMARY

The absence of interference when magnetic fields are superposed in a vacuum is demonstrated using a Braun tube. This is done by observing the displacements of the focused spot on the fluorescent screen of the tube. The experiments can be extended to include alternating magnetic fields with identical and different frequencies. The Lissajous' figures observed on the screen depend critically on the relation between the frequencies of the two magnetic fields and on their phase relation.

REQUIRED APPARATUS

Quantity	Description	Item Number
1	Training Oscilloscope	1000902
1	DC Power Supply 0 – 500 V (230 V, 50/60 Hz)	1003308 or
	DC Power Supply 0 – 500 V (115 V, 50/60 Hz)	1003307
1	Function Generator FG 100 (230 V, 50/60 Hz)	1009957 or
	Function Generator FG 100 (115 V, 50/60 Hz)	1009956
1	AC/DC Power Supply 0 – 12 V, 3 A, stab. (230 V, 50/60 Hz)	1001007 or
	AC/DC Power Supply 0 – 12 V, 3 A, stab. (115 V, 50/60 Hz)	1001006
1	Set of 15 Safety Experiment Leads, 75 cm	1002843

BASIC PRINCIPLES

A Braun tube can be used to demonstrate the principle of superposition for magnetic fields in a vacuum, by observing the deflection of the beam in the magnetic field. It is especially instructive to also perform experiments with alternating magnetic fields, as the electron beam follows the changes of the magnetic field without a significant time-lag.

In the experiment, two identical current-carrying coils are placed outside the Braun tube, and the deflection of the electron beam in the magnetic fields of the coils is observed on the tube's fluorescent screen as shifts of the focused spot. The magnetic field of the horizontal coil causes a vertical shift of the beam, while that of the vertical coil causes a horizontal shift.

When an alternating magnetic field at the mains frequency is applied to one of the coils, the focused spot is stretched out to become a vertical or horizontal line. If both coils are then connected in parallel to the alternating voltage source, the screen shows a straight line at 45° to the vertical, whereas when the coils are connected in opposition the line is at -45°, as the shifts produced by the two magnetic fields are superposed.

The experiment can be extended to study the effects of alternating magnetic fields of different frequencies. The Lissajous' figures that then appear on the screen depend critically on the relationship between the frequencies of the two magnetic fields and on their phase relationship. When the ratio of the frequencies is an integer or a simple fraction, closed figures are generated. Their exact shape also depends on the phase difference between the magnetic fields. As an example, Figure 1 shows Lissajous' figures with a frequency ratio 5:1.

If the frequency ratio is only slightly different from a simple rational value, we observe a closed figure that changes with time, at a rate that becomes slower as the difference from a simple ratio is reduced. In the experiment, this behavior is used to check the mains frequency. For this, one coil is connected to a transformer working at the mains frequency, while the second coil is connected to a signal generator whose output frequency can be read precisely.

EVALUATION

The generator frequency is adjusted relative to the mains frequency ν until we get the frequency ν_5 that gives the slowest change of a Lissajous' figure corresponding to the frequency ratio 5:1.

The mains frequency is then calculated as:

$$\nu = \frac{\nu_5}{5}$$

The measurement has a precision of ± 0.01 Hz, since ν_5 can be adjusted with a precision of ± 0.05 Hz.

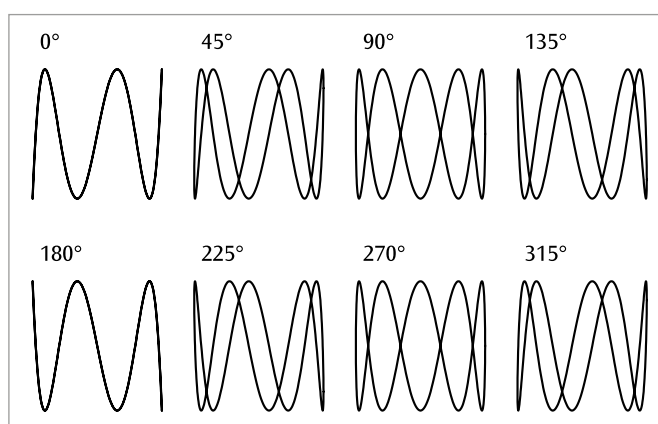
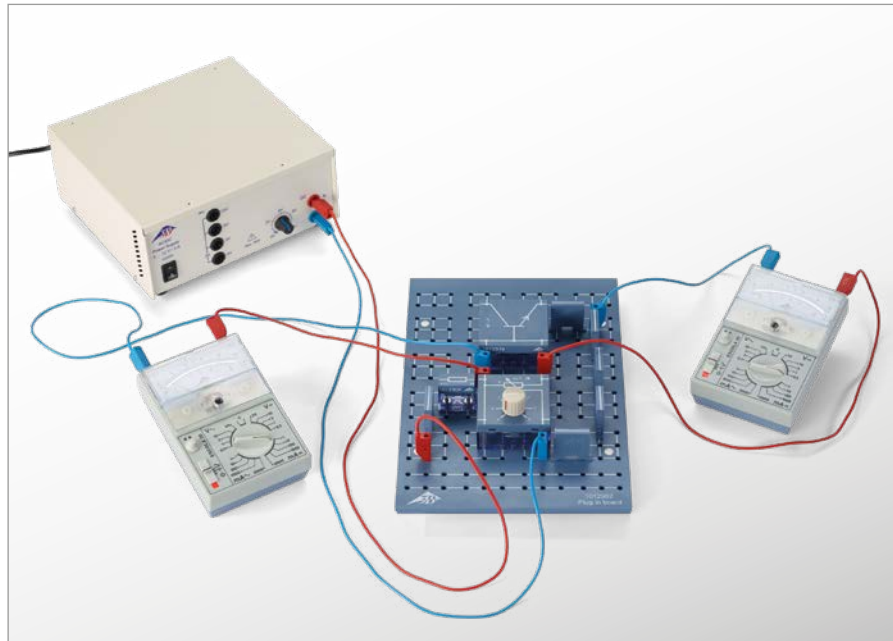


Fig. 1: Lissajous' figures for the frequency ratio 5:1 with phase differences 0°, 45°, 90°, ...

UE3080200 | BIPOLAR TRANSISTORS



OBJECTIVE

Measure the relevant characteristic curves of an npn transistor

SUMMARY

A bipolar transistor is an electronic component composed of three alternating p-doped and n-doped semiconductor layers called the base, the collector and the emitter. Depending on the sequence of the layers, the transistor may either be termed npn or pnp. The response of a bipolar transistor may be distinctively described by, for example, an input characteristic, a control characteristic, and an output characteristic. In this experiment, examples of these are to be measured for an npn transistor, displayed on a graph and evaluated.

> EXPERIMENT PROCEDURE

- Measure the input characteristic, i.e. the base current I_B as a function of the base emitter voltage U_{BE} .
- Measure the control characteristic, i.e. the collector current I_C as a function of the base current I_B for a fixed collector-emitter voltage U_{CE} .
- Measure the control characteristic, i.e. the collector current I_C as a function of the collector emitter voltage for a fixed base current I_B .

REQUIRED APPARATUS

Quantity	Description	Item Number
1	Plug-In Board for Components	1012902
1	Set of 10 Jumpers, P2W19	1012985
1	Resistor 1 k Ω , 2 W, P2W19	1012916
1	Resistor 47 k Ω , 0.5 W, P2W19	1012926
1	Potentiometer 220 Ω , 3 W, P4W50	1012934
1	Potentiometer 1 k Ω , 1 W, P4W50	1012936
1	NPN Transistor, BD 137, P4W50	1012974
1	AC/DC Power Supply 0 – 12 V, 3 A (230 V, 50/60 Hz)	1021091 or
	AC/DC Power Supply 0 – 12 V, 3 A (115 V, 50/60 Hz)	1021092
3	Analog Multimeter ESCOLA 30	1013526
1	Set of 15 Experiment Leads, 75 cm, 1 mm ²	1002840

BASIC PRINCIPLES

A bipolar transistor is an electronic component composed of three alternating p-doped and n-doped semiconductor layers called the base B, the collector C and the emitter E. The base is between the collector and emitter and is used to control the transistor. In principle a bipolar transistor resembles two diodes facing opposite directions and sharing an anode or cathode. Bipolarity arises from the fact that the two varieties of doping allow for both electrons and holes to contribute to the transport of charge.

Depending on the sequence of the layers, the transistor may either be termed npn or pnp (Fig.1). Bipolar transistors are operated as quadripoles in three basic circuits, distinguished by the arrangement of the terminals and called common emitter, common collector and common base. The names indicate which of the terminals is common to both the input and the output. Only npn transistors are considered in the following treatment.

There are four operating modes for an npn transistor, depending on whether the base-emitter or base-collector junctions are aligned in a conducting or forward-bias direction ($U_{BE}, U_{BC} > 0$) or a non-conducting or reverse bias ($U_{BE}, U_{BC} < 0$) direction (see Table 1). In forward-bias mode, electrons from the emitter migrate into the base across the transistor's forward-biased base-emitter junction ($U_{BE} > 0$), while holes from the base move into the emitter. Since the emitter has much

higher doping than the base, more electrons will migrate than holes, which minimizes recombination between the two. Because the width of the base is shorter than the diffusion length of the electrons, which count as minority carriers within the base itself, the electrons diffuse through the base into the depletion layer between the base and the collector before drifting further towards the collector itself. This is because the depletion layer only forms a barrier for majority carriers. This results in a transfer current I_T from the emitter into the collector, which is the major contributor to the collector current I_C in forward-bias mode. The transistor can therefore be regarded as a voltage controlled current source whereby the I_C at the output can be controlled by the voltage U_{BE} at the input. Electrons which recombine in the base emerge from there in a base current I_B which guarantees a constant transfer current I_T , thereby ensuring that the transistor remains stable. A small input current I_B can therefore control a much greater output current I_C ($I_C \approx I_T$), which gives rise to current amplification. The response of a bipolar transistor is described by four characteristics: The input characteristic, the control or base characteristic, the output characteristic and the feedback characteristic (see Table 2). This experiment involves measuring, by way of example, input, control and output characteristics for an npn transistor and plotting them as a graph.

Tab. 1: Four operating modes of an npn transistor

U_{BE}	U_{BC}	Operating mode
> 0	< 0	Normal mode
> 0	> 0	Saturation
< 0	> 0	Inverse mode
< 0	< 0	Off state

Tab. 2: Four characteristics of an npn transistor in normal mode

Name	Dependency	Parameter
Input characteristic	$I_B(U_{BE})$	
Control characteristic	$I_C(I_B)$	$U_{CE} = \text{const.}$
Output characteristic	$I_C(U_{CE})$	$I_B = \text{const.}$
Feedback characteristic	$U_{BE}(U_{CE})$	$I_B = \text{const.}$

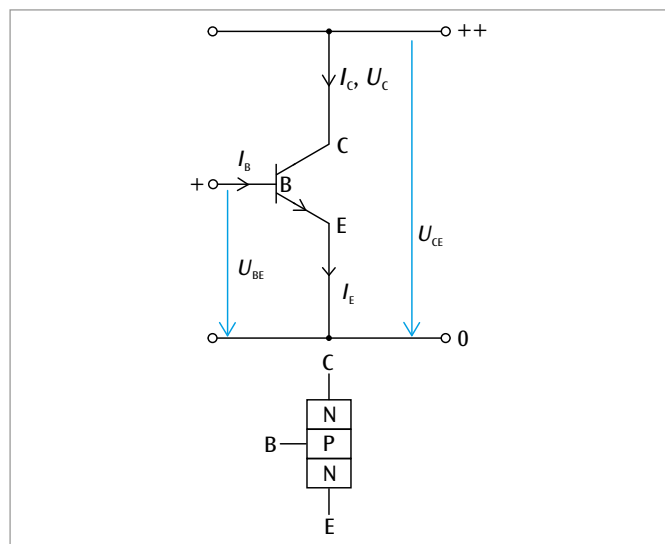


Fig. 1: Design of an npn transistor in principle, including accompanying circuit symbol plus indications of voltage and current

EVALUATION

The threshold voltage U_{Th} can be found from the input characteristic and the gain can be found from the control characteristic

$$B = \frac{\Delta I_C}{\Delta I_B}$$

The power dissipation can be found from the output characteristic $P = U_{CE} \cdot I_C$.

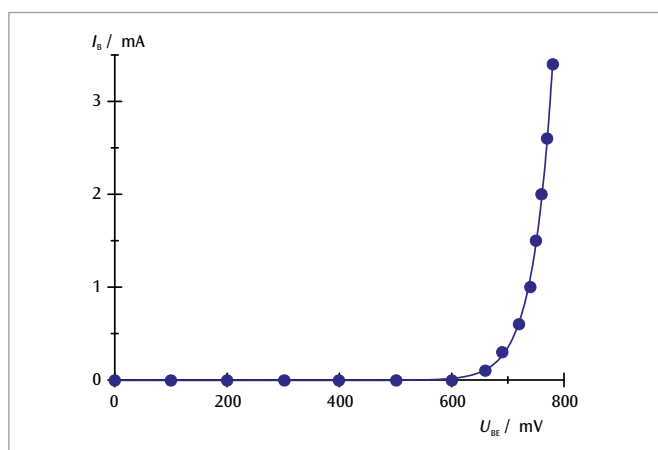


Fig. 2: Input characteristic

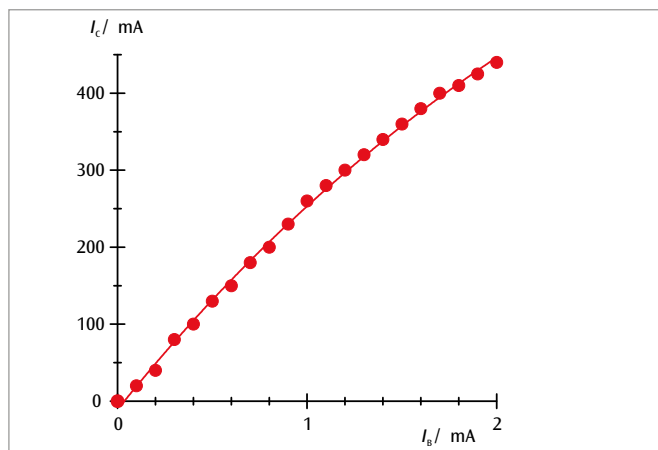


Fig. 3: Control characteristic for $U_{CE} = 5.2 \text{ V}$

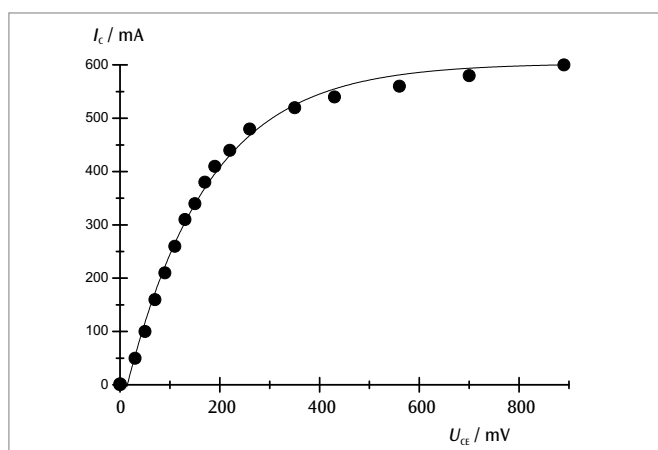
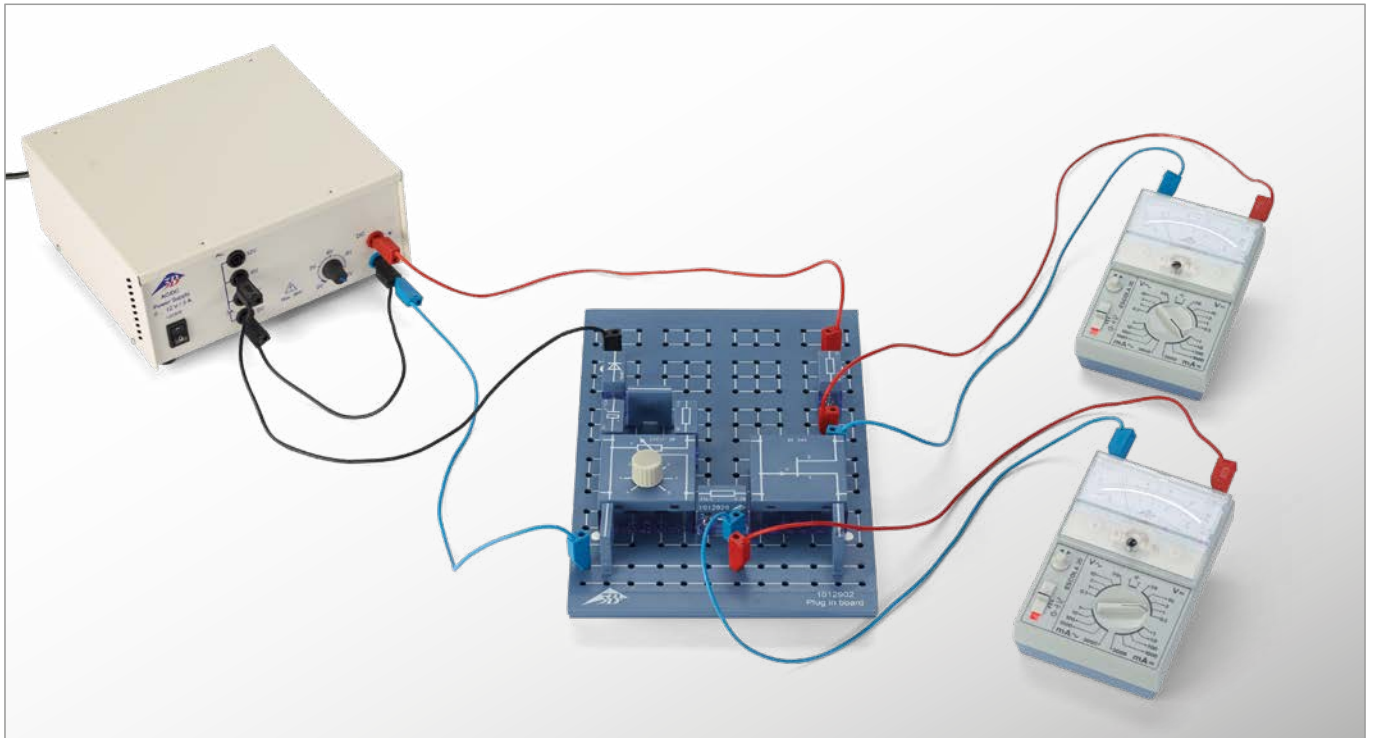


Fig. 4: Output characteristic for $I_B = 4.2 \text{ mA}$

UE3080300 | FIELD EFFECT TRANSISTORS



EXPERIMENT PROCEDURE

- Measure the drain voltage as a function of the drain current for various voltages at the gate.

OBJECTIVE

Measure the characteristics of a field effect transistor

SUMMARY

A field effect transistor (FET) is a semiconductor component in which electric current passes through a channel and is controlled by an electric field acting perpendicular to the channel. FETs have three contacts, called source, drain and gate due to their respective functions. If a voltage is applied between the source and the drain, then a drain current flows between the two. For small voltages between the drain and source, a FET acts like a simple ohmic resistor with a correspondingly linear characteristic. As the source-drain voltage increases, the channel becomes restricted and eventually is cut-off entirely. The characteristic then enters an area of saturation. When the gate voltage is non-zero, the saturation value of the drain current decreases.

REQUIRED APPARATUS

Quantity	Description	Item Number
1	Plug-In Board for Components	1012902
1	Set of 10 Jumpers, P2W19	1012985
1	Resistor 1 k Ω , 2 W, P2W19	1012916
1	Resistor 470 Ω , 2 W, P2W19	1012914
1	Resistor 47 k Ω , 0.5 W, P2W19	1012926
1	Capacitor 470 μ F, 16 V, P2W19	1012960
1	FET Transistor, BF 244, P4W50	1012978
1	Silicon Diode, 1N 4007, P2W19	1012964
1	Potentiometer 220 Ω , 3 W, P4W50	1012934
1	AC/DC Power Supply 0 – 12 V, 3 A (230 V, 50/60 Hz)	1021091 or
	AC/DC Power Supply 0 – 12 V, 3 A (115 V, 50/60 Hz)	1021092
2	Analog Multimeter ESCOLA 30	1013526
1	Set of 15 Experiment Leads, 75 cm, 1 mm ²	1002840

BASIC PRINCIPLES

A field effect transistor (FET) is a semiconductor component in which electric current passes through a channel and is controlled by an electric field acting perpendicular to the channel.

FETs have three contacts, called source (S), drain (D) and gate (G) due to their respective functions. The channel comprises a conductive link between the source and the drain. If a voltage U_{DS} is applied between source and drain, a drain current I_D flows in the channel. The current is carried by carriers of only one polarity (unipolar transistors), i.e. electrons for an n-doped semiconductor channel and holes in a p-doped channel. The cross-section or the conductivity of the channel is controlled by the electric field perpendicular to the channel. To create this field, a gate voltage U_{GS} is applied between the source and gate. The gate electrode is isolated from the channel by means of a reverse-biased pn junction or by an extra insulating layer (IGFET, MISFET, MOSFET). For insulated gate FETs the cross section of the channel is controlled by the expansion of the space-charge region of the junction, which is itself controlled by the perpendicular field. In order to ensure that the pn junction is always reverse-biased, i.e. specifically to make sure that there is no current at the gate, the gate voltage U_{GS} and the drain-source voltage U_{DS} must meet the following condition for an n-channel FET

$$(1a) \quad U_{GS} \leq 0, U_{DS} \geq 0$$

and the following for a p-channel FET

$$(1b) \quad U_{GS} \geq 0, U_{DS} \geq 0$$

If the absolute value of the drain-source voltage $|U_{DS}|$ is small, the FET acts like an ohmic resistor with a correspondingly linear characteristic. As $|U_{DS}|$ increases, the channel is restricted in size because the reverse-bias voltage between the gate and the channel increases in the direction of the drain. The space-charge region near the drain is wider than that near the source, meaning that the channel is narrower near the drain than it is near the source. At a specific voltage, where $U_{DS} = U_p$, the width of the channel becomes zero and the drain current no longer increases even though the drain-source voltage is increased. The characteristic passes out of its ohmic region into a region of saturation.

The extent of the space-charge region and therefore the size of the channel can be controlled by means of the gate voltage. As long as the gate voltage is non-zero, the channel can undergo additional constriction, making the drain-source current smaller and, in particular, the saturation current lower. The channel remains blocked irrespective of the drain-source voltage U_{DS} when $|U_{GS}| \geq |U_p|$.

The experiment involves measuring drain current I_D as a function of drain-source voltage U_{DS} for various gate voltages U_{GS} .

EVALUATION

The measurements are plotted on a graph of I_D against U_{DS} for various values of the gate voltage U_{GS} (Fig. 1). This should verify the shape of the characteristic showing how the drain current is controlled by the drain-source voltage and gate voltage.

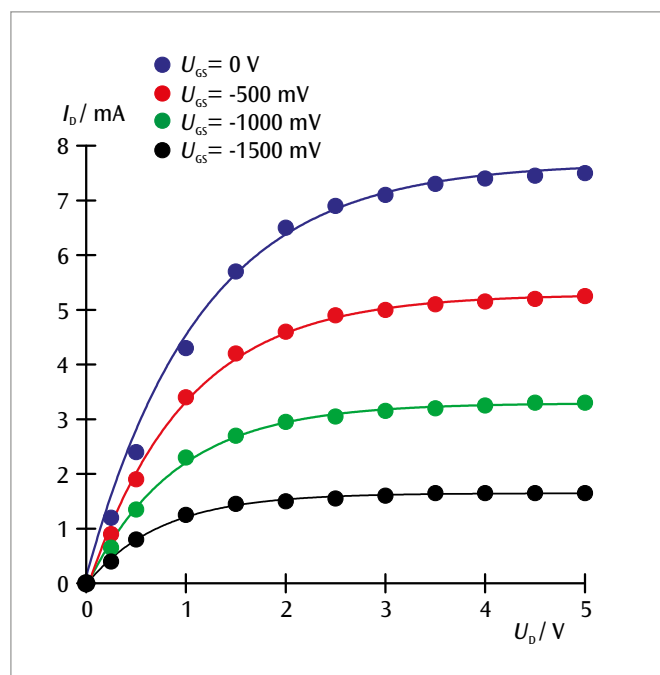
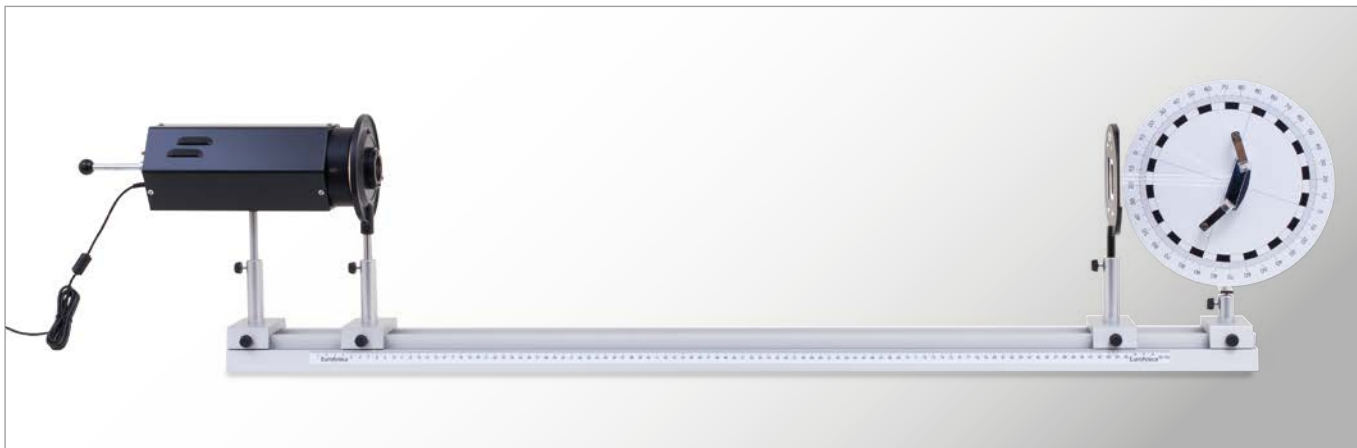


Fig. 1: Characteristic curve for FET with gate voltages 0 V (blue), -0.5 V (red), -1 V (green) and -1.5 V (black)

UE4010000 | REFLECTION IN A MIRROR



EXPERIMENT PROCEDURE

- Demonstrate the law of reflection using a plane mirror.
- Determine the focal length of a concave mirror and prove the law of reflection.
- Determine the virtual focal length of a convex mirror.

OBJECTIVE

Investigate reflection from a plane mirror and a curved mirror

SUMMARY

Light rays are reflected by a mirror in such a way that the angle of incidence is equal to the angle of reflection. This law of reflection applies not only to plane mirrors but also to curved ones. Only plane mirrors, though, reflect parallel incident rays in such a way that they remain parallel upon reflection. This is because the angle of incidence of all these parallel rays will be the same. For curved mirrors, concave and convex, parallel rays do not remain parallel after reflection. Instead, they are focussed towards a focal point.

REQUIRED APPARATUS

Quantity	Description	Item Number
1	Optical Bench U, 1200 mm	1003039
3	Optical Rider U, 75 mm	1003041
1	Optical Rider U, 35 mm	1003042
1	Optical Lamp with LED	1020630
1	Iris on Stem	1003017
1	Object Holder on Stem	1000855
1	Optical Disc with Accessories	1003036
1	Set of 5 Slit and Hole Diaphragms	1000607

BASIC PRINCIPLES

Light rays are reflected by a mirror in such a way that the angle of incidence is equal to the angle of reflection. This law of reflection applies not only to plane mirrors but also to curved ones. Only plane mirrors, though, reflect parallel incident rays in such a way that they remain parallel upon reflection. This is because the angle of incidence of all these parallel rays will be the same.

If parallel light rays strike a plane mirror at angle α , the law of reflection indicates that they should be reflected to an angle β :

$$(1) \quad \alpha = \beta$$

α : Angle of incidence, β : Angle of reflection

In this experiment the angle of reflection will be measured directly for three parallel beams and it will be determined how this angle is related to the angle of incidence.

If a light ray incident parallel to the optical axis hits a concave mirror, according to the law of reflection it is reflected symmetrically to the point of incidence and will then cross the optical axis at the following distance from the mirror:

$$(2) \quad f_{\alpha} = r - \overline{MF} = r \cdot \left(1 - \frac{1}{2 \cdot \cos \alpha} \right)$$

(See Fig. 1 for path of rays on left-hand side). For rays close to the optical axis itself, $\cos \alpha$ is close to 1, therefore

$$(3) \quad f = \frac{r}{2}$$

This is not dependent on the distance from the optical axis, which means that all parallel rays near to the optical axis will, after reflection, converge at the same point (the focal point) on the optical axis a distance f (the focal length) from the surface of the concave mirror. If parallel rays strike the mirror at an angle α to the optical axis, they will be reflected through a common point away from the optical axis. The geometric relationships for a concave mirror are similar to those for a convex mirror except that the rays diverge rather than converge after reflection. The diverging rays, however, do appear to have a point of convergence at a virtual focal point f' behind the mirror (see Fig. 1 for path of rays on right-hand side). The virtual focal length f' for a convex mirror is given by the following:

$$(4) \quad f' = -\frac{r}{2}$$

In the experiment the focal length of the concave mirror and the virtual focal length of the convex mirror will be determined from the paths of the rays on an optical disc. The validity of the law of reflection will be checked for the ray in the center.

EVALUATION

Parallel light rays incident upon a plane mirror are reflected back as parallel rays. The law of reflection applies to this process.

When a beam of parallel rays is reflected by a concave mirror, the angle of incidence is different for each of the rays and all the rays are then focussed towards a focal point. Similarly, when a beam of parallel rays is reflected by a convex mirror, the rays converge at a virtual focal point behind the mirror.

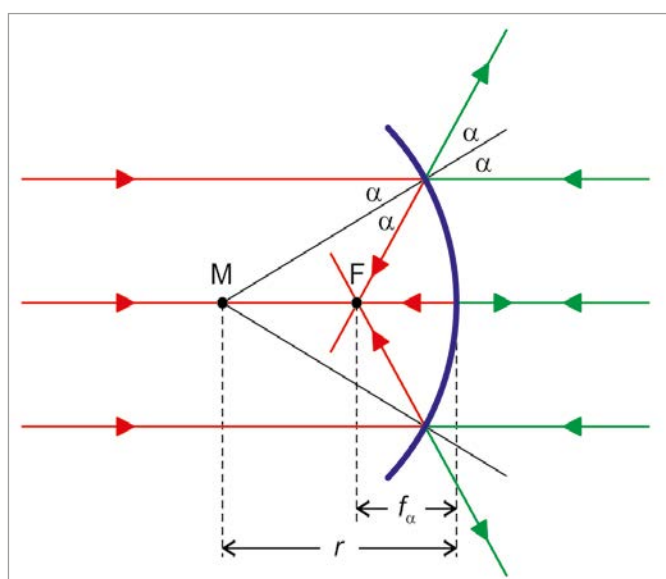


Fig. 1: Schematic for determining focal length of a concave mirror and a convex mirror

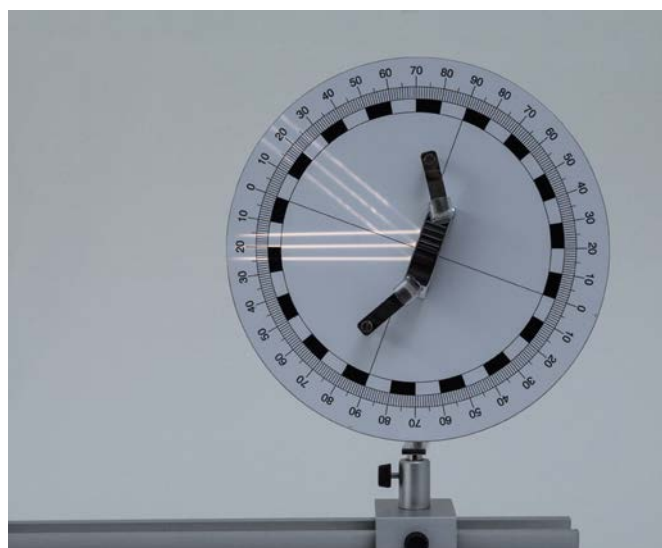


Fig. 2: Reflection of three parallel rays by a plane mirror



Fig. 3: Reflection of three parallel rays by a concave mirror

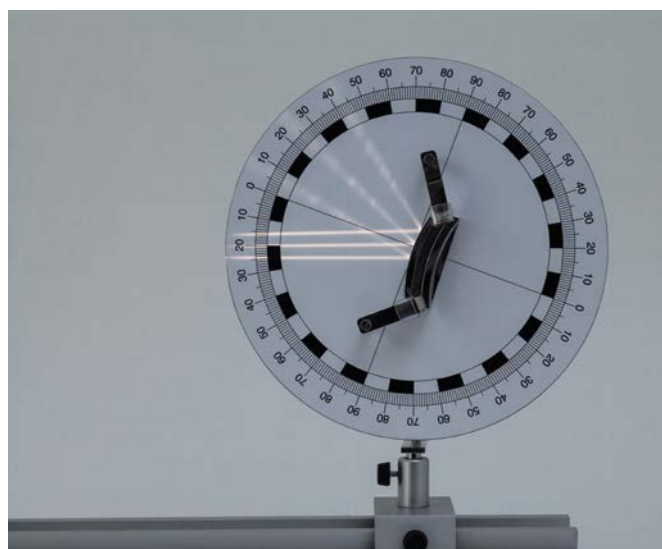
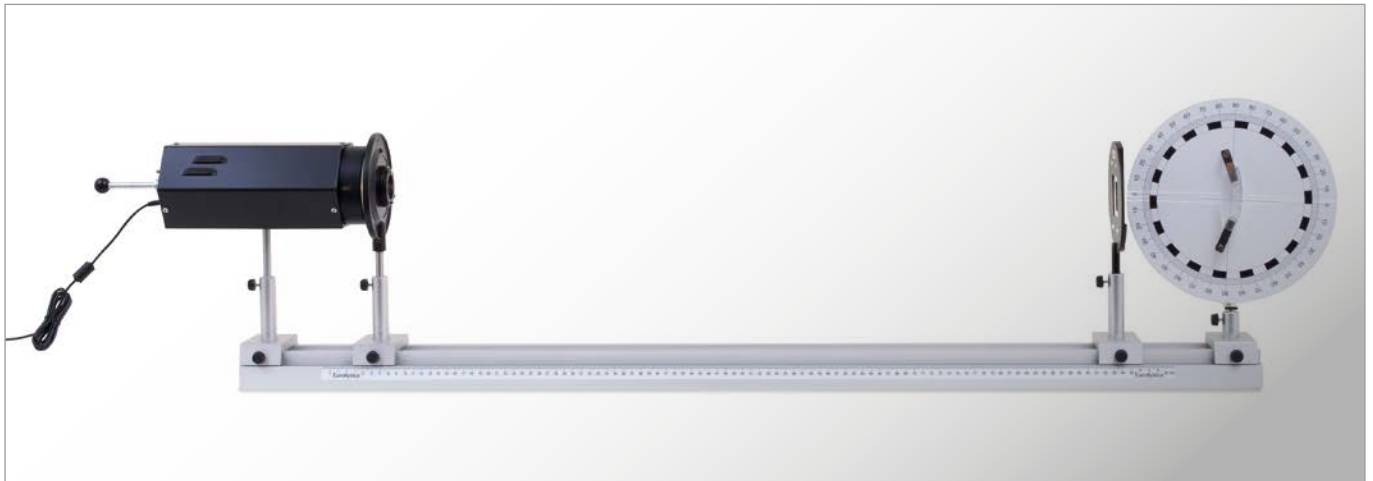


Fig. 4: Reflection of three parallel rays by a convex mirror

UE4010020 | REFRACTION OF LIGHT



› EXPERIMENT PROCEDURE

- Verify Snell's law of refraction.
- Determine the refractive index and the critical angle for total internal reflection for transparent acrylic plastic.
- Observe and measure how a beam deviates along a different parallel path when refracted by a rectangular block.
- Observe the path of light inside a prism which merely deflects a beam and in one which reverses it.
- Observe the path of light inside a convex lens and in a concave lens and determine their focal lengths.

OBJECTIVE

Investigate refraction of light by various optical components

SUMMARY

Light propagates at different speeds in different media. If a medium has low optical depth, the speed of propagation is higher than it would be in a medium of greater optical depth. A change in direction therefore takes place when a beam of light passes through a boundary between two media at any non-zero angle of incidence. The degree of deflection is dependent on the ratio of the refractive indices of these two media, as described by Snell's law of refraction. This refractive behavior will now be investigated using optical components made of transparent acrylic (perspex).

REQUIRED APPARATUS

Quantity	Description	Item Number
1	Optical Bench U, 1200 mm	1003039
3	Optical Rider U, 75 mm	1003041
1	Optical Rider U, 35 mm	1003042
1	Optical Lamp with LED	1020630
1	Iris on Stem	1003017
1	Object Holder on Stem	1000855
1	Optical Disc with Accessories	1003036
1	Set of 5 Slit and Hole Diaphragms	1000607

BASIC PRINCIPLES

Light propagates at different speeds c in different media. If a medium has low optical depth, the speed of propagation is higher than it would be in a medium of greater optical depth.

The ratio of the speed of light in a vacuum c_0 to the speed within the medium is called the absolute refractive index n . If the speed of light in the medium is c , then the following is true:

$$(1) \quad c = \frac{c_0}{n}$$

When a beam of light passes from one medium of refractive index n_1 to another one of refractive index n_2 , the beam changes direction at the boundary. This is described by Snell's law of refraction:

$$(2) \quad \frac{\sin \alpha}{\sin \beta} = \frac{n_1}{n_2} = \frac{c_2}{c_1}$$

α, n_1, c_1 : angle of incidence, refractive index and speed of propagation in medium 1

β, n_2, c_2 : angle of refraction, refractive index and speed of propagation in medium 2

A beam of light passing from a medium of relatively low optical depth into one of higher optical depth will be refracted towards a normal to the boundary surface and a beam passing from a medium of higher optical depth into one of lower optical depth would be refracted away from the normal. In the latter case, there is also a critical angle α_T , at which the beam is actually refracted along the boundary surface. At greater angles of incidence than this, refraction does not take place at all and the beam is totally reflected.

This refractive behavior is investigated in this experiment using a semi-circular body, a rectangular block with parallel sides, a prism, a converging lens and a dispersing lens, all made of transparent acrylic. The semicircular body is particularly well suited to demonstrating the law of refraction since no refraction takes place at the semicircular perimeter if the beam strikes the flat surface precisely at the center of the circle. The flat side forms the boundary between media and will be aligned at various angles to the optical axis (see Fig. 1).

As a beam of light is refracted on entering and on exiting a rectangular block, it is deflected along a line parallel to its original direction but a distance d away from that line. The deflected distance is dependent on the angle of incidence α . The following applies (see Fig. 1):

$$(3) \quad d = h \cdot \frac{\sin(\alpha - \beta)}{\cos \beta}, \quad h: \text{thickness of block}$$

A 90° prism will act in such a way as to deflect a beam of light if light beams strike it perpendicular to one of the short sides. The beam is then reflected at the hypotenuse and exits the prism having been deflected by 90°. If, however the beam strikes perpendicular to the hypotenuse, it is reflected by both the other sides and emerges from the prism travelling parallel to its original direction but going the opposite way. (see Fig. 1).

A convex lens causes parallel rays of light to be bunched together or converged by refraction, whereas a concave lens cause such rays to diverge (see Fig. 1). The rays then meet on the other side of the lens at a focal point F or can be traced back to what appears to be a virtual focal point F' in front of the lens.

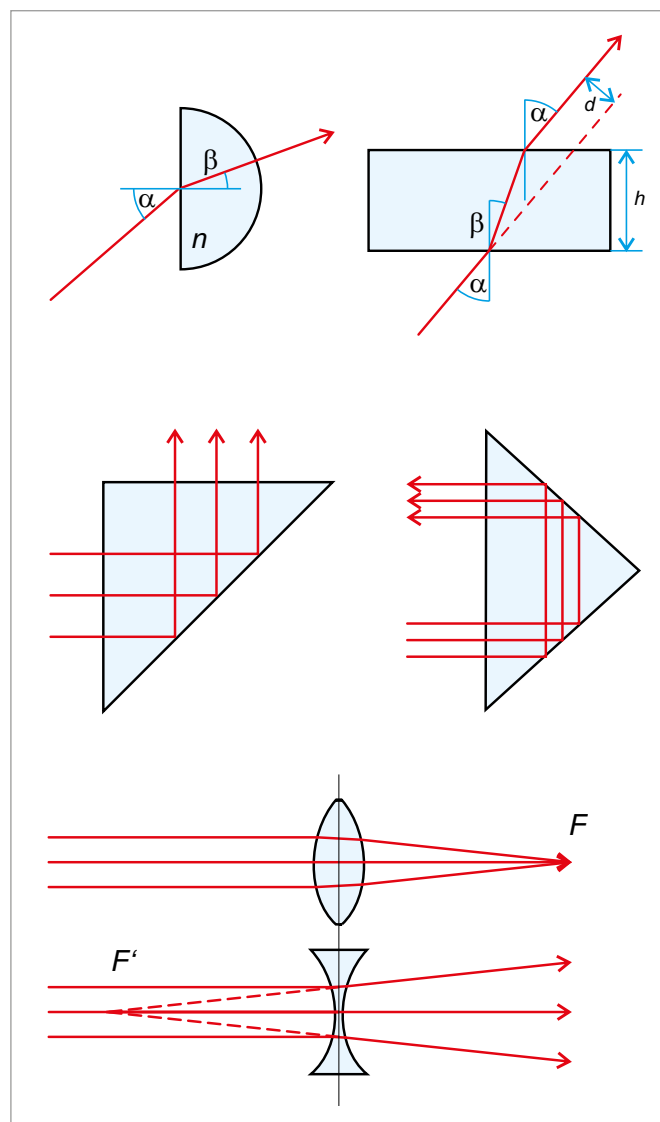


Fig. 1: Refraction by a semi-circular body, path of light through a rectangular block, deflecting and reversing prisms, path of light through a rectangular convex lens and through a concave lens

EVALUATION

If the original medium is air, for the purposes of this experiment it will be sufficiently accurate to assume that its refractive index $n_1 = 1$. If the angle of incidence is equal to the critical angle for total internal reflection α_T , the angle of refraction $\beta = 90^\circ$. From equation (2) it therefore follows that if n is the refractive index for transparent acrylic, then:

$$\sin \alpha_T = \frac{1}{n}$$

For refraction by a rectangular block, equations (2) and (3) imply the following:

$$d = h \cdot (\sin \alpha \cdot \cos \alpha \cdot \tan \beta) = h \cdot \sin \alpha \cdot \left(1 - \frac{\cos \alpha}{\sqrt{n^2 - \sin^2 \alpha}} \right)$$

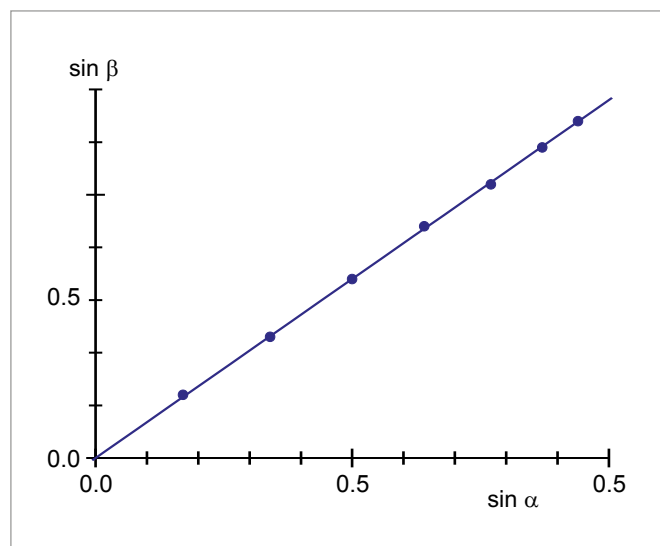
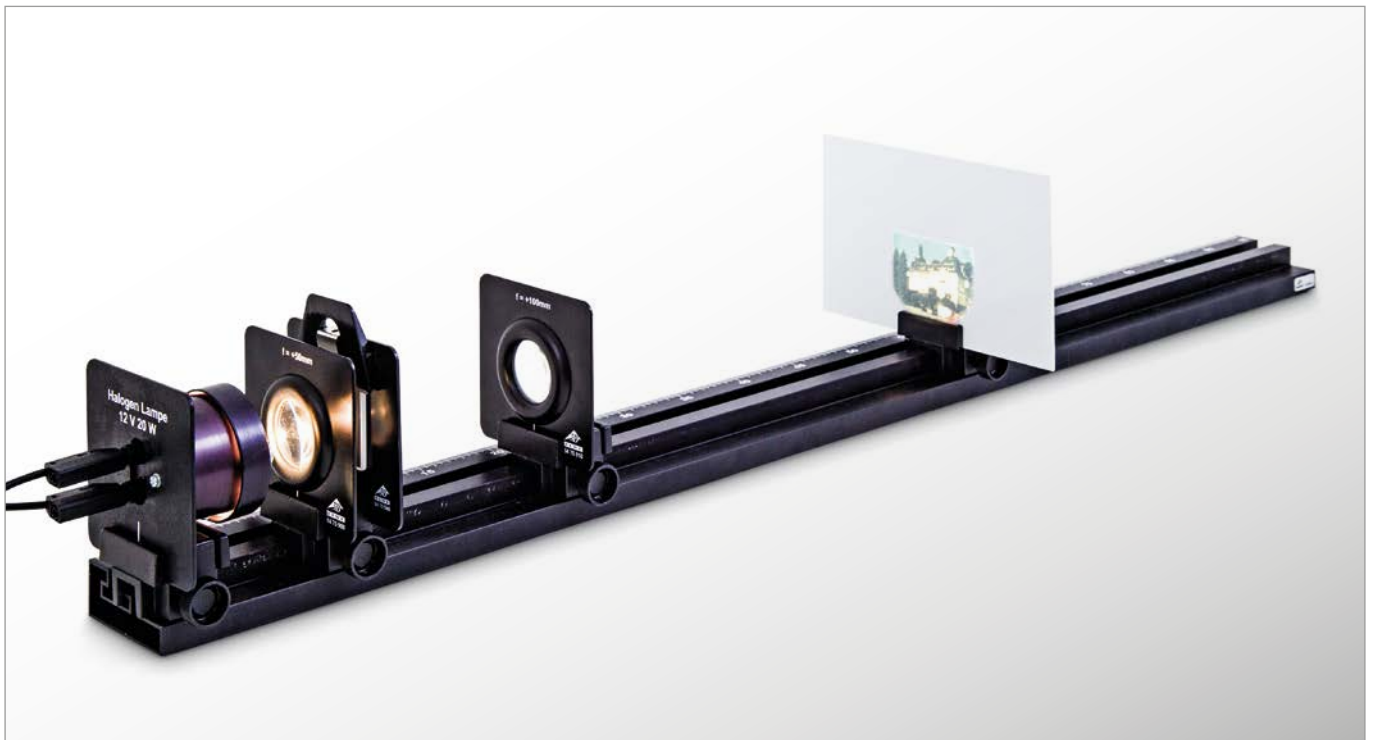


Fig. 2: Diagram for determination of refractive index n

UE4010100 | LENS EQUATION



EXPERIMENT PROCEDURE

- Determine the two positions of a thin lens where a sharp image is formed.
- Determine the focal length of a thin lens.

OBJECTIVE

Determine the focal length of a lens using the Bessel method

SUMMARY

On an optical bench it is possible to set up a light source, a lens, a screen and an object to be imaged in such a way that a well focussed image appears on the screen. Using the geometric relationships between the ray paths for a thin lens, it is possible to determine its focal length.

REQUIRED APPARATUS

Quantity	Description	Item Number
1	Optical Bench K, 1000 mm	1009696
4	Optical Rider K	1000862
1	Optical Lamp K	1000863
1	Transformer 12 V, 25 VA (230 V, 50/60 Hz)	1000866 or
	Transformer 12 V, 25 VA (115 V, 50/60 Hz)	1000865
1	Convex Lens K, $f = 50$ mm	1000869
1	Convex Lens K, $f = 100$ mm	1010300
1	Clamp K	1008518
1	Set of 4 Image Objects	1000886
1	Projection Screen K, White	1000879

BASIC PRINCIPLES

The focal length f of a lens refers to the distance between the main plane of the lens and its focal point, see Fig.1. This can be determined using the Bessel method (devised by *Friedrich Wilhelm Bessel*). This involves measuring the various separations between the optical components on the optical bench.

From Fig.1 and Fig. 2 it can be seen that the following relationship must apply for a thin lens:

$$(1) \quad a = b + g$$

a : distance between object G and image B

b : distance between lens and image B

g : distance between object G and lens

By plugging these values into the lens equation

$$(2) \quad \frac{1}{f} = \frac{1}{b} + \frac{1}{g}$$

f : focal length of lens

the following is obtained:

$$(3) \quad \frac{1}{f} = \frac{a}{a \cdot g - g^2}$$

This corresponds to a quadratic equation with the following pair of solutions:

$$(4) \quad g_{1,2} = \frac{a}{2} \pm \sqrt{\frac{a^2}{4} - a \cdot f}$$

A sharp image is obtained for each of the object distances g_1 and g_2 . The difference e between them allows the focal length to be determined:

$$(5) \quad e = g_1 - g_2 = \sqrt{a^2 - 4af}$$

The difference e is the difference between the two lens positions P_1 and P_2 , which result in a focussed image.

EVALUATION

A formula for the focal length of a thin lens can be derived using the Bessel method from equation (4)

$$f = \frac{a^2 - e^2}{4a}$$

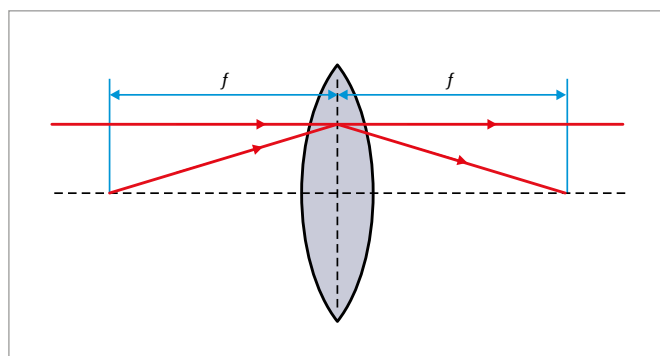


Fig. 1: Schematic showing the definition of focal length for a thin lens

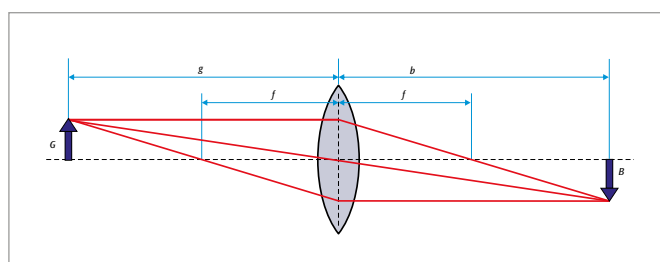


Fig.2: Schematic of ray paths through a lens

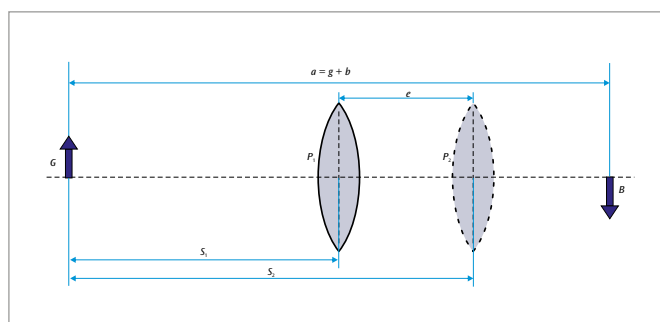
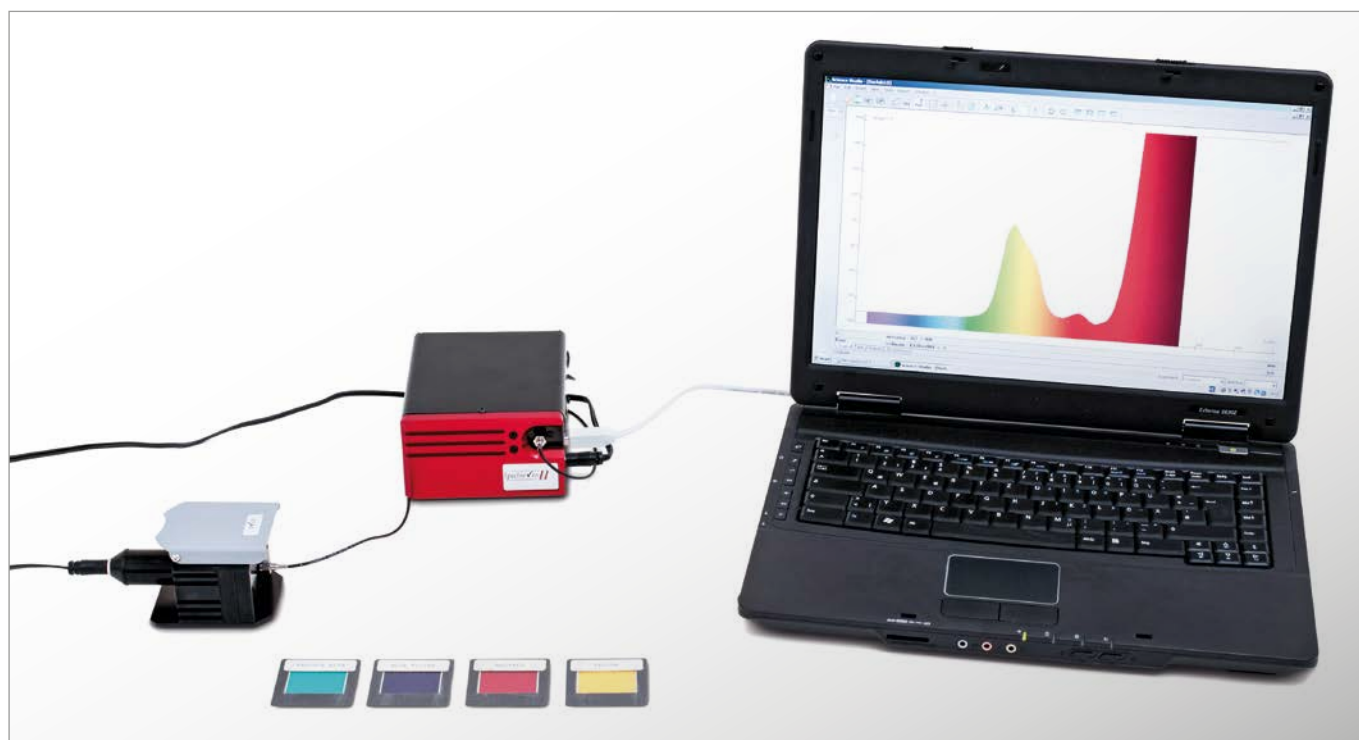


Fig.3: Schematic showing the two lens positions which result in a well focussed image on the screen

UE4020400 | TRANSMISSION SPECTRA



> EXPERIMENT PROCEDURE

- Measure and compare the transmission spectra of solid bodies.
- Measure and compare the transmission spectra of liquids.

OBJECTIVE

Record and interpret transmission spectra of transparent bodies

SUMMARY

A digital spectrophotometer is used to measure transmission spectra. In this instrument the transmitted light collected by an optical fibre is separated into its spectral components by a reflection grating using the Czerny-Turner principle and is projected as an image onto a CCD detector via two mirrors. The transmission spectrum is generated by automatic normalisation applied to the previously recorded spectrum of the light falling on the detector.

REQUIRED APPARATUS

Quantity	Description	Item Number
1	1 Digital-Spectrometer LD with Absorption Module	1019196
1	Set of 7 Color Filters	1003084
1	Macro Cuvettes, 4 ml	1018106
Additionally recommended		
	Chlorophyll	
	Potassium Permanganate	

BASIC PRINCIPLES

The observed color of an object illuminated with white light depends on its reflecting properties. The perceived color of light that has passed through an object depends on its light transmitting properties. For example, the perceived color may be red if the object is transparent to red light while other color components of the light are attenuated on passing through the object. In such a case spectral transmission is at a maximum for red light.

The unaided human eye cannot distinguish between a color sensation caused by spectrally pure light and the same sensation caused by the addition of neighboring colors of the spectrum. Therefore, it is not possible to reach conclusions about the transmission spectrum solely from the observed color. To determine it unambiguously is only possible with the help of a spectrometer.

In this experiment, transmission spectra are recorded using a digital spectrophotometer. In this instrument the transmitted light collected by an optical fibre is separated into its spectral components by a reflection grating using the Czerny-Turner principle and is projected as an image onto a CCD detector via two mirrors. The transmission spectrum is generated by automatic normalisation applied to the previously recorded spectrum of the light falling on the detector.

EVALUATION

Spectral absorptivity $A(\lambda)$ can be calculated directly from the spectral transmission coefficient $T(\lambda)$ of a body if the effect of reflection at the surface is neglected. The relationship is:

$$A(\lambda) = 1 - T(\lambda)$$

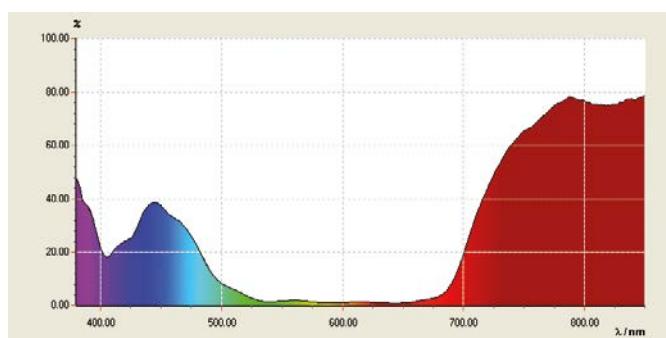


Fig. 1: Transmission spectra of a blue color film

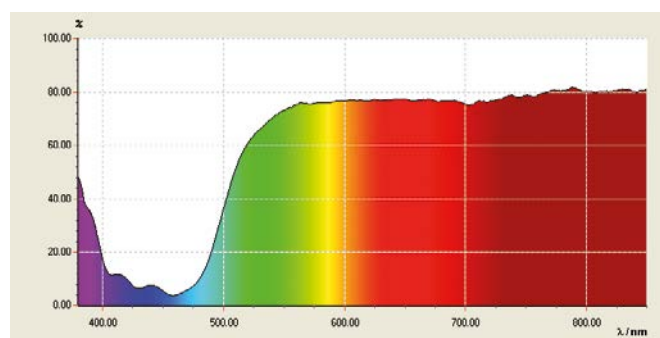


Fig. 2: Transmission spectra of a yellow color film

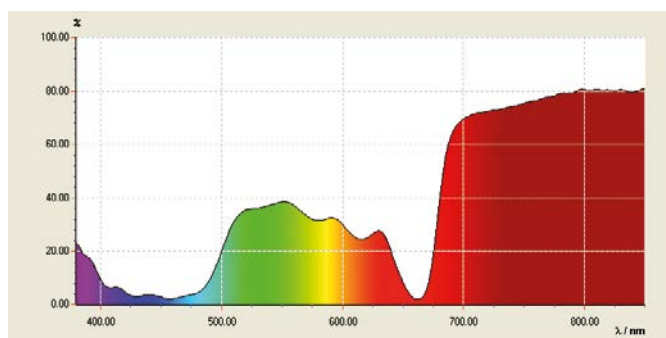


Fig. 3: Transmission spectrum of a chlorophyll solution

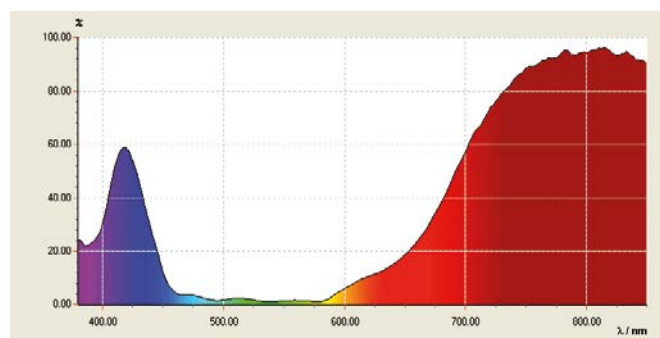


Fig. 4: Transmission spectrum of a potassium permanganate solution

UE4030100 | DIFFRACTION BY A SINGLE SLIT



EXPERIMENT PROCEDURE

- Investigate diffraction by single slits of various different widths.
- Investigate diffraction by a single slit for light of differing wavelengths.
- Investigate diffraction by a single slit and by an opaque object of the same size (Babinet's principle).

OBJECTIVE

Demonstrate the wave nature of light and determine the wavelength

SUMMARY

Diffraction of light by a single slit can be described as the superposition of coherent wavelets which, according to Huygens' principle, spread out from the illuminated slit in all directions. Depending on the angle along which they propagate, the wavelets cause either constructive or destructive interference. If the width of the slit and the distance to the screen are known, then the wavelength can be calculated based on the distance between adjacent dark bands of the interference pattern.

REQUIRED APPARATUS

Quantity	Description	Item Number
1	Laser Diode, Red	1003201 or
	Laser Diode, Red 115V	1022208
1	Laser Module, Green	1003202
1	Optical Bench K, 1000 mm	1009696
2	Optical Rider K	1000862
1	Adjustable Slit K	1008519
1	Holder K for Diode Laser	1000868

Additionally required

Wire

BASIC PRINCIPLES

Diffraction of light by a single slit can be described as the superposition of coherent wavelets which, according to Huygens' principle, spread out from the illuminated slit in all directions. This superposition leads to either constructive or destructive interference depending on the angle. Beyond the slit a system of light and dark bands can be observed on a screen.

Where the wavelets cancel – i.e. where the bands are darkest – it can be seen that for every wavelet from one half of the slit there is another wavelet from the second half which interacts with it in such a way that the combined amplitude is reduced to a minimum. This happens when the path difference Δs_n between the beam through the middle of the slit and a ray from the edge is precisely an integer multiple n of half the wavelength λ :

$$(1) \quad \Delta s_n = n \cdot \frac{\lambda}{2} = \frac{b}{2} \cdot \sin \alpha_n$$

$n = 0, \pm 1, \pm 2, \dots$: Order of diffraction
 b : Width of slit,
 α_n : Angle of propagation

The regions of maximum darkness are symmetrical about the primary ray (see Fig. 1). Their distance from the primary ray, as measured in the plane of observation is as follows:

$$(2) \quad x_n = L \cdot \tan \alpha_n$$

L : Distance between slit and plane of observation

For a small angle, the following is therefore true:

$$(3) \quad \alpha_n = x_n = \frac{\lambda \cdot L}{b} \cdot n = \Delta \cdot n \quad \text{where } \Delta = \frac{\lambda \cdot L}{b}$$

Δ : Relative distance between minima

A slit and an opaque obstruction of the same size and shape are considered complementary diffraction objects. According to Babinet's principle, the diffraction patterns of both objects, outside of the "unaffected" beam, are identical. The diffraction minima in both patterns are therefore in the same place.

In this experiment diffraction by single slits of various widths is investigated, along with diffraction of different wavelengths of light. Moreover, it will be shown that diffraction by a single slit and by an opaque object of the same width results in complementary diffraction patterns.

EVALUATION

The brightness is greatest in the direction of the primary ray. The value Δ can be determined as the gradient of the straight line graph when the distances x_n are plotted against n . Since Δ is obviously inversely proportional to the width of the slit b , the quotients Δ/L can be plotted in a graph against $1/b$ and the wavelength λ is then determined as the gradient of the graph of these measurements.

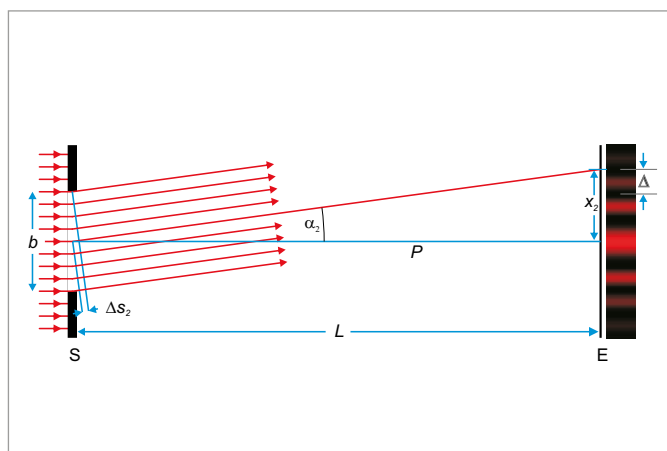


Fig. 1: Schematic diagram of diffraction of light by a single slit (S: Slit, b : Width of slit, E: Plane of observation, P : Primary beam, L : Distance of observation screen from slit, x_2 : Distance of second minimum from center, α_2 : Direction of observation for second minimum, Δs_2 : Path difference between ray through center and ray from edge).

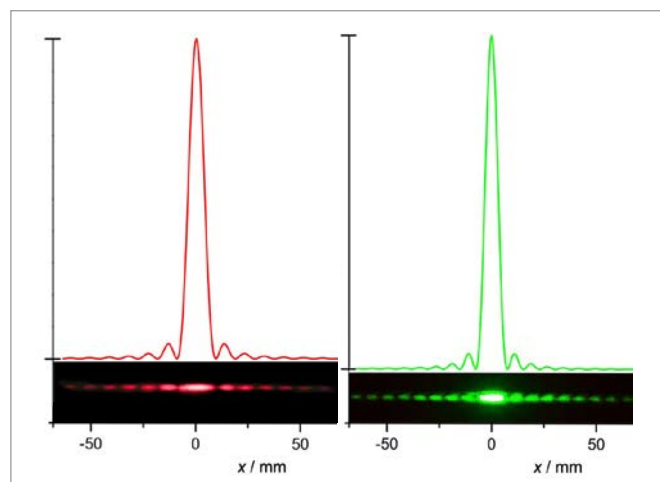


Fig. 2 Calculated and measured intensities for diffraction from a slit of width 0.3 mm with light of wavelength $\lambda = 650 \text{ nm}$ and $\lambda = 532 \text{ nm}$.

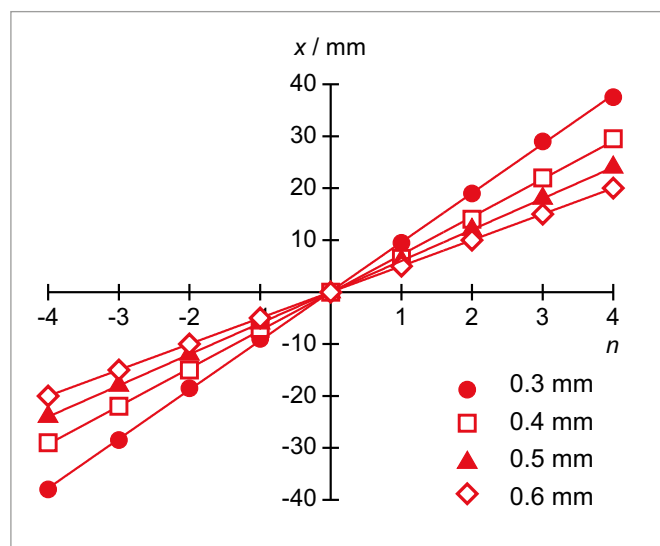


Fig. 3: Separations x_n as a function of diffraction order n for various widths of slit b where $\lambda = 650 \text{ nm}$.

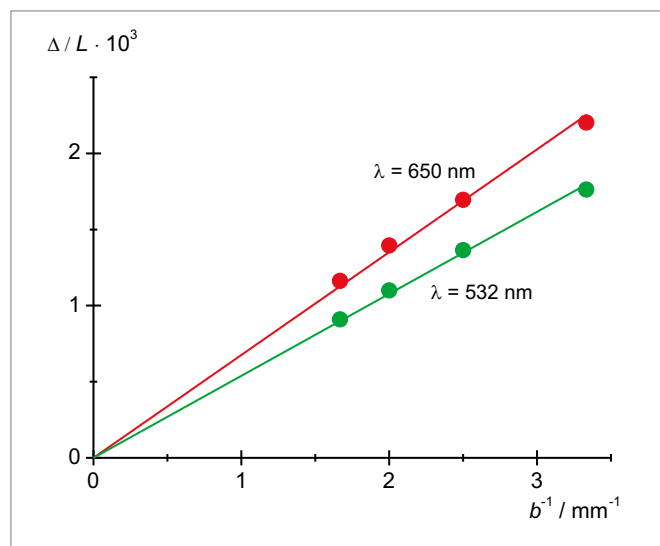


Fig. 4: Quotient of relative separation of minima Δ and distance L as a function of width of slit $1/b$.

UE4030200

DIFFRACTION BY MULTIPLE SLITS AND GRATINGS



EXPERIMENT PROCEDURE

- Investigate diffraction at a pair of slits with different distances between the slits.
- Investigate diffraction at a pair of slits with different slit widths.
- Investigate diffraction by multiple slit systems with different numbers of slits.
- Investigate diffraction by a line grating and a lattice grating.

OBJECTIVE

Demonstrate the wave nature of light and determine the wavelength

SUMMARY

The diffraction of light by multiple slits or a grating can be described by considering how the individual components of the coherent wave radiation are superimposed as they emerge from the various slits, which can each be regarded as a single point of illumination so that the waves superimpose according to the Huygens principle. The interference of the individual waves explains the pattern of bright and dark bands that is observed beyond the system of slits. If the separation between the slits and the distance to the observation screen is known, the wavelength of the light can be calculated from the distance between any two bright bands.

REQUIRED APPARATUS

Quantity	Description	Item Number
1	Laser Diode, Red 230 V	1003201 or
	Laser Diode, Red 115 V	1022208
1	Optical Bench K, 1000 mm	1009696
2	Optical Rider K	1000862
1	Clamp K	1008518
1	Holder K for Diode Laser	1000868
1	Diaphragm with 3 Double Slits of Different Widths	1000596
1	Diaphragm with 4 Double Slits of Different Spacings	1000597
1	Diaphragm with 4 Multiple Slits and Gratings	1000598
1	Diaphragm with 3 Ruled Gratings	1000599
1	Diaphragm with 2 Cross Gratings	1000601

BASIC PRINCIPLES

The diffraction of light by multiple slits or a grating can be described by considering the superimposition of individual components of the coherent wave radiation, which emerge from each point of illumination formed by the multiple slits, according to the Huygens principle. The superimposition leads to constructive or destructive interference in particular directions, and this explains the pattern of bright and dark bands that is observed beyond the system of slits.

In the space beyond a pair of slits, the light intensity at a particular angle of observation α_n is greatest when, for each individual wave component coming from the first slit, there exists an exactly similar wave component from the second slit, and the two interfere constructively. This

condition is fulfilled when the path difference Δs_n between two wave components emerging from the centers of the two slits is an integral multiple of the wavelength λ of the light (see Fig. 1), thus:

$$(1) \quad \Delta s_n(\alpha_n) = n \cdot \lambda$$

$n = 0, \pm 1, \pm 2, \dots$ is called the diffraction order.

At large distances L from the pair of slits and for small angles of observation α_n , the relationship between the path difference Δs_n and the position coordinate x_n of the n th-order intensity maximum is:

$$(2) \quad \frac{\Delta s_n}{d} = \sin \alpha_n \approx \tan \alpha_n = \frac{x_n}{L}$$

d : Distance between the slits.

Thus the maxima are spaced at regular intervals with a separation a given by:

$$(3) \quad a = x_{n+1} - x_n = \frac{\lambda}{d} \cdot L$$

This relationship is also valid for diffraction at a multiple slit system consisting of N equidistant slits ($N > 2$). Equation (1) states the condition for constructive interference of the wave elements from all N slits. Therefore, equations (2) and (3) can also be applied to a multiple slit system.

The mathematical derivation of the positions of the intensity minima is more difficult. Whereas in the case of a pair of slits there is an intensity minimum exactly halfway between two intensity maxima, for the multiple slits system a minimum is observed between the n th and the $(n+1)$ th maxima when the wave components from the N slits interfere in such a way that the total intensity is zero. This occurs when the path difference between the wave components from the centers of the slits satisfies the condition:

$$(4) \quad \Delta s = n \cdot \lambda + m \frac{\lambda}{N}$$

$$n = 0, \pm 1, \pm 2, \dots, m = 1, \dots, N - 1$$

Therefore $N-1$ minima are visible and between them are $N-2$ "minor maxima" with intensities smaller than those of the principal maxima. As the number of slits N is progressively increased, the contribution of the minor maxima gradually disappears. Then the system is no longer described as a multiple slit system but as a line grating. Finally, a lattice grating can be regarded as an arrangement of two line gratings, one rotated at 90° relative to the other. The diffraction maxima now become points on a rectangular grid with a spacing interval given by Equation (3). The intensity (brightness) of the principal maxima is modulated according to the intensity distribution function for diffraction at a single slit. The greater the slit width b , the greater the concentration of intensity towards smaller values of the angle α . For an exact derivation it is necessary to sum the amplitudes of all the wave components, taking into account the path differences, to obtain the total amplitude A . At a point on the screen defined by x , the intensity is:

$$(5) \quad I = A^2 \propto \left(\frac{\sin\left(\frac{\pi \cdot b \cdot x}{\lambda \cdot L}\right)}{\frac{\pi \cdot b \cdot x}{\lambda \cdot L}} \right)^2 \cdot \left(\frac{\sin\left(N \cdot \frac{\pi \cdot d \cdot x}{\lambda \cdot L}\right)}{\sin\left(\frac{\pi \cdot d \cdot x}{\lambda \cdot L}\right)} \right)^2$$

EVALUATION

The wavelength λ of the diffracted light can be determined from the separation a between the principal maxima, and is given by:

$$\lambda = d \cdot \frac{a}{L}$$

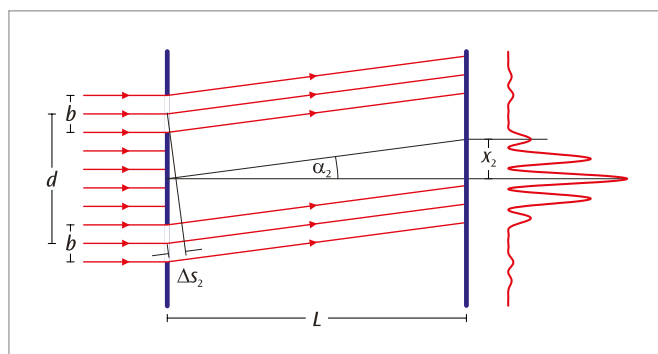


Fig. 1: Schematic diagram of the diffraction of light at a pair of slits

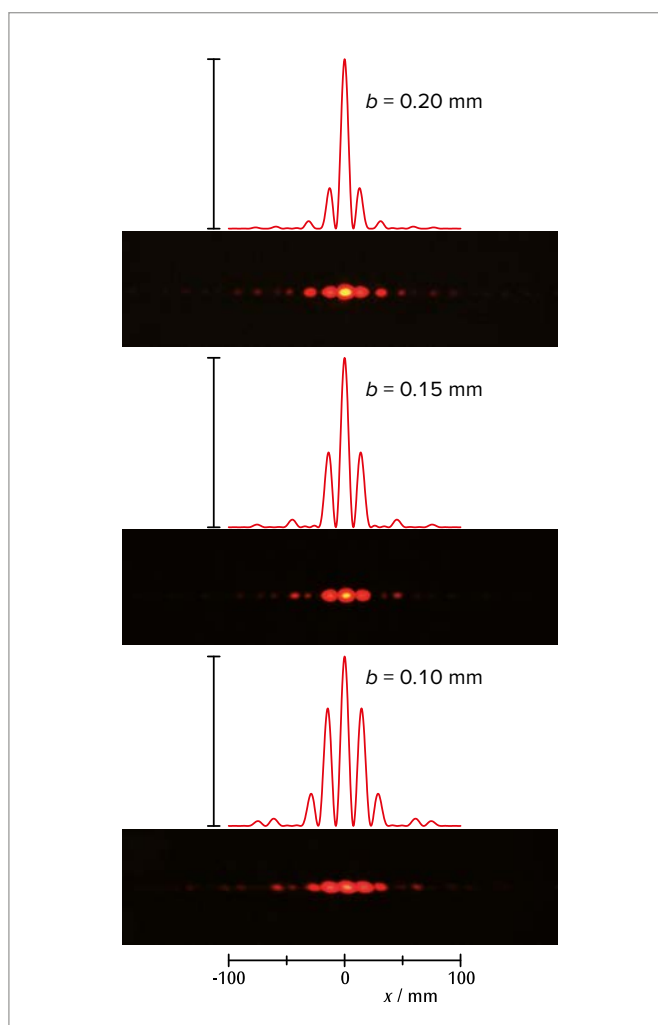


Fig. 2: Calculated and observed intensities for diffraction at a pair of slits with different distances between the slits

UE4030300 | FRESNEL BIPRISM



> EXPERIMENT PROCEDURE

- Use a Fresnel biprism to create two virtual coherent sources of light from a single point light source.
- Observation of the interference between the two split beams from the virtual light sources.
- Determine the wavelength of light from a He-Ne laser from the separation between interference bands.

OBJECTIVE

Generating interference between two beams using a Fresnel biprism

SUMMARY

Refraction of a divergent light beam by means of a biprism separates the beam into two parts which, since they are coherent, will interfere with one another. The wavelength of the light used in the experiment can be determined using the separation of the virtual light sources and the distance between adjacent interference bands.

REQUIRED APPARATUS

Quantity	Description	Item Number
1	Fresnel Biprism	1008652
1	Prism Table on Stem	1003019
1	He-Ne Laser	1003165
1	Achromatic Objective 10x / 0.25	1005408
1	Convex Lens on Stem $f = +200$ mm	1003025
3	Optical Rider D, 90/50	1002635
1	Optical Precision Bench D, 50 cm	1002630
1	Projection Screen	1000608
1	Barrel Foot, 1000 g	1002834
1	Pocket Measuring Tape, 2 m	1002603

BASIC PRINCIPLES

In one of his experiments on interference, *August Jean Fresnel* used a biprism to induce interference between two beams. He split a diverging beam of light into two parts by using the biprism to refract them. This resulted in two split beams which acted as if they were from two coherent sources and which therefore interfered with each other. By observing on a screen, he was able to see a series of peaks in the light intensity with a constant distance between them.

Whether a peak occurs in the intensity or not, depends on the difference Δ in the path travelled by each of the split beams. If the light source is a long distance L from the screen, the following is true to a good approximation:

$$(1) \quad \Delta = A \cdot \frac{x}{L}$$

Here, x refers to the coordinate of the point observed on the screen which is perpendicular to the axis of symmetry. A is the distance between the two virtual light sources, which is yet to be determined. Peaks in intensity occur at the precise points where the difference in the path travelled is a multiple of the wavelength λ :

$$(2) \quad \Delta_n = n \cdot \lambda, \text{ where } n = 0, 1, 2, \dots$$

A comparison between (1) and (2) shows that the peaks will be at the following coordinates:

$$(3) \quad x_n = n \cdot D$$

They should also be at a constant distance D apart. The following relationship is also true:

$$(4) \quad \lambda = A \cdot \frac{D}{L}$$

Equation (4) can be seen as an expression for determining the wavelength λ of the light being used. It is always applicable for interference between two beams.

Nevertheless, it is still to be established how the distance between the two virtual sources A can be measured. This can be assisted by a simple optical set-up, in which an image of both sources is obtained on the screen with the help of a converging lens so that the distance B between the images of the two sources can be measured (see Fig. 2). The following then applies:

$$(5) \quad A = B \cdot \frac{a}{b}$$

a : Object distance, b : Image distance.

NOTE

Instead of a biprism, a Fresnel mirror (1002649) can also be used to generate the two virtual light sources. The corresponding list of accessories can be found under the entry for UE4030320.

EVALUATION

In this experiment a laser is used as the source of the light. Its beam is spread out by a lens. The position of the light source is not precisely known, therefore the object distance a is not known either. It therefore needs to be calculated from the focal length f of the lens and the easily measured image distance b using the law for the formation of images:

The following therefore applies: $\frac{1}{f} = \frac{1}{a} + \frac{1}{b}$

The distances D and L can be measured directly. This means that all the variables for determining the wavelength using equation (3) are now known.

$$A = a \cdot \frac{B}{b} = \frac{f \cdot B}{b - f}$$

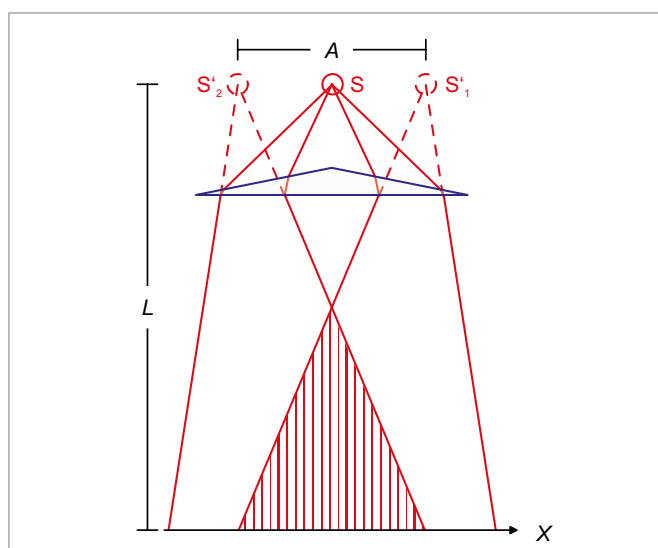


Fig. 1 : Schematic diagram of light passing through a biprism

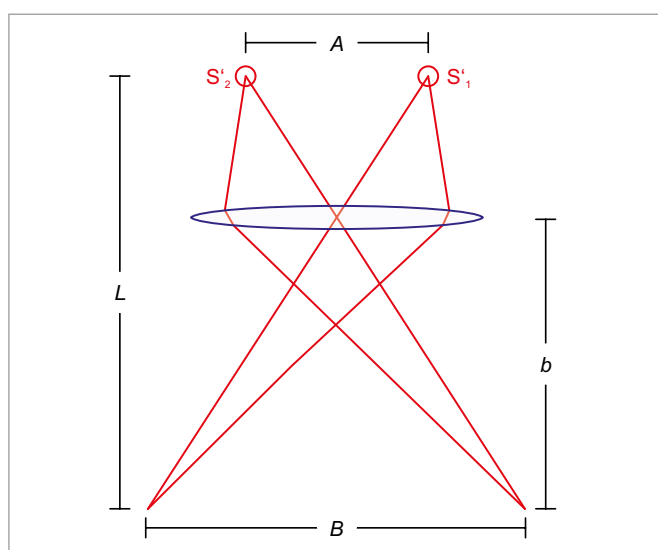
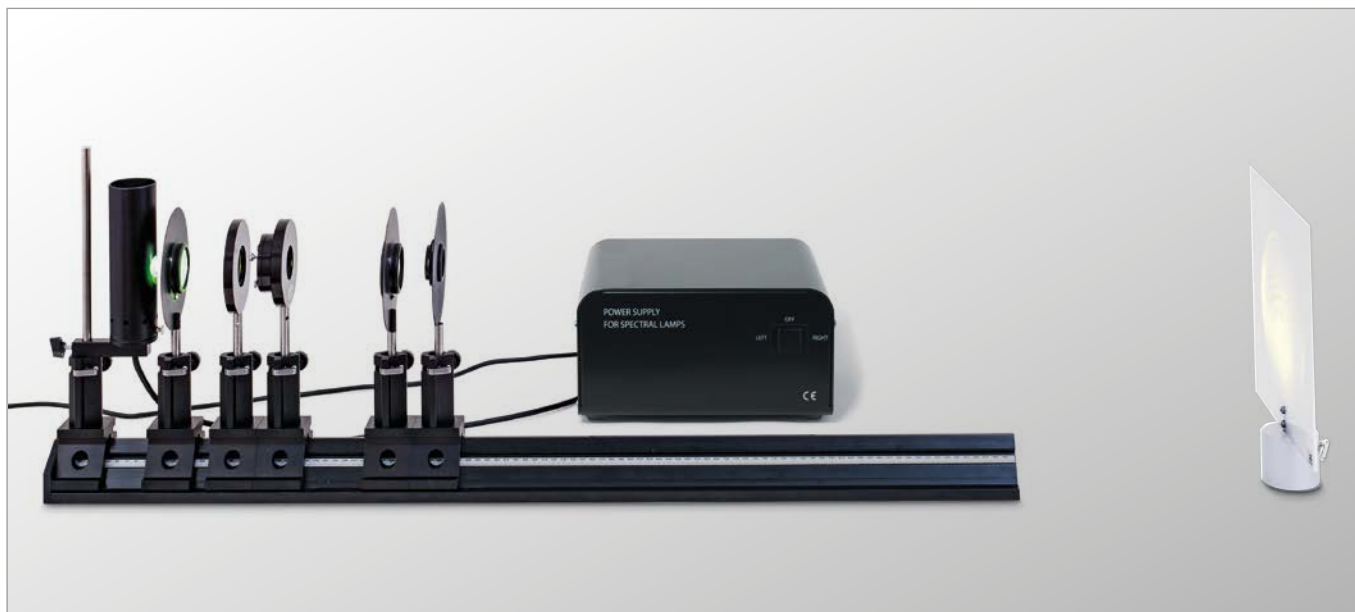


Fig. 2: Ray diagram for obtaining an image of the two virtual sources on the screen

UE4030350 | NEWTON'S RINGS



EXPERIMENT PROCEDURE

- Observe Newton's rings with monochromatic light transmitted through the apparatus.
- Measure the radius of the rings and determine the radius of curvature of the spherical body.
- Determine by how much the set up is deformed by the sphere pressing down on the plate.

OBJECTIVE

Observe Newton's rings in monochromatic light

SUMMARY

Newton's rings are generated by a set-up involving a flat glass plate and a spherical body with a large radius of curvature. If parallel monochromatic light is incident on the set-up from an angle normal to the apparatus, alternating light and dark concentric rings are generated, centered on the point where the surfaces meet. In this experiment Newton's rings are investigated using monochromatic light transmitted through the apparatus. The radius of curvature R of the spherical body can be determined from the radii r of the interference rings as long as the wavelength λ is known.

REQUIRED APPARATUS

Quantity	Description	Item Number
1	Optical Precision Bench D, 100 cm	1002628
6	Optical Rider D, 90/50	1002635
1	Control Unit for Spectrum Lamps (230 V, 50/60 Hz)	1021409 or
	Control Unit for Spectrum Lamps (115 V, 50/60 Hz)	1003195
1	Spectral Lamp Hg 100	1003545
1	Convex Lens on Stem $f=+50$ mm	1003022
1	Convex Lens on Stem $f=+100$ mm	1003023
1	Iris on Stem	1003017
1	Glass Inset for Newton's Rings Experiments	1008669
1	Component Holder	1003203
1	Interference Filter 578 nm	1008672
1	Interference Filter 546 nm	1008670
1	Projection Screen	1000608
1	Barrel Foot, 1000 g	1002834
1	Pocket Measuring Tape, 2 m	1002603

BASIC PRINCIPLES

Newton's rings are a phenomenon which can be viewed on a daily basis. They arise due to interference in light reflecting from the upper and lower boundaries of an air gap between two very nearly parallel surfaces. In white light, this produces colorful interference, since the condition for a maximum in the interference is dependent on the wavelength.

In order to deliberately generate Newton's rings, a set-up is used which involves a flat glass plate and a spherical body with a large radius of curvature. The spherical body touches the flat glass plate in such a way that an air gap results. If parallel monochromatic light is incident on the set-up from an angle normal to the apparatus, alternating light and dark concentric rings are generated, centered on the point where the surfaces meet. The darker rings are caused by destructive interference while the light ones result from constructive interference. The light waves reflected from the boundary between the spherical body and the air interfere with ones reflected from the boundary between the flat plate and the air. The interference rings can be viewed in both reflected and transmitted light. With transmission, though, the interference is always constructive at the center, regardless of the wavelength of the incident light. The separation between the interference rings is not constant. The thickness d of the air gap varies in proportion to the distance r from the point of contact between body and plate. The following can be seen from Fig. 1:

$$(1) \quad R^2 = r^2 + (R \cdot d)^2$$

R : radius of curvature

This means that when the thickness d is small, the following applies for the bright interference rings:

$$(2) \quad d = \frac{r^2}{2 \cdot R} = (n-1) \cdot \frac{\lambda}{2}$$

Therefore the radii of the bright rings are given by

$$(3) \quad r^2 = (n-1) \cdot R \cdot \lambda$$

It may be seen that the spherical body is slightly deformed at the point of contact. By rearranging equation (2) an approximation of this can be derived from the following expression:

$$(4) \quad d = \frac{r^2}{2 \cdot R} - d_0 \quad \text{for } r^2 \geq 2 \cdot R \cdot d_0$$

Therefore the radii of the bright rings are now given by:

$$(5) \quad r_i^2 = (n-1) \cdot R \cdot \lambda + 2 \cdot R \cdot d_0$$

This experiment investigates Newton's rings using transmitted light from a mercury lamp which has been rendered monochromatic with the aid of interference filters. The interference pattern is focussed onto the screen with the help of an objective lens.

EVALUATION

To determine the radius r , an average is taken of the measured radius values for the crossover point to the left and right. The magnification due to the lens is also taken into account.

Values for r^2 are then plotted as a function of $n-1$, whereby the measurements lie on straight lines of gradients $a = R \cdot \lambda$ which cross the axes at $b = 2 \cdot R \cdot d_0$. Since the wavelengths are known, it is possible to calculate the radius of curvature R . The radius of curvature is calculated to be approximately 45 m. The flattening d_0 of the sphere due to it pressing down on the plate is less than one micrometer.

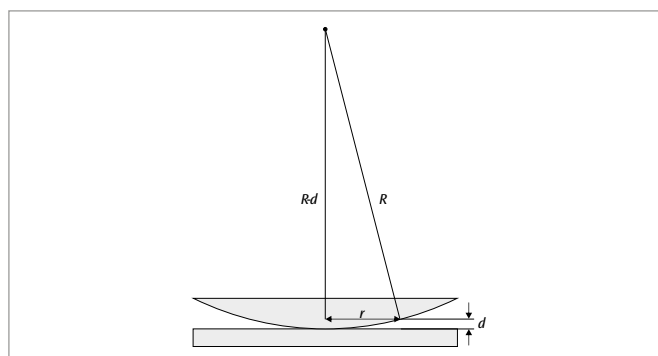


Fig. 1: Schematic illustration of the air gap between the convex lens and the flat plate

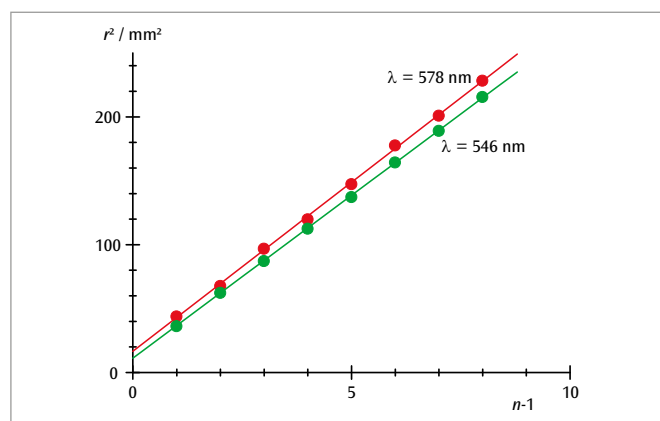


Fig. 2: Relationship between radii r^2 of bright interference rings and their number in sequence n

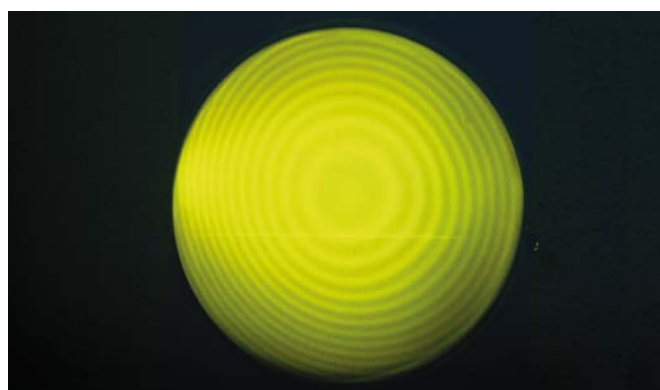
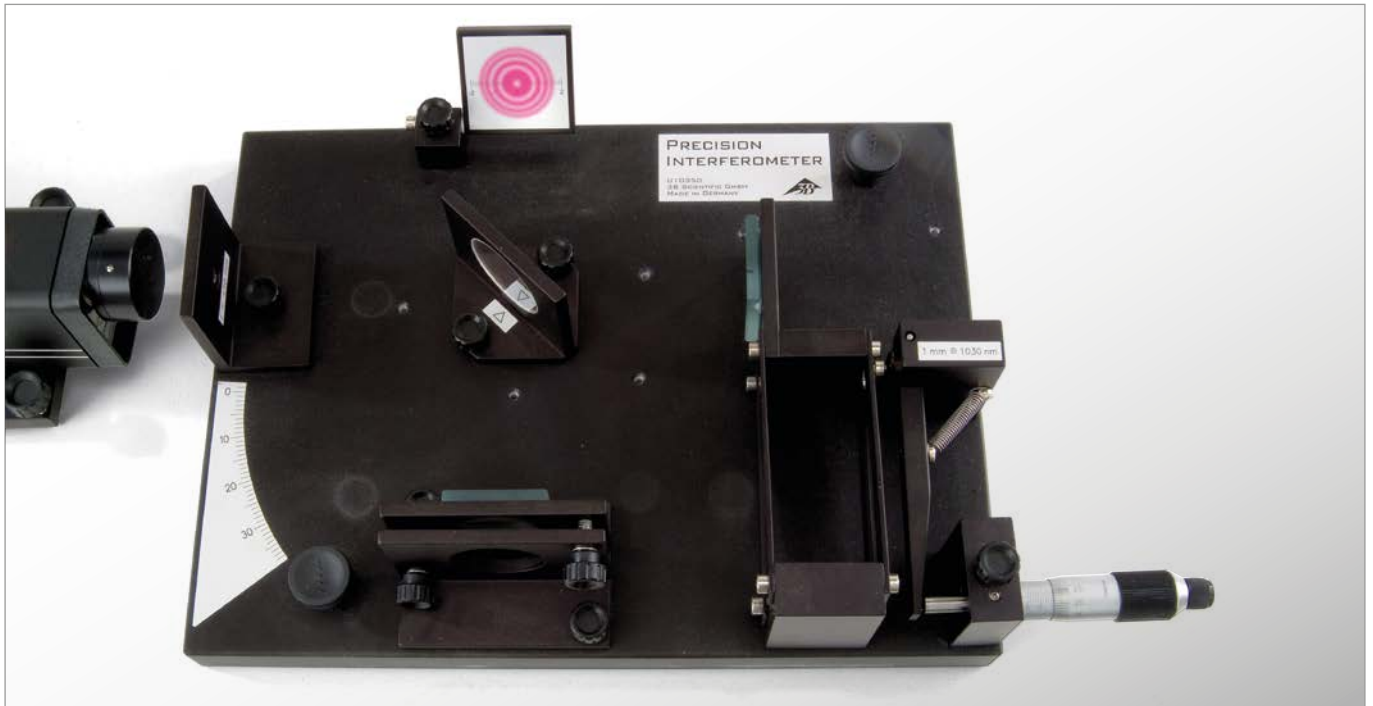


Fig. 3: Newton's rings in yellow light

UE4030410 | MICHELSON INTERFEROMETER



EXPERIMENT PROCEDURE

- Determine the wavelength of laser light.
- Determine the refractive index of air as a function of pressure.
- Determine the refractive index of glass.
- Determine the quality of the surface of a strip of adhesive tape.

OBJECTIVE

Demonstrate and investigate how a Michelson interferometer works

SUMMARY

In a Michelson interferometer a coherent light beam is separated into two rays travelling in different directions by inserting a half-silvered mirror in the path. The separated beams are reflected back along themselves and then recombined. The viewing screen then exhibits an interference pattern that changes perceptibly when the optical path lengths for each of the split beams are changed by fractions of the wavelength of light.

REQUIRED APPARATUS

Quantity	Description	Item Number
1	Interferometer	1002651
1	Accessory Set for the Interferometer	1002652
1	He-Ne Laser	1003165
1	Vacuum Hand Pump	1012856
1	Tubing, Silicone 6 mm	1002622



Glass plate in the beam path of the Michelson-interferometer.



Vacuum chamber in the beam path of the Michelson-interferometer.

BASIC PRINCIPLES

The Michelson interferometer was invented by *A. A. Michelson* originally to demonstrate whether the Earth could be observed to be in motion through an ether in which light was once thought to propagate. His design (see Fig. 1) has nevertheless proved crucial for making interferometric measurements, e.g. of changes in length, thickness of layers or refractive indices. A divergent light beam is split into two by a half-silvered mirror and the two resulting beams travel along differing paths. They are then reflected back on themselves and recombined so that interference patterns can be viewed on a screen. The resulting pattern is highly sensitive to any differences in the optical paths covered by the split beams. If the refractive index remains constant, the degree of change in the geometric paths can be calculated, e.g. changes in size of various materials due to thermal expansion. If by contrast the geometry is maintained, then refractive indices or changes in them due to pressure, temperature or density variations may be determined.

Depending on whether the optical paths are increased or decreased in length, interference lines may appear or disappear in the center of the pattern. The relationship between the change Δs in the optical paths and the wavelength λ is as follows

$$(1) \quad 2 \cdot \Delta s = z \cdot \lambda$$

The number z is a positive or negative integer corresponding to the number of interference lines appearing or disappearing on the screen. If the wavelength of light in air is to be measured by moving one of the two mirrors by a carefully defined distance Δx by means of a fine adjustment mechanism, the refractive index can be assumed to be $n = 1$ to a good approximation. The change in the optical path is thus:

$$(2) \quad \Delta s = \Delta x$$

The situation is different if an evacuated chamber of length d is inserted into only one of the split beams. By allowing air to pass into the vessel until the pressure rises to a value p , the optical path changes as follows

$$(3) \quad \Delta s = (n(p) - 1) \cdot d = A \cdot p \cdot d$$

This is because the refractive index of air at constant temperature varies with pressure in a fashion that can be represented in the following form:

$$(4) \quad n(p) = 1 + A \cdot p$$

NOTE

The supplementary kit contains a glass plate. This can be placed in the path of one light beam and rotated to a specific angle so that the portion of the optical path that passes through the glass increases while that portion of the path outside the glass decreases. The resulting change in the optical path allows the refractive index of glass to be determined. It is also possible to demonstrate the surface quality of a strip of adhesive tape attached to the glass. In practice such experiments are performed using a Twyman-Green-interferometer, which is a variant of the Michelson-interferometer.

EVALUATION

Solving Equations (1) and (2) for wavelength gives an equation for the wavelength that depends on the change in position of the mirror:

$$\lambda = \frac{2 \cdot \Delta x}{z}$$

Determining the refractive index of air: The coefficient A that appears in Equation (4) can be calculated using the following equation

$$A = \frac{z \cdot \lambda}{2 \cdot d \cdot p}$$

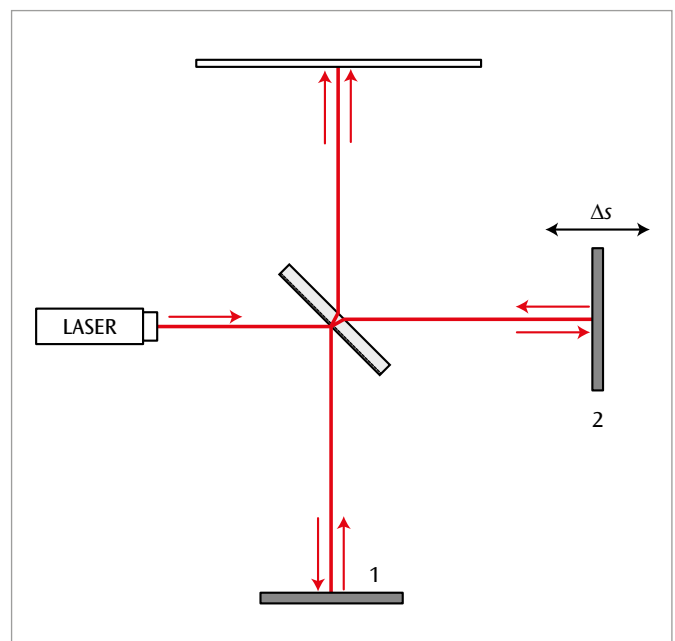


Fig. 1: Optical paths in a Michelson interferometer with a movable mirror

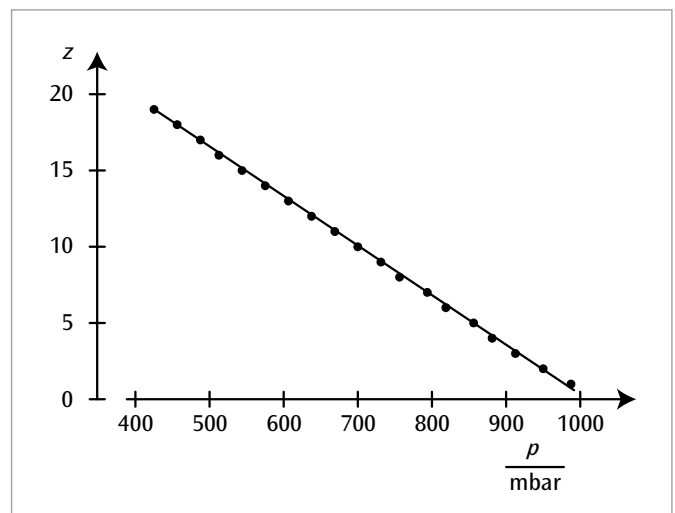


Fig. 2: Number of interference lines as a function of air pressure

UE4030520 | MACH-ZEHNDER INTERFEROMETER



EXPERIMENT PROCEDURE

- Set up and calibrate a Mach-Zehnder interferometer.
- Observe the interference pattern when the information is available, unavailable and “erased”.

OBJECTIVE

Demonstration of “quantum erasure” in an experiment by analogy

SUMMARY

Light itself can be described in quantum mechanics by means of wave equations. From this it is possible to derive the spatial distribution of the probability density in the form of the square of the modulus of the wave function. Light is therefore suitable for experiments which demonstrate quantum mechanical phenomena by analogy. Such an analogy experiment demonstrates the so-called quantum eraser effect by setting up a Mach-Zehnder interferometer and observing interference between the split beams on a screen. If two perpendicular polarizers are placed in the paths of the split beams, the interference vanishes since, in quantum mechanical terms, it is possible to determine the path a photon has taken. If a third polarising filter set at an angle of 45° is placed directly in front of the screen, this quantum information is “erased” and the interference can be seen once again.

REQUIRED APPARATUS

Quantity	Description	Item Number
1	Mach-Zehnder Interferometer	1014617
1	He-Ne-Laser	1003165

BASIC PRINCIPLES

Light itself can be described in quantum mechanics by means of wave equations. From this it is possible to derive the spatial distribution of the probability density in the form of the square of the modulus of the wave function. The combination of two beams corresponds to superposition of two wave functions. The probability density then contains a mixed term which describes the interference pattern. Light is therefore suitable for experiments which demonstrate quantum mechanical phenomena by analogy.

To demonstrate the so-called quantum eraser effect by means of an analogy experiment, a Mach-Zehnder interferometer is used. An expanded bundle of laser is used as coherent light source. With the help of beam splitter BS1, the light is divided into two split beams. Polarizer P

ensures that both split beams have the same light intensity (see Fig. 1). The two beams then follow different paths but are then brought back into superposition by a second beam splitter BS2. In terms of conventional wave optics, the electrical fields of the two split beams E_1 and E_2 are then added together:

$$(1) \quad \mathbf{E} = \mathbf{E}_1 + \mathbf{E}_2$$

In quantum mechanical terms, their wave functions Ψ_1 and Ψ_2 can also be summed as follows:

$$(2) \quad \Psi = \Psi_1 + \Psi_2$$

Therefore

$$(3) \quad |E|^2 = |E_1|^2 + |E_2|^2 + 2 \cdot E_1 \cdot E_2$$

and

$$(4) \quad |\Psi|^2 = |\Psi_1|^2 + |\Psi_2|^2 + 2 \cdot \langle \Psi_1 | \Psi_2 \rangle$$

The mixed terms in equations (3) and (4) both describe the interference pattern which can be observed on a screen. Equation 4 describes the behavior of an individual photon. Such a photon interferes with “itself” as long as it is observed by any process of measurement or if it is not possible to observe the actual path it has travelled. It is said with regard to this that “in the absence of information regarding its path, a photon behaves as a wave and exhibits interference”. If information regarding the path taken is available, however, the photon “behaves” like a classical particle and it is not possible for interference to occur. Two additional polarizers P1 and P2 placed in the paths of the split beams 1 and 2 cause the interference pattern to be affected. If the polarizers are aligned at right angles to one another, the scalar product $E_1 \cdot E_2$ vanishes in the classical description of equation (3), as does the interference term $\langle \Psi_1 | \Psi_2 \rangle$ in the quantum mechanical representation of Equation (4). This results in the disappearance of the interference pattern. In the quantum mechanical case, this is because the polarization means that it is possible to specifically determine which path, path 1 or path 2, has been taken by each photon.

However, if a third polarizer A, aligned at 45° to the others, is placed behind the second beam splitter, the interference pattern reappears. In quantum mechanical terms, this is so because polarizer A “erases” the path information, i.e. beyond polarizer A it is no longer possible to determine which path has been taken by any individual photon. In the classical representation, the third polarizer would be expected to dim the polarized split beams but they would be expected to retain their polarization.

EVALUATION

In the absence of both polarizers, P1 and P2, there will be no information available regarding the path taken by the light and interference therefore occurs. Once the two polarizers are employed, it is possible to distinguish paths and interference does not occur.

The third polarizer, A, “erases” the path information and interference occurs once more.

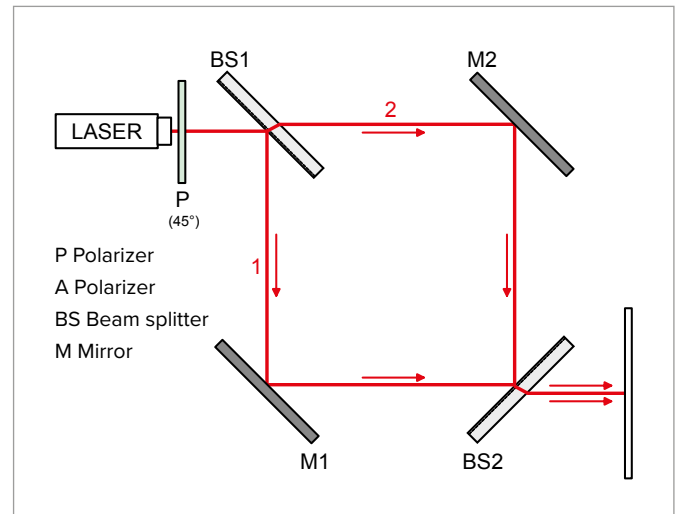


Fig. 1: Paths through the Mach-Zehnder interferometer (no path information)

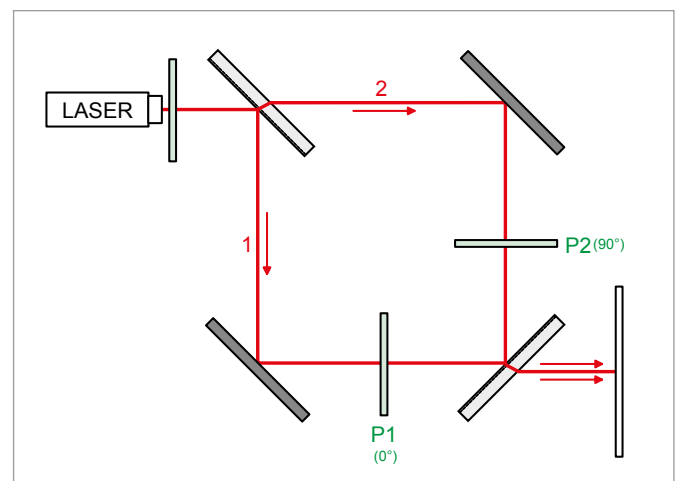


Fig. 2: Paths through the Mach-Zehnder interferometer (polarizers P1 and P2 placed in the two split beams means path information can be obtained)

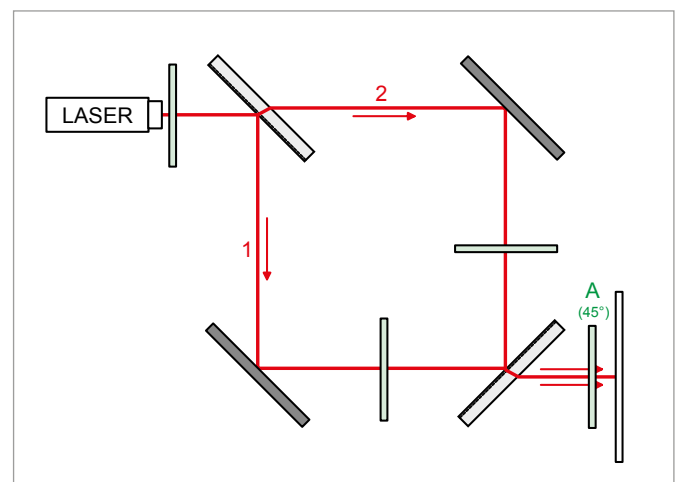


Fig. 3: Paths through the Mach-Zehnder interferometer (polarizer A “erases” the path information)

UE4040100 | MALUS' LAW



> EXPERIMENT PROCEDURE

- Measure the intensity of light I transmitted through a polarising filter as a function of the angle of rotation of the filter.
- Verify Malus' law.

OBJECTIVE

Verify Malus' law for linearly polarized light

SUMMARY

Malus' law describes how intensity I of polarized light with an initial intensity I_0 , having passed through an analyzer filter, depends on the angle of rotation of the filter. The intensity of the light is measured using a light sensor.

REQUIRED APPARATUS

Quantity	Description	Item Number
1	Optical Precision Bench D, 50 cm	1002630
4	Optical Rider D, 90/50	1002635
1	Optical LED Lamp	1020630
1	Light Sensor, Three Ranges	1021502
1	WiLab *	1022284
1	Holder for light sensor	1022269
2	Polarization Filter on Stem	1008668
1	Sensor Cable	1021514

Additionally required

1	Coach 7 License
---	-----------------

* Alternative: 1 VinciLab 1021477

BASIC PRINCIPLES

Light, being a transverse wave, can be polarized, for example by allowing it to pass through a polarising filter. In a linearly polarized light wave, both the electric field E and magnetic field B oscillate in distinct planes. The orientation direction of the electric field oscillation is called the polarization direction.

In this experiment light passes through two filters termed the polarizer and the analyzer, which are aligned at an angle of φ to one another. The polarizer only allows one linearly polarized component of the light to pass through it. The electric field of this component may be deemed to have an amplitude E_0 .

The amplitude of the component after passing through the analyzer filter is given by

$$(1) \quad E = E_0 \cdot \cos \varphi$$

This is a measure of the amount of light which can pass through the analyzer.

The intensity of the light corresponds to the square of the electric field strength. The intensity of light beyond the analyzer is therefore as follows:

$$(2) \quad I = I_0 \cdot \cos^2 \varphi$$

where I_0 is the intensity of light after passing through the polarizer. Equation (2) is a statement of Malus' law. This will be verified in the experiment by measuring the light intensity using a light sensor. In this experiment, the intensity of light measured for an angle $\varphi = 90^\circ$ should be equal to that of the ambient light. This value should be subtracted from all the other intensity measurements.

EVALUATION

Once the ambient light intensity has been subtracted from all the measurements, they are then plotted as a function of φ . The curve should then be described by equation (2). Intensity I is then plotted in another graph as a function of $\cos^2 \varphi$. In this case, the measurements lie on a straight line through the origin which has a gradient I_0 .

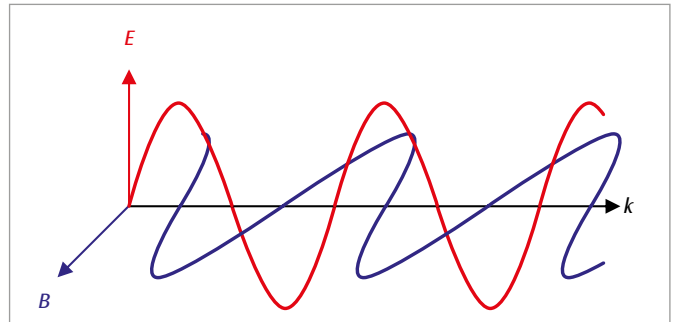


Fig. 1: Illustration showing the definition for direction of polarization

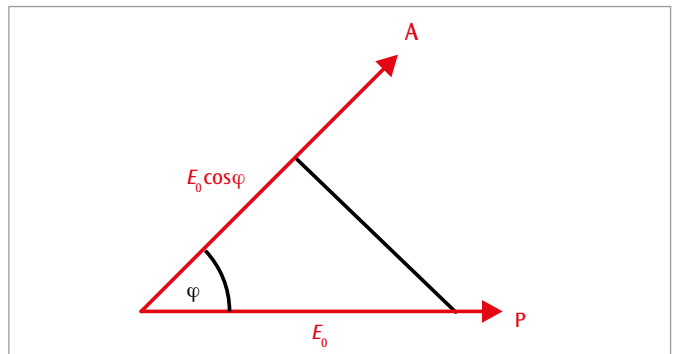


Fig. 2: Illustration of how the electric field beyond the analyzer is calculated

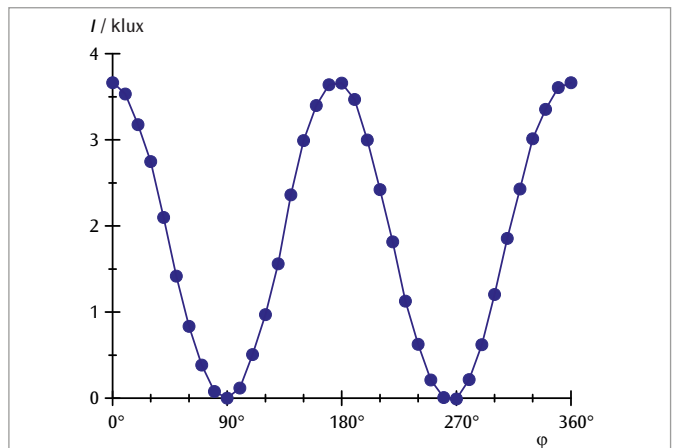


Fig. 3: Light intensity I as a function of the angle φ between the polarizer and the analyzer

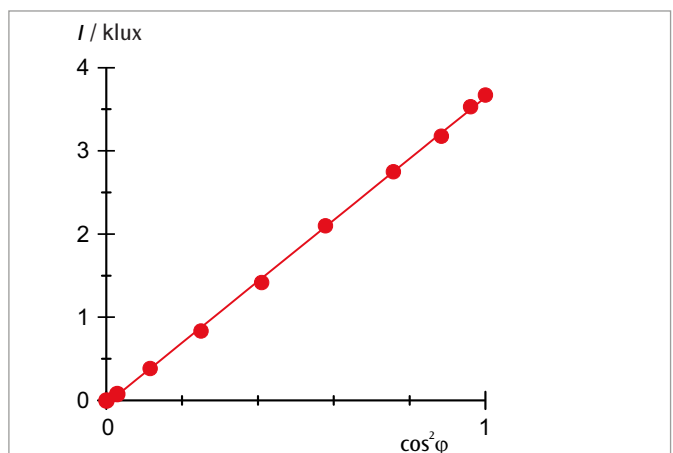


Fig. 4: Light intensity I as a function of $\cos^2 \varphi$

UE4040300 | OPTICAL ACTIVITY



EXPERIMENT PROCEDURE

- Measurement of the angle of rotation as a function of the length of the sample.
- Measurement of the angle of rotation as a function of the solution concentration.
- Determining the specific rotation for different light wavelengths.
- Comparing the directions of rotation and angles of rotation for fructose, glucose and saccharose.
- Measurement of the angle of rotation during the inversion of saccharose to give an equimolar mixture of glucose and fructose.

OBJECTIVE

Investigate the rotation of the plane of polarization by sugar solutions

SUMMARY

Sugar solutions are optically active, in other words they rotate the plane of polarization of any linearly polarized light that is passed through them. The direction of rotation depends on the molecular properties of the sugar. Thus, solutions of glucose and saccharose (sucrose) rotate the plane of polarization to the right (clockwise), whereas fructose solutions rotate it to the left (counter-clockwise), as found when the angle of rotation is measured with a polarimeter. The experiment also includes measuring the angle of rotation to study the behavior of a saccharose solution when hydrochloric acid is added. This causes a gradual reversal ("inversion") of the direction of rotation from clockwise to counter-clockwise, as the double-ring structure of the saccharose molecule is split into two, giving an equimolar mixture of glucose and fructose. The angle of rotation of the mixture is the sum of the angles of rotation of the dextro-rotatory glucose and the more strongly laevo-rotatory fructose.

REQUIRED APPARATUS

Quantity	Description	Item Number
1	Polarimeter with 4 LEDs (230 V, 50/60 Hz)	1001057 or
	Polarimeter with 4 LEDs (115 V, 50/60 Hz)	1001056
1	Graduated Cylinder, 100 ml	1002870
1	Beaker	1002872
1	Electronic Scale Scout SKX 420 g	1020859

Additionally required

Fruit Sugar (Fructose), 500 g

Grape Sugar (Glucose), 500 g

Cane Sugar (Sucrose), 500 g

BASIC PRINCIPLES

The term **optical activity** is used to describe the rotation of the plane of polarization of linearly polarized light when it passes through certain substances. This rotation is observed in solutions of chiral molecules such as sugars and in certain solids such as quartz. Substances that rotate the plane of polarization to the right (i.e. clockwise) as viewed against the direction of propagation of the light are described as **dextro-rotatory**, whereas substances with the opposite behavior are described as **laevo-rotatory**. Glucose and saccharose solutions are dextro-rotatory, whereas fructose solutions are laevo-rotatory.

The angle α through which the plane of polarization is rotated by a solution depends on the nature of the dissolved substance, and it is proportional to the concentration (mass per unit volume) c and to the length or thickness d of the sample. The relationship is expressed as:

$$(1) \quad \alpha = [\alpha] \cdot c \cdot d$$

where $[\alpha]$ is called the specific rotation of the dissolved substance. The specific rotation depends on the wavelength λ of the light and the sample temperature T , and the relationship has the form:

$$(2) \quad [\alpha] = \frac{k(T)}{\lambda^2}$$

Values of $[\alpha]$ in published tables are usually given for yellow sodium light at an ambient temperature of 25°C. If $[\alpha]$ is known, the concentration of a solution can be determined by measuring the angle of rotation in a polarimeter.

In the experiment, measurements are made on solutions of different sugars in a polarimeter under different conditions, and the angles of rotation are compared. The color of the light can be changed by choosing between four LEDs. The effect of adding hydrochloric acid to a solution of ordinary cane sugar (saccharose) is also investigated. This causes a slow reaction whereby the double-ring structure is split to give an equimolar mixture of glucose and fructose. During this process the direction of rotation becomes “inverted” from clockwise to counter-clockwise, because the angle of rotation after completion of the reaction is the sum of the angles of rotation of the dextro-rotatory glucose and the more strongly laevo-rotatory fructose.

EVALUATION

According to Equation (1), the angle of rotation of a solution of a given substance at a fixed concentration is proportional to the length of the sample, whereas for a fixed sample length it is proportional to the concentration. From the gradients of the straight lines through the origin in Figure 1, the specific rotation for each of the four wavelengths provided by the polarimeter can be calculated.

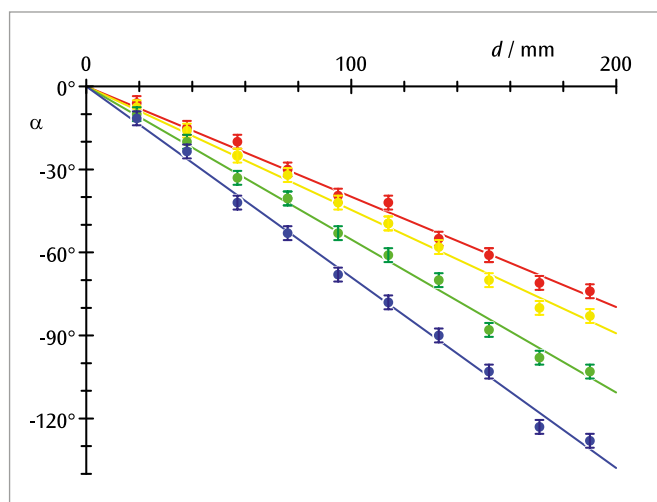


Fig. 1: Angle of rotation of a fructose solution ($c = 0.5 \text{ g/cm}^3$) as a function of sample length for four different light wavelengths

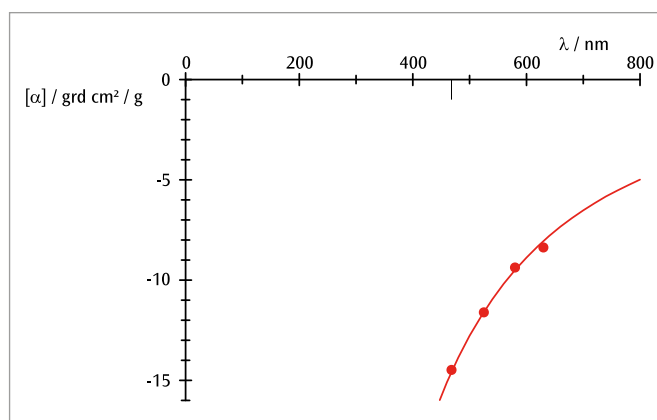


Fig. 2: Dependence of specific rotation on wavelength

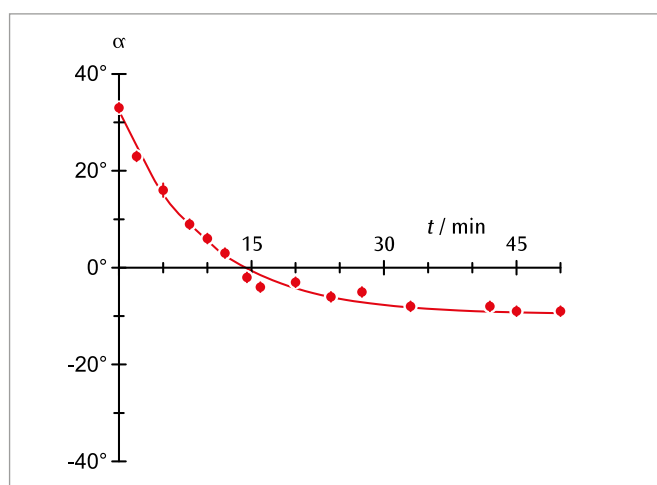


Fig. 3: Angle of rotation of a saccharose solution ($c = 0.3 \text{ g/cm}^3$, $d = 190 \text{ mm}$) during the inversion process as a function of time

UE4040500 | POCKELS EFFECT



EXPERIMENT PROCEDURE

- Demonstrate birefringence in a conoscopic beam path.
- See how the birefringence changes when an electric field is applied.
- Determine the half-wave retardation voltage.

OBJECTIVE

Demonstration of Pockels effect in a conoscopic beam path

SUMMARY

The Pockels effect is an electro-optical effect, in which an electric field within a suitable material splits a light beam into two beams polarized perpendicular to one another. This ability to produce optical birefringence derives from the differing refractive indices depending on the direction of propagation and polarization of the light. In the case of the Pockels effect, this increases linearly with the strength of the electric field as is demonstrated in this experiment using a lithium niobate crystal (LiNbO_3) placed in the path of a conoscopic beam. The interference pattern is formed by two sets of hyperbolae, from which the position of the optical axis for the birefringence can be seen directly.

REQUIRED APPARATUS

Quantity	Description	Item Number
1	Pockels Cell on Stem	1013393
1	Optical Precision Bench D, 100 cm	1002628
3	Optical Rider D, 90/50	1002635
2	Optical Rider D, 90/36	1012401
1	He-Ne Laser	1003165
1	Achromatic Objective 10x / 0.25	1005408
1	Polarization Filter on Stem	1008668
1	Convex Lens on Stem $f = +50$ mm	1003022
1	Projection Screen	1000608
1	High-Voltage Power Supply E 5 kV (230 V, 50/60 Hz)	1013412 or
	High-Voltage Power Supply E 5 kV (115 V, 50/60 Hz)	1017725
1	Pair of Safety Experiment Leads, 75 cm	1002849

BASIC PRINCIPLES

The Pockels effect is an electro-optical effect in which an electric field within a suitable material splits a light beam into two beams polarized perpendicular to one another. This ability to produce optical birefringence derives from the differing refractive indices depending on the direction of propagation and polarization of the light. In the case of the Pockels effect, this increases linearly with the strength of the electric field as is demonstrated in this experiment using a lithium niobate crystal (LiNbO_3) placed in the path of a conoscopic beam.

The crystal in this case is located inside a Pockels cell in transverse alignment, where an electric field is applied across the crystal in the direction of the optical axis for the birefringence (see Fig. 1). The light beam passing perpendicularly through the crystal splits into an ordinary and an extraordinary, i.e. one polarized in the direction of the optical axis for the birefringence and another polarized perpendicular to it. In the case of lithium niobate, the refractive index for the ordinary beam for $n_o = 2.29$ as measured at the wavelength of an He-Ne laser $\lambda = 632.8 \text{ nm}$ while that for the extraordinary beam is $n_e = 2.20$. The path difference between the ordinary and extraordinary beams is as follows:

$$(1) \quad \Delta = d \cdot (n_o - n_e)$$

where $d = 20 \text{ mm}$, the thickness of the crystal in the direction of the beam.

Demonstration of the birefringence uses a classical beam path as suggested for the purpose in numerous optics text books. The crystal is illuminated by a divergent, linearly polarized light beam and the transmitted light is observed behind an orthogonal analyzer. The optical axis of the birefringence is highly visible in the interference pattern since it stands out from the background due to its symmetry. In this experiment, it is parallel to the entry and exit surfaces on the crystal, therefore creating an interference pattern with two sets of hyperbolae rotated by 90° with respect to one another. The actual axis of the first set of hyperbolae is parallel to the optical axis of the birefringence and that of the second set is perpendicular to it. The dark bands in the sets of hyperbolae arise for beams where the difference between the optical paths of the ordinary and extraordinary beams in the crystal are an integer multiple of the wavelength. These beams retain their original linear polarization on passing through the crystal and get blocked by the analyzer.

The path difference corresponds to about 2800 wavelengths of the laser light being used. However, in general Δ is not precisely an integer multiple of the wavelength λ , but rather lies between two values $\Delta_m = m \cdot \lambda$ and $\Delta_{m+1} = (m + 1) \cdot \lambda$. For the dark lines of the first set of hyperbolae the path differences are Δ_{m+1} , Δ_{m+2} , Δ_{m+3} , etc. Those for the second set correspond to Δ_m , Δ_{m-1} , Δ_{m-2} , etc. (see Fig. 2). The position of the dark bands, or more accurately their distance from the center, depends on the difference between Δ and $m \cdot \lambda$. The Pockels effect increases or decreases the difference between the primary refractive indices $n_o - n_e$ depending on the sign of the voltage applied. This means that the difference $\Delta - m \cdot \lambda$ changes and so therefore does the position of the dark interference bands. If the so-called half-wave retardation voltage U_{π} is applied, then Δ changes by one half of the wavelength. Then the dark interference bands shift to the position of the bright bands and vice versa. This process is repeated every time the voltage is increased by U_{π} .

EVALUATION

For a voltage U_1 the dark interference bands of order +1 are located precisely in the center. For the next voltage U_2 it is those of order +2 which are in the center. Then the half-wave voltage is as follows:

$$U_{\pi} = \frac{U_2 - U_1}{2}$$

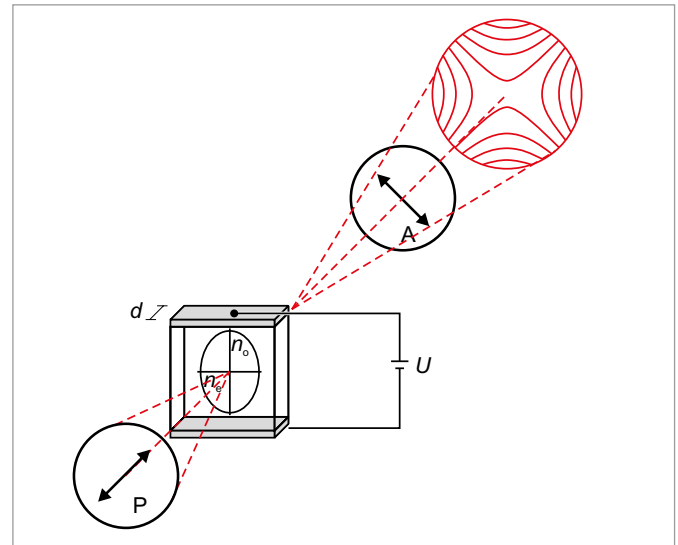


Fig. 1: Schematic of Pockels cell in a conoscopic beam path between the polarizer and analyzer

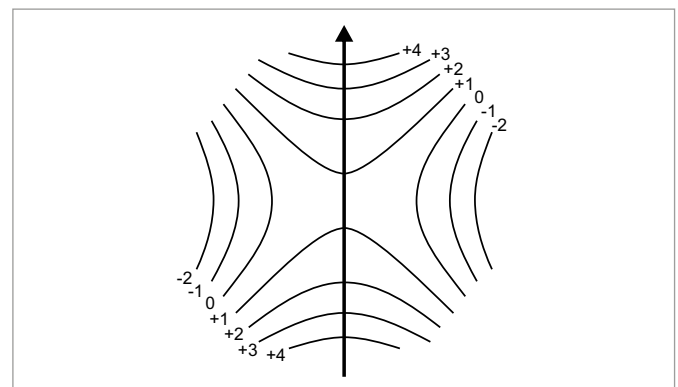


Fig. 2: Interference pattern with optical axis of crystal in the direction of the arrow. The indices of the dark interference bands indicate the path difference between the ordinary and extraordinary beams in units of the wavelength.

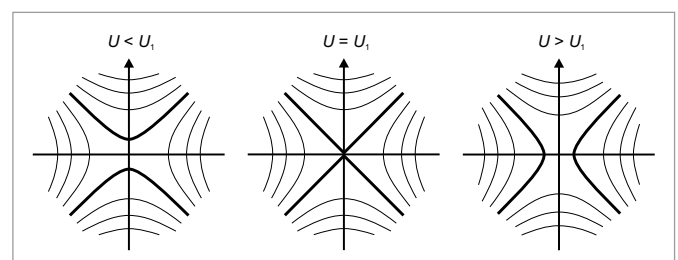


Fig. 3: Change in interference pattern due to Pockels effect. The hyperbolae indicated by thicker lines are those of order +1 in the interference pattern.

UE4040600 | FARADAY EFFECT



OBJECTIVE

Demonstrate the Faraday effect and determine the Verdet constant for flint glass

SUMMARY

Optically isotropic, transparent, non-magnetic materials become optically active in a magnetic field. They rotate the polarization plane of linearly polarized light passing through the material in the direction of the magnetic field, since the transit times of the right- and left-circularly polarized components are different. This effect is known as the Faraday effect. In this experiment, the Faraday effect is measured in flint glass. This particular type of glass is characterized by a very high and uniform optical dispersion. The frequency dependence of the refractive index n can be approximated by a Cauchy formula.

EXPERIMENT PROCEDURE

- Demonstrate the Faraday effect in flint glass.
- Measure the angle of rotation of the polarization plane in the magnetic field.
- Determine the Verdet constant for red and green light.
- Determine the Cauchy coefficient b for the refractive index.

REQUIRED APPARATUS

Quantity	Description	Item Number
1	Optical Precision Bench D, 100 cm	1002628
4	Optical Rider D, 90/50	1002635
1	Optical Base D	1009733
1	Laser Diode, Red	1003201 or
	Laser Diode, Red 115 V	1022208
1	Laser Module, Green	1003202
2	Polarization Filter on Stem	1008668
1	Projection Screen	1000608
1	Transformer Core D	1000976
2	Pair of Pole Shoes	1000978
2	Coil D, 900 Turns	1012859
1	Flint Glass Block for Faraday Effect	1012860
1	Accessories for Faraday Effect	1012861
1	VinciLab	1021477
1	Magnetic Field Sensor FW +/- 2000 mT	1021766
1	Barrel Foot, 1000 g	1002834
1	Universal Jaw Clamp	1002833
1	Set of 15 Experiment Leads, 75 cm 1 mm ²	1002840
1	DC Power Supply, 1 – 32 V, 0 – 20 A (230 V, 50/60 Hz)	1012857
	DC Power Supply, 0 – 40 V, 0 – 40 A (115 V, 50/60 Hz)	1022289
Additionally recommended		
1	Coach 7 Lite	

BASIC PRINCIPLES

Optically isotropic, transparent, non-magnetic materials become optically active in a magnetic field. They rotate the polarization plane of linearly polarized light passing through the material in the direction of the magnetic field, since the transit times of the right- and left-circularly polarized components are different. This effect is known as the Faraday effect.

The differences in transit time can be explained in a simple model by the change in the frequency that circularly polarized light experiences in the magnetic field. Light with a clockwise polarization undergoes a slight increase in frequency f by an amount called the Larmor frequency

$$(1) \quad f_L = \frac{e}{4\pi \cdot m_e} \cdot B$$

$e = 1.6021 \cdot 10^{-19}$ As: Charge of an electron

$m_e = 9.1 \cdot 10^{-31}$ kg: Rest mass of an electron

The frequency of counter-clockwise polarized light decreases by the same amount, i.e.

$$(2) \quad f_{\pm} = f \pm f_L$$

The differing frequencies can be attributed to differing refractive indices in the material. This means that the speed of propagation of waves inside the material differs as well.

With these data the rotation of the polarization plane in the optically active material can be calculated:

$$(3) \quad \varphi = 2\pi \cdot f \cdot (t_+ - t_-) = 2\pi \cdot f \cdot \frac{d}{c} \cdot (n(f_+) - n(f_-))$$

d : Length of sample,

$c = 2,998 \cdot 10^8 \frac{\text{m}}{\text{s}}$: Speed of light

Since the Larmor frequency f_L is much smaller than f , it follows that:

$$(4) \quad \begin{aligned} \varphi &= 2\pi \cdot f \cdot \frac{d}{c} \cdot \frac{dn}{df} \cdot 2 \cdot f_L \\ &= f \cdot \frac{dn}{df} \cdot \frac{e}{m_e \cdot c} \cdot B \cdot d \end{aligned}$$

The angle of rotation φ is also proportional to the magnetic field B and the length of material d through which the light passes:

$$(5) \quad \varphi = V \cdot B \cdot d$$

The constant of proportionality

$$(6) \quad V = \frac{e}{m_e \cdot c} \cdot f \cdot \frac{dn}{df}$$

is called the Verdet constant and is dependent on the dispersion of the light in the material through which it passes and on the frequency f of that light. In this experiment, measurements are made of the Faraday effect in flint glass (F_2). This particular type of glass features a high degree of very uniform optical dispersion. The frequency dependence of the refractive index n can be approximated by a Cauchy formula.

$$(7) \quad n(f) = a + \frac{b}{c^2} \cdot f^2$$

where $a = 1.62$, $b = 8920 \text{ nm}^2$

To improve the accuracy of the measurement for small angles of rotation, this experiment is set up in such a way that when the magnetic field B is positive, the polarization of the light is such that the analyzer filter causes the transmitted light to go dark at precisely 0° . When the magnetic field is switched to a negative one $-B$, the analyzer must be rotated by an angle 2φ in order to shut out the light again.

EVALUATION

From equations (6) and (7), the following can be derived:
$$V = \frac{2 \cdot e \cdot b \cdot f^2}{m_e \cdot c^3} = \frac{2 \cdot e \cdot b}{m_e \cdot c \cdot \lambda^2}$$

This means that it is possible to obtain the Cauchy coefficient b for the refractive index of the flint glass used here from the Verdet constant, as long as the wavelength λ of the light is known.

$$b = \frac{m_e \cdot c}{2 \cdot e} \cdot V \cdot \lambda^2$$

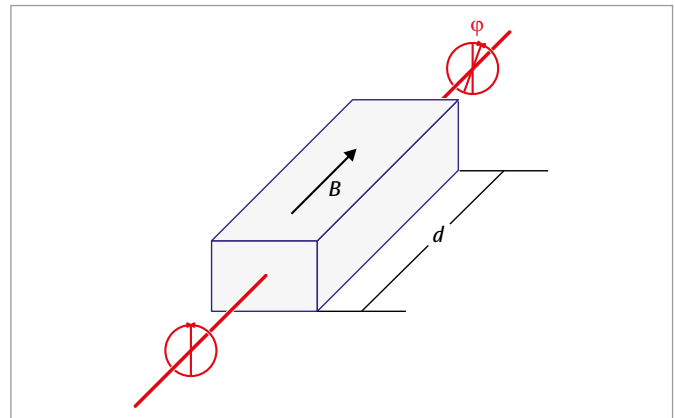


Fig. 1: Schematic diagram to illustrate the Faraday effect

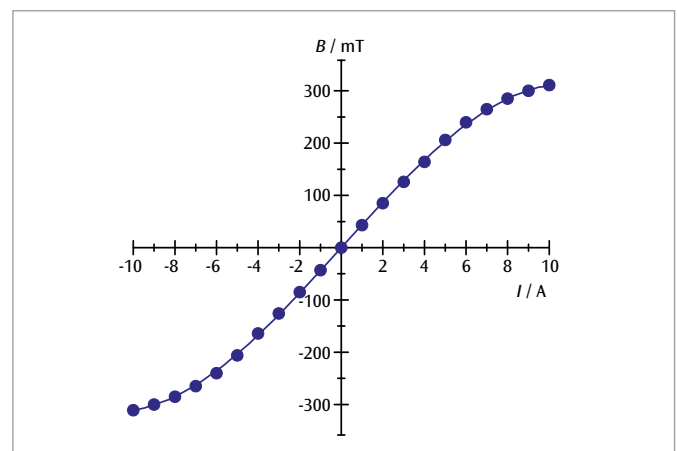


Fig. 2: Calibration curve for electromagnet

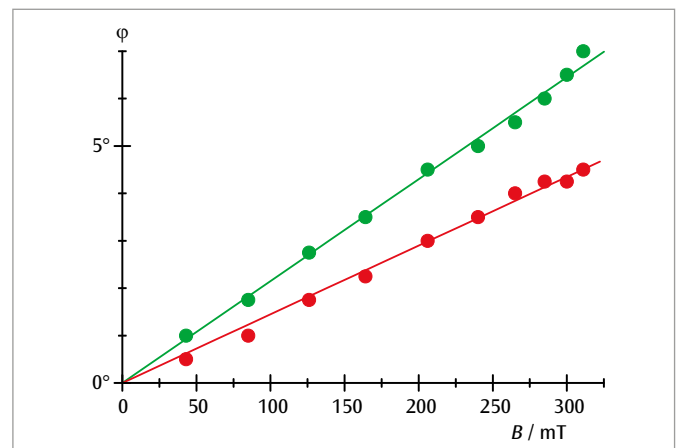
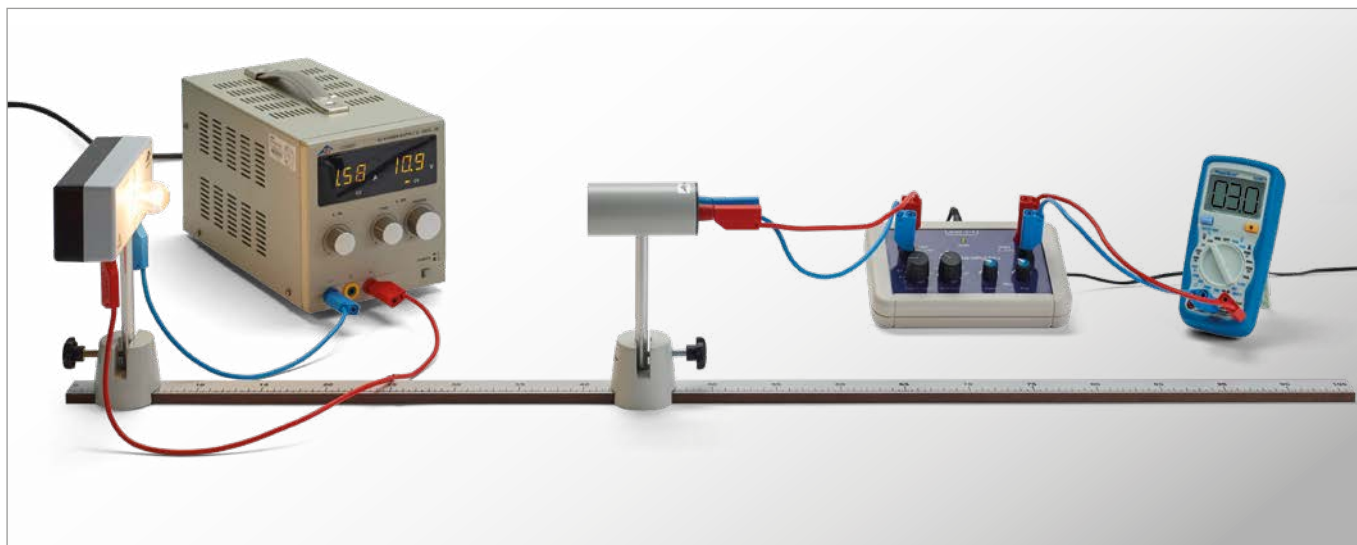


Fig. 3: Angle of rotation as a function of the magnetic field for red and green laser light

UE4050100 | INVERSE SQUARE LAW



EXPERIMENT PROCEDURE

- Calibrate an offset to compensate for ambient light.
- Measure the relative light intensity as a function of the distance.
- Plot a graph of S against $1/r^2$.

OBJECTIVE

Verify the inverse square law for the intensity of radiation from a source of light

SUMMARY

According to the inverse square law, the intensity of radiation from a light source, i.e. the power per unit area, is inversely proportional to the square of the distance from the source. This will be investigated in an experiment using an incandescent light bulb. When the distance from the lamp is much greater than the size of the filament, such a bulb can be regarded as a point source of light. In order to measure the relative intensity of the radiation, a Moll thermopile is used.

REQUIRED APPARATUS

Quantity	Description	Item Number
1	Stefan Boltzmann Lamp	1008523
1	Moll-Type Thermopile	1000824
1	Measurement Amplifier U (230 V, 50/60 Hz)	1020742 or
	Measurement Amplifier U (115 V, 50/60 Hz)	1020744
1	DC Power Supply 0 – 20 V, 0 – 5 A (230 V, 50/60 Hz)	1003312 or
	DC Power Supply 0 – 20 V, 0 – 5 A (115 V, 50/60 Hz)	1003311
1	Digital Multimeter P1035	1002781
1	HF Patch Cord, BNC/4 mm Plug	1002748
1	Ruler, 1 m	1000742
2	Barrel Foot, 500 g	1001046
1	Set of 15 Safety Experiment Leads, 75 cm	1002843

BASIC PRINCIPLES

The inverse square law describes a fundamental relationship which applies, among other things, to the intensity of light. The intensity of the light, i.e. the power detected within a unit area is inversely proportional to the square of the distance from the light source.

For this law to apply, the source needs to be radiating light uniformly in all directions and its dimensions must be negligible in comparison to its distance from the detector. In addition, there must be no absorption or reflection of light between the source and the point where the measurement is being made.

Since the source radiates uniformly on all directions, the emitted power P is distributed across the surface of a sphere at a distance r from the source.

$$(1) \quad A = 4\pi \cdot r^2$$

The light intensity is therefore given by the following

$$(2) \quad S = \frac{dP}{dA} = \frac{P}{4\pi \cdot r^2}$$

Equation (2) will be verified in this experiment using an incandescent bulb. When the distance from the lamp is much greater than the size of the filament, such a bulb can be regarded as a point source of light. In order to measure the relative intensity of the radiation, a Moll thermopile is used. Instead of the absolute intensity S , the thermopile voltage U_{th} is read off as a measure of the relative intensity.

EVALUATION

While making these measurements, it is unavoidable that the intensity of the ambient light will be detected as well as that from the source. For this reason, an offset is calibrated on the microvoltmeter before the actual measurements are made.

To check the calibration, a general straight line is drawn through the measured points.

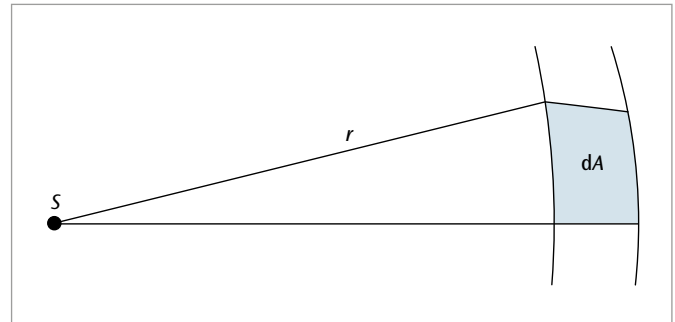


Fig. 1: Square of distance

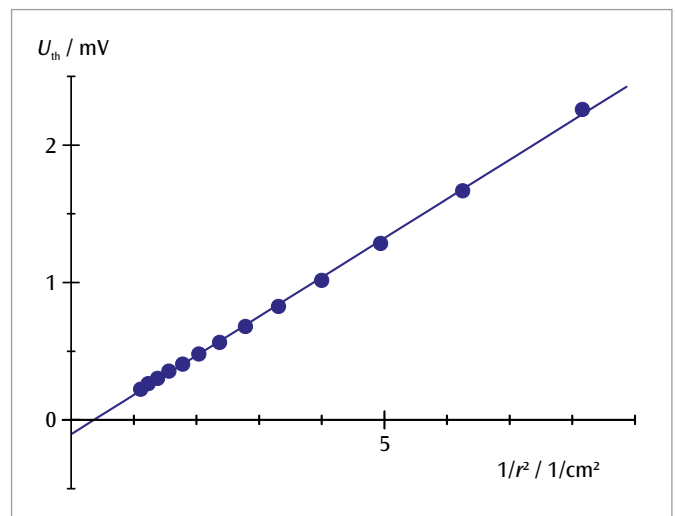


Fig. 2: Measurements plotted in a graph of U_{th} against $1/r^2$

UE4050200 | STEFAN-BOLTZMANN LAW



EXPERIMENT PROCEDURE

- Make a relative measurement of the intensity of radiation from an incandescent lamp with a tungsten filament as a function of temperature with the help of a Moll thermopile.
- Measure the resistance of the filament in order to determine the filament's temperature.
- Plot the measurements in a graph of $\ln(U_{th})$ against $\ln(T)$ and determine the exponent from the slope of the resulting straight line.

OBJECTIVE

Verify that intensity of radiation is proportional to the fourth power of the temperature, T^4

SUMMARY

The Stefan-Boltzmann law describes how the intensity of radiation from a black body depends on temperature. Similar dependence on temperature is exhibited by the intensity of radiation from an incandescent lamp with a tungsten filament. In this experiment, a Moll thermopile is used to make a relative measurement which verifies the law. The temperature of the filament can be determined from the way its resistance depends on temperature, which can be determined very accurately using a four-wire method.

REQUIRED APPARATUS

Quantity	Description	Item Number
1	Stefan Boltzmann Lamp	1008523
1	DC Power Supply 0 – 20 V, 0 – 5 A (230 V, 50/60 Hz)	1003312 or
	DC Power Supply 0 – 20 V, 0 – 5 A (115 V, 50/60 Hz)	1003311
1	Moll-Type Thermopile	1000824
3	Digital Multimeter P1035	1002781
2	Barrel Foot, 1000 g	1002834
1	Set of 15 Safety Experiment Leads, 75 cm	1002843

BASIC PRINCIPLES

Both the total intensity and the spectral distribution of the heat radiation from a body are dependent on the body's temperature and the nature of its surface. At a certain wavelength and temperature the better the body can absorb the radiation, the more radiation it can emit. A black body, a body with ideal surface characteristics, fully absorbs radiation of all wavelengths and can therefore emit the greatest amount of thermal radiation for a given temperature. Such a body is assumed when investigating how radiation of heat depends on temperature.

The Stefan-Boltzmann law describes how the intensity of radiation S from a black body depends on temperature.

$$(1) \quad S_0 = \sigma \cdot T^4$$

T : absolute temperature

$$\sigma = 5,67 \cdot 10^{-8} \frac{\text{W}}{\text{m}^2 \text{K}^4} : \text{Stefan-Boltzmann constant}$$

It is not possible to determine this intensity directly, since the body will also simultaneously be absorbing radiation from its surroundings. The intensity as measured is therefore

$$(2) \quad S_1 = \sigma \cdot (T^4 - T_0^4)$$

T_0 : absolute temperature of surroundings

Light emitted from an incandescent lamp also counts as heat radiation. In this case, the temperature of the filament is determined in such a way that a large amount of the heat is emitted in the spectrum of visible light. The way the total intensity of radiation depends on temperature is equivalent to that of a black body:

$$(3) \quad S = \varepsilon \cdot \sigma \cdot (T^4 - T_0^4)$$

This is because the filament absorbs a proportion ε of radiation of all frequencies.

An incandescent lamp of this kind with a tungsten filament will be investigated in this experiment in order to determine how the intensity of radiation depends on the temperature. A Moll thermopile is used to measure relative radiation intensity. The temperature of the filament can be determined using the temperature-dependency of its resistance:

$$(4) \quad R = R_0 (1 + \alpha \cdot (T - T_0))$$

R_0 : resistance at ambient temperature T_0

$$\alpha = 4,4 \cdot 10^{-3} \frac{1}{\text{K}} \text{ for tungsten}$$

R can be determined very accurately using a four-wire measurement.

EVALUATION

The following expression for temperature T is derived from equation (4)

$$T = \frac{R - R_0}{\alpha \cdot R_0} + T_0$$

However, equation (4) only applies as a good approximation. For more accurate results, it is possible to use a table provided in the operating instructions for the Stefan-Boltzmann lamp.

In this experiment, temperatures T are chosen to be so high that the ambient temperature T_0 can be ignored in equation (3). Instead of the absolute intensity S , the thermopile voltage U_{th} is read off as a measure of relative intensity. Equation (3) can then be rewritten as

$$U_{\text{th}} = a \cdot T^4 \text{ or } \ln(U_{\text{th}}) = \ln(a) + 4 \cdot \ln(T)$$

This means that a graph of $\ln(U_{\text{th}})$ against $\ln(T)$ will show all the measurement points along a straight line of gradient 4.

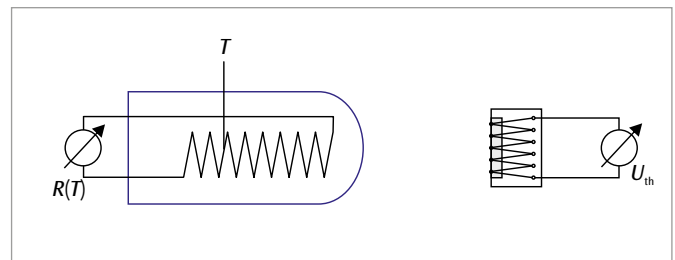


Fig. 1: Schematic of set-up

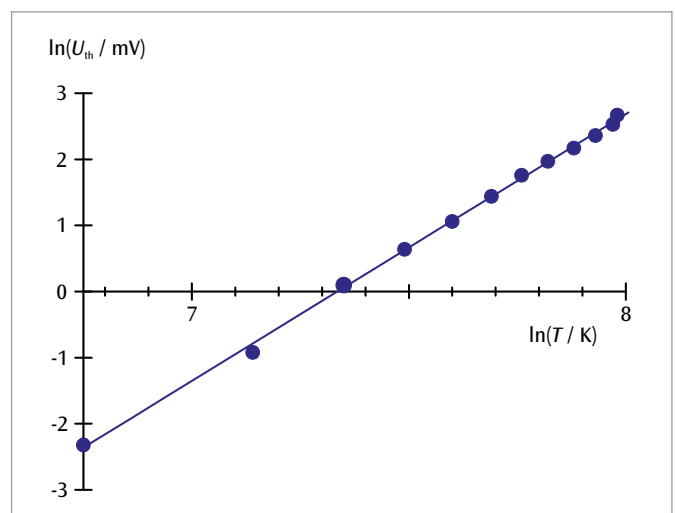


Fig. 2: Graph of $\ln(U_{\text{th}})$ against $\ln(T)$

UE4060100

DETERMINATION OF THE VELOCITY OF LIGHT



EXPERIMENT PROCEDURE

- Measuring the transit time of a short pulse of light across a known distance, by using an oscilloscope to compare it with a reference signal.
- Determining the velocity of light in air as a quotient of the distance travelled and the transit time.

OBJECTIVE

Determine the velocity of light from the transit time of short light pulses

SUMMARY

The fact that light is propagated at a finite speed can be demonstrated by a simple transit time measurement. This is achieved by using very short light pulses of only a few nanoseconds duration and determining the time for them to travel out and back over a distance of several meters, which is measured by an oscilloscope. From the transit time and the distance from the transmitter to a triple-prism reflector one can calculate the velocity of light.

REQUIRED APPARATUS

Quantity	Description	Item Number
1	Speed of Light Meter (115 V, 50/60 Hz)	1000882 or
	Speed of Light Meter (230 V, 50/60 Hz)	1000881
1	Digital Oscilloscope 2x100 MHz	1020911
1	Optical Bench U, 600 mm	1003040
2	Optical Rider U, 75 mm	1003041
1	Barrel Foot	1001045
1	Stainless Steel Rod 1500 mm	1002937
1	Universal Clamp	1002830
1	Pocket Measuring Tape, 2 m	1002603

BASIC PRINCIPLES

The fact that light is propagated at a finite speed can be demonstrated by a simple transit time measurement using modern measurement techniques. This is achieved by using very short light pulses of only a few nanoseconds duration and determining the time for them to travel out and back over a distance of several meters, which is measured by an oscilloscope.

In the experiment, the short light pulses from a pulsed LED are passed via a beam-splitter onto two photoelectric cells whose amplified signals are recorded as voltage pulses by the oscilloscope. Photocell A receives light pulses reflected back by a triple-prism reflector at a large distance, whereas photocell B records the locally generated light pulse as a reference pulse that is not delayed by transit. The oscilloscope trace is triggered by a voltage pulse from output C, which precedes the reference pulse by 60 ns.

Using a two-channel oscilloscope, one measures the transit time as the difference t between the two pulses. From this and the distance s from the transmitter to the triple-prism reflector, we can calculate the velocity of light as:

$$(1) \quad c = \frac{2 \cdot s}{t}$$

The experiment can be made more impressive by varying the distance to the reflector and observing the resulting change of the pulse separation on the oscilloscope. This can be done very easily, as careful and precise adjustments in repositioning the triple-prism reflector are not required, rather, an approximate adjustment will suffice.

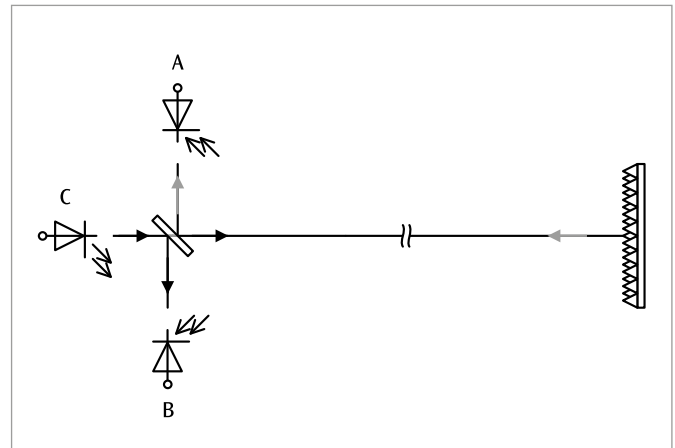


Fig. 1: Measurement principle

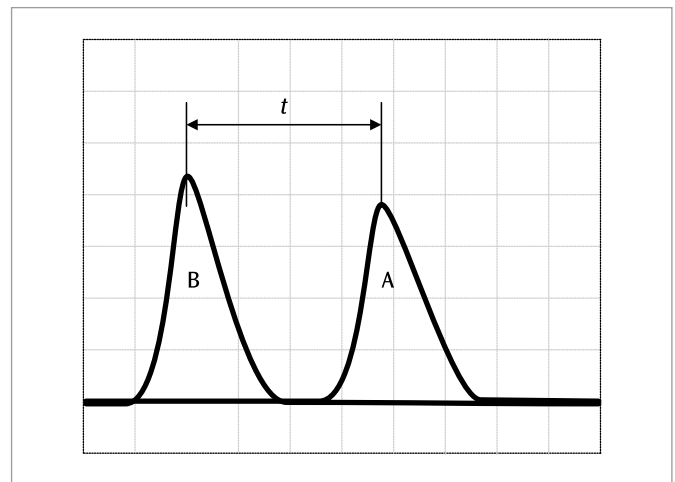
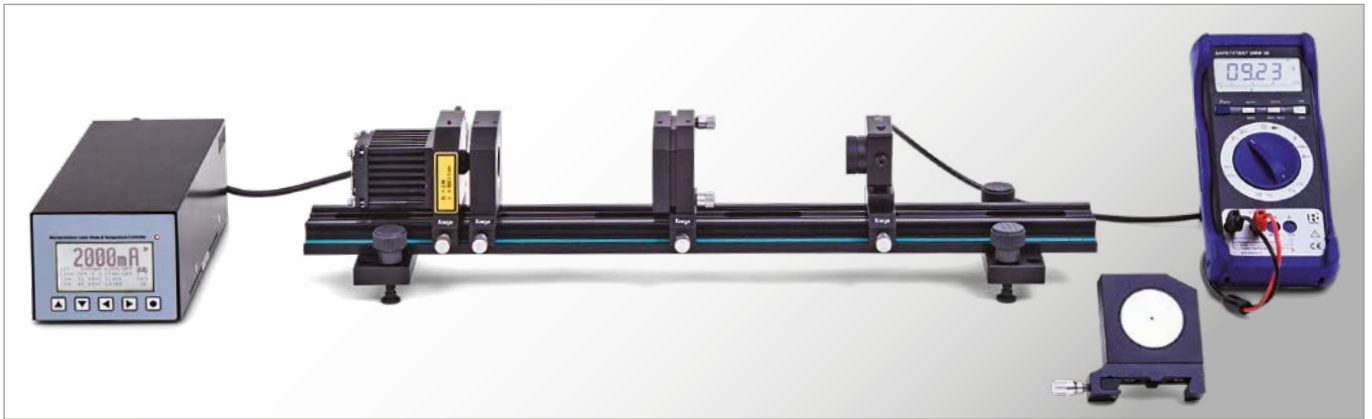


Fig. 2: Measuring the transit time with the oscilloscope

UE4070310 | ND:YAG LASERS



EXPERIMENT PROCEDURE

- Calibrate the diode laser for stable optical pumping of the Nd:YAG laser.
- Determine the lifetime of the top laser energy level ${}^4F_{3/2}$ in the Nd:YAG crystal.
- Adjust the resonator and observe the resonator modes.
- Measure the output power of the Nd:YAG laser as a function of the pumping power and determine the lasing threshold.
- Observing spiking when the laser diode is being operated in pulsed mode.



WARNING

This experiment uses a class 4 laser set-up emitting in the non-visible (infra-red) spectrum. For this reason, goggles for protection against laser light must be worn at all times. Do not look directly into the laser beam even while wearing protective goggles.

OBJECTIVE

Set up and optimize an Nd:YAG laser

SUMMARY

In this experiment an Nd:YAG laser with a diode laser pump is to be set up and optimized. Once the diode laser is calibrated for stable optical pumping and the resonator has been optimized, the system can then be used as an Nd:YAG laser. An investigation is to be made of both steady-state and non-steady-state operation and the lifetime of the top laser energy level ${}^4F_{3/2}$ in the Nd:YAG crystal will then be determined.

REQUIRED APPARATUS

Quantity	Description	Item Number
1	Laser Diode Driver and Two-Way Temperature Controller Dsc01-2.5	1008632
1	Optical Bench KL	1008642
1	Diode Laser 1000 mW	1009497
1	Nd:YAG Cristal	1008635
1	Collimator lens $f = +75$ mm	1008646
1	Laser Mirror I	1008638
1	PIN Photodiode	1008640
1	Filter RG850	1008648
1	Alignment Laser Diode	1008634
1	Transport Case KL	1008651
1	Laser Safety Goggles for Nd:YAG Laser	1002866
1	Digital Multimeter P3340	1002785
1	Digital Oscilloscope 2x100 MHz	1020911
1	HF Patch Cord, BNC/4 mm Plug	1002748
1	HF Patch Cord	1002746
1	IR Detector Card	1017879

BASIC PRINCIPLES

An Nd:YAG laser is a solid-state laser which emits an infra-red beam. The laser medium is a neodymium-doped yttrium-aluminium garnet crystal. Pumping is handled by a semiconductor laser. Usually the light emitted has a wavelength of 1064 nm.

Fig. 1 shows the energy levels for an Nd:YAG crystals with the most important transitions for optical pumping and laser operation. By means of optical pumping using light with an approxi-

mate wavelength of 808 nm, transitions can be excited between the ground state (1) and the top pumping level (4). Its lifetime is very short and rapid, non-radiating transitions take place into the upper metastable excited laser level (3). This prevents transitions occurring back into the ground state. The lasing transition of wavelength $\lambda = 1064$ nm takes place into the lower excited laser level (2). This has a very short lifetime and decays without emission into the ground state. This means that each of the levels is occupied to a certain extent. States 4 and 2, however, decay so quickly that the number of atoms in each of these states can be assumed to be close to zero. This means that the dynamic response of the laser can be described using the following rate equations for inversion density n (the difference in the number density of atoms in Nd energy levels 2 and 3) and photon density p of the laser field:

$$(1a) \quad \frac{dn}{dt} = W \cdot (N_{Nd} - n) - \sigma \cdot c \cdot p \cdot n - \frac{n}{\tau_3}$$

$$(1b) \quad \frac{dp}{dt} = \frac{L_{Nd}}{L} \cdot \sigma \cdot c \cdot p \cdot n - \frac{p}{\tau_{res}}$$

W : pumping rate

N_{Nd} : number density of Nd atoms

σ : effective cross section for emission or absorption of a photon

c : speed of light

τ_3 : lifetime of excited laser level 3

L : length of resonator

L_{Nd} : length of Nd:YAG crystal

τ_{res} : time constant for resonator losses

In (1a) the first term relates to the optical pumping, the second refers to the induced emission and the third covers the decay from the top laser level via spontaneous emission. The first term in (1b) concerns creation of a photon by induced emission, while the second describes the fall in the photon density due to losses in the resonator. For greater accuracy, it is also necessary to take into account that photons are already present at the start of the process due to spontaneous emission.

For steady-state operation and disregarding spontaneous emission, the following solution is obtained:

$$(2) \quad p = \frac{1}{\sigma \cdot c \cdot \tau_3} \cdot \frac{W - W_s}{W_s}$$

where $W_s = \frac{1}{\tau_3} \cdot \frac{n_l}{n_l - N_{Nd}}$ $n_l = \frac{L}{L_{Nd} \cdot \sigma \cdot c \cdot \tau_{res}}$

The pumping rate therefore needs to exceed a certain threshold, after which the photon density rises linearly in proportion to the pumping rate. It is not possible to measure the photon density and pumping rate directly. Therefore the experiment will demonstrate that the output power of the laser PL is linearly dependent on the pumping power above a certain threshold.

Fig. 2 shows solutions of the rate equations for non-steady-state operation. In this case there is an initial rise in the photon population inversion. Once the threshold inversion n_l has been reached, the inversion density increases linearly. There is a rapid rise in photon density and the inversion density falls to a value slightly below the threshold. As this process is repeated, the overshoot of the inversion density gradually decreases until the system settles into the steady state. The experiment will also demonstrate this so-called spiking. First, though, the wavelength of the diode laser used for the pumping is calibrated to the transition where $\lambda = 808$ nm and then the change in the spontaneous emission over time is measured with the diode laser operating in pulsed mode (Fig. 3). From these measurements

it is possible to determine the lifetime of the upper laser level. Once the resonator is set up and calibrated, spiking may be observed (Fig. 4). Finally the output power is measured as a function of the pumping power.

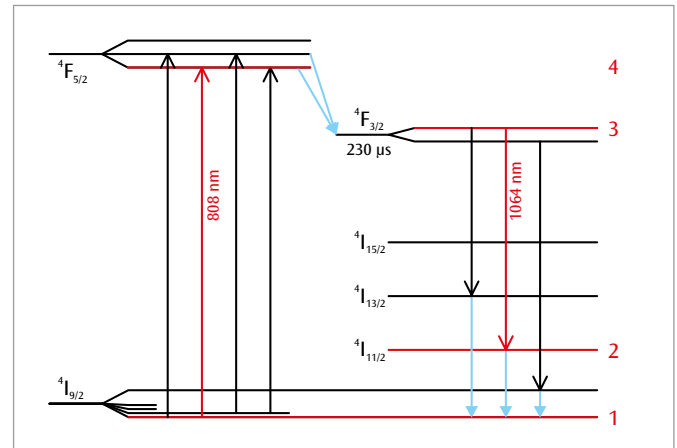


Fig. 1: Energy level diagram for Nd:YAG crystal. The transitions which are relevant to this experiment are indicated in red

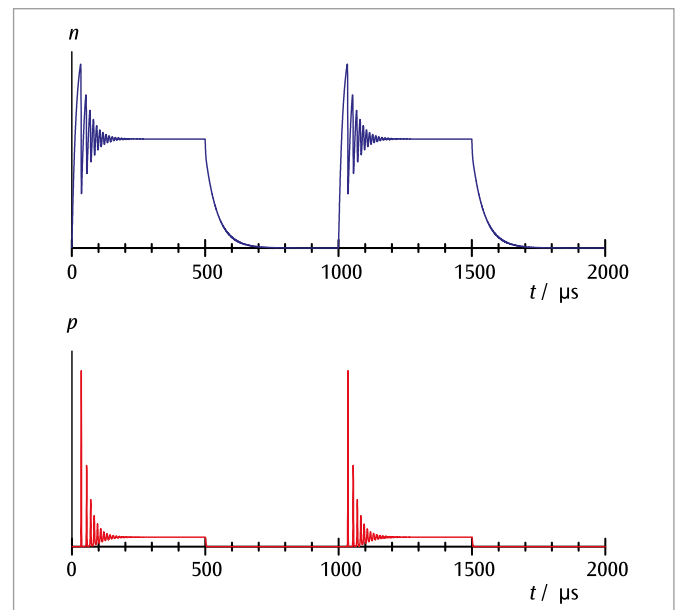


Fig. 2: Non-static solutions of the rate equations (spiking)

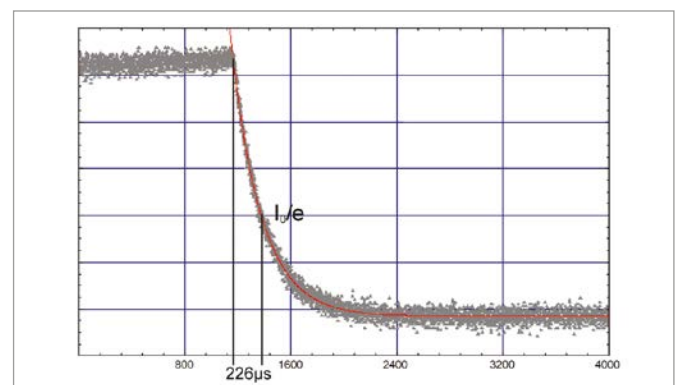


Fig. 3: Measurement of spontaneous emission in order to determine the lifetime of the upper laser level

UE4070320 | Q-SWITCHING FOR ND:YAG LASER



EXPERIMENT PROCEDURE

- Set up and optimize a Q-switching circuit for an Nd:YAG lasers using a Cr:YAG module.
- Record the pulses and determine their duration.

OBJECTIVE

Q-switching circuit for Nd:YAG laser with Cr:YAG module

SUMMARY

Q-switching of a laser makes it possible to generate short, high-energy pulses. It works by controlling the laser threshold by increasing or decreasing resonator losses. You are to implement a passive Q-switching circuit with the help of a Cr:YAG module and then record the laser pulsing over time. The energy of the pulses can be calculated from the average power and the frequency with which they are repeated.

REQUIRED APPARATUS

Quantity	Description	Item Number
1	Laser Diode Driver and Two-Way Temperature Controller Dsc01-2.5	1008632
1	Optical Bench KL	1008642
1	Diode Laser 1000 mW	1009497
1	Nd:YAG Cristal	1008635
1	Passive Q-Switch	1008637
1	Laser Mirror I	1008638
1	PIN Photodiode, Fast	1008641
1	Filter RG850	1008648
1	Alignment Laser Diode	1008634
1	Transport Case KL	1008651
1	Laser Safety Goggles for Nd:YAG Laser	1002866
1	Digital Multimeter P3340	1002785
1	Digital Oscilloscope 2x100 MHz	1020911
1	HF Patch Cord, BNC/4 mm Plug	1002748
1	HF Patch Cord	1002746
1	IR Detector Card	1017879



WARNING

This experiment involves operation of class-4 laser equipment which emits light in the (invisible) infra-red part of the spectrum. Goggles which protect against laser light should always be worn. Even when wearing such goggles, never look at the laser beam directly.

BASIC PRINCIPLES

Q-switching (also called giant pulse formation) makes it possible to generate short, high-energy laser pulses, as required in the processing of materials, for example. It works by controlling the laser threshold by increasing or decreasing resonator losses. When losses are high, it prevents the build-up of oscillation in the resonator and causes pumping energy to be stored in the laser crystal. Once the resonator is enabled by reducing the losses, a laser pulse of intensity orders of magnitude greater than the intensity in continuous mode is generated. The difference between this and spiking is that the inversion density with Q-switching far exceeds the threshold value. A distinction is made between active and passive Q-switching. Passive Q-switches are absorbers in which the capacity to absorb can be modified by means of the light in the resonator. Active switches are typically acousto-optic, electro-optic or mechanical switches, which control the transmission externally.

Use of an absorbing crystal as a passive Q-switch requires that the absorption can be saturated. That means that its effective absorption cross section must be larger than that for the light from atoms in an excited state, also that the lifetime of the excited level is both longer than the duration of the laser pulse and shorter than the frequency of repetition. A Cr:YAG crystal fulfils all these criteria.

In order to fully describe the dynamic response of the passively Q-switched laser, the rate equation for the inversion density n achievable by means of optical pumping in an Nd:YAG crystal for a photon density p in the field of the laser light (see experiment UE4070310) also needs to take into account the population density in the ground state of the Cr:YAG crystal. Due to the extremely rapid increase of the photon density, both the pumping rate and the rate of spontaneous emission can be disregarded. The threshold for the inversion density is defined as follows:

$$(1) \quad n_s = \frac{1}{\sigma \cdot c \cdot \tau_{\text{res}}}$$

τ_{res} : time constant for reduction in photon density due to resonator losses

σ : effective cross section for emission or absorption of a photon
 c : speed of light

This implies that the change in inversion density n and in the photon density p over time is given by:

$$(2a) \quad \frac{dn}{dt} = -\frac{n}{n_s} \cdot \frac{p}{\tau_{\text{res}}}$$

and

$$(2b) \quad \frac{dp}{dt} = -\left(\frac{n}{n_s} - 1\right) \cdot \frac{p}{\tau_{\text{res}}}$$

In a giant pulse, the inversion density is approximately constant and remains almost equal to the initial inversion density:

$$(3) \quad n(t) = n_i$$

Equation (2b) can then be used to determine the photon density:

$$(4) \quad p(t) = \exp\left[\left(\frac{n_i}{n_s} - 1\right) \cdot \frac{t}{\tau_{\text{res}}}\right]$$

The inversion density n_i for a giant pulse is very much greater than the threshold inversion density n_s . That means that the time it takes for the photon density to increase is much shorter than the time constant τ_{res} for resonator losses.

Another key point in time is reached when the inversion density falls back to the threshold level. Then the photon density ceases to change as described in equation (2b), i.e. no more laser photons are generated. Equation (2a) then gives us:

$$(5) \quad \frac{dn}{dt} = -\frac{p_{\text{max}}}{\tau_{\text{res}}} \quad \text{where } p(t) = p_{\text{max}}$$

The photon density therefore falls after reaching its maximum with a time constant equal to that for the resonator losses.

The maximum value for the photon density is given by the following:

$$(6) \quad p_{\text{max}} = n_s \cdot \ln\left(\frac{n_i}{n_s}\right) - (n_i - n_s)$$

This means that lasers with an upper laser level that has a very short lifetime, i.e. which only have a very small excess inversion density, do not exhibit any significant increase in output power when used in pulsed mode.

In this experiment the Cr:YAG module is added to the resonator and fine adjustment of the laser is carried out anew. The laser signal is measured using a PIN diode and traced on an oscilloscope.

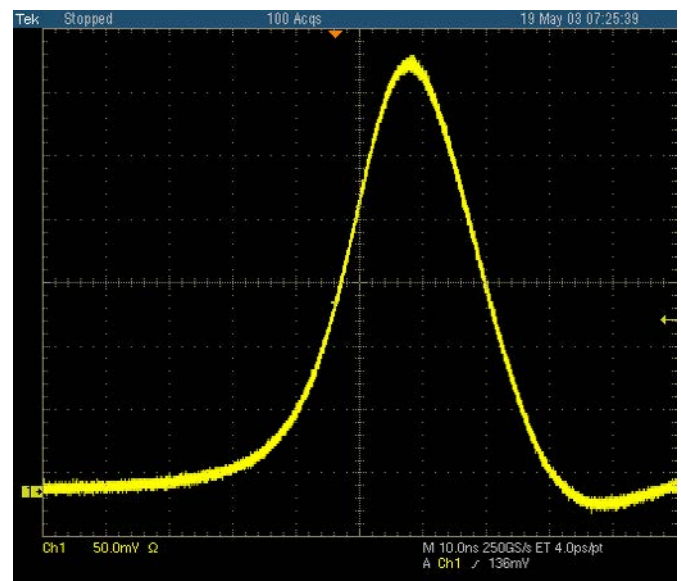
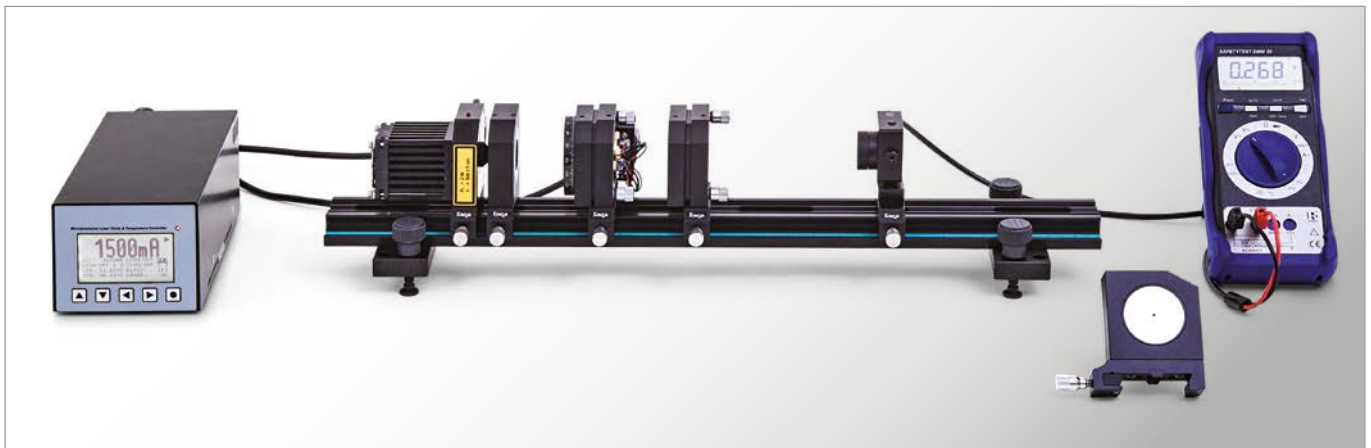


Fig. 1: Pulse over a period of time for an Nd:YAG laser with passive Q-switching

UE4070330 | ND:YAG-LASER



EXPERIMENT PROCEDURE

- Generate radiation at double the original frequency by adding a KTP crystal to the resonator.
- Measure the output power of the radiation at the doubled frequency as a function of the power associated with the fundamental wave.
- Study how the generated radiation depends on the alignment of the crystal and the temperature.

OBJECTIVE

Frequency doubling inside the resonator of a Nd:YAG laser

SUMMARY

Materials often change their optical properties in strong electromagnetic fields. For instance, it is possible for the frequency of high-intensity laser light passing through such materials to be doubled. In this experiment, a KTP (potassium titanyl phosphate) crystal is used to generate green light with a wavelength of 532 nm from the 1064-nm infra-red radiation output by an Nd:YAG laser by means of frequency doubling. The crystal is suitable in a number of respects, such as its strongly non-linear optical characteristics, and its low absorption of radiation at the original frequency and double the frequency.

REQUIRED APPARATUS

Quantity	Description	Item Number
1	Laser Diode Driver and Two-Way Temperature Controller Dsc01-2.5	1008632
1	Optical Bench KL	1008642
1	Diode Laser 1000 mW	1009497
1	Nd:YAG Cristal	1008635
1	Frequency Doubling Module	1008636
1	Laser Mirror II	1008639
1	PIN Photodiode	1008640
1	Filter BG40	1017874
1	Alignment Laser Diode	1008634
1	Transport Case KL	1008651
1	Laser Safety Goggles for Nd:YAG Laser	1002866
1	Digital Multimeter P3340	1002785
1	HF Patch Cord, BNC/4 mm Plug	1002748
1	IR Detector Card	1017879



WARNING

This experiment involves operation of class-4 laser equipment which emits light in the (invisible) infra-red part of the spectrum. Goggles which protect against laser light should always be worn. Even when wearing such goggles, never look at the laser beam directly.

BASIC PRINCIPLES

Materials often change their optical properties in strong electromagnetic fields. For instance, it is possible for the frequency of high-intensity laser light passing through such materials to be doubled. To describe such phenomena it is necessary to consider the polarization, which changes in a way which is not linearly proportional to electric field strength.

If the material is non-magnetic, the wave equation for the electric field strength E has the following form:

$$(1) \quad \Delta \mathbf{E}(\mathbf{r}, t) - \frac{1}{c^2} \cdot \frac{\partial^2 \mathbf{E}(\mathbf{r}, t)}{\partial t^2} = \frac{1}{\epsilon_0 \cdot c^2} \cdot \frac{\partial^2 \tilde{\mathbf{P}}(\mathbf{r}, t)}{\partial t^2}$$

$\tilde{\mathbf{P}}$: Polarization of the material

ϵ_0 : Electric field constant

c : Speed of light

The relationship between polarization and field strength is non-linear and is described by the following equation:

$$(2) \quad \tilde{\mathbf{P}}(t) = \epsilon_0 \cdot (\chi_1 \cdot E(t) + \chi_2 \cdot E(t)^2)$$

χ_1, χ_2 : First- and second-order susceptibilities

Correspondingly, an electric field oscillating at a frequency f and described by the equation

$$(3) \quad E(t) = E_0 \cdot \exp(i \cdot 2\pi \cdot f \cdot t)$$

produces polarization comprising two components. The component

$$(4) \quad \tilde{P}_1(t) = \epsilon_0 \cdot \chi_1 \cdot E_0 \cdot \exp(i \cdot 2\pi \cdot f \cdot t)$$

oscillates at the original frequency f and describes how the speed of light changes inside the material. The component

$$(5) \quad \tilde{P}_2(t) = \epsilon_0 \cdot \chi_2 \cdot E_0^2 \cdot \exp(i \cdot 2\pi \cdot 2f \cdot t)$$

oscillates at double the frequency, $2f$, and acts as a source for a new component of the electromagnetic field in accordance with equation (1).

When regarded at photon level, this means that two photons with a frequency f are converted into one photon with a frequency $2f$ (see Figure 1). Due to conservation of momentum, the yield here is especially large if the mismatch in phases closely approximates to zero.

$$(6) \quad \Delta k \cdot \frac{L}{2} = \left| 2 \cdot \frac{2\pi}{\lambda_f} - \frac{2\pi}{\lambda_{2f}} \right| \cdot \frac{L}{2} = \frac{2\pi}{c} \cdot f \cdot L \cdot |n_f - n_{2f}|$$

L : Length of resonator

λ_f, λ_{2f} : Wavelengths in the material at the original frequency and double the frequency

The refractive indices of the material n_f and n_{2f} should therefore match as far as possible. This can be achieved in birefringent materials with a high degree of anisotropy in three dimensions if they are suitably aligned (see Fig 2). As a consequence, the yield depends on the spatial alignment of the frequency-doubling material.

The power density P_{2f} of the new radiation has a quadratic relationship with the power density P_f of the fundamental radiation. The following applies:

$$(7) \quad P_{2f} = P_f^2 \cdot \frac{L^2}{A} \cdot C \cdot F\left(\Delta k \cdot \frac{L}{2}\right) \text{ where } F(x) = \left(\frac{\sin x}{x}\right)^2$$

A : Cross-sectional area of resonator

C : Material constant at the given wavelength

In this experiment, a crystal of KTiOPO_4 is used to generate green light with a wavelength of 532 nm from the 1064-nm infra-red radiation output by an Nd-YAG laser by means of frequency doubling. The crystal is suitable in a number of respects, such as its strongly non-linear optical characteristics, and its low absorption of radiation at the original frequency and double the frequency.

EVALUATION

To prove that the output depends on the square of the primary power P_f , use is made of the fact demonstrated in the previous experiment that the power depends on the laser diode's injection current I .

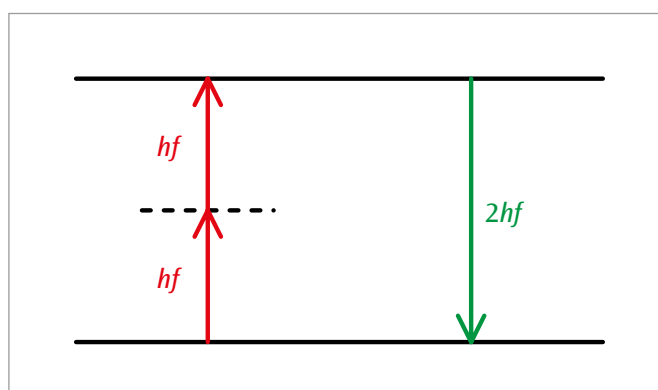


Figure 1: Schematic representation of frequency doubling

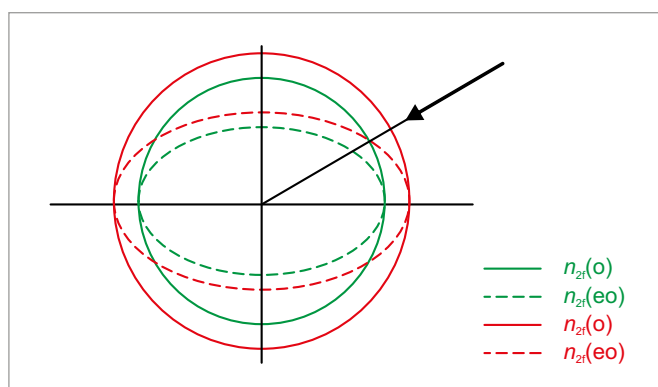


Figure 2: Schematic representation of phase matching through use of birefringence in the material

$n(o)$: Refractive index for ordinary ray

$n(eo)$: Refractive index for extraordinary ray

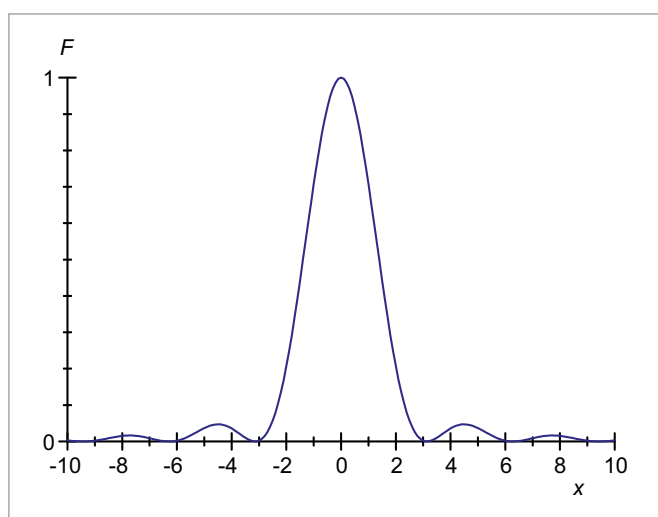


Figure 3: Representation of the function $F(x)$

UE4080100 | PRISM SPECTROMETER



OBJECTIVE

Set up and calibrate a prism spectrometer

SUMMARY

A prism spectrometer utilizes the dispersion of light into its spectral components by means of a prism to measure optical spectra. In order to measure wavelengths, it is necessary to calibrate the system since the angular dispersion is non-linear. In this experiment the known spectrum of a mercury (Hg) lamp will be used for calibration purposes and then measurements will be made for a cadmium (Cd) lamp.

EXPERIMENT PROCEDURE

- Make adjustments to a prism spectrometer and calibrate it using the spectral lines from a mercury lamp.
- Measure the minimum angle of deflection when $\lambda = 546.07$ nm.
- Determine the refractive index of flint glass when $\lambda = 546.07$ nm and the Cauchy parameters b and c for the wavelength-dependent refractive index.
- Calculate a calibration curve according to the Hartmann dispersion formula.
- Make measurements on an unknown line spectrum.

REQUIRED APPARATUS

Quantity	Description	Item Number
1	Spectrometer-Goniometer S	1008673
1	Control Unit for Spectrum Lamps (230 V, 50/60 Hz)	1021409 or
	Control Unit for Spectrum Lamps (115 V, 50/60 Hz)	1003195
1	Spectral Lamp Hg/Cd	1003546
1	Spectral Lamp Hg 100	1003545

BASIC PRINCIPLES

Prism spectrometers are used to measure optical spectra using the dispersion of light into its spectral components when it passes through a prism. This dispersion results from the fact that the refractive index is dependent on wavelength. It is non-linear and therefore the prism spectrometer needs to be calibrated in order to measure wavelengths.

Inside the spectrometer, the light being investigated passes through slit S to strike the objective O_1 . These two components form a collimator and produce a wide, parallel beam of light (see Fig. 1). After refracting at two surfaces of the prism, a parallel beam exits the prism and is focussed to an image of the slit in the focal plane of objective O_2 . This can then be viewed via the ocular lens OC. The telescope formed by objective O_2 and ocular OC is attached to a swivelling arm which is rigidly connected to the vernier scale N.

The double refraction of the light by the prism can be described by the angles α_1 , α_2 , β_1 and β_2 (see Fig. 2). The following relationships are true for an equilateral prism:

$$(1) \quad \sin \alpha_1 = n(\lambda) \cdot \sin \beta_1(\lambda) \quad ; \quad n(\lambda) \cdot \sin \beta_2(\lambda) = \sin \alpha_2(\lambda) \quad ; \quad \beta_1(\lambda) + \beta_2(\lambda) = 60^\circ$$

The angle of incidence α_1 can be altered by turning the prism with respect to the parallel beam which enters it. Angles α_2 , β_1 and β_2 are dependent on the wavelength λ since the refractive index n is wavelength-dependent.

The angle of deflection between the collimator and the telescope is determined from the angle of incidence α_1 and the exit angle α_2 .

$$(2) \quad \delta(\lambda) = \alpha_1 + \alpha_2(\lambda) - 60^\circ$$

The angle is at its minimum δ_{\min} , when the path of the beam is symmetrical with respect to the prism. At the same time the angular dispersion $d\delta/d\lambda$ will be at its maximum. Prism spectrometers are therefore adjusted in such a way that a symmetrical beam path is attained for a reference wavelength λ_0 . In this experiment, the green spectral line ($\lambda_0 = 546.07$ nm) of a

mercury lamp is chosen for this. The refractive index of the prism at the reference wavelength can be determined from the minimum angle of deflection. This is because the symmetry implies that $\beta_1(\lambda_0) = \beta_2(\lambda_0) = 30^\circ$ and $\alpha_2(\lambda_0) = \alpha_1$, therefore:

$$(3) \quad \sin \alpha_1 = n(\lambda_0) \cdot \frac{1}{2} \quad \text{where} \quad \alpha_1 = \frac{\delta_{\min}}{2} + 30^\circ$$

The dispersion means that the other spectral lines are shifted from δ_{\min} by small angles $\Delta\delta$. You will be able to read off these angles to an accuracy of minutes using the vernier scale. Since the changes in refractive index Δn remain small over the entire visible part of the spectrum, it is sufficient to consider only the linear terms in the changes. Therefore from equations 1 – 3 the following relationship can be derived between the wavelengths and deflection:

$$(4) \quad \Delta\delta(\lambda) = \Delta\alpha_2(\lambda) = \frac{\Delta n(\lambda)}{\cos \alpha_1} = \frac{\Delta n(\lambda)}{\sqrt{1 - \frac{(n(\lambda_0))^2}{4}}}$$

In the visible part of the spectrum, the refractive index n decreases as the wavelength λ increases. This can be described by the Cauchy equation in the following form:

$$(5) \quad n(\lambda) = a + \frac{b}{\lambda^2} + \frac{c}{\lambda^4}$$

In principle, it is possible to obtain a mathematical description for a calibration curve from equations (4) and (5). However, the Hartmann dispersion formula turns out to be better suited to the purpose.

$$(6) \quad \delta(\lambda) = \delta_H + \frac{K}{\lambda - \lambda_H}$$

The modifying parameters δ_H , K and λ_H in the above do not, however, have any specific physical meaning.

For this reason, in the experiment the spectral lines of the mercury lamp are utilized for calibration purposes with the help of equation (6) and afterwards the lines of an “unknown” spectrum will be measured (see Table 1).

EVALUATION

The refractive index $n(\lambda_0)$ is given from equation 3. The Cauchy parameters for the refractive index can be calculated by fitting a parabolic curve to the equation $\Delta n = n(\lambda) - n(\lambda_0) = f(1/\lambda^2)$.

Table 1: Wavelengths of lines in Cd spectrum

Color	Measurement λ / nm	Table value λ / nm
Blue (medium deflection)	466	466
Blue (large deflection)	468	468
Cyan (medium deflection)	479	480
Dark green (large deflection)	509	509
Dark green (less deflection)	515	516
Red (large deflection)	649	644

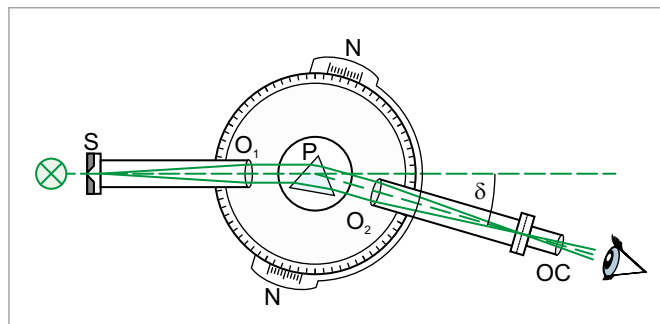


Fig. 1: Schematic of a prism spectrometer

S: Entry slit, O1: Collimator objective, P: Prism, O2: Telescope objective, OC: Telescope eyepiece (ocular), δ : Angle of deflection

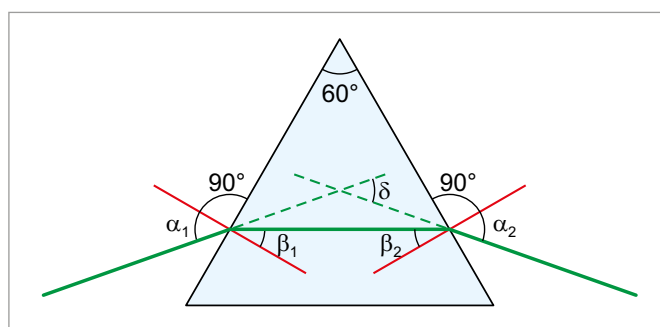


Fig. 2: Beam path through prism

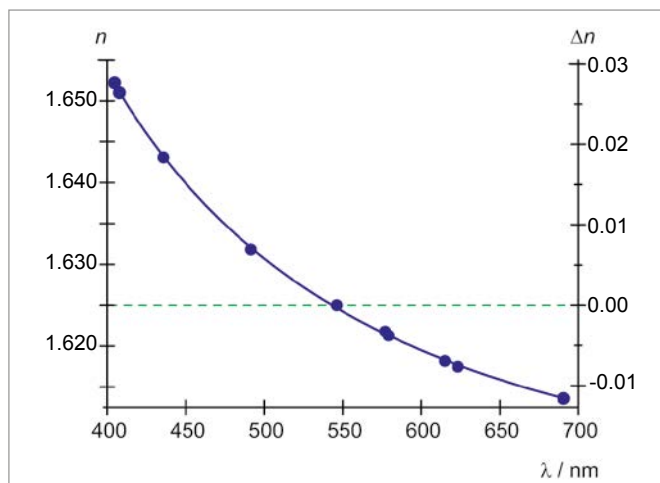


Fig. 3: Wavelength-dependent refractive index for flint glass prism

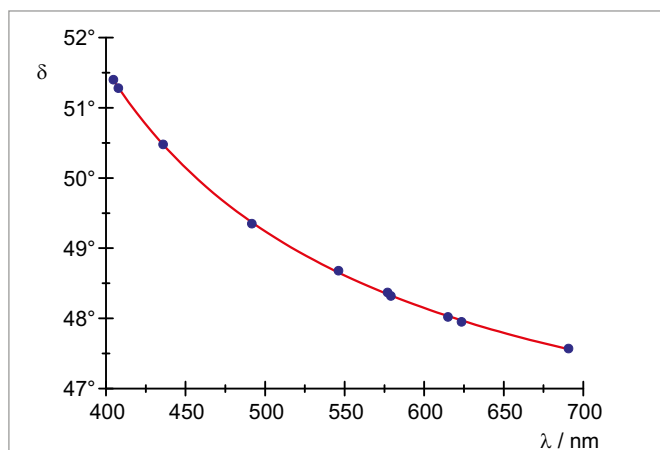


Fig. 4: Calibration curve for prism spectrometer

UE5010200 | PLANCK'S CONSTANT



> EXPERIMENT PROCEDURE

- Measure the cut-off value of the decelerating voltage as a function of the wavelength of light.
- Plot the results in a graph of energy against frequency.
- Determine Planck's constant and the work required to emit an electron.
- Demonstrate that the energy of the electrons does not depend on the intensity of the light.

OBJECTIVE

Determine Planck's constant using the decelerating voltage method

SUMMARY

In a modified version of a classic set-up, light of known frequency passes through a ring-shaped anode to collide with a cathode, where it causes electrons to be released due to the photo-electric effect. The energy of the electrons can be determined by applying a decelerating voltage, which compensates for the flow of electrons towards the anode until no electrons are flowing. This demonstrates that the cut-off value of the decelerating voltage which corresponds to a current of zero is not dependent on the intensity of the light. The energy of the electrons is therefore similarly independent of intensity. By obtaining the cut-off voltages for light of varying frequency, it is possible to calculate Planck's constant.

REQUIRED APPARATUS

Quantity	Description	Item Number
1	Planck's Constant Apparatus (230 V, 50/60 Hz)	1000537 or
	Planck's Constant Apparatus (115 V, 50/60 Hz)	1000536

BASIC PRINCIPLES

The photoelectric effect exhibits two important properties, which were discovered in 1902 by *Lenard*. The number of electrons emitted from the cathode material as a result of the photoelectric effect is proportional to the intensity of the incident light. However, the energy is dependent on the frequency of the light and not on its intensity. In 1905, *Einstein* used a hypothesis based on the description of black body radiation discovered by *Planck* to explain this and thereby laid important foundations for quantum mechanics.

Einstein assumed that light propagates in the form of photons possessing energy proportional to the frequency of the light. If a photon of energy

$$(1) \quad E = h \cdot f$$

$h = 6.626 \times 10^{-34}$ Js: Planck's constant

strikes an electron inside the cathode material, its energy can be transferred to the electron, which is then emitted from the cathode with kinetic energy

$$(2) \quad E_{\text{kin}} = h \cdot f - W$$

The work W required for emission of the electron is a quantity which is dependent on the nature of the material, its value for caesium for example is approximately 2 eV.

In this experiment, the above relationship is used to determine Planck's constant h . Light of a specific frequency f passes through a ring-shaped anode and strikes a cathode, causing electrons to be released. The resulting current from cathode to anode is then measured using a nanoammeter and a decelerating voltage U_0 is applied in order to reduce the current to zero. The light from various LEDs is used. The spectrum of the respective components is sufficiently narrow that a distinctive wavelength λ can be assigned to each of them, from which the frequency can be obtained as follows:

$$(3) \quad f = \frac{c}{\lambda}$$

$$c = 2.998 \times 10^8 \text{ m/s}$$

The intensity of the light from the diodes can be varied between 0% and 100%, meaning that it is possible to investigate how the energy of the electrons depends on the intensity of the light.

EVALUATION

In each case, the current is compensated to a value of zero at the cut-off value of the decelerating voltage U_0 . This definition can be summarized using equations (2) and (3) as follows

$$e \cdot U_0 = h \cdot f - W = h \cdot \frac{c}{\lambda} - W$$

where $e = 1.602 \times 10^{-19}$ As: elementary charge

Planck's constant can therefore be determined from the slope of a graph where values $E = e \cdot U_0$ are plotted along the y-axis and values of $f = \frac{c}{\lambda}$ are plotted along the x-axis.

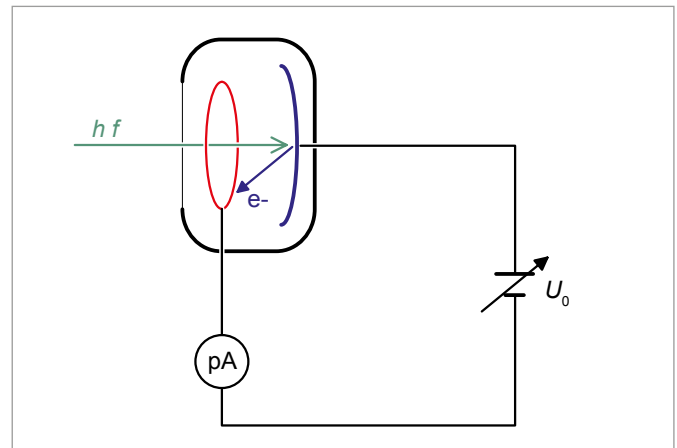


Fig. 1: Schematic of set-up for measurements

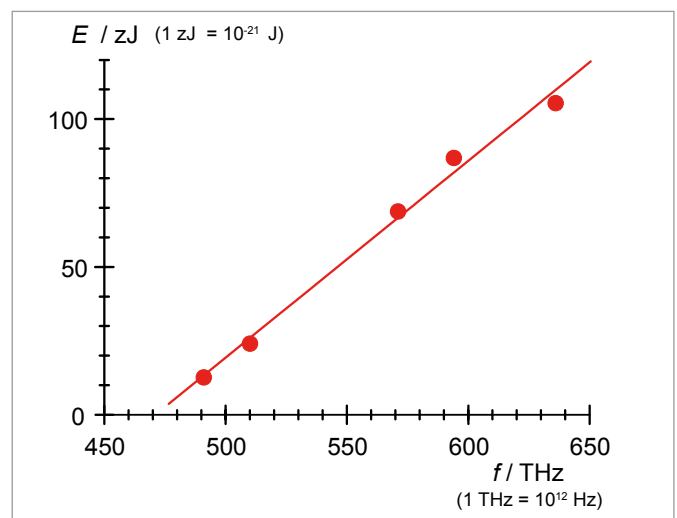


Fig. 2: Graph of energy against frequency

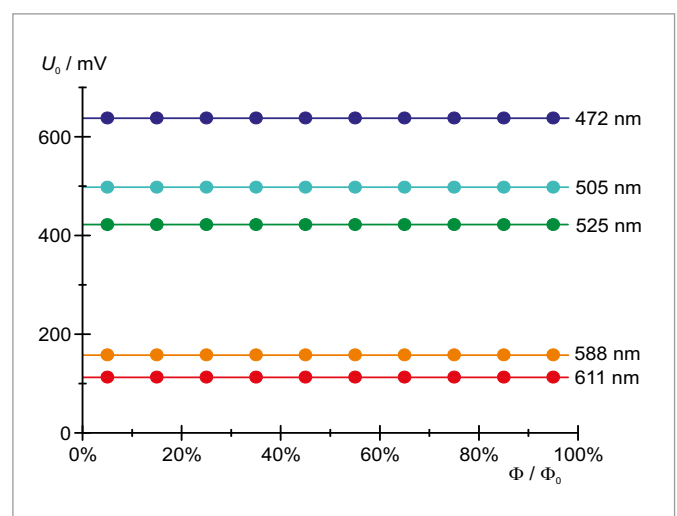


Fig. 3: Cut-off voltage U_0 as a function of intensity

UE5010400 | MILLIKAN'S EXPERIMENT



OBJECTIVE

Carry out Millikan's experiment to confirm the value of the elementary charge with the help of charged oil drops

SUMMARY

Between the years 1910 and 1913, *Robert Andrews Millikan* managed to measure the elementary electric charge to an unprecedented accuracy and thereby confirmed the quantum nature of charge. The experiment which now bears his name is based on measuring the quantity of charge carried by charged drops of oil, which are able to rise through the air under the influence of an electric field from a plate capacitor and descend when the field is absent. The Millikan apparatus used for this version of the experiment utilizes a compact piece of equipment which is based on Millikan's design and which does not require any radioactive source.

EXPERIMENT PROCEDURE

- Produce and select suitable oil drops and observe them in an electric field.
- Measure the speed with which they rise in the electric field and descend without it.
- Confirm the value of the elementary charge.

REQUIRED APPARATUS

Quantity	Description	Item Number
1	Millikan's Apparatus (230 V, 50/60 Hz)	1018884 or
	Millikan's Apparatus (115 V, 50/60 Hz)	1018882

BASIC PRINCIPLES

Between the years 1910 and 1913, *Robert Andrews Millikan* managed to measure the elementary electric charge to an unprecedented accuracy and thereby confirmed the quantum nature of charge. He was awarded the Nobel Prize in physics for his work. The experiment which now bears his name is based on measuring the quantity of charge carried by charged drops of oil, which are able to rise through the air under the influence of an electric field from a plate capacitor and descend when the field is absent. The value he obtained for the elementary charge $e = (1.592 \pm 0.003) \cdot 10^{-19}$ C differs by only 0.6% from the accepted modern value.

The forces which act on a droplet of oil (which we shall assume to be spherical) situated in the electric field of a plate capacitor are the force of gravity,

$$(1) \quad F_G = m_2 \cdot g = \frac{4}{3} \cdot \pi \cdot r_0^3 \cdot \rho_2 \cdot g$$

m_2 : Mass of oil drop, r_0 : Radius of oil drop, ρ_2 : Density of oil, g : Acceleration due to gravity

the drop's buoyancy in air,

$$(2) \quad F_A = \frac{4}{3} \cdot \pi \cdot r_0^3 \cdot \rho_1 \cdot g$$

ρ_1 : Density of air

the force exerted by the electric field E ,

$$(3) \quad F_E = q_0 \cdot E = \frac{q_0 \cdot U}{d}$$

q_0 : Charge on oil drop, U : Voltage between the plates of the capacitor, d : Separation of the capacitor plates

and Stokes' force of friction

$$(4) \quad F_{R1,2} = 6 \cdot \pi \cdot \eta \cdot r_0 \cdot v_{1,2}$$

η : Viscosity of air, v_1 : Speed of ascent, v_2 : Speed of descent

When an oil drop rises in an electric field, the equilibrium equation involves the following forces:

$$(5) \quad F_G + F_{R1} = F_E + F_A$$

During descent the equation is as follows:

$$(6) \quad F_G = F_{R2} + F_A$$

This means we can find the radius of the drop and its charge:

$$(7) \quad r_0 = \sqrt{\frac{9 \cdot \eta \cdot v_2}{2 \cdot (\rho_2 - \rho_1) \cdot g}}$$

and

$$(8) \quad q_0 = \frac{6 \cdot \pi \cdot \eta \cdot d \cdot (v_1 + v_2)}{U} \cdot r_0$$

Very small radii r_0 are of the same order of magnitude as the mean free path of air molecules. This means a correction needs to be made to the Stokes' friction. The corrected radius r and charge q are then given by the following:

$$(9) \quad r = \sqrt{r_0^2 + \frac{A^2}{4}} - \frac{A}{2} \quad \text{where } A = \frac{b}{p}$$

$$b = 82 \mu\text{m} \cdot \text{hPa} = \text{constant}, p: \text{Air pressure}$$

$$(10) \quad q = q_0 \cdot \left(1 + \frac{A}{r}\right)^{-1.5}$$

The Millikan apparatus used for this version of the experiment uses a compact piece of equipment which is based on Millikan's design and which does not require any radioactive source. The charged oil drops are produced with the help of an atomizer, after which the random charge they assume is no longer affected by external influences. As in Millikan's own set-up, the droplets are introduced into the experiment chamber from above. Suitable oil drops are selected and their charge determined by observing them through a measuring microscope. For each of the drops chosen, the time to rise a certain distance in the electric field is measured, as is the time it takes to descend by the same distance with the field absent. The distance is taken to be that between two adjacent scale markings on the ocular. The polarity of the capacitor plates is selected in accordance with the sign of the charge. An alternative is to apply a field sufficient to cause the drops being measured to hover stationary in one place.

The times measured for ascent and descent of a charged drop, the voltage applied across the plates and the other parameters relevant to evaluating the results, temperature, viscosity and pressure are displayed on the touch-sensitive screen.

EVALUATION

The speeds of ascent and descent are obtained from the times t_1 and t_2 measured for the ascent or descent to occur:

$$v_{1,2} = \frac{s}{V \cdot t_{1,2}}$$

s : Distance between two selected markings on the ocular scale, $V = 2$: Objective magnification

From these the charge q on the oil drop is calculated using equation (10).

The charges q_i determined from these measurements (Table 1) are all divided by a whole number n_i in such a way that the resulting values exhibit a minimum of variation about the mean value. The degree of spread about the mean is indicated by the standard deviation. The best estimate for elementary charge e and the standard deviation Δe can be determined from the values e_i obtained from individual measurements along with their individual deviations from the mean Δe_i (Table 1) by forming a weighted mean as below:

$$e \pm \Delta e = \frac{\sum w_i \cdot e_i}{\sum w_i} \pm \frac{1}{\sqrt{\sum w_i}} \quad \text{where } w_i = \left(\frac{1}{\Delta e_i}\right)^2$$

Using the values from Table 1, this results in:

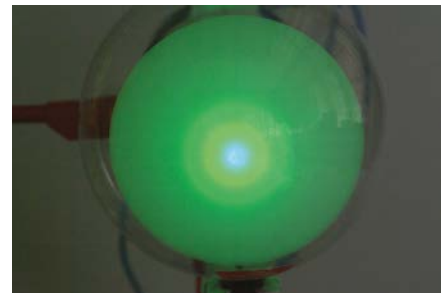
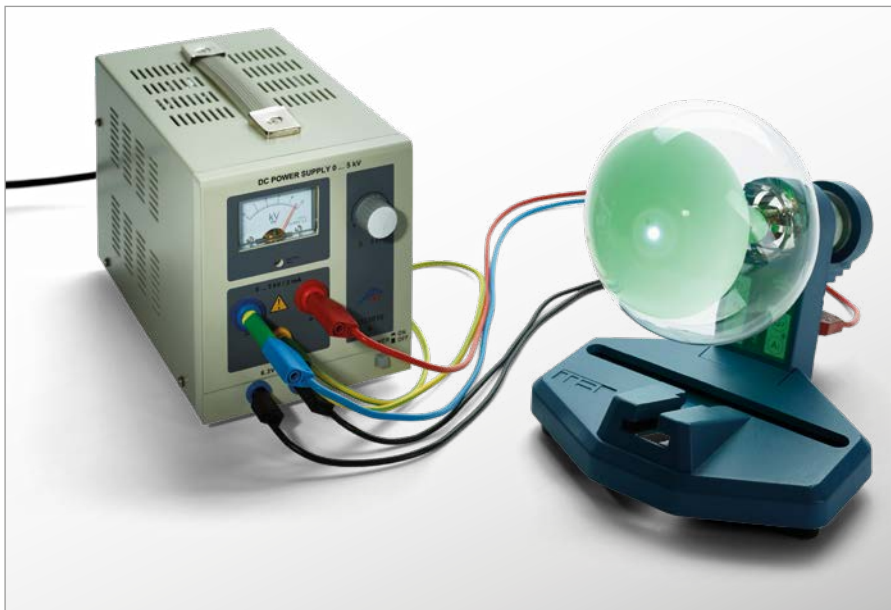
$$e \pm \Delta e = \frac{1286}{799} \pm \frac{1}{28} = (1.61 \pm 0.04) \cdot 10^{-19} \text{ C}$$

The result is therefore all the more significant, the greater the number of measurements that are made, i.e. the larger the quantity of samples and the smaller the number n of differing charges on the drops. Due to measurement uncertainties, particularly in the distance between capacitor plates and readings from the microscope scale, it would be expected that $n \leq 7$.

Table 1: Charges q_i measured for ten different oil drops and the value e_i determined for the elementary charge.

i	Polarity	q_i 10^{-19} C	Δq_i 10^{-19} C	n	e_i 10^{-19} C	Δe_i 10^{-19} C
1		-11.1	0.9	-7	1.59	0.13
2		-7.9	0.6	-5	1.58	0.12
3		-6.2	0.4	-4	1.55	0.10
4		3.5	0.2	2	1.75	0.10
5		4.9	0.3	3	1.63	0.10
6		6.3	0.5	4	1.58	0.13
7		6.6	0.4	4	1.65	0.10
8		7.6	0.6	5	1.52	0.12
9		10.2	0.8	6	1.70	0.13
10		10.6	0.8	7	1.51	0.11

UE5010500 | ELECTRON DIFFRACTION



OBJECTIVE

Observe the diffraction of electrons on polycrystalline graphite and confirm the wave nature of electrons

> EXPERIMENT PROCEDURE

- Measuring the diameters of the two diffraction rings for different accelerator voltages.
- Determining the wavelength of the electrons for different accelerator voltages by applying the Bragg condition.
- Confirming the de Broglie equation for the wavelength.

SUMMARY

The diffraction of electrons on a polycrystalline graphite foil provides evidence for the wave nature of electrons. It is possible to observe two diffraction rings surrounding a central spot on the axis of the beam on the fluorescent screen of the electron diffraction tube. These rings are caused by the diffraction of electrons at those lattice planes of the microcrystals in the graphite foil that satisfy the Bragg condition. The phenomenon is similar to the results obtained in the Debye-Scherrer diffraction of X-rays by a crystalline powder.

REQUIRED APPARATUS

Quantity	Description	Item Number
1	Electron Diffraction Tube S*	1013889
1	Tube Holder S	1014525
1	High Voltage Power Supply 5 kV (230 V, 50/60 Hz)	1003310 or
	High Voltage Power Supply 5 kV (115 V, 50/60 Hz)	1003309
1	Set of 15 Safety Experiment Leads, 75 cm	1002843

* Please ask also for a quote with our electron tubes D.

BASIC PRINCIPLES

In 1924 *Louis de Broglie* put forward the hypothesis that particles can in principle also possess wave properties, and that the wavelength depends on the momentum. His theories were later confirmed by *C. Davisson* and *L. Germer* by observing the diffraction of electrons by crystalline nickel.

According to de Broglie, the relation between the wavelength λ of a particle and its momentum p is given by:

$$(1) \quad \lambda = \frac{h}{p}$$

h : Planck's constant.

For electrons that have been accelerated by a voltage U_A , this leads to the equation

$$(2) \quad \lambda = \frac{h}{\sqrt{2 \cdot m \cdot e \cdot U_A}}$$

m : Mass of the electron, e : Elementary electric charge.

For example, if the accelerator voltage is 4 kV, one can assign to the electrons a wavelength of about 20 pm.

In the experiment, the wave nature of electrons in an evacuated glass tube is demonstrated by observing their diffraction by polycrystalline graphite. On the fluorescent screen of the tube one observes diffraction rings around a central spot on the axis of the beam. The diameter of the rings depends on the accelerator voltage. They are caused by diffraction of electrons at those lattice planes of the microcrystals that satisfy the Bragg condition:

$$(3) \quad 2 \cdot d \cdot \sin \vartheta = n \cdot \lambda$$

ϑ : the Bragg angle, n : Diffraction order,

d : Distance between the lattice planes

(see Fig. 2). The diameter of the diffraction ring corresponding to the Bragg angle ϑ is given by:

$$(4) \quad D = 2 \cdot L \cdot \tan 2\vartheta$$

L : Distance between the graphite foil and the fluorescent screen.

As graphite has a crystal structure with two different lattice plane distances, $d_1 = 123$ pm and $d_2 = 213$ pm (see Fig. 3), the first-order diffraction pattern ($n = 1$) consists of two diffraction rings with diameters D_1 and D_2 .

EVALUATION

From the diameters of the two diffraction rings and the distances between the lattice planes, we can determine the wavelength λ by applying the Bragg condition. For small diffraction angles the following equation is valid:

$$\lambda = 2 \cdot d_{1/2} \cdot \sin \left(\frac{1}{2} \cdot \arctan \left(\frac{D_{1/2}}{2 \cdot L} \right) \right)$$

The experimental wavelengths thus calculated can be compared with the values calculated from the theoretical expression (2).

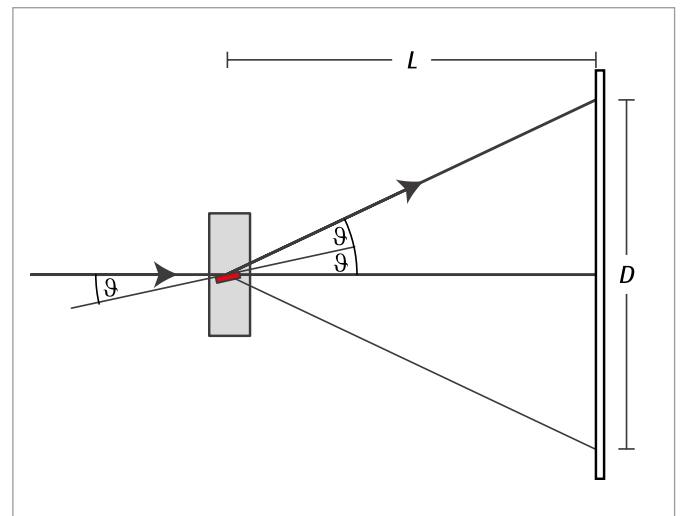


Fig. 2: Bragg reflection at a “favorable” group of lattice planes in a typical crystallite of the graphite foil

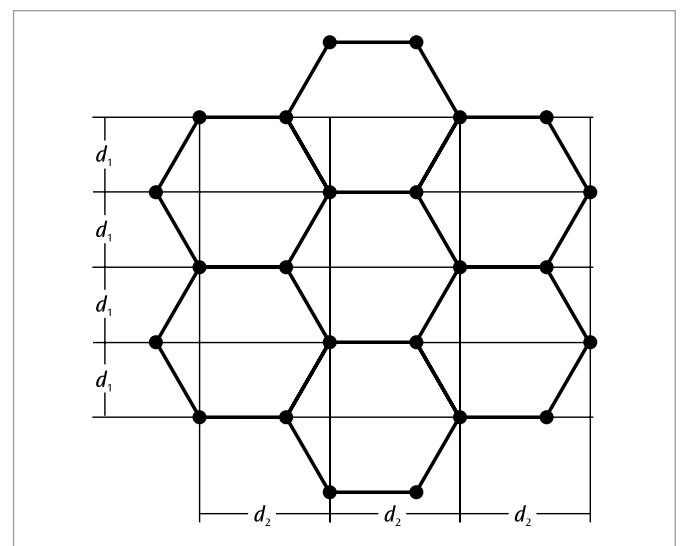


Fig. 3: The crystal structure of graphite

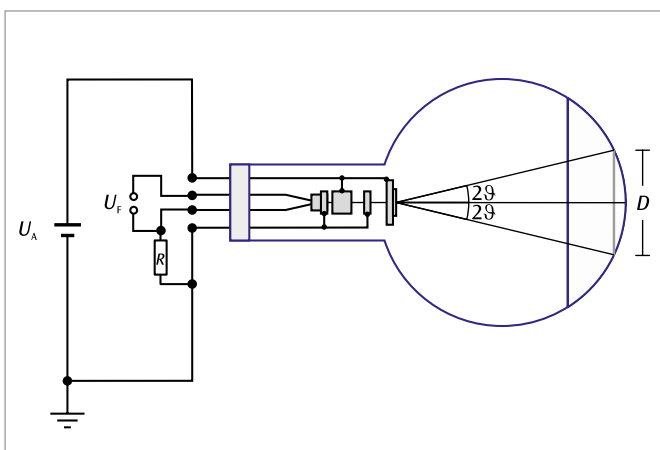


Fig. 1: Schematic diagram of the electron diffraction tube

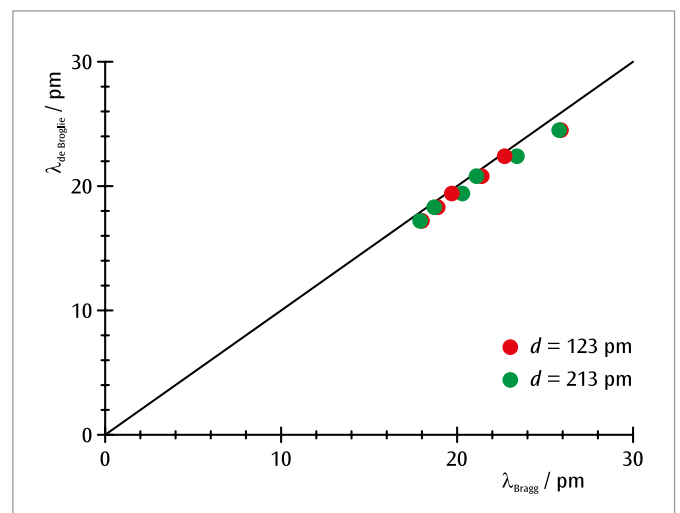


Fig. 4: The relation between wavelengths determined experimentally using the Bragg condition and the theoretical de Broglie wavelengths

UE5020100 | LINE SPECTRA I



EXPERIMENT PROCEDURE

- Record the line spectrum of hydrogen.
- Determine the frequencies of the H_{α} , H_{β} , H_{γ} and H_{δ} lines of the Balmer series for hydrogen.
- Calculate the Rydberg constant.
- Record and interpret line spectra of inert gases and metal vapors.

OBJECTIVE

Record and interpret the Balmer series of lines for hydrogen other line spectra in the visible region

SUMMARY

The line spectra of light-emitting atoms are uniquely characteristic for each specific chemical element, although they become increasingly complex for elements with higher atomic numbers. By contrast, that part of the line spectrum of hydrogen atoms that lies within the visible region can be explained simply on the basis of the Bohr model of the atom.

REQUIRED APPARATUS

Quantity	Description	Item Number
1	Digital-Spectrometer LD	1018103
1	Spectrum Tube Power Supply (230V, 50/60 Hz)	1000684 or
	Spectrum Tube Power Supply (115V, 50/60 Hz)	1000683
1	Spectrum Tube Hydrogen	1003409
1	Barrel Foot, 1000 g	1002834
Additionally recommended:		
1	Spectrum Tube Helium	1003408
1	Spectrum Tube Neon	1003413
1	Spectrum Tube Argon	1003403
1	Spectrum Tube Krypton	1003411
1	Spectrum Tube Mercury	1003412
1	Spectrum Tube Bromine	1003404
1	Spectrum Tube Iodine	1003410

BASIC PRINCIPLES

Light emitted by atoms of an electronically excited gas gives rise to spectra consisting of many individual lines, which are clearly distinguishable from one another, although they may be quite tightly packed in some parts of the spectrum. The lines are uniquely characteristic for each chemical element, because each line corresponds to a transition between particular energy levels in the electron shell of the atom.

The emission spectrum of hydrogen atoms has four lines, H_{α} , H_{β} , H_{γ} and H_{δ} , in the visible region. The spectrum continues into the ultra-violet region to form a complete series of spectral lines. In 1885 *J. J. Balmer* discovered that the frequencies of this series fit an empirical formula:

$$(1) \quad \nu = R \cdot \left(\frac{1}{2^2} - \frac{1}{n^2} \right)$$

$$n = 3, 4, 5, 6 \dots$$

$R = 3290$ THz: Rydberg constant.

Later, with the aid of the Bohr model of the atom, it was shown that the frequency series could be explained simply in terms of the energy released by an electron when it undergoes downward transitions from higher shells to the second shell of a hydrogen atom.

The line spectrum of a helium atom, which contains only one more electron than hydrogen, is already much more complex, because the spin of the two electrons can be oriented in parallel or anti-parallel, so that they occupy completely different energy levels in the helium atom. The complexity increases further for all other chemical elements. However, in every case the line spectrum is uniquely characteristic of the element.

EVALUATION

When the frequencies ν of the Balmer series are plotted as a function of $1/n^2$, with the H_{α} line assigned to $n = 3$, the H_{β} line to $n = 4$, and so on, the points lie on a straight line (see Fig. 1).

The gradient of the line corresponds to the Rydberg constant R . The intercept where the curve crosses the x-axis is at about 0.25, as a consequence of the fact that the transitions of the Balmer series go down to the $n = 2$ energy level.

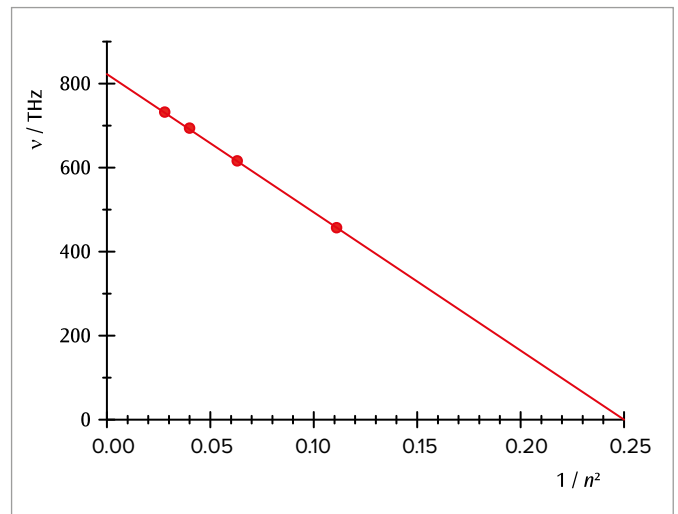


Fig. 1: Transition frequencies of the Balmer series as a function of $1/n^2$

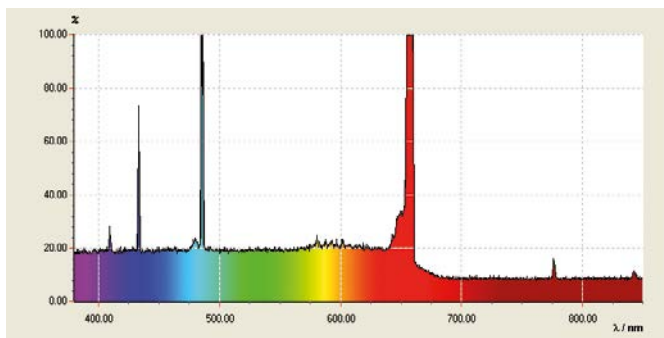


Fig. 2: Line spectrum of hydrogen atoms

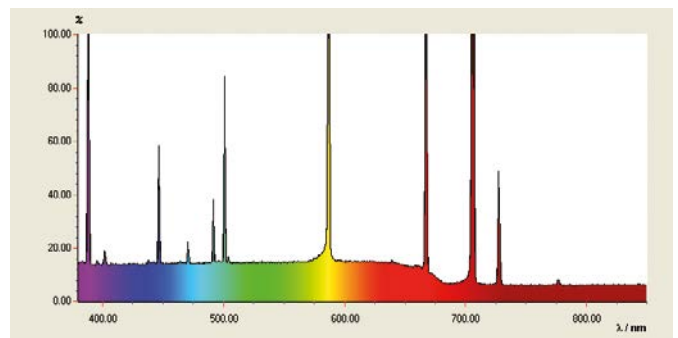


Fig. 3: Line spectrum of helium

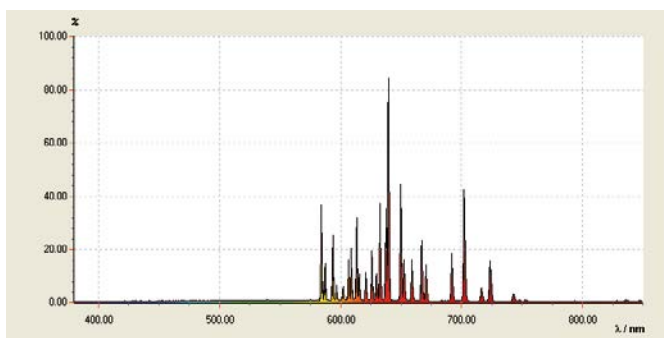


Fig. 4: Line spectrum of neon

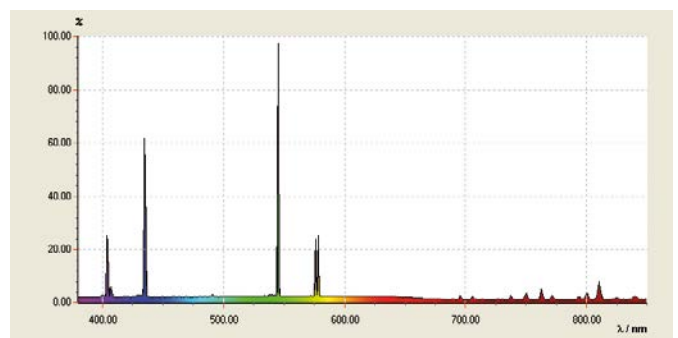


Fig. 5: Line spectrum of mercury vapor

UE5020150 | LINE SPECTRA II



> EXPERIMENT PROCEDURE

- Demonstrate the fine structure of the sodium D-lines.
- Measure absorption lines in the spectrum of the sun.
- Carry out high-precision measurements for other atoms.

OBJECTIVE

Carry out high-precision measurements of absorption and emission lines

SUMMARY

The resolution of a spectrometer is often assessed in terms of whether the two sodium D-lines can be distinguished. This experiment uses a digital spectrometer with the resolution to do this.

REQUIRED APPARATUS

Quantity	Description	Item Number
1	Digital-Spectrometer HD	1018104
1	Control Unit for Spectrum Lamps (230 V, 50/60 Hz)	1021409 or
	Control Unit for Spectrum Lamps (115 V, 50/60 Hz)	1003195
1	Spectral Lamp Na	1003541
2	Barrel Foot, 1000 g	1002834
Additionally recommended:		
1	Spectral Lamp Hg 100	1003545
1	Spectral Lamp Hg/Cd	1003546

BASIC PRINCIPLES

The resolution of a spectrometer characterizes the performance of such a device. It is a measure of the minimum separation in terms of wavelength which must be exhibited by two adjacent spectral lines in order for them to be distinguished. One particularly well known pair of lines is the doublet making up the sodium D line. The separation in wavelength between these two lines is 0.6 nm. The resolution of a spectrometer is often assessed in terms of whether these two lines can be separated.

The sodium D-line occurs due to the transition of sodium 3s electrons from the excited 3p state down to the ground state. Since electron spin and orbital angular momentum are linked (Spin-orbit interaction), the 3p state is separated into two finely distinguished states with overall spin $j = 1/2$ and $j = 3/2$. The energy difference between these two adjacent states is 0.0021 eV and the wavelengths associated with decay to the ground state are 588.9950 nm (D2) and 589.5924 nm (D1).

In this experiment a digital spectrometer capable of distinguishing the fine structure of the sodium D-line is used. Spectral dispersion of the incident light is effected by inserting a grating with 1200 lines/mm into a Czerny-Turner monochromator. It is possible to measure the spectral range between 400 nm and 700 nm across a CCD array of 3600 pixels. That means there is one pixel available for each wavelength interval of 0.08 nm. This enables a resolution of 0.5 nm to be achieved, enabling the fine structure of the sodium D-line to be measured.

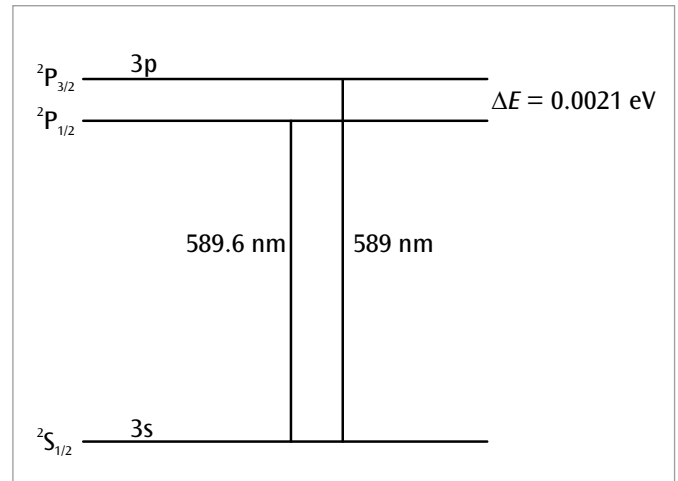


Fig. 1: Simplified energy level diagram for sodium

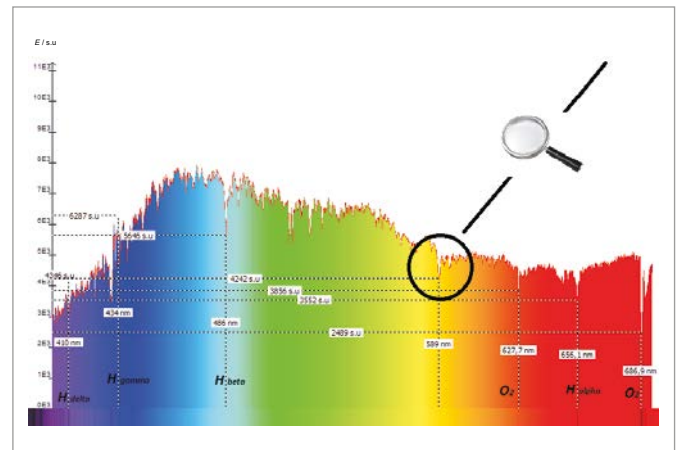


Fig. 2: Absorption lines in the spectrum of the sun

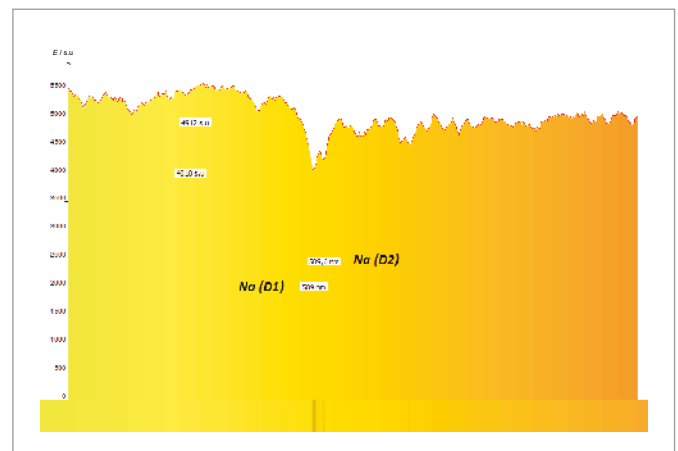
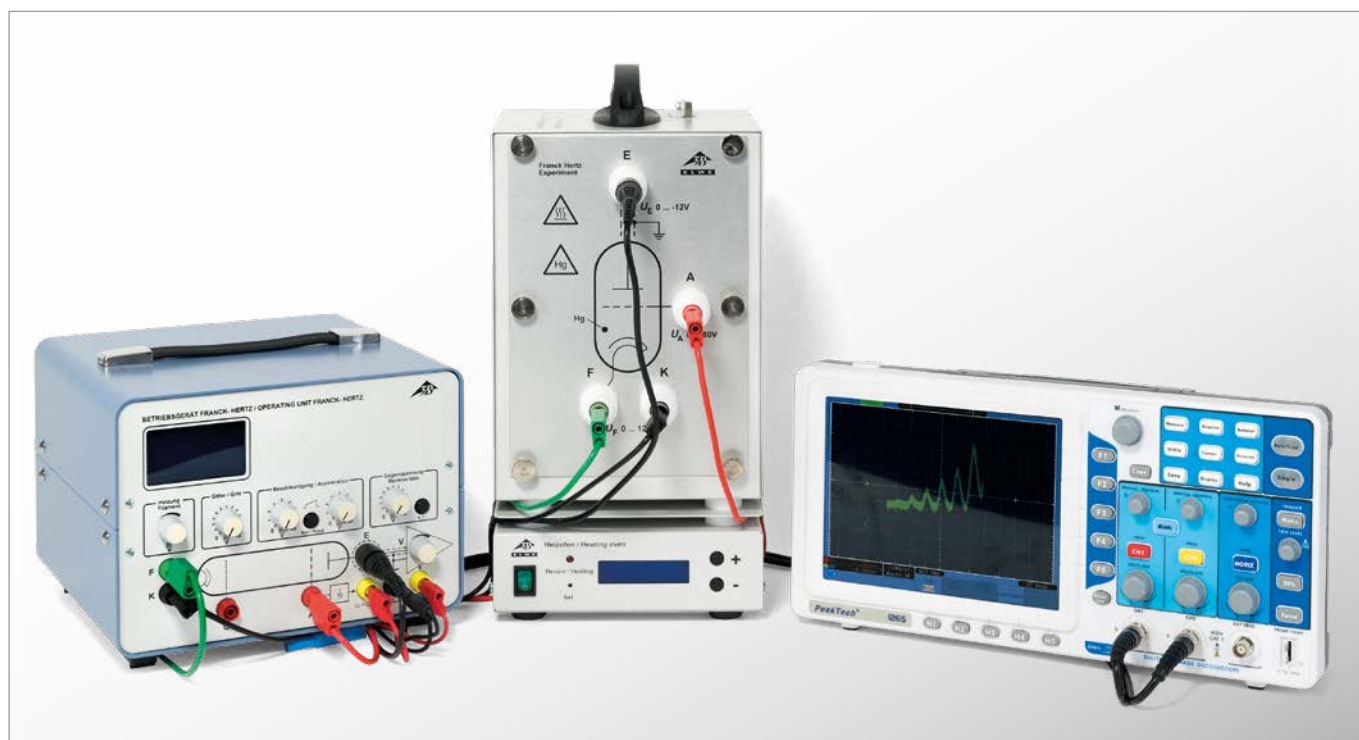


Fig. 3: Sodium absorption lines in the spectrum of the sun

UE5020300

FRANCK-HERTZ EXPERIMENT FOR MERCURY



> EXPERIMENT PROCEDURE

- Measure target current I as a function of the voltage U between cathode and grid.
- Determining the separation ΔU of current maxima or minima.
- Compare the voltage intervals with the excitation energies of mercury atoms.

OBJECTIVE

Record and evaluate the Franck-Hertz curve for mercury

SUMMARY

The Franck-Hertz experiment for mercury involves observing how energy is transferred from electrons as a result of inelastic collision while passing through mercury vapor. The transfer of energy occurs in discrete steps corresponding to the excitation by such collision of distinct energy level transitions in the mercury atoms. The experiment thus provides confirmation of the Bohr model of the atom and the discrete energy levels described by that model.

REQUIRED APPARATUS

Quantity	Description	Item Number
1	Franck-Hertz Tube with Mercury Filling and Heating Chamber (230 V, 50/60 Hz)	1006795 or
	Franck-Hertz Tube with Mercury Filling and Heating Chamber (115 V, 50/60 Hz)	1006794
1	Power Supply Unit for Franck-Hertz Experiment (230 V, 50/60 Hz)	1012819 or
	Power Supply Unit for Franck-Hertz Experiment (115 V, 50/60 Hz)	1012818
1	Digital Oscilloscope 2x30 MHz	1020910
1	Digital Multimeter P3340	1002785
1	HF Patch Cord	1002746
2	HF Patch Cord, BNC/4 mm Plug	1002748
1	Set of 15 Safety Experiment Leads, 75 cm	1002843

BASIC PRINCIPLES

James Franck and Gustav Hertz reported in 1914 that electrons passing through mercury vapor transferred energy in discrete steps and that this is associated with observing the emission of mercury's ultra-violet spectral line ($\lambda = 254 \text{ nm}$). Niels Bohr realized several months later that this was a confirmation of the atomic model he had developed. The Franck-Hertz experiment with mercury has thus become a classic experiment for the confirmation of quantum theory.

An evacuated glass tube contains a heated cathode C, a grid G and a target electrode A placed in that sequence (see Fig. 1). Electrons are emitted from the cathode and are accelerated by a voltage U towards the grid. Having passed through the grid they reach the target and thus contribute to a target current I if their kinetic energy is sufficient to overcome a decelerating voltage U_{GA} between the grid and the target. In addition a glass tube with a droplet of mercury is included and this is heated to generate a vapor pressure of approximately 15 hPa.

As the voltage U increases the target current I initially increases since more and more atoms are attracted out of the space charge field around the cathode by the electric field.

At a certain value $U = U_1$ some atoms attain sufficient kinetic energy just in front of the grid so that they are able to provide sufficient energy to excite the mercury atoms by inelastic collision. The target current then drops to near zero since after such a collision, the electrons no longer have the energy to overcome the decelerating voltage.

As the voltage increases more, the electrons acquire enough energy to excite the mercury atoms further away from the grid. After such collisions they are accelerated again and can once again acquire enough energy to reach the target so the target current rises again.

At a still higher voltage $U = U_2$ the electrons can acquire so much energy after the first collision that they are able to excite another mercury atom. The target current once again drops drastically but rises once more as the voltage further increases. This continues for a third time at a still higher voltage and again the target current drops dramatically.

NOTE

The first minimum is not at 4.9 V itself but is shifted by an amount corresponding to the so-called contact voltage between the cathode and grid.

EVALUATION

The voltages U_1, U_2, U_3, \dots , at which the current dramatically drops in the recorded $I(U)$ -characteristics all appear at a constant interval $\Delta U = 4.9 \text{ V}$. This interval corresponds to the excitation energy $E_{\text{Hg}} = 4.9 \text{ eV}$ ($\lambda = 254 \text{ nm}$) at which mercury atoms are raised from the base state 1S_0 to the first 3P_1 -state. The following equation applies:

$$(1) \quad E_{\text{Hg}} = e \cdot \Delta U$$

e: Elementary electron charge

The results can thus be traced to discrete energy absorption by mercury atoms due to inelastic collision and the associated transfer of a fixed amount of energy from the electrons.

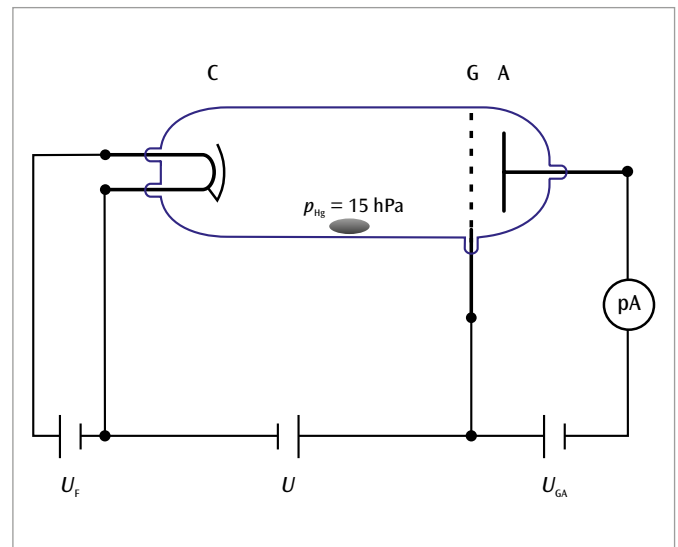


Fig. 1: Schematic of set up for measuring the Franck-Hertz curve for mercury

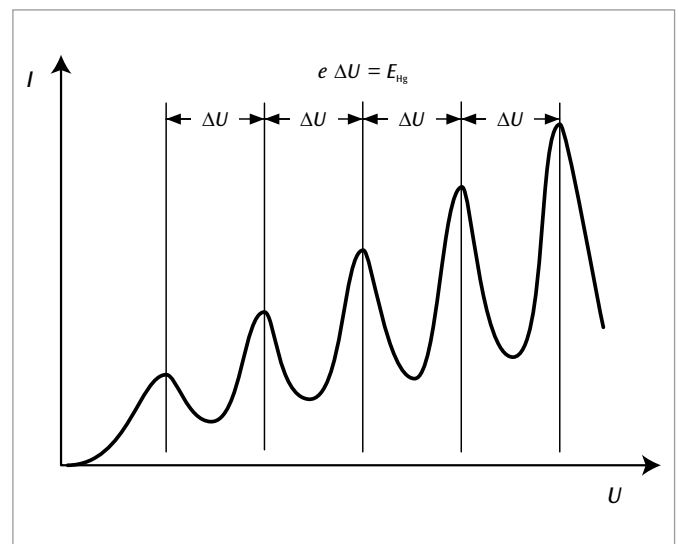


Fig. 2: Target current I as a function of the accelerating voltage U

UE5020400

FRANCK-HERTZ EXPERIMENT FOR NEON



> EXPERIMENT PROCEDURE

- Measure target current I as a function of the voltage U between cathode and grid.
- Compare the distribution of current maxima with the excitation energies of neon atoms.
- Observe the light emitted by the excited neon atoms.
- Determine the number of light-emitting levels for various accelerating voltages.

OBJECTIVE

Record and evaluate the Franck-Hertz curve for neon and observe emission of light

SUMMARY

The Franck-Hertz experiment for neon involves observing how energy is transferred from electrons as a result of inelastic collision while passing through neon gas. The transfer of energy occurs in discrete steps corresponding to the excitement by such collision of distinct energy level transitions in the neon atoms. The excited atoms then emit visible light.

REQUIRED APPARATUS

Quantity	Description	Item Number
1	Franck-Hertz Tube with Ne Filling	1000912
1	Power Supply Unit for Franck-Hertz Experiment (230 V, 50/60 Hz)	1012819 or
	Power Supply Unit for Franck-Hertz Experiment (115 V, 50/60 Hz)	1012818
1	Digital Oscilloscope 2x30 MHz	1020910
1	Digital Multimeter P3340	1002785
1	HF Patch Cord	1002746
2	HF Patch Cord, BNC/4 mm Plug	1002748
1	Set of 15 Safety Experiment Leads, 75 cm	1002843

BASIC PRINCIPLES

In the Franck-Hertz experiment neon atoms are excited by inelastic collision with electrons. The excited atoms emit visible light that can be viewed directly. Thus it is possible to detect zones where the light and therefore the excitation is more intense. The distribution of such zones between the cathode and the grid depends on the difference in potential between the two.

An evacuated glass tube that has been filled with neon gas to a pressure of 10 hPa contains a heated cathode C, a control grid S, a grid G and a target electrode A arranged in that sequence (see Fig. 1). Electrons are emitted from the cathode and are accelerated by a voltage U towards the grid. Having passed through the grid they reach the target and thus contribute to a target

current I if their kinetic energy is sufficient to overcome a decelerating voltage U_{GA} between the grid and the target.

The $I(U)$ -characteristic (see Fig. 2) has a similar pattern to the original Franck-Hertz experiment using mercury gas but this time the intervals between minima where the current falls to almost zero for a specific voltage $U = U_1$ corresponding to the electrons reaching sufficient kinetic energy to excite a neon atom by inelastic collision just before reaching the grid are about 19 V. Simultaneously it is possible to observe a faint orange light close to the grid since the energy transition to the base state of a neon atom results in the emission of such light. The zone of illumination moves towards the cathode as the voltage U increases and the target current I rises once more.

For a higher voltage $U = U_2$ the target current also drops drastically and it is possible to see two zones of illumination. The electrons can in this case retain enough energy after an initial collision to excite a second neon atom.

As the voltages are further increased, other minima in the target current along with further zones of illumination can be observed.

NOTE

The first minimum is not at 19 V itself but is shifted by an amount corresponding to the so-called contact voltage between the cathode and grid. The emission lines in the neon spectrum can easily be observed and measured using a spectroscope (1003184) when the maximum voltage U is used.

EVALUATION

The $I(U)$ -characteristic exhibits various maxima and minima and the interval between the minima is about $\Delta U = 19$ V. This corresponds to excitation energy of the 3p energy level of a neon atom (see Fig. 3) so that it is highly likely that this level is being excited. Excitement of the 3s-level cannot be neglected entirely and gives rise to some fine detail in the structure of the $I(U)$ -characteristic.

The zones of illumination are zones of greater excitation and correspond to drops in voltage in the $I(U)$ -characteristic. One more zone of illumination is created every time U is increased by about 19 V.

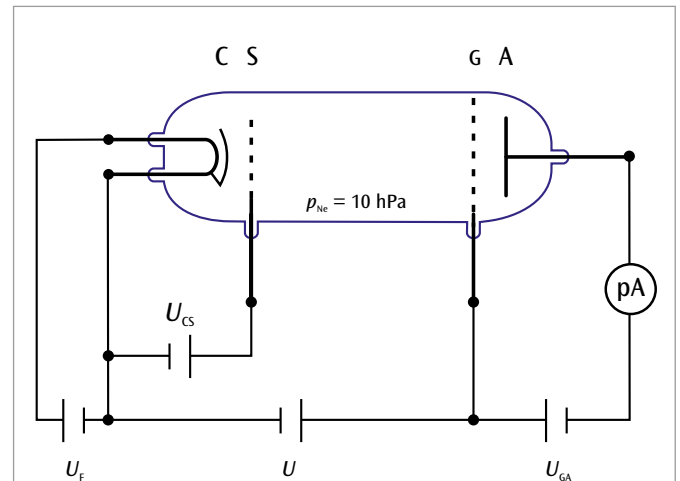


Fig. 1: Schematic of set up for measuring the Franck-Hertz curve for neon

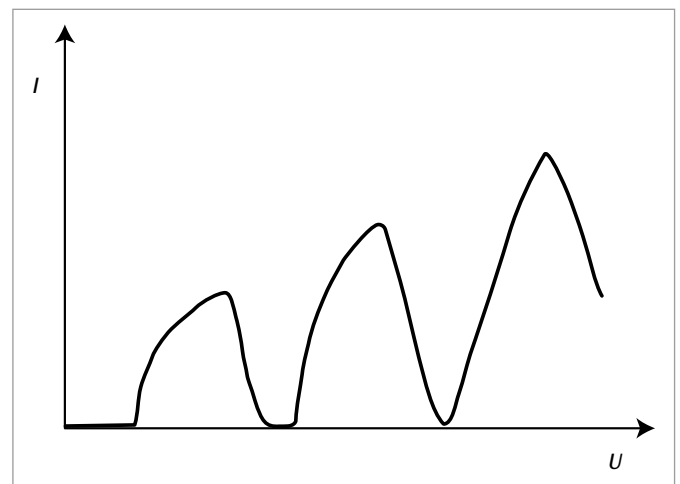


Fig. 2: Target current I as a function of the accelerating voltage U

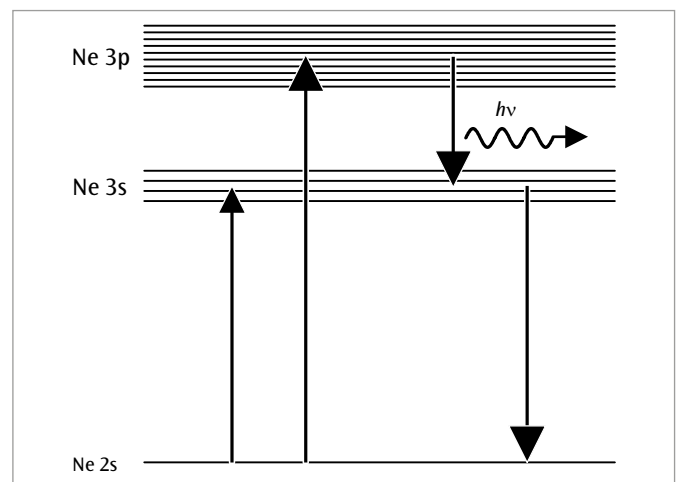
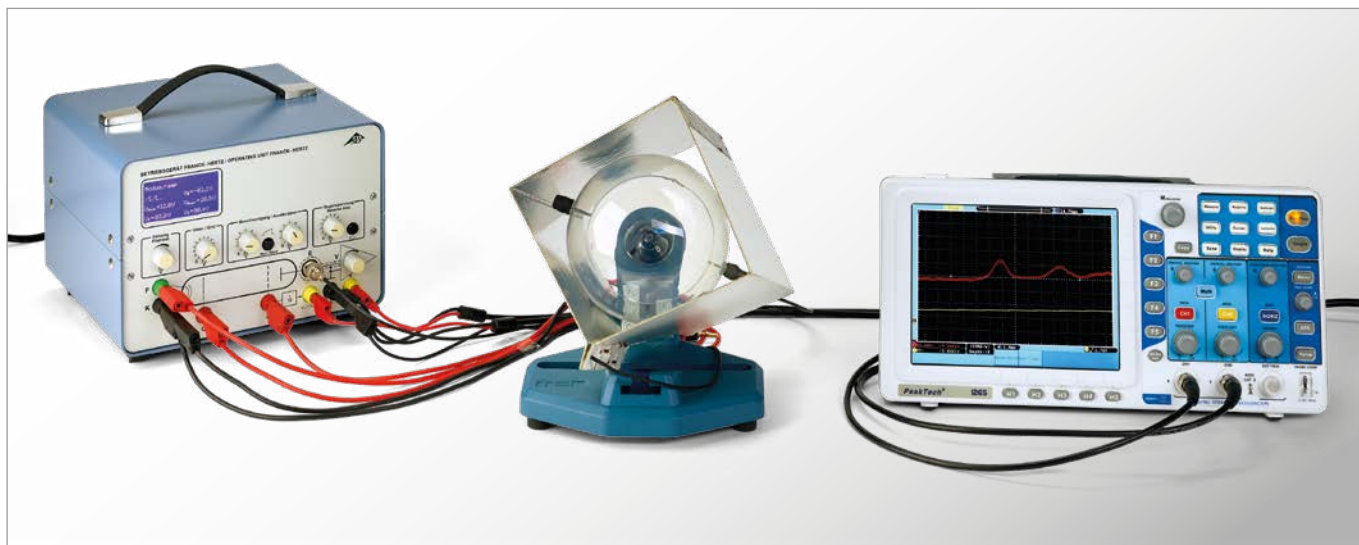


Fig. 3: Energy levels in neon atoms

UE5020500 | CRITICAL POTENTIALS



> EXPERIMENT PROCEDURE

- Measure the collector current I_R as a function of the accelerating voltage U_A .
- Compare the positions of the current maxima with the known critical potentials of the helium atom.
- Identify the doublet structure in the term scheme of helium (ortho and para helium).

OBJECTIVE

Determine the critical potentials of a helium atom

SUMMARY

The expression “critical potential” is a general name for all the excitation and ionization energies in the electron shells of an atom. The corresponding electronic states can be excited in various ways, for example by inelastic collisions with electrons. If the kinetic energy of the electron corresponds to a critical potential, the electron can lose all its kinetic energy in an inelastic collision. An experiment set-up originally designed by Gustav Hertz is used here to determine critical potentials. Our improved design allows for the separation of the 2^1S para helium and the 2^3P ortho helium level.

REQUIRED APPARATUS

Quantity	Description	Item Number
1	Critical Potential Tube S with He-Filling	1022131
1	Tube Holder S	1014525
1	Power Supply Unit F/H Experiment (230 V, 50/60 Hz)	1012819 or
	Power Supply Unit F/H Experiment (115 V, 50/60 Hz)	1012818
1	Digital Oscilloscope 2x30 MHz	1020910
2	HF Patch Cord, BNC/4 mm Plug	1002748
1	Set of 15 Safety Experiment Leads, 75 cm	1002843

BASIC PRINCIPLES

The expression “critical potential” is a general name for all the excitation and ionization energies in the electron shells of an atom. The corresponding electronic states of the atom can be excited in various ways, for example by inelastic collisions with electrons. If the kinetic energy of the electron corresponds exactly to a critical potential, the electron can transfer all its kinetic energy to the atom in an inelastic collision. Using an experiment set-up originally designed by *Gustav Hertz*, this effect can be used to determine the critical potentials.

In a tube that has been evacuated and then filled with helium, free electrons are accelerated by a voltage U_A to form a divergent beam passing through a space at a constant potential. To prevent the walls of the tube becoming charged, the inner surface is coated with a conducting material and connected to the anode A (see Fig. 1). In the tube there is a ring-shaped collector electrode R, through which the divergent beam can pass without touching it, even though the ring is at a slightly higher potential.

However, a small current I_R , with a value in the order of picoamperes, is measured at the collector ring, and is found to depend on the accelerating voltage U_A . It shows characteristic maxima, which are caused by the fact that the electrons can undergo inelastic collisions with helium atoms during their passage through the tube. The kinetic energy E of an electron is as follows:

$$(1) \quad E = e \cdot U_A$$

e : Elementary electron charge

If this energy corresponds exactly to a critical potential of the helium atom, all the kinetic energy may be transferred to the helium atom. In this instance the electron can then be attracted and collected by the collector ring, thus contributing to an increased collector current I_R . As the accelerating voltage is increased, successively higher levels of the helium atom can be excited, until finally the kinetic energy of the electron is enough to ionize the helium atom. As the accelerating voltage is increased further, the collector current shows a steady increase.

EVALUATION

The positions of the observed current maxima are compared with literature values for the excitation energies and the ionization energy of the helium atom. Account must be taken of the fact that the maxima will be shifted relative to the quoted values by an amount corresponding to the so-called contact voltage between the cathode and the anode.

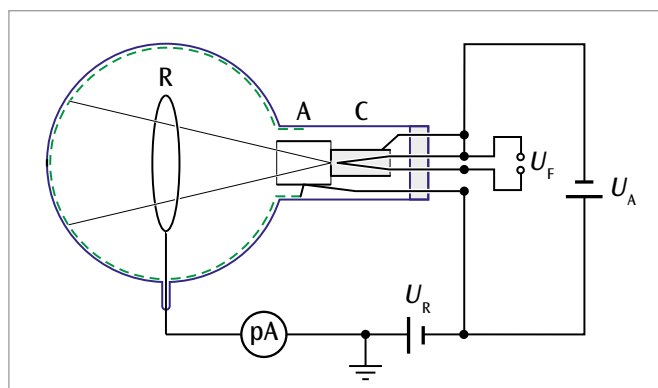


Fig. 1: Schematic diagram of critical potential tube

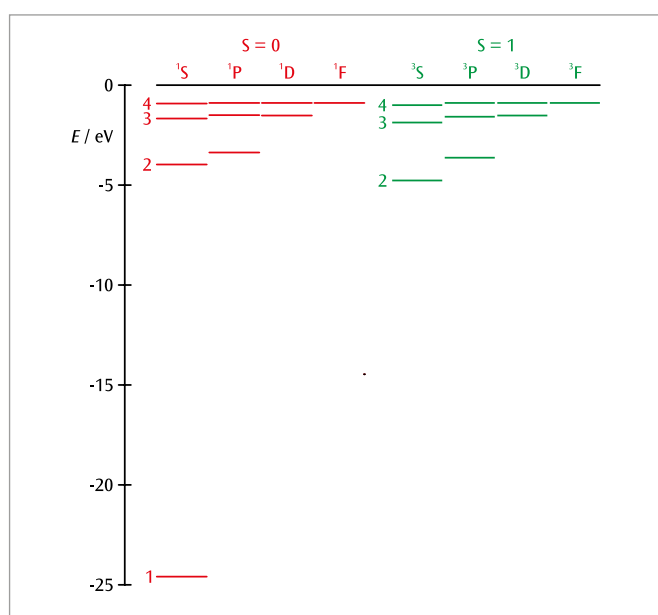


Fig. 2: The term scheme of helium
red: total spin $S = 0$ (para helium),
green: total spin $S = 1$ (ortho helium)

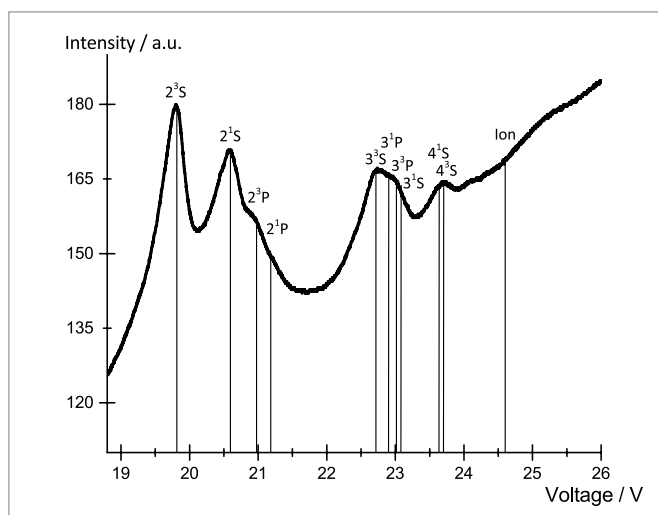


Fig. 3: Collector current I_R as a function of accelerating voltage U_A . Please note the separation of the 2^1S para helium and the 2^3P ortho helium resonances.

UE5020700 | NORMAL ZEEMAN EFFECT



OBJECTIVE

Observe the doublet and triplet splitting of the red cadmium line in an external magnetic field due to the normal Zeeman effect.

SUMMARY

The splitting of the spectral lines – into a doublet (longitudinal Zeeman effect) or a triplet (transversal Zeeman effect) due to the so-called “normal” Zeeman effect – is observed. For this, a cadmium lamp is placed into a magnetic field and a Fabry-Pérot etalon is used to analyze

> EXPERIMENT PROCEDURE

- With no external magnetic field applied, use the Fabry-Pérot etalon to observe the characteristic interference rings of the light emitted from the cadmium atoms.
- Switch on the field and observe the splitting of the interference rings into the characteristic doublet of the longitudinal Zeeman effect.
- Rotate the magnet including the cadmium lamp. Study the horizontal Zeeman effect by observing the splitting into a triplet.

FURTHER STUDIES:

- Investigate the polarization of the doublet and triplet components by means of the quarter-wavelength plate with polarizing attachment and the polarization filter.
- Spectroscopy with a Fabry-Pérot interferometer: Determine the energy splitting in dependence of the external magnetic field by measuring the Radius of the Interference Rings (UE5020700–2).
- Determine the value of the Bohr magneton.

the emitted light. By ramping up the magnetic field strength the continuous splitting can be seen directly in the interference ring pattern. In addition, this equipment allows further studies, which are described in detail in the experiment manual. They include the investigation of polarization properties, the measurement of the actual energy shift of the spectral lines and the determination of the value of the Bohr magneton.

REQUIRED APPARATUS

Quantity	Description	Item Number
1	Cadmium Lamp with Accessories (230 V, 50/60 Hz)	1021366 or
	Cadmium Lamp with Accessories (115 V, 50/60 Hz)	1021747
1	U Core D	1000979
2	Coil D 900 Turns	1012859
1	Electromagnet Accessory for Zeeman Effect	1021365
1	DC Power Supply, 32 V, 20 A (230 V, 50/60 Hz)	1012857 or
	DC Power Supply, 0 – 40 V, 0 – 40 A (115 V, 50/60 Hz)	1022289
1	Set of 15 Experiment Leads, 75 cm 1 mm ²	1002840
1	Fabry-Pérot Etalon	1020903
2	Convex Lens on Stem, $f=100\text{mm}$	1003023
1	Quarter Wavelength Filter on Stem	1021353
1	Polarising Attachment	1021364
1	Polarisation Filter on Stem	1008668
1	Optical Precision Bench D, 1000 mm	1002628
1	Optical Base D	1009733
5	Optical Rider D, 90/36	1012401
1	Holder and Filter for Moticam	1021367
1	Digital Camera Moticam 1	1021162

BASIC PRINCIPLES

The Zeeman effect refers to the splitting of atomic energy levels or spectral lines due to the action of an external magnetic field and is named after P. Zeeman, the scientist who discovered it in 1896.

The normal Zeeman effect occurs only at the transitions between atomic states with the total spin $S = 0$. The total angular momentum $J = L + S$ then corresponds to the orbital angular momentum L , i.e. $J = L$. It generates a magnetic moment

$$(1) \quad \mu = \frac{\mu_B}{\hbar} J$$

where the Bohr magneton is given by

$$(2) \quad \mu_B = -\frac{1}{2} \cdot \frac{e}{m_e} \cdot \hbar$$

$\hbar = h/2\pi$: reduced Planck's constant, e : elementary charge, m_e : mass of electron

In an external magnetic field (Fig. 3)

$$(3) \quad B = \begin{pmatrix} 0 \\ 0 \\ B \end{pmatrix}$$

the magnetic moment has the energy

$$(3) \quad E = \mu \cdot B = \mu_z \cdot B$$

Due to space quantization, the component J_z of the total angular momentum parallel to the magnetic field can only have the values

$$(4) \quad J_z = M_J \cdot \hbar \quad \text{with } M_J = -J, -(J-1), \dots, (J-1), J$$

J : total angular momentum quantum number

In this case, the energy level of the total angular momentum quantum number J thus splits into $2J+1$ equidistant components, which differ by the magnetic quantum number M_J (Fig. 2). With eq. (1), it follows that

$$(6) \quad \mu_z = \frac{\mu_B}{\hbar} \cdot J_z,$$

whereby according to eq. (3)

$$(7) \quad E = \mu_z \cdot B = \frac{\mu_B}{\hbar} \cdot J_z \cdot B$$

and finally with eq. (4):

$$(8) \quad E = \mu_B \cdot M_J \cdot B$$

Therefore the energy interval between adjacent levels is:

$$(9) \quad \Delta E = \mu_B \cdot B$$

The normal Zeeman effect can be observed in the red spectral line of cadmium. It corresponds to the transition $^1D_2 \rightarrow ^1P_1$ with the wavelength $\lambda = 643.8 \text{ nm}$ (Fig. 2). According to eq. (4), level 1D_2 splits into five components and level 1P_1 splits into three components, each with the equidistant energy interval given by eq. (9).

According to the selection rules for electrical dipole radiation, the permissible transitions between these levels are ones with

$$(10) \quad \Delta M_J = \begin{cases} +1 & \text{(clockwise circularly polarized light, } \sigma^+) \\ 0 & \text{(linearly polarised light, } \pi) \\ -1 & \text{(anti-clockwise circularly polarized light, } \sigma^-) \end{cases}$$

whereby the light emitted is polarized as indicated above. Thus, we observe a total of three spectral lines (Fig. 2): one π component that is not shifted and, according to $E = \hbar \cdot \omega$, two σ components shifted by

$$(11) \quad \Delta\lambda = \pm \frac{\lambda^2}{2\pi \cdot \hbar \cdot c} \cdot \Delta E$$

c : speed of light in vacuum

with a corresponding longer or shorter wavelength. In a magnetic field of flux density $B = 1 \text{ T}$, applying eq. (9) and (2) to eq. (11) results in a shift of only $|\Delta\lambda| = 0.02 \text{ nm}$. The spatial distribution of the emitted light is different for the π component and the two σ components. In classical terms, the case $\Delta M_J = 0$ corresponds to a Hertzian dipole oscillating parallel to the magnetic field. Accordingly, linearly polarized light is emitted perpendicular to the magnetic field, and no light is emitted parallel to the magnetic field (Fig. 3). The cases $\Delta M_J = \pm 1$ correspond to two dipoles oscillating perpendicularly to each other with a phase difference of 90° . Accordingly, light is emitted both parallel and perpendicular to the direction of the magnetic field. That light is circularly polarized parallel to the direction of the magnetic field, i.e. counter-clockwise circularly polarized for $\Delta M_J = -1$ and clockwise circularly polarized for $\Delta M_J = +1$.

EVALUATION

In the experiment, the splitting is observed using a digital camera fitted with a Fabry-Pérot etalon and imaging optics. The Fabry-Pérot etalon is designed to meet the resonance condition for the specific wavelength 643.8 nm of the red Cd line. As it passes through the Fabry-Pérot etalon, the light from the cadmium lamp creates interference rings that split like the spectral lines according to the external magnetic field and are recorded by the optics of the camera sensor. The electromagnets can be rotated on their axes to permit observation parallel or perpendicular to the external magnetic field.

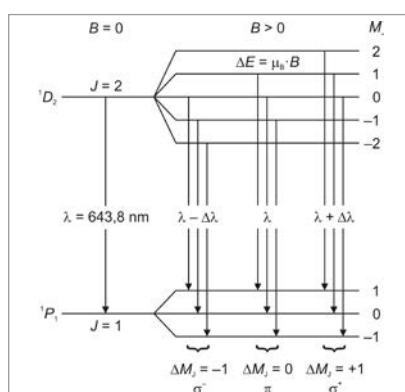


Fig. 1: Normal Zeeman effect in the red spectral line of cadmium. Splitting of energy levels and transitions permitted according to the selection rules for electrical dipole radiation



Fig. 2: No external magnetic field: Observation of the interference rings of the red cadmium line created by the Fabry-Pérot etalon. As an orientation aid, the second interference ring from the centre is indicated with a frame.

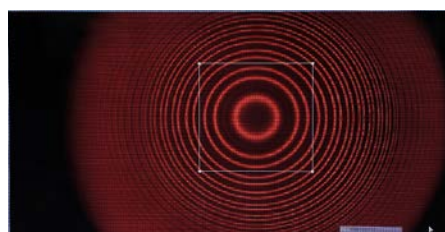


Fig.3.: Longitudinal Zeeman effect: Observation of the doublet splitting of the red cadmium line in an external magnetic field.

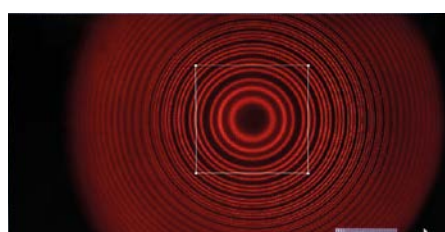
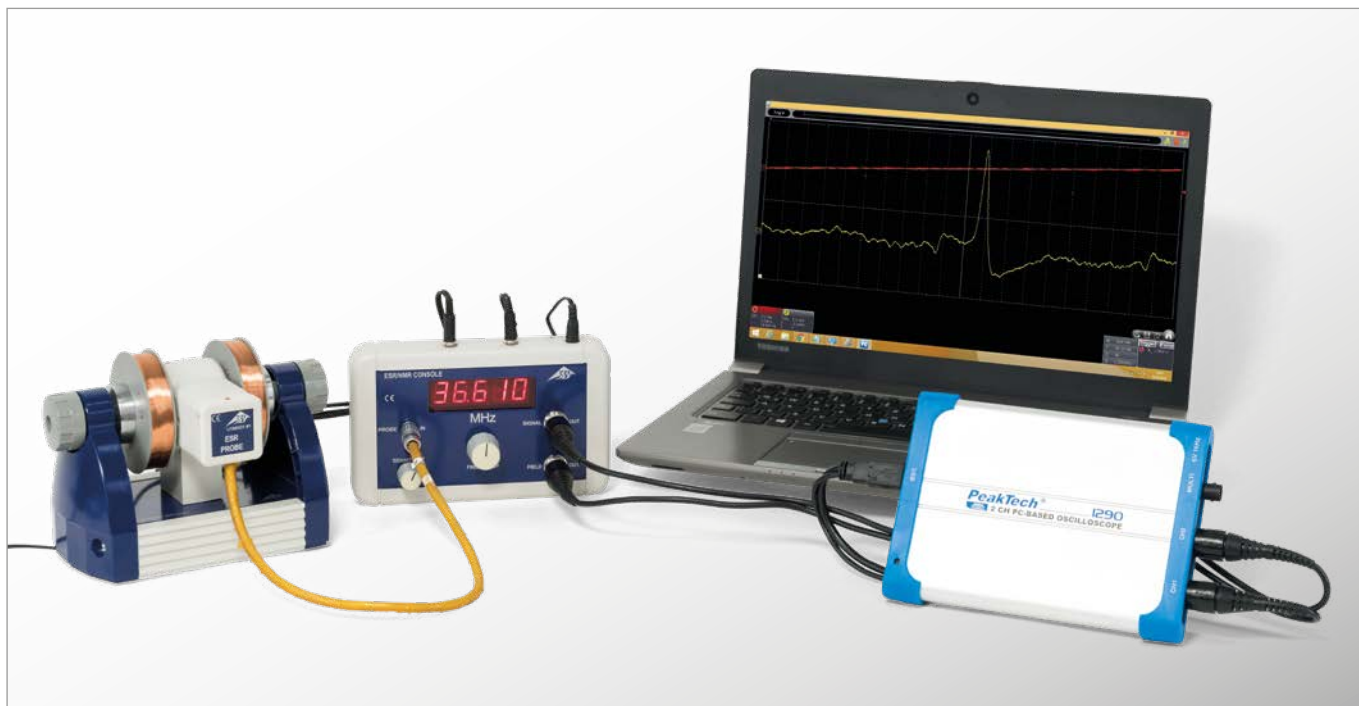


Fig.4: Horizontal Zeeman effect: Observation of the triplet splitting of the red cadmium line in an external magnetic field.

UE5030100 | ELECTRON SPIN RESONANCE



> EXPERIMENT PROCEDURE

- Observe the resonance curve of DPPH.
- Determine the resonant frequency as a function of the magnetic field.
- Determine the Landé g -factor for free electrons.

OBJECTIVE

Demonstrate electron spin resonance in DPPH

SUMMARY

Electron spin resonance (ESR) is based on the energy absorption by substances with unpaired electrons, which are inside an external magnetic field produced by a DC source. The energy is absorbed from a high-frequency AC-generated field which is fed in perpendicular to the field from the DC source. If the frequency of the alternating field is equal to the resonant frequency, the impedance of the transmitting coil filled with the test material changes in accordance with a resonance curve and a peak will be visible on an oscilloscope screen. One suitable material for this is diphenyl-picryl-hydrazyl (DPPH).

REQUIRED APPARATUS

Quantity	Description	Item Number
1	ESR/NMR Basic Set (230 V, 50/60 Hz)	1000638 or
	ESR/NMR Basic Set (115 V, 50/60 Hz)	1000637
1	ESR Supplementary Set	1000640
1	PC Oscilloscope, 2x25 MHz	1020857
2	HF Patch Cord	1002746

BASIC PRINCIPLES

Electron spin resonance (ESR) is based on the energy absorption by substances with unpaired electrons, which are inside an external magnetic field produced by a DC source. The energy is absorbed from a high-frequency AC-generated field which is fed in perpendicular to the field from the DC source. If the frequency of the alternating field is equal to the resonant frequency, the impedance of the transmitting coil filled with the test material changes in accordance with a resonance curve and a peak will be visible on an oscilloscope screen. The cause of resonance absorption is the “tipping over” of the magnetic moments between spin states of a free electron. The resonant frequency depends on the strength of the DC-generated field and the width of the resonance signal is related to the uniformity of the field.

The magnetic moment of an electron with purely spin-related magnetism assumes discrete values in a magnetic field B :

$$(1) \quad E_m = -g_j \cdot \mu_B \cdot m \cdot B, \quad m = -\frac{1}{2}, \frac{1}{2}$$

Bohr magneton: $\mu_B = 9.274 \cdot 10^{-24} \frac{\text{J}}{\text{T}}$
Landé g -factor: $g_j = 2.0023$

The interval between the two levels is therefore

$$(2) \quad \Delta E = g_j \cdot \mu_B \cdot B$$

Resonance occurs when the frequency f of the alternating field being fed in meets the following condition:

$$(3) \quad h \cdot f = \Delta E$$

$$\text{Planck's constant: } h = 6.626 \cdot 10^{-34} \text{ Js}$$

In this experiment, electron spin resonance will be demonstrated in diphenyl-picrylhydrazyl (DPPH), an organic compound, the molecules of which include an unpaired electron. The basic magnetic field is generated inside a pair of Helmholtz coils and is moved between zero and a maximum value of $B_{\text{max}} = 3.5 \text{ mT}$ using a saw-tooth wave-form. Now it is possible to look for a frequency f , at which resonance absorption takes place at a distinct position along the saw-tooth curve, i.e. for a pre-selected magnetic field.

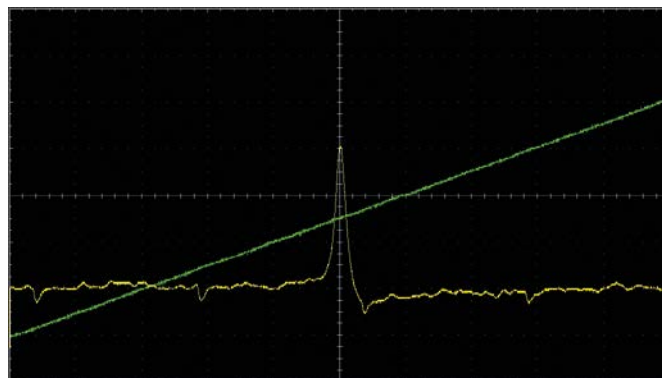


Fig. 1: Absorption signal and the magnetic field trace over time for electron spin resonance in DPPH

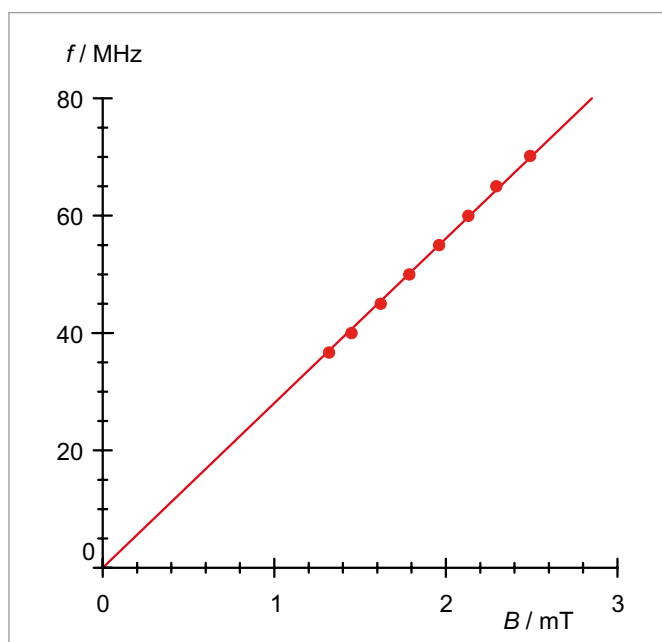


Fig. 2: Resonant frequency f as a function of the magnetic field B

EVALUATION

The following relationship between the resonance frequency f and the magnetic field B can be derived from (2) and (3).

$$f = g_j \cdot \frac{\mu_B}{h} \cdot B$$

The measurements therefore lie along a straight line through the origin to within the measurement tolerances. The Landé g -factor can be determined from the slope of this graph.

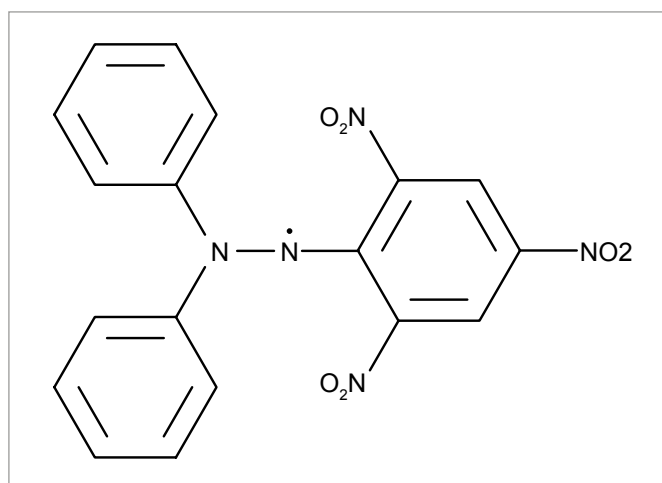
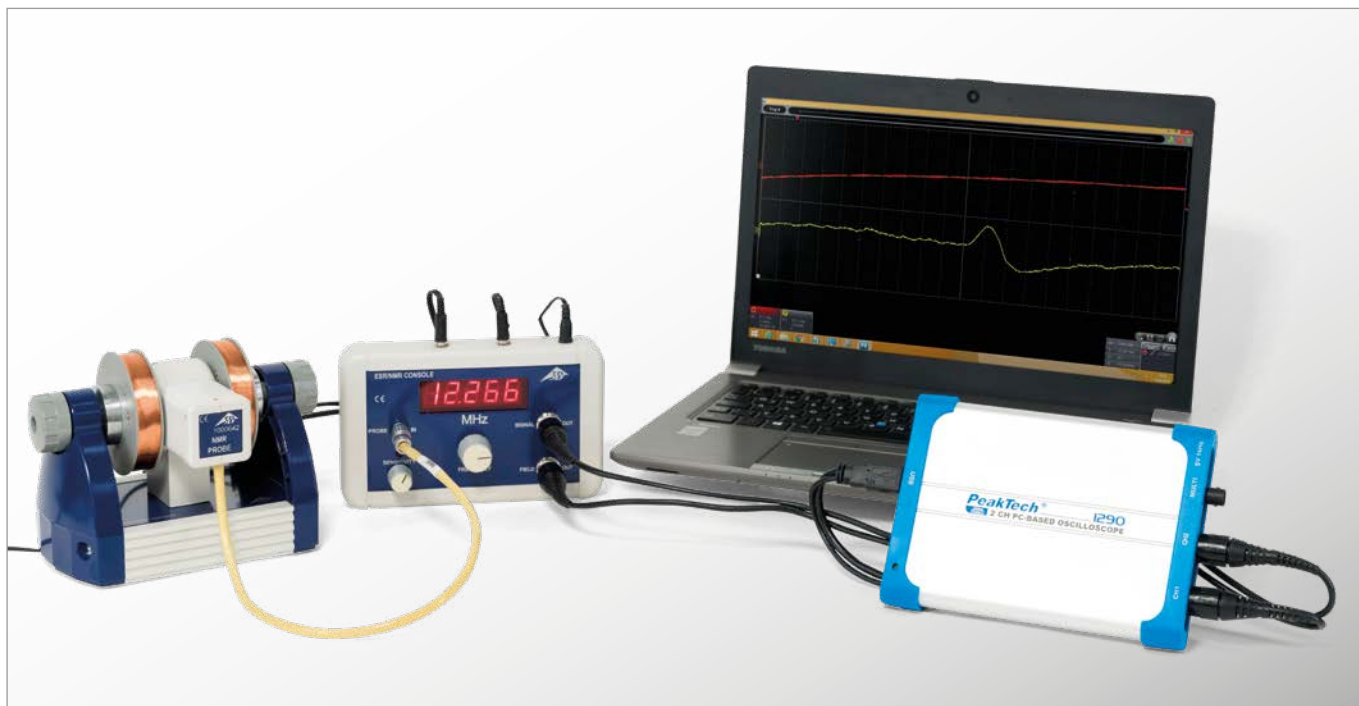


Fig.3: Molecular structure of DPPH

UE5030200 | NUCLEAR MAGNETIC RESONANCE



> EXPERIMENT PROCEDURE

- Demonstrate nuclear magnetic resonance in glycerine, polystyrene and Teflon.
- Determine the resonant frequencies in a constant magnetic field.
- Make a comparison between the g -factors of ^1H and ^{19}F nuclei.

OBJECTIVE

Demonstrate and compare nuclear magnetic resonance in glycerine, polystyrene and Teflon

SUMMARY

Nuclear magnetic resonance (NMR) is based on the energy absorption by substances with nuclear magnetism, which are inside an external magnetic field produced by a DC source. The energy is absorbed from a high-frequency AC-generated field which is fed in perpendicular to the field from the DC source. If the frequency of the alternating field is equal to the resonant frequency, the impedance of the transmitting coil filled with the test material changes in accordance with a resonance curve and a peak will be visible on an oscilloscope screen. Suitable materials for this include glycerine, polystyrene and Teflon, whereby the magnetic moment of ^1H or ^{19}F nuclei is used.

REQUIRED APPARATUS

Quantity	Description	Item Number
1	ESR/NMR Basic Set (230 V, 50/60 Hz)	1000638 or
	ESR/NMR Basic Set (115 V, 50/60 Hz)	1000637
1	NMR Supplementary Set	1000642
1	PC Oscilloscope, 2x25 MHz	1020857
2	HF Patch Cord	1002746

BASIC PRINCIPLES

Nuclear magnetic resonance (ESR) is based on the energy absorption by substances with nuclear magnetism, which are inside an external magnetic field produced by a DC source. The energy is absorbed from a high-frequency AC-generated field which is fed in perpendicular to the field from the DC source. If the frequency of the alternating field is equal to the

resonant frequency, the impedance of the transmitting coil filled with the test material changes in accordance with a resonance curve and a peak will be visible on an oscilloscope screen. The cause of resonance absorption is a transition between energy states of the nucleus' magnetic moment inside a magnetic field. The resonant frequency depends on the strength of the DC-generated field and the width of the resonance signal is related to the uniformity of the field.

The magnetic moment of a nucleus with nuclear spin I assumes discrete values in a magnetic field B :

$$(1) \quad E_m = -g_l \cdot \mu_k \cdot m \cdot B, \quad m = -I, -I+1, \dots, I$$

Nuclear magneton: $\mu_k = 5,051 \cdot 10^{-27} \frac{\text{J}}{\text{T}}$
 g -factor of atomic nucleus: g_l

The interval between the two levels is therefore

$$(2) \quad \Delta E = g_l \cdot \mu_k \cdot B$$

When the energy levels meet the condition for resonance, another magnetic field of frequency f applied perpendicular to the uniform field excites the transition between energy states. Resonance occurs when the frequency f precisely fulfils the following condition:

$$(3) \quad h \cdot f = \Delta E$$

Planck's constant: $h = 6.626 \cdot 10^{-34} \text{ Js}$.

In this experiment nuclear magnetic resonance will be demonstrated in glycerine, polystyrene and Teflon, whereby the ^1H isotope contributes to the resonance in glycerine and polystyrene while the ^{19}F isotope is the contributor in Teflon. The uniform magnetic field is largely generated by permanent magnets. Added to this is a magnetic field which varies in a saw-tooth pattern between zero and a maximum value generated inside a pair of Helmholtz coils. Now a frequency f can be found where resonance absorption takes place in a pre-selected magnetic field, which, for simplicity, we will take to be in the middle of the saw-tooth wave.

EVALUATION

The g -factors for the nuclei involved are quoted in literature to be as follows: $g_l(^1\text{H}) = 5.5869$ und $g_l(^{19}\text{F}) = 5.255$.

From (2) und (3) the following applies for the resonant frequency f in a magnetic field B .

$$f = g_l \cdot \frac{\mu_k}{h} \cdot B$$

The resonant frequencies for various nuclei in the same magnetic field therefore have the same ratios as the g -factors:

$$\frac{f(^{19}\text{F})}{f(^1\text{H})} = \frac{g_l(^{19}\text{F})}{g_l(^1\text{H})} = 94\%$$

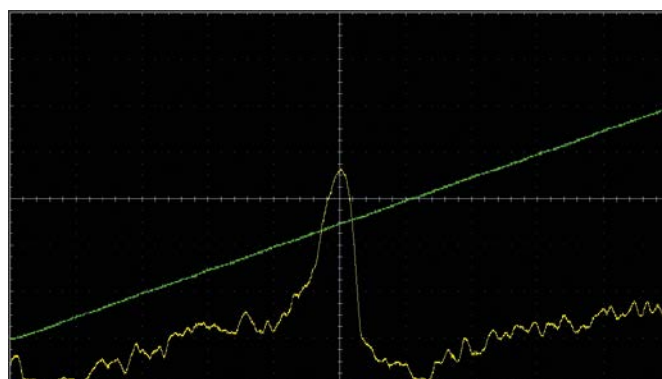


Fig. 1: Nuclear magnetic resonance in glycerine
($f = 12.854 \text{ MHz}$)

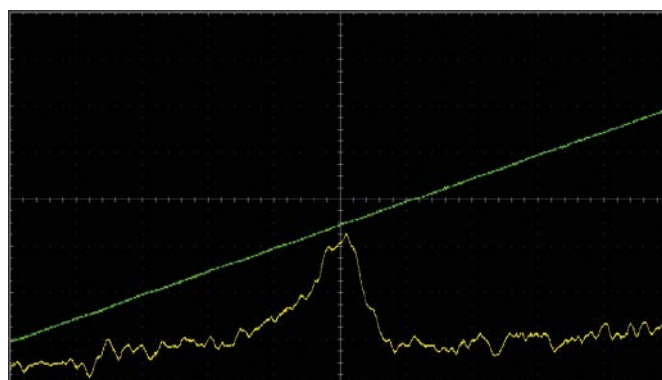


Fig. 2: Nuclear magnetic resonance in polystyrene
($f = 12.854 \text{ MHz}$)

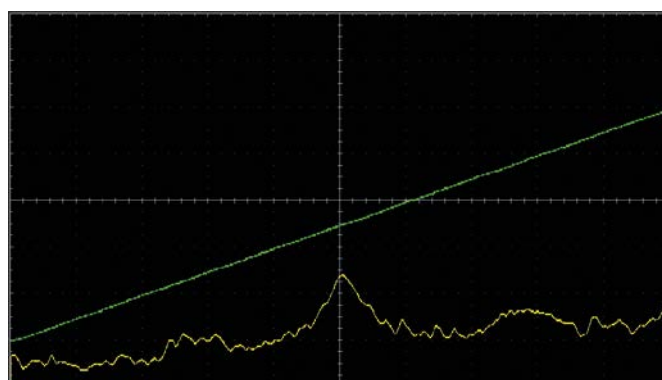


Fig. 3: Nuclear magnetic resonance in Teflon
($f = 12.1 \text{ MHz}$)

UE6020100

ELECTRICAL CONDUCTION IN SEMICONDUCTORS



OBJECTIVE

Determine band separation in germanium

SUMMARY

Semiconductors only exhibit measurable electrical conductivity at high temperatures. The reason for this dependence on temperature is the band structure of the electron energy levels, which comprise a conduction band, a valence band and an intermediate zone, which in pure, undoped semiconductor materials cannot be occupied by electrons at all. As the temperature increases, more and more electrons are thermally excited from the valence band into the conduction band, leaving behind “holes” in the valence itself. These holes move under the influence

of an electric field as if they were positive particles and contribute to the current much as electrons do. In order to determine the conductivity of pure, undoped germanium, this experiment involves sending a constant current through the crystal and measuring the voltage drop as a function of temperature. The data measured can be described by an exponential function to a good approximation, whereby the separation of bands appears as a key parameter.

EXPERIMENT PROCEDURE

- Measure the electrical conductivity of undoped germanium as a function of temperature.
- Determine the band separation between the valence band and conduction band.

NOTE

In practice, the intrinsic conductivity of pure, undoped semiconductors is of minor importance. As a rule, the crystals have imperfections which adversely affect the flow of current. Often, highly pure crystals are specifically targeted by addition of donor or acceptor atoms to make them more conductive. The effect of such doping becomes apparent when the investigations described here are carried out to include comparison of n and p-doped germanium. The conductivity of the doped crystals at room temperature is much higher than that of pure crystals, although at high temperatures, it approaches the intrinsic conductivity, see Fig. 4. The way that Hall coefficients depend on temperature is investigated in greater detail in Experiment UE6020200.

REQUIRED APPARATUS

Quantity	Description	Item Number
1	Undoped Germanium on Printed Circuit Board	1008522
1	Hall Effect Basic Apparatus	1009934
1	Barrel Foot, 1000 g	1002834
1	Transformer with Rectifier 3/ 6/ 9/ 12 V, 3 A (230 V, 50/60 Hz)	1003316 or
	Transformer with Rectifier 3/ 6/ 9/ 12 V, 3 A (115 V, 50/60 Hz)	1003315
1	Digital Multimeter P3340	1002785
1	Pair of Safety Experiment Leads, 75 cm	1002849
1	Pair of Safety Experimental Leads, 75 cm, red/blue	1017718
Additionally recommended		
1	P-Doped Germanium on Printed Circuit Board	1009810
1	N-Doped Germanium on Printed Circuit Board	1009760
1	VinciLab	1021477
1	Sensor Cable	1021514
1	Voltage Sensor 500 mV, differential	1021681
2	Voltage Sensor 10 V, differential	1021680
1	Coach 7 License	

BASIC PRINCIPLES

Electrical conductivity is highly dependent on the nature of the material. It is therefore common to classify materials according to their conductivity. Solid bodies for which conductivity only becomes measurable at relatively high temperatures are classified as semiconductors. The reason for this dependence on temperature is the band structure of the electron energy levels, which comprise a conduction band, a valence band and an intermediate zone, which in pure, undoped semiconductor materials cannot be occupied by electrons at all.

In the ground state, the valence band is the highest band occupied by electrons and the conduction band is the next band up, which is unoccupied. The separation between these bands is labelled E_g and depends on the material itself. For germanium this quantity is approximately 0.7 eV. As the temperature increases, more and more electrons are thermally excited from the

valence band into the conduction band, leaving behind “holes” in the valence itself. These holes move under the influence of an electric field E as if they were positive particles and contribute to the current much as electrons do (see Fig.1).

$$(1) \quad j = \sigma \cdot E$$

σ : Electrical conductivity of semiconductor material

Electrons and holes move with differing average drift velocities:

$$(2) \quad v_n = -\mu_n \cdot E \quad \text{and} \quad v_p = \mu_p \cdot E$$

μ_n : Mobility of electrons
 μ_p : Mobility of holes

This ability to conduct, which results from electrons being thermally excited from the valence band into the conduction band, is called intrinsic conduction.

In a state of thermal equilibrium, the number of electrons in the conduction band is equal to the number of holes in the valence band, so that the current density in the case of intrinsic conduction can be written out as follows:

$$(3) \quad j_i = -e \cdot n_i \cdot v_n + e \cdot n_i \cdot v_p = e \cdot n_i \cdot (\mu_n + \mu_p) \cdot E$$

i.e. the intrinsic conductivity σ is

$$(4) \quad \sigma_i = e \cdot n_i \cdot (\mu_n + \mu_p)$$

The temperature dependence of the current carrier density n_i for electrons or holes is given by the following:

$$(5) \quad n_i = 2 \cdot \left(\frac{2\pi}{h^2} \cdot \sqrt{m_n m_p} \cdot kT \right)^{\frac{3}{2}} \cdot \exp\left(-\frac{E_g}{2kT}\right)$$

Boltzmann constant: $k = 8,617 \cdot 10^{-5} \frac{\text{eV}}{\text{K}}$
 h : Planck's constant

m_n : Effective mass of electrons

m_p : Effective mass of holes

T : Sample temperature

The mobilities μ_n and μ_p also depend on temperature. In the temperature range above room temperature, the following applies:

$$(6) \quad \mu \sim T^{-\frac{3}{2}}$$

The dominant term with regard to temperature dependence, however, is the exponential expression. This means that the intrinsic conductivity at high temperature can be expressed in the following form:

$$(7) \quad \sigma_i = \sigma_0 \cdot \exp\left(-\frac{E_g}{2kT}\right)$$

In this experiment to determine the conductivity of pure, undoped germanium, a constant current I is sent through the crystal and the voltage drop U is measured as a function of temperature. The conductivity σ can be calculated from the measured data thanks to the relationship

$$(8) \quad U = a \cdot E \quad \text{resp.} \quad I = b \cdot c \cdot j$$

a, b, c : dimensions of crystal

$$(9) \quad \sigma = \frac{I}{U} \cdot \frac{a}{b \cdot c}$$

EVALUATION

Equation (7) can be rewritten in the following form:

$$\ln \sigma = \ln \sigma_0 - E_g \cdot \frac{1}{2kT}$$

Therefore $y = \ln \sigma$ is plotted against $x = \frac{1}{2kT}$ and the band separation E_g can be found from the gradient of the resulting straight line.

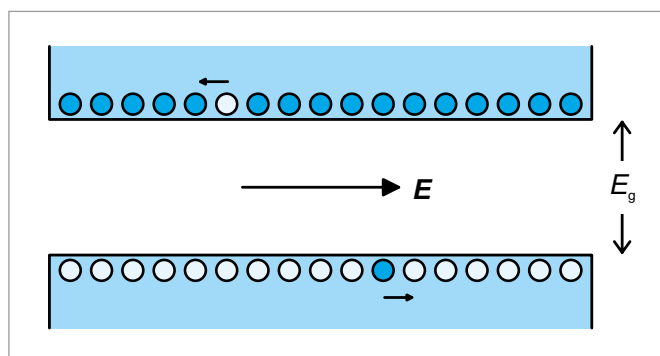


Fig. 1: Structure of semiconductor bands with one electron in the conduction band and a hole in the valence band, both of which drift due to the influence of an electric field E

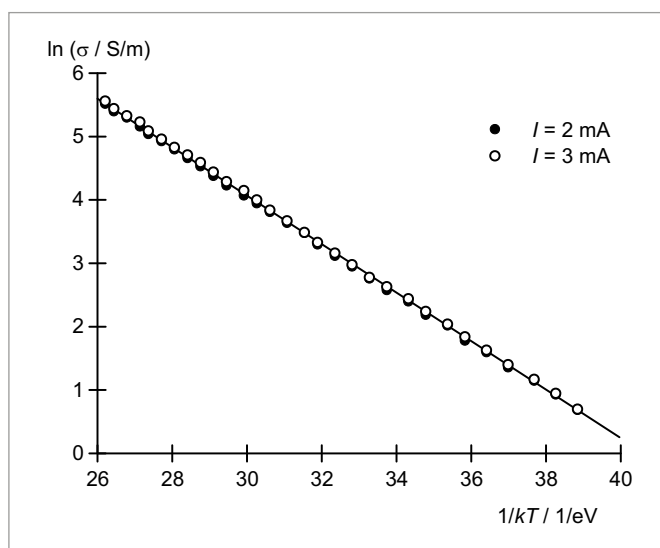


Fig. 2: Representation for the determination of band separation E_g in germanium

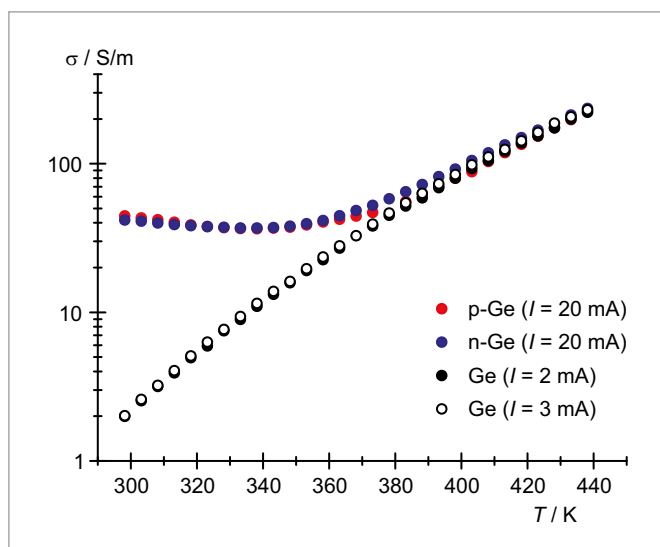


Fig. 3: Comparison between conductivities of pure and doped germanium

UE6020200 | HALL-EFFECT IN SEMICONDUCTORS



EXPERIMENT PROCEDURE

- Demonstrating the Hall effect in doped germanium.
- Measuring the Hall voltage as a function of the current and magnetic field at room temperature.
- Determining the sign, density and mobility of charge carriers at room temperature.
- Measuring the Hall voltage as a function of sample temperature.
- Determining the inversion temperature; differentiating between extrinsic and intrinsic conduction in the case of p -doped germanium.

NOTE

The temperature dependence of the electrical conductivity of the employed germanium crystals is investigated in experiment UE6020100.

OBJECTIVE

Investigating electrical conduction mechanisms in doped germanium with the Hall effect

SUMMARY

The Hall effect occurs in electrically conductive materials located in a magnetic field B . The Hall voltage's sign changes depending on whether the same current I is borne by positive or negative charge carriers. Its value depends on the charge carrier density. The Hall effect is consequently an important means of determining the mechanisms of charge transport in doped semiconductors. In this experiment, doped germanium crystals are examined at temperatures between 300 K and 450 K to ascertain the differences between electrical conduction enabled by doping, and intrinsic conduction enabled by thermal activation of electrons causing their transfer from the valence band into the conduction band.

REQUIRED APPARATUS

Quantity	Description	Item Number
1	Hall Effect Basic Apparatus	1009934
1	N-Doped Germanium on Printed Circuit Board	1009760
1	P-Doped Germanium on Printed Circuit Board	1009810
1	Magnetic Field Sensor FW \pm 2000 mT	1021766
2	Coil D with 600 Taps	1000988
1	U Core	1000979
1	Pair of Pole Shoes and Clamping Brackets for Hall Effect	1009935
1	Transformer with Rectifier 3/ 6/ 9/ 12 V, 3 A (230 V, 50/60 Hz)	1003316 or
	Transformer with Rectifier 3/ 6/ 9/ 12 V, 3 A (115 V, 50/60 Hz)	1003315
1	DC Power Supply 0 – 20 V, 0 – 5 A (230 V, 50/60 Hz)	1003312 or
	DC Power Supply 0 – 20 V, 0 – 5 A (115 V, 50/60 Hz)	1003311
1	Digital Multimeter P3340	1002785
1	VinciLab	1021477
2	Sensor Cable	1021514
1	Voltage Sensor 500 mV, differential	1021681
2	Voltage Sensor 10 V, differential	1021680
2	Set of 15 Safety Experiment Leads, 75 cm	1002843
Additionally required		
1	Coach 7 License	

BASIC PRINCIPLES

The Hall effect occurs in electrically conductive materials located in a magnetic field B . This effect is attributable to the Lorentz force which deflects the charge carriers producing an electric current I through a material sample perpendicularly with respect to the magnetic field and the current's direction. Charge separation results in an electric field E_H which is perpendicular to the current's direction and compensates the Lorentz force, while generating a Hall voltage U_H between the sample's edges. The Hall voltage's sign changes depending on whether the same current I is borne by positive or negative charge carriers. Its value depends on the charge carrier density. The Hall effect is consequently an important means of determining the mechanisms of charge transport in conductive materials, and used often to study doped semiconductors.

This experiment examines doped germanium crystals at temperatures between 300 K and 450 K. The crystals are present in the form of flat samples which have a length a , width b and thickness d , and which longitudinally conduct a current I . The magnetic field B pervades each sample perpendicularly with respect to the current. The resultant Hall voltage is:

$$(1) \quad U_H = R_H \cdot \frac{B \cdot I}{d}$$

The Hall coefficient is:

$$(2) \quad R_H = \frac{1}{e} \cdot \frac{n_p \cdot \mu_p^2 - n_n \cdot \mu_n^2}{(n_p \cdot \mu_p + n_n \cdot \mu_n)^2}$$

$$e = 1.602 \cdot 10^{-19} \text{ ampere-second (elementary charge)}$$

The densities n_n and n_p respectively of the electrons in the conduction band and electron holes in the valence band, as well as the mobilities μ_n and μ_p respectively of the electrons and corresponding holes are material quantities which depend on the sample temperature T .

Measured besides the Hall voltage in the experiment is the longitudinal voltage drop U in the sample in order to determine the electrical conductivity:

$$(3) \quad \sigma = e \cdot (n_n \cdot \mu_n + n_p \cdot \mu_p)$$

Also determined in this process is the Hall mobility:

$$(4) \quad \mu_H = R_H \cdot \sigma = \frac{n_p \cdot \mu_p^2 - n_n \cdot \mu_n^2}{n_p \cdot \mu_p + n_n \cdot \mu_n}$$

The charge carrier densities n_n and n_p are influenced by the doping, i.e. inclusion of foreign atoms in the crystal. In the case of p-doping, acceptor atoms bind electrons from the valence band and thereby produce electron holes in that band. In the case of n-doping, donor atoms each supply one electron to the conduction band.

The doped crystals are electrically neutral, i.e. their negative and positive charges cancel each other out. Accordingly:

$$(5) \quad n_n + n_A = n_p + n_D$$

n_A : Concentration of acceptors

n_D : Concentration of donors

Furthermore, n_n and n_p are coupled by a mass action law, the number of electron-hole pairs which form and recombine per unit of time being equal during temperature-dependent equilibrium. The following applies:

$$(6) \quad n_n \cdot n_p = n_i^2$$

n_i is the charge carrier density in the case of purely intrinsic conduction (see experiment UE6020100)

In general, therefore:

$$(7) \quad n_n = \sqrt{n_i^2 + \frac{(n_A - n_D)^2}{4}} + \frac{n_D - n_A}{2}$$

$$(8) \quad n_p = \sqrt{n_i^2 + \frac{(n_A - n_D)^2}{4}} + \frac{n_A - n_D}{2}$$

At room temperature, the concentrations n_A and n_D are significantly higher than the charge carrier density in the case of purely intrinsic conduction n_i . Consequently:

$$(9) \quad R_H = -\frac{1}{n_D \cdot e}, \quad \mu_H = -\mu_n$$

with n-doping at 300 K

$$(10) \quad R_H = \frac{1}{n_A \cdot e}, \quad \mu_H = \mu_p$$

with p-doping at 300 K.

The charge carriers' sign and density can therefore be read directly from the Hall coefficient. The charge carriers' mobility is equivalent to the Hall mobility.

EVALUATION

As more carriers become available for conducting electricity with increasing temperature, the Hall voltage decreases until it attains a value of zero.

In the case of p-doped germanium, the Hall voltage's sign changes because increasing intrinsic conduction leads to a dominant influence of the electrons whose mobility μ_n is higher. Electrical conduction enabled by doping dominates below the inversion temperature, while intrinsic conduction dominates above the inversion temperature.

At high temperatures, the n-doped and p-doped crystals are no longer distinguishable because:

$$n_n = n_p = n_i, \quad R_H = -\frac{1}{n_i \cdot e} \cdot \frac{\mu_n - \mu_p}{\mu_n + \mu_p}, \quad \mu_H = -(\mu_n - \mu_p)$$

The temperature dependence of the mobilities μ_n and μ_p is not evident in the Hall coefficient, because in both cases: $\mu \sim T^{-\frac{3}{2}}$ (also see experiment UE6020100)

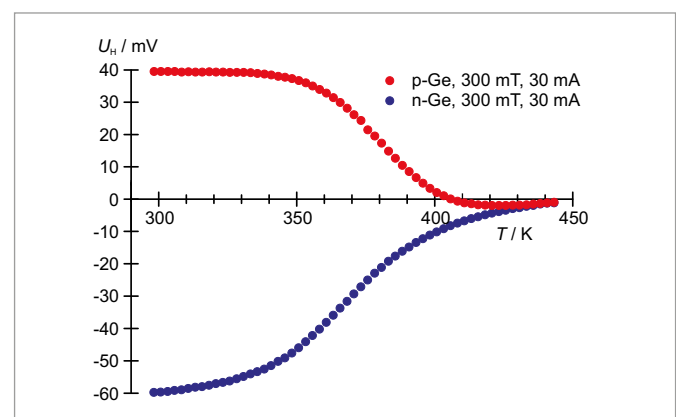
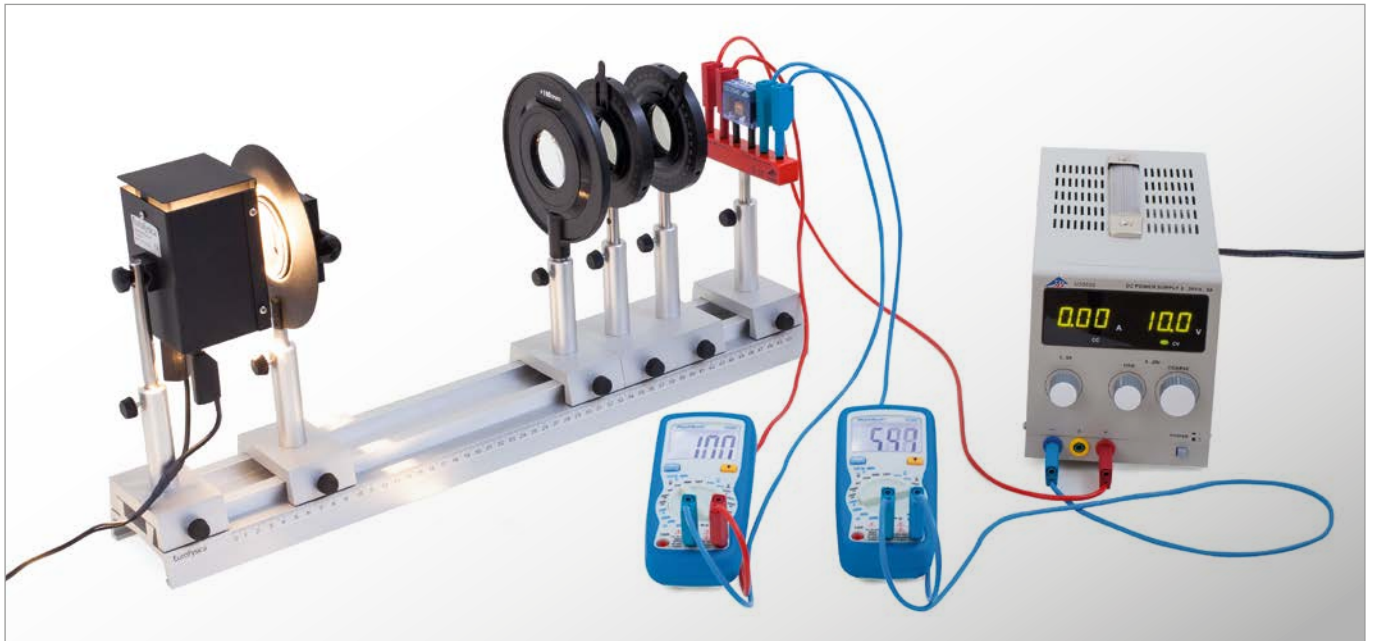


Fig. 1: Hall voltage in p- and n-doped germanium as a function of the temperature T

UE6020400 | PHOTOCONDUCTIVITY



EXPERIMENT PROCEDURE

- Measure current as a function of voltage for various intensities of light.
- Measure current as a function of light intensity for various voltages.

OBJECTIVE

Record the characteristic curve for a photoresistor

SUMMARY

Photoconductivity utilizes absorption of light by means of the inherent photoelectric effect in a semiconductor to create electron-hole pairs. One specific semiconductor mix which exhibits the photoelectric effect particularly strongly is cadmium sulphide. This material is used in the construction of photoresistors. In this experiment, a CdS photoresistor is illuminated with white light from an incandescent bulb. The intensity of this illumination of the photoresistor is then varied by crossing two polarising filters placed one behind the other in the beam.

REQUIRED APPARATUS

Quantity	Description	Item Number
1	Optical Bench U, 600 mm	1003040
6	Optical Rider U, 75 mm	1003041
1	Experimental Lamp, Halogen	1003038
2	Transformer 12 V, 60 VA (230 V, 50/60 Hz)	1020595 or
	Transformer 12 V, 60 VA (115 V, 50/60 Hz)	1006780
1	Adjustable Slit on Stem	1000856
1	Convex Lens on Stem $f = +150$ mm	1003024
1	Polarization Filter on Stem	1008668
1	Holder for Plug-in Components	1018449
2	Photoresistor LDR 05, P2W19	1012940
1	DC Power Supply 0 – 20 V, 0 – 5 A (230 V, 50/60 Hz)	1003312 or
	DC Power Supply 0 – 20 V, 0 – 5 A (115 V, 50/60 Hz)	1003311
2	Digital Multimeter P1035	1002781
3	Pair of Safety Experimental Leads, 75 cm, red/blue	1017718

BASIC PRINCIPLES

Photoconductivity utilizes absorption of light by means of the photoelectric effect in a semiconductor to create electron-hole pairs. In some semiconductors, this effect is dominated by boundaries of discontinuities in the material. The effect is then not only dependent on the basic material, but also on its microstructure and on impurities. Ionization of these impurities acts in a similar way to doping for a few milliseconds, increasing the electrical conductivity of the material. One specific semiconductor mix which exhibits the inherent photoelectric effect particularly strongly is cadmium sulphide, which is used to make photoresistors.

Absorption increases the conductivity of the semiconductor in a manner described by the following equation:

$$(1) \quad \Delta\sigma = \Delta p \cdot e \cdot \mu_p + \Delta n \cdot e \cdot \mu_n$$

e : Elementary charge,
 Δn : Change in electron concentration,
 Δp : Change in hole concentration,
 μ_n : Electron mobility, μ_p : Hole mobility

When a voltage U is applied, the photoelectric current is given by the following:

$$(2) \quad I_{ph} = U \cdot \Delta\sigma \cdot \frac{A}{d}$$

A : Cross-section of current path,
 d : Length of current path

The semiconductor therefore acts in a circuit like a light-dependent resistor, the value of its resistance decreasing when light shines upon it. The dependence of current on light intensity Φ at a constant voltage may be expressed in the form

$$(3) \quad I_{ph} = a \cdot \Phi^\gamma \text{ where } \gamma \leq 1.$$

Here the value γ is indicative of the recombining processes within the semiconductor material.

In this experiment, a CdS photoresistor is illuminated with white light from an incandescent bulb. Measurements are made of how current I through a CdS photoresistor depends on the applied voltage U at constant light intensity Φ and how it depends on intensity Φ at constant voltage U . The intensity is varied by crossing two polarising filters placed one behind the other in the light beam.

If the maximum power dissipation of 0.2 W is exceeded, the photoresistor will be damaged. For this reason the intensity of the incident light in the experiment is limited by means of an adjustable slit directly behind the light source.

EVALUATION

The current-voltage characteristics of a CdS photoresistor are along a straight line through the origin, as implied by equation (2).

In order to describe the characteristics for current and light intensity, the term $\cos^2\alpha$ is calculated for use as a relative measure of light intensity. In this case, α is the angle between the directions of polarization of the two filters. However, even when they are fully crossed, the filters will not block all the light. Also, it is not possible to avoid entirely the intrusion of residual light from the room in which the experiment is taking place. Under such circumstances, equation (3) needs to be modified to

$$I = a \cdot \Phi^\gamma + b \text{ with } \gamma \leq 1.$$

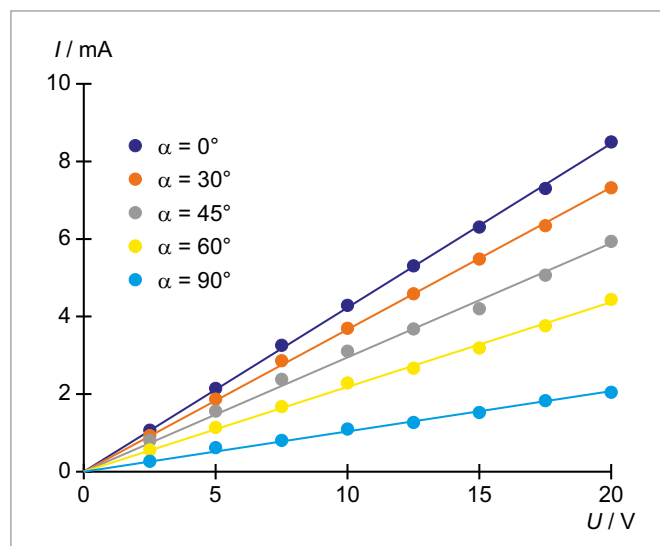


Fig. 1: Current-voltage characteristics of a CdS photoresistor for various intensities of light.

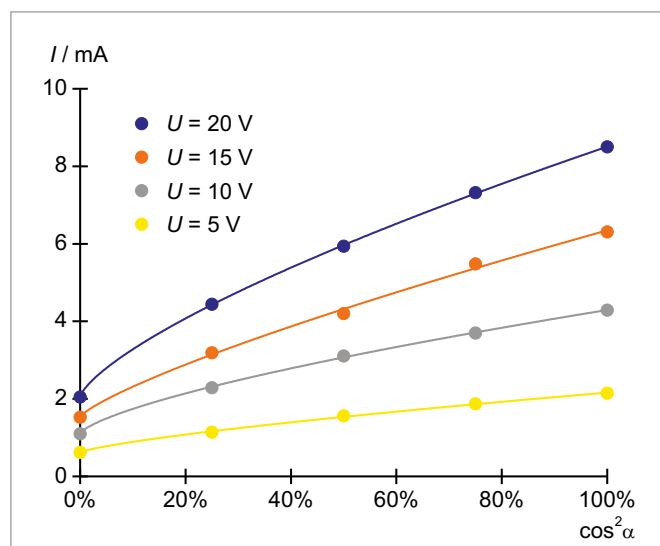


Fig. 2: Characteristics for current and light intensity of a CdS photoresistor at various voltages.

UE6020500 | SEEBECK EFFECT



OBJECTIVE

Record characteristics for various thermocouples and determine their sensitivity

> EXPERIMENT PROCEDURE

- Measure the thermocouple voltage U_{th} as a function of temperature T_1 and confirm that there is a linear relationship between for each of three different thermocouples.
- Determine the sensitivity S from the plots of U_{th} and T_1 .
- Estimate the reference temperature T_2 from the measured curves.

SUMMARY

If the ends of a metal wire are at different temperatures, since the thermally generated motions of the electrons have different velocities, thermal diffusion will occur between the hot and cold ends of the wire. The current resulting from this diffusion causes the cold end to be negatively charged with respect to the warmer end. The thermal diffusion voltage that arises is proportional to the difference in temperature between the two ends with the constant of proportionality being known as the Seebeck coefficient. If wires of two different metals are joined together, with contact points held at different temperatures, and a voltmeter is connected between the two unjoined ends, the result is a thermocouple. The voltmeter will then display a voltage which is directly proportional to the difference in temperature between the contact points. The experiment investigates this phenomenon with three different combinations of metals.

REQUIRED APPARATUS

Quantity	Description	Item Number
1	Set of 3 Thermocouples	1017904
1	Thermometer -20 – 110°C	1003384
1	Thermometer Clip	1003528
1	Set of 10 Beakers, Tall Form	1002873
1	Magnetic Stirrer with Heater (230 V, 50/60 Hz)	1002807 or
	Magnetic Stirrer with Heater (115 V, 50/60 Hz)	1002806
1	Measurement Amplifier U (230 V, 50/60 Hz)	1020742 or
	Measurement Amplifier U (115 V, 50/60 Hz)	1020744
1	Digital Multimeter P3340	1002785

BASIC PRINCIPLES

If the ends of a metal wire are at different temperatures, since the thermally generated motions of the electrons have different velocities, thermal diffusion will occur. Since the thermal motion of electrons at the hot end is faster than that of those at the cooler end, more electrons on average move from the warm end to the cold end than the other way round. The current resulting from this diffusion causes the cold end to be negatively charged with respect to the warmer end resulting in a voltage between the two ends. This increasingly acts against the flow of electrons until the diffusion current ceases to flow.

The thermal diffusion voltage U_{td} is proportional to the difference in temperature $T_1 - T_2$ between the ends, with the constant of proportionality being known as the Seebeck coefficient k :

$$(1) \quad U_{td} = k \cdot (T_1 - T_2)$$

U_{td} : Thermal diffusion voltage,
 k : Seebeck coefficient,
 T_1 : Temperature at hot end
 T_2 : Temperature at cold end

If wires of two different metals are joined together, with contact points held at different temperatures, a thermoelectric current will result. The metal with the larger thermal diffusion voltage will determine the direction of the current flow. If a voltmeter is then connected between the ends, the result is a thermocouple. Due to the high input resistance, very little current will then flow and the voltmeter will indicate a voltage which is directly proportional to the difference in temperature between the contact points:

$$(2) \quad U_{th} = U_{td,B} - U_{td,A} = (k_B - k_A) \cdot (T_1 - T_2)$$

U_{th} : Thermocouple voltage,
 $U_{td,A}, U_{td,B}$: Thermal diffusion voltages for metals A and B
 k_A, k_B : Seebeck coefficients for metals A and B

Only the differential between the Seebeck coefficients

$$(3) \quad k_{BA} = k_B - k_A$$

which appears in equation (2) can be measured without difficulty. This corresponds to the sensitivity of a thermocouple consisting of metals A and B, given by the following:

$$(4) \quad S = \frac{dU_{th}}{dT_1}$$

It is common to use platinum, Pt, as the reference material, whereby the coefficients are given as K_{APt} . This experiment involves measuring sensitivities S for three different pairs of metals. Water in a beaker will be heated to a temperature T_1 and one end of the thermocouple will be immersed in that. The other end of the thermocouple will be connected to the measurement amplifier U in order to measure the voltage. The sockets of this amplifier are at a constant temperature T_2 .

EVALUATION

The thermocouple voltage will be plotted against temperature in a graph of U_{th} against T_1 for each of the three thermocouples. A straight line is drawn to fit each set of points and the sensitivities of each element can then be determined from the gradients of the lines.

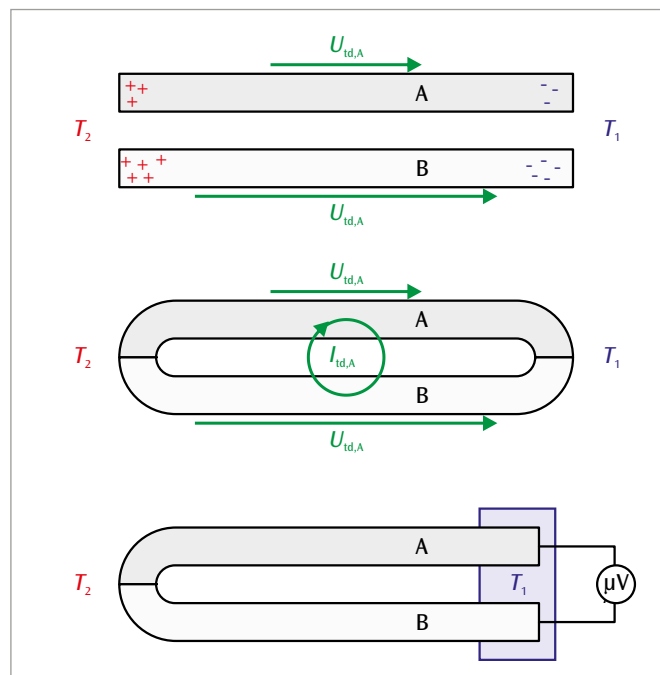


Fig. 1: Thermal diffusion in metal wires (top), thermoelectric current (center) and thermocouple voltage in a loop made of two different metals (bottom)

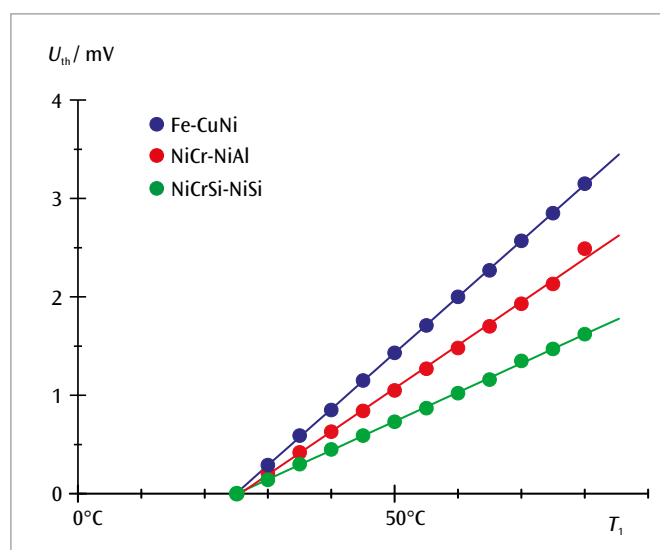
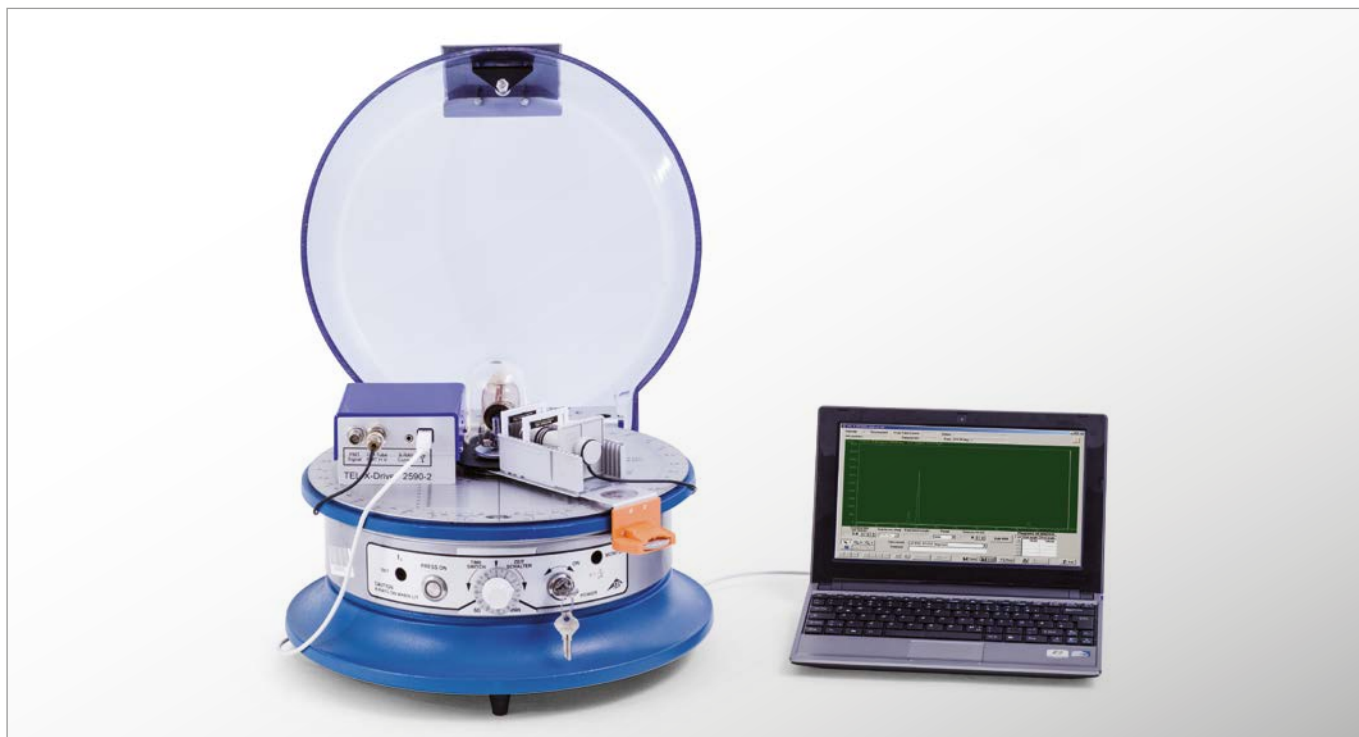


Fig. 2: Thermocouple voltages as a function of temperature for Fe-CuNi, NiCr-NiAl and NiCrSi-NiSi thermocouples. The measured curves cross the T_1 axis of the graph at the reference temperature $T_2 = 23^\circ\text{C}$

UE7010100 | BRAGG REFLECTION



> EXPERIMENT PROCEDURE

- Record diffraction spectra of the X-rays produced by a copper anode upon passing through crystals with a salt-like structure.
- Determine the lattice constants and make a comparison with the size of the crystals' components.

OBJECTIVE

Determine the lattice constants for crystals with a structure similar to salt (NaCl)

SUMMARY

Measurement of Bragg reflection is a key method for investigating monocrystals using X-rays. It involves X-rays being reflected by the various lattice planes, whereby the secondary waves reflected by individual layers undergo constructive interference when the Bragg condition is fulfilled. If the wavelength of the X-rays is known, it is possible to calculate the separation between lattice planes. In this experiment, various crystals which share the structure of salt (NaCl) are investigated and compared.

REQUIRED APPARATUS

Quantity	Description	Item Number
1	X-Ray Apparatus (230 V, 50/60 Hz)	1000657 or
	X-Ray Apparatus (115 V, 50/60 Hz)	1000660
1	Basic Set Bragg	1008508
1	Crystallography Accessories	1000666
1	Bragg Drive	1012871

BASIC PRINCIPLES

A key method for investigating monocrystals using X-rays was devised by *H. W.* and *W. L. Bragg*. They developed an interpretation of how atoms or ions were arrayed in a crystal which took the form of parallel layers in a structure containing the component atoms of the crystal lattice. Incoming plane waves of X-rays would then be reflected from these layers but the wavelength of the X-rays would remain unaffected.

The direction of the incident and reflected rays, parallel to the wave fronts, would be expected to meet the condition "angle of incidence = angle of reflection". The secondary waves reflected from the various lattice layers would also be expected to interfere with one another,

whereby the interference would be constructive when the path difference Δ between the secondary waves is an integer multiple of the wavelength λ .

The path difference can be deduced with the help of Fig. 1, where it can be seen that

$$(1) \quad \Delta = 2 \cdot d \cdot \sin\vartheta$$

d : interplanar distance

ϑ : angle of incident and reflected rays

This means the condition for constructive interference is

$$(2) \quad 2 \cdot d \cdot \sin\vartheta_n = n \cdot \lambda$$

Therefore, if monochromatic X-rays of known wavelength are used, the interplanar distance d can be found by measuring the angles.

In practice, this is done by turning the crystal by an angle ϑ with respect to the angle of incidence, while at the same time moving the Geiger-Müller detector by an angle of 2ϑ , see Fig. 2. Condition (2) is therefore precisely met when the Geiger counter registers maximum intensity.

This experiment uses the characteristic X-rays produced by an X-ray tube with a copper anode. This produces K_α radiation of wavelength $\lambda = 154 \text{ pm}$ and K_β radiation of wavelength $\lambda = 138 \text{ pm}$. Use of a nickel filter allows much of the K_β radiation to be suppressed, since the absorption edge of nickel lies between the two aforementioned wavelengths. In addition to their characteristic radiation, all X-ray tubes also emit “bremsstrahlung” (literally braking radiation) distributed over a continuous spectrum. This is evident as background beneath the peaks in the measured curves, which represent the characteristic lines. This experiment investigates cubic monocrystals which have been sliced parallel to their (100) face. This makes the lattice planes which are relevant for Bragg reflection easy to identify. In order to improve the accuracy of the measurement, multiple orders of diffraction are considered.

The crystals provided include LiF and NaCl crystals. Supplementary measurements can also be made using KCl and RbCl crystals. All of these have the same crystal lattice structure, in which the two varieties of atom occupy alternating positions in the lattice. The interplanar distance d is therefore equal to half of the lattice constant a .

EVALUATION

Using equation (2) the following equation can be derived for determining the lattice constants:

$$a = 2 \cdot d = \lambda_{K\alpha} \cdot \frac{n}{\sin\vartheta_n}$$

A comparison between the values obtained for NaCl, KCl and RbCl indicates that the lattice constant correlates with the size of the alkali metal ions. The lattice constants for LiF and NaCl also differ because the component atoms of the crystal are of different sizes.



Fig. 5: NaCl crystal

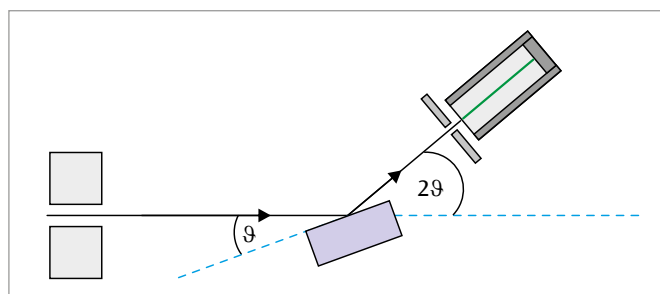


Fig. 1: Measuring principle

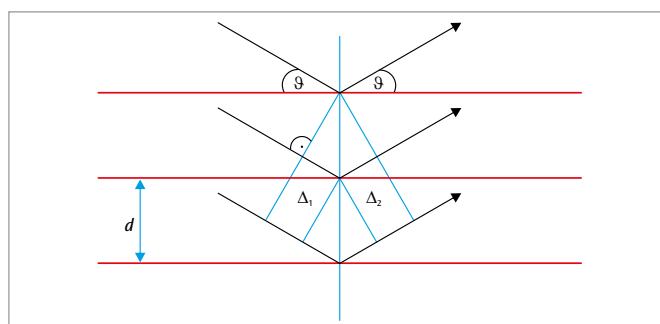


Fig. 2: Diagram showing derivation of Bragg condition

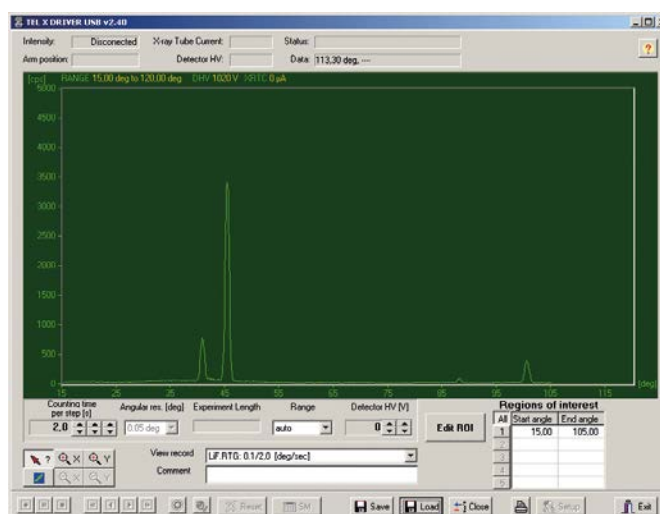


Fig. 3: Bragg curve for NaCl

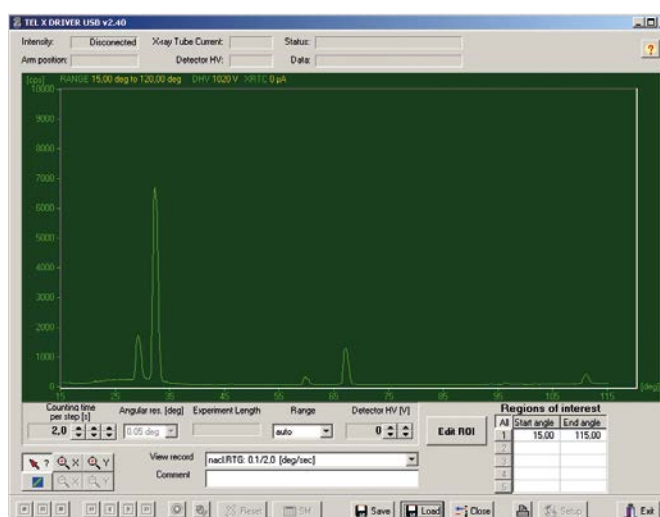
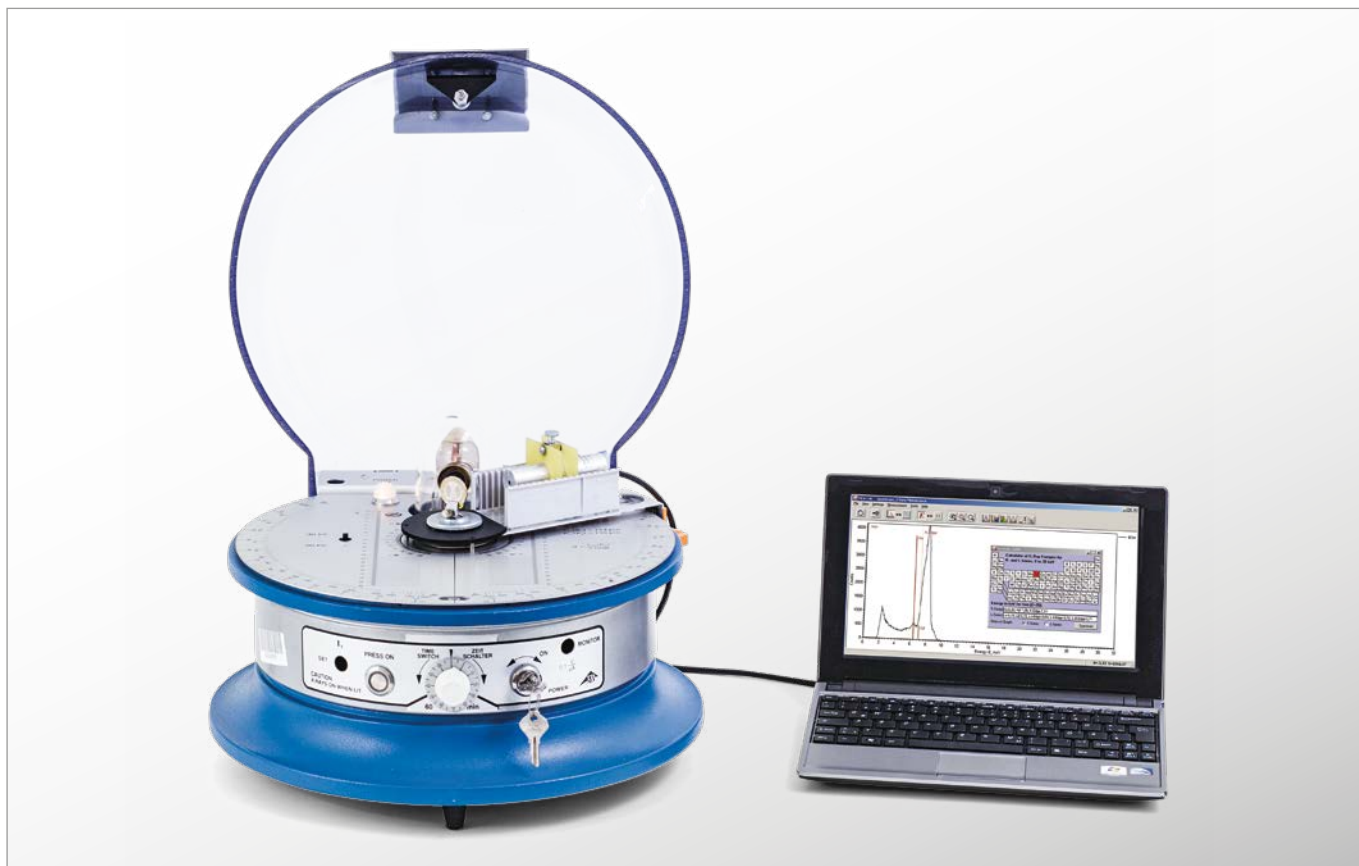


Fig. 4: Bragg curve for LiF

UE7020100 | X-RAY FLUORESCENCE



> EXPERIMENT PROCEDURE

- Record X-ray fluorescence spectra for various material samples.
- Identify the chemical components on the basis of characteristic X-ray lines.

OBJECTIVE

Non-destructive analysis of chemical composition

SUMMARY

Chemical elements can be uniquely identified on the basis of their characteristic X-ray radiation. This is because the energy of that radiation is dependent on the atomic number of the element. X-ray fluorescence analysis involves exciting this characteristic X-ray radiation by bombarding the material to be investigated with highly energetic X-ray quanta. This experiment analyzes the chemical composition of multiple material samples. Comparisons are made between wrought iron and stainless steel, copper, brass and bronze, as well as a variety of coins.

REQUIRED APPARATUS

Quantity	Description	Item Number
1	X-Ray Apparatus (230 V, 50/60 Hz)	1000657 or
	X-Ray Apparatus (115 V, 50/60 Hz)	1000660
1	Basic Set Bragg	1008508
1	X-Ray Energy Detector	1008629
1	Set of Fluorescence Samples	1012868

Additionally recommended

Coins

BASIC PRINCIPLES

Chemical elements can be uniquely identified on the basis of their characteristic X-ray radiation. This is because the energy of that radiation is dependent on the atomic number of the element. This means that the chemical composition of a material can be determined by measuring the characteristic X-ray radiation. Chemical bonds between the elements are not relevant to this since they do not involve the inner shells of atoms where X-ray transitions occur.

X-ray fluorescence analysis involves exciting this characteristic X-ray radiation by bombarding the material to be investigated with highly energetic X-ray quanta. The excitation energy needs to be higher than the characteristic radiation to be expected, meaning that it may not be possible to excite high-order transitions in the K series of elements.

The analysis therefore needs to concentrate on transitions in the L series, see Fig. 1.

An X-ray energy detector is provided for this experiment in order to record the energy spectra. The incident X-ray radiation causes interactions between electron/hole pairs in the atoms of crystals forming a silicon PIN photodiode. The overall charge associated with these is proportional to the X-ray energy. The charge is converted into a voltage pulse proportional to the X-ray energy which can then be transmitted to a computer as a digital value. Evaluation software is used to plot the distribution of pulses of specific amplitude. When the energy is calibrated, this distribution is equivalent to the energy spectrum we are seeking.

This experiment uses an X-ray tube with a copper anode as its source of radiation. The chemical composition of multiple material samples are analyzed and comparisons made between wrought iron and stainless steel, copper, brass and bronze, as well as a variety of coins.

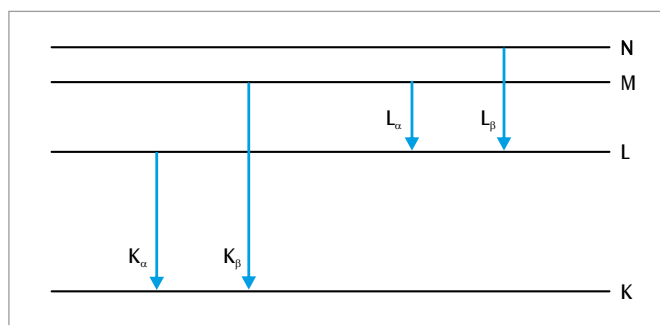


Fig. 1: Simplified energy band diagram for an atom with characteristic X-ray lines

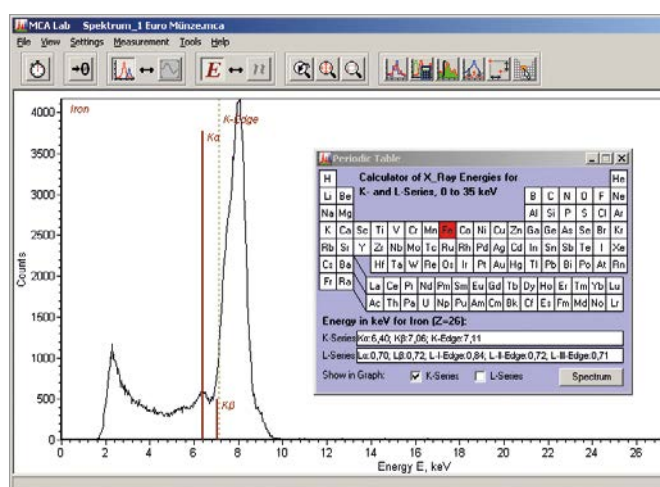


Fig. 2: X-ray fluorescence spectrum for a one euro coin

EVALUATION

The evaluation software allows the measured energy levels to be compared with values quoted in literature for the characteristic radiation wavelengths of the materials in question.

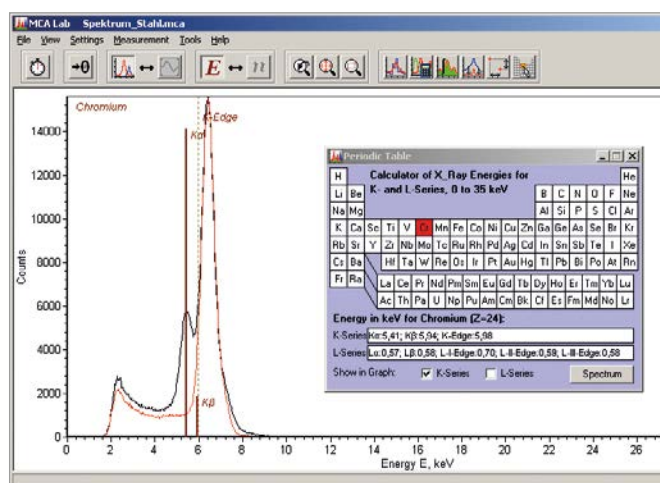
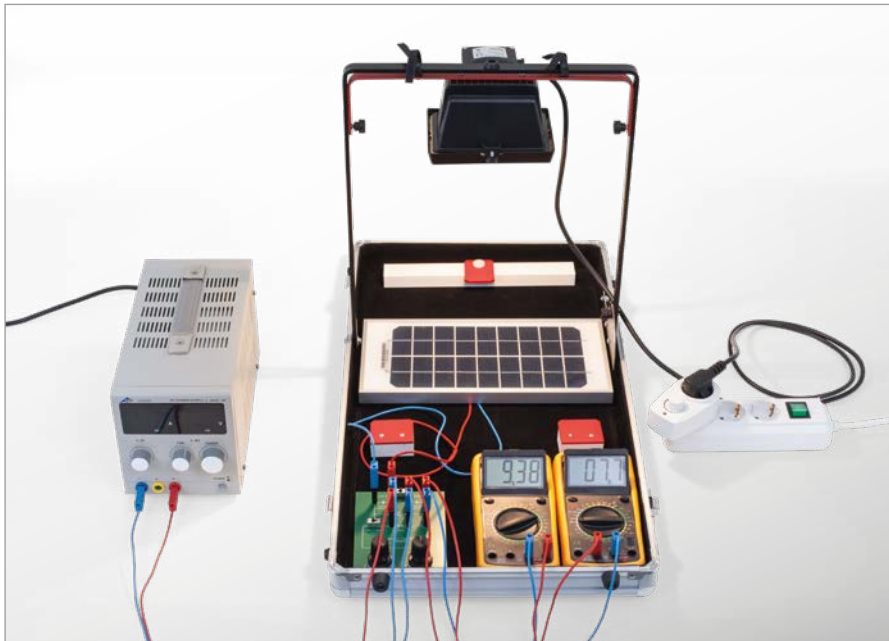


Fig. 3: X-ray fluorescence spectra for wrought iron (red) and stainless steel (black)



OBJECTIVE

Record the characteristics of a photovoltaic module (solar cell) as a function of the luminosity

SUMMARY

A photovoltaic system converts light energy from sunlight to electrical energy. To do this, solar cells are used which are comprised of, for example, suitably doped silicon and consequently correspond to an up-scaled photodiode. Light absorbed by the solar cell releases charge carriers from their crystal bonds which result in a photoelectric current flowing opposite the forward direction of the p-n junction. It is the diode current of the solar cell that limits current output to an external load. When at the so-called no-load or idle voltage U_{OC} , this current reaches a

> EXPERIMENT PROCEDURE

- Measuring the $I-U$ characteristics of a photovoltaic module (solar cell) at various illumination levels.
- Comparing the measured characteristics with a calculation in accordance with the single-diode model.
- Determining the relationship between the no-load voltage and the short-circuit current for various illumination levels.

zero value because the photoelectric current and the diode current precisely offset each other and only becomes negative when a voltage is applied that is above the no-load voltage. When a positive current range is reached, the solar cell can be operated as a generator that outputs electrical power to an external load. In the experiment, the voltage-current characteristics of this generator are measured as a function of the illumination level and described with a set of simple parameters.

REQUIRED APPARATUS

Quantity	Description	Item Number
1	SEK Solar Energy (230 V, 50/60 Hz)	1017732 or
	SEK Solar Energy (115 V, 50/60 Hz)	1017731
1	DC Power Supply 0 – 20 V, 0 – 5 A (230 V, 50/60 Hz)	1003312 or
	DC Power Supply 0 – 20 V, 0 – 5 A (115 V, 50/60 Hz)	1003311

BASIC PRINCIPLES

The term photovoltaic is a combination of the Greek work phos (light) and the Italian name Volta. This is in honor of *Alessandro Volta*, who, among other things, invented the first functional electrochemical battery. A photovoltaic system converts limitlessly available and free light energy from sunlight into electrical energy without causing any CO₂ emissions. To do this solar cells are needed, which in most cases are made of suitably doped silicon and thus corresponds to a scaled-up photodiode. Prior to reaching the external contacts of the solar cell, first the light absorbed by the solar cell releases charge carriers from their crystal bonds (internal photoeffect), due to the electrical field achieved through suitable dosing of the p-n junction the electrons drift to the n-doped side and the holes drift to the p-doped side (Fig. 1). This is how a photoelectric current arising flows in the reverse direction to the forward direction of the p-n junction, which can output the electrical power to an external load.

The photoelectric current I_{ph} is proportional to the illumination level Φ :

$$(1) \quad I_{ph} = \text{const} \cdot \Phi$$

It is superpositioned by the diode current in the forward or conducting direction:

$$(2) \quad I_d = I_s \cdot \left(\exp\left(\frac{U}{U_T}\right) - 1 \right)$$

I_s : Saturation current,

U_T : Temperature voltage

and grows ever stronger the more voltage U between the contacts exceeds the diffusion voltage U_D . Thus the current I output available for external loads is limited by the diode current:

$$(3) \quad I = I_{ph} - I_D = I_{ph} - I_s \cdot \left(\exp\left(\frac{U}{U_T}\right) - 1 \right)$$

It reaches the value zero for so-called no-load or idle voltage U_{OC} because the photo-electric current and the diode current mutually offset each other and only becomes negative if a voltage $U > U_{OC}$ is applied.

In the range of positive currents the solar cell can be operated as a generator to output electrical energy to an external load. Eq. (3) expresses the I - U characteristic of this generator. Since in actual practice the photo-electric current I_{ph} is considerably higher than the saturation current I_s , we can derive from (3) the following relationship for the idle voltage:

$$(4) \quad U_{oc} = U_T \cdot \ln\left(\frac{I_{ph}}{I_s}\right).$$

If the terminals of solar cell are short-circuited, the cell supplies the short-circuit current I_{SC} , which corresponds to the photo-electric current since $U = 0$ according to Equation (3). Consequently, we obtain:

$$(5) \quad U_{oc} = U_T \cdot \ln\left(\frac{I_{SC}}{I_s}\right) \text{ where } I_{SC} = I_{ph}$$

Eq. 2 describes the diode response within the framework of the so-called standard model. Here the saturation current I_s happens to be a material variable, which depends on the geometrical and electrical data of the solar cell. For the temperature voltage U_T , the following holds true:

$$(6) \quad U_T = \frac{m \cdot k \cdot T}{e}$$

$m = 1 \dots 2$: Ideal factor, k : Boltzmann's constant, e : Elementary charge, T : Temperature in Kelvin

In a more precise examination of the characteristic, leakage currents at the edges of the solar cells and point-like short-circuits of the p-n junction would be taken into consideration, which can be modelled using a parallel resistance R_p . Eq. 3 then becomes

$$(7) \quad I = I_{ph} - I_s \cdot \left(\exp\left(\frac{U}{U_T}\right) - 1 \right) - \frac{U}{R_p}$$

So in order to achieve effectively utilisable voltages in the range between 20 and 50 V, in practice we see a significant number of solar cells connected in series. Such a series connection configuration comprised of 18 solar cells is illuminated in the experiment using a halogen lamp of variable luminosity and the current-voltage characteristics of the module are recorded at varying luminosities.

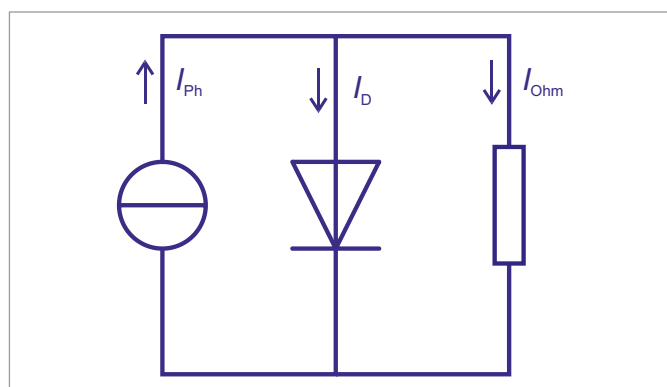


Fig. 3: Equivalent circuit diagram for the photovoltaic module

EVALUATION

The family of current-voltage characteristics from the photo-voltaic module (Fig. 2) can be described using Equation 7, if regardless of the luminosity the same set of parameters i.e. I_s , U_T and R_p is inserted and the photo-electric current I_{ph} is selected as a function of the luminosity. Of course the temperature voltage is the 18 times the value estimated in Eq. 6 because the module consists of 18 solar cells connected in series.

A parallel circuit comprised of an ideal power source, a series connection of 18 semi-conductor diodes and an ohmic resistor, see Fig. 3 is provided as an equivalent circuit diagram for the photovoltaic module. The power source supplies a luminosity-dependent current in the reverse direction.

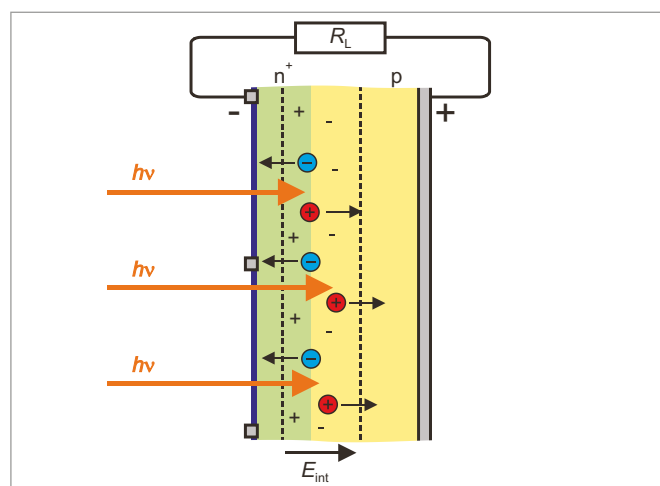


Fig. 1: Schematic depiction of a solar cell as a semi-conductor element, n^+ : heavily n-doped area, p : p-doped area, \ominus : mobile hole produced by light absorption, \oplus : free electron produced by light absorption, + : stationary positive charge, - : stationary negative charge, E_{int} : electrical field imposed by the space-charge differential, R_L -load resistance

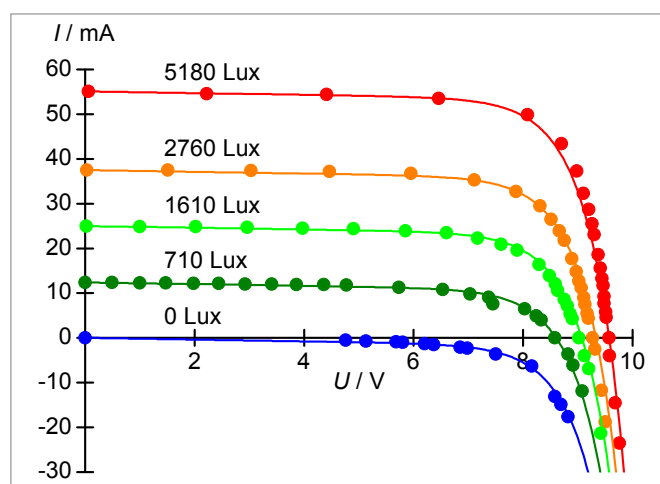
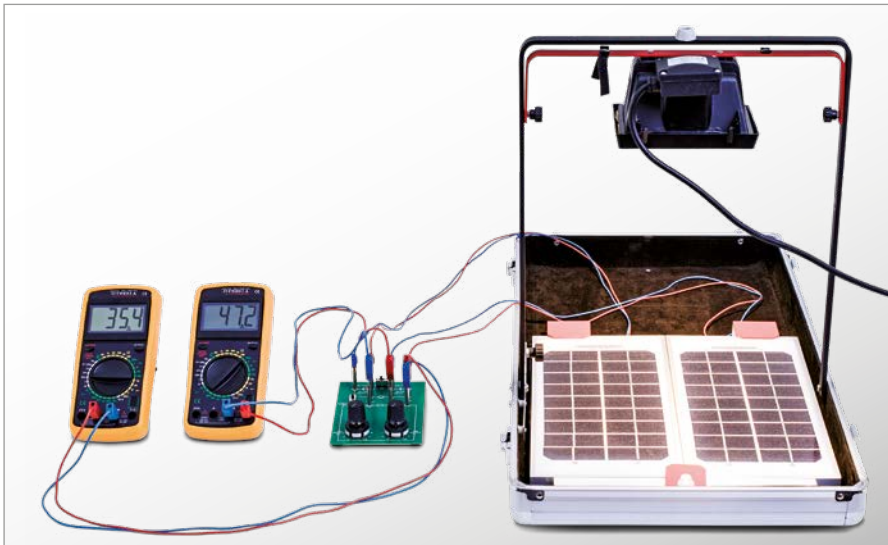


Fig. 2: Current-voltage family of characteristics of a photovoltaic module for five different luminosities

UE8020200 | PHOTOVOLTAIC SYSTEMS



OBJECTIVE

Investigate how partial shading affects photovoltaic systems

EXPERIMENT PROCEDURE

- Measure and analyze the $I-U$ characteristic and $P-R$ characteristic for a series circuit containing two photovoltaic modules.
- Measure and analyze the characteristics with the modules partially in shade both with and without by-pass diodes.
- Demonstrate the reverse bias voltage for an unprotected module in shadow.
- Determine the loss of power resulting from partial shading.

SUMMARY

In photovoltaic installations, multiple solar modules are usually connected in series in a long line. The modules themselves are made up of many solar cells connected in series. In practice, it is possible for such systems to be partially in shadow. Individual parts of the system are then exposed to less light and therefore generate little current, which then limits the current in the whole series circuit. This can be avoided by means of by-pass diodes. In this experiment, two modules each consisting of 18 solar cells are formed into a simple photovoltaic system. They can optionally be connected in series with or without by-pass diodes and are then illuminated with light from a halogen lamp.

REQUIRED APPARATUS

Quantity	Description	Item Number
1	SEK Solar Energy (230 V, 50/60 Hz)	1017732 or
	SEK Solar Energy (115 V, 50/60 Hz)	1017731

BASIC PRINCIPLES

In photovoltaic installations, multiple solar modules are usually connected in series in a long line. The modules themselves are made up of many solar cells connected in series.

Calculation of current and voltage for such a series circuit follows from Kirchhoff's laws, taking into account the current-voltage characteristic of the solar cells. The same current I flows through all the modules in the series circuit and the voltage is given by

$$(1) \quad U = \sum_{i=1}^n U_i$$

n : Number of modules

This is the sum of all the voltages U_i between the terminals of the individual modules.

The current-voltage characteristic of a solar cell or module can be easily explained by means of an equivalent circuit diagram made up of a constant voltage source supplying a photoelectric voltage and a "semiconductor diode" connected in parallel with it but in reverse-bias direction. Resistive losses which occur are represented by a resistor, also connected in parallel in the system (see Experiment UE8020100 and Fig. 1). The photoelectric current is proportional to the intensity of the illuminating light. When the intensity is the same for all modules, then they all respond alike and individually supply the same voltage. Equation 1 then implies:

$$(2) \quad U = n \cdot U_1$$

In practice, however, it is possible for such systems to be partially in shadow. Individual modules in the system are then exposed to less light and therefore generate little photoelectric current, which then limits the current in the whole series circuit. This limiting of current causes differing voltages U_i to be generated by the individual modules. In the extreme case, the voltages across fully illuminated modules, even under short-circuit conditions ($U = 0$), can attain values going as far as the open-circuit voltage, see Fig. 2. The sum of these voltages is in reverse-bias direction across the modules in shadow. This can lead to enormous amounts of heating and can destroy the capsules in which the solar cells are contained or even the cells themselves. To protect against this, photovoltaic systems are equipped with by-pass diodes, which allow the current to by-pass elements which are in shadow.

In this experiment, two modules each consisting of 18 solar cells are formed into a simple photovoltaic system. They can optionally be connected with or without by-pass diodes in series and are then illuminated with light from a halogen lamp. Initially the two modules are both illuminated with the same bright intensity of light, but later one module is put into shadow such that it only supplies half the amount of current. In all cases I - U characteristics are plotted from short-circuit to open-circuit range and compared. Power values are also calculated as a function of the load resistance to determine the amount of power loss as a result of the shading and to determine the effect of the by-pass diodes. For the case of a short-circuit, the voltage across the shaded module is also measured separately. It reaches -9 V if the module is not protected by a by-pass diode.

EVALUATION

If a module only supplies half the amount of photoelectric current, for example, it will be responsible for determining the short-circuit current for the whole series circuit in the absence of any by-pass diodes.

With by-pass diodes, the fully illuminated module can supply its higher current until this starts to decrease when the open-circuit voltage of the individual module is reached.

The mathematical model for evaluating the measurements in Figs. 3 and 4 takes into account Kirchhoff's laws and utilizes the current-voltage characteristic for the individual modules obtained in Experiment UE8020100 with parameters I_S , U_T and R_p . To take account of the by-pass diodes, their own characteristics are used.

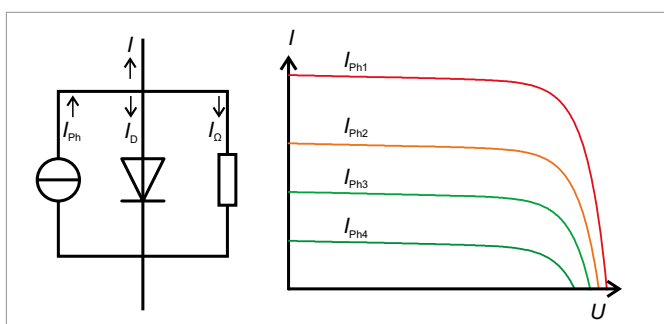


Fig. 1: Equivalent circuit diagram and characteristics of a solar cell

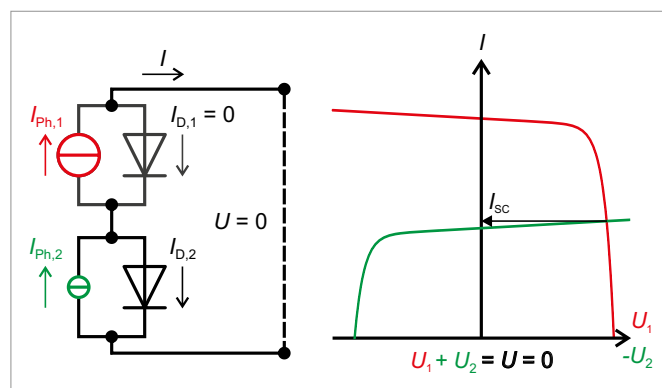


Fig. 2: Schematic diagram of partial shading of two modules with no by-pass diodes under short-circuit conditions ($U = 0$). The characteristic of the shaded model (green) is shown reversed. Here it represents a voltage of U_2 in the reverse-bias direction.

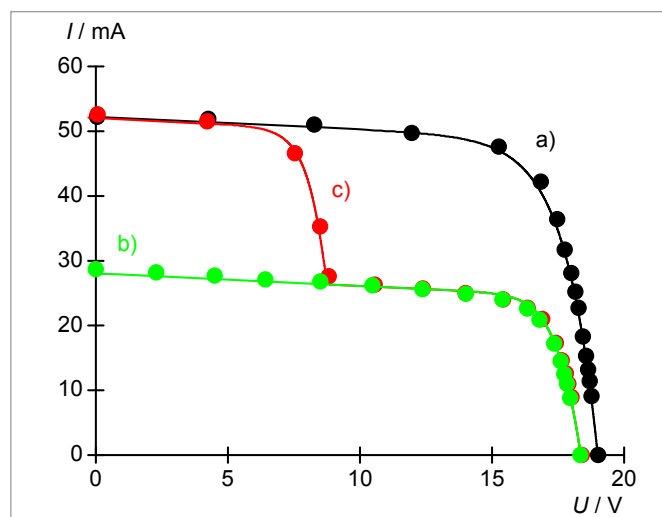


Fig. 3: I - U characteristic for series circuit containing two solar modules a) with no shading, b) partial shading without by-pass, c) partial shading with by-pass

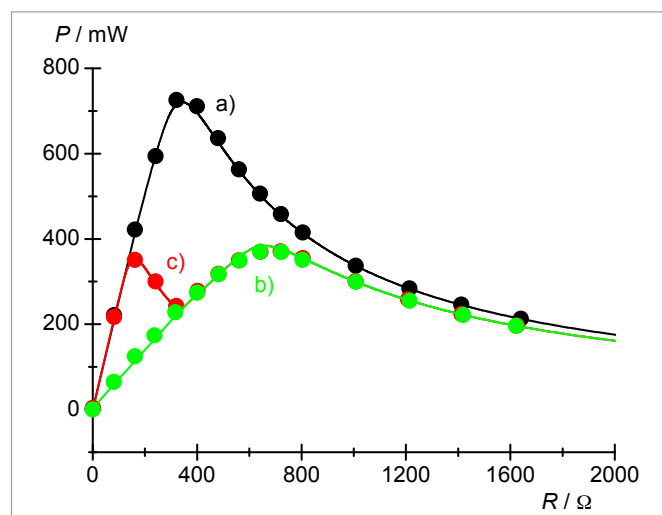
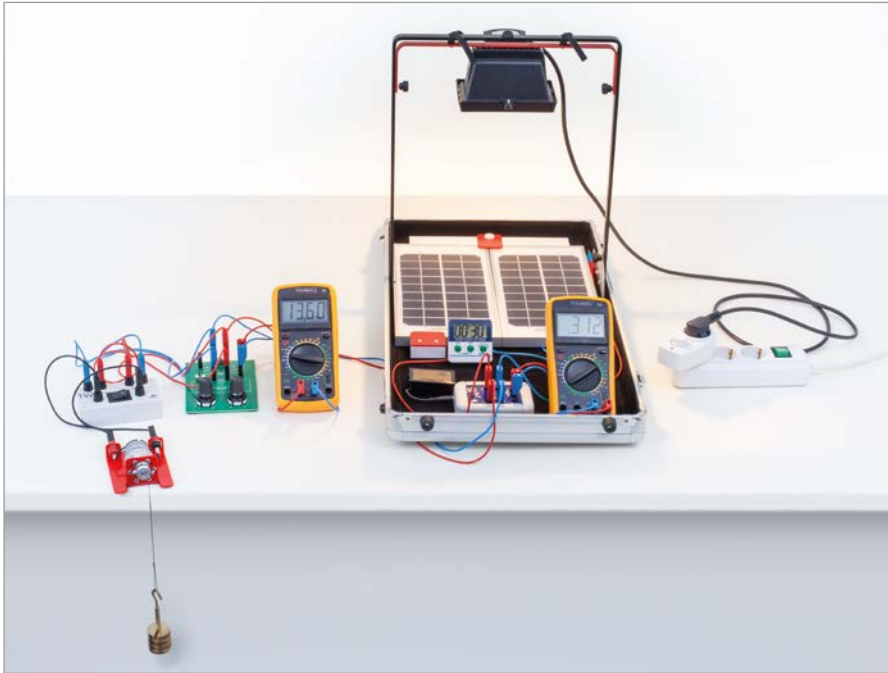


Fig. 4: P - R characteristic for series circuit containing two solar modules a) with no shading, b) partial shading without by-pass, c) partial shading with by-pass

UE8020250 | PHOTOVOLTAIC SYSTEMS



OBJECTIVE

Investigation of an island grid or microgrid used to generate and store electrical energy

> EXPERIMENT PROCEDURE

- Determining the operating current of the electronic charge meter and the minimum illuminance required for operation.
- Investigating the current balance of the island grid for various resistive loads and different luminosities in lab operation.
- Measuring the solar power being delivered and the charging or discharging current as a function of the load current for different illuminance levels.

SUMMARY

Island grids or microgrids are power supply systems without any connection to a public utility grid and incorporate both generation and storage of electrical energy. Frequently photovoltaic modules are used to generate power and accumulators are used for energy storage. In order to simulate such an island grid in an experiment, two photovoltaic modules are used to charge up a nickel-metal hydride battery. A DC motor is deployed as the connected load which discharges the accumulator, while an electronic charge meter measures the electrical charging and discharging of the battery. Thanks to a series connection of the two modules a reliable charging of the accumulator is achieved also when there is less illuminance, since idle voltage is still far above the accumulator voltage level.

REQUIRED APPARATUS

Quantity	Description	Item Number
1	SEK Solar Energy (230 V, 50/60 Hz)	1017732 or
	SEK Solar Energy (115 V, 50/60 Hz)	1017731
1	Coulombmeter with Rechargeable Battery	1017734
1	Geared Motor with Pulley	1017735
1	Set of Slotted Weights, 5 x 50 g	1018597
1	Cord, 100 m	1007112
1	Two-pole Switch	1018439
1	Set of 15 Experiment Leads, 75 cm, 1 mm ²	1002840
1	Timer	1003009

BASIC PRINCIPLES

Island grids are off-grid power supply systems without a connection to a public utility grid. They include power generation and storage and are normally deployed when connection to the public utility grid is either impossible or inefficient, or when this offers insufficient flexibility and mobility. Photovoltaic modules are frequently used to generate power and accumulators for storing energy in this context. To emulate this kind of off-grid island system two photovoltaic modules are used in the experiment, each having a nominal power of 5 W

for charging a nickel-metal hydride battery with a capacitance of 220 mAh. A DC motor functions as a connected load discharging the accumulator while an electronic charge meter is used to measure current charging and discharging. We dispense with the charge controller usually deployed in this context.

The voltage U_{Accu} of the accumulator has a nominal rating of 8.4 V, but depends on the charging state as well as the charge current I_{Accu} and conventionally reaches up to 10 V. It determines the voltage in all circuit branches connected in parallel (see Fig. 1):

$$(1) \quad U_{Accu} = U_{Op} = U_L = U_{Solar}$$

The current supplied I_{Solar} is used as the basic operating current I_{Op} for the electronic charge meter, as charging current I_{Accu} for the accumulator and as current I_L flowing through the connected resistive load. The electric balance

$$(2) \quad I_{Solar} = I_{Accu} + I_{Op} + I_L$$

This also applies for cases of negative charge current I_{Accu} , i.e. in cases where the accumulator is discharging power.

The operating current $I_{Op} = 10$ mA is defined by the electronic circuit of the charge meter, while the load current I_L depends on the ohmic resistance R_L of the connected load. The accumulator is thus charged up when the photovoltaic system supplies power and the load resistance is not too low.

To ensure reliable charging of the accumulator during lower illuminance levels, it is important to configure the photovoltaic system so that its idle voltage U_{OC} is significantly higher than the voltage U_{Accu} . A comparison with the characteristics measured in the experiment UE8020100 shows that this can be reasonably reached by connecting the two modules in series configuration. Then the solar power supplied I_{Solar} is, in good approximation, proportional to the luminosity E and under laboratory conditions reaches values up to 50 mA, which are optimal for rapid charging of the accumulator.

A DC motor and a cascade resistor configuration are used as resistive loads with which the charging current/load current characteristics of the island grid is sampled and furthermore verified that the solar current supplied is independent of the resistive load. In the results the minimum brightness can be specified, for example, which is needed to charge the accumulator in the absence of all loads.

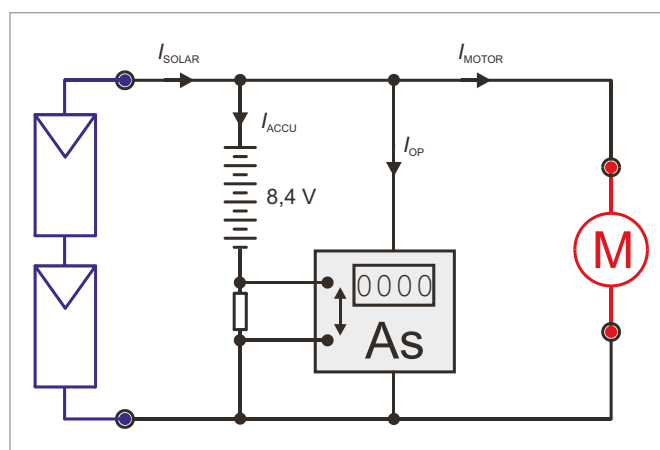


Fig. 1: Block circuit diagram of island grid

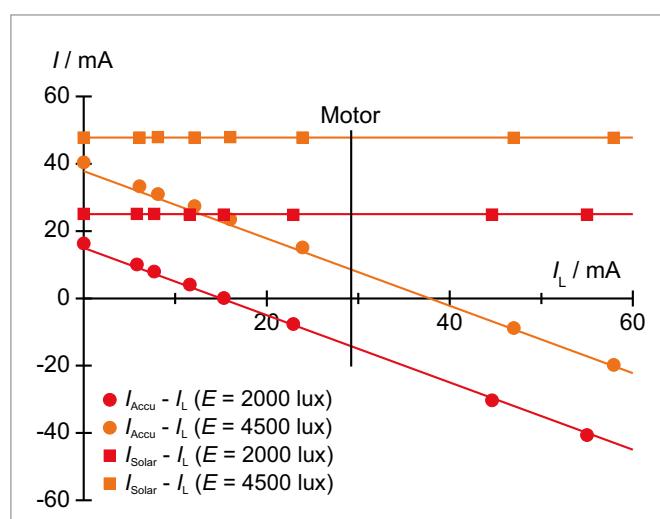


Fig. 2: Load characteristics of island grid

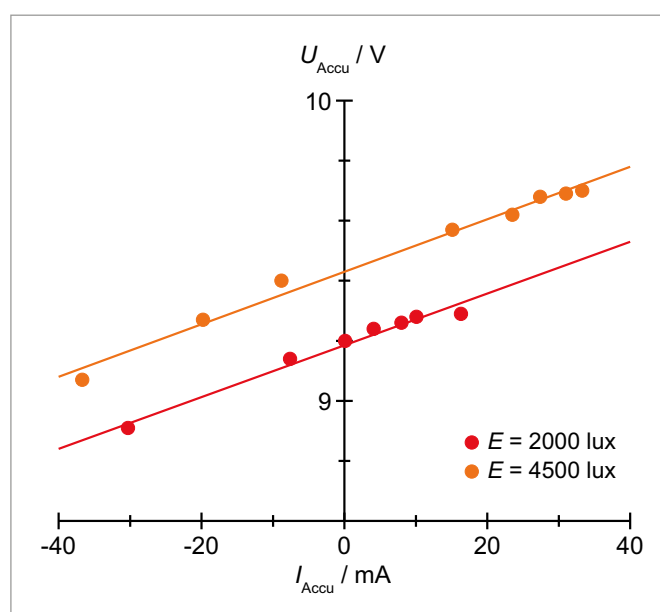


Fig. 3: Characteristics of the accumulator, measured at different luminosities. Depending on the accumulator's charging state, these characteristics are shifted up or down on the y-axis.

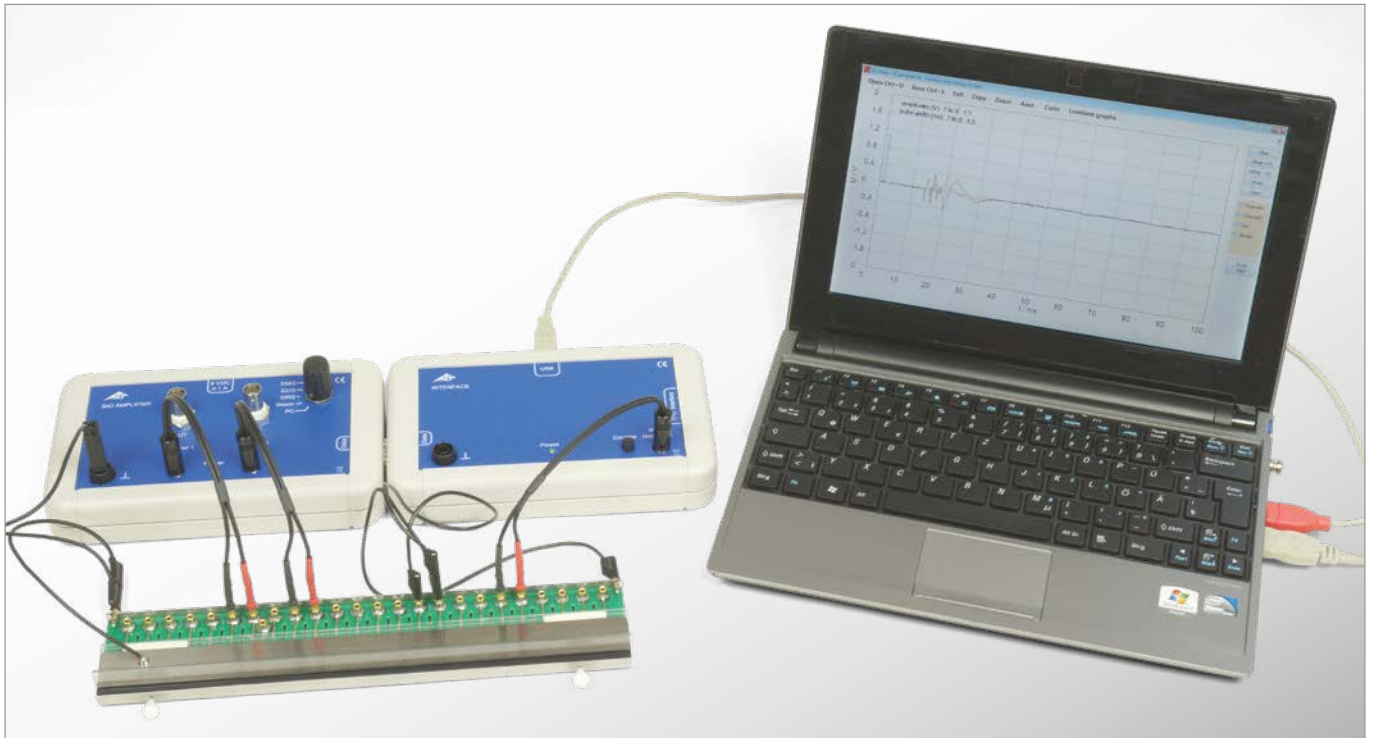
NOTE

When operating the photovoltaic module in sunlight outdoors, considerably higher electrical currents are reached. Here the accumulator should not be connected without additional resistive load which should ensure that the charging current does not exceed $I_{Accu} = 44$ mA.

EVALUATION

The operating current of the charging meter is determined from the charge flowing in 30 s out of the accumulator, if neither module nor load are connected.

UE9010100 | NEUROPHYSIOLOGY



> EXPERIMENT PROCEDURE

- Record the action potentials in earthworm giant nerve fibers after electrical and tactile stimulation.
- Option: Record a simple electro-myogram and electrocardiogram in humans.

WARNING

Electrophysiological experiments on humans must not be performed without reliable isolation from the mains voltage! Use measured values and measurement curves solely for educational purposes, never use the values to assess the state of health of a person!

OBJECTIVE

Investigate the action potentials in earthworm giant nerve fibers after electrical and tactile stimulation

SUMMARY

In this adaptation of Luigi Galvani's famous frog leg experiment an earthworm's giant nerve fiber is first irritated electrically. The resulting action potentials are amplified and measured with an interface. In the next step the earthworm is stimulated tactilely, which also leads to an action potential. Optionally, a simple electrocardiogram and a simple electromyogram on humans can be recorded.

REQUIRED APPARATUS

Quantity	Description	Item Number
1	Measurement Chamber for Earthworm Experiments	1020601
1	Bio-Amplifier (230 V, 50/60 Hz)	1020599 or
	Bio-Amplifier (115 V, 50/60 Hz)	1020600
1	Bio-Measurement Interface	1020602
1	Stimulation Equipment for Earthworm Experiments	1020603
	Giant Earthworms	
Additionally recommended		
1	Connecting Cable for Electro Cardiograms	1020605
1	Set of 30 Electrodes for ECG/EMG	5006578

BASIC PRINCIPLE

As early as 1790 the Bolognese researcher *Luigi Galvani* had demonstrated on the leg of a frog that electrical processes were involved in the functioning of nerves and muscles. Even today, similar specimens are used for research into nerve function and muscle contraction. One alternative to this is to carry out experiments on a live earthworm.

In the first part of the experiment a giant earthworm is brought into contact with an array of electrodes, which are connected to a bio-amplifier and a bio-measurement interface. The giant nerve fiber of the earthworm is then stimulated with different voltage signals at one end. As soon as the voltage exceeds a certain threshold an action potential can be observed. In the next step the earthworm is stimulated tactilely on the posterior and anterior end which also leads to the buildup of an action potential. As the skin thickness at both ends of the worm differ from each other it can be observed that also the action potentials have a different behavior.

The nerves of the earthworm have a simpler structure than those of the frog, thus allowing measurement of the nerve impulses in individual nerve fibers. The function of nerve potentials for the reflexes exhibited by the intact worm can be demonstrated. Cellular mechanisms for habituation can be measured.

During the experiment the worm remains alive and unharmed. Afterwards it can be released to its natural habitat.

EVALUATION

Figure 1 shows the earth worm's reactions to electrical stimulations. In the upper graph the stimulation was too weak to evoke a nerve potential, a just 0.1V higher stimulation in the lower graph was sufficient to start an action potential.

In figure 2 the action potentials after tactile stimulation at the anterior end (lower graph) and at the tail (upper graph) are shown. After stimulation at the anterior end recording takes place in the more posterior parts of the worm while recordings after tail stimulations are done in the anterior parts.

An example for an electromyogram of a slowly contracted biceps is shown in figure 3.

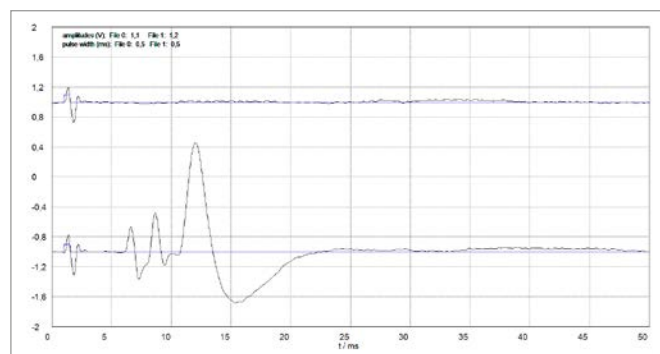


Fig. 1: Reactions to electrical stimulations

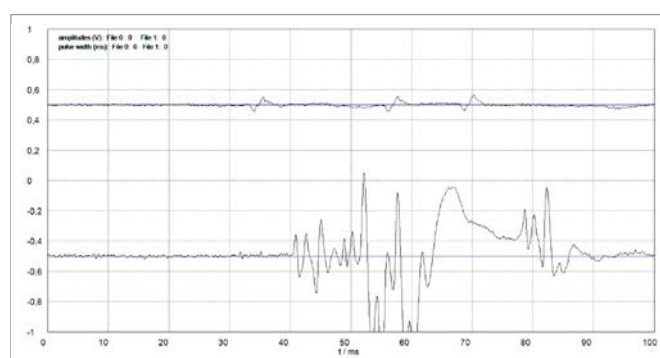


Fig. 2: Reactions to tactile stimulation at the anterior end (lower graph) and at the tail (upper graph)

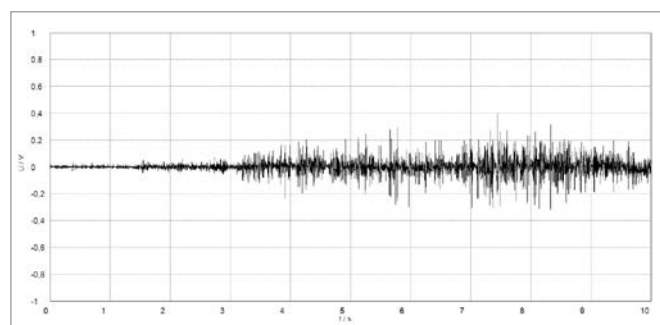
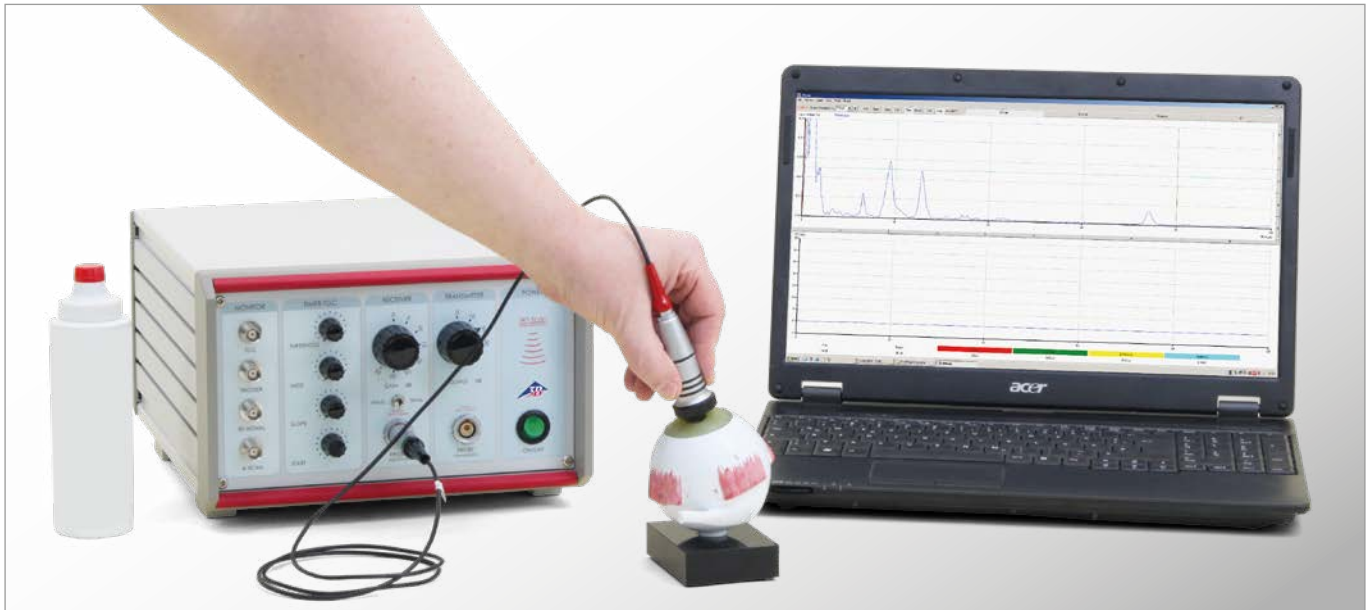


Fig. 3: Electromyogram of a slowly contracted biceps

UE9020100 | ULTRASONIC BIOMETRY



> EXPERIMENT PROCEDURE

- Measure the biometric ratios in the human model eye by using a pulse-echo method.
- Calculate the geometry of individual objects in the eye.

OBJECTIVE

Determining the internal dimensions in a model eye

SUMMARY

In this experiment a typical application of A-scan ultrasound biometry in medical diagnostics used in ophthalmology is given. At an eye dummy all parts of the healthy eye are measured and correction calculations shall be done.

REQUIRED APPARATUS

Quantity	Description	Item Number
1	Ultrasonic Echoscope GS200	1018616
1	Ultrasonic Probe 2MHz GS200	1018618
1	Model Eye for Ultrasonic Biometry	1012869
1	Ultrasonic Coupling Gel	1008575

BASIC PRINCIPLE

Ultrasound is used also in ophthalmology. Its largest importance lies in the area of biometry, in the measurement of distances in the eye. The distance between cornea and retina is very significant for the calculation of the characteristics of the artificial lens implanted to patients with cataract. Sonography is necessary in this case since the cornea or the lens are too cloudy for the use of optical methods. Investigations of the aqueous, vitreous humor and the thickness of the lens are nowadays often done with new methods of laser light or ultrasonic B-mode imaging.

The given measured time of flight of the echoes of the A-scan cannot be calculated as distance in a simple way, because of different velocities in the different media (cornea, lens, vitreous humor). Therefore a corrective calculation is necessary. Two velocities are given for the dummy: -lens: 2500 m/s, -humors: 1410 m/s. These values and the time of flight from the measured A-scan image shall be used to determine the distances with the help of the following equation:

$$(1) \quad s = v \frac{\Delta t}{2}$$

In medical diagnostics “averages” are often used known from experience. This average velocity shall be calculated for the dummy with the following equation:

$$(2) \quad v = \frac{v_1(t_1 + (t_3 - t_2)) + v_2(t_2 - t_1)}{t_3}$$

Ultrasonic coupling gel is used to connect the probe to the cornea of the dummy. Slowly move the probe over the cornea to look for the optimal signals (2 large lens peaks and one smaller from the retina). After measuring the time of flight of the peaks the real distances can be calculated.

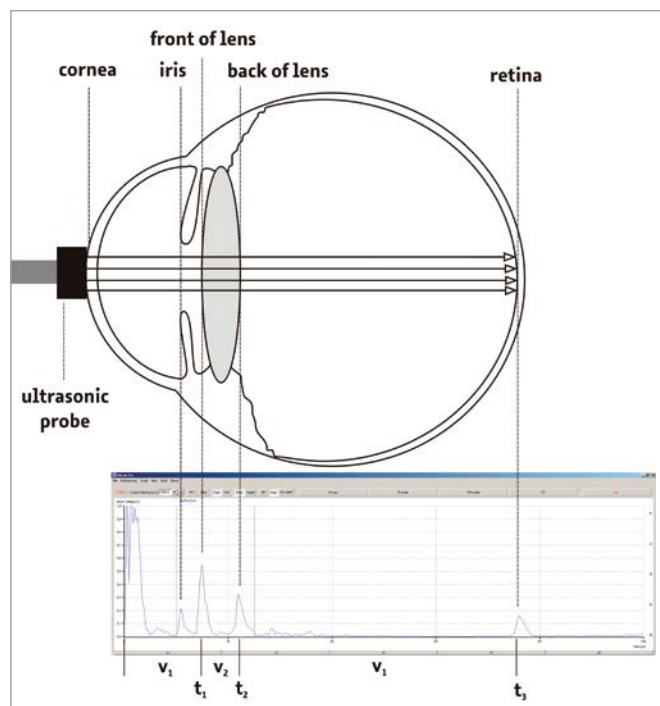


Fig. 1: A-mode image and schematic diagram of the human eye

EVALUATION

The time of flight of each peak was measured and the averaged velocity was calculated with the equation (2). The result was adjusted to the A-scan device, it was switched to the depth scale and the depth of each peak was measured.

velocities in m/s			
(aqueous/ vitreous humor)	1410 m/s		
(lens)	2500 m/s		
values:	front of lens	back of lens	retina
time in 10^{-6} s	13.7	21.1	74.8
average velocity	1518 m/s		
measured depth in mm	11.9	15.9	42.5
real depth in mm	9.66	18.91	56.77
thickness/ distance in mm	9.66	9.25	37.86

UE9020200

ULTRASONIC COMPUTER TOMOGRAPHY



> EXPERIMENT PROCEDURE

- Record an ultrasonic CT image.
- Analyze different measuring parameters.
- Investigate the influence of filtering and image processing.

OBJECTIVE

Investigate the formation of an ultrasonic CT image and its relevant parameters

SUMMARY

The several steps of the formation of a computed tomography are illustrated. The difference between damping and sound velocity as measuring parameters is analyzed. The influence of filtering and image processing is investigated.

REQUIRED APPARATUS

Quantity	Description	Item Number
1	Ultrasonic Echoscope GS200	1018616
1	CT Controller	1017783
1	CT Scanner	1017782
1	CT Measuring Trough	1017785
1	CT Sample	1017784
2	Ultrasonic Probe 2MHz GS200	1018618
1	Ultrasonic Coupling Gel	1008575

BASIC PRINCIPLE

X-ray CT, MRT and PET are computer-aided imaging methods used in medical diagnostics, industry and research. Processes such as radiation absorption, nuclear magnetic resonance or particle emission are used to produce cross-sectional images by means of appropriately measurable physical quantities. Ultrasonic computer tomography is another CT method. It differs from X-ray CT in that instead of the attenuation of X-rays, the attenuation and times of flight of ultrasonic signals in the test object are measured. With the ultrasonic CT, line scans are recorded at different angles and put together to form a cross-sectional image. In this process, the sample arranged between transmission and receiving probe is moved and turned under computer control. The overlaying of the projections of individual scans can be followed step by step on the PC.

To form the image the attenuation of sound and the sound velocity are utilized. The attenuation coefficient of sound μ results from the measured amplitude A and the amplitude without sample A_0 after the law of attenuation:

$$(1) \quad \mu \propto \ln \frac{A_0}{A}$$

For the generation of the sound velocity tomogram the time of flight is used as the measuring quantity and the following is valid:

$$(2) \quad c \propto \frac{t_0}{t}$$

where t_0 is the measured time of flight without the sample (the path length s is constant).

The sample (damping or velocity sample) is attached to the sample holder and by means of the scanner control is positioned exactly between the two sensors. Then the sample holder is moved half of the scanning way, the accuracy of scanning and the number of angle intervals are adjusted and the CT scan is started. During the measurements the individual line scans are observed and the generation of the tomograms by superposition of the projections of line scans is studied. The resulting images are optimized by means of various filters and by brightness and contrast adjustments, then the damping tomogram is compared with the velocity tomogram.

EVALUATION

The transmission signal (the diagram left above in Fig. 1) has been measured with regard to maximal amplitude and time of flight of the maximal amplitude and from this a line profile (scan at one angle, 500 μm point distance) has been built (diagram left below). The superposition by means of the CT-algorithm (25 angle intervals) yields for sound attenuation to the image left above (non filtered, contrast changed) and for the sound velocity to the image right above (also non filtered, contrast changed). Filtering the attenuation image improves the contrast so the edges become visible (reflection losses). The inner part hardly distinguishes from the surrounding water, in the sound velocity image (right) the sample and the inclusion are clearly visible as homogeneous regions of a different sound velocity.

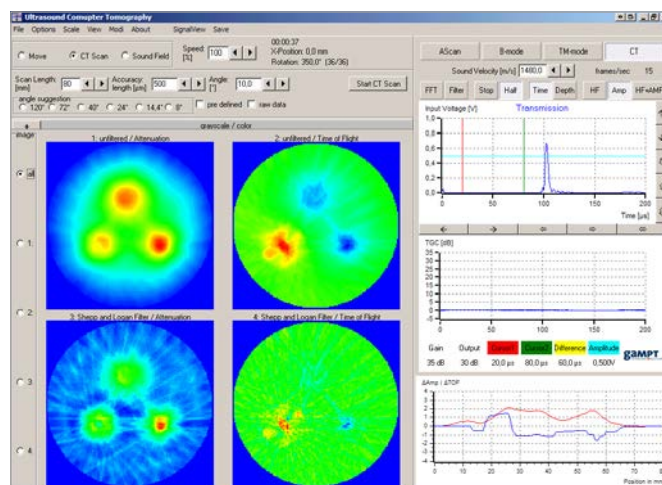
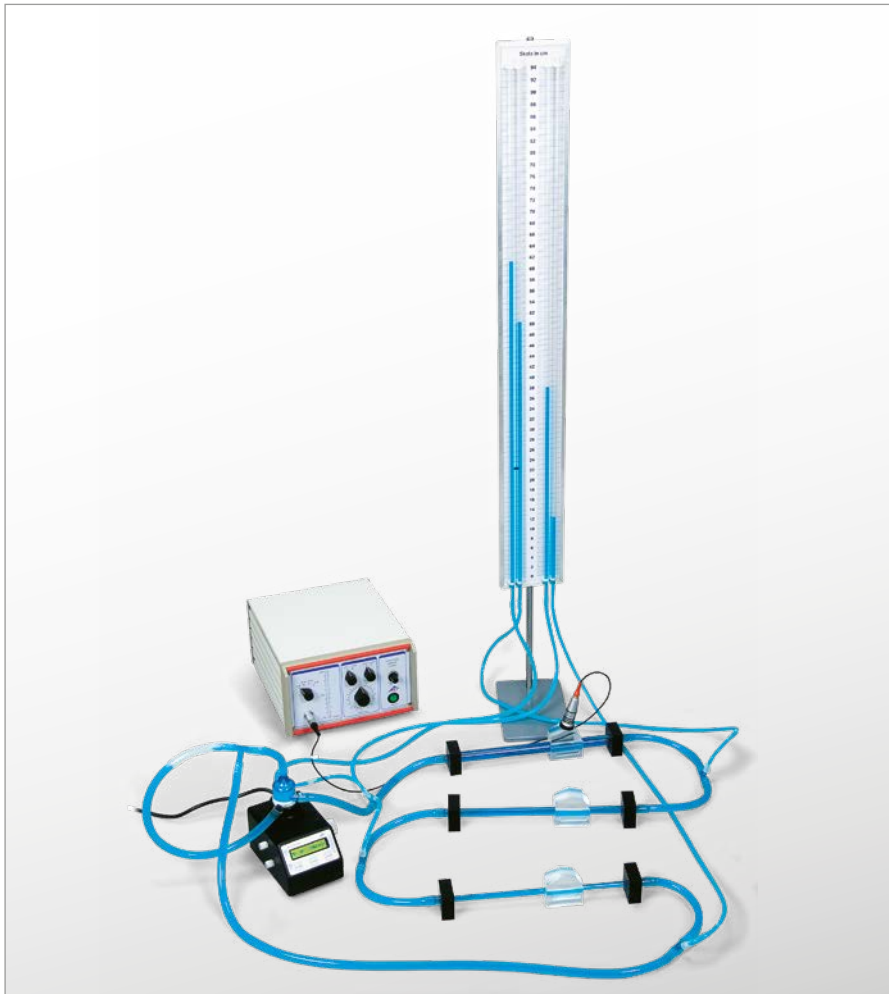


Fig. 1: Screenshot with attenuation and time-of-flight tomograms of the CT sample



OBJECTIVE

Investigate the fundamental characteristics of stationary and laminar flowing liquids by using the ultrasonic Doppler method

EXPERIMENT PROCEDURE

- Measure the Doppler frequency shift for different pump speeds and the pressure drops by standpipes.
- Determine flow rates, flow resistances, and dynamic viscosity of the doppler liquid by using the continuity equation, Bernoulli's equation and the Hagen-Poiseuille equation.
- Calculate the Reynold numbers for different flow velocities and pipe diameters.

SUMMARY

Flow measurements according to the ultrasonic Doppler method are used to demonstrate fundamental laws governing the flow of liquids in pipes and their dependence on the flow velocity and the pipe geometry. The relationship between flow velocity and tube cross section (continuity condition) as well as between flow resistance and tube diameter (law of Hagen-Poiseuille) are examined.

REQUIRED APPARATUS

Quantity	Description	Item Number
1	Ultrasonic Doppler Apparatus	1022330
1	Ultrasonic Probe, 2 MHz	1018618
1	Set of Doppler Prisms and Flow Tubes	1002572
1	Riser Tubes for Pressure Measurement	1002573
1	Doppler Phantom Fluid	1002574
1	Centrifugal Pump	1002575
1	Ultrasonic Coupling Gel	1008575

BASIC PRINCIPLE

The applications of the Doppler Effect in the medical diagnostics are at the investigation of running movements and moving structures as in cardiologic diagnostics, arterial and venous blood vessels, brain blood circulation and postoperative blood vessel control.

A stationary flowing liquid is characterized by a constant flow of liquid at each point of the system. Therefore the continuity equation for two different tube areas A_1 and A_2 results as:

$$(1) \quad A_1 v_1 = A_2 v_2 = \dot{V} = \text{const.}$$

v_1 and v_2 being the mean velocities in the respective section and \dot{V} the flow rate (volume per time unit). The static pressure in a flowing liquid is always smaller than in a motionless liquid, and reduces the greater the flow velocity is (Bernoulli equation). For the flow through a horizontal tube (without gravity pressure) the total pressure p_0 is:

$$(2) \quad p + \frac{1}{2} \rho v^2 = p_0$$

Only in a friction-less liquid p_0 is constant. In a flow pertaining to friction the total pressure decreases in dependence on the viscosity η , the length l , the cross-section A of the passing through region and the flow rate \dot{V} . For liquids with not too high flow velocities (laminar flow) in narrow tubes the Hagen-Poiseuille law is valid for the pressure drop Δp :

$$(3) \quad \Delta p = R \dot{V}$$

$$(4) \quad R = \frac{8 l}{\pi r^4} \eta$$

where r is the radius of the tube and l is the length. That means that a reduction of the diameter of the vessel to half results in an enhancement of the flow resistance to 16 times. By this principle blood vessels regulate the blood distribution between extremities and inner organs. A circulation is built consisting of 3 tube lines of equal lengths but different diameters. At the beginning and end of each line is a measuring point of equal diameter. At the tube lines the mean velocity is measured for 3 different flow rates (3 different voltages at the centrifugal pump) by means of the Doppler prism and the FlowDop. Knowing the measured flow velocities the flow rate can be determined after (1) and compared. At the measuring points the pressure drop due to the flow resistance can be measured. Calculating the flow rate from (1) the flow resistance can be determined after (4) and from this using the known geometry the dynamical viscosity of the liquid is obtained.

EVALUATION

From the flow rates measured and the specific crosssectional areas, the corresponding flow can be calculated. This is nearly equivalent in this experimental setup for all pipe diameters for the same settings of the centrifugal pump, thus satisfying the continuity equation. As a further result, the diagram below shows the flow resistance R determined for different pipe diameters and different flows. This shows the strong dependence on the pipe radius r to be expected from the Hagen-Poiseuille equation:

$$R \sim \frac{1}{r^4}$$

Fig.1 shows that the flow rate calculated from the measured velocity and the area is nearly the same at all tube diameters for equal voltages and therefore the continuity equation is fulfilled.

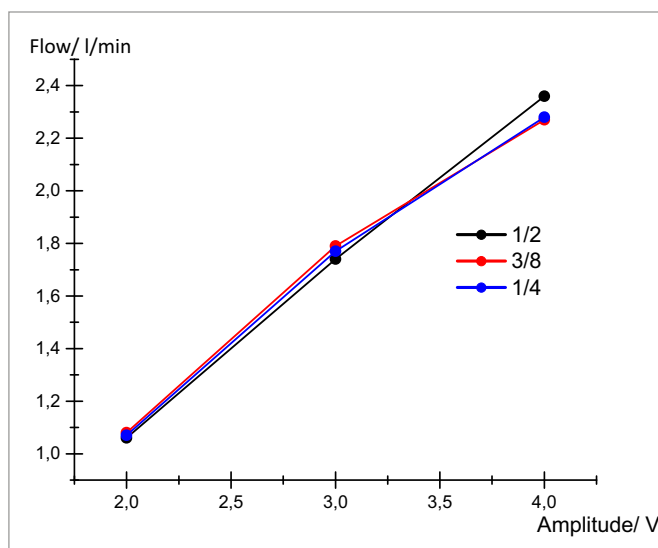


Fig1.: Flow rates for different tube diameters

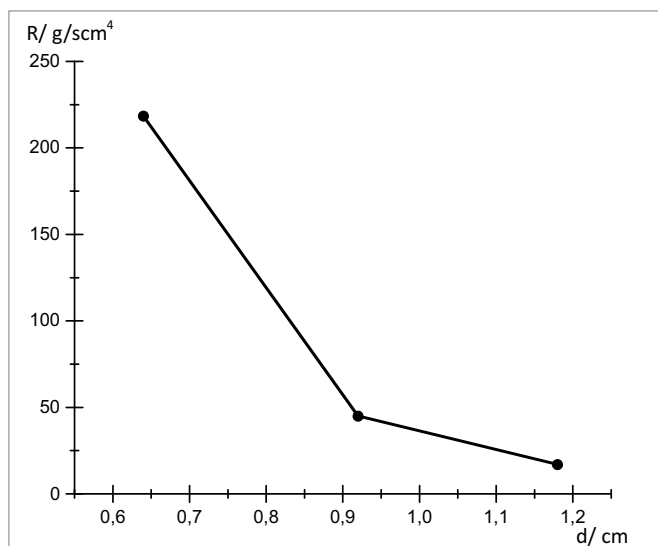


Fig1.: Flow rates for different tube diameters

UE9020400 | DOPPLER SONOGRAPHY



> EXPERIMENT PROCEDURE

- Doppler sonographic examinations of a human model arm.
- Measurement of the flow velocity of blood.
- Diagnosis of stenosis (vascular stricture) in an arm.
- Recording of Doppler spectra and pulse curves.

OBJECTIVE

Investigating a model arm

SUMMARY

The goal of the experiment is to learn how blood flow measurements are made with Doppler ultrasound. A realistic arm model is used to show the differences between continuously (venous) and pulsatile (arterial) flow and between normal blood flow and a stenosis.

REQUIRED APPARATUS

Quantity	Description	Item Number
1	Ultrasonic Doppler Apparatus	1022330
1	Arm Phantom Set	1022331
1	Centrifugal Pump	1002575
1	Ultrasonic Coupling Gel	1008575

BASIC PRINCIPLE

Doppler sonography uses the Doppler Effect to assess whether structures (usually blood) are moving towards or away from the ultrasonic probe, and its relative velocity. By calculating the frequency shift of a particular sample volume, for example a jet of blood flow over a heart valve, speed and direction of this sample volume can be determined and visualized. Doppler frequency shift is the difference in ultrasonic frequency between transmitted and received echoes, i.e. the echo frequency minus the transmitted frequency. The Doppler frequency is proportional to the blood flow velocity.

Doppler sonography is particularly useful in cardiovascular studies (sonography of the vasculature system and heart) and essential in many areas such as determining reverse blood flow in the liver vasculature in portal hypertension. The Doppler information is displayed graphically using spectral Doppler or as an image using color Doppler. For the experiment a pump is switched on and the speed is adjusted in a middle range (approx. 4000 min^{-1}). The mode is GK (continuously, venous). With the Doppler probe and coupling gel the arm model is scanned for a vessel with a significant audio signal.

The flow in the spectral image is analyzed for negative and positive components. The probe direction is then switched by 180° . Then the vessel is scanned for changes in the spectral image (stenosis) and the differences between the images of the "healthy" vessel and the stenosis will be characterized.

Lastly the pump is switched to P_1 and P_2 mode (pulsatile) the images are analyzed and the pulse rate is determined.

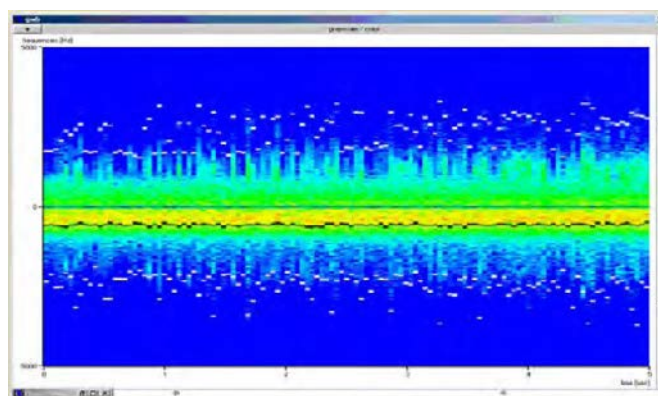


Fig. 1: Doppler spectrum of blood flow in veins

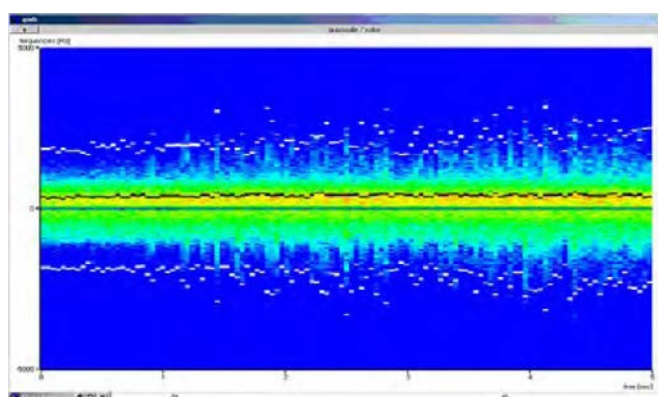


Fig. 2: Spectral distribution with rotated probe

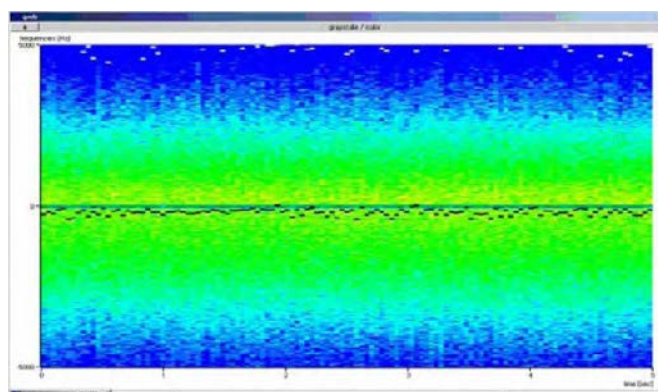


Fig. 3: Doppler spectrum of a stenosis

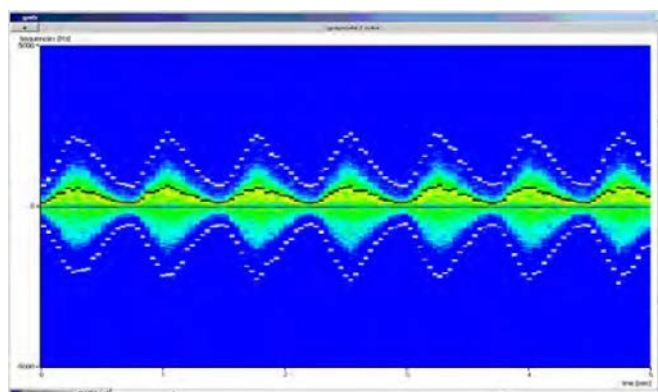


Fig. 4: Pulsatile flow

EVALUATION

Figure 1 shows a continuously (venous) flow with a mean Doppler shift of approx. -700Hz . The minus in the Doppler shift means a flow away from the probe.

Figure 2 is the spectral distribution with rotated probe. Flow towards the probe (the same Doppler shift, but positive).

Figure 3 is the Doppler spectral figure of a stenosis. The differences to a normal (healthy) figure like shown in figure 1 are:

1. A local increase of the maximum Doppler shift (maximum flow velocity).
2. A decrease of mean frequency and a broadening of the spectra.
3. An increase of reflux phenomenon (negative and positive parts of the spectra).

Figure 4 shows the pulsatile flow of P_1 with a pulse rate of ca. 90min^{-1} .

STUDENT EXPERIMENT

MECHANICAL OSCILLATIONS AND WAVES



> CONTENTS:

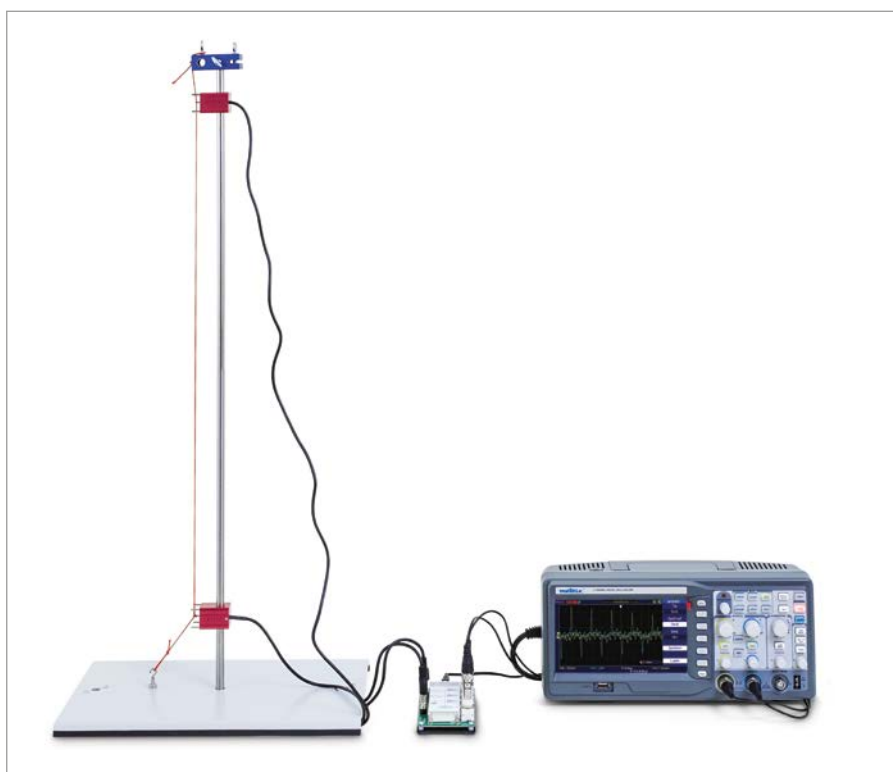
- 1 MEC Control Unit
- 1 Plug-in Power Supply
- 2 Dynamic Force Sensors
- 1 Eccentric Axle Motor
- 1 Induction Coil
- 1 Stopwatch
- 4 Coil Springs
- 1 Set of 10 Weights, 50 g
- 1 Base Plate
- 1 Cross-strut
- 2 Stand Rods with External Threads
- 2 Stand Rods with External and Internal Threads
- 2 Double Clamps
- 1 Magnetic Hooks
- 1 Bar Magnet
- 1 Rubber Cord
- 1 Roll of Twine
- 1 Thread Eyelet
- 1 Squirrel Cage Ring
- 1 Ruler
- 2 BNC Cable, 1 m
- 1 BNC/4-mm Cable

- > CD-ROM CONTAINING ALL DIFFERENT SETS OF INSTRUCTIONS IS INCLUDED!

Large equipment set for carrying out 23 fundamental experiments on the properties of mechanical oscillations and waves. Stored in a tough Grattell tray with foam inlay featuring recesses moulded to the shape of the apparatus and covered by a transparent lid. Includes CD with experiment instructions.

SEK Mechanical Oscillations and Waves (230 V, 50/60 Hz) 1016652

SEK Mechanical Oscillations and Waves (115 V, 50/60 Hz) 1018476



Reflection of waves along a rope

INCLUDES INSTRUCTION FOR 23 EXPERIMENTS ON MECHANICAL OSCILLATIONS AND WAVES:

- Determining spring constants (2x)
- Oscillations of a spring pendulum *
- Oscillations of two "identical" spring pendulums * / **
- In-phase and 180° out-of-phase oscillations of two "identical" spring pendulums * / **
- Excitation of a motionless spring pendulum by a moving one * / **
- Superposition of the oscillations of two spring pendulums * / **
- Spring pendulums connected in line * / **
- Spring pendulums connected parallel to one another * / **
- Intrinsic oscillation of a spring pendulum *
- Types of oscillation for a coil spring pendulum *
- String pendulums (2x)
- Seconds pendulums
- Galileo's interrupted pendulum
- Damped oscillations of string pendulums (2x) *
- Standing waves along a rope (2x) *
- Reflection of waves along a rope *
- Speed of propagation of waves along a rope (2x) *
- Oscillation of strings *

Equipment Mechanical Oscillations and Waves:

1016652 SEK Mechanical Oscillations and Waves (230 V, 50/60 Hz)

or

1018476 SEK Mechanical Oscillations and Waves (115 V, 50/60 Hz)

Dual-channel Oscilloscope, e.g.

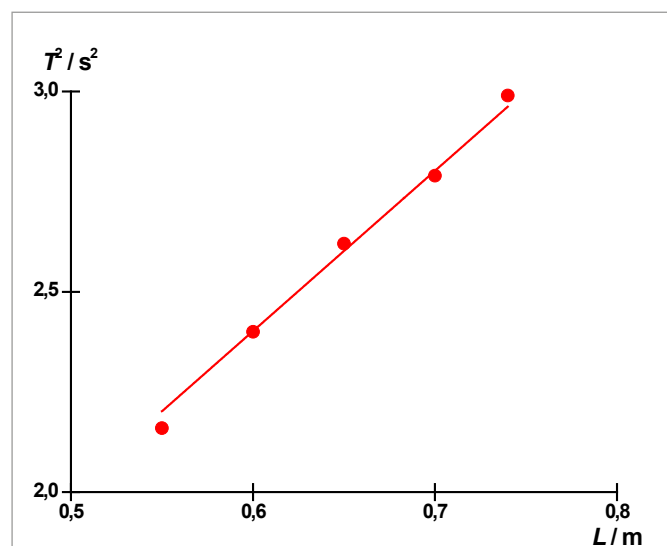
1020910 Digital Oscilloscope 2x30 MHz

(for experiments marked *)

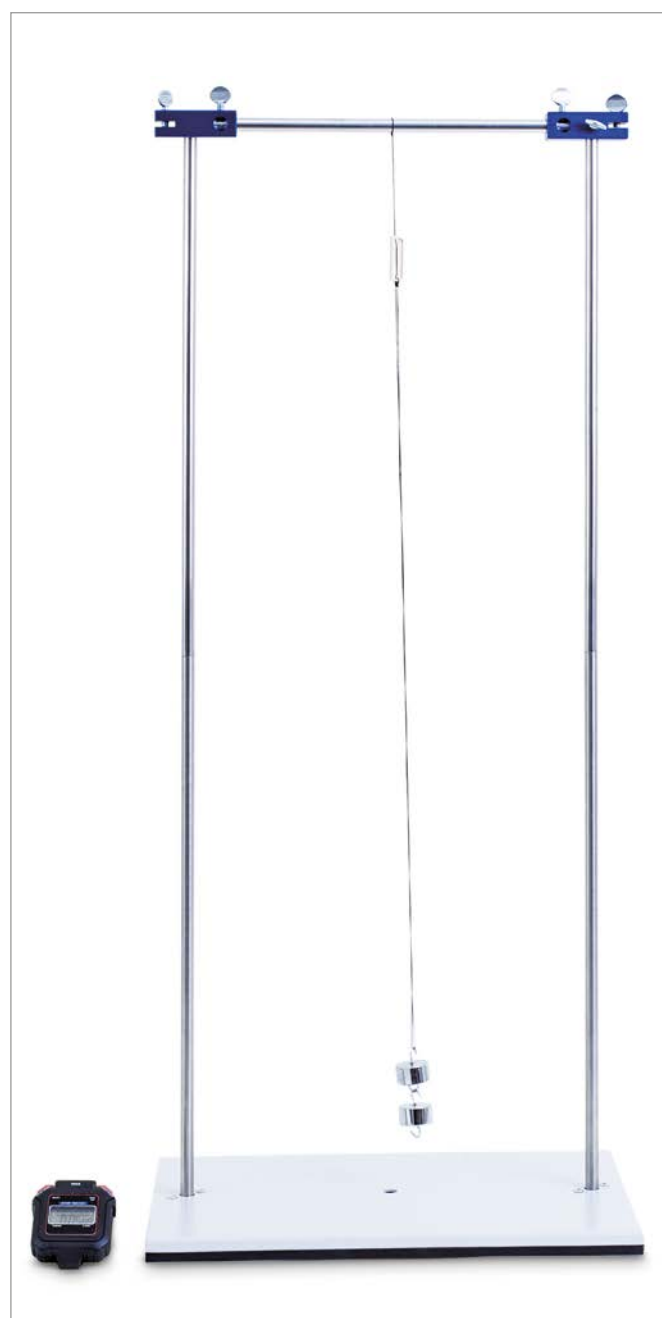
1013526 Analog Multimeter ESCOLA 30

(for experiments marked **)

PLEASE ASK FOR QUANTITY DISCOUNTS
ON CLASS SETS OF 8 PIECES OR MORE.



Squares of the period as a function of the length of the pendulum



String pendulum

STUDENT EXPERIMENT KIT SYSTEM

ULTRASONIC WAVES



> INCLUDES:

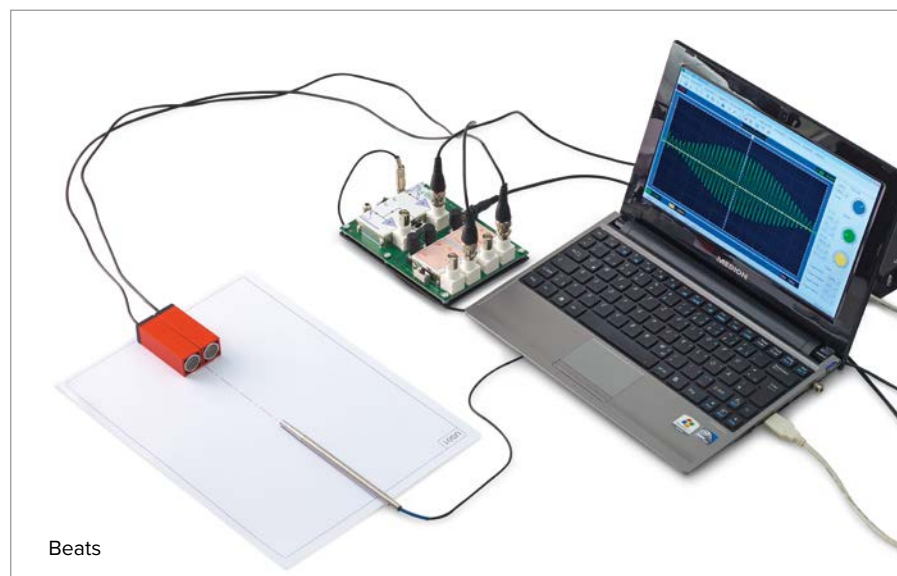
- 1 Ultrasonic Control Unit
- 2 Ultrasonic Transmitters, 40 kHz
- 1 Ultrasonic Pen
- 1 Holder for Ultrasonic Pen
- 1 Holder Base for Ultrasonic Pen
- 1 Microphone Probe
- 2 Beam Splitters
- 3 Clamps for Beam Splitters
- 1 Fresnel Zone Plate
- 1 Concave Mirrors
- 2 Side Pieces for Double Slit/Reflectors
- 1 Center Post for Double Slit
- 1 Clap for Double Slit
- 1 Ultrasonic Absorber
- 2 BNC Cables, 1 m
- 1 Cable, BNC/4-mm
- 1 Plug-in Power Supply

- > CD-ROM CONTAINING ALL DIFFERENT SETS OF INSTRUCTIONS IS INCLUDED!

Large equipment set incorporating 30 student experiments for demonstrating the fundamental properties of waves using the example of 40 kHz ultrasonic waves. Stored in a tough Gratnell tray with foam inlay featuring recesses moulded to the shape of the apparatus and covered by a transparent lid. Includes CD with experiment instructions. Includes two ultrasonic transmitters, a rod-shaped microphonic sensor for recording and analysing oscillations using a standard oscilloscope and an ultrasonic pen for recording wave fronts along the desktop in the form of lines of the same phase (isophases). Many of the experiments can also be carried out without using an oscilloscope. In order to measure ultrasonic amplitudes, it is sufficient in many cases to use an analog voltmeter for alternating current if it has a wide enough frequency range.

1016651 (230 V, 50/60 Hz)

1014529 (115 V, 50/60 Hz)



Beats

INCLUDES INSTRUCTIONS FOR 30 EXPERIMENTS ON ULTRASONIC WAVES

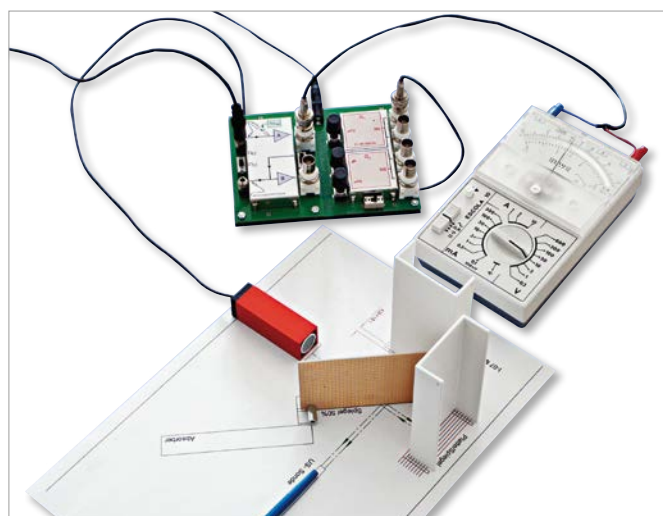
- Display of sound oscillations on an oscilloscope *)
- Relationship between oscillations and waves *)
- Comparison of oscillations at two points along a wave *)
- Analysis of phase relationships using an ultrasonic “pen” *)
- Determination of wavelength and velocity of sound
- How velocity of sound depends on temperature
- Transmission characteristic of ultrasonic transmitters **)
- Resonance curve for ultrasonic transducers *)
- Transmission and reflection of ultrasonic waves **)
- Absorption of ultrasonic waves **)
- Superimposition of sinusoidal oscillations *)
- Constructive and destructive reinforcement when sinusoidal oscillations are superimposed *)
- Recording of wave fronts using ultrasonic pen
- Generation and detection of straight wave fronts
- Diffraction of ultrasonic waves by an edge
- Diffraction of ultrasonic waves by a single slit
- Interference between two beams **)
- Law of reciprocity for interference between two beams **)
- Diffraction by a double slit **)
- Phase relationships for diffraction by a double slit / *)
- Phase relationships for diffraction by a double slit / **)
- Formation of images by a spherical concave mirror **)
- Plotting of Fresnel zones **)
- Formation of images by a Fresnel zone plate **)
- Interference of ultrasonic waves by Lloyd’s mirror **)
- Design of a simple interferometer **)
- Design of a Michelson interferometer **)
- Elimination of interference by interrupting the path *)
- Generation of standing ultrasonic waves **)
- Beats in ultrasonic waves *)
- Doppler effect in ultrasonic waves

Additionally required:

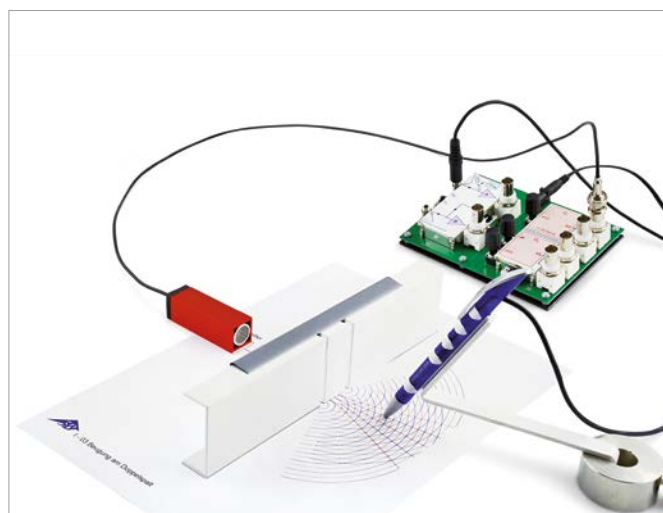
1017264 Dual-Channel Oscilloscope (for experiments marked *)

1006811 Multimeter ESCOLA 2 (for experiments marked **)

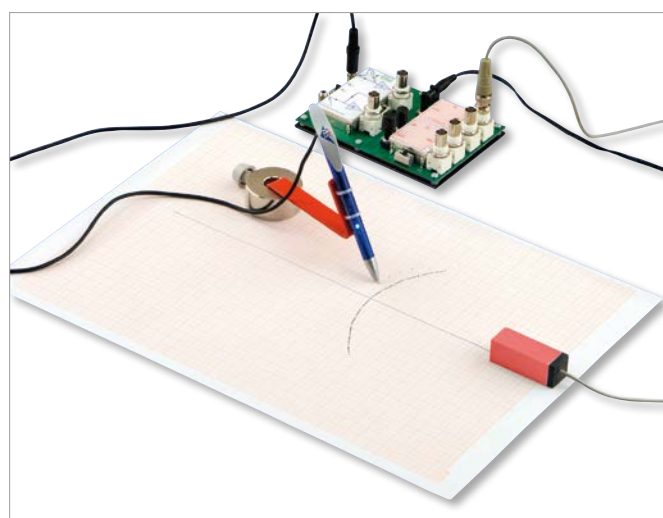
PLEASE ASK FOR QUANTITY DISCOUNTS ON CLASS SETS OF 8 PIECES OR MORE.



Michelson Interferometer



Diffraction by a double slit



Recording of wave front

STUDENT EXPERIMENT KIT SYSTEM

KRÖNCKE OPTICAL SYSTEM



> CONTENTS:

- 1 Optical Lamp
- 1 Transformer 12 V, 25 VA
- 1 Optical Bench, 1000 mm
- 6 Optical Slides
- 2 Clamps
- 2 Converging Lenses, $f = 50$ mm
- 2 Converging Lenses, $f = 100$ mm
- 2 Converging Lenses, $f = 150$ mm
- 1 Converging Lens, $f = 300$ mm
- 1 Converging Lens, $f = 500$ mm
- 1 Diverging Lens, $f = -100$ mm
- 1 Diverging Lens, $f = -500$ mm
- 1 Diaphragm with 1 Slit
- 1 Diaphragm with 3 Slits
- 1 Photograph in Slide Frame
- 1 Transparent Screen
- 1 White Screen
- 1 Set of 4 Color Filters
- 1 Ruler, 15 mm
- 1 Set of Holes arranged to form the Number "1"
- 1 Pinhole Aperture, $d = 1$ mm
- 1 Pinhole Aperture, $d = 6$ mm

- > CD-ROM CONTAINING ALL DIFFERENT SETS OF INSTRUCTIONS IS INCLUDED!

BASIC SET FOR KRÖNCKE OPTICAL SYSTEM

The Kröncke optical system provides robust reliability that has been tried and tested for decades and offers all the precision needed for student exercises and practical courses in numerous experiments on ray and wave optics. The experiments are carried out in traditional fashion using the white light of an incandescent lamp, the filament of which can be projected through an adjustable slit to observe interference in particular.

All optical components are mounted in diaphragms with no stems and can easily be adjusted vertically and with precision into the optical light path when mounted on optical riders. Optical riders can freely move on the U-profile rail of an optical bench and can be attached with a minimum of force.

RAY OPTICS:

- Pinhole camera
- Imaging with converging lenses
- Image aberrations
- Images in the eye (eye model)
- Correction of vision
- Magnifying glasses
- Microscopes
- Astronomical telescopes
- Terrestrial telescopes
- Slide projectors

Equipment ray optics:

- 1009932 Basic Set for Kröncke Optical System (230 V, 50/60 Hz)
- or
- 1009931 Basic Set for Kröncke Optical System (115 V, 50/60 Hz)

POLARIZATION:

- Polarization of transverse waves
- Polarizer and analyzer
- Visibility of polarized light in turbid water
- Double refraction
- Rotation of planes of polarization by a sugar solution

Equipment polarization:

1009932 Basic Set for Kröncke Optical System (230 V, 50/60 Hz)
or
1009931 Basic Set for Kröncke Optical System (115 V, 50/60 Hz)
1009701 Supplementary Set for Polarization

SUPPLEMENTARY SET FOR POLARIZATION

Supplementary set to the Kröncke optics basic set (1009932 resp. 1009931) for carrying out student experiments on the polarization of light waves.

Contents:

- 1 Pair of polarising filters
- 1 Pinhole aperture, 10 mm
- 1 Rectangular cuvette
- 1009701

INTERFERENCES:

- Fresnel mirror
- Diffraction by small openings and plates
- Diffraction by an air gap
- Diffraction by the wire
- Diffraction by multiple slits
- Diffraction by the grating
- Optical resolution
- Determining the wavelength of light

Equipment interference:

1009932 Basic Set for Kröncke Optical System (230 V, 50/60 Hz)
or
1009931 Basic Set for Kröncke Optical System (115 V, 50/60 Hz)
1009700 Supplementary Set for Interference

SUPPLEMENTARY SET FOR INTERFERENCE

Supplementary set to the Kröncke optics basic set (1009932 resp. 1009931) for carrying out student experiments on the interference of light waves.

Contents:

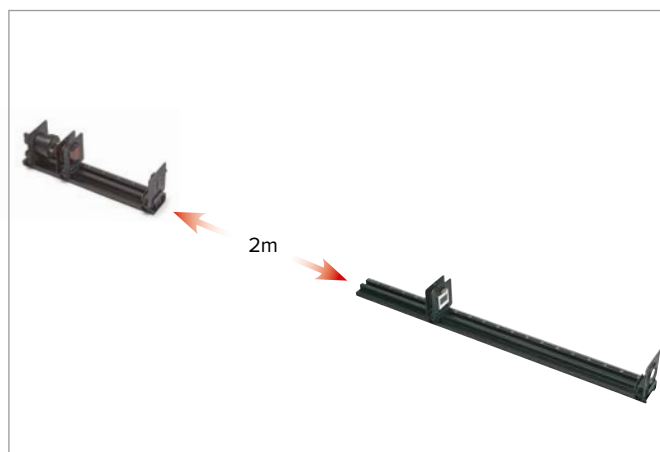
- 1 Optical bench, 500 mm
- 1 Adjustable slit
- 1 Diaphragm with 9 circular discs
- 1 Diaphragm with 9 circular holes
- 1 Diaphragm with 3 individual slits and 1 double slit
- 1 Diaphragm with 4 multiple slits and grating
- 1 Diaphragm with 3 ruled gratings
- 1 Micrometer screw
- 1 Fresnel mirror
- 1009700



Visibility of polarized light in turbid water



Slide projectors

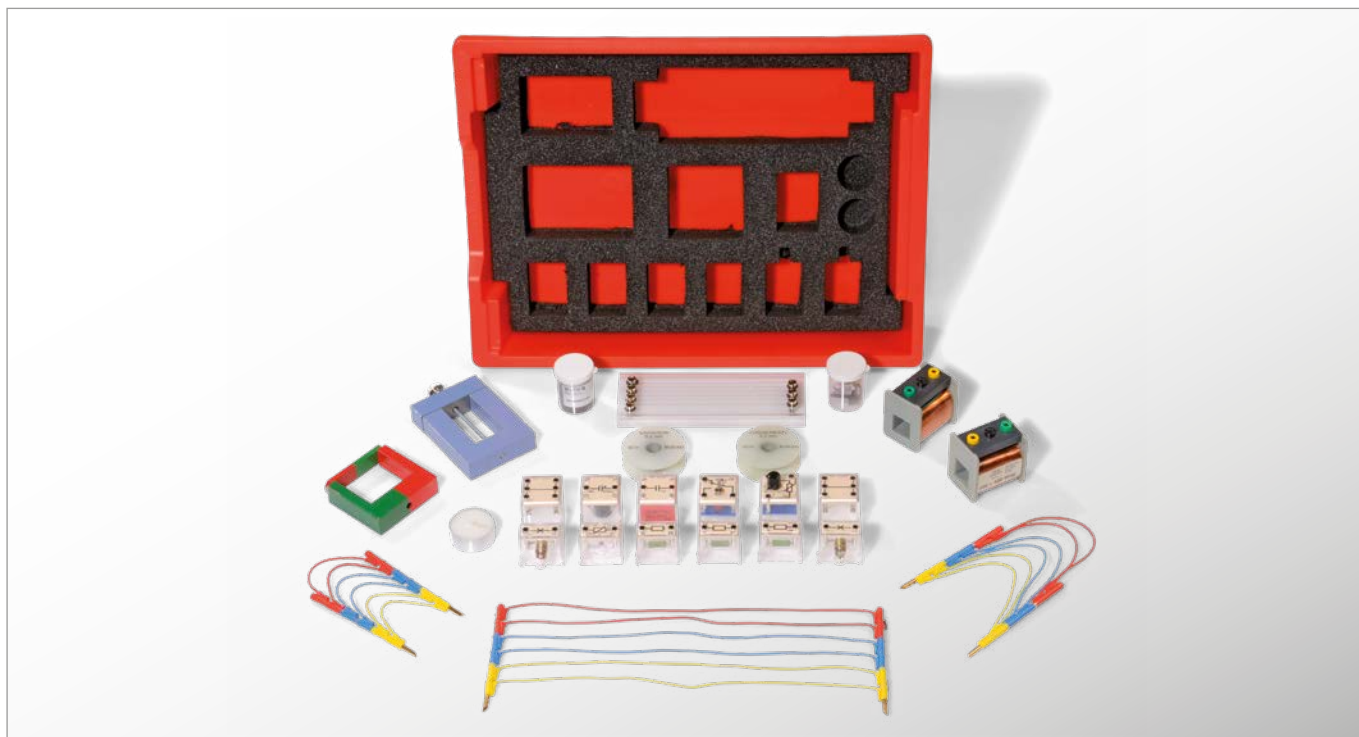


Diffraction by a multiple slit

PLEASE ASK FOR QUANTITY DISCOUNTS
ON CLASS SETS OF 8 PIECES OR MORE.

STUDENT EXPERIMENT KIT SYSTEM

ELECTRICITY AND MAGNETISM



> CONTENTS:

- 1 Set of Experiment Leads
- 1 Bar Magnet, 65x16x5 mm approx.
- 1 Horseshoe Magnet, ALNICO, flat
- 1 Resistor Board
- 1 Transformer Core, 20x20 mm
- 1 Tightening Screw
- 1 Coil, 200/400/600 windings
- 1 Coil, 400/400/800 windings
- 2 Current Branches (plug-in components)
- 1 Potentiometer, 100 Ω (plug-in component)
- 1 Switch (plug-in component)
- 1 Capacitor, 4700 μF (plug-in component)
- 1 Capacitor, 10 μF (plug-in component)
- 1 Resistor, 33 Ω (plug-in component)
- 1 Resistor, 47 Ω (plug-in component)
- 1 Resistor, 1 k Ω (plug-in component)
- 1 NTC-resistor, 100 Ω (plug-in component)
- 2 Lamp Sockets, E10 (plug-in components)
- 1 Storage Box with 1 Set of Threads with Washer, 2 Threaded Bushes, 2 Threaded Pins, 2 Paper Clips, 2 Aluminium Electrodes, constantan wire
- 50 g of Iron Filings
- 50 m of Chrome/Nickel Wire, 0.2 mm
- 50 m of Iron Wire, 0.2 mm
- 1 Tea Candle

Set of equipment for carrying out 41 student experiments on electricity and magnetism. In a tough plastic box containing a foam insert with cut-outs for the equipment and featuring a transparent lid. Includes CD with experiment instructions. The experiments are set up and performed in a space saving fashion but are still clearly laid out on the SEK base plate (1000789).
1008532

SEK Power Supply

AC/DC power supply for SEK electricity and magnetism kit (1008532).

- Voltage limitation to 25 V AC and 60 V DC
 - Safety transformer conforming to EN 61558-2-6
 - Safe isolation between power supply and output circuits
- Voltages: 1.5/ 3.0/ 4.5/ 6.0 V AC/DC

SEK Power Supply (230 V, 50/60 Hz) 1021686

or

SEK Power Supply (115 V, 50/60 Hz) 1021687



> CD-ROM CONTAINING ALL DIFFERENT SETS OF INSTRUCTIONS IS INCLUDED!

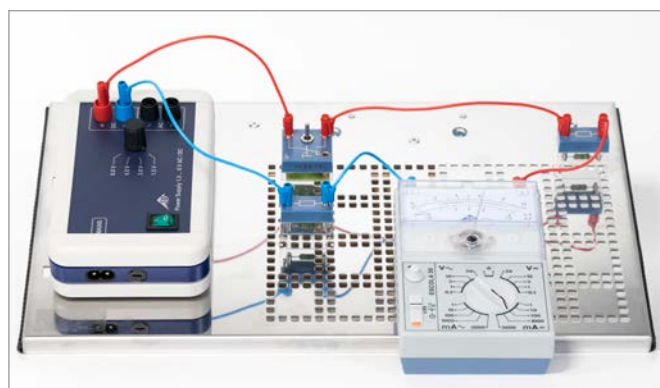
INCLUDES 41 EXPERIMENTS ON THE SUBJECT OF ELECTRICITY AND MAGNETISM:

- Closed circuits
- Conductors and insulators
- Circuits with no branches
- Circuits with branches
- Current in a circuit with no branches
- Current in a circuit with branches
- Initial voltage and terminal voltages
- Voltage in a circuit with no branches
- Voltage in a circuit with branches
- Voltage dividers
- Ohm's law
- Temperature dependence of a resistor (iron wire)
- Current-voltage diagram for a light bulb
- Current-voltage diagram for a thermistor
- Law of resistance
- Resistance in a circuit with no branches
- Resistance in a circuit with branches
- Resistance and voltage in a circuit with no branches
- Resistance and current in a circuit with branches
- Voltage dividers with and without a load
- Voltage-time diagram for charging and discharging of a capacitor
- Current-time diagram for charging and discharging of a capacitor
- Relationship between charge and voltage
- Capacitor in the DC and AC circuit (response)
- Test bodies in a magnetic field
- Magnetic poles
- Magnetic field of a horseshoe magnet and a bar magnet
- Magnetic dipoles
- A coil used as a magnet
- Forces in the magnetic field of a coil
- Induction due to relative motion
- Induction due to changes in magnetic field
- Induction law
- Ohmic resistance in AC and DC circuits
- Capacitors in AC and DC circuits (resistance)
- Coils in AC and DC circuits
- How a transformer works
- Voltage and number of windings for a transformer with no load
- Transformer under load
- Transformer under heavy load
- Thermoelectricity

Equipment Electricity:

- 1008532 SEK Electricity and Magnetism
 - 1000789 SEK Base Plate
 - 1013526 Analogue Multimeter ESCOLA 30
 - 1021686 SEK Power Supply (230 V, 50/60 Hz)
- or
- 1021687 SEK Power Supply (115 V, 50/60 Hz)

PLEASE ASK FOR QUANTITY DISCOUNTS
ON CLASS SETS OF 8 PIECES OR MORE.



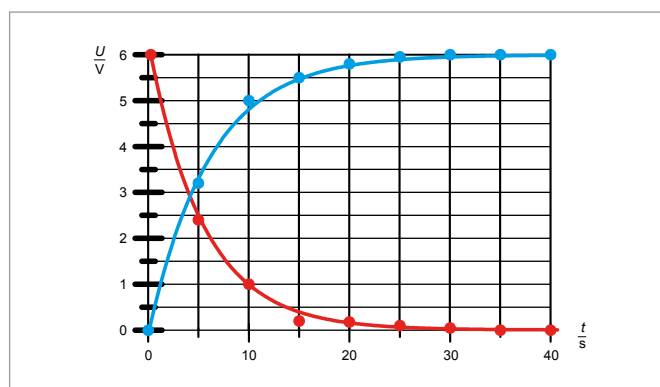
Electric current in circuits with no branches



Laws of resistance



Charging and discharging of a capacitor (voltage)



Capacitor: charging (blue) and discharging (red)

STUDENT EXPERIMENT KIT SYSTEM

ELECTRONICS



> CONTENTS:

- 1 Set of 10 Jumpers
- 1 Resistor 100 Ω , 2 W
- 1 Resistor 470 Ω , 2 W
- 1 Resistor 1 k Ω , 2 W
- 1 Resistor 4.7 k Ω
- 1 Resistor 10 k Ω , 0.5 W
- 1 Resistor 47 k Ω , 0.5 W
- 1 Electrolytic Capacitor 100 μ F, 35 V
- 1 Electrolytic Capacitor 470 μ F, 16 V
- 1 E 10 Socket, socket upward facing
- 1 Set of 10 bulbs, 12 V; 100 mA
- 1 Set of 10 bulbs, 4 V; 40 mA
- 1 Single-Pole Rocker Switch
- 1 Single-Pole Push-Button Switches, normally open
- 1 Single-Pole Push-Button Switches, normally closed
- 4 Si-Diodes 1N 4007
- 1 Ge-Diode
- 1 Zener Diode ZPD 6.2
- 1 LED green
- 1 LED, red
- 1 LDR 05 Photoresistor
- 1 NTC Thermistor 2.2 k Ω
- 1 PTC Thermistor 100 Ω
- 1 Potentiometer 220 Ω , 3 W
- 1 NPN Transistor BD 137
- 1 PNP Transistor BD 138
- 1 BF 244 Field Effect Transistor
- 1 TYN 1012 Thyristor
- 1 Single-Pole Change-Over Switch
- 1 Set of Earpiece Headphones

Set of apparatus for carrying out 11 fundamental student experiments on electronics. Stored in a tough Gratnell tray with foam inlay featuring recesses moulded to the shape of the apparatus and covered by a transparent lid. Circuits are assembled using components in plug-in housings plugged into a plug-in board. Power is supplied via an external power supply. Includes a CD with instructions for the experiments.

P-1021672

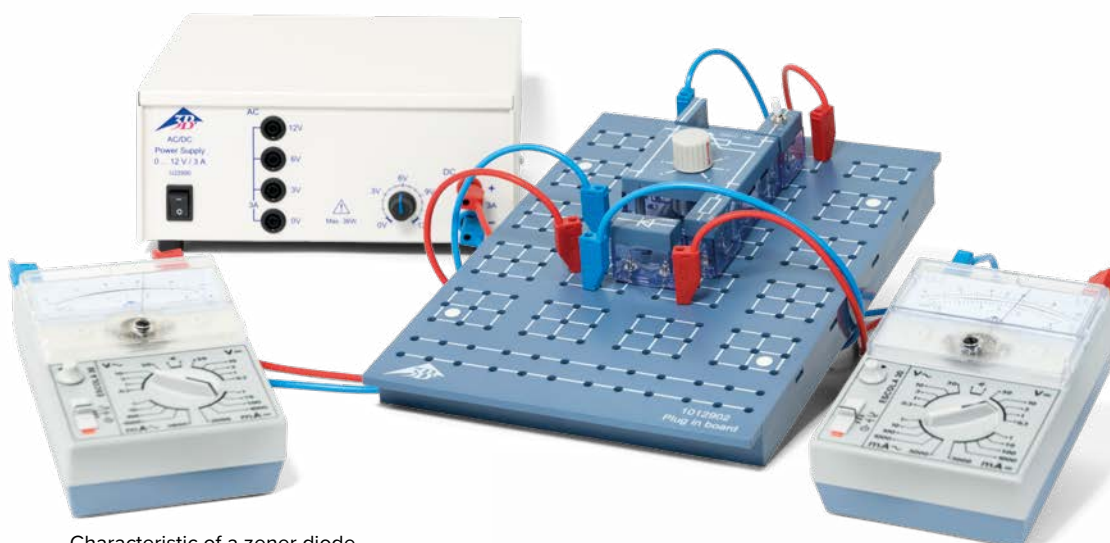
INCLUDES INSTRUCTIONS FOR 11 EXPERIMENTS ON ELECTRONICS:

- Characteristic of an LED
- Characteristic of a zener diode
- Check how current flows through a transistor
- Characteristics of a transistor
- LDR photoresistor (light dependent resistor)
- Thyristors in DC circuits
- Temperature response of NTC and PTC thermistors
- Delayed switching processes
- Characteristics of a field effect transistor
- Check for mains hum

EQUIPMENT ELECTRONICS:

- 1021672 SEK - Electronics
- 1012902 Plug-in Board for Components
- 1021091 AC/DC Power Supply, 0 - 12 V, 3 A (230 V; 50/60 Hz)
- or
- 1021092 AC/DC Power Supply, 0 - 12 V, 3 A (115 V; 50/60 Hz)
- 1013526 Analog Multimeter 30 (2x)
- 1002840 Set of 15 Experiment Leads, 75 cm

> CD-ROM CONTAINING ALL DIFFERENT SETS OF INSTRUCTIONS IS INCLUDED!



Characteristic of a zener diode



Check how current flows through a transistor

PLEASE ASK FOR QUANTITY DISCOUNTS ON CLASS SETS OF 8 PIECES OR MORE.



Thyristors in DC circuits

STUDENT EXPERIMENT KIT SYSTEM

SOLAR ENERGY



> CONTENTS:

- 1 Halogen Spotlight
- 2 Solar Modules
- 2 Digital Multimeters
- 1 Lux Meter
- 1 Digital Thermometer
- 1 Terminal Board with Resistor Cascade
- 1 Power Adjuster
- 1 Jumper
- 1 Set of Experiment Leads
- 1 Cross Piece
- 1 Support Brace
- 1 Set of Items for Covering Modules
- 1 Case

> CD-ROM CONTAINING ALL DIFFERENT SETS OF INSTRUCTIONS IS INCLUDED!

Large equipment set for carrying out 16 fundamental experiments on solar energy. The basic parameters and properties of solar modules and the aspects which affect their energy efficiency can all be demonstrated by experiment. Contained in a rugged metal case including foam inlay with recesses in the shape of the apparatus. The system allows you to assemble experiments easily and in a compact set-up on or in the lid of the kit's carry case. Includes CD with experiment instructions.

SEK Solar Energy (230 V, 50/60 Hz) 1017732

SEK Solar Energy (115 V, 50/60 Hz) 1017731

INCLUDES INSTRUCTION FOR 16 EXPERIMENTS ON SOLAR ENERGY:

- Illuminance of various light sources
- Parameters affecting the power generated by a solar module
- Shading of solar modules connected in series
- Effect of shading on the terminal voltage of a solar module
- Effect of illuminance on the open-circuit voltage and short-circuit current for a solar module
- Effect of angle of incidence on the open-circuit voltage and short-circuit current for a solar module
- Open-circuit voltage and short-circuit current for solar modules connected in series and in parallel
- Current-voltage characteristic for a solar module
- Current-voltage characteristic for solar modules in series
- Current-voltage characteristic for solar modules in parallel
- Optimum load resistance when the angle of incidence changes
- How the open-circuit voltage and short-circuit current for a solar module depend on temperature
- How power output from solar modules depends on temperature
- Voltage-current characteristic for illuminated and non-illuminated solar modules *
- Setting up a stand-alone power supply network **
- Energy conversion ***

EQUIPMENT SOLAR ENERGY:

1017732 SEK Solar Energy (230 V, 50/60 Hz)

or

1017731 SEK Solar Energy (115 V, 50/60 Hz)

1003312 DC Power Supply 0-20 V (230 V, 50/60 Hz)

or

1003311 DC Power Supply 0-20 V (115 V, 50/60 Hz)

(for experiments marked *)

1017734 Coulombmeter with Rechargeable Battery

1002811 Digital Stopwatch (for experiments marked **)

1017735 Geared Motor with Pulley

1018597 Set of Weights 1 g to 500 g, slotted with Holder

1007112 Experiment Cord

1002811 Digital Stopwatch (for experiments marked ***)

COULOMBMETER WITH RECHARGEABLE BATTERY

Coulombmeter for measuring the flow of current when storing energy in a rechargeable battery. Charge or consumption can be displayed by means of a voltmeter. Depending on the measuring range selected, 1 Vn the voltmeter corresponds to either 0.1, 1 or 10 ampere seconds (As).

Measuring ranges: 1/10/100 As (max. measurable charge ± 499 As)

Power supply: 9 V rechargeable battery via DC co-axial power socket

Load current: max. 500 mA

Charging current for

battery: max. 50 mA

External power source: Solar panel or DC power supply (max. 12 V DC) with current limiting to 50 mA when there is no load on the coulombmeter

Connectors: 4-mm safety sockets

Dimensions: approx. 105x75x45 mm³

Weight: 200 g including rechargeable battery and housing

1017734

GEARED MOTOR WITH PULLEY

The geared motor with string pulley is used in conjunction with the Solar Energy Student Experiment Kit as a load for demonstrating conversion of energy. The motor is mounted on a base plate and has a pulley attached for a string. Power is supplied via 4-mm safety sockets. Weights of up to approximately 1 kg can be lifted.

Power supply: max. 12 V DC

Load current: max. 50 mA

Torque: 0.41 Nm

Speed: 76.1 rpm with no load

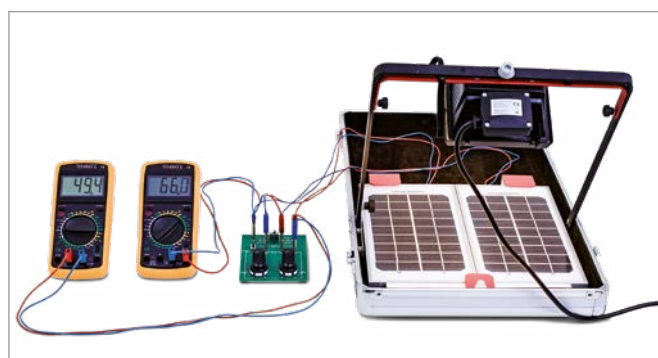
Connectors: 4-mm safety sockets

Dimensions: approx. 105x75x45 mm³

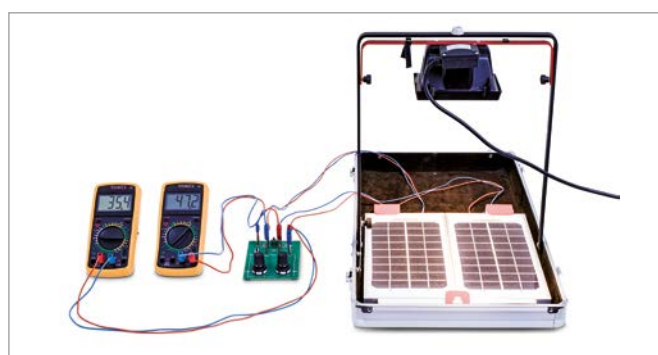
Weight: approx. 220 g

1017735

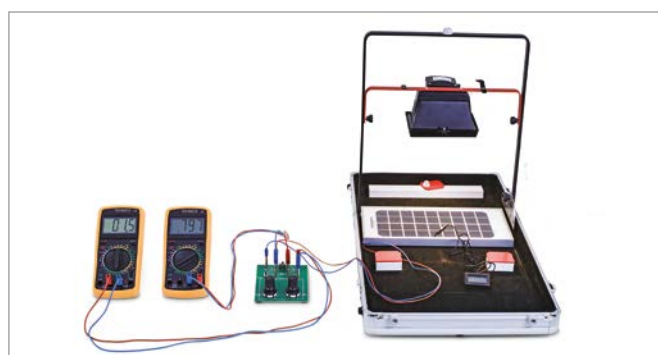
PLEASE ASK FOR QUANTITY DISCOUNTS
ON CLASS SETS OF 8 PIECES OR MORE.



Optimum load resistance when the angle of incidence changes



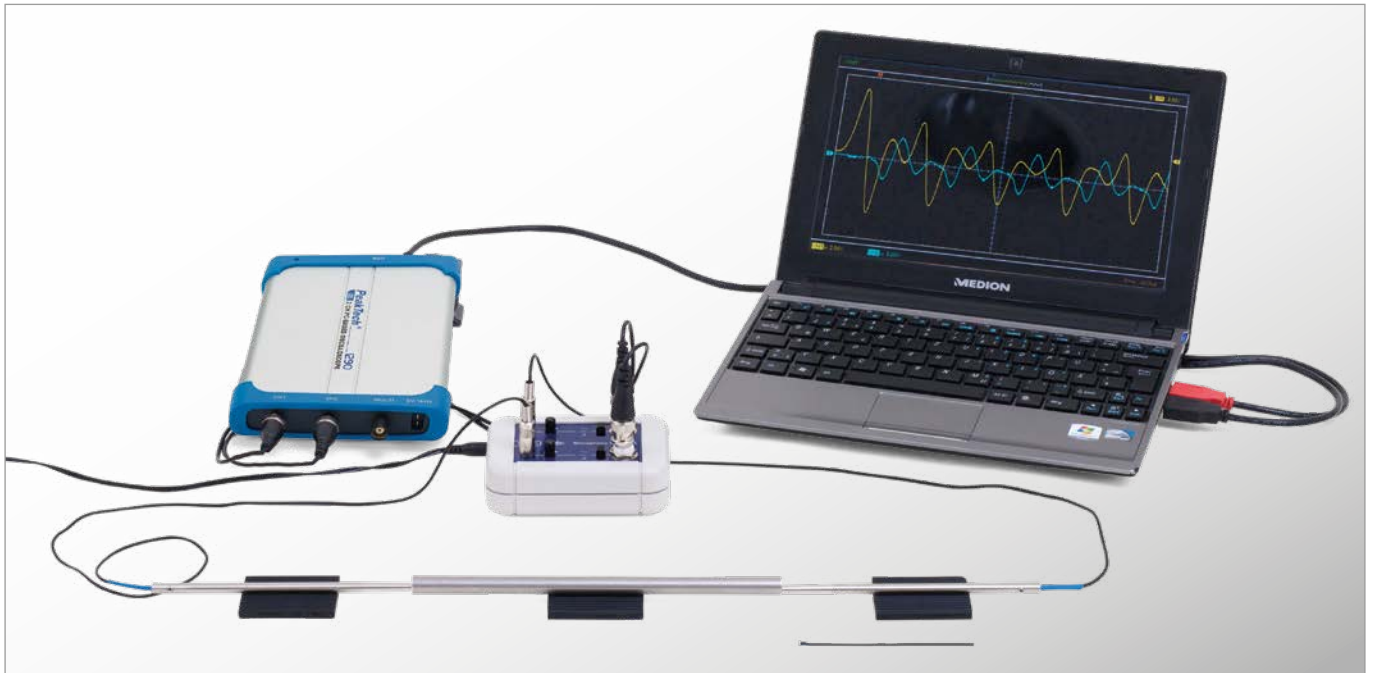
Current-voltage characteristic for solar modules in series



How power output from solar modules depends on temperature

STUDENT EXPERIMENT KIT SYSTEM

SOUND PROPAGATION IN SOLID BODIES



> CONTENTS:

- 6 Test Rods, 200 mm, made of Glass, Transparent Acrylic (perspex), PVC, Wood (Beech), Stainless Steel and Aluminium
- 4 Test Rods, 100 mm, Made of Copper, Brass, Stainless Steel and Aluminium
- 1 Test Rod, 400 mm made of Stainless Steel
- 2 Beaters
- 2 Microphone Probes
- 1 Microphone Boxes
- 1 Plug-in Power Supply 12 V AC
- 3 Rubber Mats, 50x40x5 mm³

> COMPACT SET-UP ON LAB BENCHES

EQUIPMENT SET “SOUND PROPAGATION IN RODS”

Equipment set for investigating propagation of sound and determining the speed of sound in solid rods of various materials. The set includes various test rods, two microphone probes and a microphone box for connection to an oscilloscope. Contained in a sturdy plastic case with foam inlays in the shape of the apparatus and a transparent lid.

Equipment Set “Sound Propagation in Rods” (230 V, 50/60 Hz) 1018469
or

Equipment Set “Sound Propagation in Rods” (115 V, 50/60 Hz) 1018468

Additionally required:

Dual-channel oscilloscope, e.g.
1020857 PC Oscilloscope, 2x25 MHz

EXPERIMENT TOPICS:

- Speed of propagation of sound pulses in various rods
- Comparison between the propagation of longitudinal and transverse waves
- Standing sound waves in short rods
- Polarity of reflections at the ends of the rods
- Multiple reflection at the ends of longer rods



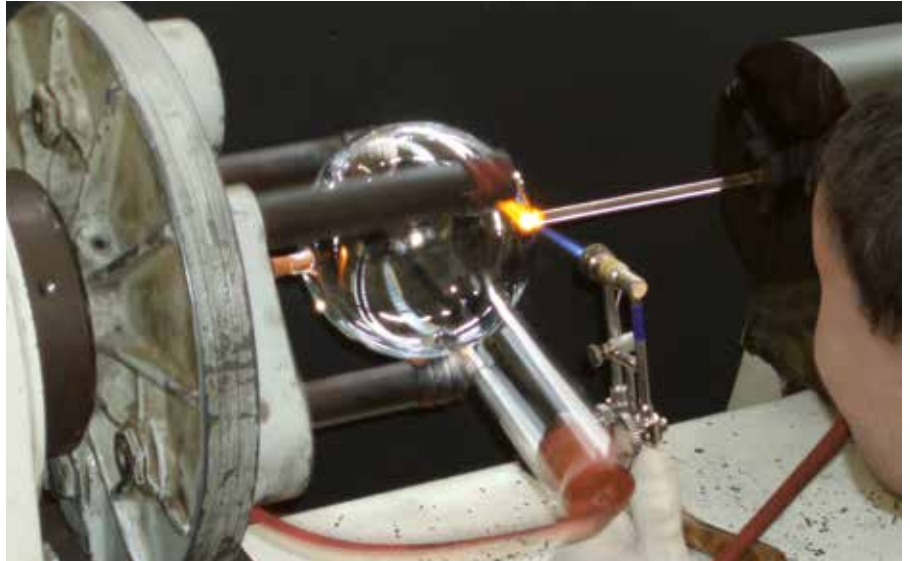
NON-CONTACT AND LOW-ATTENUATION MEASUREMENT OF SOUND WAVES!

3B SCIENTIFIC PHYSICS PRODUCTION IN GERMANY, KLINGENTHAL



MANUFACTURING A TELTRON® ELECTRON TUBE AT 3B SCIENTIFIC IN GERMANY

Electron tubes are produced at only a very small number of places in the world. Only specially trained technicians with many years of experience have the skills that are needed for this technologically advanced manufacturing process, which ensures that every TELTRON® electron tube that you receive from us will have the same consistently high quality.



ASSEMBLY PRODUCTION AT THE CNC PROCESSING CENTRE

The universally recognised high quality of the teaching equipment produced is achieved through a combination of modern process technology with the best traditional craftsmanship. The skills and facilities of the CNC Processing Centre in Klingenthal guarantee not only the mechanical precision that is essential for high-quality physical instruments, but also cost-effective series production with consistently high quality.

A CAD/CAM WORKSTATION

A direct extension from the principles of CAD (Computer Aided Design) is CAM (Computer Aided Manufacturing), here shown being applied to controlling a flat-bed milling machine. This manufacturing technology makes it possible to fulfill special project requirements with speed and with the usual high precision.



MALTESE-CROSS TUBE EXPERIMENT

Demonstrate the straight-line propagation of electrons in the absence of any field

› More on page 170

